BNL-52672
Formal Report

Proceedings of RIKEN BNL Research Center Workshop Volume 43

RIKEN Winter School

Quark-Gluon Structure of the Nucleon and QCD

March 29-31, 2002

Organizers:

Hideto En'yo, Naohito Saito, T.-A. Shibata, and Koichi Yazaki

RIKEN BNL Research Center

Building 510A, Brookhaven National Laboratory, Upton, NY 11973-5000, USA

Available electronically at-

http://www.doe.gov/bridge

Available to U.S. Department of Energy and its contractors in paper from-

U.S. Department of Energy
Office of Scientific and Technical Information
P.O. Box 62
Oak Ridge, TN 37831
(423) 576-8401

Available to the public from-

U.S. Department of Commerce
National Technical Information Service
5285 Port Royal Road
Springfield, VA 22131
(703) 487-4650

Printed on recycled paper

Preface to the Series

The RIKEN BNL Research Center (RBRC) was established in April 1997 at Brookhaven National Laboratory. It is funded by the "Rikagaku Kenkyusho" (RIKEN, The Institute of Physical and Chemical Research) of Japan. The Center is dedicated to the study of strong interactions, including spin physics, lattice QCD, and RHIC physics through the nurturing of a new generation of young physicists.

During the first year, the Center had only a Theory Group. In the second year, an Experimental Group was also established at the Center. At present, there are seven Fellows and eight Research Associates in these two groups. During the third year, we started a new Tenure Track Strong Interaction Theory RHIC Physics Fellow Program, with six positions in the first academic year, 1999-2000. This program has increased to include ten theorists and one experimentalist in the current academic year, 2001-2002. Beginning this year there is a new RIKEN Spin Program at RBRC with four Researchers and three Research Associates.

In addition, the Center has an active workshop program on strong interaction physics with each workshop focused on a specific physics problem. Each workshop speaker is encouraged to select a few of the most important transparencies from his or her presentation, accompanied by a page of explanation. This material is collected at the end of the workshop by the organizer to form proceedings, which can therefore be available within a short time. To date there are forty-two proceeding volumes available.

The construction of a 0.6 teraflops parallel processor, dedicated to lattice QCD, begun at the Center on February 19, 1998, was completed on August 28, 1998.

T. D. Lee
August 2, 2001

*Work performed under the auspices of U.S.D.O.E. Contract No. DE-AC02-98CH10886.

CONTENTS

Introduction

The RIKEN School on "Quark-Gluon Structure of the Nucleon and QCD" was held from March 29th through 31st at the Nishina Memorial Hall of RIKEN, Wako, Saitama, Japan, sponsored by RIKEN (the Institute of Physical and Chemical Research). The school was the second of a new series with a broad perspective of hadron and nuclear physics.

The purpose of the school was to offer young researchers an opportunity to learn theoretical aspects of hadron physics based on QCD and related experimental programs being or to be carried out by Japanese groups.

We had 3 theoretical courses, each consisting of 3 one-hour lectures, and 6 experimental courses, each consisting of a one-hour lecture. The list of the lecturers together with the titles of their lectures are given below.

Lecturers

T. Hatsuda (Univ. of Tokyo)	"Introduction to Hot and Dense QCD"
M. Oka (Tokyo Inst. of Technology)	"Properties of Hadrons in Non-Perturbative QCD"
D. Soper (Univ. of Oregon)	"Basics of QCD Perturbation Thoery"
Y. Akiba (KEK)	"Heavy Ion Physics at RHIC"
Y. Goto (RBRC/RIKEN)	"First Polarized Proton Collisions at RHIC"
N. Horikawa (Nagoya Univ.)	"The Gluon Polarization Measurement by COMPASS and the Experimental Test of GDH Sum Rule"
T. Hotta (RCNP, Osaka Univ.)	"Laser Electron Photon Experiments at SPring-8"
T.-A. Shibata (Tokyo Inst. of Technology)	"Recent Results on Spin Structure of the Nucleon from HERMES"
H. Yamazaki (Kakuriken, Tohoku Univ.)	"Hadron Physics at Kakuriken (Laboratory of Nuclear Science)"

Totally 55 students attended the school and actively participated in the program. The number was more than three times the previous one. We had expected that the broader choice of the subjects would attract more students but the increase was beyond our expectation, suggesting that the easily accessible location and the choice of the period were also important.

The lecturers gave excellent courses which were both pedagogical and inspiring. Though almost all the students were Japanese, we asked all the lecturers to prepare the transparencies in English and some of the Japanese lecturers to speak in English so that we could involve Prof. Soper in the discussions during the lectures. There were relatively long intervals between the lectures and the lecturers were kind enough to talk to students and respond to their questions during the breaks.

Senior participants, Drs. H. Fujii, M. Hirai, T. Hirano, N. Ishii, A. Kohama, K. Sudou and Y. Yasui, stimulated the discussions and helped younger students understand the lectures.

At the end of the school, we asked the participants to write their opinions about the school. The responses were all positive with some comments on the choice of subjects, period and location. They were satisfied by the well-prepared lectures and the stimulating atmosphere. The mixture of theoretical and experimental lectures was both instructive and useful. Some students wanted to have a longer experimental course on a general subject together with topical ones. The location was not exciting but was convenient and enabled many students in Tokyo region to attend the school. The period just after the JPS meeting was welcomed by most of the participants. These comments are to be taken into consideration in planning this school series in future.

We are grateful to RIKEN for the financial support which enabled us to organize this school. The school was held as an activity related to the collaboration with the RIKEN-BNL Research Center and we thank the director of the Center, Professor T.D. Lee, for the approval of publishing this proceedings as a volume of the RBRC Workshop Proceedings Series and general support. We are obliged to the lecturers and the students, both young and senior, for making the school exciting and fruitful.

Special thanks are due to Ms.Y. Kishino and Ms.N. Kiyama, who did most of the administrative works and took care of drinks and snacks during the breaks, and Ms.S. Asaka and Ms.E. Nagahama of the International Cooperation Office for their help during the school. Mr.Y. Takubo and Mr.T. Watanabe of the Tokyo Institute of Technology did important jobs of preparing the announcements of the school and the copies of the transparencies for the lectures, which were distributed to all participants before the lectures started.

Hideto En'yo, Naohito Saito, Toshi-Aki Shibata,
Yasushi Watanabe and Koichi Yazaki

RIKEN,
June, 2002

Introduction to Hot and Dense QCD

Tetsuo Hatsuda[1] – *Univ. of Tokyo*

RIKEN Spring School, Wako/Japan, March 29-31, 2002

abstract

An over view of the recent progress in Quantum Chromodynamics (QCD) at finite temperature and baryon density is given. The 1st lecture is devoted to general introduction to the phase transition in QCD. In the 2nd lecture, plasma properties at high temperature is discussed on the basis of the weak coupling perturbation theory. In the 3rd lecture, critical phenomena assciated with the QCD phase transtion are described. Applications to early universe, relativistic heavy ion collisions and the structure of neutron stars are also discussed.

contents

[1] hatsuda@phys.s.u-tokyo.ac.jp

quenched heavy-quark potential

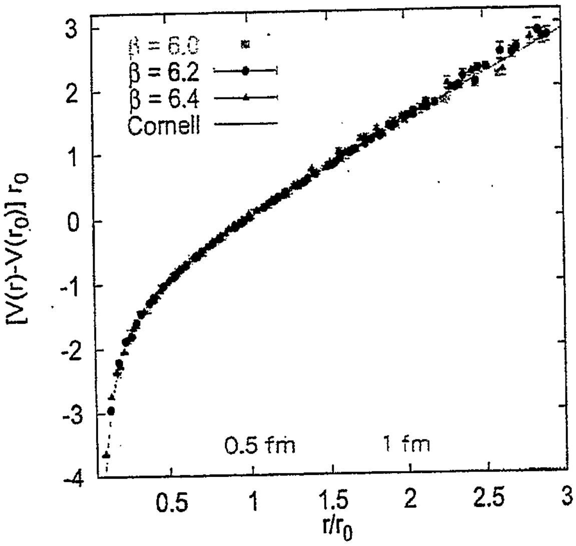

G.S. Bali, Phys Rep ('01)

quenched light-hadron spectrum

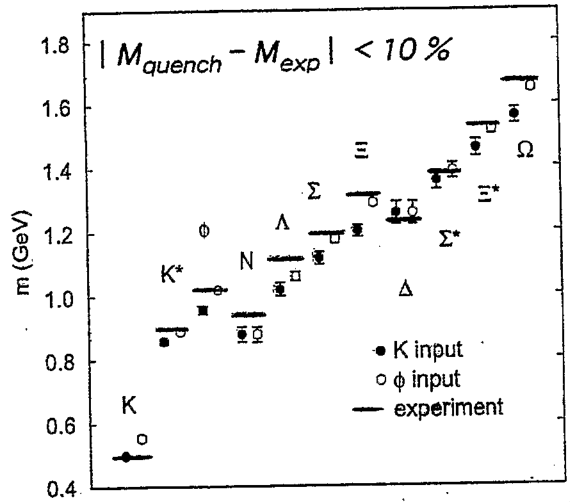

CP-PACS Coll., PRL 84 ('00)

Open problems

String breaking in full QCD ?

SESAM &T$_\chi$L, UKQCD, MILC Coll.

$| M_{full} - M_{exp} | < | M_{quench} - M_{exp} |$?

CP-PACS Coll., hep-lat/0105015 ('01).

$$\alpha_s(\mu) = \frac{\#}{\ln(\mu^2/\Lambda^2)} + \cdots$$

$\mu \sim Q$ (DIS,

$\sim T$ (QGP

$\sim p_F$ (QM,

QCD running coupling

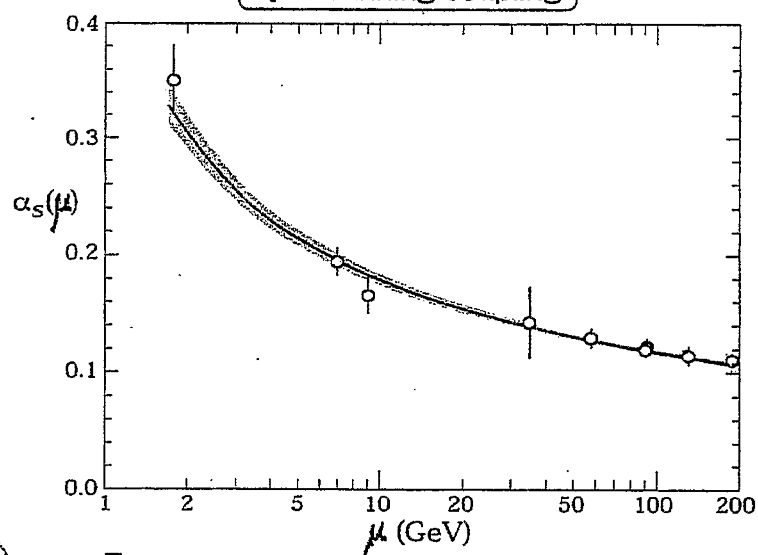

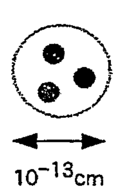

confinement of
quarks & gluons
at Λ_{QCD}~200 MeV

asymptotic free
quarks & gluons

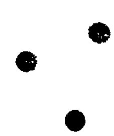

phase transition to Quark-gluon plasma

$$\begin{cases} T_c \simeq 200\,\mathrm{MeV} & \sim\ 10^{12}\,\mathrm{K} \\ \rho_c \simeq (3\text{-}6)\,\rho_0 & \sim\ 10^{12}\,\mathrm{kg/cm^3} \end{cases}$$

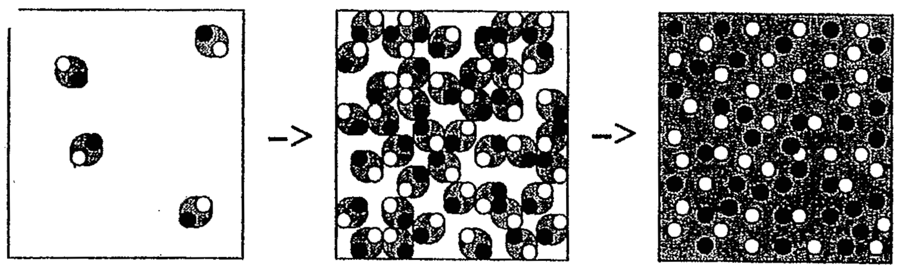

$T < T_c$ $\qquad$ $T \sim T_c$ $\qquad$ $T > T_c$

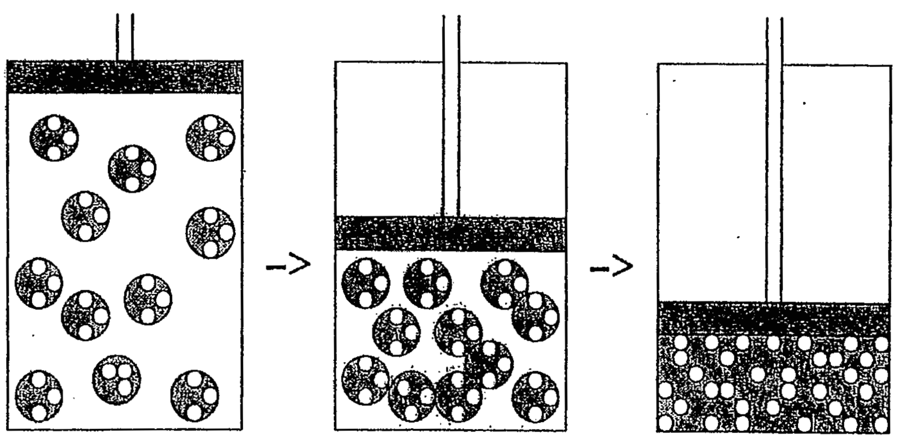

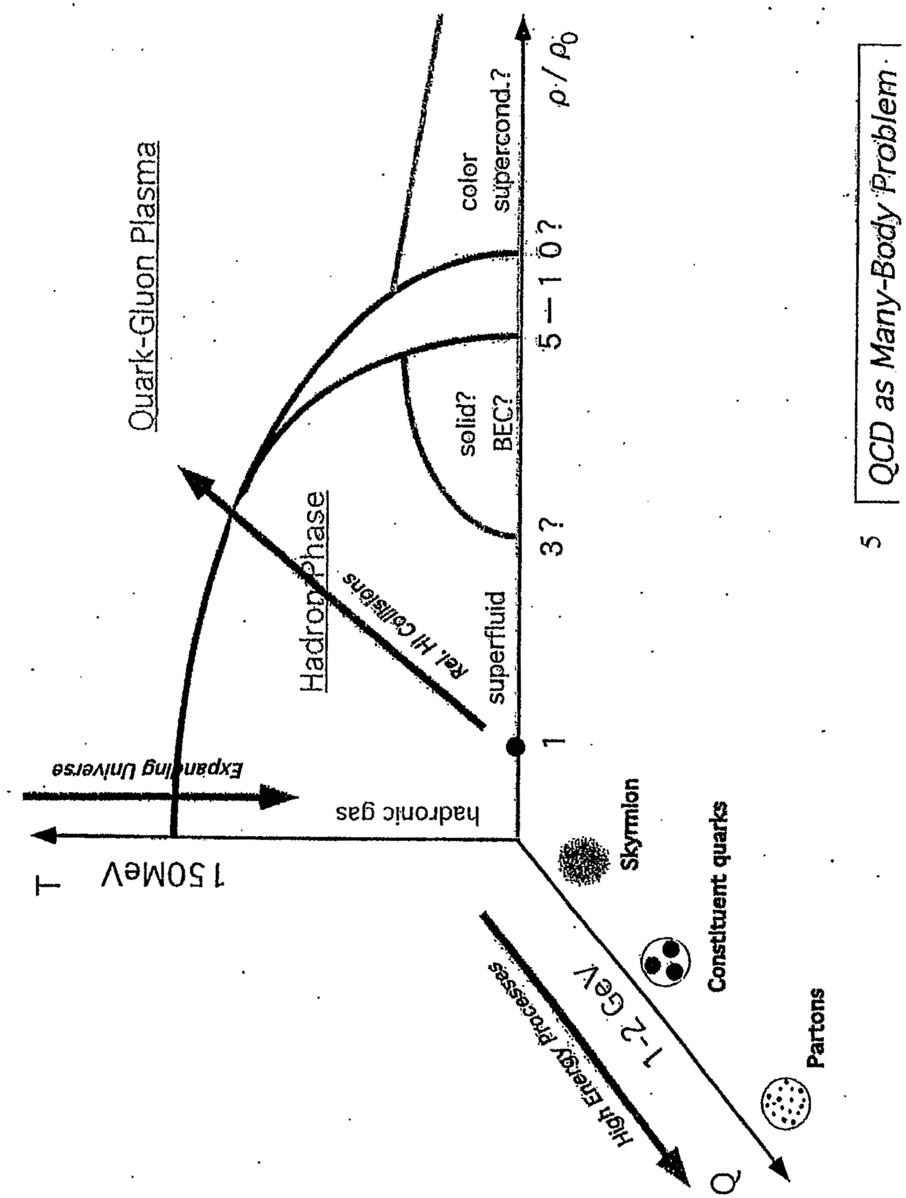

宇宙史

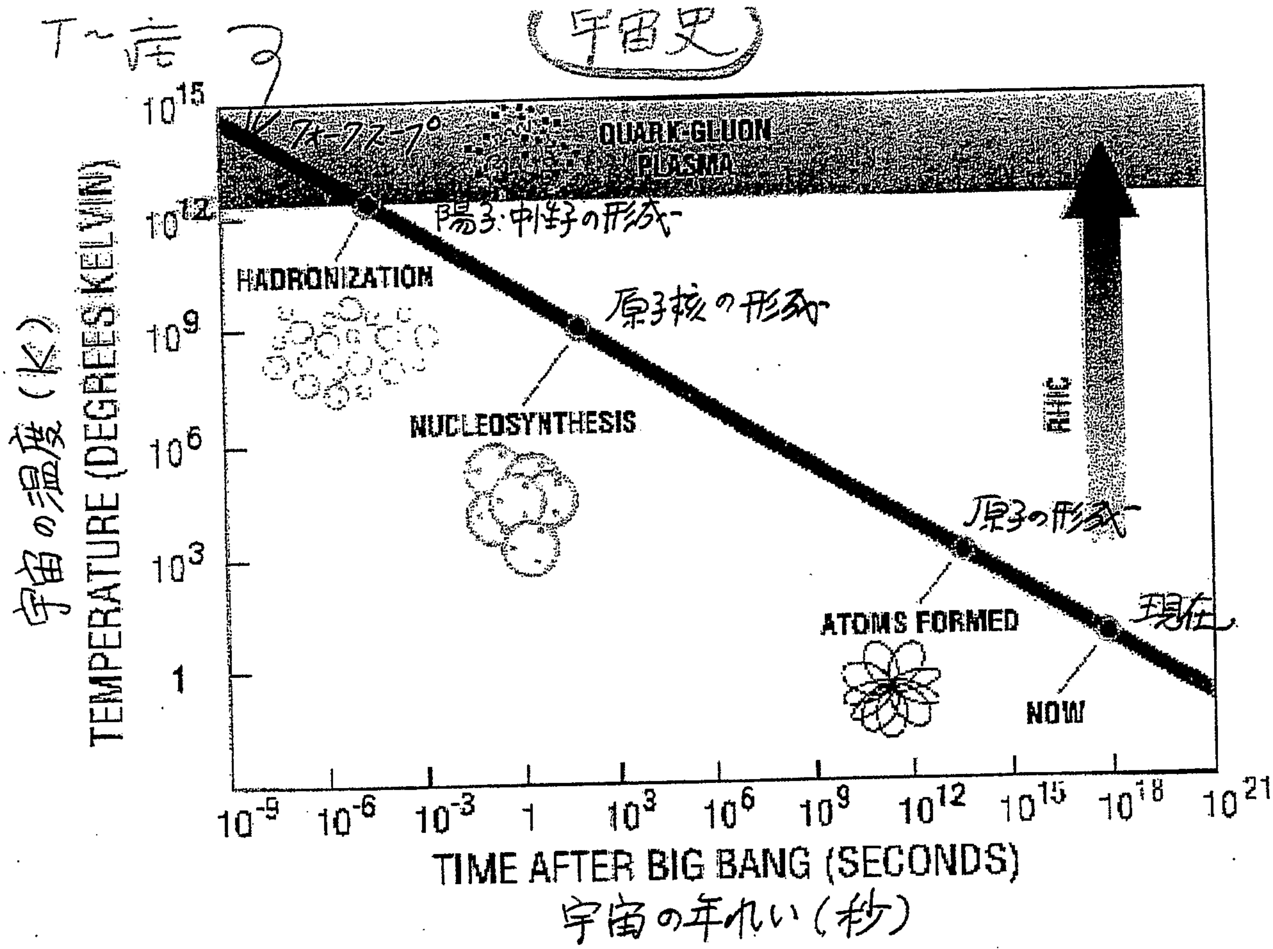
T~京
クォークスープ
QUARK-GLUON PLASMA
陽子・中性子の形成
HADRONIZATION
原子核の形成
NUCLEOSYNTHESIS
RHIC
原子の形成
ATOMS FORMED
現在
NOW
宇宙の温度(K)
TEMPERATURE (DEGREES KELVIN)
10^{15}
10^{12}
10^9
10^6
10^3
1
10^{-9} 10^{-6} 10^{-3} 1 10^3 10^6 10^9 10^{12} 10^{15} 10^{18} 10^{21}
TIME AFTER BIG BANG (SECONDS)
宇宙の年れい(秒)


Isolated Neutron Star RX J185635-3754 HST •
PRC97-32 • ST ScI OPO • September 25, 1997
F. Walter (State University of New York at Stony Brook) and NASA

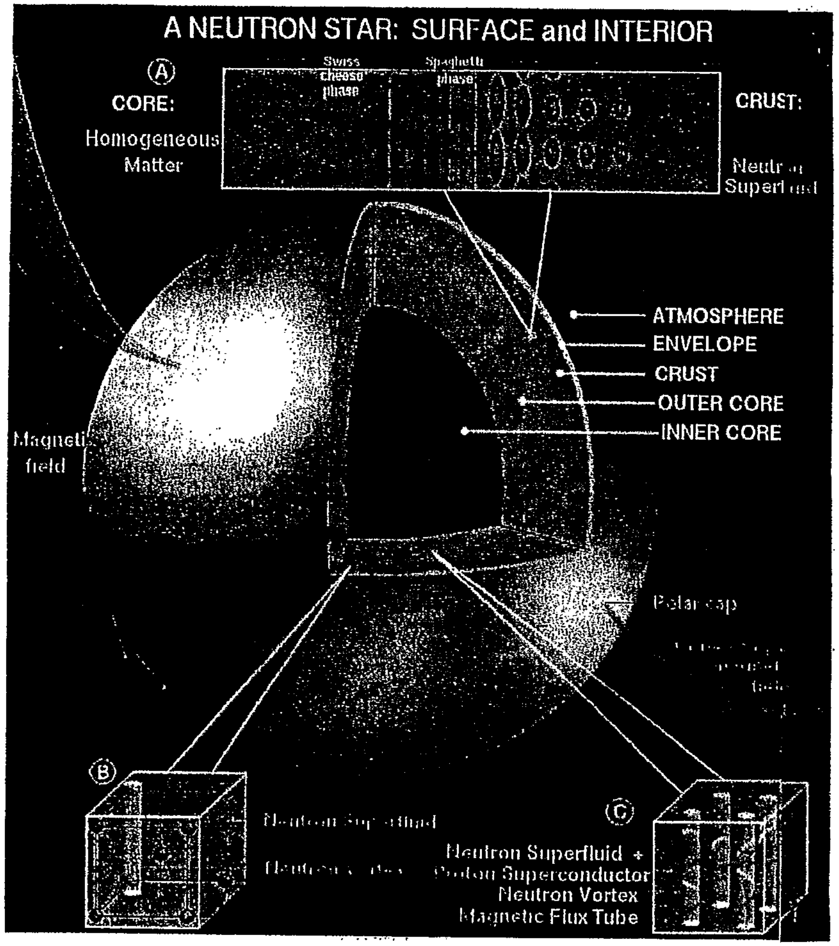

米国ブルックヘブン国立研究所

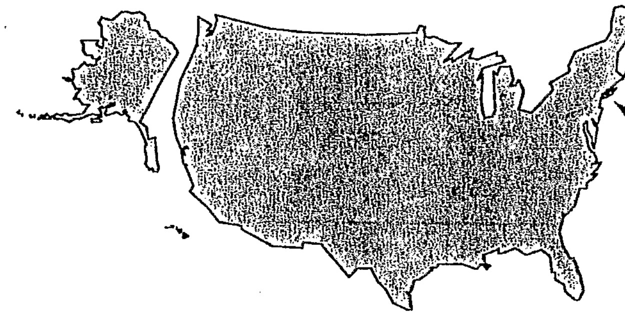

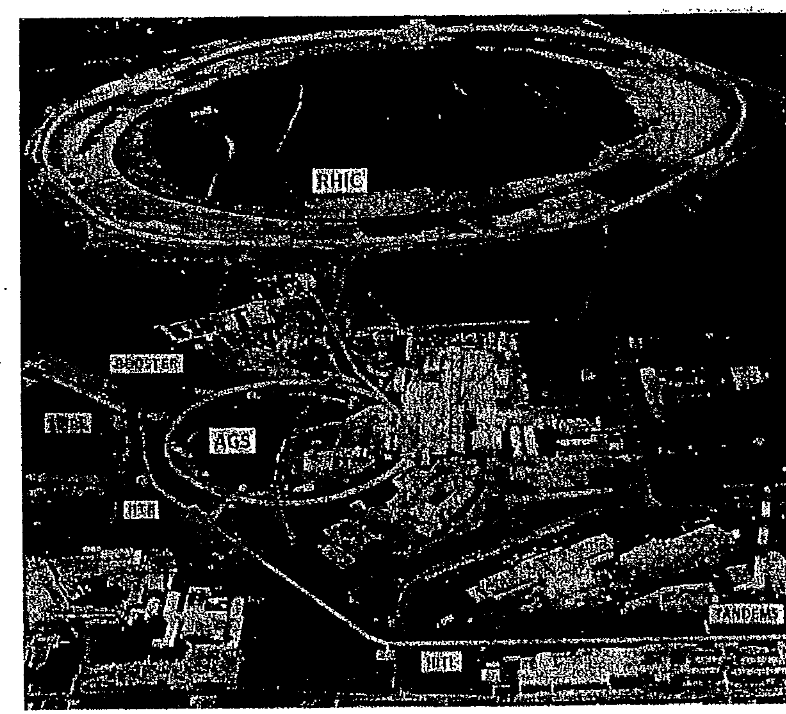

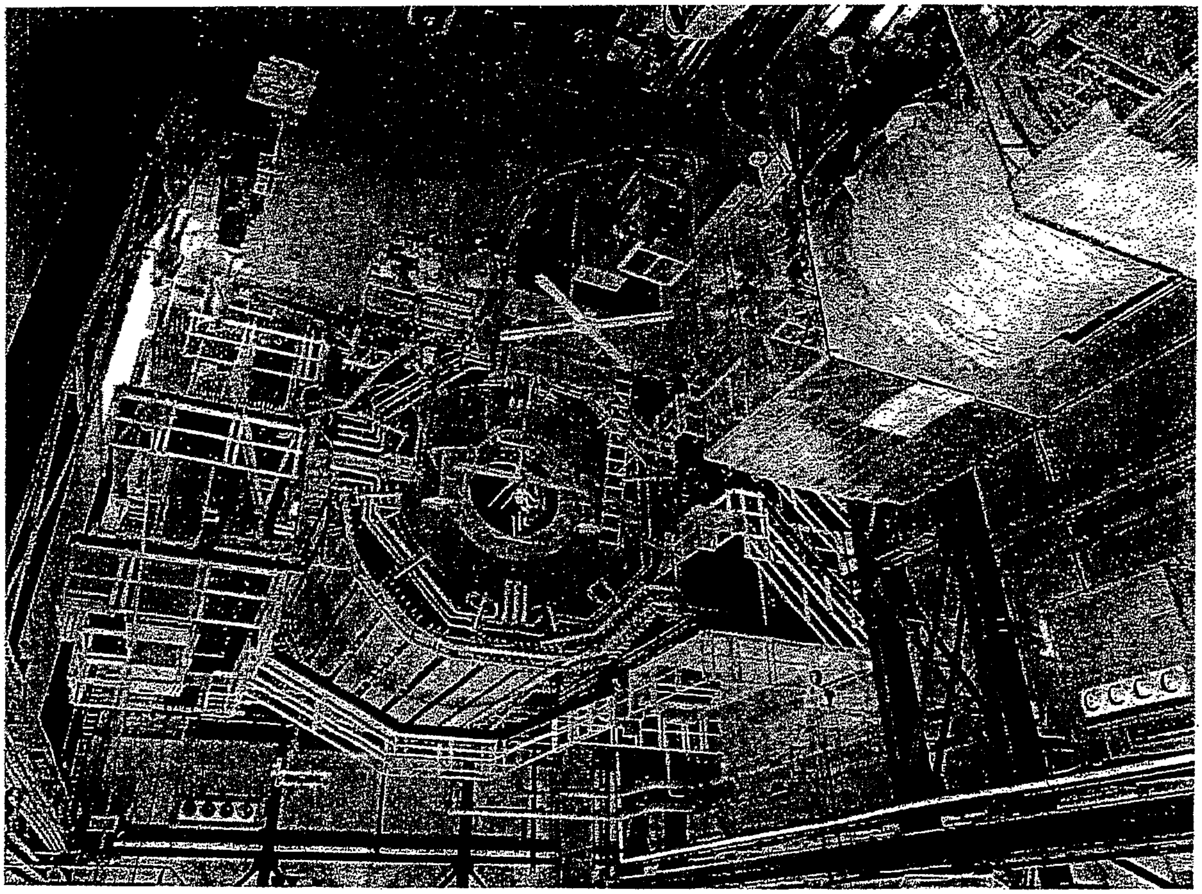

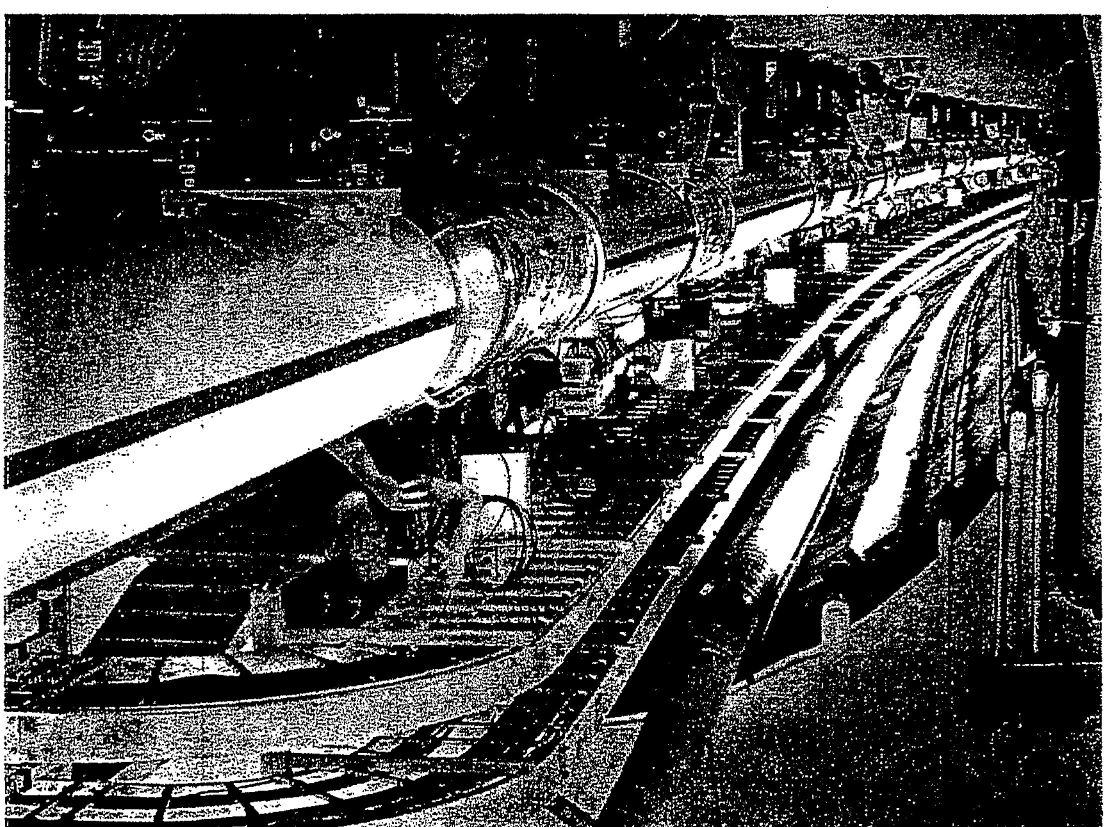

TPC Performance: Au +Au at $\sqrt{s_{NN}}$ = 130 GeV

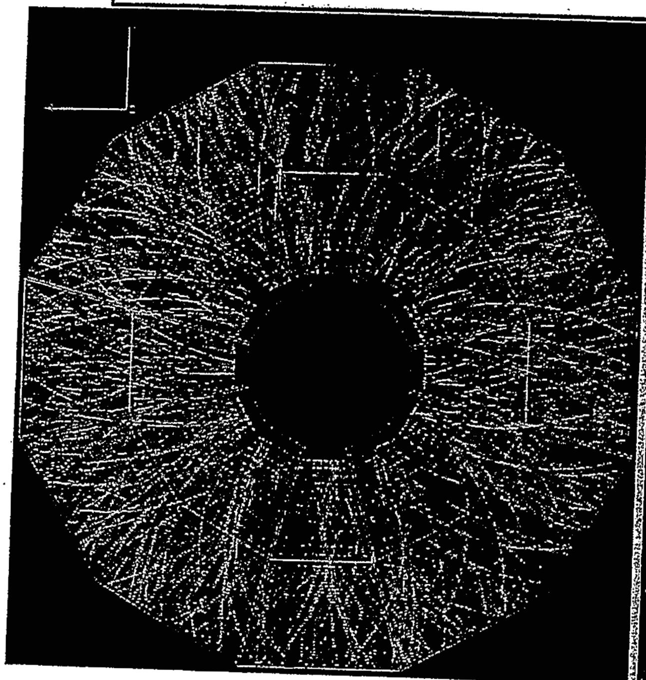

Run: 1186017, Event: 32, central

colors ~ momentum: low - - - high

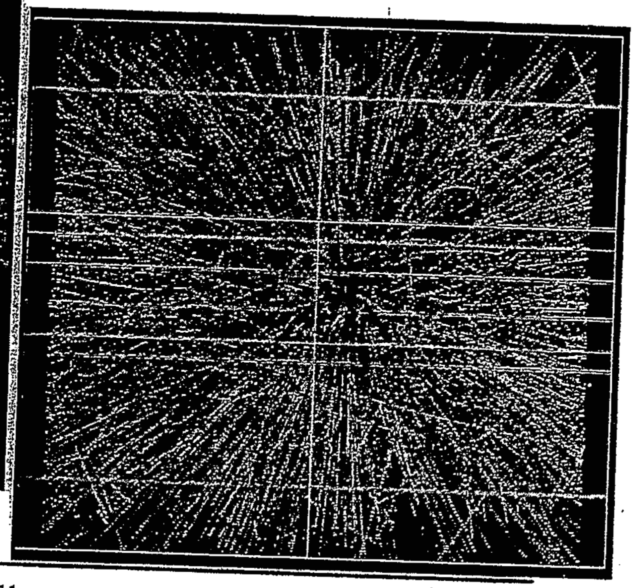

STAR

October 4, 2000 11 Thomas S. Ullrich

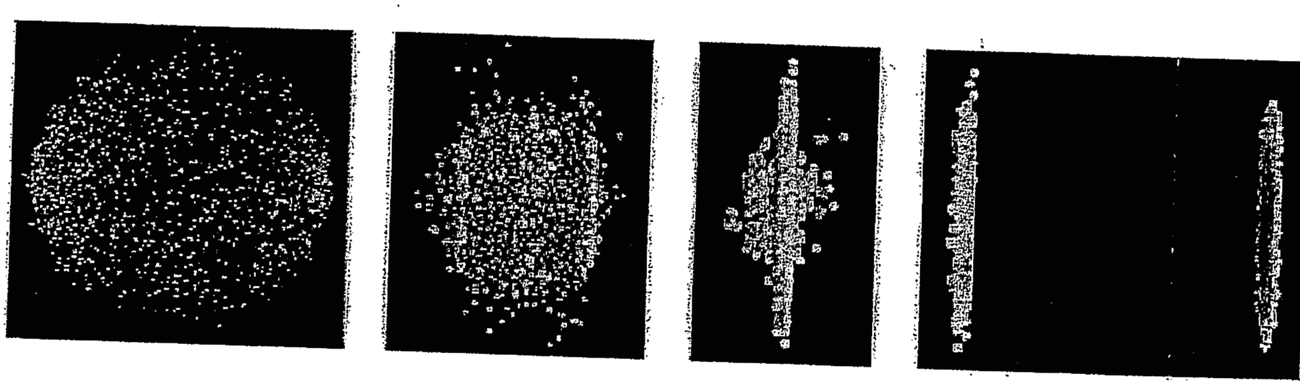

Phase Transition at $T \neq 0$

① Back of an envelope

percolation model

string model

② Piece of paper

bag equation of state

③ Super computer (~100 hours CPU time)

lattice QCD

④ Real world

Percolation of pions

- pion number density (massless pion)

$$n_\pi(T) = d_\pi \int \frac{d^3p}{(2\pi)^3} \frac{1}{e^{p/T}-1}$$

$$= d_\pi T^3 \frac{4\pi}{8\pi^3} \underbrace{\int_0^\infty dx \frac{x^2}{e^x-1}}_{\Gamma(3)\zeta(3)}$$

$$= \frac{d_\pi \zeta(3)}{\pi^2} T^3 \quad //$$

note
$n_\pi(T) \sim \left(\frac{T}{\hbar}\right)$
"intrinsically qua

$$* \int_0^\infty dx \frac{x^{n-1}}{e^x \pm 1} = \Gamma(n)\zeta(n) \times \begin{cases} 1-2^{1-n} & (+) \\ 1 & (-) \end{cases}$$

$$\begin{cases} \zeta(2) = \pi^2/6, \quad \zeta(4) = \pi^4/90, \cdots \\ \zeta(3) = 1.202\cdots, \quad \zeta(5) = 1.037\cdots \\ \Gamma(n) = (n-1)! \end{cases}$$

- percolation temperature (closed packed)

$$n_\pi(T_c) \times \frac{4}{3}\pi R_\pi^3 = 1$$

$$T_c = \left(\frac{\pi}{4\underset{\uparrow \atop 1.202\cdots}{\zeta(3)}}\right)^{1/3} \frac{1}{\underset{\uparrow \atop 0.65\,fm}{R_\pi}} \simeq 264\,MeV \quad //$$

Continuum percolation

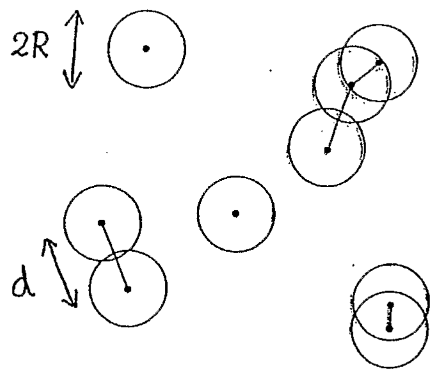

Figure 1. Division of a configuration into clusters.

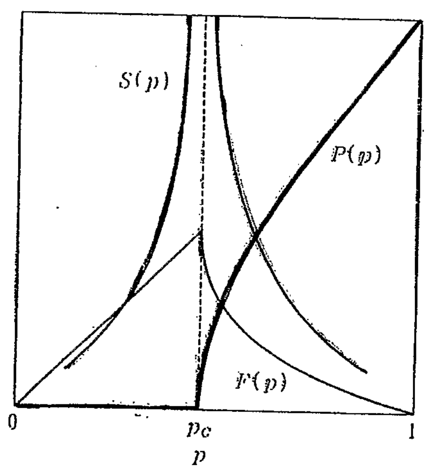

$\left(p = \frac{n}{n_{c.p.}}\right)$

$P(p)$: prob. to find a particle in infinite cluster

$S(p)$: averaged size of finite-size clusters

$F(p) = p - P(p)$: prob. to find a particle in finite cluster

Percolation model

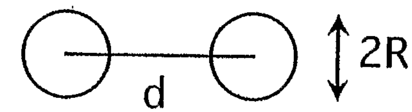

	percolation・start (infinite cluster)	percolation・end (close-packed)
$n_c V$	0.35 ± 0.06 Pike-Seager, PRB ('74)	1.0
n_c (R=0.65fm)	$0.3/\mathrm{fm}^3$	$0.89/\mathrm{fm}^3$
d_c	1.84 fm	1.3 fm

$\Downarrow$ $\Downarrow$

T_c=160-180 MeV: a rough estimate

Energy-entropy argument in string picture

$$F = E - TS$$

- non-interacting open strings (string tension σ)

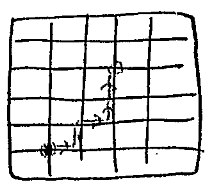

$\updownarrow a$

$\leftarrow$ d-space dim.

$$Z = \sum_L \sum_{\substack{\text{all open}\\ \text{string with}\\ \text{length } L}} e^{-\frac{L\sigma a}{T}}$$

$\leftarrow (2d-1)^L$ possibilities for non-backtracking random walk

$$= \sum_L \exp\left[-\frac{1}{T}\left(\underbrace{L\sigma a - LT\ln(2d-1)}\right)\right]$$

$$F_L = \underset{\text{Energy}}{L\sigma a} - \underset{\text{entropy}}{LT\ln(2d-1)}$$

$$\equiv L\,\sigma_{eff}(T)\,a$$

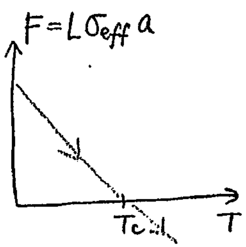

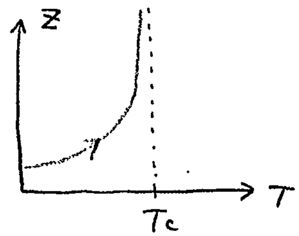

$$T_c = \frac{\sigma a}{\ln(2d-1)} \sim \frac{(m_\pi + m_\rho)/2}{\ln(2d-1)} = 280\,\text{MeV} \,/\!/$$

Basic Thermodynamics ($T\neq 0$, $\mu = 0$ case)

- 0-th law : $A \leftrightarrow B$, $B \leftrightarrow C$ equilibrium $\rightarrow$ $B \leftrightarrow C$ equilib.
- 1-st law : conservation of energy
- 2nd law : increasing entropy
- 3rd law : $S(T\rightarrow 0) \rightarrow 0$

- Thermodynamic identity

$$dS(E,V) = \left.\frac{\partial S}{\partial E}\right|_V dE + \left.\frac{\partial S}{\partial V}\right|_E dV \equiv \frac{1}{T}dE + \frac{P}{T}dV$$

or $\boxed{TdS = dE + PdV}$

- free energy

$$\boxed{F(T,V) \equiv E - TS} \rightarrow \boxed{dF = -SdT - PdV}$$

1st+2nd law $\rightarrow$ $S_{max} = F_{min}$

also $Z(T,V) = \mathrm{Tr}[e^{-H/T}] = e^{-F(T,V)/T}$

- phase equilibrium

$$\boxed{P_I = P_{II}, \quad T_I = T_{II}}$$

- Useful relations

(i) $p = -\left.\frac{\partial F}{\partial V}\right|_T = -\left.\frac{\partial f(T)V}{\partial V}\right|_T = -f(T) \rightarrow \boxed{F(T,V) = -PV}$

(ii) $S = -\left.\frac{\partial F}{\partial T}\right|_V = V\left.\frac{\partial P}{\partial T}\right|_V \rightarrow \boxed{s(T) = \left.\frac{\partial P}{\partial T}\right|_V}$

(iii) $F = E - TS \rightarrow -p = \varepsilon - sT \rightarrow \boxed{\varepsilon + P = sT}$

Stefan-Boltzmann (SB) law

- pion energy density $\quad (m_\pi = 0)$

$$\varepsilon_\pi(T) = d_\pi \int \frac{d^3p}{(2\pi)^3} |\vec{p}| \frac{1}{e^{p/T}-1}$$

$$= d_\pi T^4 \frac{1}{2\pi^2} \underbrace{\int_0^\infty dx \frac{x^3}{e^x-1}}_{\Gamma(4)\zeta(4) = 3! \frac{\pi^4}{90}}$$

$$= 3 d_\pi \frac{\pi^2}{90} T^4 \quad //$$

Bag equation of state at $T \neq 0$

For simplicity, assume massless pion $(m_\pi \ll T_c)$
assume massless quarks

◎ Equation of state in hadron phase

$$\boxed{\begin{cases} P_H = d_\pi \frac{\pi^2}{90} T^4 & + B \\ \varepsilon_H = 3 d_\pi \frac{\pi^2}{90} T^4 & - B \\ s_H = 4 d_\pi \frac{\pi^2}{90} T^3 & + 0 \end{cases}}$$

SB gas

$$\langle \Theta_{\mu\nu} \rangle_0 = \begin{pmatrix} \varepsilon_{vac} & & & 0 \\ & P_{vac} & & \\ & & P_{vac} & \\ 0 & & & P_{vac} \end{pmatrix} = -B g_{\mu\nu}$$

(vacuum pressure and energy density)

(note 1)
entropy does not have constant
$S_H(T \to 0) = 0$ the third law of thermodynamics

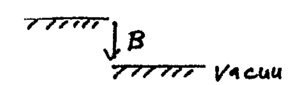

(note 2)
degeneracy factor

$$d_\pi = N_f^2 - 1 \quad : \# \text{ of NG-bosons}$$

13

Equation of state in QGP phase

$$\boxed{\begin{cases} P_Q = d_Q \dfrac{\pi^2}{90} T^4 \\ \varepsilon_Q = 3 P_Q, \quad s_Q = 4 P_Q / T \end{cases}}$$ SB gas

$$d_Q = d_{gluon} + \frac{7}{8} d_{quark} \quad : \text{degeneracy factor}$$

$$\begin{cases} d_{gluon} = \underset{\text{spin}}{2} \times \underset{\text{color } SU(N_c)}{(N_c^2 - 1)} \\ d_{quark} = \underset{\text{spin}}{2} \times \underset{q\,\&\,\bar{q}}{2} \times \underset{\text{color}}{N_c} \times \underset{\text{flavor}}{N_f} \end{cases}$$

	$N_c = 3$, $N_f = 2$	$N_c = 3$, $N_f = 3$
d_π	3	8
d_Q	37	47.5
d_{glue}	16	16
d_{quark}	24	36

- phase equilibrium

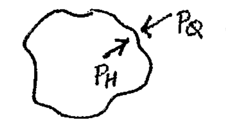

$$P_H = P_Q, \quad T_H = T_Q$$

favored phase at fixed T → large pressure
(small free energy $f = -P$)

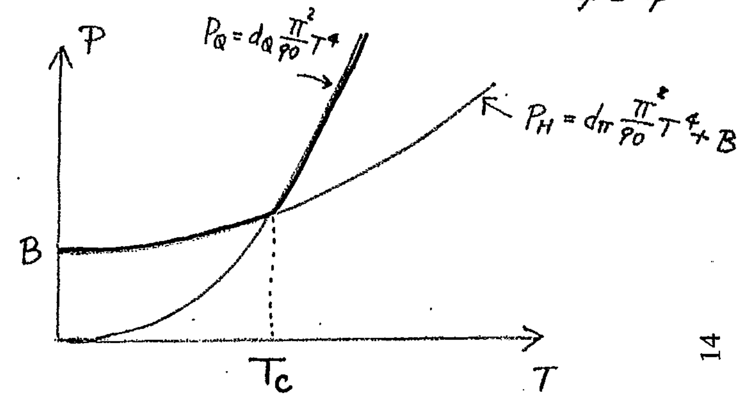

- critical temperature

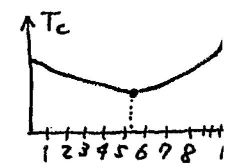

$$T_c^4 = \frac{90}{\pi^2} \frac{B}{\frac{7}{8} 4 N_c N_f + 2(N_c^2 - 1) - (N_f^2 - 1)}$$

$$= \underset{N_c=3,\, N_f=2}{\left(\frac{90}{\pi^2} \frac{1}{34}\right) B}, \quad \underset{N_c=3,\, N_f=3}{\left(\frac{90}{\pi^2} \frac{1}{39.5}\right) B}$$

$$\Rightarrow \boxed{\begin{aligned} T_c &\simeq 144\,\text{MeV} \quad (N_f = 2) \\ &\simeq 139\,\text{MeV} \quad (N_f = 3) \end{aligned}} \quad \text{for } B^{1/4} = 200\,\text{Me}$$

$$\leftrightarrow \varepsilon_c \simeq (1\,\text{GeV} \sim 2\,\text{GeV}) / fm^3 \leftrightarrow \varepsilon_{nm} = 0.16\,\text{Ge}$$

- energy and entropy

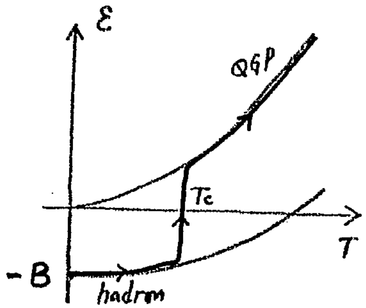

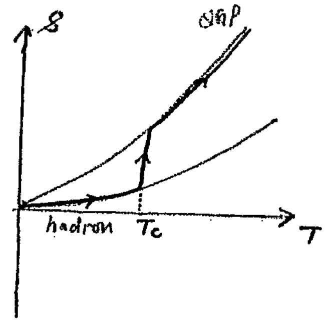

1st order phase transition
with latent heat $\Delta\varepsilon = \varepsilon_{QGP}(T_c) - \varepsilon_H(T_c)$

$$= 3P_{Q}(T_c) - [3P_H(T_c) - 4B]$$

$$= 4B$$

- For $m_\pi \gg T_c \Rightarrow$ neglect pions at low T

$$T_c^4 = \frac{90}{\pi^2}\,\frac{B}{\frac{7}{8}4N_cN_f + 2(N_c^2-1)} < T_c^4(\text{massless pion})$$

- For pure gauge system

$$T_c^4(\text{pure gauge}) = \frac{90}{\pi^2}\,\frac{B}{2(N_c^2-1)} > T_c^4(\text{massless pion})$$

- various corrections:

(hadronic interactions, resonances in Hadronic phase
perturbative QCD corrections in QGP phase

⇩

change T_c, order etc

Effect of the π-π interaction to the SB gas

Gerber & Leutwyler; Nucl. Phys. B321 ('89) 387

$$Z = \mathrm{Tr}\,(e^{-H/T})$$

$$= \int [dU]\, \exp\left[-\int d^4x_E\, \mathcal{L}_{eff}\right]$$

$$\mathcal{L}_{eff} = \mathcal{L}^{(2)} + \mathcal{L}^{(4)} + \mathcal{L}^{(6)} + \cdots$$

$m_\pi = 0$

$$\mathcal{L}^{(2)} = \frac{1}{4} f_\pi^2\, \mathrm{Tr}\,(\partial_\mu U \partial_\mu U^+)$$

$$\mathcal{L}^{(4)} = l_1 (\mathrm{Tr}\,\partial_\mu U \partial_\mu U^+)^2 + l_2 \mathrm{Tr}\,(\partial_\mu U \partial_\nu U^+)\,\mathrm{Tr}\,(\partial_\mu U^+ \partial_\nu U) + l_3\, \mathrm{Tr}\,(\partial_\mu U^+ \partial_\mu U\, \partial_\nu U^+ \partial_\nu U)$$

......

15

$F =$ 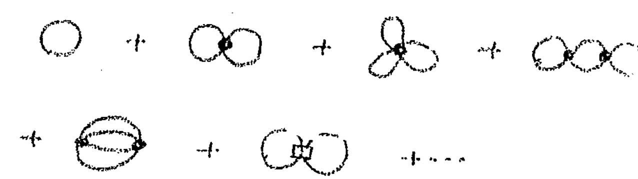

$\bullet = \mathcal{L}^{(2)}$, $\square = \mathcal{L}^{(4)}$

$$\boxed{\begin{aligned} P &= \frac{\pi^2}{30} T^4 \left[1 + \frac{T^4}{36 f_\pi^4} \ln \frac{\Lambda_p}{T} + O(T^6)\right] \\ \varepsilon &= \frac{\pi^2}{10} T^4 \left[1 + \frac{T^4}{108 f_\pi^4}\left(7 \ln \frac{\Lambda_p}{T} - 1\right) + \cdots\right] \\ s &= \frac{5}{12}\pi^2 T^3 \left[1 + \frac{T^4}{180 f_\pi^4}\left(8 \ln \frac{\Lambda_p}{T} - 1\right) + \cdots\right] \end{aligned}}$$

$\Lambda_p = 275 \pm 65$ MeV

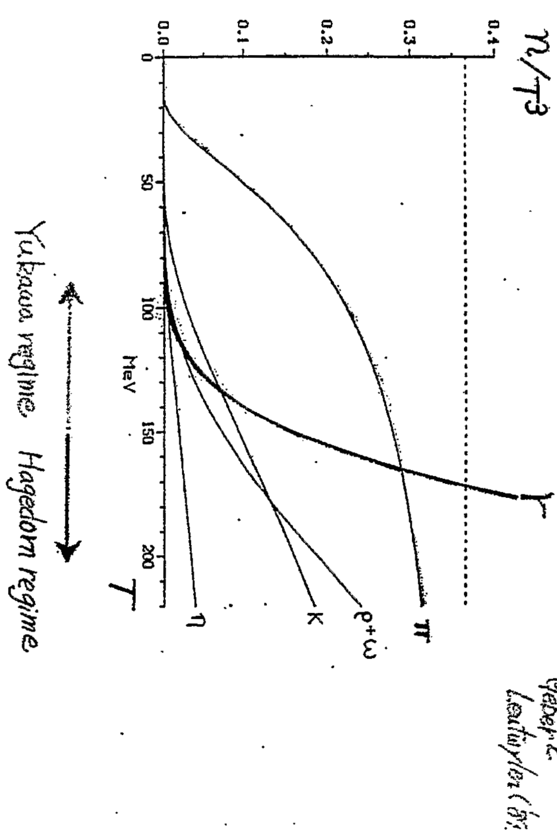

$$n_{tot}(T) = \int_0^\infty dm\, n(m;T)\, \rho(m)$$

$$n(m;T) \propto e^{-m/T}, \quad \rho(m) = \frac{C}{m^\alpha} e^{m/\tau}$$

Hagedorn ('65)

QCD thermodynamics

on the lattice

QCD on the Lattice

4-d Euclidean lattice

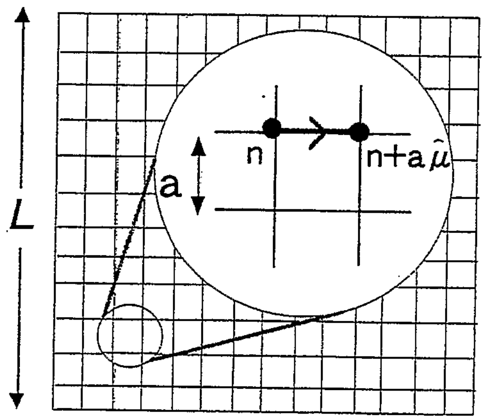

Discretization

$A_\mu(x) \rightarrow U_\mu(n) = \exp(i\, a\, A_\mu)$

$q(x) \rightarrow q(n)$

$T=0$: $L^3 \times L = (N_s a)^4$

$T\neq 0$: $L^3 \times 1/T = (N_s a)^3 \times (N_t a)$

Monte Carlo integration

$$Z = \int [dU]\,[dq d\bar{q}]\; e^{-S_{Dirac}(q,\bar{q},U) - S_{YM}(U)}$$

$$= \int [dU]\; \det Q(U)\; e^{-S_{YM}(U)}$$

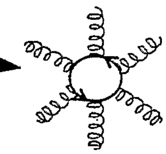

- Quenched QCD : $\det Q \rightarrow 1$
- Full QCD : $\det Q \neq 1$

Light quarks

- Wilson & Staggered (KS) : chiral sym. when $a \rightarrow 0$
- Domain wall (5-d lattice) : chiral sym. when $L_5 \rightarrow \infty$

Extrapolation

$\boxed{a \ll R,\, 1/T \ll L}$

0.05 fm 3 fm (quenched)

- Continuum limit : $a \rightarrow 0$ $(g(a) \rightarrow 0)$
- Thermodynamic limit : $L \rightarrow \infty$

Improved action

$S_{imp} = S_{standard} + \Sigma\, a^n c_n S_n$

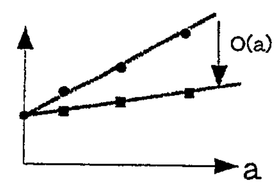

Lattice QCD : First principle numerical simulation

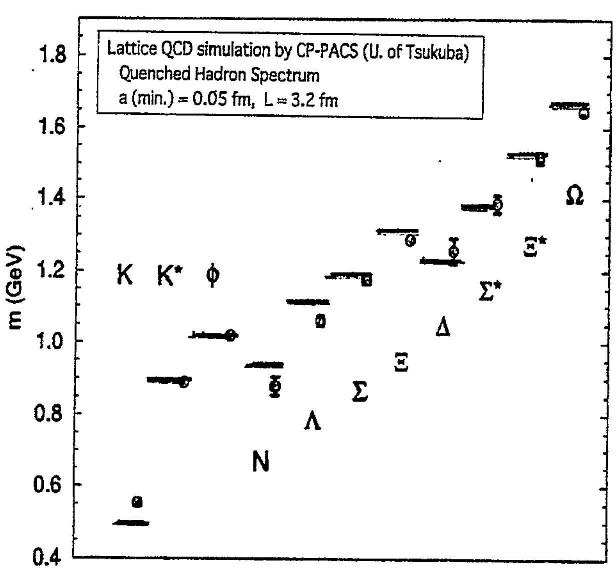

$|M_{th} - M_{exp.}| < 10\ \%$

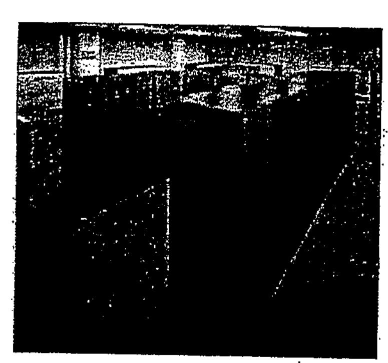

π

Aoki et al., PRL 84 ('00)

— CP-PACS Collaboration —

CP-PACS @ Univ. Tsukuba

Hot QCD

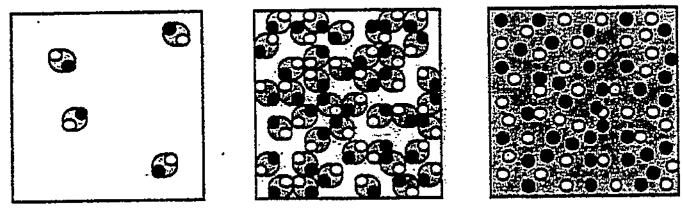

Low T expansion

$$\varepsilon_{\mathrm{sub}}{}^{(N_f=2)} = 3\,\frac{\pi^2}{30}T^4$$

$$\times\left[1+\frac{T^4}{108 f_\pi^4}\ln\left(\frac{275\,\mathrm{MeV}}{T e^{1/7}}\right)^7 + O(T^6)\right]$$

Gerber & Leutwyler, NPB ('89)

High T expansion

$$\varepsilon_{\mathrm{sub}}{}^{(N_f=2)} = (16+21)\,\frac{\pi^2}{30}T^4$$

$$\times\left[1-2.97\left(\frac{\alpha_s}{\pi}\right)+20.0\left(\frac{\alpha_s}{\pi}\right)^{3/2} + (132+39.0\ln\frac{\alpha_s}{\pi})\left(\frac{\alpha_s}{\pi}\right)^2 - 474\left(\frac{\alpha_s}{\pi}\right)^{5/2}\right]$$

Arnold & Zhai, PRD ('95): Braaten & Nieto, PRD ('96)

Heavy resonances ?

Resummation ?

IR problem at $O(\alpha_s{}^3)$

T.H. PRD ('97) : Kasterning, PRD ('97,
Anderson et al., PRD ('00)
Blaizot et al., PRD ('01) ···

Linde, PLB ('80); Braaten, PRL ('95)

Stefan–Boltzmann gas for free quark & gluons

$$\frac{\epsilon_{SB}}{T^4} = \frac{3p_{SB}}{T^4} = \left(16+\frac{21}{2}n_f\right)\frac{\pi^2}{30}$$

QCD equation of state on the lattice

Karsch, hep–ph/0103314

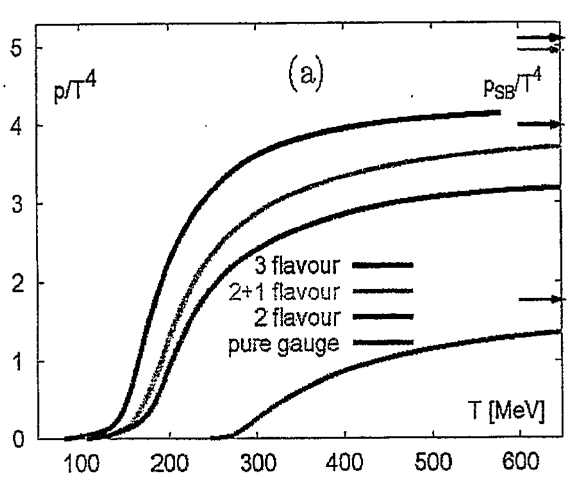

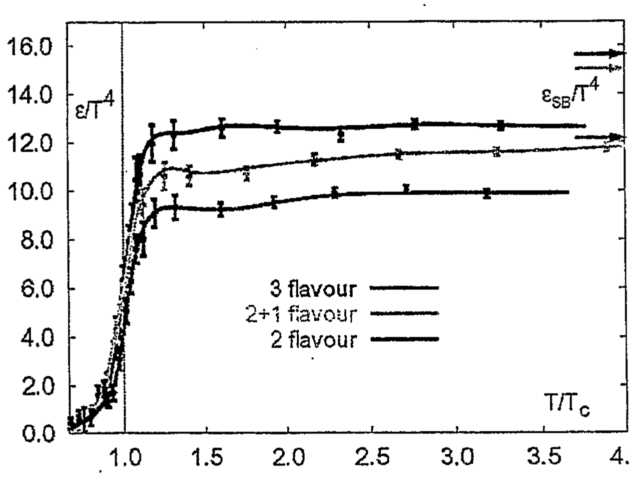

$N_f=2$

$T_c = 173 \pm 8$ MeV →

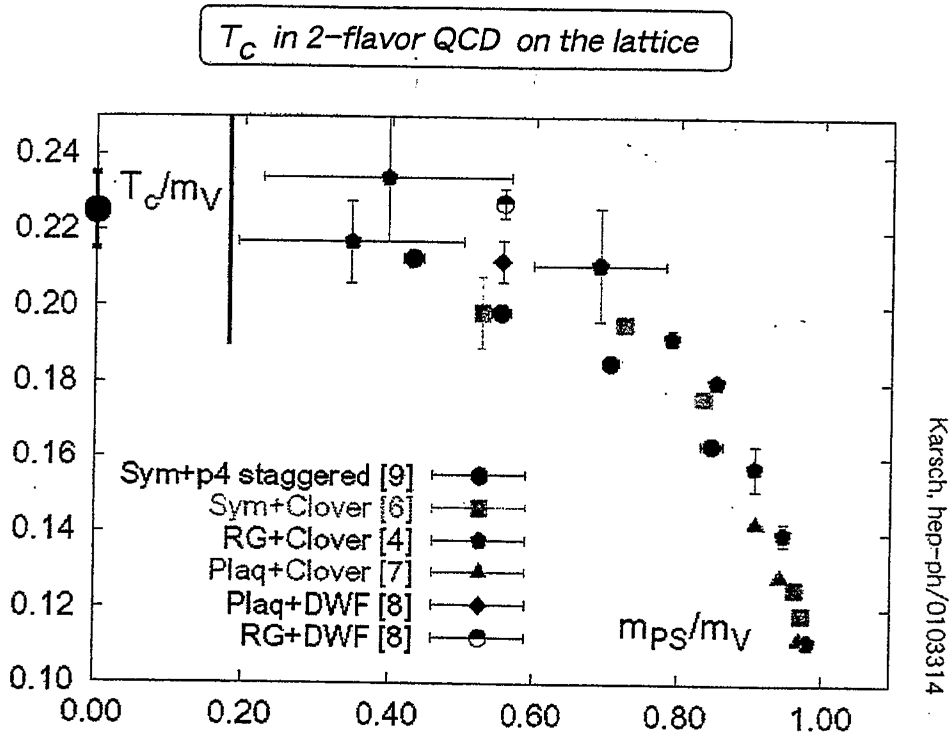

←

$m_{u,d}$ small

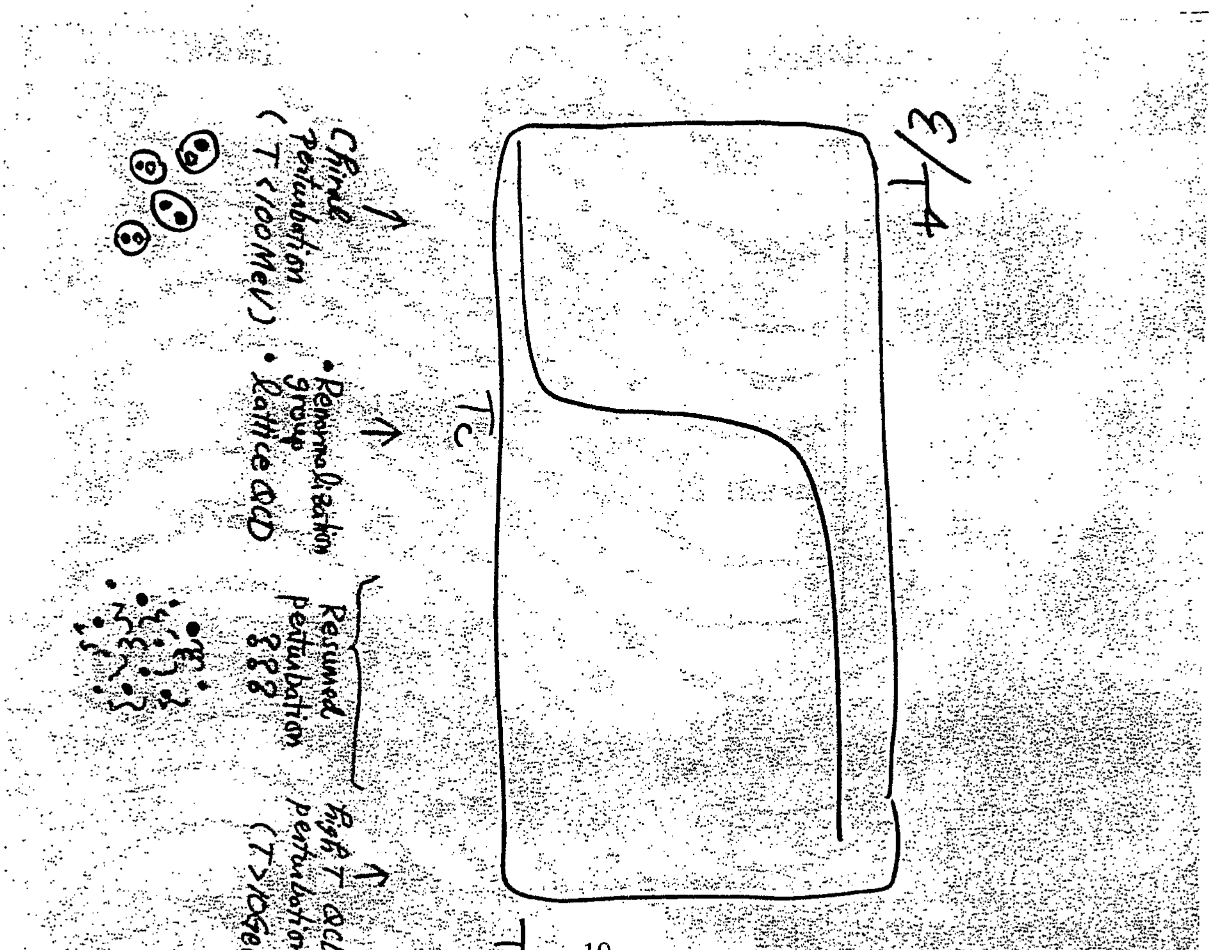

QCD plasma in perturbation theory at high T

hope: $g(T\to\infty)\to 0$
⇨ perturbation works for $T \gg T_c$.

① Static : $\omega = 0$
- Debye screening in QCD $\quad \omega_D \sim gT$

② Dynamic : $\omega \neq 0$
- plasmon and plasmino $\quad \omega_{pl} \sim gT$
$\gamma_{pl} \sim \alpha_s T$

③ "Doubt" on pert. theory for $T \lesssim 10$ GeV
- Asymptotic nature of the expansion
$F(T) = T^4 [g^2 + g^3 + g^4 + g^5 + \cdots]$
→ Improvement (Padé)
- IR problem in higher orders
(magnetic sector)
→ open problem
QCD_3 ?

Plasma screening and oscillation

- classical
screening : Debye & Hückel, Z. Phys. (1923)
oscillation : Tonks & Langmuir, Phys. Rev. (1929)

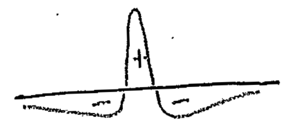

20

- YM theory at high T ("semi-classical")

Vlasov eq. + Maxwell eq. : Blaizot & Iancu, (19.
↑
collisionless
Boltzmann eq.
with mean-field

Loops : Braaten & Pisarski (1990–)

QED plasma in Debye-Hückel approach

- static Maxwell eq.

$$\partial_\nu F^{\nu\mu}(x) = j^\mu(x)$$

$$\vec{\nabla}\cdot\vec{E}(\vec{x}) = -\nabla^2\phi(\vec{x}) = \underset{\text{total}}{\rho(\vec{x})} = \underset{\substack{\text{external}\\\text{charge}\\\text{density}}}{\rho_s(\vec{x})} + \underset{\substack{\text{induced}\\\text{charge}\\\text{density}}}{\rho_{ind}(\vec{x})}$$

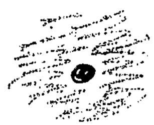

- Induced charge

$$\rho_{ind}(\vec{x}) = \underset{\text{spin}}{2}\int\frac{d^3p}{(2\pi)^3}\left[e\,\underset{\text{positron}}{n_+(\vec{p},\vec{x})} - e\,\underset{\text{electron}}{n_-(\vec{p},\vec{x})}\right]$$

$$n_\pm(\vec{p},\vec{x}) = \frac{1}{e^{(|\vec{p}|\pm e\phi(\vec{x}))/T}+1} \quad \leftarrow \text{solution of the Vlasov eq.}$$

$T \gg e\phi$, $T \gg \nabla \sim eT$ (small amp., weak coupling) (∇: soft)

$$\rho_{ind}(\vec{x}) \simeq 4e^2\phi(\vec{x})\int\frac{d^3p}{(2\pi)^3}\frac{dn(\vec{p})}{dp}$$

$$= -4e^2\phi(\vec{x})\frac{T^2}{2\pi^2}\int_0^\infty dx\,\frac{x^2e^x}{(e^x+1)^2}$$

$$= -4e^2\phi(\vec{x})\frac{T^2}{\pi^2}\underbrace{\int_0^\infty dx\,\frac{x}{e^x+1}}_{=(1-\frac{1}{2})\Gamma(2)\zeta(2)=\frac{\pi^2}{12}}$$

$$= -\frac{e^2}{3}T^2\phi(\vec{x})$$

- Self-consistent equation

$$-\nabla^2\phi(\vec{x}) = \rho_s(\vec{x}) - \frac{e^2}{3}T^2\phi(\vec{x})$$

$$\boxed{[-\nabla^2 + m_D^2]\phi(\vec{x}) = \rho_s(\vec{x})}$$

($m_D = eT/\sqrt{3}$: Debye mass)

- For point charge at $\vec{x}=0$

$$\rho_s(\vec{x}) = Q\,\delta(\vec{x})$$

$$\phi(\vec{x}) = \frac{Q}{4\pi r}e^{-m_D r}, \quad \rho_{ind}(\vec{x}) = -\frac{m_D^2 Q}{4\pi r}e^{-m_D r}$$

- Interaction between $+Q$ and $-Q$

$$V_{Q\bar{Q}}(\vec{x}) = -\frac{Q^2}{4\pi r}e^{-m_D r}$$

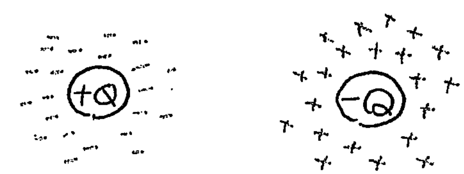

Finite T perturbation

- partition function

$$K = \langle \beta | e^{-iHt} | \alpha \rangle$$

$$\updownarrow$$

$$Z = Tr(e^{-H/T}) = \sum_\alpha \langle \alpha | e^{-H/T} | \alpha \rangle$$

$$t \leftrightarrow -i\frac{1}{T}, \quad |\beta\rangle \to |\alpha\rangle$$

$$\Downarrow$$

Euclidian path integral with
periodic (anti-periodic) b.c.

$$\boxed{\begin{aligned} Z &= Tr(e^{-H/T}) \\ &= \int [d\phi]\, e^{-\int_0^{1/T} dx_4 \int d^3x\, \mathcal{L}_E} \end{aligned}}$$

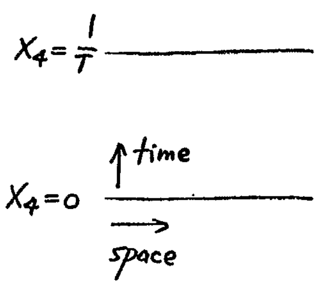

$$\phi(x_4 = \tfrac{1}{T}, \vec{x}) = \pm\, \phi(x_4 = 0, \vec{x})$$

boson ($+$), fermion ($-$)

$$\left\{ \begin{array}{l} * \text{ boson} \\ \quad Tr\mathcal{O} = \sum_n \langle n | \mathcal{O} | n \rangle = \int d\phi^* d\phi\, e^{-\phi^*\phi} \langle \phi | \mathcal{O} | \phi \rangle \\ * \text{ fermion} \\ \quad Tr\mathcal{O} = \sum_n \langle n | \mathcal{O} | n \rangle = \int d\xi^* d\xi\, e^{-\xi^*\xi} \langle -\xi | \mathcal{O} | \xi \rangle \end{array} \right.$$

- Matsubara frequency

$$\boxed{f(x_4, \vec{x}) = \frac{1}{(1/T)} \sum_{n=-\infty}^{\infty} \int \frac{d^3k}{(2\pi)^3}\, e^{i\vec{k}\cdot\vec{x}} f(k_4^{(n)}, \vec{k})}$$

$$k_4^{(n)} = \begin{cases} 2\pi n T & \text{for boson} \\ 2\pi(n+\frac{1}{2})T & \text{for fermion} \end{cases}$$

- Feynman rules

propagator :

$$\underset{\substack{\text{Minkowski} \\ T=0}}{\frac{1}{k_0^2 - \vec{k}^2}} \longrightarrow \underset{\substack{\text{Euclidian} \\ T=0}}{\frac{-1}{k_4^2 + \vec{k}^2}} \longrightarrow \underset{T \neq 0}{\frac{-1}{(2\pi n T)^2 + \vec{k}^2}}$$

integral :

$$\int dk_0 d^3k \longrightarrow i\int dk_4 d^3k \longrightarrow iT \sum_{n=-\infty}^{\infty} \int d^3k$$

- 2 point functions

Matsubara

$$-\mathcal{G}(\tau,\vec{x}) = \langle T_\tau \phi(\tau,\vec{x})\phi^\dagger(0,\vec{0})\rangle$$

Retarded (Advanced)

$$i\,G^R(t,\vec{x}) = \langle R\,\phi(t,\vec{x})\phi^\dagger(0,\vec{0})\rangle$$

$$= \theta(t)\langle [\phi(t,\vec{x}),\phi^\dagger(0,\vec{0})]_\pm\rangle \quad \begin{matrix}\leftarrow \text{bose}\\ \leftarrow \text{fermi}\end{matrix}$$

$$G^A = (G^R)^*$$

Causal

$$i\,G^C(t,\vec{x}) = \langle T\,\phi(t,\vec{x})\phi^\dagger(0,\vec{0})\rangle$$

$$G^C(\omega,\vec{k}) = [1\mp e^{-\omega/T}]^{-1}G^R + [1\mp e^{\omega/T}]^{-1}G'$$

- AGDF Theorem

$$\boxed{\mathcal{G}(\omega_n>0,\vec{k}) \xrightarrow[A.C.]{} G^R(\omega,\vec{k})}$$

- Analytic structure

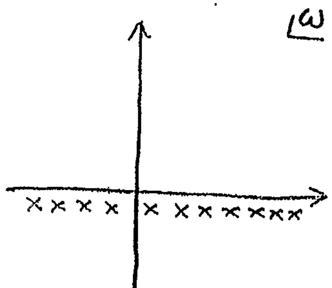

$$\begin{cases} G^R(\omega,\vec{k}) = \displaystyle\int_{-\infty}^{\infty}\frac{d\omega'}{2\pi}\,\frac{\rho(\omega',\vec{k})}{\omega-\omega'+i\varepsilon} \\ \mathcal{G}(\omega_n,\vec{k}) = \displaystyle\int_{-\infty}^{\infty}\frac{d\omega'}{2\pi}\,\frac{\rho(\omega',\vec{k})}{i\omega_n-\omega'} \end{cases}$$

Case for gauge theory

- Euclidian def.

$$(x_\mu)_E = (\tau,\vec{x}),\quad (\partial_\mu)_E = (\partial_\tau,\vec{\nabla})$$

$$(\gamma_\mu)_E = (\gamma_4,\vec{\gamma}),\quad (A_\mu)_E = (A_4,\vec{A})$$

- Minkowski → Euclidian

$$t\to -i\tau,\quad A^0\to -iA_4,\quad (\gamma^0)_M\to -i(\gamma_4)_E$$

then

$$\begin{cases} (A^\mu B_\mu)_M \to -(A_\mu B_\mu)_E, & (\partial^\mu A_\mu)_M \to (\partial_\mu A_\mu)_E \\ \{\gamma^\mu,\gamma^\nu\}_M = 2g^{\mu\nu} \to \{\gamma_\mu,\gamma_\nu\}_E = -2\delta_{\mu\nu} & \\ (\gamma^\mu A_\mu)_M \to -(\gamma_\mu A_\mu)_E, & (\gamma^\mu\partial_\mu)_M \to (\gamma_\mu\partial_\mu)_E \end{cases}$$

- Partition function

$$Z = \int [dA\,dq\,d\bar{q}\,d\bar{c}\,dc]\; e^{-\int_0^\beta d\tau\int d^3x\,\mathcal{L}}$$

$$\mathcal{L} = \bar{q}(-i\gamma_\mu D_\mu + m_q)q + \frac{1}{4}F_{\mu\nu}F_{\mu\nu} + \bar{c}\,\partial_\mu D_\mu c + \frac{1}{2\alpha}(\partial_\mu$$

$$\xrightarrow[\text{free}]{} \bar{q}(-i\gamma\partial + m_q)q - \frac{1}{2}A_\mu\partial^2 A_\mu + \bar{c}\,\partial^2 c$$

plasmon and plasmino

polarization function $\Pi_{\mu\nu}(P)$: $P^\mu = (p^0, \vec{p})$

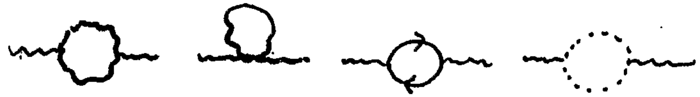

$\downarrow$

$$\begin{cases} \Pi_L(P) \equiv \Pi_{00}(P) \\ \Pi_T(P) \equiv \frac{1}{2}\left(\delta_{ij} - \frac{p^i p^j}{p^2}\right) \Pi_{ij}(P) \end{cases}$$

- For $T \gg p_0, p \quad \leftrightarrow \quad g \ll 1$

$$\boxed{\begin{aligned} \Pi_L(p_0,p) &= -3\omega_{pl}^2 \left[1 - F(p_0/p)\right] \\ \Pi_T(p_0,p) &= \frac{3}{2}\omega_{pl}^2 \frac{p_0^2}{p^2}\left[1 - \left(1 - \frac{p^2}{p_0^2}\right)F(p_0/p)\right] \end{aligned}} \leftarrow \text{gauge independent}$$

where $F(x) = \frac{x}{2} \ln\left|\frac{x+1}{x-1}\right| - i\pi\theta(1-x)$

$\omega_{pl} = \underset{\text{QED}}{\frac{e}{3}T} \; , \; \underset{\text{QCD}}{\frac{g}{3}T\sqrt{N_c + \frac{1}{2}N_f}} \leftarrow$ plasma frequency

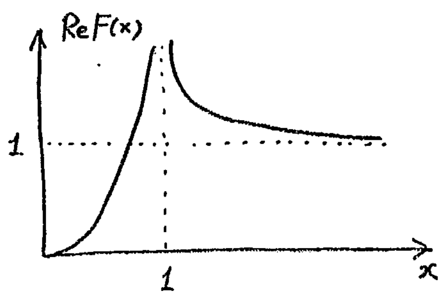

- Relation to propagator

e.g. in Coulomb gauge

free propagator $\sim\!\sim$ $\begin{cases} D_{00}(P) = \frac{1}{p^2}, & D_{0i}(P) = 0 \\ D_{ij}(P) = \frac{1}{P^2}\left(\delta_{ij} - \frac{p^i p^j}{p^2}\right) \end{cases}$

$\downarrow$

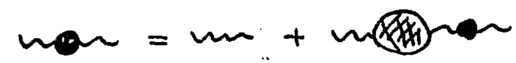

$$\begin{cases} D^*_{00}(P) \equiv D^*_L = \dfrac{1}{p^2 - \Pi_L} & p^2 = |\vec{p}|^2 \\ D^*_{ij}(P) = \left(\delta_{ij} - \frac{p^i p^j}{p^2}\right) D^*_T = (\;\cdot\;) \dfrac{1}{P^2 - \Pi_T} & P^2 = p_0^2 - \vec{p}^2 \end{cases}$$

- static limit of $\Pi_{T,L}$

$$\begin{cases} \Pi_L(p_0=0,p) = -3\omega_{pl}^2 \Rightarrow D^*_L = [p^2 + \underbrace{3\omega_{pl}^2}]^{-1} \equiv [p^2 + \omega_D^2]^{-1} \\ \Pi_T(p_0=0,p) = 0 \quad \Rightarrow D^*_T = [-P^2]^{-1} = [p^2]^{-1} \end{cases}$$

- longitudinal mode is screened
  ω_D : Debye mass
- transverse mode is not screened

Properties of QCD Plasma

QCD Debye screening :

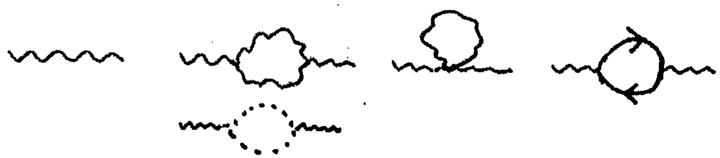

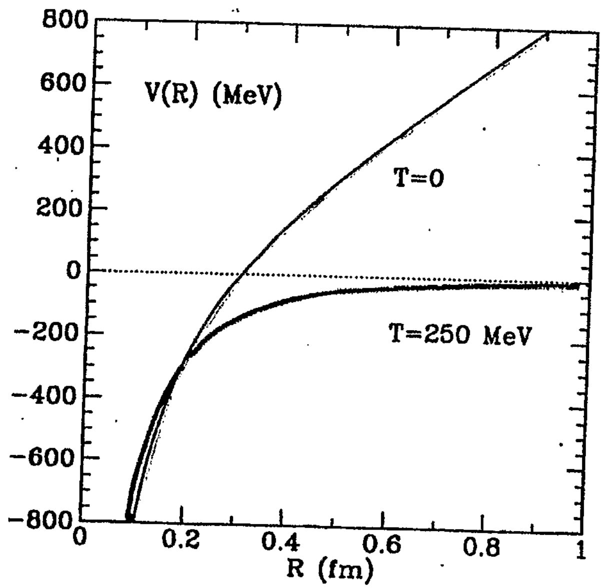

$$\lambda_D = \frac{1}{\sqrt{(N_c + N_f/2)/3}\; gT}, \qquad V_{Q\bar{Q}}(r) \propto \frac{1}{r}\exp(-r/\lambda_D)$$

⇒ J/ψ properties   Matsui-Satz ('86)
Hashimoto, Miyamura, Hirose & Kanki ('86)

- non static case

dispension relations

$$\begin{cases} P^2 = \Pi_L(P_0, P) \rightarrow P_0^2 = \omega_{pl}^2 + \frac{3}{5}p^2 + \cdots & \text{long. mode} \\ P^2 = \Pi_T(P_0, P) \rightarrow P_0^2 = \omega_{pl}^2 + \frac{6}{5}p^2 + \cdots & \text{trans. mode} \end{cases}$$

$\uparrow$
$|\vec{p}| \simeq 0$

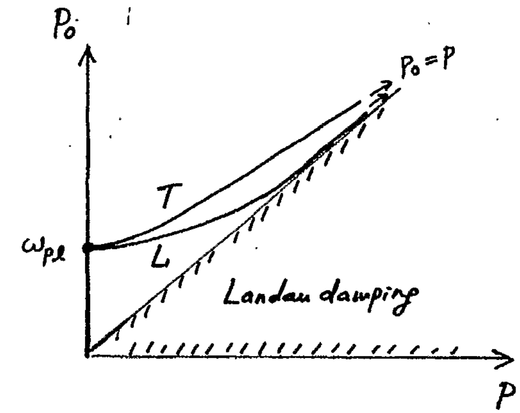

no damping in $O(g)$ at high T

(note) Landau damping

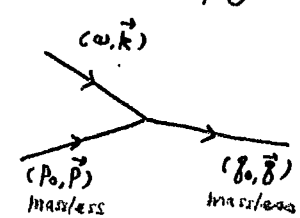

$\omega + P_0 = q_0, \quad \vec{k} + \vec{p} = \vec{q}$

$\downarrow$

$\omega^2 - \vec{k}^2 = (q_0 - P_0)^2 - (\vec{q} - \vec{p})^2$

$= -2|\vec{q}||\vec{p}|(1 - \cos\theta) < 0$

(Landau damping occurs for $\omega^2 < k^2$ in massless plasma.

- *Fermion case*

$$\boxed{\Sigma(p_0,p) = \omega_F^2\left[\gamma^0 \frac{1}{p_0} F(p_0/p) - \vec{\gamma}\cdot\hat{p}\,\frac{1}{p}\left(F(p_0/p)-1\right)\right]}$$

for $T \gg p, p_0$

where $\omega_F = \underset{QED}{\frac{e}{2\sqrt{2}}T}\,,\ \underset{QCD}{\frac{g}{\sqrt{6}}T}$ ← plasma frequency

- *static limit*

$$\Sigma(p_0=0,p) = +\vec{\gamma}\cdot\hat{p}\,\frac{1}{p}\,\omega_F^2$$

$$\downarrow$$

$$S(p_0=0,p) = \frac{-1}{\vec{\gamma}\cdot\vec{p}\,(1+\omega_F^2/p^2)} = \vec{\gamma}\cdot\vec{p}\,\frac{1}{p^2+\omega_F^2}$$

- *non static case*

$$S(p_0,p) = \left[\gamma^0\left(p_0-\frac{\omega_F^2}{p_0}F\right) - \vec{\gamma}\cdot\hat{p}\left(p+\frac{\omega_F^2}{p}(F-1)\right)\right]^{-1}$$

$$\xrightarrow[p\to 0]{} \quad p_0 = \begin{cases}\omega_F + \frac{1}{3}p\\ \omega_F - \frac{1}{3}p\end{cases}$$

$$\xrightarrow[p\to\infty]{} \quad p_0 = p$$

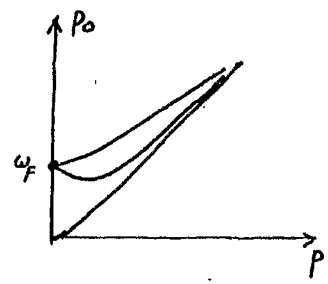

Elementary Modes at high T

QCD Plasmon	Plasmino
	
$m_{pl} = \frac{1}{\sqrt{3}}\,gT$	$m_{plm} = \frac{1}{\sqrt{6}}\,gT$
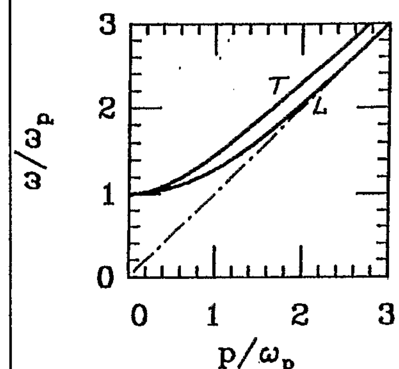	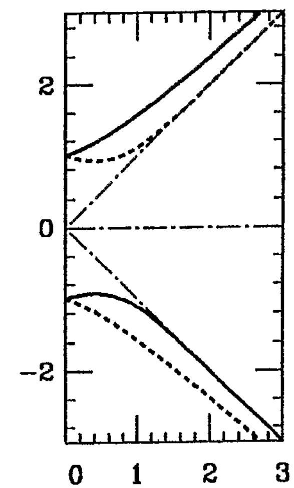

QCD Plasma is at T~ 300 MeV is composed of plasmon and plasmino: m ~ 300 MeV ?

• multiple scale in hot plasma (T: large, $g \ll 1$)

T hard

$\Downarrow$

gT soft $\sim \omega_D$

$\Downarrow$

g^2T supersoft $\sim \omega_M$

$\Downarrow$

$\vdots$

• Interaction among soft particles

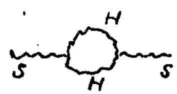

: plasmon mass

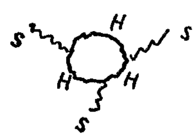

$\sim$ (tree) $\frac{g^2T^2}{P^2_{soft}} \sim$

$$\left(\begin{aligned} \Gamma_{\mu\nu\rho}(P,Q,R) &= 2\omega_{pl}^2 \int \frac{d\Omega}{4\pi} \hat{K}_\mu \hat{K}_\nu \hat{K}_\rho \\ &\times \left[\frac{i\,\omega_r}{(P\cdot\hat{K})(R\cdot\hat{K})} - \frac{i\,\omega_q}{(P\cdot\hat{K})(Q\cdot\hat{K})} \right] \\ \hat{K}^\mu &= (-i, \hat{k}) \end{aligned} \right)$$

• Hard Thermal loop (HTL) resummation

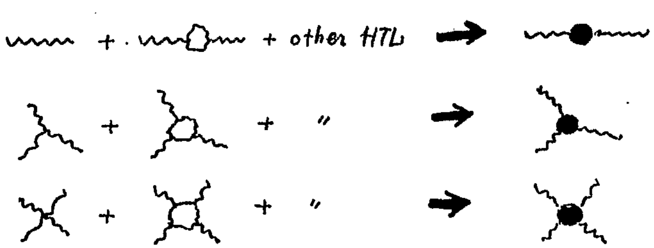

— Pert. theory based on these vertices —

• Plasmon/plasmino damping rates

• lowest order damping = 0 (kinematically forbidden)

• real damping occures in

e.g. $gg \to gg$, $gg \to ggg$ etc

• calculation in HTL method

$\Pi(\omega \sim gT, \vec{p}=0) =$

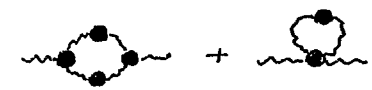

$\Downarrow$

$$\boxed{\begin{aligned} \omega(p) &= \mathrm{Re}\,\omega(p) - i\gamma(p) \\ \gamma_{L,T}(p=0) &= 3.32\,\alpha_s T \quad (N_f=0) \\ \gamma_q(p=0) &= 1.9\,\alpha_s T \quad (N_f=2,3) \end{aligned}}$$

Braaten-Pisarski ('9

Problems in high T perturbation

① Bad convergence

good only for T > 30 GeV ?

② IR divergence

at $O(g^6)$ in $F(T)$

at $O(g^2)$ in $m_{mag}(T)$

QCD free energy at high T ($N_f=3$)

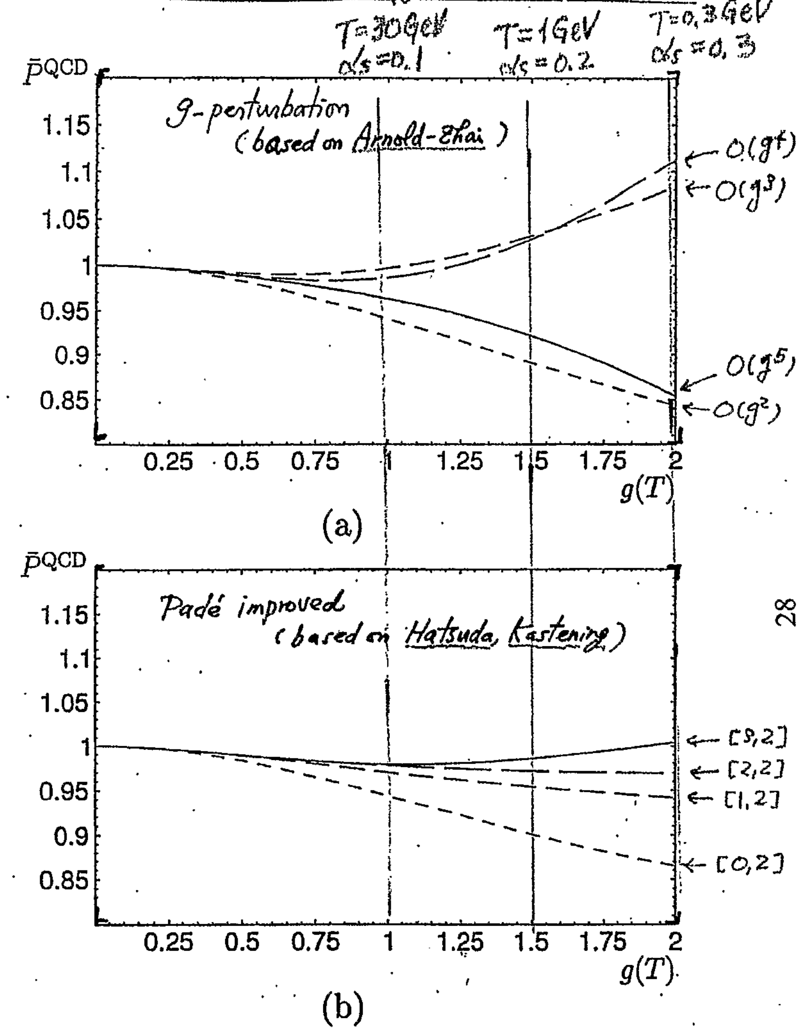

FIG. 1. a) The perturbative results for the pressure of QCD($N_f = 3$) up to order g^5 (full line). Short, medium, and long dashes give the results up to g^2, g^3, and g^4, respectively. b) The corresponding Padé approximants [0, 2], [1, 2], [2, 2], and [3, 2].

taken from Rebhan, hep-ph/9808

Free energy up to $O(g^5)$

$$F(T) = -\frac{8\pi^2}{45}T^4\left[F_0 + F_2\left(\frac{g(\mu)}{2\pi}\right)^2 + F_3\left(\frac{g(\mu)}{2\pi}\right)^3 + F_4\left(\frac{g(\mu)}{2\pi}\right)^4 + F_5\left(\frac{g(\mu)}{2\pi}\right)^5\right]$$

Boltzmann (1884) — Shuryak (1978) — Kapusta (1979) — Arnold-Zhai (1994, 1995) — Zhai-Kastening, Braaten-Nieto (1995, 1996)

$$\begin{cases} F_0 = 1 + \frac{21}{32}N_f \\ F_2 = -\frac{15}{4}\left(1+\frac{5}{12}N_f\right) \\ F_3 = 30\left(1+\frac{1}{6}N_f\right)^{3/2} \\ F_4 = 237.2 + 15.97N_f - 0.415N_f^2 + 135\left(1+\frac{1}{6}N_f\right)\ln\frac{g}{2\pi}\left(1+\frac{1}{6}N_f\right)^{1/2} \\ \qquad - \frac{165}{8}\left(1+\frac{5}{12}N_f\right)\left(1-\frac{2}{33}N_f\right)\ln\frac{\mu}{2\pi T} \\ F_5 = \left(1+\frac{1}{6}N_f\right)^{1/2}\left(-799.2 - 21.96N_f - 1.926N_f^2\right) \\ \qquad + \frac{495}{2}\left(1+\frac{1}{6}N_f\right)^{3/2}\left(1-\frac{2}{33}N_f\right)\ln\frac{\mu}{2\pi T} \end{cases}$$

- expansion by g
- increasing coeff.
- explicit μ-dep.

Why odd powers arise? (Gell-Mann - Brückner summation)

 with 

$O(g^4)$ but IR div.

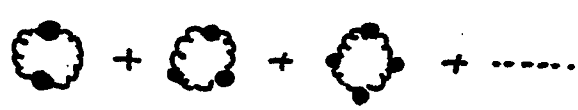

$$= F_{ring} \sim T\int\frac{d^3k}{(2\pi)^3}\left\{\ln\left(1+\frac{\omega_D^2}{k^2}\right) - \frac{\omega_D^2}{k^2}\right\}$$

$$\sim T\omega_D^3 \sim g^3T^4$$

$$\omega_D \sim gT$$

$\Rightarrow$ Systematic GB resummation in QCD

① $L = \left[L_{free} + \frac{1}{2}m_D^2A_4^2\right] + \left[L_{int} - \frac{1}{2}m_D^2A_4^2\right]$ Arnold et al ('95)

IR problem at $O(g^6)$
(by Linde)

$$F = T^4 [\underbrace{a + bg^2 + \cdots}_{\text{bad convergence}} + \underbrace{f}_{\text{IR div.!}} g^6 + \cdots]$$

∞

Linde's IR problem ('80)

$$F(T) \propto T^4 [F_0 + F_2 \left(\frac{g}{2\pi}\right)^2 + \cdots + F_5 \left(\frac{g}{2\pi}\right)^5 + F_6 \left(\frac{g}{2\pi}\right)^6 + \cdots]$$

- consider

$$\sim \underline{\underline{g^6 T^4 \left(\frac{g^2 T}{m}\right)^{l-3}}}, \quad (l > 3)$$

- IR cutoff m?

$m^2 = m_{el}^2 \sim T^2 (g^2 + g^4 + \cdots)$ $\qquad$ $m^2 = m_{mag}^2 \sim T^2 (\cancel{g^2} + g^4 + \cdots)$

$\Rightarrow$ new resummation necessary!
at $O(g^6)$ for $F(T)$

Infrared problem (Linde '80)

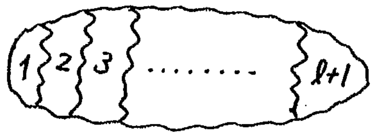

leading IR part : $n=0$ mode

$$\sim g^{2l}\left(T\int_m d^3p\right)^{l+1}\frac{1}{(p^2)^{3l}}\; p^{2l}$$

g^{2l} ← $2l$ vertices; $(\ldots)^{l+1}$ ← $(l+1)$-loops; $(p^2)^{3l}$ ← $3(l-1)+3$ propagators; p^{2l} ← $2l$ vertices with $\partial A\cdot A\cdot A$ type

$$\sim g^{2l}\,T^{l+1}\left(\int_m dp\right)^{l+1}\frac{1}{p^{2(l+1)}}$$

$$\Downarrow$$

$$\begin{cases} l<3 : & \text{IR convergent} \\ l=3 : & g^6T^4\ln(T/m) \\ l>3 : & g^{2l}T^{l+1}\dfrac{1}{m^{l-3}} \sim g^6T^4\left(\dfrac{g^2T}{m}\right)^{l-3} \end{cases}$$

- electric sector $m=\omega_D \simeq gT \neq 0 \rightarrow$ O.K.
  magnetic sector $m=\omega_M = \text{"}\alpha\text{"}\, g^2T \rightarrow$ trouble!
- Also, "α" cannot be obtained pert. theory

$$\begin{cases} l=1 : & g^4T^2\ln(T/m) \\ l>1 : & g^4T^2\left(g^2T/m\right)^{l-1} \end{cases}$$

the same problem

Dimensional Reduction of QCD at high T

Appelquist-Pisarski ('81)
Nadkarni ('83, '88)
Landsman ('89), Reisz ('92)

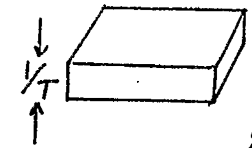

$$S_{QCD} = -\int_0^{1/T} d\tau \int d^3x\, \mathcal{L}\left(A_\mu(\tau,\vec{x}),\, q(\tau,\vec{x})\right)$$

$\omega_F = 2\pi T(n+\frac{1}{2})$
$\omega_B = 2\pi T n$

$\downarrow$ $n\neq 0$ mode decouple.

$$S_{eff} \sim -\frac{1}{T}\int d^3x\left\{\frac{1}{4}F_{ij}^2(\vec{x}) + \frac{1}{2}(D_iA_0(\vec{x}))^2 + V(A_0(\vec{x}), A_i(\vec{x}))\right\}$$

- QCD_3 with scalar field A_0
  with $g_3^2 = g_4^2\,T$
- $V(A_0, A_i)$ calculated in pert. theory

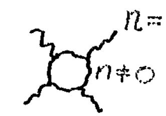

$$V \sim aA_0^2 + bA_0^4 \quad (a,b>0)$$

Non pert. nature of QCD_4 at high T (NP scale $\sim g_4^2T$)	$\Leftrightarrow$	Confining nature of dimensionally reduced theory at $T=0$ (coupling $g_3^2 = g_4^2T$)

Applications
lattice Reisz ('92)
continuum Ishii, Hatsuda, ...

Order of the QCD phase transition

Energy density on the Lattice

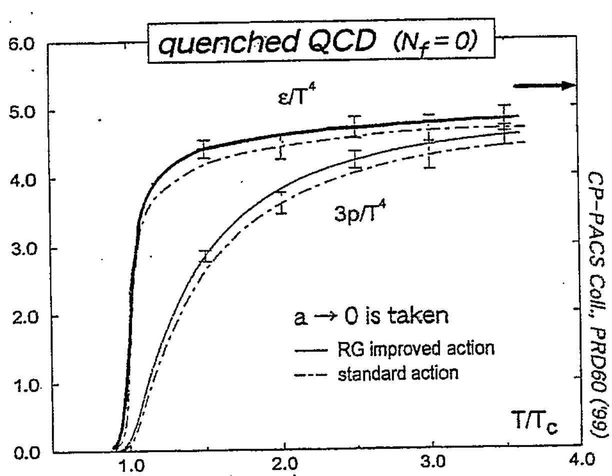

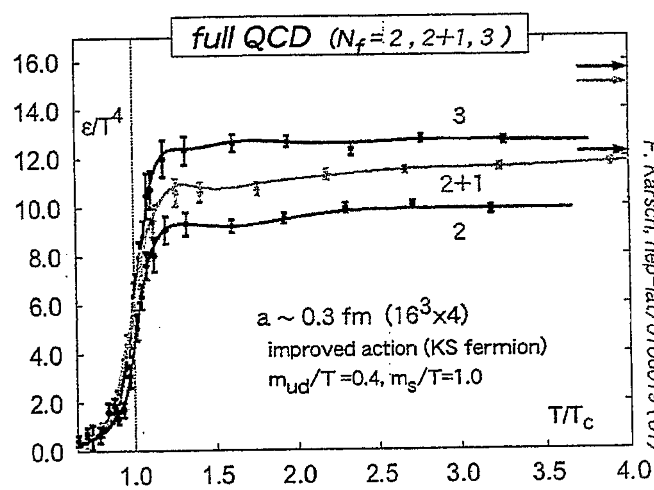

glueball gas gluon plasma resonance gas quark–gluon plasma

Are they phase transitions ?

What is the order parameter ? Tc ?

[II] Order of the phase transition

	Pure gauge ($m_q=\infty$)	full QCD ($m_q=0$)	real world ($m_q\neq 0$, small)
Order parameter	$\langle \mathrm{Tr} P e^{i\int d\tau A_4}\rangle$	$\langle \bar{q}q\rangle$	$\langle \bar{q}q\rangle$
Symmetry	$Z(N_c)$	chiral symmetry	approximate chiral symmetry
Effective theory	N_c-state Potts model	linear σ-model	linear σ-model

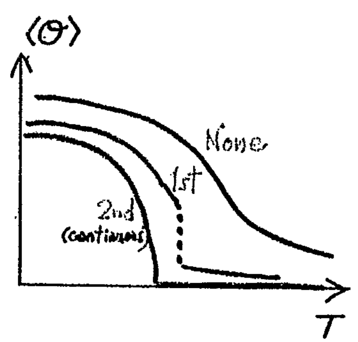

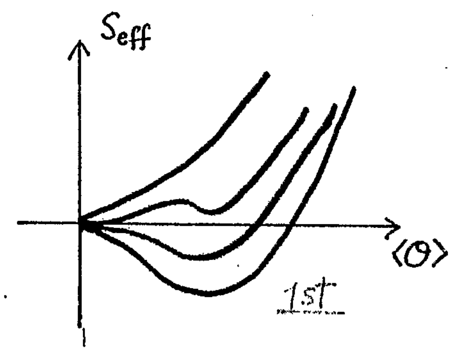

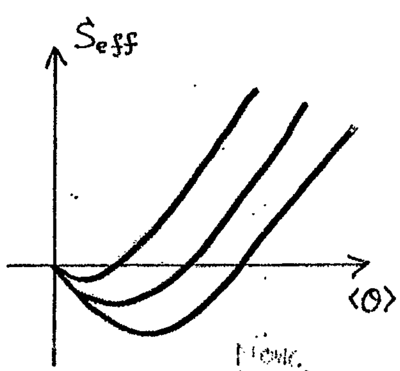

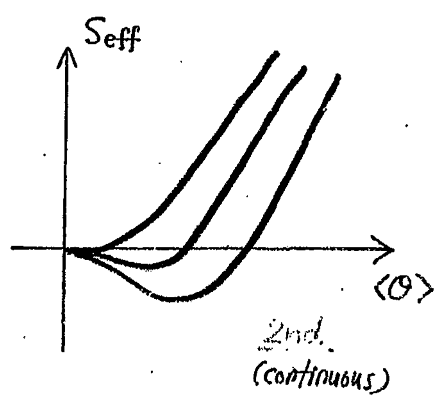

Confinement
- deconfinement
phase transition

33

$$\langle L\rangle \sim e^{-F_Q/T}$$

Z_N-symmetry in YM theory

- QED

∘ periodic gauge trans. $V(\vec{x},\tau) = e^{i\Lambda(\vec{x},\tau)}$

with $\Lambda(\vec{x},\beta) = \Lambda(\vec{x},0)$

$$\begin{cases} A_\mu \to V(A_\mu + i\partial_\mu)V^\dagger \\ L(\vec{x}) \to V(0)L(\vec{x})V^\dagger(\beta) = e^{-i[\Lambda(\vec{x},\beta)-\Lambda(\vec{x},0)]}L(\vec{x}) \end{cases}$$

$$= L(\vec{x}) \quad \leftarrow \text{invariant}$$

where $L(\vec{x}) = \exp\left[i\int_0^\beta d\tau\, A_4(\vec{x},\tau)\right]$

"Polyakov-line"

∘ aperiodic gauge trans.

$$\boxed{V(\vec{x},\tau+\beta) = e^{i\theta}\, V(\vec{x},\tau)}$$

$$A_\mu(\vec{x},\tau) \to A_\mu(\vec{x},\tau) + \partial_\mu\Lambda(\vec{x},\tau) \equiv A'_\mu(\vec{x},\tau)$$

$$A_\mu(\vec{x},\tau+\beta) \to A_\mu(\vec{x},\tau+\beta) + \partial_\mu\Lambda(\vec{x},\tau+\beta)$$

$$= A'_\mu(\vec{x},\tau) + \partial_\mu\theta$$

✓ therefore A_μ is still periodic if $\underline{\theta = \text{const}}$

✓ but $L(\vec{x}) \to e^{i\theta}L(\vec{x})$

- QCD

∘ periodic gauge trans. $V(\vec{x},\tau) \in SU(N)$

$V(\vec{x},\tau+\beta) = V(\vec{x},\tau)$

$$\begin{cases} A_\mu \to V(A_\mu + i\partial_\mu)V^\dagger \\ \text{Polyakov-line} \end{cases}$$

$$\boxed{\begin{aligned} \Omega(\vec{x}) &= P\exp\left[i\int_0^\beta A_4^a t^a d\tau\right] = P\exp\left[i\int_0^\beta A_4 \right. \\ L(\vec{x}) &= \mathrm{tr}\, \Omega(\vec{x}) \end{aligned}}$$

$$L(\vec{x}) \longrightarrow \mathrm{tr}\left[V(\vec{x},0)\,\Omega(\vec{x})\,V^\dagger(\vec{x},\beta)\right]$$

$$= L(\vec{x}) \quad \text{if } V \text{ is periodic}$$

QCD action is obviously invariant under V

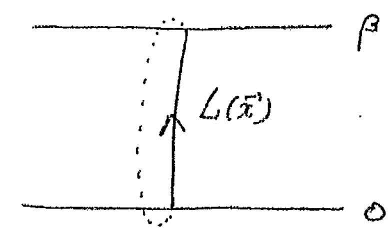

o aperiodic gauge trans.

$$\boxed{V(\vec{x},\tau+\beta) = z\, V(\vec{x},\tau)} \qquad \in SU(N)$$

since $V \in SU(N)$, $\underline{z z^{+} = 1}$, and $\underline{\det z = 1}$ ①

Conditions for z:

$$\begin{cases} A_\mu(\vec{x},\tau) \to V(\vec{x},\tau)\left(A_\mu(\vec{x},\tau) + i\partial_\mu\right)V^{+}(\vec{x},\tau) = A'_\mu(\vec{x},\tau) \\ A_\mu(\vec{x},\tau+\beta) \to V(\vec{x},\tau+\beta)\left(A_\mu(\vec{x},\tau+\beta) + i\partial_\mu\right)V^{+}(\vec{x},\tau+\beta) \end{cases}$$

$$= z\, V(\vec{x},\tau)\left[A_\mu(\vec{x},\tau) + i\partial_\mu\right]V^{+}(\vec{x},\tau)\, z^{+}$$

$$= z\, \underset{\underset{A'_\mu(\vec{x},\tau)}{\Downarrow}}{A'_\mu(\vec{x},\tau)}\, z^{+} + i\, \underset{\underset{0}{\downarrow}}{z\partial_\mu z^{+}}$$

$z t^a z^{+} = t^a$ or $\underline{z \underset{\widehat{SU(N)}}{G} z^{+} = G}$ ②

$\underline{z\partial_\mu z^{+} = 0}$ ③

①②③ → z is a center of $SU(N)$

$$\boxed{z = e^{2\pi i n/N}\, \mathbb{1}} \quad (n = 0, 1, 2, \cdots, N-1)$$

$$\left\{ \begin{array}{l} A_\mu : \text{periodic} \\ \text{QCD action invariant} \\ L(\vec{x}) \to z L(\vec{x}) \end{array} \right\}$$

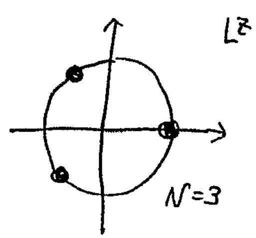

under this aperiodic gauge trans.

Physical meaning of $L(\vec{x})$

McLerran-Svetitsky

Consider static heavy quark $\hat{\Psi} = e^{-m\tau}\hat{\varphi}$

eq. of motion

$$\left[i\frac{\partial}{\partial\tau} - \hat{A}^4(\vec{x},\tau)\right]\hat{\varphi}(\vec{x},\tau) = 0$$

$$\downarrow$$

$$\hat{\varphi}_\alpha(\vec{x},\tau) = T\exp\left[i\int_0^\tau d\tau' \hat{A}^4(\vec{x},\tau')\right]_{\alpha\beta}\hat{\varphi}_\beta(\vec{x},0)$$

$$\equiv \Omega_{\alpha\beta}(\vec{x},\tau)\hat{\varphi}_\beta(\vec{x},0)$$

partition func.

$H = H_{gauge} + \int \hat{\varphi}^{+}\hat{A}_4\hat{\varphi}\, d\tau d^3x$

complete set with 1-heavy quark

$$e^{-\beta F(\vec{x})} \sim \sum_n \langle n| e^{-\beta H} |n\rangle$$

$$= \sum_m \langle m| \hat{\varphi}_\alpha(\vec{r},0)\, e^{-\beta H}\, \hat{\varphi}_\alpha^{+}(\vec{r},0) |m\rangle$$

complete set with heavy q.

$$= \sum_m \langle m| e^{-\beta H}\hat{\varphi}_\alpha(\vec{r},\beta)\hat{\varphi}_\alpha^{+}(\vec{r},0)|m\rangle$$

$e^{\beta H} O(\tau) e^{-\beta H} = O(\tau+\beta)$

$H = H_{gauge} + H_{int}$
H_{int} acts l.h.s. and vanishes!

$$= \sum_m \langle m| e^{-\beta H}\Omega_{\alpha\beta}(\vec{x})\underbrace{\hat{\varphi}_\beta(\vec{r},0)\hat{\varphi}_\alpha^{+}(\vec{r},0)}_{\delta_{\alpha\beta}}|m\rangle$$

$$= \sum_m \langle m| e^{-\beta H_{gauge}}\Omega_{\alpha\alpha}(\vec{x},\beta)|m\rangle$$

$$= \mathrm{Tr}\left[e^{-\beta H_{gauge}}\Omega_{\alpha\alpha}(\vec{x},\beta)\right]$$

$$= \langle L(\vec{x})\rangle$$

confined phase $F \to \infty \to \langle L\rangle = 0$

deconfined phase F: finite $\to \langle L\rangle$ finite

- On the lattice

gauge trans. $\quad U^{\mu}(n) \to V(n)\, U^{\mu}(n)\, V^{\dagger}(n+\mu)$

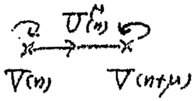

example of aperiodic V

$$U^{0}(\vec{x},\tau_0) \to z\, U^{0}(\vec{x},\tau_0) \quad \text{for specific time slice } \tau_0$$

$$L(\vec{x}) = \mathrm{tr} \prod_{\tau=0}^{N_\tau - 1} U^{\mu=0}(\vec{x},\tau) \longrightarrow z\, L(\vec{x}) .$$

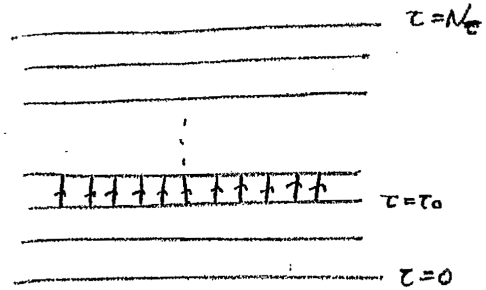

	Confined	Deconfined
T	$T < T_c$	$T > T_c$
F_Q	∞	finite
$\langle L \rangle$	0	finite
Z_N	unbroken	broken (spontaneously)

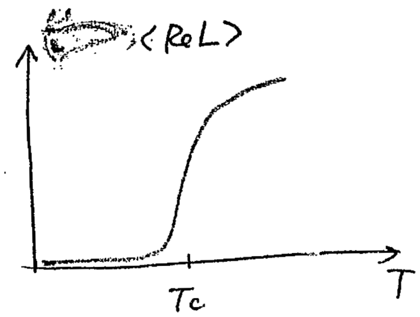

$SU_c(2)$

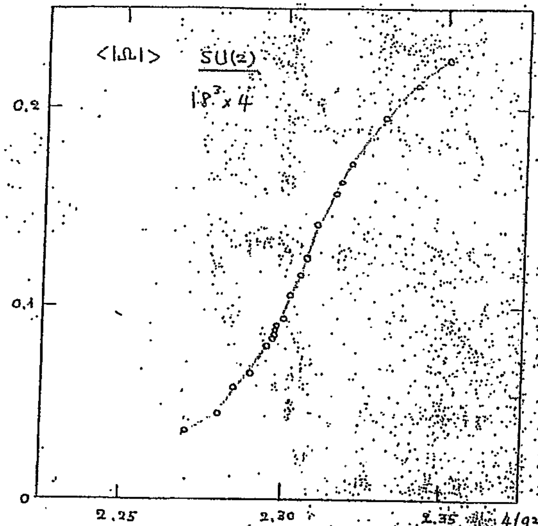

second-order? $\langle|\Omega|\rangle \sim (\beta-\beta_c)^{\beta}$, $\beta>\beta_c$?

$= 0$ $\beta<\beta_c$?

$SU_c(3)$

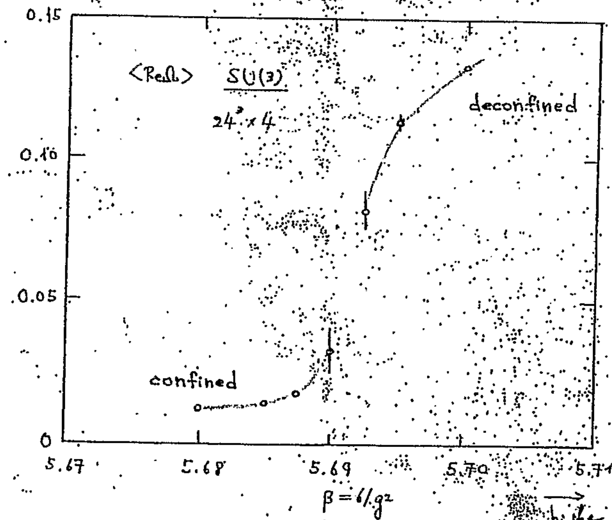

first-order with a jump?

pure gauge

Ukawa '93

pure SU(3) theory, Polyakov line

~~<|Ω|>~~ <ReΩ>

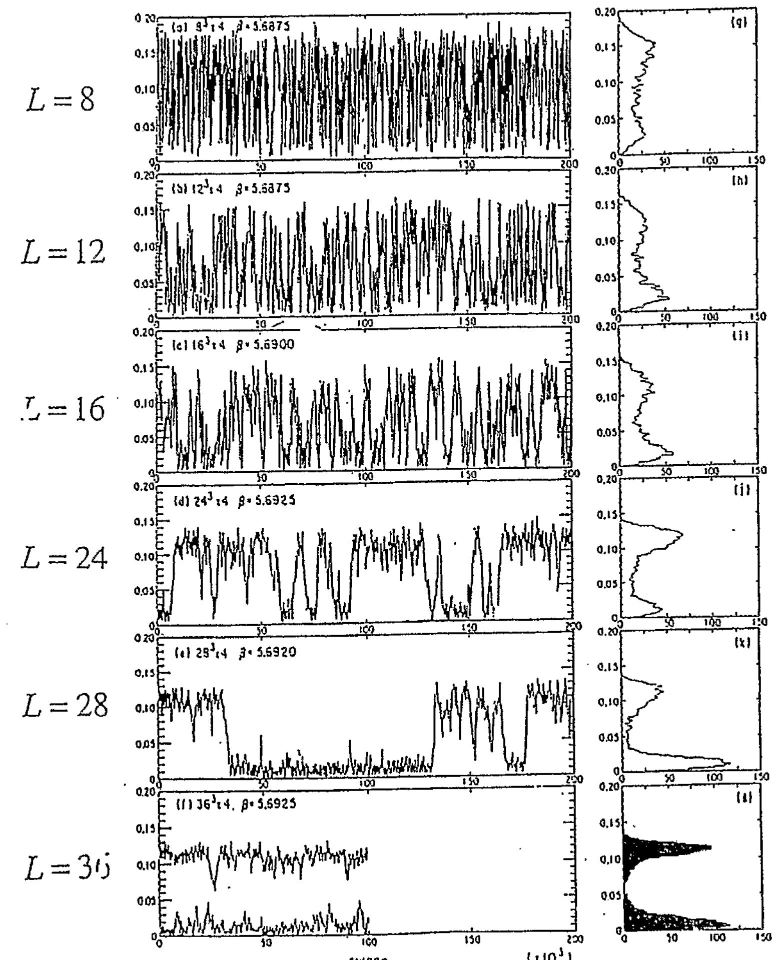

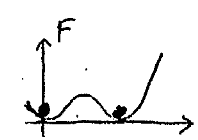

Ukawa et al (9

Finite size scaling analysis

scaling of peak height : $\rho = 1$ expected for 1st order

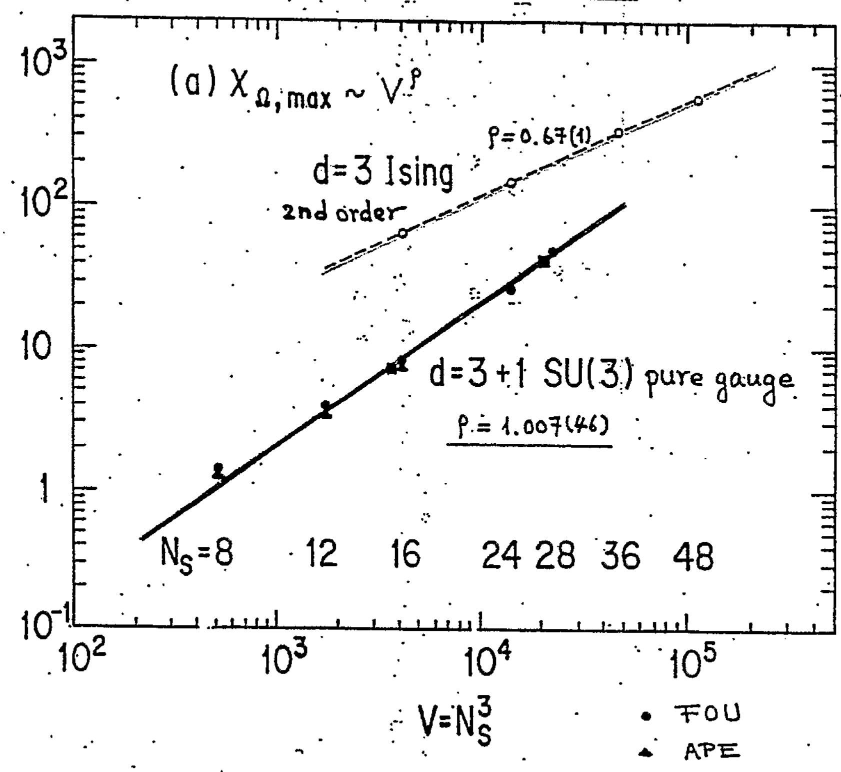

Fig. 5(a)

What kind of phase transitions ?

quenched QCD

$e^{-F_q(T)/T}$: heavy-quark free-energy

$= 0 \quad \Leftrightarrow$ conf. (Z(3) restored)

$\neq 0 \quad \Leftrightarrow$ deconf. (Z(3) broken)

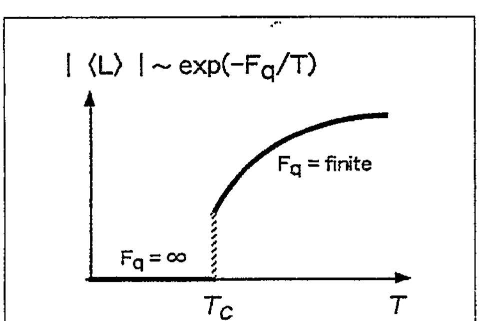

$T_c = 271 \pm 2$ MeV, 1st order

- $a \to 0$, $L \to \infty$ taken
- typical lattice size : $32^3 \times 8$

full QCD

$\langle \bar{q}q \rangle$: q–$\bar{q}$ pairing

$\neq 0 \quad \Leftrightarrow$ "super" (χ-sym. broken)

$= 0 \quad \Leftrightarrow$ "normal" (χ-sym. restored)

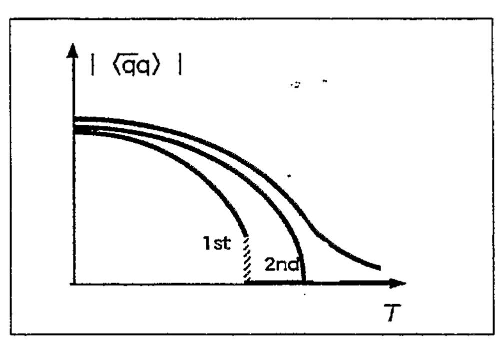

$N_f = 3$: $T_{pc} =$ 154 ± 8 MeV "1st order" (KS)

$N_f = 2$: $T_{pc} =$ 173 ± 8 MeV "2nd order" (KS)

171 ± 4 MeV "2nd order" (Wilson)

- $a \sim 0.3$ fm (improved action)
- typical lattice size : $16^3 \times 4$

CP-PACS Coll, PRD63 (01)
Karsch et al, hep-lat/0012023 (C

String breaking in QCD at $T \neq 0$

QCD string in hot medium

linear string at T=0 : (E_{min})

$V(r) \to \sigma r$

fluctuating string at $T\neq 0$ ($F_{min} = E - TS$)

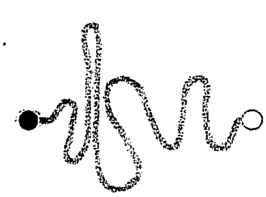

$$\frac{\sigma(T)}{\sigma(0)} = \left(1 - \frac{T^2}{T_c^2}\right)^{\beta} \to 0.5$$

1.21 0.99

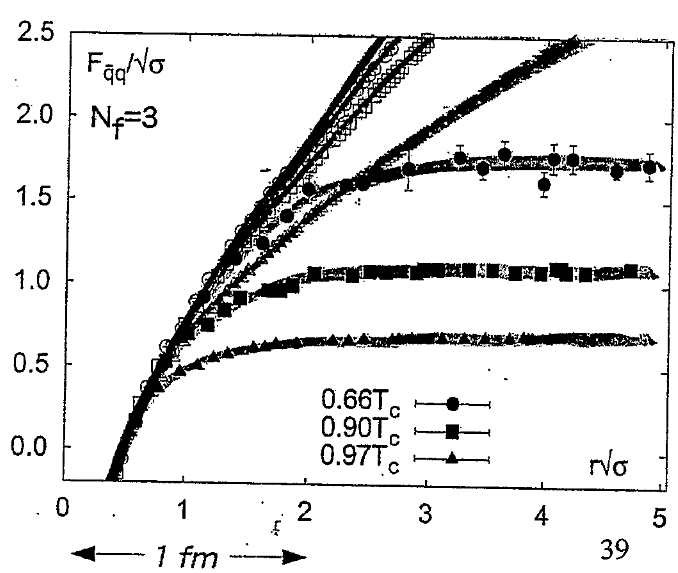

string breaking at $T\neq 0$

$V(r) \to$ const.

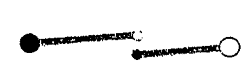

Karsch et al.,
hep-lat/0012023 ('00), hep-lat/0106019 ('01)

Level shift/crossing in $c\bar{c}$ system $\Longleftrightarrow$ charmonium below T_c

Miyamura et al., PRL 57 ('86); Vogt & Jackson, PL B206 ('88)
Sivirtsev et al., PL B484 ('00); Hayashigaki, PL B487 ('00)

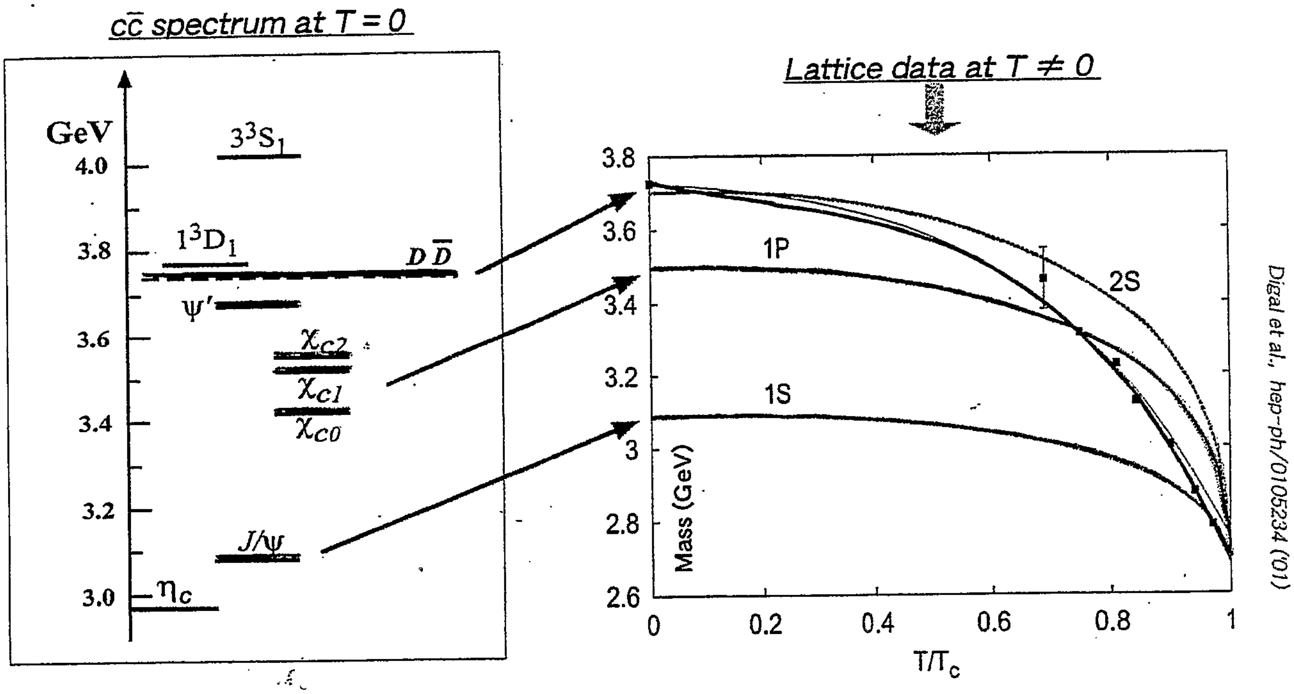

Chiral phase transition

$\langle \bar{q} q \rangle$

What is chiral symmetry ?

▼ massless quarks : chirality (handedness) = helicity

▼ pert. QCD : chirality conserving ($q = q_R + q_L$)

$$L_{QCD} = L(q_R) + L(q_L) + m\bar{q}_R q_L$$

▼ Chiral symmetry ⇔ conservation of R, L currents

$$q_R \rightarrow e^{i\alpha} q_R, \qquad q_L \rightarrow e^{i\beta} q_L$$

▼ non-pert. QCD : chirality mixing

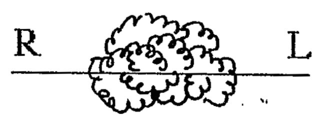

⇔ generation of the "constituent" mass M :

M (350 MeV) ≫ m (10 MeV)

⇔ Non-zero quark condensate : $\langle \bar{q}_R q_L \rangle \neq 0$

existence of the pion

Nambu-Goldstone Theorem

QCD vacuum structure

NP QCD : chirality mixed   P QCD : chirality conserved

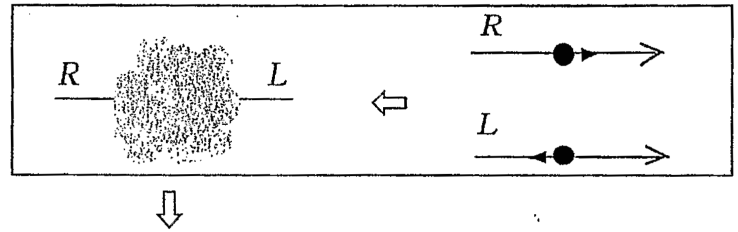

- quark condensate : $\langle \bar{q}q \rangle = \langle \bar{q}_R q_L + \bar{q}_L q_R \rangle = -(225 \pm 25\ \mathrm{MeV})^3$
- Nambu-Goldstone boson : pion
- massive qasi-particle : constituent quark with M (350 MeV)
- hadron spectrum :

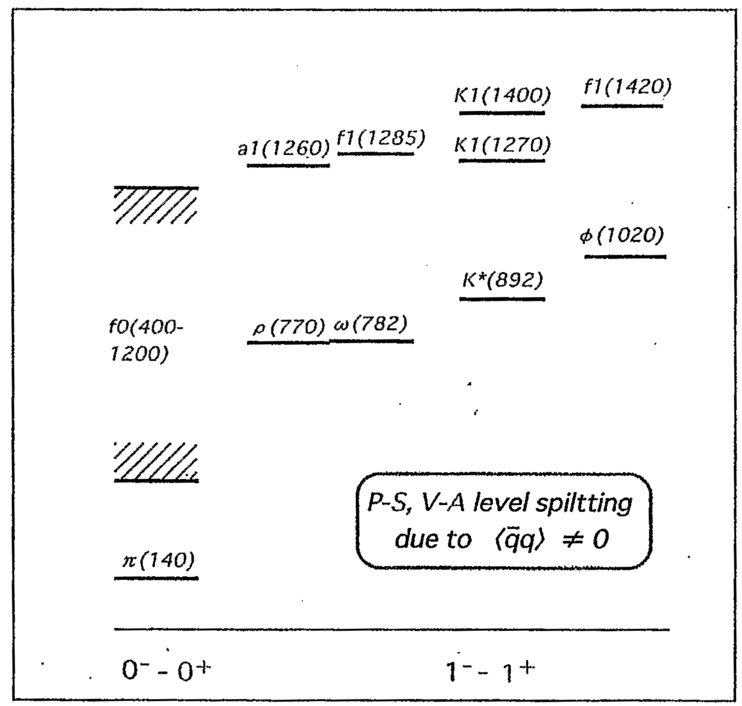

$q\bar{q}$ excitations

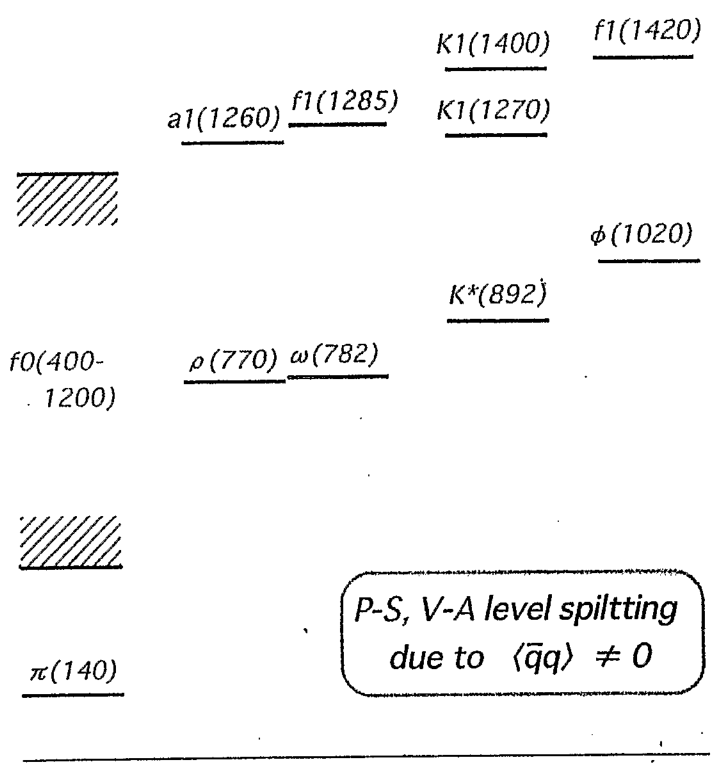

Chiral mass formulas

$$m_\pi^2 \approx \hat{m}\langle\bar{q}q\rangle_0 / f_\pi^2 \qquad m_\rho^2 \approx \left[\frac{448}{27}\pi^3\alpha_s\langle\bar{q}q\rangle_0^2\right]^{1/3}$$

$$m_{a1}^2 \approx \left[\frac{2816}{27}\pi^3\alpha_s\langle\bar{q}q\rangle_0^2\right]^{1/3}$$

⇧ small quark-mass

⇧ QCD sum rules in large N_c

Symmetry breaking & restoration

▼ QCD

Order Parameter

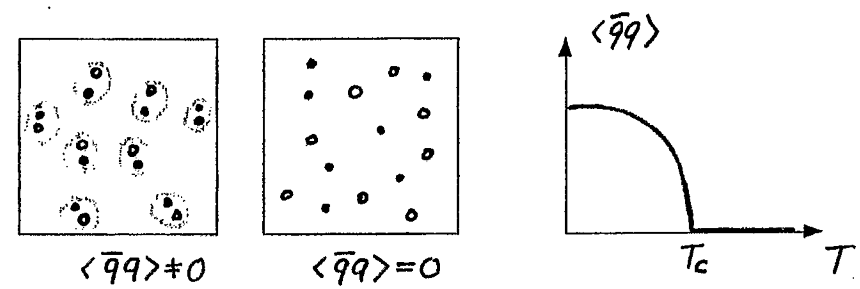

▼ Superconductors

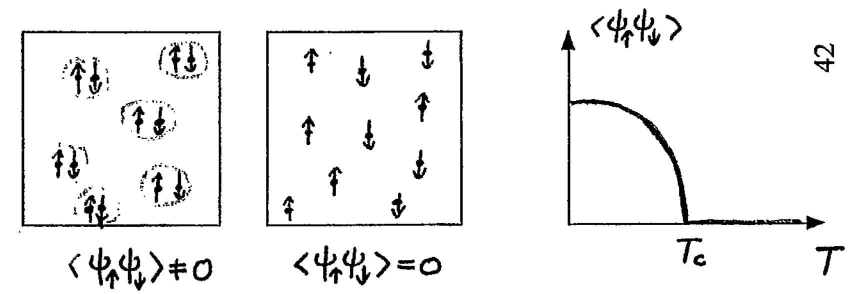

▼ Spin systems

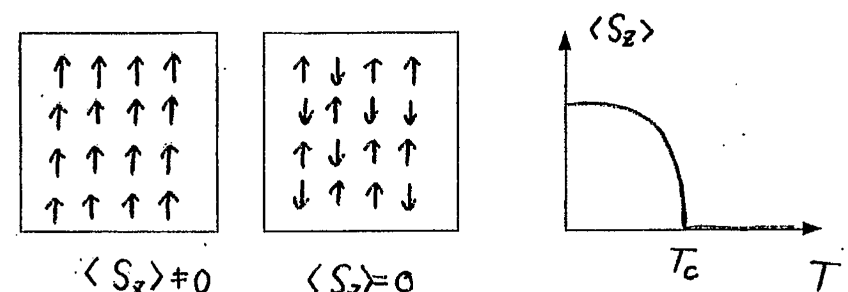

Chiral Phase Transition in QCD

system	$N_f = 3$ $m_{u,d} = m_s = 0$	$N_f = 2$ $m_{u,d} = 0,\ m_s = \infty$	$N_f = 2+1$ $m_{u,d} \sim 5$ MeV, $m_s \sim 100$ MeV
symmetry	$SU_L(3) \times SU_R(3)$	$SU_L(2) \times SU_R(2) \sim O(4)$	*approximate* $SU_L(3) \times SU_R(3)$
order parameter and effective theory	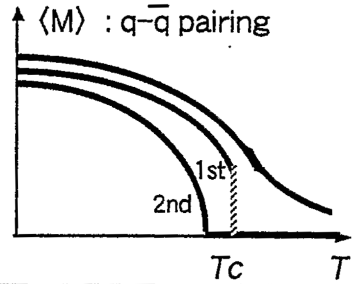	3-d σ model : $M \sim \langle q_L q_R \rangle$ $L_{eff} = \mathrm{tr}\, \nabla M^\dagger \nabla M + a\, \mathrm{tr}\, M^\dagger M + b\, \mathrm{tr}\,(M^\dagger M)^2 + c\,(\mathrm{tr}\, M^\dagger M)^2 + \cdots$ *Pisarski & Wilczek, PR D29 ('84)*	
order	1st	2nd	1st or crossover ?
T_{pc}	154 ±8 MeV (KS)** (improved action, a ~ 0.3 fm, $m_q \to 0$ taken)	171±4 MeV (Wilson)* 173±8 MeV (KS)** (improved action, a ~ 0.3fm , $m_q \to 0$ taken)	?

** CP-PACS, PRD63 ('00), ** Karsch et al., hep-lat/0012023 ('00)*

Phase structure at finite T (from lattice QCD)

Karsch et al., hep-lat/0012023 ('00)

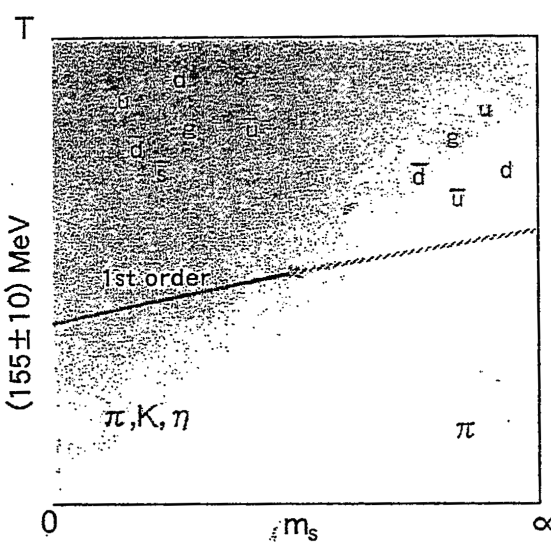

Phase structure at finite ρ (from effective theories)

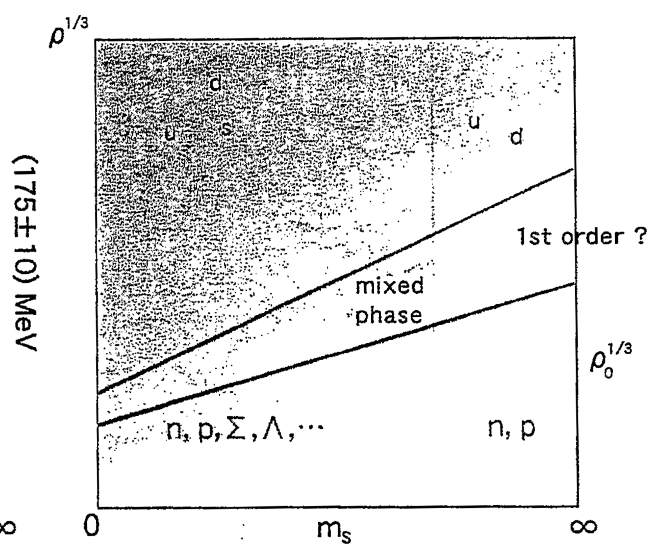

In-medium hadrons

Chiral partners in the vacuum

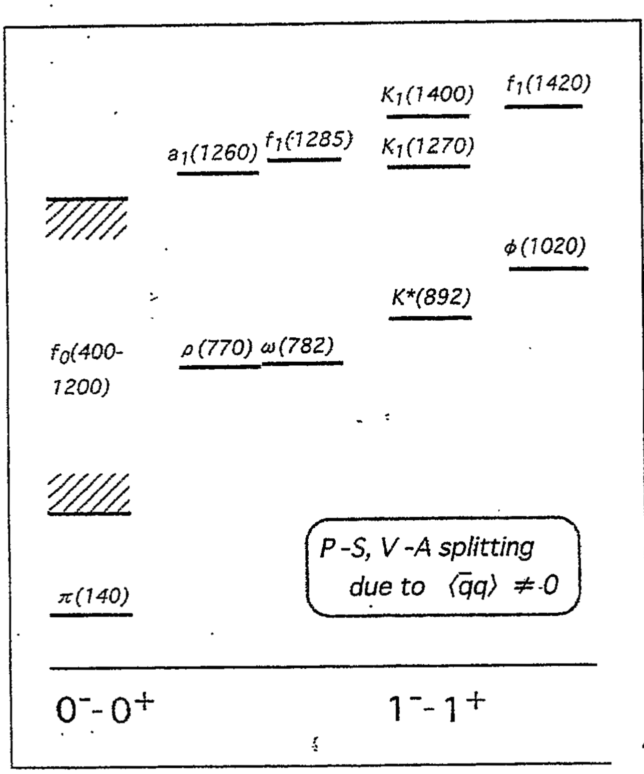

Hadronic correlations in the medium

- $\langle \bar{q}q \rangle \to 0$

  $\Leftrightarrow$ Chiral degeneracy

  $\langle S(x)S(y) \rangle \sim \langle P(x)P(y) \rangle$
  $\langle A(x)A(y) \rangle \sim \langle V(x)V(y) \rangle$

- change of $\langle \bar{q}q \rangle$

  $\Leftrightarrow$ Individual spectrum

  $\langle S(x)S(y) \rangle$, $\langle P(x)P(y) \rangle$
  $\langle A(x)A(y) \rangle$, $\langle V(x)V(y) \rangle$

NJL · Hatsuda & Kunihiro, PRL ('85)
QSR · Hatsuda, Koike & Lee, NPB ('92)

Hadronic susceptibility (χ_H)

$$\int \langle S(x_E)S(0)\rangle d^4x_E \rightarrow \int \langle P(x_E)P(0)\rangle d^4x_E$$

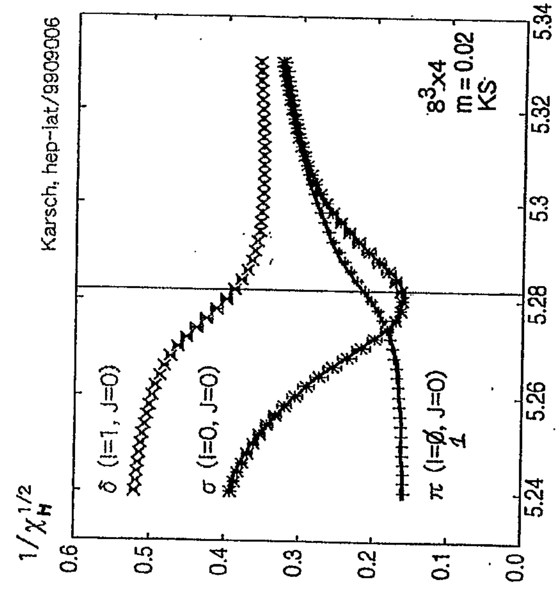

Dilepton spectrum

$$\frac{dR}{d^4x d^4q} \propto \mathrm{Im}\ F.T. \langle V(t,\vec{x})V(0)\rangle$$

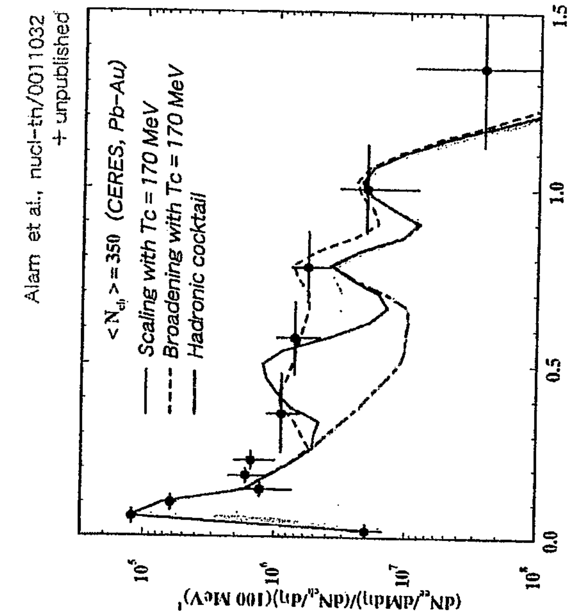

Past and Future Experiments

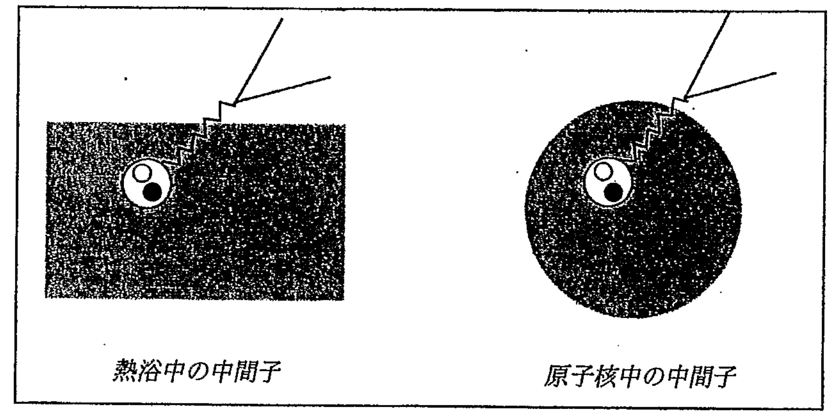

Past

- CERES (SPS@CERN) : $S + Au \rightarrow e^+e^- + X$ PRL ('95)
  ρ, ω, φ — $Pb + Au \rightarrow e^+e^- + X$ NPA ('98)
- "σ" CHAOS (TRIUMF) : $\pi^+ + (H, C, Ca, Pb) \rightarrow \pi^+\pi^- + X$ PRL ('96), NPA ('00)
- CB (BNL) $\pi + (\text{"}) \rightarrow \pi^0\pi^0 + X$
- TAPS (Mainz) $\gamma + (\text{"}) \rightarrow \pi^0\pi^0 + X$ PRL ('00)

On going

- ρ, ω, φ E325 (KEK-PS) : $p + A \rightarrow e^+e^- + X,\ K^+K^- + X$ ('97-) PRL ('01)

Planned

- PHENIX (RHIC@BNL) : $A + A \rightarrow e^+e^- + X$
  ρ, ω, φ
- GSI : $d + A \rightarrow {}^3He + (A\text{-}1)$
  ρ, ω — $\pi^- + A \rightarrow e^+e^- + (A\text{-}1) + n$
- Spring-8 : $\gamma + A \rightarrow 2\gamma + X,\ 4\gamma + X$
  "σ"

Hadronic correlations in lattice QCD

$$D(\tau) = \int \left\langle \bar{q}\Gamma q(\tau,\vec{x})\bar{q}\Gamma q(0)\right\rangle d^3x$$

$$\sim e^{-m\tau} \qquad (\tau \to \infty)$$

$$= \int_0^\infty e^{-\omega\tau} A(\omega)\, d\omega \qquad (\text{any } \tau)$$

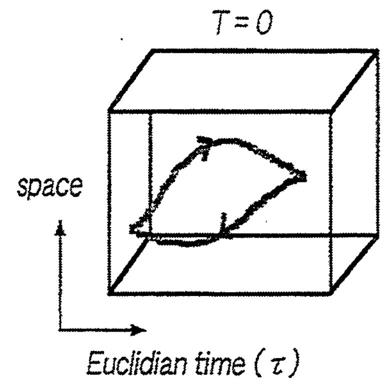

Ill-posed problem


T. Bayes 1702-1761


C.E. Shannon, 1916-2001

<u>M</u>aximal <u>E</u>ntropy <u>M</u>ethod : P [A | D]

- <u>No</u> parametrization of A (ω)
- <u>unique</u> solution for D (τ) → A (ω)
- <u>error estimate</u> on A (ω)

<u>Reviews :</u>
Optics and astrophysics: N. Wu, Springer ('97)
Spin systems: Jarrell & Gubernatis, Phys. Rep. 269 ('96)
Lattice QCD: Asakawa, Nakahara and T.H., Prog. Part. Nucl. Phys. 47 ('01)

MEM Image Reconstruction


The Image of Saturn

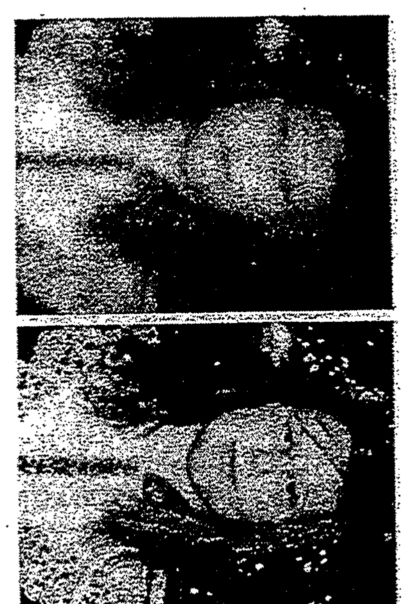
The girl's portrait

From N. Wu, "The Maximum Entropy Method" (1997)

► Test with mock data

$$\begin{array}{cccc} & \text{Laplace Trans.} & \text{Truncation \& Noise} & \text{MEM} \\ A_{in}(\omega) & \rightarrow\ D_{in}(\tau) & \rightarrow\ D_{mock}(\tau_i) & \rightarrow\ A_{out}(\omega_n) \end{array}$$

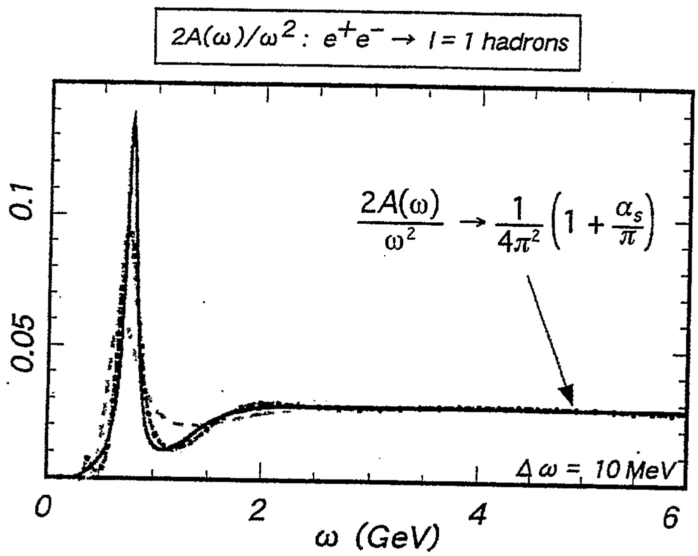

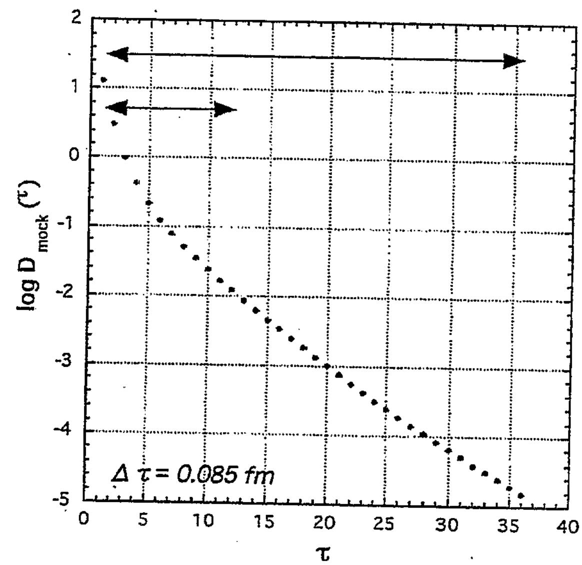

Spectral functions
in π & ρ channels at $T=0$

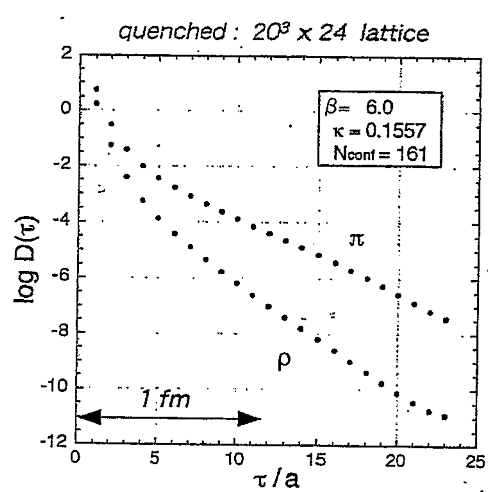

MEM

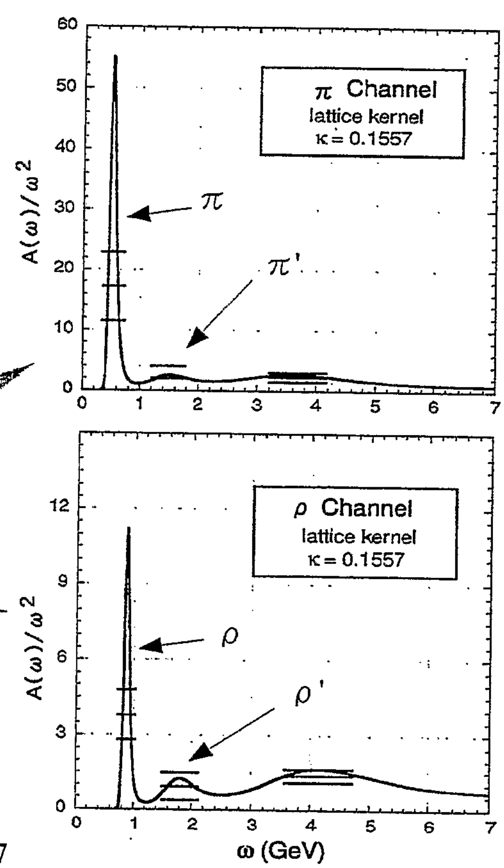

Asakawa, Nakahara & T.H., PRD ('99), hep-lat/0011040 ('00)
CP-PACS Coll., hep-lat/0105030 ('01)

Hadronic correlations at finite T in lattice QCD

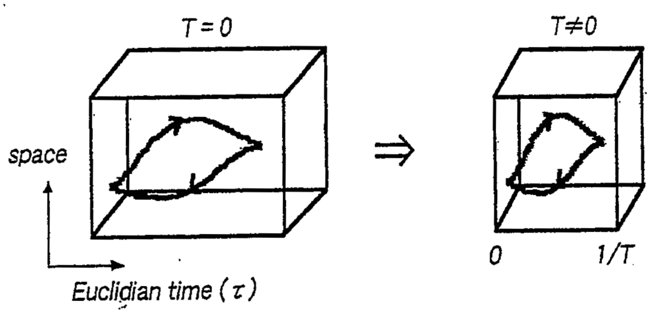

$$D(\tau;T) = \int_0^\infty \frac{e^{-\omega\tau} + e^{+\omega(\tau - 1/T)}}{1 - e^{-\omega/T}} A(\omega;T)\, d\omega$$

Lattice QCD + MEM provides a clue to study in-medium hadrons (ρ , J/Ψ , ⋯)

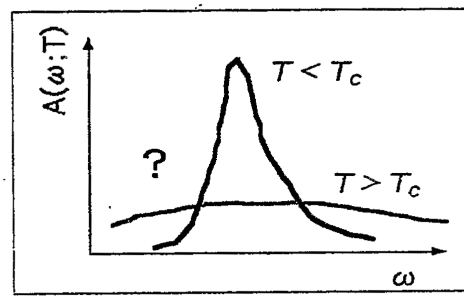

studies are started on anisotropic lattice:

Asakawá, Nakahara & T.H., on CP-PACS.

($\pi, \rho, \omega, \phi, J/\psi$ $\quad 32^3 \times 32, \times 48, \times 64, \times 96$
$\beta = 7.0, \quad a_s/a_\tau = 4$)

QCD phenomenology at $T \neq 0, \rho \neq 0$
and its relation to { experiments / observations

① Early Universe.

② Relativistic heavy ion collisions

③ Signatures of phase transition

- J/ψ suppression ↔ deconfine
- spectral change of ρ, ω, ϕ ↔ chiral restor

$\rho, \omega, \phi, J/\psi \to \ell^+\ell^-$

④ Physics of Neutron Stars

QCD Phase Transition in Early Universe

Big Bang vs Little Bang

$$T = \left(\frac{45}{16G\pi^3 d}\right)^{1/4} \times \frac{1}{t^{1/2}}$$

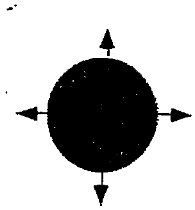

$$T = \left(T_0^3 \tau_0\right)^{1/3} \times \frac{1}{\tau^{1/3}}$$

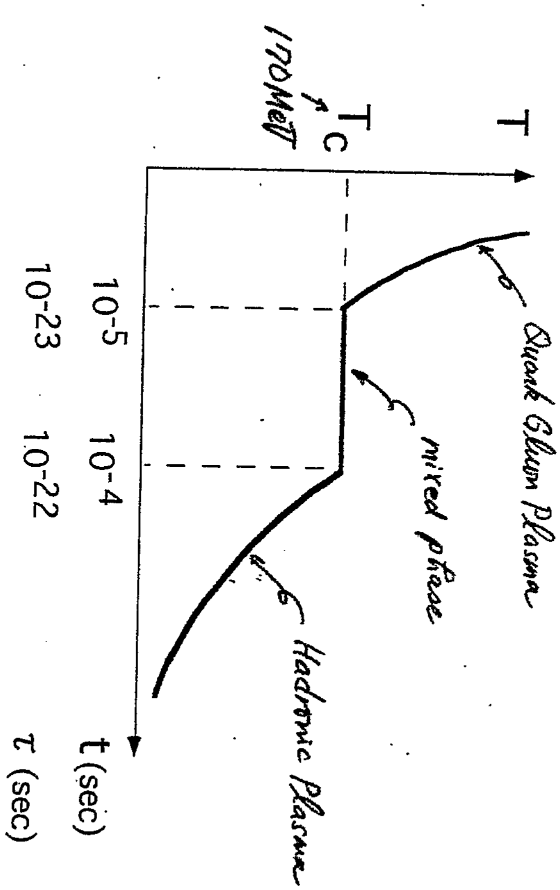

Early Universe

- Robertson-Walker metric

$$ds^2 = dt^2 - a^2(t)\left[\frac{dr^2}{1-kr^2} + r^2(d\theta^2 + \sin^2\theta\, d\phi^2)\right]$$

$a(t)$: scale parameter, $k \begin{smallmatrix} >0 \\ =0 \\ <0 \end{smallmatrix}$ open / flat / close

- Hubble constant $\boxed{H(t) = \dot{a}(t)/a(t)}$

$H(t=\text{now}) \simeq (50-100)\ \text{km/sec/Mpc}$

$(1\,\text{Mpc} = 3\times10^{19}\,\text{km})$

- Einstein equation

$$\boxed{\begin{cases} \ddot{a} = -\frac{4\pi}{3} G(\mathcal{E}+3P)\,a \\ \left(\frac{\dot{a}}{a}\right)^2 = \frac{8\pi}{3} G\,\mathcal{E} - \frac{k}{a^2} \end{cases}} \rightsquigarrow \boxed{\frac{d\mathcal{E}}{da} = -3\,\frac{\mathcal{E}+P}{a}}$$

cons. of energy-mom. tensor

- Ideal gas equation of state

$$\boxed{\begin{matrix}\mathcal{E} = 3P \\ = \cancel{\tfrac{4}{8}ST}\end{matrix}} \quad \text{with} \quad \begin{cases} \mathcal{E} = d\,\frac{\pi^2}{30}T^4 \\ d = d_B + \frac{7}{8}d_F \end{cases}$$

$= \cancel{\tfrac{1}{4}ST}$

$\frac{3}{4}ST$

- Solution for idea gas case

$$\begin{cases} a(t) \propto \sqrt{t} \\ \mathcal{E} \propto a^{-4} \\ T \propto a^{-1} \end{cases}$$

also, total entropy is conserved:

$S_{tot} \propto a^3T^3 = \text{constant}$

$\Downarrow$

$$\boxed{T = \frac{1}{2}\left(\frac{45}{\pi^3 d\,G}\right)^{1/4}\frac{1}{\sqrt{t}}}$$

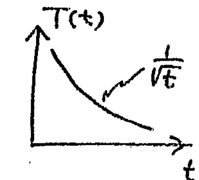

- 1st order phase transition

total entropy conservation: $s\,a^3 = \text{const}$.

$$[f\,S_H + (1-f)\,S_Q]\,a^3 = s_0\,a_0^3$$

$t = t_I : f = 0$
$t = t_F : f = 1$ $\gg$ $S_Q\, t_I^{3/2} = S_H\, t_F^{3/2}$

$\Downarrow$

$$\frac{t_F}{t_I} = \left(\frac{S_Q}{S_H}\right)^{2/3} \sim O(10)$$

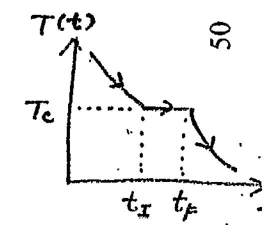

50

Baryon number ratio at $T=T_c$

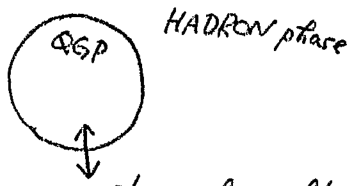

chemical equilibrium $\mu_B = 3\mu_Q,\ T=T_c$

$T \gg \mu$ case :

$$\langle n_B \rangle_{QGP} = d_Q \frac{\mu_Q}{12} T^2 \qquad \left(\underset{u,d\ \text{gas}}{d_Q = 2\times2\times3\times2 = 24} \right)$$

↑ baryon # density in QGP — relativistic

$$\langle n_B \rangle_{HAD} = d_B \frac{2\mu_B}{T} \left(\frac{m_N T}{2\pi} \right)^{3/2} e^{-m_N/T} \qquad \left(\underset{n,p\ \text{gas}}{d_B = 2\times2\times2 = 8} \right)$$

↑ baryon # density in Hadron gas — non-rel.

$$\Downarrow$$

$$r \equiv \left. \frac{\langle n_B \rangle_{HAD}}{\langle n_B \rangle_{QGP}} \right|_{T=T_c} = \underbrace{3 \left(\frac{2m_N}{\pi T_c} \right)^{3/2}}_{24} \underbrace{e^{-m_N/T_c}}_{0.002} = \underline{5\%}$$

for $T_c = 150\,\text{MeV}$

相対論的重イオン衝突 ($T \rightarrow 100\sim300$ MeV)

▼ A-A 衝突における時間発展： Bjorken ('83) ·····

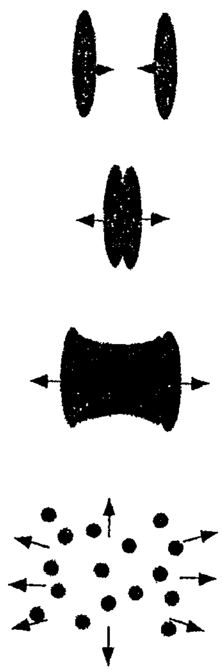

① Pre-equilibrium (t=0.1~1 fm)
parton cascade

② Plasma/Mixed phase (t=1~20 fm)
relativistic hydrodynamics

③ Hadronization (t=20~40 fm)
relativistic Boltzmann eq.

▼ 現在／将来の実験：

	nucleus	E_{tot}(GeV)	T_0 (MeV)	year
AGS (BNL)	$^{197}Au + ^{197}Au$	4 A	150	running
SPS (CERN)	$^{208}Pb + ^{208}Pb$	17 A	190	running
RHIC (BNL)	$^{197}Au + ^{197}Au$	200 A	230	~~1999~~ 2000
LHC (CERN)	$^{208}Pb + ^{208}Pb$	7000 A	260	2005 ?

[IV] Current/Future projects

Parameters and conditions expected for experiments at AGS, SPS, RHIC and LHC.

Machine	Beam – Target	$\sqrt{s}$ [GeV/A]	$(dN/dy)_o$	ϵ_o [GeV/fm³]	T_o [Mev]
AGS	^{28}Si – ^{197}Au	5	70	0.9	150
SPS	^{32}S – ^{238}U	20	200	2.4	190
AGS	^{197}Au – ^{197}Au	4	230	0.8	150
SPS	^{208}Pb – ^{208}Pb	17	700	2.4	190
RHIC	^{197}Au – ^{197}Au	200	1400	5.1	230
LHC	^{208}Pb – ^{208}Pb	6300	2600	9.0	260

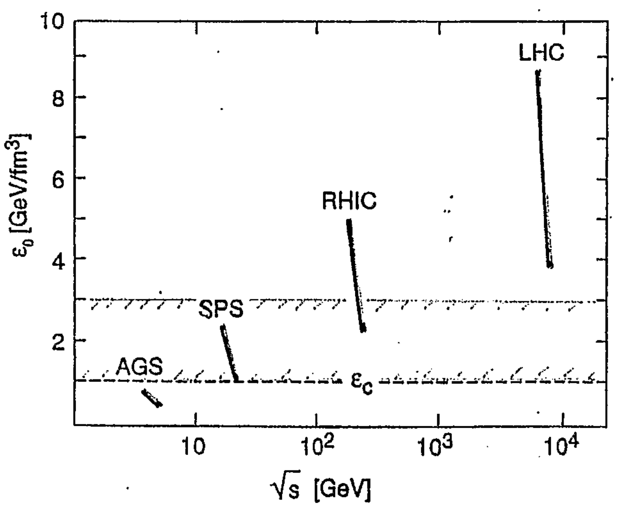

$T_c = 200$ MeV

$T_c = 150$ MeV

$\mathcal{E}_0 \sim \langle m_T \rangle \left(\frac{dN}{dy}\right)_0 / \pi R^2 \tau_0 \qquad \tau_0 \simeq 1\,fm.$

parton cascade & Thermalization

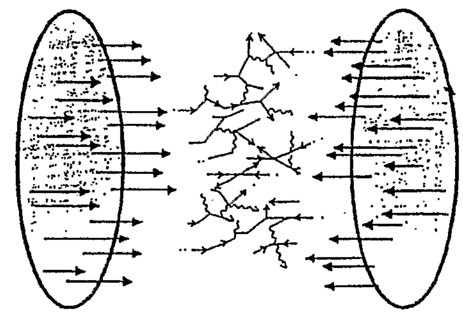

Relativistic transport

$p^\mu \partial_\mu F_a(r,p) = I_a(r,$

$(a = g, q, \bar{q})$

Geiger & Kapusta (

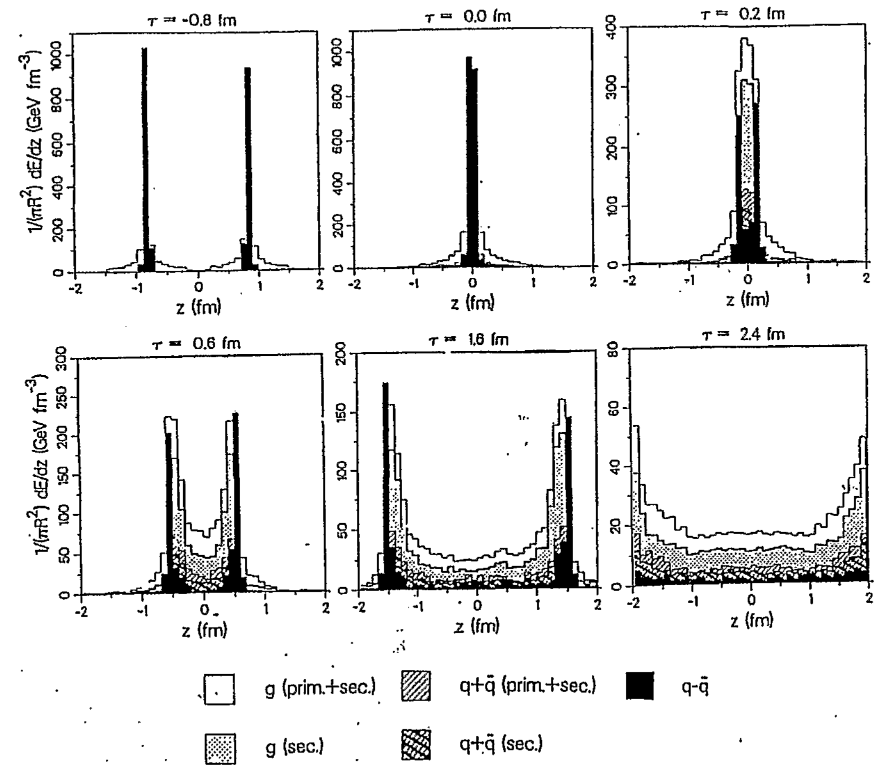

Energy density (z) in Au+Au (b=0) $s^{1/2}$ = 200 A GeV

Mean Free Path in Hot Plasma

local thermal equilibrium $\leftrightarrow$ $\lambda_{q,g} \ll$ system size
(hydro. assumption) $\qquad\qquad\qquad\qquad \sim 10\,fm$

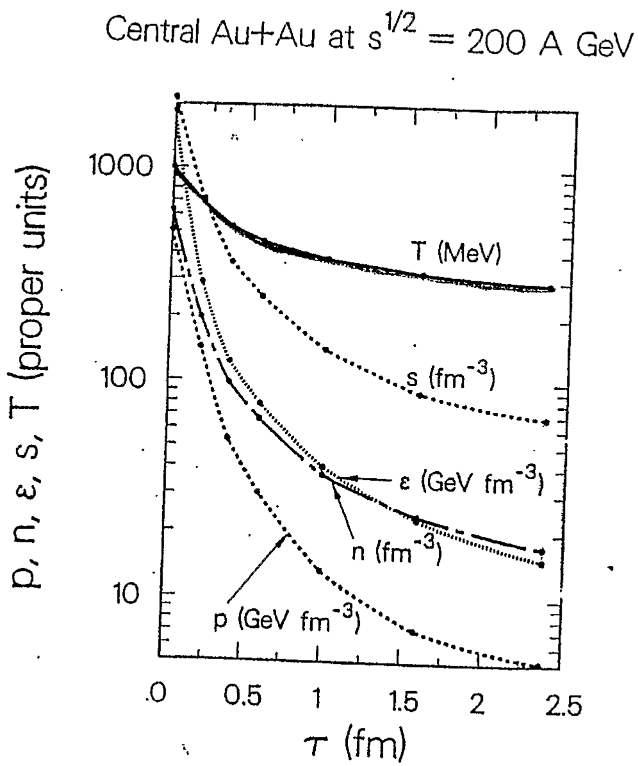

Geiger & Kapusta
PRD ('93)

- **Rough estimate**

(i) q-q cross section

$$\sigma_{qq} \simeq \sigma_{pp}/9 \sim 45\,mb/9 = \underline{5\,mb = 0.5\,fm^2}$$

(ii) quark number density

$$n_q \sim \frac{\varepsilon_q}{\langle p \rangle} \underset{\substack{\uparrow \\ T=200\,MeV \\ N_f=3}}{\sim} \frac{3\,GeV/fm^3 \times \left(\frac{36}{47.5}\right)}{3 \times 200\,MeV} = \underline{3.8/fm^3}$$

(iii) mean free path

$$\underline{\lambda_q} = [\sigma_{qq} n_q]^{-1} = [0.5 \times 3.8]^{-1} fm = \boxed{0.5\,fm}$$

- **From damping rate**

$$\left\{ \begin{array}{l} \underline{\lambda_g} \sim \gamma_{L,T}^{-1} = [3.32\,\alpha_s T]^{-1} = \begin{cases} \underline{0.86\,fm} & T = 200\,MeV \\ 0.6\,fm & T = 400\,MeV \end{cases} \\ \underline{\lambda_q} \sim \gamma_q^{-1} = [1.9\,\alpha_s T]^{-1} = \begin{cases} \underline{1.5\,fm} & T = 200\,MeV \\ 1.05\,fm & T = 400\,MeV \end{cases} \end{array} \right.$$

$$\uparrow$$

$\alpha_s(2\pi T) = 0.35 \quad (T = 200\,MeV)$
$\qquad\quad\;\; = 0.25 \quad (T = 400\,MeV)$

Scaling hydrodynamics

- Assumption : perfect fluid
  (local thermal equilibrium, no viscosity)

$\Downarrow$

$$\begin{cases} \partial_\mu T^{\mu\nu}(x) = 0 & : \text{energy-mom. cons.} \\ \partial_\mu j_B^\mu(x) = 0 & : \text{baryon \# cons.} \end{cases}$$

where $T^{\mu\nu}(x) = -P(x) g^{\mu\nu} + (\varepsilon(x) + P(x))\, u^\mu(x) u^\nu(x)$

$j_B^\mu(x) = n_B(x)\, u^\mu(x)$

with $u^\mu(x) = \gamma(x)\,(1, \vec{v}(x)) = \dfrac{1}{\sqrt{1-v^2(x)}}\,(1, \vec{v}(x))$

$\uparrow$ local fluid velocity

(i) cons. of entropy $\quad \partial_\mu (s(x) u^\mu(x)) = 0$

(ii) cons. of baryon # $\quad \partial_\mu (n_B(x) u^\mu(x)) = 0$

(iii) flow eq. $\quad (-g^{\mu\nu} + u^\mu u^\nu)\, \partial_\mu P(x) + (\varepsilon + P)\, u^\mu \partial_\mu u^\nu = 0$

- 1-dimensional scaling solution

$\tau = \sqrt{t^2 - z^2}$

$u^\mu(x) \equiv (\cosh\eta(x), 0, 0, \sinh\eta(x)) \leftarrow u^\mu u_\mu = 1$

and

find a scaling solution

$s = s(\tau),\ n_B = n_B(\tau) \quad \leftarrow$ indep. of η

- solution

(i) + (ii) $\longrightarrow \eta(x) = y \qquad$ with $y = \frac{1}{2}\ln\left(\frac{t+z}{t-z}\right)$

$$\begin{cases} \text{(i)} \longrightarrow \tau \dfrac{ds}{d\tau} + s = 0 \\ \text{(ii)} \longrightarrow \tau \dfrac{dn_B}{d\tau} + n_B = 0 \end{cases}$$

(iii) $\longrightarrow$ trivially satisfied

$\Downarrow$

$$\boxed{\eta = \frac{1}{2}\ln\left(\frac{t+z}{t-z}\right), \quad s = \frac{s_0 \tau_0}{\tau}, \quad n_B = \frac{n_B^0 \tau_0}{\tau}}$$

For ideal gas : $s \sim T^3,\ \varepsilon \sim T^4$

$\Downarrow$

$$\boxed{T = T_0 \left(\frac{\tau_0}{\tau}\right)^{1/3}, \quad \varepsilon = \varepsilon_0 \left(\frac{\tau_0}{\tau}\right)^{4/3}}$$

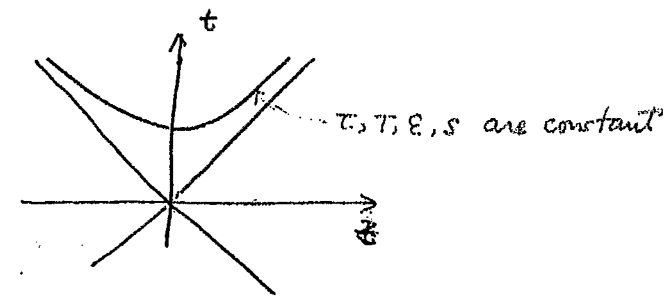

[redacted]

- mixed phase

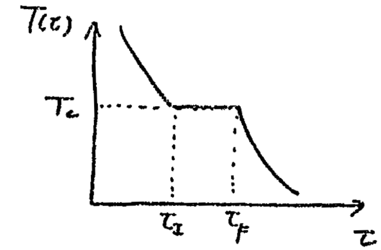

$$[f S_H + (1-f) S_Q]\tau = S_0 \tau_0 \qquad \text{entropy cons. } S\tau = \text{const.}$$

$$\left.\begin{array}{l} \tau = \tau_I : f = 0 \\ \tau = \tau_F : f = 1 \end{array}\right\} \Rightarrow S_Q \tau_I = S_H \tau_F$$

$$\downarrow$$

$$\boxed{\frac{\tau_F}{\tau_I} = \frac{S_Q}{S_H} \sim O(10)}$$

- estimate of τ_I

$$T(\tau) = T_0 \left(\tau / \tau_0 \right)^{-1/3}$$

$$\downarrow$$

$$\underline{\tau_I} = \tau_0 \left(T_0 / T_c \right)^3 \simeq 1\,\text{fm} \times \left(\frac{300\,\text{MeV}}{150\,\text{MeV}} \right)^3 = \underline{8\,\text{fm}}$$

sensitive
to τ_0 and T_0
(initial condition)

Estimate of the energy density (Bjorken)

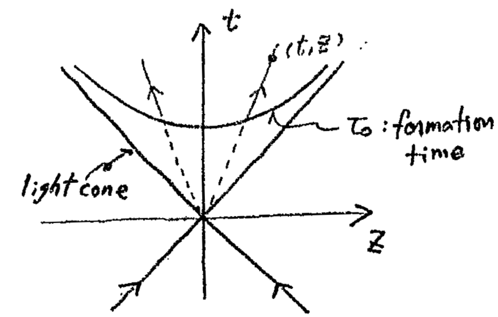

Consider high-energy p-p (p-$\bar{p}$) head on collision

55

- produced hadron mom.

$$q^\mu = (E, q_L, \vec{q}_T), \quad E^2 - q_L^2 = m^2 + q_T^2 \equiv \underbrace{m_T^2}_{\text{transverse mass}}$$

$$\Rightarrow \boxed{\begin{cases} E = m_T \cosh y \\ q_L = m_T \sinh y \end{cases}} \quad \text{with} \quad \begin{array}{l} y \text{ (rapidity)} \\ = \frac{1}{2} \ln \left(\frac{E + q_L}{E - q_L} \right) \\ = \frac{1}{2} \ln \left(\frac{1 + v_L}{1 - v_L} \right) \end{array}$$

- free streaming after freezeout

$$\begin{cases} \tau = \sqrt{t^2 - z^2} \\ y = \frac{1}{2} \ln \left(\frac{1 + v_L}{1 - v_L} \right) \simeq \frac{1}{2} \ln \left(\frac{t + z}{t - z} \right) \end{cases}$$

$$\Downarrow$$

$$\boxed{\begin{cases} t = \tau \cosh y \\ z = \tau \sinh y \end{cases}}$$

- number of particles in the rapidity interval $y \sim y+\Delta y$

$$\Delta N = \left(\frac{dN}{dy}\right)\Delta y \quad \leftarrow \text{measurable}$$

- Internal (or "thermal") energy in the interval

$\leftrightarrow$ transverse mass $\langle m_T \rangle$

$\uparrow$ average m_T per particle in $y \sim y+\Delta y$

$$\Delta E = \langle m_T \rangle \frac{dN}{dy}\Delta y$$

- Volume at $\tau = \tau_0$

$$\Delta V = (\pi R^2)\underbrace{\Delta z}_{z=\tau \sinh y} \simeq \pi R^2 \tau_0 \Delta y$$

- Energy density at $\tau = \tau_0$

$$\boxed{\varepsilon_0 = \frac{\Delta E}{\Delta V} = \frac{\langle m_T \rangle}{\tau_0 \pi R^2}\frac{dN}{dy}}$$

p-p (p-$\bar{\text{p}}$) collision $\longrightarrow$ A-A collision

$E_{CM} = 100\,\text{GeV}$

$\frac{dN}{dy} \simeq 6$

$R \simeq 0.8\,\text{fm}$, $\langle m_T \rangle = 0.4\,\text{GeV}$

$\tau_0 \simeq 1\,\text{fm}$

$\Downarrow$

$\varepsilon_0 \simeq 1\,\text{GeV}/\text{fm}^3$

$E_{CM} = 100\,\text{GeV}/A$

$\left(\frac{dN}{dy}\right)_{UU} \cong A\left(\frac{dN}{dy}\right)_{pp}$

$\Downarrow$

$\boxed{\varepsilon_0 \simeq 3.3\,\text{GeV}/\text{fm}^3}$

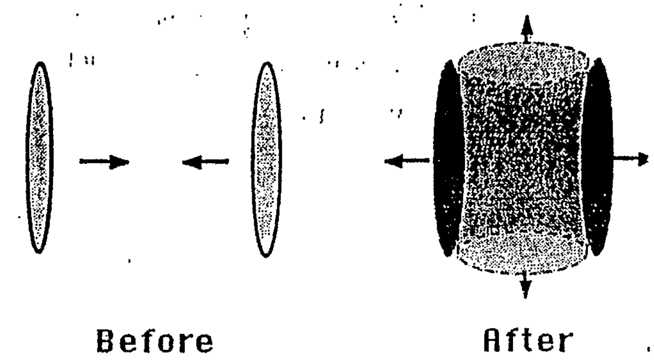

Figure 2.3.

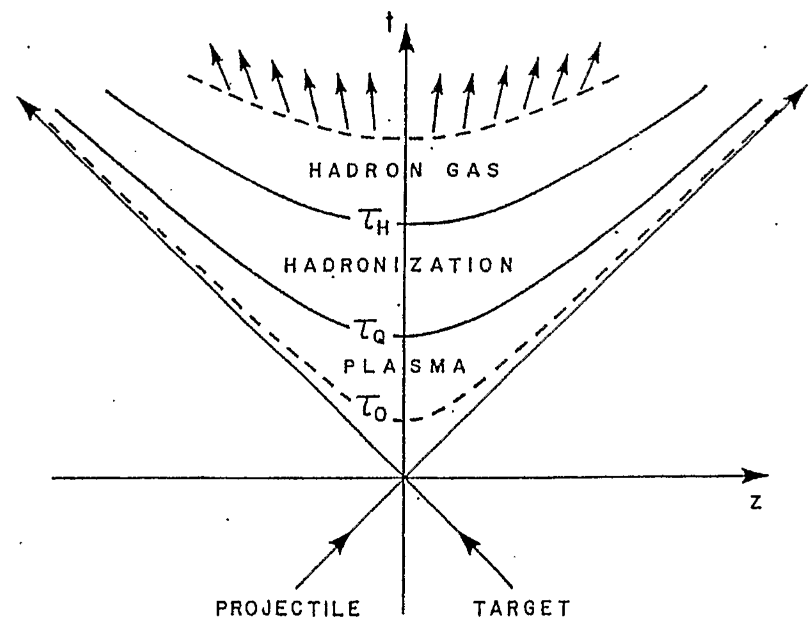

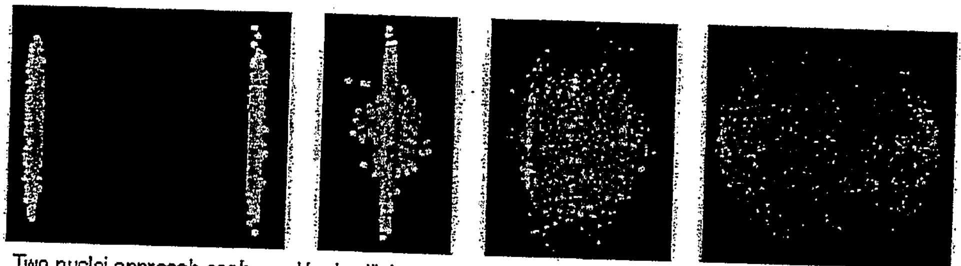

Two nuclei approach each other, relativistically contracted to thin pancakes

Hard collisions dominate first instants of collision

Produced particles reinteract at hard and soft scales

Final state particles freeze-out and stream towards the detectors...

Peter Steinberg/BNL

PHOBOS

Relativistic Hydrodynamics in (1+3)-dim.

$\partial_\mu T^{\mu\nu}=0, \quad \partial_\mu j^\mu_B=0$

Time evolution of energy density

Au+Au 130 GeV, $b=7.5$ fm

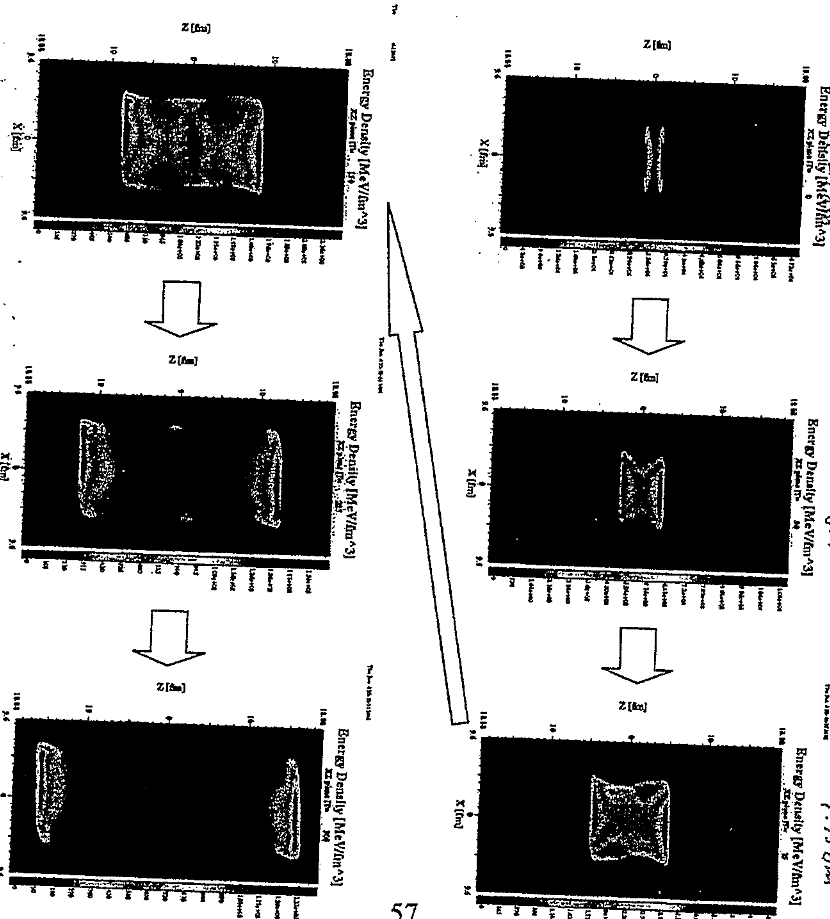

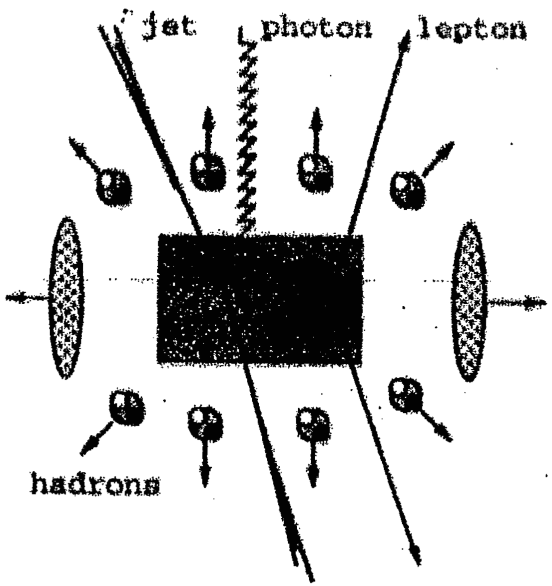

Detect everything!

- lepton pairs, photon
- pion, kaon
- strange baryons
- jet
- ⋮

Expectations

$\varepsilon_{RHIC} \simeq (2\text{-}5)\,GeV/fm^3$

$\varepsilon_{LHC} \simeq (4\text{-}9)\,GeV/fm^3$

$> \varepsilon_c \equiv (1\text{-}3)\,GeV/fm^3$

Mean free path

$\lambda_g \lesssim 1\,fm < 10\,fm$

$\longrightarrow$ local equilibrium

Chemical Freezeout in A–A Collisions

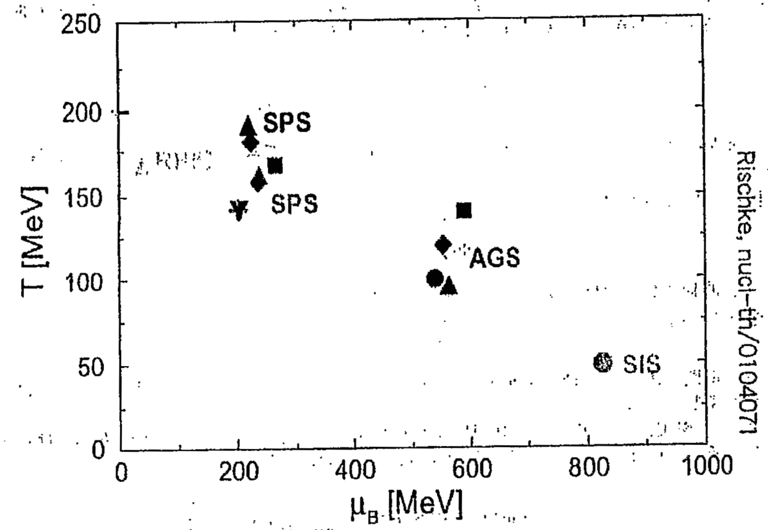

Au+Au, 2.3 AGeV	● [1] Cleymans et al., PRC 59 (99) 1663
	■ [2] Gorenstein et al., JPG 24 (98) 1777
	◆ [3] Becattini et al., hep-ph/0002267
Au+Au, 5 AGeV	▲ [4] Kabana et al., hep-ph/0010247
	● [5] Cleymans et al., PLB 388 (96) 5
	◆ [6] Becattini, JPG 23 (97) 1933
S+S, 20 AGeV	▼ [7] Sollfrank, EPJC 9 (99) 159
	▲ [8] Panagiotou et al., PRC 53 (96) 1353
	■ [9] Braun-Munzinger et al., PLB 465 (99) 15
Pb+Pb, 17 AGeV	◆ [3]
	▲ [4]
	+ [10] Letessier et al., IJMPE 9 (00) 107
Au+Au, 130 AGeV	▲ [4]
	◆ [11] Becattini et al., ZPC 74 (97) 319

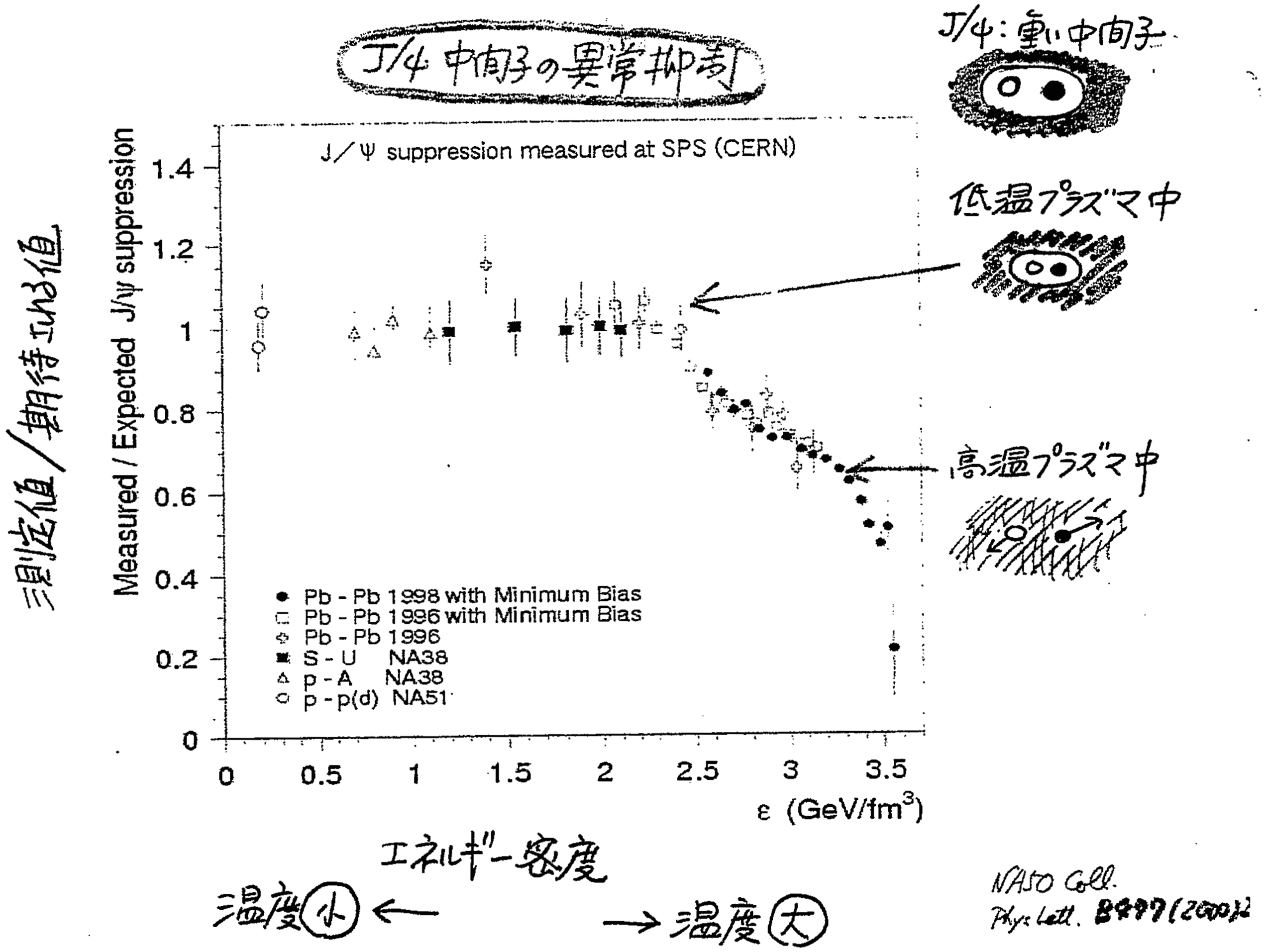

Finite Baryon Density

Neutron Star Structure

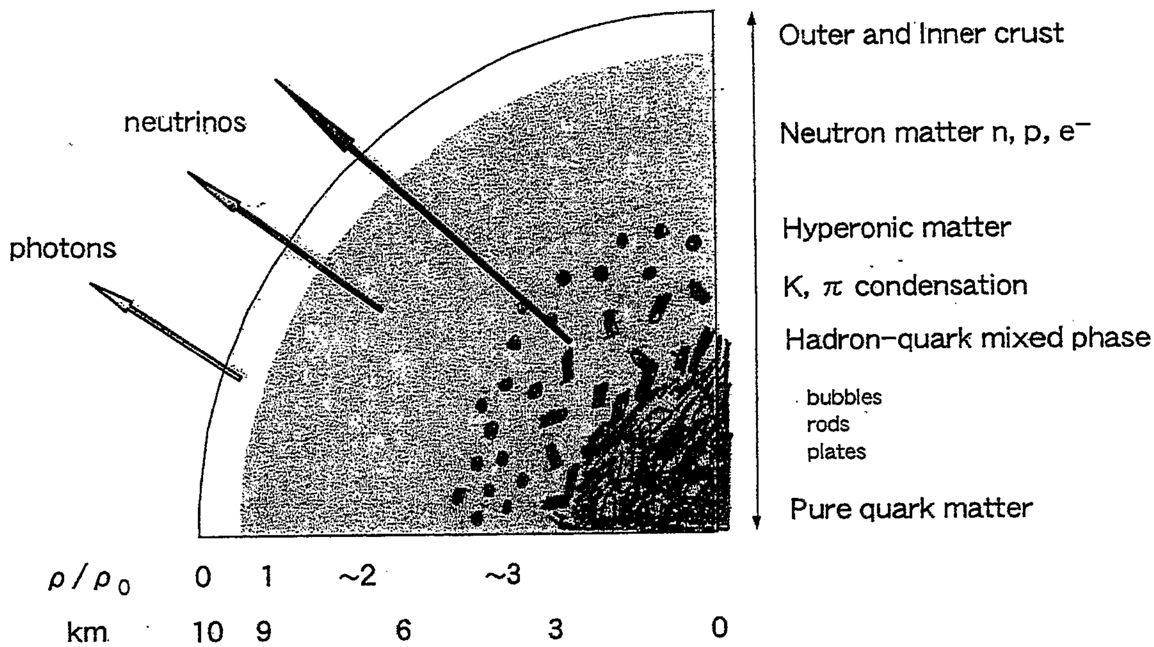

● TOV equation + EOS ($E(\rho)$ or $P(\rho)$) ⇨ M, R, $\rho(r)$

Standard neutron star matter : n, p, e^- with $n \rightleftarrows p + e^-$

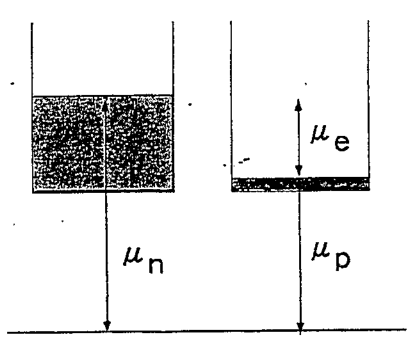

Pandharipande et al., astro-ph/9905177 ('99)

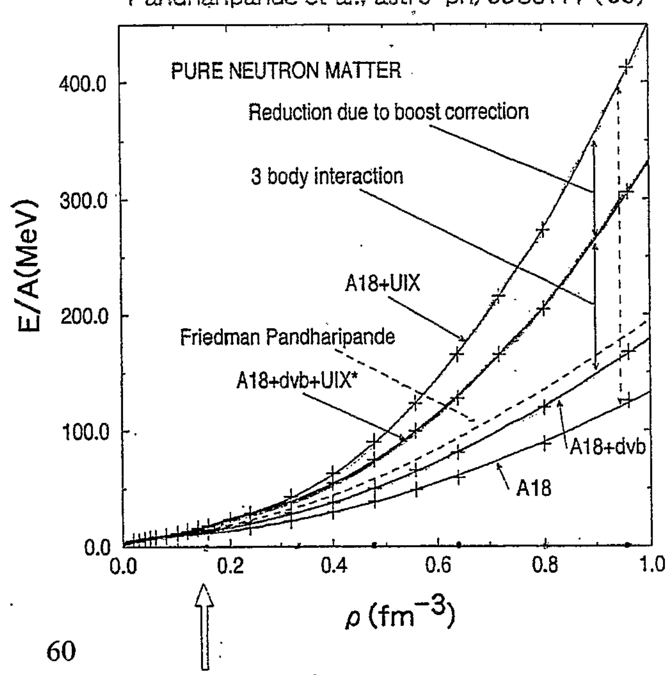

$\rho_0 = 0.16$ fm^{-3} (Dilute !)

Recent progress

- modern N-N int. (> 1994)
  (4301 N-N data fittied with χ^2/dof ~1)
- relativistic corrections
- N-N-N interactions
- precise many body techniques
  (variational method, BHF+PPHH, DBHF)

Hyperonic matter : n, p, Σ^-, Λ, e^- with $\Sigma^- \rightleftarrows n + e^-$, $\Lambda \rightleftarrows n$

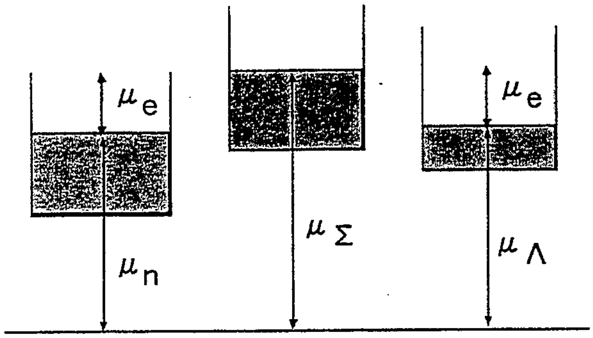

Glendenning, nucl-th/0009082 ('00)

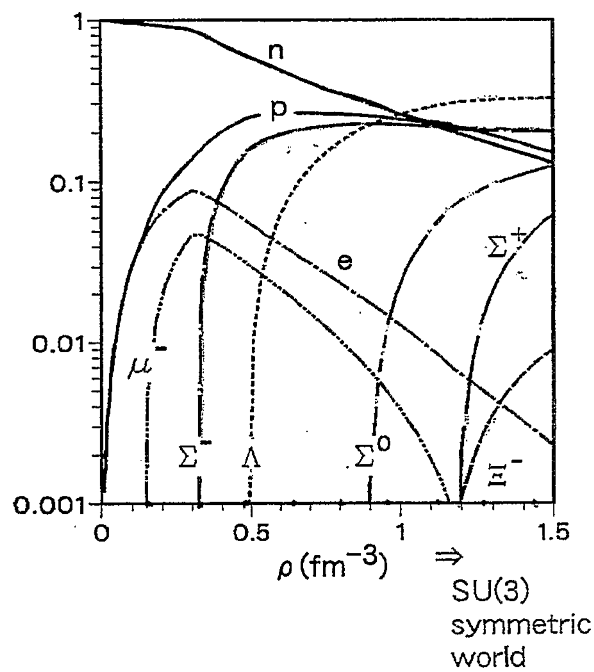

Remarks

- Hyperon mixing may start at (2–3) ρ_0
- Y–N int. not well understood
  (need more hyper-nucleus data : JHF !)

Kaon condensation : n, p, K^- with $n \rightleftarrows p + K^-$

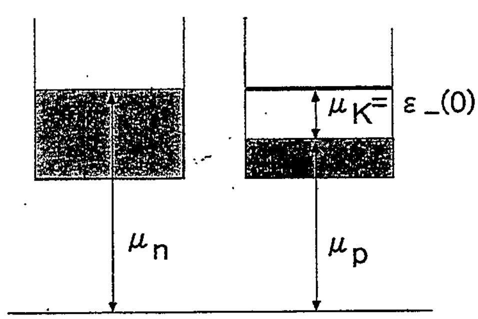

Yasuhira, nucl-th/0010030 ('00)

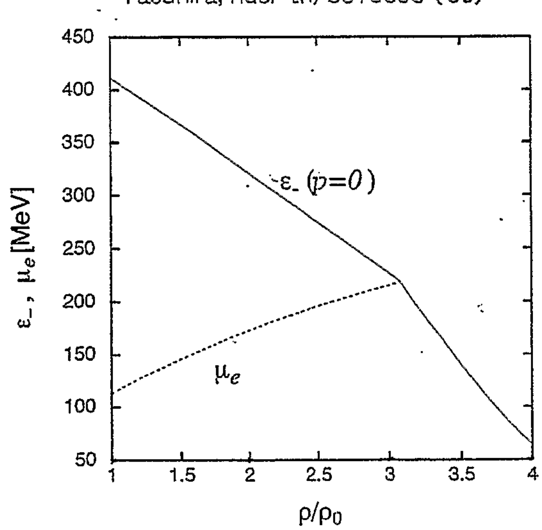

Remarks

- Condensation may start at (3–5) ρ_0
- $\varepsilon_-(0)$ (< m_K) not well determined

Kaon condensed Stars

Fujii, Maruyama, Muto & Tatsumi ('95)

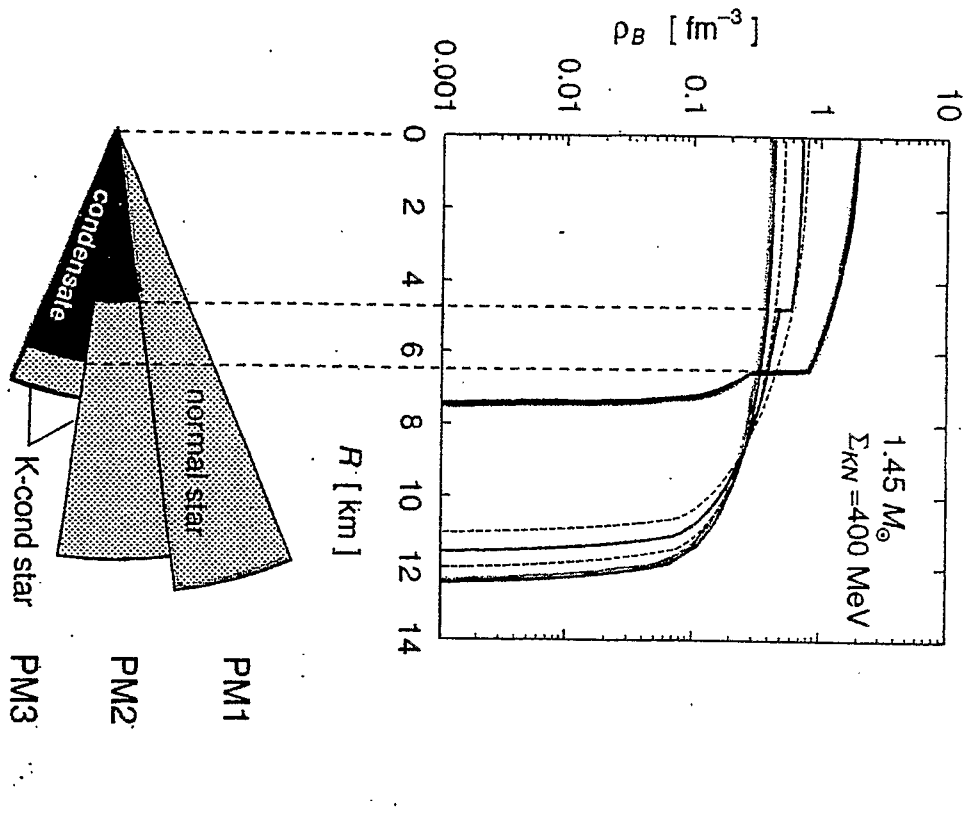

Quark matter : u, d, s, e^- with $d \rightleftarrows u + e^-, d \rightleftarrows u + e^-, s \rightleftarrows d$

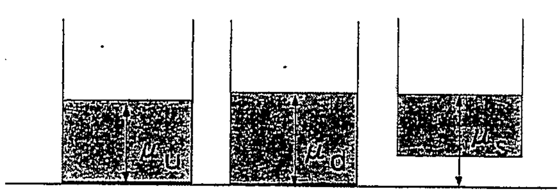

Heiselberg and Pandharipande,
astro-ph/0003276 ('00)

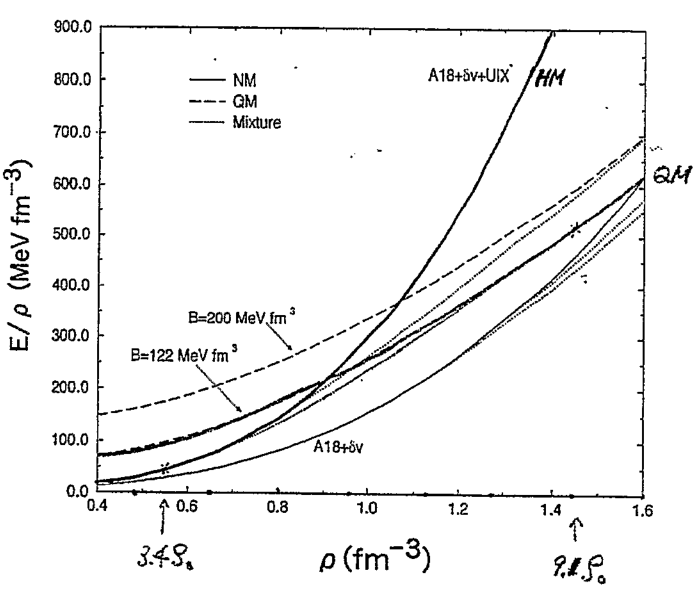

Remarks

- Mixed phase may start even at $\sim 3\ \rho_0$
- sensitive to hadronic EOS

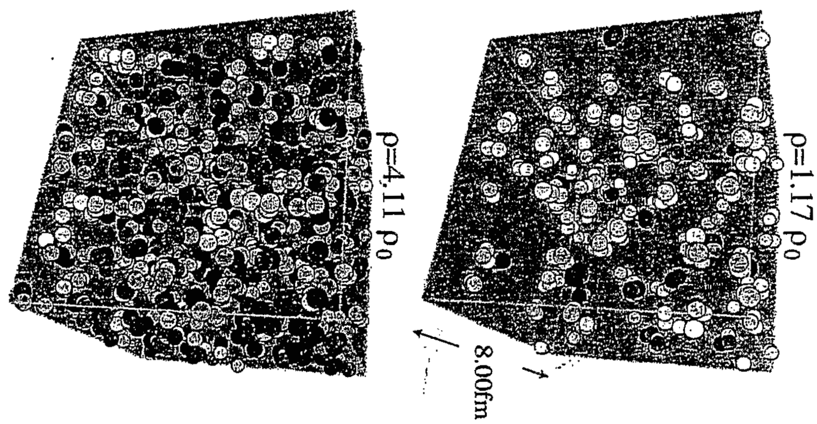

Color Molecular Dynamics simulation
Maruyama & Hatsuda,
nucl-th/9908021
Phys. Rev. C61, 062201 (2000)

M−R relation

Thorsett & Chakrabarty, APJ ('99)

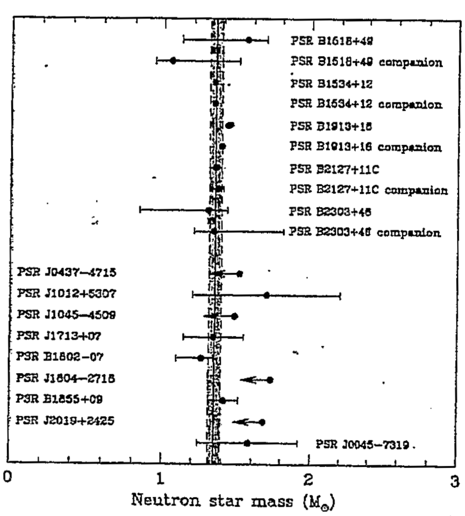

$M = 1.35 \pm 0.04\, M_\odot$

Pethick et al., astr-ph/9905177 ('99)

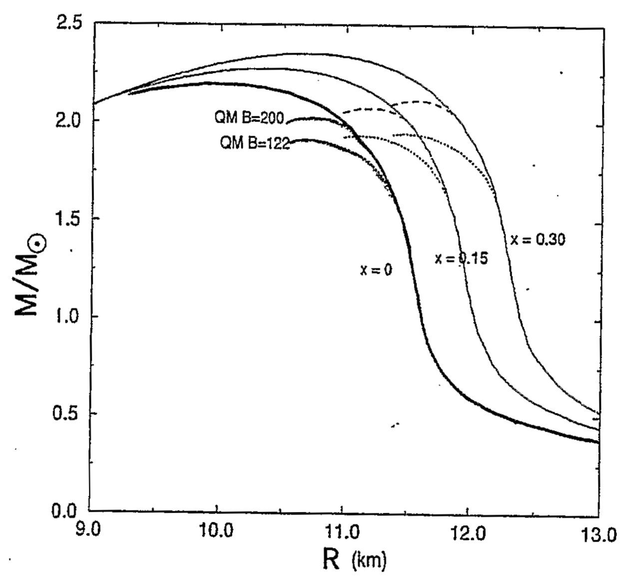

● Phase change
⇒ low $E(\rho)$ ⇒ soft EOS
⇒ small M & R, large ρ_c

nucleon superfluid

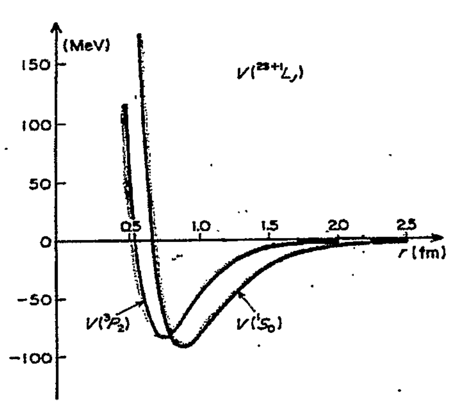

Takatsuka & Tamagaki, PTP Suppl. ('93)

quark superfluid

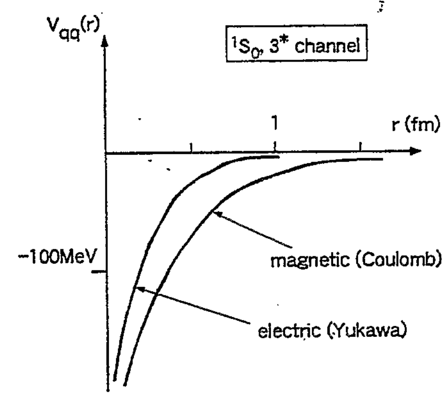

review:
Rajagopal & Wilczek, hep-ph/0011333 ('00)

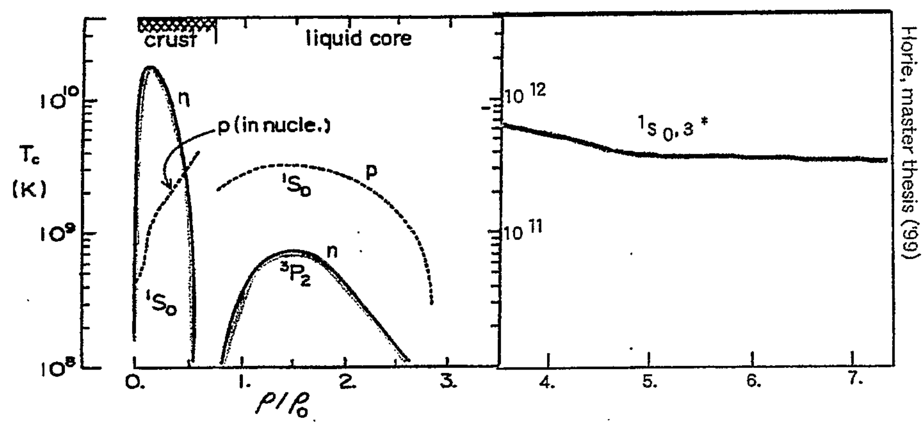

Cooling of N★ by ν-emission

- URCA process "perfect sink of money"

$$n \to p + e^- + \bar{\nu}_e$$
$$e^- + p \to n + \nu_e$$

kinematically forbidden at.
(charge neutraity
& chemical equilibri

- modified URCA process

luminocity

$$L_\nu^{\overline{URCA}} \simeq 5.3 \times 10^{39}\ \mathrm{erg \cdot s^{-1}} \times \left(\frac{M}{M_\odot}\right)\left(\frac{\rho_0}{\rho}\right)^{1/3}\left(\frac{T}{10^9 K}\right)^8$$

↕

(emissivity

$$\varepsilon_\nu^{\overline{URCA}} \simeq 7.4 \times 10^{20}\ \mathrm{erg \cdot cm^{-3} \cdot s^{-1}} \left(\frac{\rho}{\rho_0}\right)^{2/3} T_9$$

- pion condensation

$$L_\nu^\pi \simeq 1.5 \times 10^{46}\ \mathrm{erg \cdot s^{-1}}\ \sin^2\Theta \times \left(\frac{M}{M_\odot}\right)\left(\frac{\rho_0}{\rho}\right) T_9^6$$

$\langle\pi^-\rangle = \sin\Theta$

- quark matter

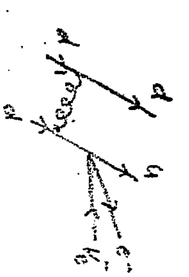

$$L_\nu^Q \simeq 1.3 \times 10^{44}\ \mathrm{erg \cdot s^{-1}} \times \left(\frac{M}{M_\odot}\right) T_9^6$$

$\alpha_s = 0.1$

Neutrino cooling

- direct URCA ($x_p > 0.14$)

  $n \to p + e^- + \bar{\nu}_e$

- modified URCA

  $n + n \to n + p + e^- + \bar{\nu}_e$

- hyperon URCA

  $\Lambda \to p + e^- + \bar{\nu}_e$

- π, K cond.

  $\langle \pi^- \rangle + n \to n + p + e^- + \bar{\nu}_e$

  $\langle K^- \rangle + n \to n + p + e^- + \bar{\nu}_e$

- quark

  $d + d \to d + u + e^- + \bar{\nu}_e$

all quenched by "super" : $e^{-\Delta/T}$

See, Page et al., PRL85 ('00)

A4: mURCA with super
B4/C4: dURCA with super
D4: hyperon dURCA without super

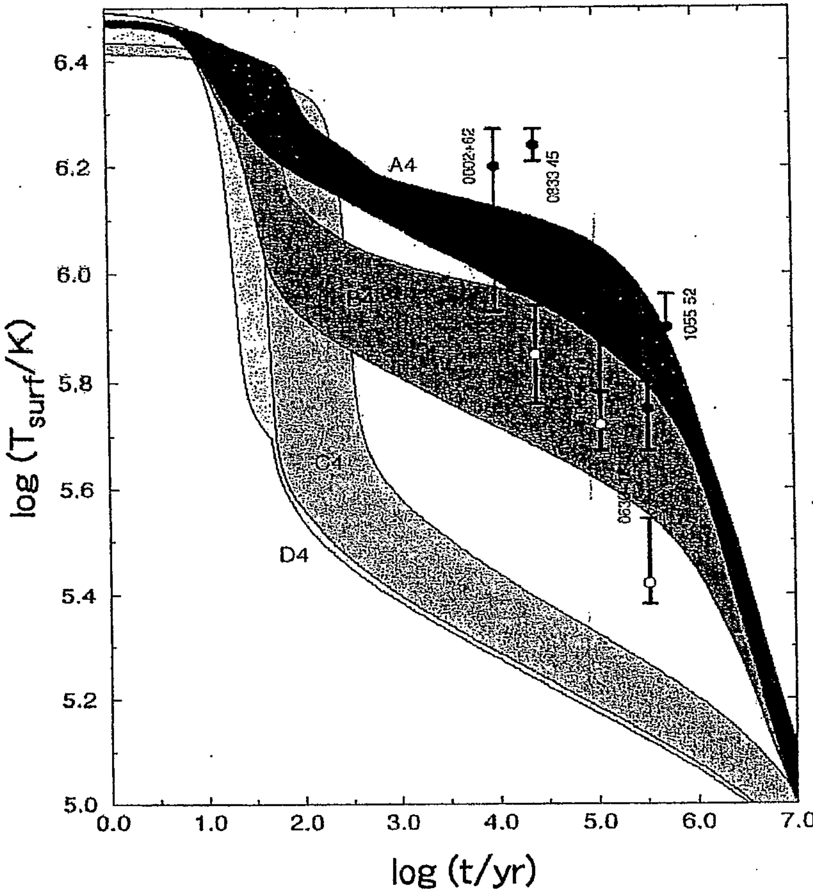

Schaab, Weber & Weigel, ('98)

- sensitive to EOS
- hard to nail down the key process

Drake et al,
astro-ph/0205159

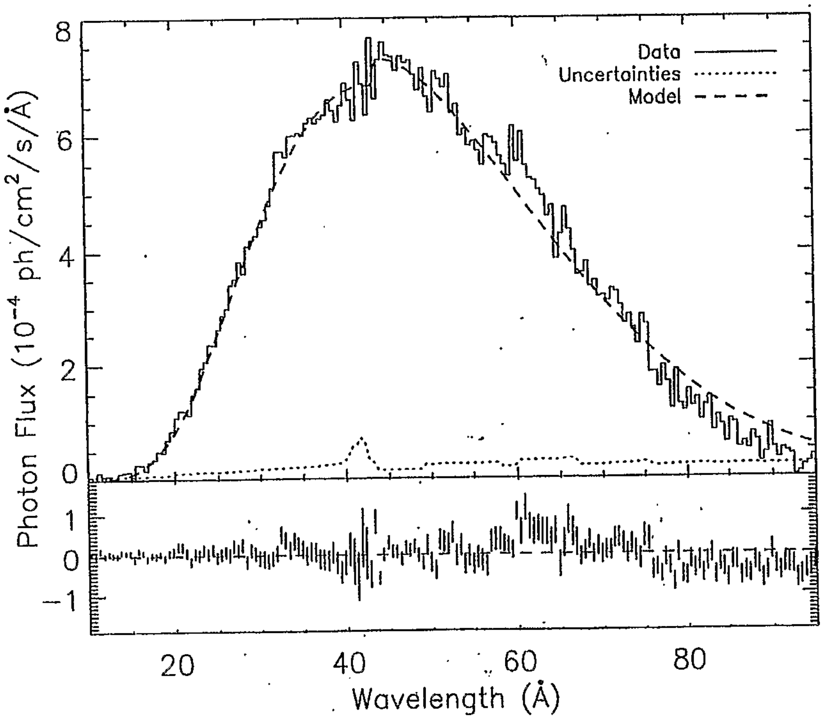

Fig. 1.— The combined positive and negative order spectra of RX J1856.5−3754 binned at 0.5 Å intervals shown with the best fit blackbody model with parameters corresponding to method (2) in §4 and residuals (observations−model). The deviations from this model are consistent with Poisson statistics after allowing for calibration uncertainties at the C K-edge and over broader wavelength intervals. The apparent edge at 60 Å results primarily from one of the HRC-S plate gap boundaries and small residual QE differences between positive and relative negative order outer plates.

Modern Physics Letters A, Vol. 2, No. 11 (1987) 805–809

STRANGE STARS AND THE NEUTRINO BURST FROM SUPERNOVA 1987a

T. HATSUDA,
National Laboratory for High Energy Physics (KEK), Ibaraki, 305, Japan

Received 3 August 1987

Possibility of strange star formation in the recently discovered LMC supernova is examined. If the proto-neutron star first formed is converted into a strange star about 1 sec after the core bounce, a large energy release with $E_{tot} \sim 10^{53}$ erg having QCD origin occurs. The high energy $\bar{\nu}$-events of long duration observed by Kamiokande II and IMB detectors can be naturally understood by the formation of the hot strange star.

Observations of the supernova explosions and their remnants give us rich information about our understanding of the fate of stars, the nature of the gravitational collapse, properties of high density matter, and weakly interacting particles such as neutrinos, axions, majorons and so on. Recently, the Kamiokande II Collaboration[1] and the IMB Collaboration[2] have reported a neutrino burst prior to the optical observations of supernova (SN1987a) in the large Magellanic cloud (LMC).[3]

A characteristic feature of the Kamiokande II data is that it has a bunch structure; the first 6 events ($0 \sim 0.686$ sec), the second 3 events ($1.541 \sim 1.915$ sec) with rather high mean energy and the third scattered 3 events ($9.219 \sim 12.439$ sec). If one excludes the first two events, the angular distribution is consistent with isotropy; we can then identify them as $\bar{\nu}_e$-events which are detected through the inverse β-process ($\bar{\nu}_e p \to n e^+$) in the water. The mean energies of the observed events, with an assumption that all of them are caused by $\bar{\nu}_e p \to n e^+$ process, become 13.4 MeV (1st bunch), 27.2 MeV (2nd bunch) and 12.0 MeV (3rd bunch).[4] On the other hand, the IMB data shows no such bunch structures but consists of relatively high energy events (20–40 MeV) which span an interval of 6 sec. The overall features of these data seem to be consistent with the standard explosion and cooling theory of the type II supernova.[6,7] However, there are some controversial points for the late events (the ones after 1 sec in the Kamiokande II data[6a] and all the IMB data,[8] or at least the ones after 5 sec in the Kamiokande II data[6b]); In fact, the standard cooling of the proto-neutron star gives too small mean energy and small number of events[9] to explain the late events, which may suggest that the core temperature is higher than expected or other non-standard mechanism of neutrino emission is present.[6]

In this letter, we will not stick to the bunch structure but take the late and relatively high energy events seriously and suggest a possibility of the formation of a strange star.

New ideas

- **Strange** quark star (u,d,s) — review: Madsen, hep-ph/9809032 ('98)
- **Ferromagnetic** quark star — Tatsumi, Phys. Lett. B ('00)
- **Crystal** structure in superconducting quark matter — Alford et al., hep-ph/0009357 ('00)
- Coherent $\Lambda-\Sigma$ mixing in hyperonic matter — Akaishi et al., PRL 84 ('00)
- **Delayed collapse** to BH — Brown & Bethe, ApJ ('94); Yasuhira & Tatsumi, nucl-th/0009090 ('00)

Things to be done

i. n,p : NNN-force ⇦ light nuclei ⇦ QMC method — Wiringa et al., nucl-th/0002022 ('00)

ii. hyperon : YN & YY forces ⇦ hyper nuclei ⇦ Japan Hadron Facilities

iii. hadron → quark ⇦ lattice QCD ⇦ New method ? — Engels et al., et al., hep-lat/9903030 ('99)

Summary

Many-body problems of quarks & gluons based on QCD

Theoretical developments (past 5 years)

high T	high ρ
▸ improved perturbation theory	▸ high precision hadronic matter calculations
▸ extensive lattice QCD simulations	▸ new ideas in hadronic/quark matter

Experimental/Observational developments (past 5 years)

- SPS@CERN found "evidences" of high T matter
- RHIC@BNL started to operate [redacted]
- NNN and YN interactions are start to be constrained
- Neutron star properties: mass, T_{surf}, B etc

Expected progresses in coming 5 years

- Quark-gluon plasma will be found and studied at RHIC
- New era in lattice QCD simulations (from 10% to 1 %)
- Determination of YN and YY interactions at JHF

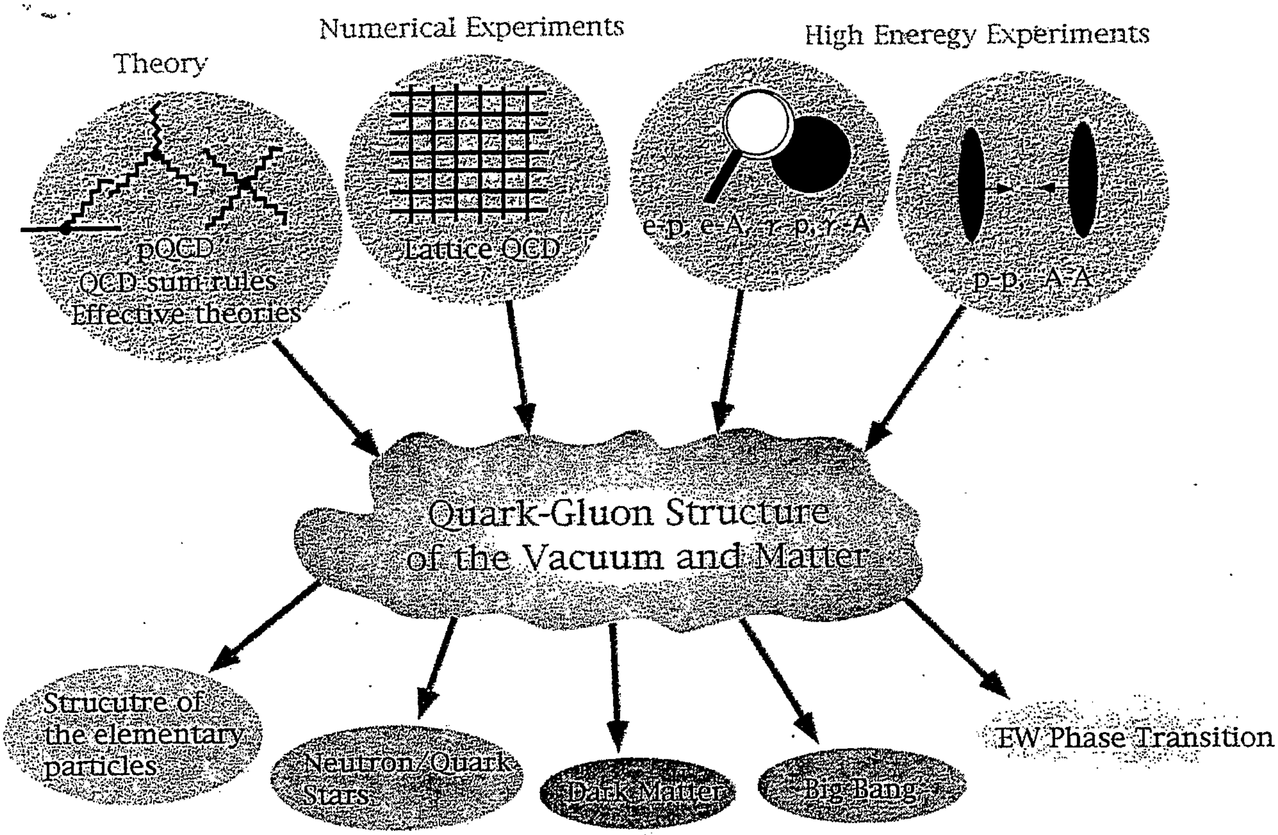
Theory
Numerical Experiments
High Energy Experiments
pQCD
QCD sum rules
Effective theories
Lattice QCD
p-p, A-A
Quark-Gluon Structure
of the Vacuum and Matter
Strucutre of
the elementary
particles
Neutron/Quark
Stars
Dark Matter
Big Bang
EW Phase Transition

Properties of Hadrons in Nonperturbative QCD

Makoto Oka
Department of Physics, Tokyo Institute of Technology,
Meguro, Tokyo 152-8551
oka@th.phys.titech.ac.jp

Abstract

Main aims of the hadron physics are (1) to understand hadron spectrum, structure and interactions in the language of the quantum chromodynamics (QCD), the fundamental theory of the strong interaction, and (2) to explore rich phase structure of multi-hadron systems and hadronic matter. The first subject is quite old, while the second is relatively new and studied heavily recently as hot and/or dense hadronic matter can be produced in the heavy ion laboratories.

The reason why the QCD phase structure is complicated is that the QCD vacuum is highly nontrivial. Although the QCD lagrangian looks simple and symmetric, most symmetries of QCD are explicitly realized in the ground state. Accordingly the QCD vacuum has quark condensates, gluon condensate, and nontrivial topological objects.

While the QCD vacuum structure is most intriguing object, what we observe in laboratories are hadrons, the low-energy excited states upon the complicated QCD vacuum. Thus the properties of the hadrons are what we need to study in the language of QCD. This is what I concentrate in these lectures.

In the first lecture, I overview properties of QCD and hadrons. I especially emphasize the symmetries of QCD and their realization in hadron spectra. In the second and third lectures, I concentrate on two topics. One is chiral symmetry of baryon and baryon resonances, where I discuss classification of baryons in linear representations of chiral symmetry and its consequences. In the third lecture, I will turn to the strong interaction corrections to the nonleptonic weak interactions of hyperons. I will discuss how the QCD corrections are relevant to observables of hyperon decays. I also discuss a new type of nonleptonic weak decay observed in the decay of hypernuclei.

Properties of Hadrons in Nonperturbative QCD

Makoto Oka
Tokyo Institute of Technology

CONTENTS

QCD SU(3) color gauge field theory

$$\mathcal{L} = -\frac{1}{2}\mathrm{Tr}\{G^{\mu\nu}G_{\mu\nu}\} + \bar{q}(i\gamma\cdot D - M)q$$

$$G^{\mu\nu}(x) \equiv \partial^\mu A^\nu - \partial^\nu A^\mu + ig[A^\mu, A^\nu] \qquad A^\mu(x) \equiv \sum_{\alpha=1}^{8}\frac{\lambda^\alpha}{2}A^{\alpha\mu}$$

$$q(x) \equiv \begin{pmatrix} q_R(x) \\ q_B(x) \\ q_G(x) \end{pmatrix} \qquad D_\mu q(x) \equiv (\partial_\mu + igA_\mu)q(x)$$

Local gauge invariance $U(x) \in SU(3)_{color}$

$$q(x) \to q'(x) = U(x)q(x)$$

$$A_\mu(x) \to A'_\mu(x) = U(x)A_\mu(x)U^{-1}(x) + \frac{i}{g}\partial_\mu U(x)U^{-1}(x)$$

$$D_\mu q(x) \to U(x)D_\mu q(x)$$

Asymptotic Freedom and Color Confinement

$$\alpha_s(Q^2) = \frac{12\pi}{(33-2N_f)\ln\frac{Q^2}{\Lambda^2}} + \text{(higher order terms)}$$

$$\Lambda = \Lambda_{QCD} \approx 280\mathrm{MeV}$$

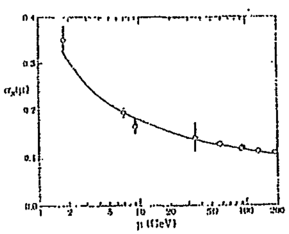

Large Q^2 (> 10 (GeV/c)^2)
weak interaction perturbative
deep inelastic lepton scattering
Bjorken scaling· Feyman parton picture

Small Q^2 (~ 1 (GeV/c)^2)
strong interaction nonperturbative
- *color confinement*
- *non-trivial vacuum structure*
- *complex hadron spectrum*

Color Confinement

quark - antiquark interaction at large distances

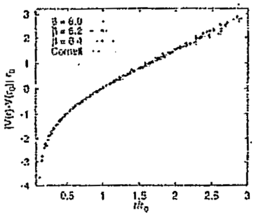

confining potential from Lattice QCD

no colored hadrons
no free quarks or gluons

Nontrivial Vacuum

quark condensates — break chiral symmetry

$\langle \bar{u}u \rangle \equiv \langle 0| : \bar{u}u : |0\rangle \approx \langle \bar{d}d \rangle \approx (-230\mathrm{MeV})^3 \qquad \langle \bar{s}s \rangle \approx 0.8 \langle \bar{u}u \rangle$

gluon condensate — breaks scale invariance

$\langle G^2 \rangle \equiv \langle 0| : \frac{\alpha_s}{\pi} G^{\alpha\mu\nu} G^{\alpha}_{\mu\nu} : |0\rangle \approx (330\mathrm{MeV})^4$

nontrivial topology — ex. instanton solutions

Hadrons as Soft Excited Modes

QCD vacuum = Ground state

Spontaneous Breaking of Chiral symmetry — $\langle 0|\bar{q}q|0\rangle \neq 0$ at $T = 0$
Anomalous $U_A(1)$ Breaking
Flavor Symmetry Breaking — $\langle 0|\bar{q}q|0\rangle = 0$ at $T > T_c$

$\Updownarrow$

Hadrons = Low energy excited states

Pseudoscalar Mesons: π, K, η, η'

Scalar Mesons: σ, κ, a_0, f_0

Baryons: N, Δ, N^*, Λ etc.

Nontrivial Topology

Instanton solution in Euclid QCD

$\int G_{\mu\nu} \tilde{G}_{\mu\nu} d^4x \neq 0$ — gluon condensate

Instanton couples to Fermion zero mode — 't Hooft — η'

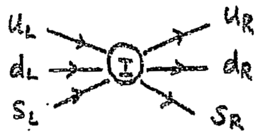

flavor singlet

$\mathcal{L}_{\mathrm{int}} \propto \det_{i,j}\{\bar{q}^i_R q^j_L\} + c.c.$ — breaks $U_A(1)$ symmetry

Kobayashi-Maskawa-'t Hooft interaction

Diversity of Hadron Spectrum

Heavy quark mesons — J/ψ ($c\bar{c}$), ... $b\bar{b}$, ...

Linear confinement + Coulomb Potential gluon exchange

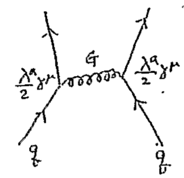

$U(r) = \sigma r - \frac{e}{r}$ — Cornell potential

$-e = -\frac{4}{3}\alpha_s$ meson
$-\frac{2}{3}\alpha_s$ baryon

Heavy quark potential from Lattice QCD
Wilson loop

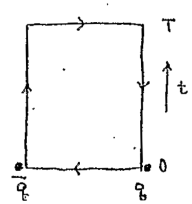

$\propto e^{-\sigma L T}$

Light mesons and baryons

pseudoscalar mesons	$\pi\ \eta\ \eta'$ ...	8+1 nonets
scalar mesons	$\sigma\ a_0\ f_0$ ...	
baryons	N, N*, ...	

Symmetries are not manifest !

- Color gauge symmetry ⇔ Quark confinement
  - ⇒ Regge trajectories
- Chiral symmetry ⇔ Quark condensate
  - ⇒ Light pseudoscalar mesons
- $U_A(1)$ symmetry ⇔ Anomaly
  - ⇒ Heavy η' meson, flavor mixing
- Flavor SU(3) symmetry ⇔ Quark mass
  - ⇒ Constituent quark model

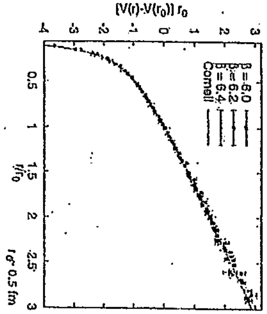
G.S. Bali / Physics Reports 343 (2001) 1–136

Fig. 4.2. The quenched Wilson action SU(3) potential, normalized to $V(r_0) = 0$.

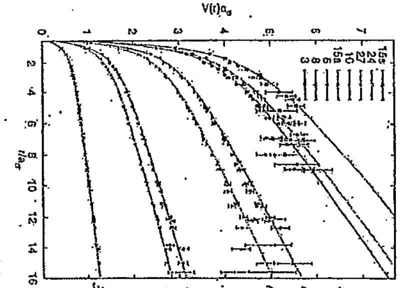
G.S. Bali / Physics Reports 343 (2001) 1–136

Fig. 5.7. Static potentials between sources in various representations of SU(3) in lattice units, $a_\sigma \approx 0.085$ fm.

Casimir scaling prop to $\langle -\sum_a T_1^a T_2^a \rangle$

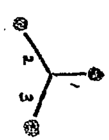
$L_{min} = \mathrm{Min}\,(L_1 + L_2 + L_3)$

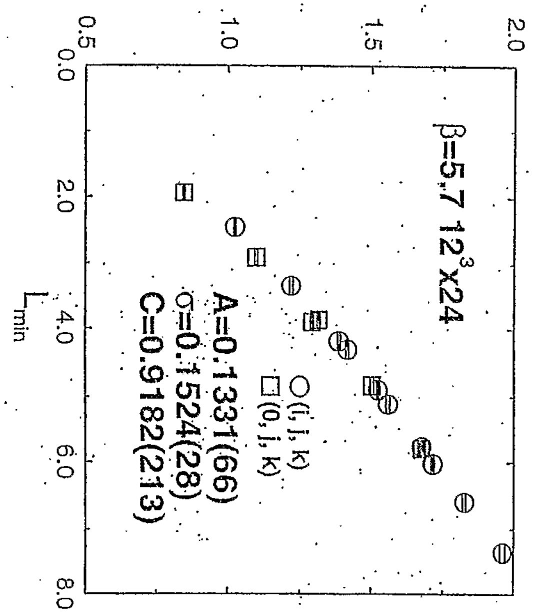
Three-Quark Potential in SU(3) Lattice QCD
T. T. Takahashi, H. Matsufuru, Y. Nemoto, and H.Suganuma
Phys.Rev.Lett. 86 (2001) 18-21

Meson spectrum

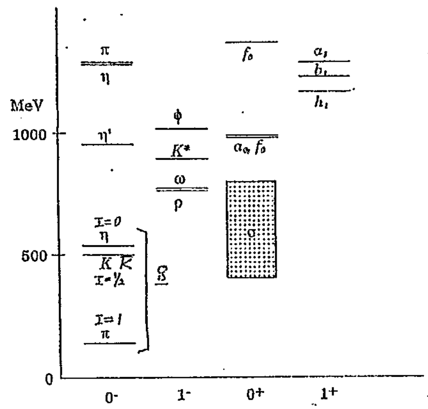

Light pseudoscalar mesons
flavor nonet 8 + 1 :
NG bosons

The η' meson is heavy:
$U_A(1)$ problem

The $\eta - \eta'$ meson mixing:
Flavor mixing

Chiral Symmetry of QCD

N_f flavor quarks

$$q(x) = q_R(x) + q_L(x) \qquad q_{\substack{R\\L}} \equiv \frac{1 \pm \gamma^5}{2} q$$

$SU(N_f)_R \times SU(N_f)_L$ transform: global symmetry

$$\begin{array}{cc} \Psi & \Psi \\ R & L \end{array}$$

$$\begin{cases} q_R \longrightarrow R\, q_R & \bar{q}_R \longrightarrow \bar{q}_R R^\dagger \\ q_L \longrightarrow L\, q_L & \bar{q}_L \longrightarrow \bar{q}_L L^\dagger \end{cases}$$

$$\left.\begin{array}{l} \bar{q}\gamma^\mu q = \bar{q}_R \gamma^\mu q_R + \bar{q}_L \gamma^\mu q_L \\ \bar{q}\gamma^\mu \gamma^5 q = \bar{q}_R \gamma^\mu q_R - \bar{q}_L \gamma^\mu q_L \end{array}\right) \text{ Chiral invariant} \quad \text{even}$$

$$\left.\begin{array}{l} \bar{q}q = \bar{q}_L q_R + \bar{q}_R q_L \\ \bar{q}\gamma^5 q = \bar{q}_L q_R - \bar{q}_R q_L \end{array}\right) \text{ Chiral non inv.} \quad \text{odd}$$

$$\mathcal{L}_{mass} = -m\,\bar{q}q \quad : \text{ chiral odd}$$

If $M=0$, then QCD is chiral invariant.

$$\mathcal{L} = -\frac{1}{2}\mathrm{Tr}\{G^{\mu\nu}G_{\mu\nu}\} + \bar{q}(i\gamma \cdot D - M)q \qquad M \equiv \begin{pmatrix} m_u & & \\ & m_d & \\ & & m_s \end{pmatrix}$$

$m_u, m_d \ll \Lambda_{QCD} \qquad SU(2)_R \times SU(2)_L$

$m_s \lesssim \Lambda_{QCD} \qquad SU(3)_R \times SU(3)_L$

Extended symmetry

$$\bar{q}Mq = \bar{q}_L M q_R + \bar{q}_R M^\dagger q_L \qquad (M^\dagger \neq M)$$

$$M \longrightarrow LMR^\dagger \quad \text{"extended"}$$

QCD mass term is invariant under Ext. chiral trans.

Noether Currents and Conserved Charges

$$J^{a\mu}_{\substack{L\\R}} \equiv \bar{q}_{\substack{L\\R}} \gamma^\mu T^a q_{\substack{L\\R}} \qquad T^a \equiv \frac{\tau^a}{2} \quad a=1,2,3 \quad SU(2)$$

$$\frac{\lambda^a}{2} \quad a=1,2,\cdots,8 \quad SU(3)$$

$$\partial_\mu J^{a\mu}_{\substack{L\\R}} = 0$$

$$J^{a\mu}_V \equiv J^{a\mu}_R + J^{a\mu}_L \qquad J^{a\mu}_A \equiv J^{a\mu}_R - J^{a\mu}_L$$

vector $\qquad$ axialvector

$$Q^a_{\substack{L\\R}} \equiv \int d^3x\, J^{a0}_{\substack{L\\R}} \qquad Q^a_V = F^a \ : \text{ flavor}$$

$$Q^a_A \quad : \text{ axial charge}$$

$$[Q^a_{\substack{R\\L}}, Q^b_{\substack{R\\L}}] = i f_{abc} Q^c_{\substack{R\\L}}$$

$$[Q^a_V, Q^b_V] = i f_{abc} Q^c_V$$

$$[Q^a_V, Q^b_A] = i f_{abc} Q^c_A$$

$$[Q^a_A, Q^b_A] = i f_{abc} Q^c_V$$

Spontaneous symmetry breaking

no parity degeneracy $\qquad Q^a_A P = -P Q^a_A$

$$Q^a_A |0\rangle \neq 0$$

or

$$\int d^3x\, \langle 0 | [J^{a0}_A(\vec{x},0), \phi^b(0)] | 0 \rangle \neq 0$$

$$\phi^b(0) = \bar{q}\gamma^5 T^a q \qquad \text{pion}$$

$$[Q^a_A, \phi^b] \sim \delta^{ab}\, \bar{q}q$$

quark condensates break chiral symmetry

$$\langle \bar{u}u \rangle \equiv \langle 0| : \bar{u}u : |0\rangle \approx \langle \bar{d}d \rangle \approx (-230\text{MeV})^3 \qquad \langle \bar{s}s \rangle \approx 0.8 \langle \bar{u}u \rangle$$

The Goldstone theorem
shows existence of a zero mode
for each broken symmetry generator

$N_f=2$ $\quad \langle 0 | A_\mu^a(0) | \pi^b(p) \rangle = \delta^{ab}\, i f_\pi p_\mu$

3 NG bosons $\pi^\pm, \pi^0$

$N_f=3$ 8 NG bosons $\pi^\pm, \pi^0$, $K^\pm, K^0, \bar{K}^0$, η

The remaining conserved generators form a subgroup H
The NG modes belong to an irreducible rep. of H

$N_f=2$ $\quad I=1$

$N_f=3$ $\quad \underline{8}$

$\mathrm{U_A}(1)$ Anomaly

singlet term

$\mathrm{U_A}(1)$ symmetry is broken by ANOMALY

$U_A(1)$: グルーオン

$$J_A^{\mu 0} = \bar{q}\gamma^\mu\gamma^5 q$$

$$\partial_\mu J_A^{\mu 0} = 2im_q\bar{q}\gamma^5 q + \frac{\alpha_s}{2\pi} N_f \,\mathrm{Tr}\{G_{\mu\nu}\tilde{G}^{\mu\nu}\}$$

$U_V(1)$: Baryonic current

$$J_V^{\mu 0} = \bar{q}\gamma^\mu q$$

$$\partial_\mu J_V^{\mu 0} = 0$$

Chiral Symmetry of QCD

$$\begin{array}{ccccccccc} SU(N_f)_R & \times & SU(N_f)_L & \times & U(1)_V & \to & SU(N_f)_V & \times & U(1)_V \\ Q_R & & Q_L & & & & Q_V & & \\ N_f^2-1 & & N_f^2-1 & & & & N_f^2-1 & & \end{array}$$

$N_f^2-1(=8)$ NG bosons

$\mathrm{U_A}(1)$ Problem

Symmetry of QCD Lagrangian and
Spontaneous Symmetry Breaking

$$\begin{array}{ccccc} U(N_f)_R & \times & U(N_f)_L & \to & U(N_f)_V \\ Q_R & & Q_L & & Q_V \\ N_f^2 & & N_f^2 & & N_f^2 \end{array}$$

η' is too heavy.

Weinberg limit on the η' mass

$$m(\eta') < \sqrt{\frac{3}{2}} m_8$$

985MeV $\quad\sim$ 700MeV

Nontrivial Topology

Instanton solution in Euclid QCD

$$\int G_{\mu\nu}\tilde{G}_{\mu\nu} d^4x \neq 0$$

gluon condensate

Instanton couples to Fermion zero mode 't Hooft

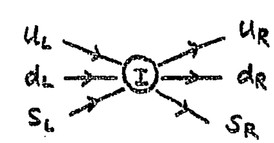

flavor singlet

$\mathcal{L}_{\rm int} \propto \det_{i,j}\{\bar{q}_R^i q_L^j\}$ + c.c. **breaks $\mathrm{U_A}(1)$ symmetry**

Kobayashi-Maskawa-'t Hooft interaction

Scalar and Pseudoscalar mesons

PS $\pi(138)$ $K(495)$ $\eta(547)$ $\eta'(958)$

S $a_0(980)$ $\kappa(\sim 800)$ $\sigma(\sim 600)$ $f_0(980)$

Higgs particles of chiral symmetry breaking

Proceedings of YITP Workshop (2000)
M. Ishida
Igi - Hikasa

$J/\psi \to \omega\pi\pi$ $m_\sigma \sim 400-700$ MeV
$\to \phi\pi\pi$ f_0 dominant

Nambu-Jona-Lasinio

Proc. Yukawa 2000
M. Ishida
Igi - Hikasa

σ meson, π-π scattering
~600 MeV

Baryon and Dibaryon systems

III can reproduce baryon spectrum as well.
Rosner-Shuryak, Oka-Takeuchi

$$H_{III} \propto \bar\psi_R(1)\bar\psi_R(2)\left[1+\frac{3}{32}\lambda_1\cdot\lambda_2+\frac{9}{32}(\lambda_1\cdot\lambda_2)(\vec\sigma_1\cdot\vec\sigma_2)\right]\psi_L(2)\psi_L(1)+h.c.$$

equivalent to color-magnetic int.

Puzzles on the spin-orbit forces of baryons can be solved.
Takeuchi
weak LS force inside the nonstrange baryons
strong LS and ALS forces between baryons

The H-dibaryon acquires repulsive 3-body interaction.
Oka-Takeuchi, Takeuchi-Kubodera-Nussinov
$H = uuddss$ flavor singlet
III repulsion ~ 50 MeV

75

OZI and III

III gives a strong mixing of flavors in the isoscalar sector

Ideal Mixing	$\xRightarrow{\text{flavor mixing}}$	SU(3)
$\frac{\bar u u+\bar d d}{\sqrt{2}}$		$\frac{\bar u u+\bar d d-2\bar s s}{\sqrt{6}}$
$\bar s s$		$\frac{\bar u u+\bar d d+\bar s s}{\sqrt{3}}$

OZI violation due to III is weak in the vector and axialvector mesons.

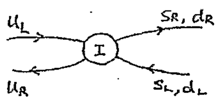

$\Leftarrow$ S, PS channels

Possibility of strong $U_A(1)$ breaking
Nemoto-Takizawa-Oka

Analyses of η decays and η_1 - η_8 mixing angle

The mixing angle is mass dependent.

$$\theta(m_\eta^2) \neq \theta(m_{\eta'}^2)$$

Mass of η is not sensitive to the mixing angle.

Analyses in the 3-flavor NJL model with the KMT interaction

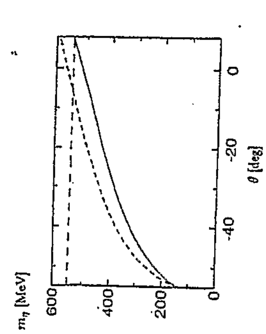

FIG. 6. Dependence of the η-meson mass on the mixing angle. The solid line indicates the result calculated in the NJL model and the short-dashed line indicates that in the $1/N_C$ expansion approach. The horizontal long-dashed line shows the experimental η meson mass.

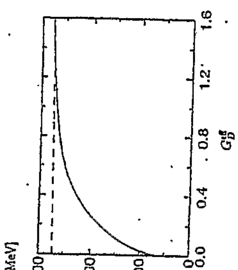

FIG. 4. Dependence of the η-meson mass on the dimensionless coupling constant $G_D^{\rm eff}$. The horizontal dashed line indicates the experimental value.

Lagrangian does not cause the flavor mixing and therefore the ideal mixing is achieved. The "η" is purely $u\bar{u}+d\bar{d}$

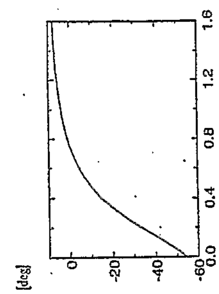

FIG. 5. Dependence of the mixing angle θ on the dimensionless coupling constant $G_D^{\rm eff}$.

NJL

$U_R(3) \times U_L(3)$ Hatsuda-Kunihiro
+ quark mass
+ III (KMT) interaction

$$\mathcal{L} = \mathcal{L}_0 + \mathcal{L}_4 + \mathcal{L}_6$$

$$\mathcal{L}_0 = \bar{q}(i\partial\!\!\!/ - m)q$$

$$\mathcal{L}_4 = \frac{1}{2} G_S [(\bar{q}\lambda^a q)^2 + (\bar{q} i\gamma^5 \lambda^a q)^2]$$

$$\mathcal{L}_6 = G_D \left[\det_f (\bar{q}(1-\gamma^5)q) + h.c. \right]$$

Chiral Symmetry Breaking (by G_S)
Constituent quark mass

$$M = m - G_S\langle\bar{q}q\rangle$$
$$= m + G_S \lim_{x\to 0} \mathrm{Tr}(iS_F^M(x))$$
$$= m + i\frac{G_S}{4\pi^2}\int d^4p \frac{M}{p^2-M^2+i\varepsilon} \times \begin{pmatrix}\text{color-flavor}\\ \text{factor}\end{pmatrix}$$

if $m=0$

$$M = M\frac{G_S}{\pi^2}\int_0^\Lambda \frac{p^2 dp}{\sqrt{p^2+M^2}} \qquad \Lambda: \text{cut off}$$

$$G_S^c = \frac{2\pi^2}{\Lambda^2} \qquad \text{if } G_S > G_S^c, \ \boxed{M \neq 0}$$

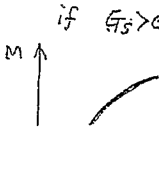

Mean field approximation
for quark propagator

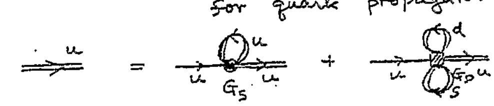

Gap equation

$$M_u = m_u - 2G_S\langle\bar{u}u\rangle - \underline{2G_D\langle\bar{d}d\rangle\langle\bar{s}s\rangle}$$

Mesons in ladder approximation

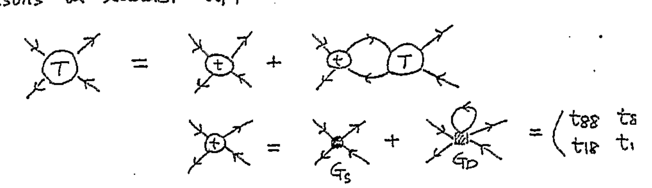

$$T = t + tGT \qquad \text{or} \qquad [1 - tG(q^2)]T = t$$

$\det[1 - tG(q^2)] = 0$ determines $q^2 = m_\eta^2$.

Flavor Mixing

$$T = \begin{pmatrix} A(q^2) & B(q^2) \\ B(q^2) & C(q^2)\end{pmatrix} \xrightarrow[\text{diagon.}]{} \begin{pmatrix} D_\eta(q^2) & 0 \\ 0 & D_{\eta'}(q^2)\end{pmatrix}$$

$$\tan 2\theta(q^2) = \frac{2B(q^2)}{C(q^2) - A(q^2)}$$

T has a pole at $q^2 = m_\eta^2$
$\theta(q^2 = m_\eta^2)$ is the $\eta_1 - \eta_8$ mixing angle for η

The residue of the pole

$$g_\eta^2 \equiv \lim_{q^2\to m_\eta^2} (q^2 - m_\eta^2) D_\eta(q^2)$$

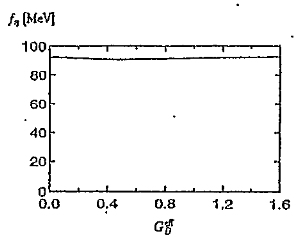

FIG. 7. Dependence of the η decay constant f_η on the dimensionless coupling constant G_D^{eff}.

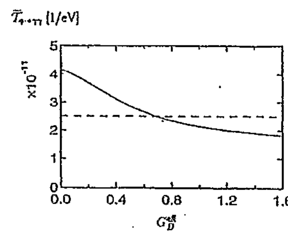

FIG. 8. Dependence of the $\eta \to \gamma\gamma$ decay amplitude on the dimensionless coupling constant G_D^{eff}. The horizontal dashed line indicates the experimental value.

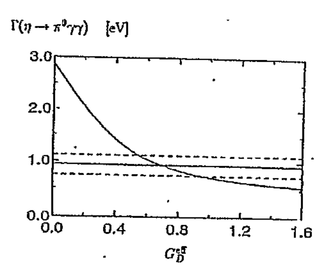

FIG. 13. Dependence of the $\eta \to \pi^0\gamma\gamma$ decay width on the dimensionless coupling constant G_D^{eff}. The horizontal solid line indicates the experimental value and the dashed lines indicate its error widths.

Puzzle of the Scalar Meson Nonet

Mass spectrum is not consistent with the $^3P_0$ quark model with SU(3) breaking due to the $m_s > m_{u,d}$

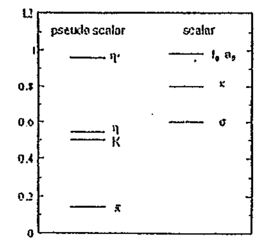

$$f_0 \sim \bar{s}s$$

$$a_0 \sim (\bar{u}u - \bar{d}d)/\sqrt{2}$$

$$m(f_0) \sim m(a_0)$$

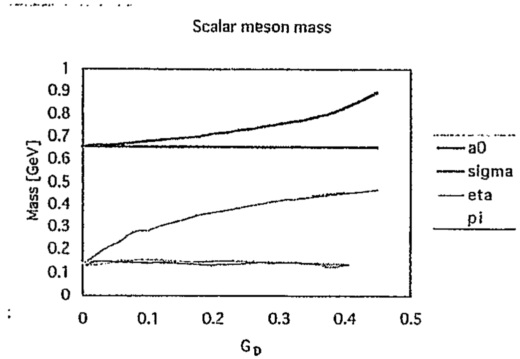

Chiral Symmetry of Baryon and Baryon Resonances

Makoto Oka
Tokyo Institute of Technology

Atsushi Hosaka (RCNP, Osaka Univ.)
Daisuke Jido (IFIC, Valencia, Spain)
Yukio Nemoto (Riken-BNL Center)
Hungchong Kim (Yonsei Univ.)

Phys. Rev. Lett. 80 (1997) 448
Nucl. Phys. A640 (1998) 77
Phys. Rev. D57 (1998) 4124
hep-ph/0007127 (Nucl. Phys. A) 671 (2000)
Prog. Theor. Phys., to be publsihed 106 (2001) 823 - 873 -

1. Introduction

QCD phase diagram for high T and/or μ

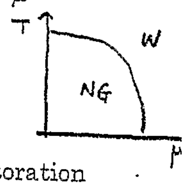

Chiral symmetry
NG phase ⇒ Wigner phase
$\langle\bar{q}q\rangle \neq 0$ $\langle\bar{q}q\rangle = 0$

Hadron spectrum at the symmetry restoration
degenerate parity partners
belongs to the same chiral multiplet

Mesons $SU(2)_L \times SU(2)_R$
(π, σ) 0^- 0^+ $\left(\frac{1}{2}, \frac{1}{2}\right)$
(ρ, a_1) 1^- 1^+ $(1,0) \oplus (0,1)$

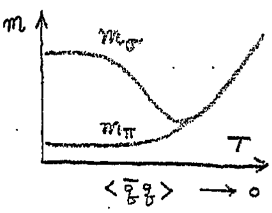

Baryons $N(940)$ $\frac{1}{2}^+$ ⇔ $N(1535)$ $\frac{1}{2}^-$?

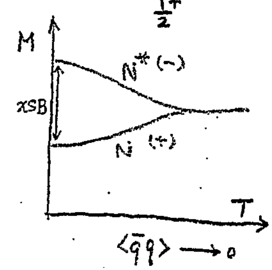

Gottlieb et al. (1987)
Jido et al. (1996)

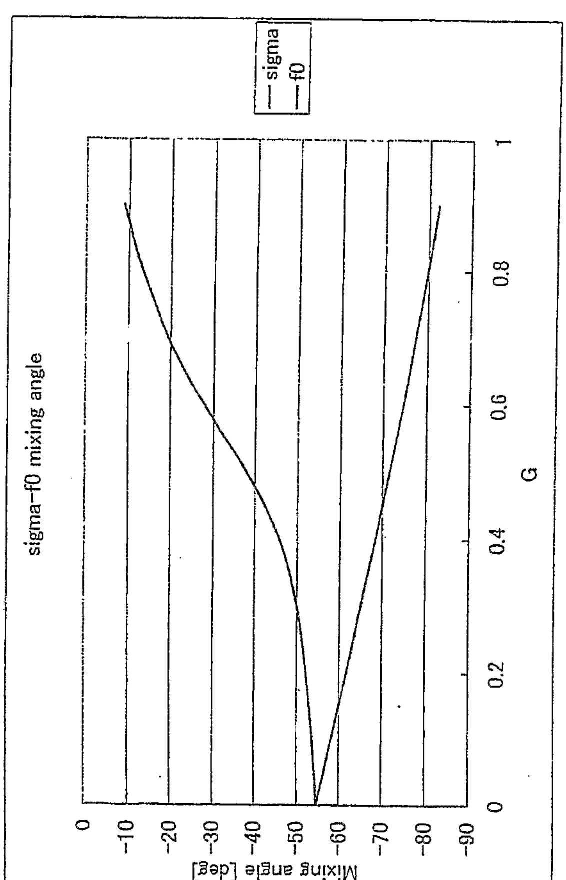

Conclusion

Strong $U_A(1)$ Breaking and Flavor Mixing

Pseudo-scalar nonet
The mixing angle has strong q^2 dependence
The radiative decays of η indicate the strong $U_A(1)$ breaking.
$\frac{G_D\langle\bar{s}s\rangle}{G_S} \simeq 0.54 \Longleftrightarrow \simeq 0.1$ for $\theta \simeq -20°$
$\theta(m_\eta^2) \simeq 0$ ... η is ≃ octet.

Scalar nonet
III induces the a_0–σ mass difference.
Mass of σ does not change but the mixing is significant.
$\bar{s}s$ mixing in σ is about 15 %.

QCD Sum Rules

Shifman - Vainshtein - Zakharov (1979)

Correlation function of composite operators

$$\Pi(p) \equiv i \int d^4x e^{ip\cdot x} \langle 0|T(J(x)J(0))|0\rangle$$

$J(x)$: Interpolating field (= composite operator)

(1) OPE (Operator Product Expansion) side

$$p_E^2 \equiv -p^2 \to \infty$$

$$\Pi(p_E^2) = \sum_n C_n(p_E^2)\langle 0|O_n(0)|0\rangle \qquad O_n : \text{Local operator}$$

(2) Phenomenological side
parametrization of the spectral function at $\mathbf{p^2 = m^2}$

$$\Pi(p^2) = \frac{1}{\pi}\int ds \frac{\rho(s)}{s-p^2} \qquad \rho(s)\text{: Spectral function}$$

$$\rho(s) = \lambda\delta(s-m^2) + \theta(s-s_0)\rho(s) \qquad \mathbf{s_0 : threshold}$$

Interpolating field operators

Mesons

$$J_\rho(x) = \bar{q}(x)\gamma^\mu\frac{\vec{\tau}}{2}q(x) \qquad \textbf{I=1 vector meson}$$

$$J_\pi(x) = \bar{q}(x)\gamma^5\frac{\vec{\tau}}{2}q(x) \qquad \textbf{I=1 pseudoscalar meson}$$

Baryons Ioffe

$$J_N(x;t) = \varepsilon^{abc}[(u_a(x)Cd_b(x))\gamma_5 u_c(x) + t(u_a(x)C\gamma_5 d_b(x))u_c(x)],$$

$$\begin{aligned} J_\Lambda(x) = \varepsilon_{abc}[&(d_a(x)Cs_b(x))\gamma_5 u_c(x) + (s_a(x)Cu_b(x))\gamma_5 d_c(x) \\ &-2(u_a(x)Cd_b(x))\gamma_5 s_c(x) \\ &+t\{(d_a(x)C\gamma_5 s_b(x))u_c(x) + (s_a(x)C\gamma_5 u_b(x))d_c(x) \\ &-2(u_a(x)C\gamma_5 d_b(x))s_c(x)\}] \end{aligned}$$

2. Chiral symmetry of Baryons

$SU(N_f = 2)$ axial transformation

$$[Q_5^a, q] = \frac{1}{2}\gamma_5\tau^a q \equiv \Gamma_5^a q \qquad \Gamma_5^a \equiv \frac{1}{2}\gamma_5\tau^a$$

$$q = \begin{pmatrix} u \\ d \end{pmatrix}$$

3 quark local opeartor for baryons

$$B^\alpha(x) \equiv \underbrace{(q^T(x)C\gamma_5 q(x))}_{\text{scalar diquark } 0^+\ I=0} q^\alpha(x)$$

α : Dirac
$C = \gamma^0\gamma^2$ antisym
color singlet

$$[Q_5^a, (q^T(x)C\gamma_5 q(x))] = 0$$

$$[Q_5^a, B] = (q^T(x)C\gamma_5 q(x))\Gamma_5^a q = \Gamma_5^a B$$

$$g_A = 1$$

Alternative choice

$$\underline{B}^\alpha(x) \equiv (q^T(x)Cq(x))\gamma_5 q^\alpha(x)$$

$$[Q_5^a, \underline{B}] = \Gamma_5^a \underline{B}$$

T.D. Cohen, X. Ji   PR D55 (1997)

Two point correlator

$$T(p) \equiv i\int d^4x\ e^{ipx}\,\theta(x^0)\,\langle 0|B(x)\bar{B}(0)|0\rangle$$

$$\Downarrow\ p^0 = \sqrt{s}\quad \vec{p} = 0$$

$$= \gamma^0 A(\sqrt{s}) + B(\sqrt{s})$$

Spectral representation

$$= \frac{1}{\pi}\int \frac{1+\gamma^0}{\sqrt{s}-m-i\varepsilon}\rho^{(+)}(m)\,dm \qquad \text{positive parity baryons}$$

$$-\frac{1}{\pi}\int \frac{1-\gamma^0}{\sqrt{s}-m-i\varepsilon}\rho^{(-)}(m)\,dm \qquad \text{negative parity baryons}$$

$$\frac{1}{2}\,\mathrm{Im}\,[A(m) \pm B(m)] = \rho^{(\pm)}(m)$$

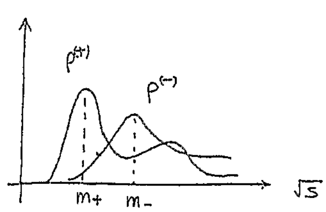

If $B(m) = 0$ then $\rho^{(+)} = \rho^{(-)}$
parity degeneracy

(3) **Analyticity of the correlator**
dispersion relation

$$\Pi(p^2) = \frac{1}{\pi}\int_0^\infty ds \frac{\mathrm{Im}\Pi(s)}{s-p^2}$$

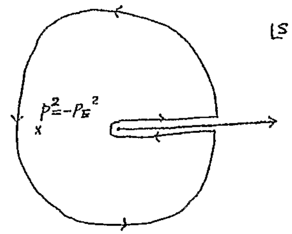

QCD duality threshold s_0

$$\mathrm{Im}\Pi^{\mathrm{OPE}}(s) = \mathrm{Im}\Pi^{\mathrm{PH}}(s) \quad \text{for } s > s_0$$

$$\int_0^{s_0} \frac{\mathrm{Im}\Pi^{\mathrm{OPE}}(s)}{s-p^2} ds = \int_0^{s_0} \frac{\mathrm{Im}\Pi^{\mathrm{PH}}(s)}{s-p^2} ds$$

ρ meson

$$m_\rho^2 = M^2 \times$$
$$\left[\left(1+\frac{\alpha_s}{\pi}\right)\left(1-\left(1+\frac{s_0}{M^2}\right)e^{-s_0/M^2}\right) - \frac{8\pi^2}{M^4}\langle m\bar{q}q\rangle - \frac{\pi^2}{8M^4}\left\langle \frac{\alpha_s}{\pi} G_{\mu\nu}G^{\mu\nu}\right\rangle \right]$$
$$\times \left[\left(1+\frac{\alpha_s}{\pi}\right)\left(1-e^{-s_0/M^2}\right) + \frac{8\pi^2}{M^4}\langle m\bar{q}q\rangle + \frac{\pi^2}{8M^4}\left\langle \frac{\alpha_s}{\pi} G_{\mu\nu}G^{\mu\nu}\right\rangle \right]^{-1}$$

Reinders - Rubinstein - Yazaki
Phys. Rep. 127 (1985)

mass, coupling
$\Updownarrow$
condensates

L.J. Reinders et al., Hadron properties from QCD sum rules 55

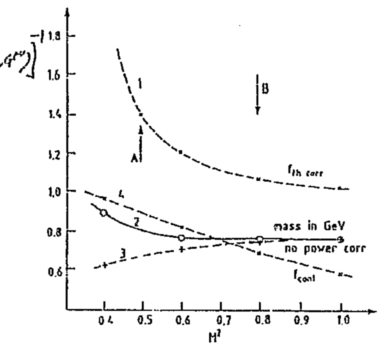

Fig. 11. The ρ meson mass with and without power corrections. The continuum threshold $s_0 = 1.5\,\mathrm{GeV}^2$. Also shown are the functions f_{cont} and $f_{th\,corr}$ defined in the text. The region between the arrows A and B is considered to be reliable for determining the resonance parameters. Figure adapted from [1].

(4) **To improve:**
Borel transformation M^2

$$\Pi(p^2=-p_E^2) \to \mathcal{B}_{M^2}\Pi \equiv \tilde{\Pi}(M^2) = \lim_{p_E^2, n\to\infty, M^2 \equiv p_E^2/n = \text{finite}} \frac{(p_E^2)^{n+1}}{n!}\left(-\frac{d}{dp_E^2}\right)^n \Pi(p_E^2)$$

Borel sum rule for the imaginary part of T

$$\mathcal{B}_{M^2}\int_0^{s_0} \frac{\mathrm{Im}\Pi(s)}{s+p_E^2} ds = \int_0^{s_0} e^{-s/M^2}\mathrm{Im}\Pi(s) ds$$

$$\int_0^{s_0} e^{-s/M^2}\mathrm{Im}\Pi^{\mathrm{OPE}}(s) ds = \int_0^{s_0} e^{-s/M^2}\mathrm{Im}\Pi^{\mathrm{PH}}(s) ds$$

QCD Sum Rule for Baryons

positive and negative parity baryons

$$J_- \equiv i\gamma_5 J_+$$

$$\Pi_+(p) = p_\mu\gamma^\mu\Pi_1(p^2) + \Pi_2(p^2),$$
$$\Pi_-(p) = -\gamma_5\Pi_+(p)\gamma_5 = p_\mu\gamma^\mu\Pi_1(p^2) - \Pi_2(p^2).$$

old-fashioned correlator Jido - Kodama - Oka

$$\Pi(p) = i\int d^4x e^{ip\cdot x}\theta(x_0)\langle 0|J_B(x)\bar{J}_B(0)|0\rangle$$

$$\begin{aligned}\mathrm{Im}\,\Pi(p_0) &= \sum_n \left[(\lambda_n^+)^2\frac{\gamma_0+1}{2}\delta(p_0-m_n^+) + (\lambda_n^-)^2\frac{\gamma_0-1}{2}\delta(p_0-m_n^-)\right] \\ &\equiv \gamma_0 A(p_0) + B(p_0),\end{aligned}$$

Phenomenological side

$$A(p_0) = \frac{1}{2}\sum_n[(\lambda_n^+)^2\delta(p_0 - m_n^+) + (\lambda_n^-)^2\delta(p_0 - m_n^-)]$$
$$B(p_0) = \frac{1}{2}\sum_n[(\lambda_n^+)^2\delta(p_0 - m_n^+) - (\lambda_n^-)^2\delta(p_0 - m_n^-)]$$

OPE side

$$A^{\rm OPE}(p_0) = \frac{5+2t+5t^2}{2^{10}\pi^4}p_0^5\theta(p_0) + \frac{5+2t+5t^2}{2^9\pi^2}p_0\theta(p_0)\langle\frac{\alpha_s}{\pi}GG\rangle - \frac{5+2t-7t^2}{12}\delta(p_0)\langle\bar{q}q\rangle^2,$$
$$B^{\rm OPE}(p_0) = -\frac{7t^2-2t-5}{32\pi^2}p_0^2\theta(p_0)\langle\bar{q}q\rangle - \frac{3(1-t^2)}{32\pi^2}\theta(p_0)\langle\bar{q}g\sigma\cdot Gq\rangle.$$

A : **chiral even terms**
B : **chiral odd (symmetry breaking) terms**

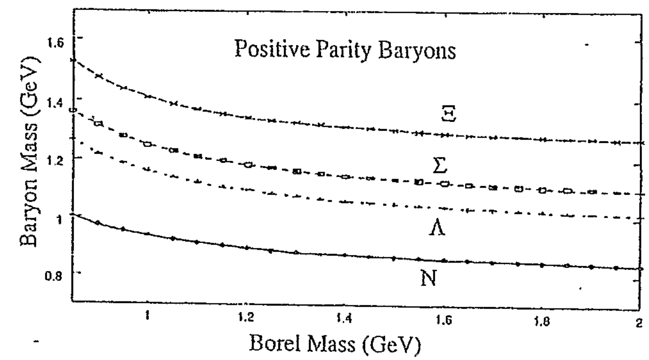

chiral symmetry breaking

Borel Sum Rules for m^+ and m^-

$$\frac{1}{2}[\tilde{A}^{\rm OPE}(M,s_0^+) + \tilde{B}^{\rm OPE}(M,s_0^+)] = (\lambda^+)^2\exp[-\frac{(m^+)^2}{M^2}],$$
$$\frac{1}{2}[\tilde{A}^{\rm OPE}(M,s_0^-) - \tilde{B}^{\rm OPE}(M,s_0^-)] = (\lambda^-)^2\exp[-\frac{(m^-)^2}{M^2}],$$

Choice of QCD parameters

$\langle\bar{q}q\rangle$	m_0	m_s	χ	χ_5
(-0.244 GeV)^3	0.9 GeV	0.1 GeV	0.75	0.8

$m_0^2 \equiv \langle\bar{q}g\sigma\cdot Gq\rangle/\langle\bar{q}q\rangle$ $\quad\chi \equiv \langle\bar{s}s\rangle/\langle\bar{q}q\rangle$ $\quad\chi_5 \equiv \langle\bar{s}g\sigma\cdot Gs\rangle/\langle\bar{q}g\sigma\cdot Gq\rangle$

vacuum saturation $\quad\langle(\bar{q}q)^2\rangle = \langle\bar{q}q\rangle^2$

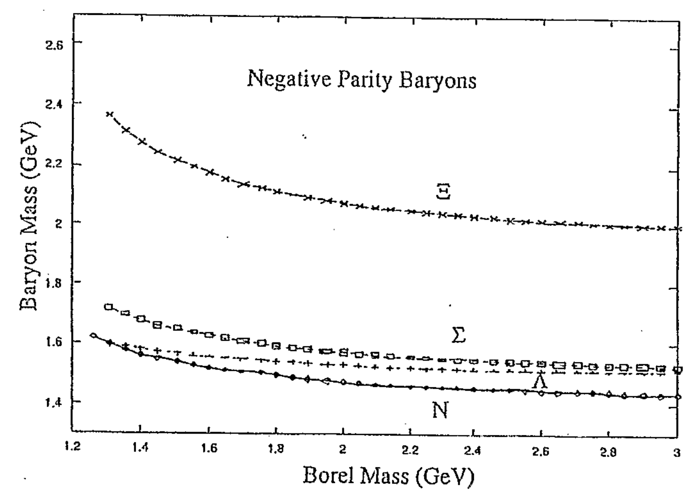

QCD sum Rule for Negative Parity Baryons

D. Jido et al.
CEBAF/INT N^* physics
hep-ph/9611322

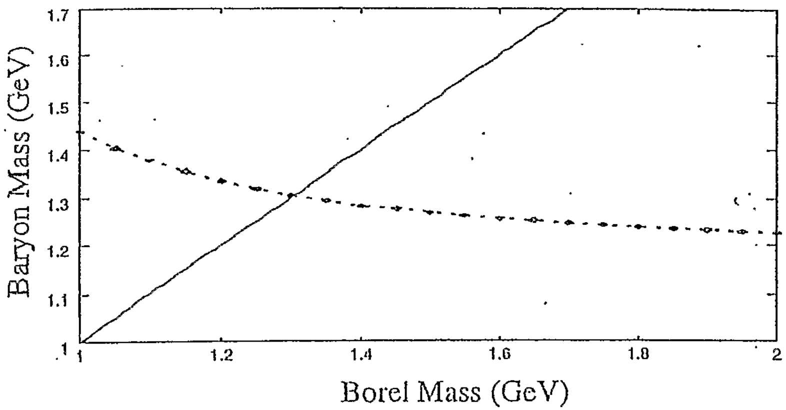

Figure 3: The Borel mass M dependence of the singlet Λ_S- masses. The solid l
denotes $M = m_B$.

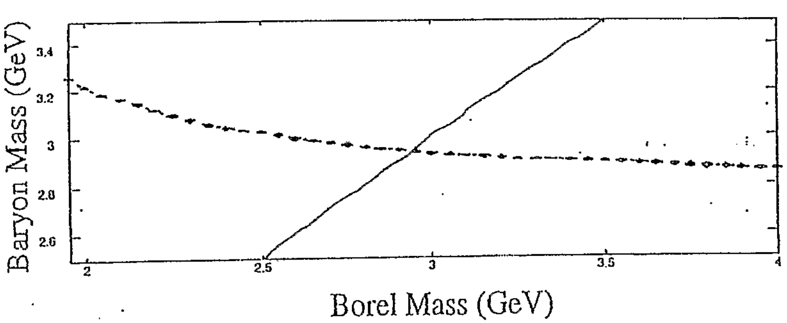

Table 2:

unit : GeV

Baryon	Sum rule	Exp.	IK Quark Model
flavor octet baryons			
N_+	0.94	0.94	
Λ_+	1.12	1.12	
Σ_+	1.21	1.19	
Ξ_+	1.32	1.32	
N_-	1.54	1.535	1.49
Λ_-	1.55	1.67	1.65
Σ_-	1.63	1.62	1.65
Ξ_-	1.63	—	1.78
flavor singlet baryons			
Λ_{S-}	1.31	1.405	1.49
Λ_{S+}	2.94	—	

Linear σ- model

$SU(2)_R \times SU(2)_L$

$$\mathcal{L} = \frac{i}{2}\,\bar{\psi}\,\gamma\cdot\overleftrightarrow{\partial}\,\psi + g\,\bar{\psi}\,(\phi^0 + i\,\vec{\tau}\cdot\vec{\phi}\,\gamma^5)\,\psi$$
$$+ \frac{1}{2}(\partial_\mu \phi^\alpha)^2 - C^2(\phi^2 - v^2)^2$$

Chiral Transform

$$\psi \longrightarrow e^{i\gamma^5 \frac{\vec{\tau}}{2}\cdot\vec{\alpha}}\,\psi$$

$$\begin{pmatrix}\phi^0\\ \vec{\phi}\end{pmatrix} \longrightarrow \begin{pmatrix}\cos\alpha & \hat{\alpha}\sin\alpha\\ -\hat{\alpha}\sin\alpha & \cos\alpha\end{pmatrix}\begin{pmatrix}\phi^0\\ \vec{\phi}\end{pmatrix}$$

Noether current

$$\vec{A}^\mu = \bar{\psi}\,\gamma^\mu\gamma^5\frac{\vec{\tau}}{2}\,\psi + \phi^0\,\partial^\mu\vec{\phi} - \partial^\mu\phi^0\,\vec{\phi}$$

$$\partial_\mu \vec{A}^\mu = 0$$

For $v^2 > 0$

$$\langle 0|\,\phi^0\,|0\rangle = v$$

$$\phi^{0\prime} \equiv \phi^0 - v$$

$$\mathcal{L} = \frac{i}{2}\,\bar{\psi}\,\gamma\cdot\overleftrightarrow{\partial}\,\psi + g\,v\,\bar{\psi}\psi$$
$$+ g\,\bar{\psi}\,(\phi^{0\prime} + i\,\vec{\tau}\cdot\vec{\phi}\,\gamma^5)\,\psi$$
$$+ \frac{1}{2}\left\{(\partial_\mu\phi^{0\prime})^2 + (\partial_\mu\vec{\phi})^2\right\}$$
$$- C^2\left((\phi^{0\prime})^2 + 2v\,\phi^{0\prime} + \vec{\phi}^{\,2}\right)^2$$

Fermion mass $\quad M = -g v = -g\langle 0|\phi^0|0\rangle$

Boson masses $\quad \phi^{0\prime} \quad m_0' = \sqrt{8 v C^2}$

$\vec{\phi} \quad m_i = 0 \quad$ NG boson

Explicit Symmetry Breaking

$$\mathcal{L}_{CSB} = a\,\phi^0$$

$$V(\vec{\phi}=0) = C^2\,(\phi^{0\,2}-v^2)^2 - a\,\phi^0$$

$$\Rightarrow \vec{\phi} \text{ mass} \qquad m_i = \sqrt{\frac{a}{\langle\phi^0\rangle}} = m_\pi$$

PCAC

$$\partial_\mu \vec{A}^\mu = a\,\vec{\phi} = m_\pi^2\,\langle\phi^0\rangle\,\vec{\phi}$$

Pion decay

$$\langle 0|\,\vec{A}^\mu\,|\vec{\pi}(p)\rangle = i\,p^\mu\,\langle\phi^0\rangle = i\,p^\mu f_\pi$$

$$\partial_\mu \vec{A}^\mu = m_\pi^2\, f_\pi\, \vec{\phi}$$

Fermion mass $\quad M = -g\,f_\pi$

Goldberger - Treiman

Linear Sigma Model Lagrangian

$$\mathcal{L} = \bar{B}\,i\partial\!\!\!/\,B - g\,\bar{B}\,(\sigma + i\vec{\tau}\cdot\vec{\pi}\,\gamma^5)\,B + \mathcal{L}(\sigma,\pi)$$

$$\langle\sigma\rangle = f_\pi \neq 0 \qquad \text{SSB}$$

$$\mathcal{L} = \bar{B}\,(i\partial\!\!\!/ - m)\,B - g\,\bar{B}\,(\sigma' + i\vec{\tau}\cdot\vec{\pi}\,\gamma^5)\,B + \cdots$$

$$m = g\langle\sigma\rangle = g\,f_\pi \qquad \sigma' = \sigma - \langle\sigma\rangle$$

Nonlinear Representation

$$U = \frac{1}{f_\pi}\,(\sigma + i\vec{\tau}\cdot\vec{\pi}) = \xi^2 \qquad \xi^\dagger\xi = \xi\xi^\dagger = 1$$

unitary

$$\Psi_R \equiv \xi\,B_R \qquad \Psi_L \equiv \xi^\dagger\,B_L$$

$$\bar{B}\,i\partial\!\!\!/\,B = \bar{\Psi}\,(i\partial\!\!\!/ - V\!\!\!/)\,\Psi + \bar{\Psi}\,A\!\!\!/\,\gamma^5\,\Psi$$

$$V_\mu \equiv \frac{1}{2i}\,(\xi^\dagger\partial_\mu\xi + \xi\,\partial_\mu\xi^\dagger) \sim \frac{i}{f_\pi^2}\,\vec{\pi}\times\partial_\mu\vec{\pi}$$

$$A_\mu \equiv \frac{1}{2i}\,(\xi^\dagger\partial_\mu\xi - \xi\,\partial_\mu\xi^\dagger) \sim \frac{1}{f_\pi}\,\partial_\mu\vec{\pi}$$

$$-g\,\bar{B}\,(\sigma + i\vec{\tau}\cdot\vec{\pi}\,\gamma^5)\,B = -g\,f_\pi\,\bar{\Psi}\Psi = -m\,\bar{\Psi}\Psi$$

$$\mathcal{L} = \bar{\Psi}\,(i\partial\!\!\!/ - V\!\!\!/ - m)\,\Psi + \bar{\Psi}\,A\!\!\!/\,\gamma^5\,\Psi + \cdots$$

$$g_A = 1$$

3. Linear Sigma Models for N and N^*

$$[Q_5^a, N] = \frac{1}{2}\gamma_5\tau^a N$$

chiral transform

$$N(x) = N_L(x) + N_R(x) \qquad N_{\substack{R\\L}} = \frac{1\pm\gamma_5}{2}N$$

$$N_L(x) \to L\, N_L(x) \qquad L \in SU(N_f)_L$$
$$N_R(x) \to R\, N_R(x) \qquad R \in SU(N_f)_R$$

$\bar{N} N = \bar{N}_L N_R + \bar{N}_R N_L$ is not chiral invariant

N becomes massless in the Wigner phase.

Linear Sigma Model

$N_f = 2$

$$\bar{N}(\sigma + i\vec{\tau}\cdot\vec{\pi}\gamma^5)N = \bar{N}_L(\sigma + i\vec{\tau}\cdot\vec{\pi})N_R + \bar{N}_R(\sigma - i\vec{\tau}\cdot\vec{\pi})N_L$$

$$= f_\pi(\bar{N}_L U N_R + \bar{N}_R U^\dagger N_L) \qquad \text{invariant}$$

$$U \equiv \frac{1}{f_\pi}(\sigma + i\vec{\tau}\cdot\vec{\pi}) \to LUR^{-1}$$

SSB

$$\langle\sigma\rangle = \sigma_0 \ (= f_\pi) \neq 0$$

$$L = \bar{N}(i\partial\!\!\!/ - m)N - g\bar{N}(\sigma' + i\vec{\tau}\cdot\vec{\pi}\gamma^5)N + \cdots$$

$$m = g\sigma_0 \qquad \sigma' \equiv \sigma - \langle\sigma\rangle$$

Chiral Symmetry of N and N^*

Case 1 : Naïve Assignment

$$\boxed{\begin{array}{ll} N_{1R} \to RN_{1R} & N_{1L} \to LN_{1L} \\ N_{2R} \to RN_{2R} & N_{2L} \to LN_{2L} \end{array}} \quad \begin{array}{l} \text{positive parity} \\ \text{negative parity} \end{array}$$

No mass term allowed

$$L = \bar{N}_1 i\partial\!\!\!/ N_1 + \bar{N}_2 i\partial\!\!\!/ N_2 + a\bar{N}_1(\sigma + i\gamma_5\pi^a\tau^a)N_1$$
$$+ b\bar{N}_2(\sigma + i\gamma_5\pi^a\tau^a)N_2$$
$$+ c(\bar{N}_1(\sigma + i\gamma_5\pi^a\tau^a)N_2 + \bar{N}_2(\sigma + i\gamma_5\pi^a\tau^a)N_1) + L_M$$

mass matrix

$$M \sim \sigma_0\begin{pmatrix} a & \gamma_5 c \\ -\gamma_5 c & b \end{pmatrix}$$

π coupling

$$C \sim \begin{pmatrix} a & \gamma_5 c \\ -\gamma_5 c & b \end{pmatrix} i\gamma_5\tau^a\pi^a$$

diagonalization $\to$ mass eigenstates

$$\sinh\delta = \frac{a+b}{2c}$$

$$\begin{pmatrix} N_+ \\ N_- \end{pmatrix} = \frac{1}{\sqrt{2\cosh\delta}}\begin{pmatrix} -e^{-\delta/2} & \gamma_5 e^{\delta/2} \\ \gamma_5 e^{\delta/2} & e^{-\delta/2} \end{pmatrix}\begin{pmatrix} N_1 \\ N_2 \end{pmatrix}$$

$$m_\pm = \frac{1}{2}\sigma_0\left(\sqrt{(a+b)^2 + 4c^2} \pm (a-b)\right)$$

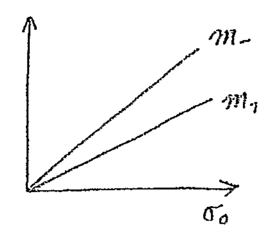

$g_\pm = 0$ no off-diagonal πNN^* coupling

two independent "Naive" baryons

3rd lecture

Case 2 : <u>Mirror</u> Assignment

C. DeTar and T. Kunihiro
B.W. Lee

$N_{1R} \to RN_{1R}$	$N_{1L} \to LN_{1L}$	positive parity
$N_{2R} \to LN_{2R}$	$N_{2L} \to RN_{2L}$	negative parity

$$[Q_5^a, N_1] = \frac{1}{2}\gamma_5 \tau^a N_1 \qquad [Q_5^a, N_2] = -\frac{1}{2}\gamma_5 \tau^a N_2$$

$g_A = -1$

off diagonal mass term

$$m_0(\overline{N}_2\gamma_5 N_1 - \overline{N}_1\gamma_5 N_2)$$
$$= m_0(\overline{N}_{2L} N_{1R} - \overline{N}_{2R} N_{1L} - \overline{N}_{1L} N_{2R} + \overline{N}_{1R} N_{2L})$$

chiral invariant

Mass eigenstates (in the Wigner phase)

$$[Q_5^a, N_+] = \frac{\tau^a}{2} N_- \qquad [Q_5^a, N_-] = \frac{\tau^a}{2} N_+$$

$N_+ \longleftrightarrow N_-$

chiral partner

$$N_+ = \frac{1}{\sqrt{2}}(N_1 + \gamma_5 N_2) \qquad \text{positive parity}$$

$$N_- = \frac{\gamma_5}{\sqrt{2}}(N_1 - \gamma_5 N_2) \qquad \text{negative parity}$$

$$L = \overline{N}_1 i\partial N_1 + \overline{N}_2 i\partial N_2 + m_0(\overline{N}_2\gamma_5 N_1 - \overline{N}_1\gamma_5 N_2)$$
$$+ a\overline{N}_1(\sigma + i\gamma_5\pi^a\tau^a)N_1 + b\overline{N}_2(\sigma + i\gamma_5\pi^a\tau^a)N_2 + L_M$$

mass matrix

$$M \sim \begin{pmatrix} a\sigma_0 & \gamma_5 m_0 \\ -\gamma_5 m_0 & b\sigma_0 \end{pmatrix}$$

π coupling

$$C \sim \begin{pmatrix} a & 0 \\ 0 & b \end{pmatrix}$$

Mass eigenstates

$$\begin{pmatrix} N_+ \\ N_- \end{pmatrix} = \frac{1}{\sqrt{2\cosh\delta}} \begin{pmatrix} -e^{-\delta/2} & \gamma_5 e^{\delta/2} \\ \gamma_5 e^{\delta/2} & e^{-\delta/2} \end{pmatrix} \begin{pmatrix} N_1 \\ N_2 \end{pmatrix} \qquad \sinh\delta = \frac{a+b}{2}\frac{\sigma_0}{m_0}$$

$$m_\pm = \frac{1}{2}\left(\sqrt{(a+b)^2\sigma_0^2 + 4m_0^2} \pm (a-b)\sigma_0\right)$$

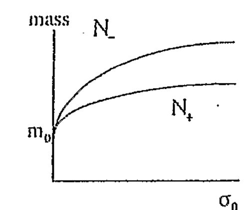

Axial charges have the opposite sign.

$$[Q_5^a, N_+] = +\frac{\tau^a}{2}\left(\tanh\delta\,\gamma_5 N_+ + \frac{1}{\cosh\delta} N_-\right)$$

$$[Q_5^a, N_-] = +\frac{\tau^a}{2}\left(-\tanh\delta\,\gamma_5 N_- + \frac{1}{\cosh\delta} N_+\right)$$

$g_\pm \neq 0$

Goldberger–Treiman relation

$$f_\pi g_{\pi NN^*} = (m_- - m_+)\, g_{ANN^*}$$

Local Quark Operator for Mirror Baryon

$$[Q_5^a\ ,\ \bar{q}q\,] = -i\ \ \bar{q}\,i\gamma_5\tau^a q$$

$$[Q_5^a\ ,\ \bar{q}\,i\gamma_5\tau^b q] = \ i\,\delta^{ab}\,\bar{q}q$$

$$\underbrace{S \equiv \bar{q}q \qquad \Pi^a \equiv \bar{q}\,i\gamma_5\tau^a q}_{\text{color singlet}} \qquad \Gamma_5^a \equiv \frac{1}{2}\gamma_5\tau^a$$

$$[Q_5^a\ , S + i\gamma_5\tau^b\,\Pi^b] = -\,\{\Gamma_5^a\,, S + i\gamma_5\tau^b\,\Pi^b\}$$

$$\boxed{\begin{aligned} B^* &\equiv (S + i\gamma_5\tau^b\,\Pi^b\,)\,B \\ &= (\bar{q}q)\,(q^T C\,\gamma_5\,q)\,q \\ &\qquad + (\bar{q}\,i\gamma_5\tau^b q)\,(q^T C\,\gamma_5\,q)\,i\gamma_5\tau^b q \end{aligned}}$$

$$\begin{aligned} [Q_5^a\ , B^*\,] &= -\{\Gamma_5^a\,, S + i\gamma_5\tau^b\,\Pi^b\}\,B \\ &\qquad + (S + i\gamma_5\tau^b\,\Pi^b\,)\,\Gamma_5^a\,B \\ &= -\,\Gamma_5^a\,(S + i\gamma_5\tau^b\,\Pi^b\,)\,B \\ &= -\,\Gamma_5^a\,B^* \end{aligned}$$

$$g_A = -1$$

A Realistic N and N* model

N (940) $\frac{1}{2}^+$ $I=\frac{1}{2}$

N^*(1535) $\frac{1}{2}^-$ $I=\frac{1}{2}$

$\hookrightarrow N\eta\ ,\ N\pi$

H. Kim, et al. NP A640 (1998) 77

Naive	Mirror	exp
$g_{NN}^A = 1$	$g_{NN}^A = \tanh\delta < 1$	$(g_{NN}^A)_{\rm exp.} = 1.26$
$g_{NN^*}^A = 0$	$g_{NN^*}^A = \dfrac{1}{\cosh\delta}$	$(g_{NN^*}^A) \sim 0.2$

New terms with derivatives

Naive

$$d_1\bar{N}_1\Pi_2 N_1 + d_2\bar{N}_2\Pi_2 N_2 + d_3(\bar{N}_1\Pi_2\gamma_5 N_2 + h.c.)$$

$$\Pi_2 = (\tau\cdot\pi\partial\sigma - \sigma\tau\cdot\partial\pi)\gamma_5 - \tau\cdot(\pi\times\partial\pi)$$

Mirror

$$d_1\bar{N}_1\Pi_2 N_1 + d_2\bar{N}_2\Pi_2 N_2 + d_3(\bar{N}_1\Pi_1\gamma_5 N_2 + h.c.)$$

$$\Pi_1 = i\partial\sigma\gamma_5 + \tau\cdot\partial\pi$$

Naive

$$g_{NN}^A = 1 + d_1\sigma_0^2 \qquad 1.26 \ \rightarrow\ 1 \quad \text{quenching}$$

$$g_{NN^*}^A = d_3\sigma_0^2 \qquad 0.2\ \rightarrow\ 0$$

Mirror

$$g_{NN}^A = \tanh\delta + \frac{2\sigma_0 d_3}{\cosh\delta} - \sigma_0^2\,\frac{d_1 e^{\delta} - d_2 e^{-\delta}}{\cosh\delta} \qquad 1.26\ \rightarrow\ 0$$

$$g_{NN^*}^A = \frac{1}{\cosh\delta} + 2\sigma_0 d_3\tanh\delta + \sigma_0^2\,\frac{d_1 + d_2}{\cosh\delta} \qquad 0.2\ \rightarrow\ 1$$

Nucleons at finite density

Relativistic Hartree approximation

$$E=\lambda(\sigma_0^2-f_\pi^2)+\underset{\downarrow}{E_v^+}+\underset{\downarrow}{E_v^-}+4\int_0^{k_f}\frac{d^3k}{(2\pi)^3}\sqrt{k^2+m_+^{*2}}$$

$\lambda = m_\sigma{}^2/8\,f_\pi{}^2$ vacuum energy from N^+ and N^-

Parameters $a, b, d_1, d_2, d_3, (m_0)$

$m_+ = 939\text{MeV}$ $g^A_{NN} = 1.26$

$m_- = 1535\text{MeV}$ $g^A_{NN^*} = 0.217$ $g^A_{NN} = -g^A_{N^*N^*}$

m_0 : free parameter indep of chiral symmetry breaking

Results

$m_-^* - m_+^*$ decreases as $\sigma_0 \to 0$

$N^* \to N\eta$ suppressed in nuclear medium.

g^A_{NN} shows quenching
(for large m_0, large quenching)

$g^A_{NN^*}\begin{cases}\text{decreases in the naive case}\\ \text{increases in the mirror case}\end{cases}$

$g_{\pi NN^*}$

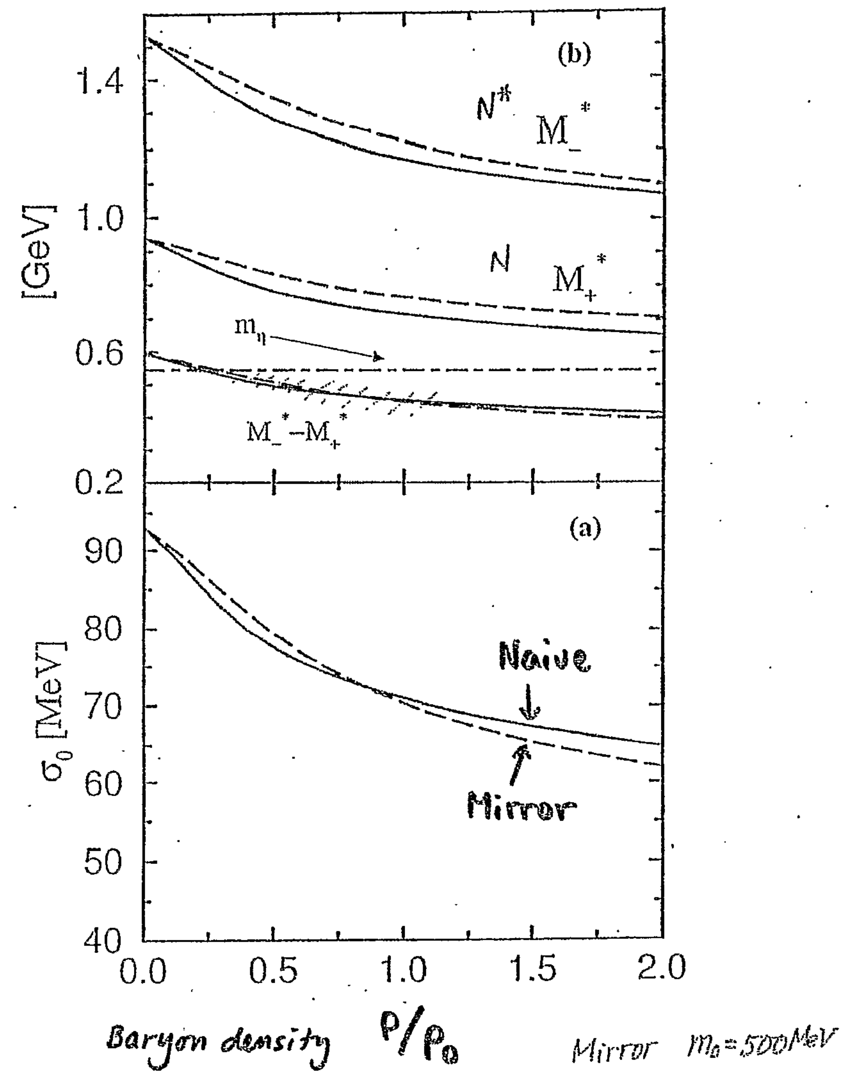

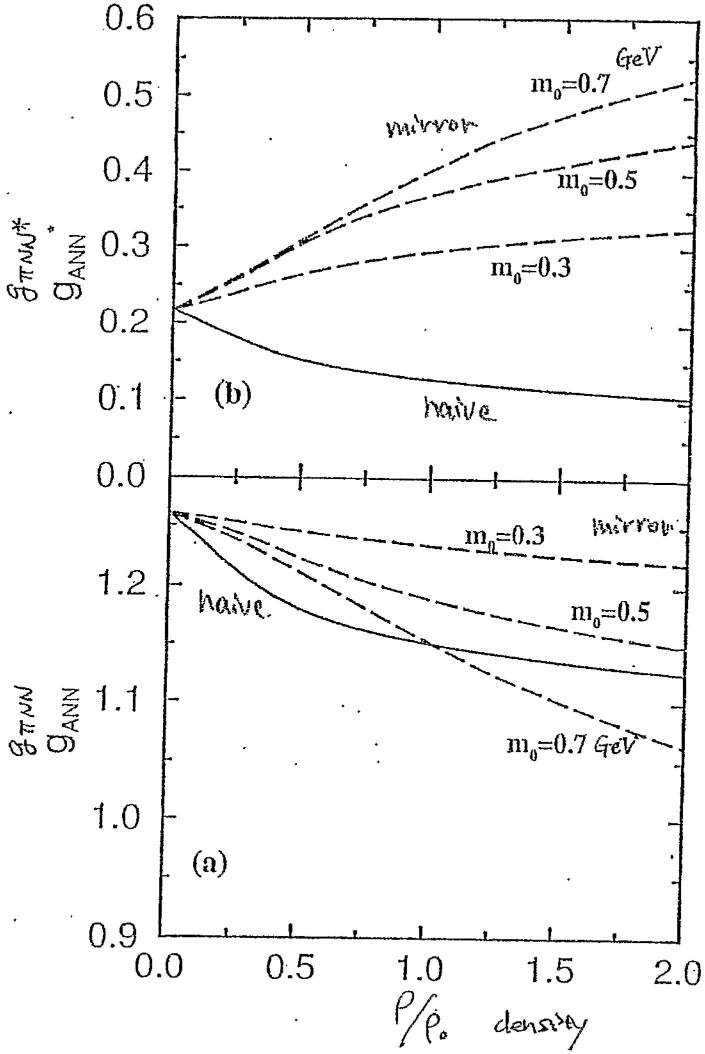

mirror
6 parameters 4 inputs m_N, m_{N^*}, g^A_{NN}, $g^A_{NN^*}$
$g_A^{NN} = -g_A^{N^*N^*}$

Signature for Mirror (N, N^*)

- In chiral symmetry restoration
  (N, N^*) forms a parity doublet
  with nonzero mass m_0 ?
  indep of χSB

- $g(\pi NN^*)$ is enhanced in nuclear matter
  $N^* \to N\eta$ is suppressed

  $$\frac{\Gamma(N^* \to N\eta)}{\Gamma(N^* \to N\pi)}$$ decreases

- $\overset{g_{AN^*N^*}}{g(\pi N^*N^*)} \approx - \overset{g_{ANN}}{g(\pi NN)}$ opposite sign

  $\gamma + N \to N + \pi + \eta$
  $\pi + N$

$\gamma + N \longrightarrow N + \pi + \eta$

γ^*

Jido, Hosaka, Oka

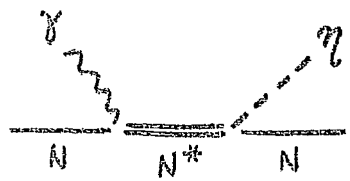

$N^*(1535)$

+ (soft) pion

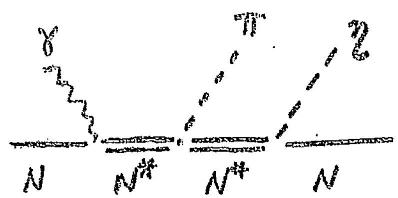

$g_{\pi N^* N^*}\, g_{N^* N \eta}$

interfere

$g_{\pi NN}\, g_{N^* N \eta}$

+ (many) other diagrams

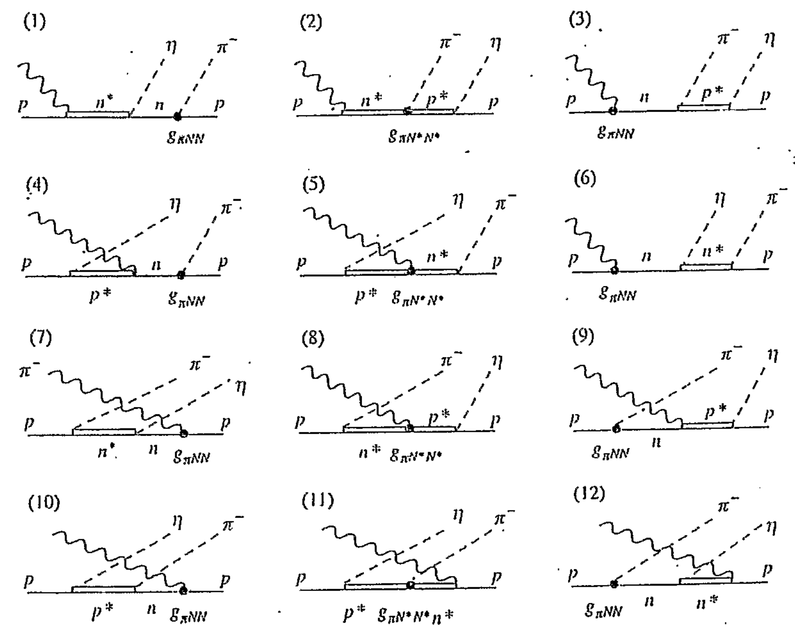

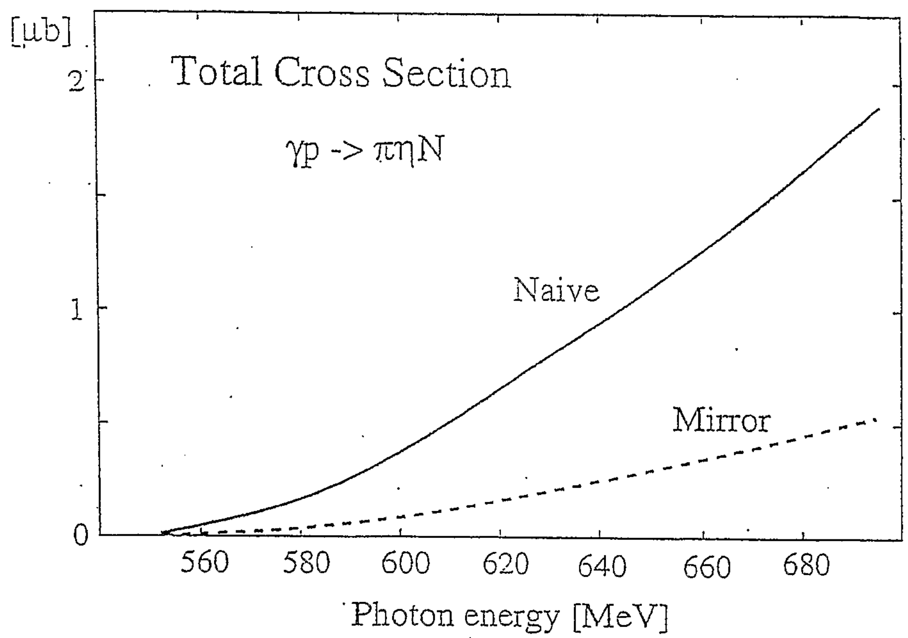
[μb]
Total Cross Section
γp -> πηN
Naive
Mirror
Photon energy [MeV]

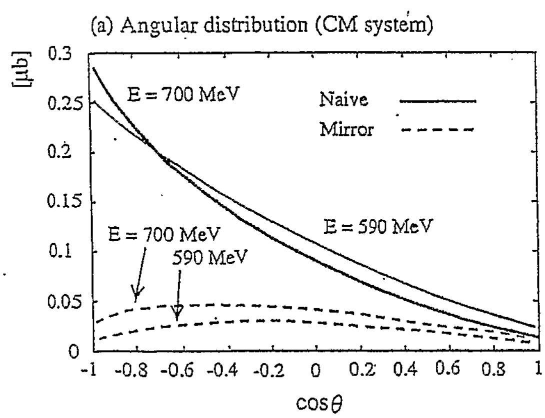
(a) Angular distribution (CM system)
[μb]
E = 700 MeV
Naive
Mirror
E = 590 MeV
E = 700 MeV
590 MeV
cos θ

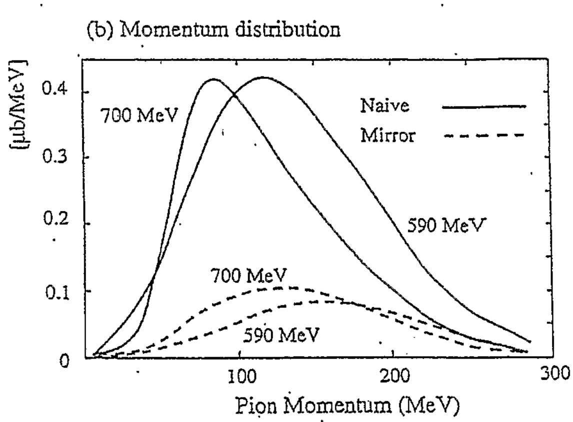
(b) Momentum distribution
[μb/MeV]
700 MeV
Naive
Mirror
590 MeV
700 MeV
590 MeV
Pion Momentum (MeV)

March, 2002

QCD Effects on the Weak Decays of Hyperons and Hypernuclei

Why do we need QCD in weak interactions?

Soft-pion and chiral effective theory

Quark model approach to hypernuclear decays

1. Introduction

Strangeness nuclear (hadron) physics

Strangeness is most sensitive to QCD.

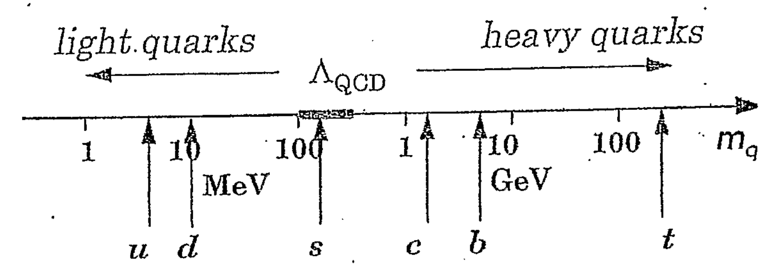

$m_s \sim \Lambda_{QCD}$

u, d quarks follow *SU(2)* isospin invariance.
isospin symmetry binding

s quark is sensitive to dynamical contents
as *SU(3)* symmetry is partially broken.

ex. chiral perturbation theory

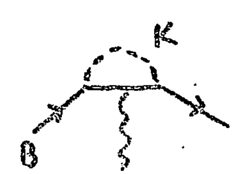

$\sim \ln \frac{m_K^2}{\mu^2}$

93

Strangeness decays

$s \longrightarrow u\, W^-$

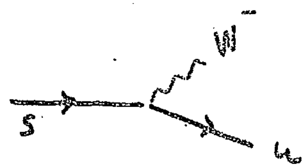

Weak interactions of hadrons are good probes of QCD.

– Semileptonic decays of hadrons

β decay of baryons $\begin{matrix} n \longrightarrow \\ \Lambda \longrightarrow \end{matrix} p\ e^-\ \nu_e$
parity violation
current conservation PCAC

– Nonleptonic decays

$K \longrightarrow \pi\ \pi$ CP violation

$\Lambda \longrightarrow N\ \pi$ $\Delta I = 1/2$ rule

Nonleptonic weak interactions of hadrons
can be studied only through *strangeness*
except for parity violating *NN* forces

2. Weak decay of strangeness

$\Delta S = 1$ weak transition

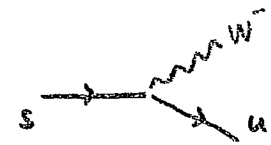

charged current

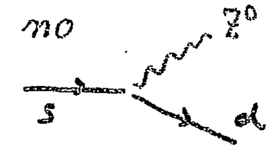

GIM forbidden

semileptonic weak interactions of hadrons

$K^- \longrightarrow \pi^0\ \mu^-\ \nu_\mu$
$\longrightarrow \mu^-\ \nu_\mu$

$\Lambda \longrightarrow p\ e^-\ \nu_e$

$\langle \text{hadron} | A^\mu | \text{hadron} \rangle \sim g_A\, \chi_p^\dagger\, \vec{\sigma}\, \chi_\Lambda$

nonleptonic weak interactions

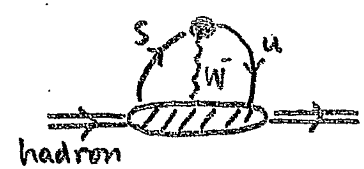

$K^0 \longrightarrow \pi^+\ \pi^-$
$\Lambda \longrightarrow p\ \pi^-$

as $m_W^2 >> \Lambda^2_{QCD}$

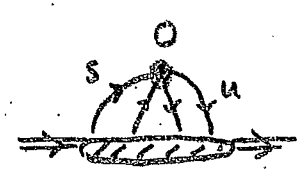

4-quark local operator

$O = (\bar{u}\, \Gamma\, s)\ (\bar{d}\, \Gamma\, u)$

$\Gamma \sim \gamma^\mu (1-\gamma^5)$ etc.

ΔI=1/2 rule for ΔS=1 weak transition

Standard Theory

no neutral current for flavor changing transition
GIM

$s \to u + W^-$ $\quad W^- \to d + \bar{u}$

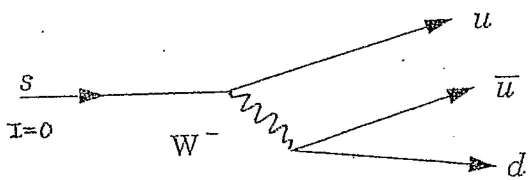

ΔI=1/2 or 3/2

		ratio
$\Delta I = \frac{1}{2}$	$\left(\frac{1}{2}\,\frac{1}{2}\,1\ \text{-}1 \,\middle|\, \frac{1}{2}\ \text{-}\frac{1}{2}\right) = \sqrt{\frac{2}{3}}$	2
$\Delta I = \frac{3}{2}$	$\left(\frac{1}{2}\,\frac{1}{2}\,1\ \text{-}1 \,\middle|\, \frac{3}{2}\ \text{-}\frac{1}{2}\right) = \sqrt{\frac{1}{3}}$	1

$\Lambda \to N + \pi$

$(\Lambda \to p + \pi^-) : (\Lambda \to n + \pi^0)$

$= 2:1$ for $\Delta I = \frac{1}{2}$

$= 1:2$ for $\Delta I = \frac{3}{2}$

$= 64\% : 36\%$ exp.

QCD corrections

QCD at work

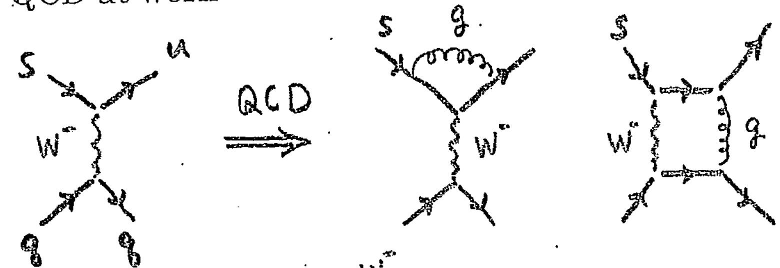

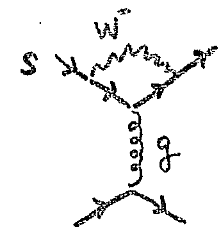

penguin diagram
(Vainshtein et al. 1977)

Perturbative QCD *(Gaillard-Lee, Altarelli-Maiani 1974)*

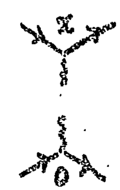

$$\int e^{iq\cdot x}\, T\,[\,W_\mu(x)\, W^\mu(0)\,]\, d^4x = \sum_m C_m(q^2;\mu^2)\ \hat{O}_m(\mu^2)$$

$$\hat{O}_m(\mu^2) = \ :\bar{q}\,\Gamma_m\, q\ \bar{q}\,\Gamma_m\, q:_{\mu^2}$$

local operator renormalized at $q^2=\mu^2$

hadron matrix elements evaluated at $\mu^2 \sim 1\ \mathrm{GeV}^2$

$$\langle \text{hadrons} \,|\, T \,|\, \text{hadrons} \rangle = \sum_m \underbrace{C_m(q^2;\mu^2)}_{\text{renormalization group equation}} \langle \text{hadrons} \,|\, \hat{O}_m \,|\, \text{hadrons} \rangle_{\mu^2}$$

Chiral structure of currents

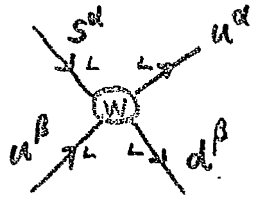

$$\gamma^\mu_L = \gamma^\mu(1-\gamma^5)$$

$$\hat{O} = (\bar{u}^\alpha \gamma^\mu_L s^\alpha)(\bar{d}^\beta \gamma_{L\mu} u^\beta) \equiv (\bar{u}^\alpha s^\alpha)_L (\bar{d}^\beta u^\beta)_L$$

α, β : color

Fierz equivalence

$$\hat{O} = (\bar{u}^\alpha s^\alpha)_L (\bar{d}^\beta u^\beta)_L = (\bar{d}^\beta s^\alpha)_L (\bar{u}^\alpha u^\beta)_L$$

symmetric under $u \longleftrightarrow d$ exchange
$\alpha \longleftrightarrow \beta$ in the final state

	$\Delta I = 1/2$ *antisym*	$\Delta I = 1/2 + 3/2$ *sym*
final I_f	0	1
color	$\bar{3}$	6
spin	0	0
$(\lambda_i \lambda_j)(\sigma_i \sigma_j)$	−8 *attractive*	4 *repulsive*

gluons (QCD) do not change chirality *but change color*

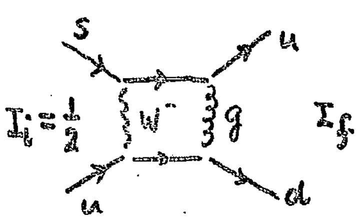

gluon exchange interaction
spin-dependence

$$-\alpha_s (\lambda_i \cdot \lambda_j)(\vec{\sigma}_i \cdot \vec{\sigma}_j)$$

attractive for $I_f = 0$ and repulsive for $I_f = 1$

Final $I_f = 0$ is enhanced by QCD $\Delta I = 1/2$

valence quarks in the baryon

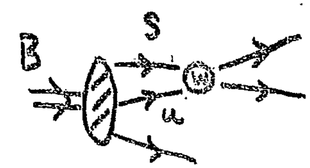

color singlet baryon
has no $C=6$ pair
$C=\bar{3}$ only

$I_f = 0$ only and pure $\Delta I = 1/2$

Miura-Minamikawa (1967), Pati-Woo(1971)

penguin diagram

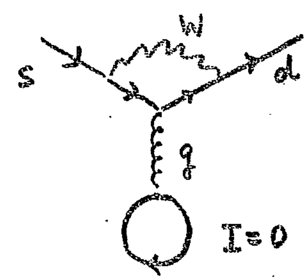

$s \longrightarrow d$ purely $\Delta I = 1/2$

$I=0$ $I=\frac{1}{2}$

Effective Weak Hamiltonian for $\Delta S = 1$

$$H_{eff}^{\Delta S=1} = -\frac{G_f}{\sqrt{2}} \sum_{r=1, r\neq 4}^{6} K_r O_r$$

he four-quark operators, O_k ($k = 1, 2, 3, 5$ and 6) are defined by [21]

$SU(3)$

$$\underline{8} \begin{cases} O_1 = (\bar{d}_\alpha s_\alpha)_{V-A}(\bar{u}_\beta u_\beta)_{V-A} - (\bar{u}_\alpha s_\alpha)_{V-A}(\bar{d}_\beta u_\beta)_{V-A} \\ O_2 = (\bar{d}_\alpha s_\alpha)_{V-A}(\bar{u}_\beta u_\beta)_{V-A} + (\bar{u}_\alpha s_\alpha)_{V-A}(\bar{d}_\beta u_\beta)_{V-A} \\ \quad + 2(\bar{d}_\alpha s_\alpha)_{V-A}(\bar{d}_\beta d_\beta)_{V-A} + 2(\bar{d}_\alpha s_\alpha)_{V-A}(\bar{s}_\beta s_\beta)_{V-A} \end{cases}$$

$$\underline{27} \quad O_3 = O_3(\Delta I = \tfrac{1}{2}) + O_3(\Delta I = \tfrac{3}{2})$$

$$\begin{cases} \underset{I=1/2}{27} \quad O_3\ (\ \Delta I = \tfrac{1}{2}) = \tfrac{1}{3} \times \\ \qquad [(\bar{d}_\alpha s_\alpha)_{V-A}(\bar{u}_\beta u_\beta)_{V-A} + (\bar{u}_\alpha s_\alpha)_{V-A}(\bar{d}_\beta u_\beta)_{V-A} \\ \qquad + 2(\bar{d}_\alpha s_\alpha)_{V-A}(\bar{d}_\beta d_\beta)_{V-A} - 3(\bar{d}_\alpha s_\alpha)_{V-A}(\bar{s}_\beta s_\beta)_{V-A}] \\ \underset{I=3/2}{27} \quad O_3\ (\ \Delta I = \tfrac{3}{2}) = \tfrac{5}{3} \times \\ \qquad [(\bar{d}_\alpha s_\alpha)_{V-A}(\bar{u}_\beta u_\beta)_{V-A} + (\bar{u}_\alpha s_\alpha)_{V-A}(\bar{d}_\beta u_\beta)_{V-A} \\ \qquad - (\bar{d}_\alpha s_\alpha)_{V-A}(\bar{d}_\beta d_\beta)_{V-A}] \end{cases}$$

96

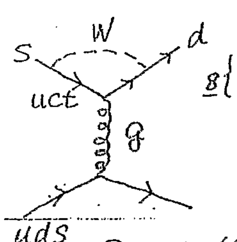

Penguin (QCD)

$$\underline{8} \begin{cases} O_5 = (\bar{d}_\alpha s_\alpha)_{V-A}(\bar{u}_\beta u_\beta + \bar{d}_\beta d_\beta + \bar{s}_\beta s_\beta)_{V+A} \equiv Q_5 \\ O_6 = (\underbrace{\bar{d}_\alpha s_\beta)_{V-A}(\bar{u}_\beta u_\alpha}_{\text{Color}} + \bar{d}_\beta d_\alpha + \bar{s}_\beta s_\alpha)_{V+A} \equiv Q_6 \end{cases}$$

$\to$ Scalar + Pseudoscalar

$(\bar{u}_\alpha s_\alpha)_{V-A} \equiv (\bar{u}_\alpha \gamma^\mu (1-\gamma_5)\, s_\alpha)$ etc.

K_r : Wilson coefficients (Paschos et al.)

$\boxed{K_1 = -0.284}$ $K_2 = 0.009$ $K_3 = 0.026$

$K_5 = 0.004$ $\boxed{K_6 = -0.021}$

(ΔI=1/2) / (ΔI=3/2) Ratio

K decay

$K^0 \longrightarrow \pi^+\pi^-\,,\ \pi^0\pi^0$ $\quad \Delta I = 1/2 + 3/2$

$K^+ \longrightarrow \underbrace{\pi^+\pi^0}_{I=2}$ $\quad \Delta I = 3/2$ only

S wave only + Bose Einstein Symmetry

$$\frac{K^0 \to \pi^+\pi^-}{K^+ \to \pi^+\pi^0} \sim 20 \quad \text{(exp)}$$

Hyperon decay

$\Lambda \longrightarrow N\pi$

$\Sigma \longrightarrow N\pi$

$$\frac{\Delta I = 1/2}{\Delta I = 3/2} \sim 20$$

Nonperturbative Effects

- Quark model calculations
  - final state interactions
  - color-symmetry in the valence quark model
  - MMPW theorem
- Chiral symmetry
  - soft-pion theorem

3. Nonperturbative QCD effects

hadronic corrections at low $q^2=\mu^2$

Hadron matrix elements

$$\langle \text{hadrons} \,|\, \sum_m C_m \hat{O}_m \,|\, \text{hadrons} \rangle_{\mu^2 = 1\,\text{GeV}^2}$$

gluonic effects

$K \longrightarrow \pi\pi$ decay matrix elements

enhancement of Q_6 operator (LQCD)

Penguin: S–PS vertex $\Delta I = 1/2$

final state interactions

$K \longrightarrow \pi\pi\,(I=0)$

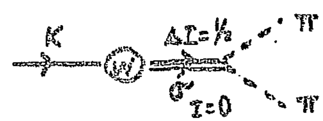

final state attraction

or a scalar σ (~ 600 MeV) resonance

(Morozumi–Lim–Sanda, 1990)

(Takizawa–Inoue–Oka, 1994)

chiral symmetry

soft-pion theorem **for Baryons**

Soft-Pion Theorem

PCAC + reduction formula

π matrix element $\rightarrow$ no π matrix element

$$\langle \alpha\, \pi^a(q) \,|\, \mathcal{O} \,|\, \beta \rangle$$

$$= i \int d^4x\, e^{iq\cdot x} (\Box + m_\pi^2) \langle \alpha |\, T[\phi_\pi^a(x)\, \mathcal{O}(0)] \,|\beta\rangle$$

$q \longrightarrow 0$ soft-pion limit

$$\longrightarrow i \int d^4x\, e^{iq\cdot x} (\Box + m_\pi^2) \frac{1}{f_\pi m_\pi^2} \langle \alpha |\, T[\partial_\mu A_a^\mu(x)\, \mathcal{O}(0)] \,|\beta\rangle$$

$$= \frac{-i}{f_\pi} \frac{1}{(2\pi)^{3/2}} \langle \alpha |\, [Q_5^a, \mathcal{O}(0)] \,|\beta\rangle$$

$$+ \lim_{q\to 0} \frac{q_\mu}{f_\pi} \int d^4x\, \frac{e^{iq\cdot x}}{(2\pi)^{3/2}} \langle \alpha |\, T[A_a^\mu(x)\, \mathcal{O}(0)] \,|\beta\rangle$$

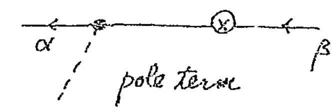

Soft Pion for $Y \to N\pi$ decays

PV amplitude: *soft-pion relation*

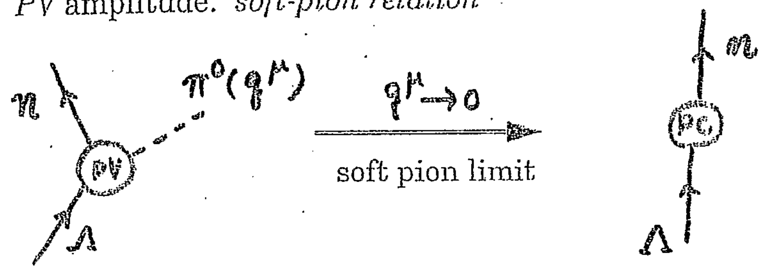

$$\left\langle n\pi^0(q)\right| H^{PV} \left|\Lambda\right\rangle \to \frac{-i}{f_\pi}\left\langle n\right|\left[Q_5^0 , H^{PV}\right]\left|\Lambda\right\rangle = \frac{-i}{2f_\pi}\left\langle n\right| H^{PC} \left|\Lambda\right\rangle$$

H_{WEAK} left-handed currents $\bar{q}_L^a \gamma^\mu q_L^b$ and QCD corrections (flavor singlet)

$$\left[Q_R^a , H_W\right] = 0$$
$$\left[Q_5^a , H_W\right] = \left[Q_R^a - Q_L^a , H_W\right] = -\left[Q_L^a , H_W\right] = -\left[I^a , H_W\right]$$
$$I^a = Q_R^a + Q_L^a$$
$$\left[Q_5^a , H^{PV}\right] = -\left[I^a , H^{PC}\right]$$

$$\left\langle n\right|\left[Q_5^0 , H^{PV}\right]\left|\Lambda\right\rangle = -\left\langle n\right|\left[I^a , H^{PC}\right]\left|\Lambda\right\rangle = -\frac{1}{2}\left\langle n\right| H^{PC}\left|\Lambda\right\rangle$$

$\Delta I = 1/2$ ***rule follows with MMPW mechanism***

PC amplitude: *pole dominance approximation*

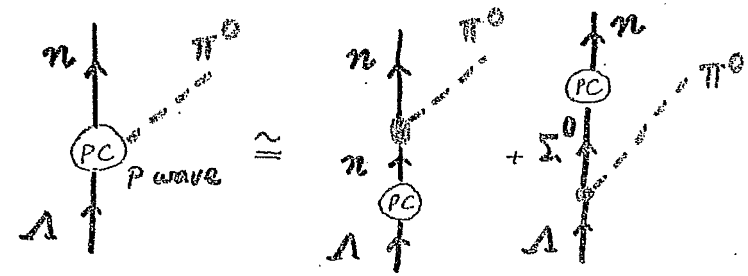

$$\left\langle n\pi^0(q)\right| H^{PC} \left|\Lambda\right\rangle = \left\langle n\pi^0\right| n\rangle \frac{i}{m_\Lambda - m_n}\left\langle n\right| H^{PC}\left|\Lambda\right\rangle$$
$$+\left\langle n\right| H^{PC}\left|\Sigma^0\right\rangle \frac{i}{m_n - m_\Sigma}\left\langle \Sigma^0\pi^0\right|\Lambda\rangle$$

$\Delta I = 1/2$ only (MMPW)

$\Sigma^+ \to n + \pi^+$ decay

PV exp. 0.13

$$\left\langle n\pi^+\right| H^{PV}\left|\Sigma^+\right\rangle \to \frac{i}{f_\pi}\left\langle n\right|\left[I^- , H^{PC}\right]\left|\Sigma^+\right\rangle$$
$$= \frac{i}{f_\pi}\left[\left\langle p\right| H^{PC}\left|\Sigma^+\right\rangle - \sqrt{2}\left\langle n\right| H^{PC}\left|\Sigma^0\right\rangle\right] = 0$$

if $\Delta I = 1/2$: $H^{PC}(\Delta I = \frac{1}{2}, \Delta I_3 = -\frac{1}{2})$

$$\left[I^- , H^{PC}\right] = 0 \qquad \left\langle p\right| H^{PC}\left|\Sigma^+\right\rangle = \sqrt{2}\left\langle n\right| H^{PC}\left|\Sigma^0\right\rangle$$

PC exp. 42.2

$$\left\langle n\pi^+(q)\right| H^{PC}\left|\Sigma^+\right\rangle = \left\langle n\pi^+\right| p\rangle \frac{i}{m_\Sigma - m_p}\left\langle p\right| H^{PC}\left|\Sigma^+\right\rangle$$
$$+\left\langle n\right| H^{PC}\left|\Sigma^0\right\rangle \frac{i}{m_n - m_\Sigma}\left\langle \Sigma^0\pi^+\right|\Sigma^+\rangle + (\Sigma^0 \to \Lambda)$$

4. Nonmesonic Weak Decay of Hypernuclei

$\Lambda N \to NN$

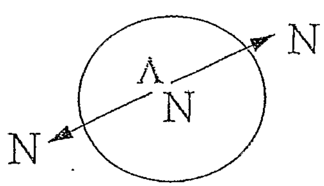

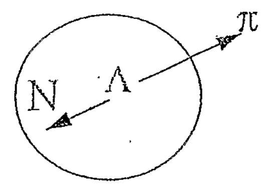

$p_N \approx 400$ MeV / c
Short distance

$p_N \approx 100$ MeV / c
Pauli blocked

Conventional Approach

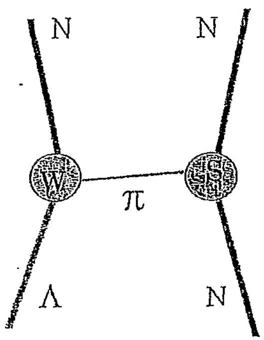

One Pion Exchange

(Block-Dalitz, 1963)

strong tensor transition

$\Lambda p \ ^3S_1 \to np \ ^3S_1, \ ^3D_1$

$\Gamma_n / \Gamma_p \approx 0.1$
much smaller than
experiment

Heavy Mesons $K + \rho + \omega + K^* + 2\pi(\sigma) + \ldots$

(McKeller-Gibson, 1984) (Takeuchi-Takaki-Bando, 1985)
(Dubach et al., 1996) (Parreno-Ramos-Bennhold, 1997)
(Shmatikov, 1994) (Itonaga-Ueda-Motoba, 1995)

Nuclear Force $\pi + \rho + \omega + 2\pi(\sigma) + \ldots$

Quark Exchange Force

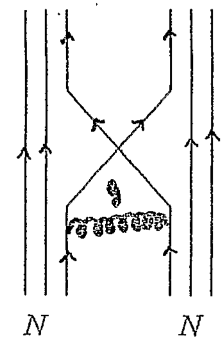

NN Short-range repulsion

(Oka-Yazaki, 1980)

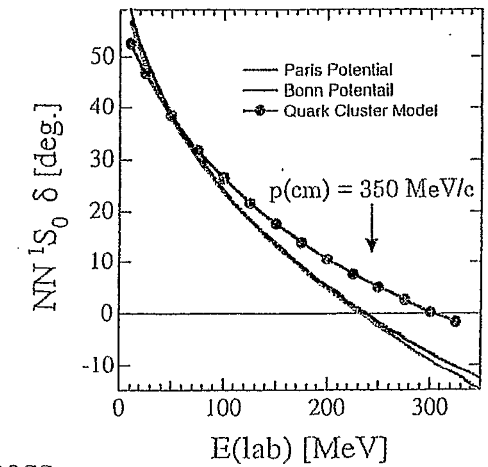

Direct Quark Process

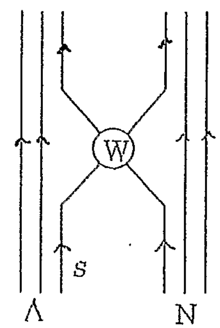

W = Effective 4–quark weak vertices including the one-loop QCD corrections

$s\,u \longrightarrow d\,u$
$s\,d \longrightarrow d\,d$ transitions

(Cheung-Heddle-Kisslinger, 1983)
(Oka-Inoue-Takeuchi, 1994)
(Maltman-Shmatikov, 1994)

→ Decays of Light Hypernuclei

→ Decays of Lambda in Nuclear Matter

(Inoué, Oka, Motoba, Itonaga, 1998, Sasaki, Inoue, Oka, 1999, 2000)

Chiral Perturbation Theory Approach

Baryonic Weak Effective Lagrangian

J. Bijnens, et al (1985)
E. Jenkins (1992)

$SU(3)$

$$\mathcal{L}_{\rm Weak} = d\,{\rm Tr}\left(\bar{B}\{h_+, B\}\right) + f\,{\rm Tr}\left(\bar{B}[h_+, B]\right)$$
$$+(\text{higher order terms})$$

$$h_+ \equiv \xi^\dagger h \xi + \xi^\dagger h^\dagger \xi \quad , \quad h \equiv \begin{pmatrix} 0 & 0 & 0 \\ 0 & 0 & 1 \\ 0 & 0 & 0 \end{pmatrix} \; s \to d$$

$$\xi^2 \equiv U = \exp\left(\frac{i\Phi}{f_\pi}\right)$$

Φ : 3× 3 meson octet fields in SU(3)

B : 3× 3 baryon octet fields in SU(3)

Assume $h \to L h L^\dagger$: left handed $\underline{8}$ $\Delta I = 1/2$ only

then h_+ is transformed as matter field

$$h_+ \to K h_+ K^\dagger \cdot \quad B \to K B K^\dagger$$

Thus $\mathcal{L}_{\rm Weak}$ is chiral invariant.

Hyperon Weak Decay Amplitudes

Borosoy and Holstein (1999)

$$\frac{f}{F_\pi} = 0.92 \times 10^{-7} \quad , \quad \frac{d}{f} = -0.42$$

lowest order

Mode	A^{exp}	A^{th}	B^{exp}	B^{th}
$\Lambda^0 \to p\pi^-$	3.25	3.38	22.1	23.0
$\Lambda^0 \to n\pi^0$	-2.37	-2.39	-15.8	-16.0
$\Sigma^+ \to n\pi^+$	0.13	0.00	42.2	4.3
$\Sigma^+ \to p\pi^0$	-3.27	-3.18	26.6	10.0
$\Sigma^- \to n\pi^-$	4.27	4.50	-1.44	-10.0
$\Xi^0 \to \Lambda^0\pi^0$	3.43	3.14	-12.3	3.3
$\Xi^- \to \Lambda^0\pi^-$	-4.51	-4.45	16.6	-4.7
	S		P	

Table 5: Decay amplitudes for Nonleptonic Hyperon Decay (in units of 10^{-7}). The theoretical amplitudes are the values arising from a lowest order chiral fit.

S wave amplitudes are well reproduced.

P wave amplitudes have large corrections from
higher order contributions.
positive parity baryon resonances

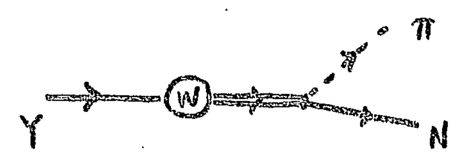

Weak hyperon-nucleon interactions

hadronic matrix element for $\Lambda N \longrightarrow NN$

of 4-quark operators at $\mu^2 \sim 1\,\mathrm{GeV}^2$

expansion in terms of ranges of interaction
or momentum transfer q^2

$$\langle NN \mid \sum_m C_m \hat{O}_m \mid \Lambda N \rangle_{\mu^2}$$

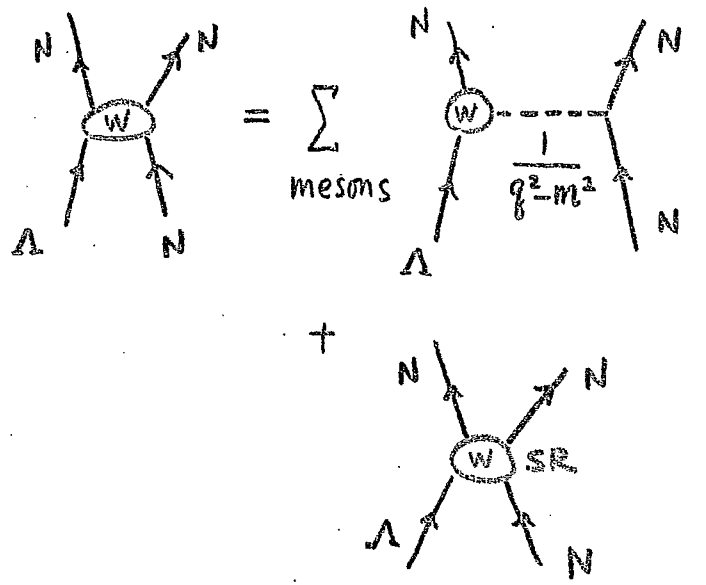

- $q \sim 400\,\mathrm{MeV}/c$
  strong repulsion in NN force
  from Quark Exchange
  M.O. K.Yazaki (1980)
- Saturation of Γ (A → large)

Direct Quark (DQ) Process

Inoue - Takeuchi - Oka (19

valence quark model
nonrelativistic kinematics
SU(6) wave functions

p/m_q expansion of H_w ($\Delta S=1$) with $m_q \sim 350\,\mathrm{MeV}/c^2 \sim \frac{M_B}{3}$

quark antisymmetrization via quark cluster wave fuction

Ⓦ : 4 quark operators
$su \to ud$
$sd \to dd$

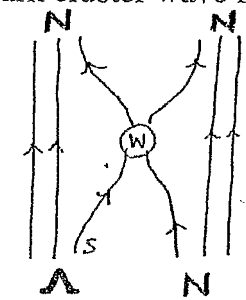

Transition potential

$T_{fi} = \langle \Psi_f \mid H_w (\Delta S=1) \mid \Psi_i \rangle$

for NN (L=0,1) ⟵ ΛN (L=0) J=0, 1

nonlocal due to antisymmetrization

PC + PV parts $\Delta I = 1/2$ and $3/2$

range ~ 0.5 fm (size of quark wave function)

$$V_{LSJ \to L'S'J}(r, r') = V_{local}(r) \frac{\delta(r-r')}{r^2} + \underbrace{V_{der}(r) \frac{\delta(r-r')}{r^2} \partial_r}_{PV} + V_{nonlocal}(r, r')$$

Strong $\Delta I = 3/2$ contribution in J=0 transitions

$\Lambda N \ {}^1S_0 \longrightarrow NN \ {}^1S_0$: a

$\qquad\qquad\qquad\quad\ {}^3P_0$: b

Decay of Light Hypernuclei

K. Sasaki, T. Inoue, M. O. T. Motoba, K. Itonaga (1998, 2000)

OPE (π) induces

strong ***tensor*** transition

$^3S_1 \rightarrow {}^3D_1$ only in $\Lambda p \rightarrow np$

enhances Γ_p

OKE (*K*)

tensor contribution with opposite sign

reduces Γ_p

enhances parity violating (*PV*) transition: new

$^3S_1 \rightarrow {}^3P_1$ both in Λp (f_p) and Λn (f_n)

DQ

$^3S_1 \rightarrow {}^3P_1$ (f_p and f_n) transition dominant

not violating $\Delta I = 1/2$

enhances $\Gamma_n / \Gamma_p \approx 1$

and $PV/PC \sim 6.8$

J=0 transition amplitudes (*a* and *b*) are small

but are dominantly $\Delta I = 3/2$

$\pi + K + DQ$

$\Gamma_p \approx 0.304\,\Gamma_\Lambda$
$\Gamma_n \approx 0.219\,\Gamma_\Lambda$
$\Gamma_n / \Gamma_p \approx 0.72$

$^5_\Lambda He$

proton asymmetry $\alpha_p \simeq$ 0.68 (>0 exp) KEK E307

$PV/PC \approx 4.8$

$$\frac{\Gamma_{n0}}{\Gamma_{p0}} \simeq 0.1 \longleftrightarrow 2 \text{ in } \Delta I = \frac{1}{2}$$

Sasaki – Inoue – Oka NPA 669 (2000) 331 (E) A678

J=0 & 1

Table 1: Nomesonic Decay Width of $^5_\Lambda$He in unit of Γ_Λ

	channel	π	π+K	DQ	π+DQ	π+K+DQ
$^1S_0 \rightarrow {}^1S_0$	a_p	0.002	0.004	0.004	0.010	0.015
$^1S_0 \rightarrow {}^3P_0$	b_p	0.007	0.000	0.005	0.024	0.008
$^3S_1 \rightarrow {}^3S_1$	c_p	0.005	0.009	0.004	0.000	0.001
$^3S_1 \rightarrow {}^3D_1$	d_p	0.241	0.073	0.000	0.241	0.073
$^3S_1 \rightarrow {}^1P_1$	e_p	0.060	0.077	0.001	0.078	0.097
$^3S_1 \rightarrow {}^3P_1$	f_p	0.013	0.044	0.015	0.056	$\boxed{0.110}$
$^1S_0 \rightarrow {}^1S_0$	a_n	0.003	0.007	0.004	0.000	0.001
$^1S_0 \rightarrow {}^3P_0$	b_n	0.013	0.000	0.004	0.003	0.002
$^3S_1 \rightarrow {}^3P_1$	f_n	0.027	0.089	0.028	0.109	$\boxed{0.217}$
	Γ_p	0.328	0.207	0.030	0.410	0.304
	Γ_n	0.044	0.097	0.036	0.112	0.219
	total	0.372	0.304	0.066	0.523	0.523
	n/p	0.133	0.466	$\boxed{1.216}$	0.274	0.720
	asy	-0.441	-0.362	-0.398	-0.769	-0.678

Γ_p : $\Lambda p \rightarrow pn$

Γ_n : $\Lambda n \rightarrow nn$

Table 1: Nomesonic Decay Width of ${}^{5}_{\Lambda}$He in unit of Γ_Λ

${}^{5}_{\Lambda}$He	total	Γ_p	Γ_n	Γ_n/Γ_p	α
π	0.372	0.328	0.044	0.133	-0.441
π+K	0.304	0.207	0.097	0.466	-0.362
DQ	0.066	0.030	0.036	1.216	-0.398
π+K+DQ	0.523	0.304	0.219	0.720	-0.678
EXP [1]	0.41±0.14	0.21±0.07	0.20±0.11	0.93±0.55	—
EXP [2]	0.50±0.07	0.17±0.04	0.33±0.04	1.97±0.67	—
EXP [3]	—	—	—	—	0.24±0.22

Table 2: Nomesonic Decay Width of ${}^{4}_{\Lambda}$He in unit of Γ_Λ

${}^{4}_{\Lambda}$He	total	Γ_p	Γ_n	Γ_n/Γ_p	α
π	0.272	0.250	0.022	0.089	-0.417
π+K	0.155	0.145	0.009	0.064	-0.357
DQ	0.032	0.021	0.011	0.516	-0.373
π+K+DQ	0.218	0.214	0.004	0.019	-0.679
β= -0.1	0.261	0.256	0.005	0.021	-0.679
1 % Σ β= 0.1	0.178	0.175	0.003	0.017	-0.656
EXP [2]	0.19±0.04	0.15±0.02	0.04±0.02	0.27±0.14	—

2 Σ-Mixing in Light Hypernuclei

<u>Σ hypernuclei</u> real (~on-shell) Σ

$^{4}_{\Sigma}\mathrm{He}$ ***Nagae et al. (1998)***

<u>A=3</u> virtual Σ mixing

or three-body force in $^{3}_{\Lambda}\mathrm{H} = (p, n, \Lambda) + (p, n, \Sigma)$

coupled channel calculation

by ***Miyagawa et al. (1995)***

<u>A=4</u>

charge symmetry breaking in $^{4}_{\Lambda}\mathrm{He} - ^{4}_{\Lambda}\mathrm{H}$

due to $\Sigma^{\pm}, \Sigma^{0}$ mass differences

4-body coupled channel calculation

by ***Hiyama et al. (2000)***

J=0+ strong Σ mixing ~ 1.8 %

J=1+ weaker ~ 1.1 %

coherent Σ mixing by ***Akaishi et al. (2000)***

differs from $^{5}_{\Lambda}\mathrm{He}$ (I=0)

<u>Coherent</u> Σ mixing by ***Akaishi et al. (2000)***

overbinding problem of S-shell hypernuclei

$^{5}_{\Lambda}\mathrm{He}$ binding energy suppressed by incoherent Σ mixing

$^{4}_{\Lambda}\mathrm{He}$ binding energy enhanced by coherent mixing of Σ

0^+ 1 ~ 2 %

1^+ ~0.01 %

$$\underset{I=1/2}{|^{4}_{\Lambda}\mathrm{He}\rangle} = \alpha\,|\underset{I=0}{\Lambda} + \underset{1/2}{^{3}\mathrm{He}}\rangle + \beta\,|\underset{I=1}{\Sigma} + \underset{1/2}{^{3}\mathrm{He}}\rangle$$

$$\underset{I=0}{|^{5}_{\Lambda}\mathrm{He}\rangle} = |\underset{I=0}{\Lambda} + \underset{0}{^{4}\mathrm{He}}\rangle \quad \cancel{|\underset{I=1}{\Sigma} + \underset{0}{^{4}\mathrm{He}}\rangle}$$

<u>Spin-orbit interactions</u>

ΛN $\Leftrightarrow$ ΣN coupling in ALS interactions

antisymmetric LS force $(\vec{\sigma}_\Lambda - \vec{\sigma}_N)\cdot\vec{L}$

induces ${}^3P_1 \leftrightarrow {}^1P_1$ mixing

$$\begin{aligned} V_{SO} &= V_{SLS}(\vec{\sigma}_\Lambda + \vec{\sigma}_N)\cdot\vec{L} + V_{ALS}(\vec{\sigma}_\Lambda - \vec{\sigma}_N)\cdot\vec{L} \\ &= (V_{SLS}+V_{ALS})\,\vec{\sigma}_\Lambda\cdot\vec{L} + (V_{SLS}-V_{ALS})\,\vec{\sigma}_N\cdot\vec{L} \end{aligned}$$

SU(3) relations for ${}^3P_1 \leftrightarrow {}^1P_1$ matrix elements

$$\begin{aligned} \langle \Lambda N\,{}^1P_1|V|\Lambda N\,{}^3P_1\rangle &= V_0 \\ \langle \Sigma N\,{}^1P_1|V|\Lambda N\,{}^3P_1\rangle &= -V_0 \\ \langle \Lambda N\,{}^1P_1|V|\Sigma N\,{}^3P_1\rangle &= 3V_0 \\ \langle \Sigma N\,{}^1P_1|V|\Sigma N\,{}^3P_1\rangle &= -3V_0 \end{aligned}$$

Oka-Tani-Takeuchi

Strong ALS potential due to quark exchange force

QCM calculation *Takeuchi (2000)*

ALS is enhanced by ΣN coupling

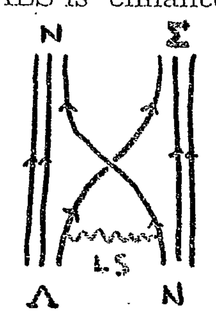

${}^4_\Lambda$He

coherent Σ mixing

$$|{}^4_\Lambda\mathrm{He}(0^+)\rangle = \alpha\,|\Lambda \oplus {}^3\mathrm{He}\rangle + \beta\,|\Sigma \oplus {}^3\mathrm{He}\rangle$$

$$\begin{aligned} |\Sigma \oplus {}^3\mathrm{He}\rangle = {} & \sqrt{\tfrac{2}{9}}|(\Sigma^+p)^0(nn)^0\rangle + \sqrt{\tfrac{1}{9}}|(\Sigma^0n)^0(pp)^0\rangle \\ & -\sqrt{\tfrac{1}{9}}|(\Sigma^+n)^0(pn)^0\rangle - \sqrt{\tfrac{1}{18}}|(\Sigma^0p)^0(pn)^0\rangle \\ & +\sqrt{\tfrac{1}{3}}|(\Sigma^+n)^1(pn)^1\rangle - \sqrt{\tfrac{1}{6}}|(\Sigma^0p)^1(pn)^1\rangle \end{aligned}$$

$\Sigma^+p \to pp$ decay

$$|\beta|^2\,\frac{2}{9} \lesssim 0.5\,\%$$

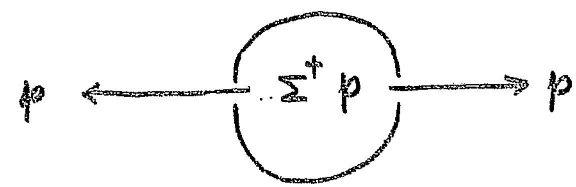

π^+ decay of Light Hypernuclei

${}^4_\Lambda He \longrightarrow \pi^+ p\, n\, n$ ~ 5% of π^- decay
S wave $E_\pi < 20$ MeV

Single Λ decay $\longrightarrow$ $p\pi^-$ or $n\pi^0$ does not emit π^+

need a two-body process
$\Lambda p \longrightarrow nn\pi^+$

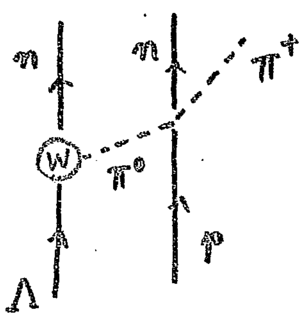

charge exchange

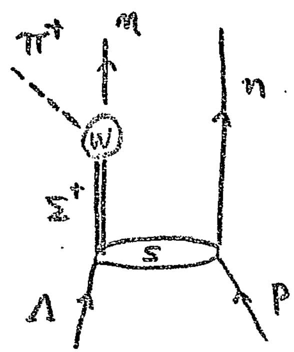

Σ^+ *mixing*

Soft pion limit for $\Lambda\, p \to n\, n\, \pi^+$ process

$$\langle n n\, \pi^+(q) \,|\, H_W \,|\, \Lambda p \rangle$$

$$\xrightarrow[q^\mu \to 0]{} -\frac{i}{\sqrt{2} f_\pi} \langle nn | [Q_5^-, H_W] | \Lambda$$

$$[Q_5^-, H_W] = -[I^-, H_W]$$

$H_W(\Delta I_3 = -\tfrac{1}{2})$ lowers I_3 by $\tfrac{1}{2}$

$$\begin{cases} \Delta I = \tfrac{1}{2} & [I^-, H_W(\Delta I = \tfrac{1}{2}, \Delta I_3 = -\tfrac{1}{2})] = 0 \\ \Delta I = \tfrac{3}{2} & [I^-, H_W(\Delta I = \tfrac{3}{2}, \Delta I_3 = -\tfrac{1}{2})] \end{cases}$$

$$= \sqrt{3}\, H_W(\Delta I = \tfrac{3}{2}, \Delta I_3 = -$$

$$\langle n n\, \pi^+(q) | H_W | \Lambda p \rangle$$

$$\to \frac{i\sqrt{3}}{\sqrt{2} f_\pi} \underbrace{\langle nn}_{I_3 = -1} | H_W(\Delta I = \tfrac{3}{2}, \Delta I_3 = -\tfrac{3}{2}) | \underbrace{\Lambda p \rangle}_{I_3 = +\frac{1}{2}}$$

Only the ΔI=3/2 part of the Hamiltonian survives in the ***soft-pion*** limit.

excellent probe of $\Delta I = 3/2$ process

$\Delta I = \frac{1}{2}, \frac{3}{2}$ in ${}^{4}_{\Lambda}He$ ${}^{4}_{\Lambda}H$ ${}^{5}_{\Lambda}He$ decays

		data	$DQ+{}^{\pi}_{K}$
${}^{5}_{\Lambda}He$	$\Gamma_p^5 = \rho_5 \left(\frac{1}{2}\Gamma_{p0} + \underline{\frac{3}{2}\Gamma_{p1}} \right)$	0.2	0.26
$pp\,nn\,\Lambda$	$\Gamma_n^5 = \rho_5 \left(\frac{1}{2}\Gamma_{n0} + \frac{3}{2}\Gamma_{n1} \right)$	0.2	0.08
${}^{4}_{\Lambda}He$	$\Gamma_p^4 = \rho_4 \left(\frac{1}{2}\Gamma_{p0} + \underline{\frac{3}{2}\Gamma_{p1}} \right)$	0.15	0.18
$pp\,\underbrace{n\Lambda}_{J=0}$	$\Gamma_n^4 = \rho_4 \Gamma_{n0}$	0.04	0.01
		$(\Delta I = \frac{1}{2}$	
${}^{4}_{\Lambda}H$	$\Gamma_p^{4\prime} = \rho_4 \Gamma_{p0}$	(0.02)	0.05
$nn\,\underbrace{p\Lambda}_{J=0}$	$\Gamma_n^{4\prime} = \rho_4 \left(\frac{1}{2}\Gamma_{n0} + \frac{3}{2}\Gamma_{n1} \right)$	(0.15)	0.05

unit $\Gamma_\Lambda(\text{free})$

$$\frac{\rho_5}{\rho_4} = \frac{\Gamma_p^5}{\Gamma_p^4} = \frac{\Gamma_n^5}{\Gamma_n^{4\prime}}$$

$$\frac{\Gamma_{n0}}{\Gamma_{p0}} = \frac{\Gamma_n^4}{\Gamma_p^{4\prime}} = 2 \quad \Delta I = \frac{1}{2}$$

$$\sim \frac{1}{5} \quad DQ + \pi + K$$

Conclusion

Hadronic weak interactions of strange particles
require nonperturbative QCD interference.

Hyperon decays
Qualitative behaviors are fairly well understood.

Two problems remain for quantitative study.
S/P problem
$(\Delta I=3/2)/(\Delta I=1/2)$ ratio

Hypernuclear decays
Novel direct quark interaction at short distances

Phenomenological problems
Γ_n/Γ_p resolved
proton asymmetry

$\Delta I=3/2$ may be as strong as $\Delta I=1/2$.
S-shell hypernuclei
π^+ decays

Coherent Σ mixing effects are significant
in A=4 hypernuclei
$\Sigma^+ p$ --> pp decays

Basics of QCD perturbation theory

D. E. Soper
Institute of Theoretical Science, University of Oregon
Eugene, OR 97403 USA

A prediction for experiment based on perturbative QCD combines a particular calculation of Feynman diagrams with the use of general features of the theory that allow the Feynman diagrams to be related to experiment. The calculational part is easy at leading order, not so easy at next-to-leading order or even higher orders. The subject of how to do these calculations is interesting, but is not included in these lectures. Rather, I discuss the general features of the theory that make a calculation relevant. These features include the renormalization group and the running coupling; the existence of infrared safe observables; and the isolation of hadron structure in parton distribution functions. The key idea is that QCD describes processes on a wide range of momentum scales. Furthermore, these processes can occur in the same event. Thus we need to sort out the role that processes at different momentum scales play in determining a measured cross section. Along the way we will learn about some useful kinematical concepts: light-cone coordinates and rapidity. We will study three important types of experiments. I begin with e^+e^- annihilation, which is simple because it has no hadrons in the initial state. Then I turn to deeply inelastic scattering, including the definition of the structure functions that are used for its description. Finally, I discuss the production in hadron-hadron collisions of heavy particles and of jets.

Basics of QCD perturbation theory

D. E. Soper

RIKEN, March 2002

Abstract

A prediction for experiment based on perturbative QCD combines

• a particular calculation of Feynman diagrams (easy at leading order, not so easy at next-to-leading order).

• use of general features of the theory that allow the Feynman diagrams to be related to experiment:

  • renormalization group and the running coupling;
  • existence of infrared safe observables;
  • isolation of hadron structure in parton distribution functions.

I will discuss these structural features of the theory that allow a comparison of theory and experiment. Along the way we will discover something about certain important processes: e^+e^- annihilation, deeply inelastic scattering, and jet production in hadron-hadron collisions.

Disclaimer. We will not learn how to do significant calculations in QCD perturbation theory. Three hours is not enough for that.

How final states form

Exploring the QCD final state with e^+e^- annihilation

A) Structure of the cross section.
B) Null plane coordinates.
C) Space-time picture of the singularities.
D) The long time problem and infrared safe observables.

Electron-positron to three partons

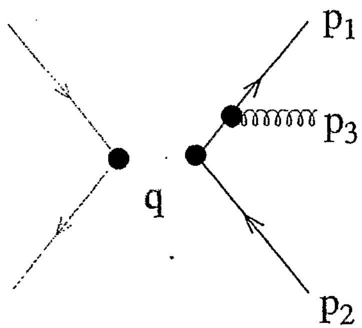

$$\frac{1}{\sigma_0}\frac{d\sigma}{dE_3\,d\cos\theta_{13}} = \frac{\alpha_s}{2\pi}C_F\frac{f(E_3,\theta_{13})}{E_3(1-\cos\theta_{13})}$$

where $f(E_3,\theta_{13})$ is finite for $E_3 \to 0$ and for $\theta_{13} \to 0$.

Collinear singularity, $\theta_{13} \to 0$:

$$\int_a^1 d\cos\theta_{13}\ \frac{d\sigma}{dE_3\,d\cos\theta_{13}} = \log(\infty).$$

Soft singularity, $E_3 \to 0$:

$$\int_0^a dE_3\ \frac{d\sigma}{dE_3\,d\cos\theta_{13}} = \log(\infty).$$

That's great, but is there a general reason for it?

Why is $e^+e^- \to 3$ partons singular?

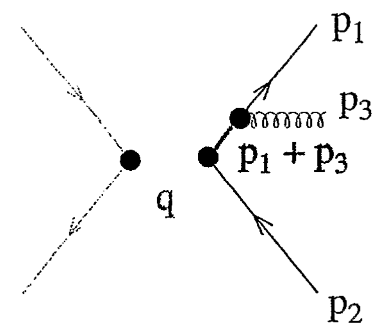

$\mathcal{M}$ contains a factor $1/(p_1+p_3)^2$ where

$$(p_1+p_3)^2 = 2p_1\cdot p_3 = 2E_1E_3(1-\cos\theta_{13}).$$

Also, a numerator factor $\propto \theta_{13}$ in the collinear limit. So

$$|\mathcal{M}|^2 \propto \left[\frac{\theta_{13}}{E_3\theta_{13}^2}\right]^2$$

for $E_3 \to 0$ or $\theta_{13} \to 0$.
Integration:

$$\int \frac{E_3^2 dE_3 d\cos\theta_{13} d\phi}{E_3} \sim \int E_3 dE_3 d\theta_{13}^2 d\phi.$$

Together:

$$d\sigma \sim \int E_3 dE_3 d\theta_{13}^2 d\phi \left[\frac{\theta_{13}}{E_3\theta_{13}^2}\right]^2 \sim \int \frac{dE_3}{E_3}\ \frac{d\theta_{13}^2}{\theta_{13}^2}\ d\phi.$$

Note the universal nature of these factors.

Interlude: Null plane coordinates

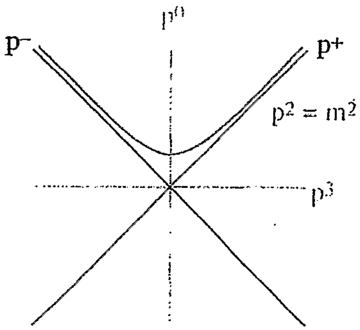

Use $p^\mu = (p^+, p^-, p^1, p^2)$ where

$$p^\pm = (p^0 \pm p^3)/\sqrt{2}.$$

• For a particle with large momentum in the $+z$ direction and limited transverse momentum, p^+ is large and p^- is small.
• Often one *chooses* the + axis so that a particle or group of particles of interest have large p^+ and small p^- and p_T.
• Covariant square:

$$p^2 = 2p^+p^- - \mathbf{p}_T^2.$$

• p^- for a particle on its mass shell:

$$p^- = \frac{\mathbf{p}_T^2 + m^2}{2p^+}.$$

Kinematics of null plane coordinates, continued.

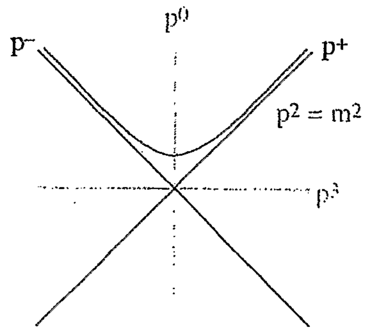

• For a particle on its mass shell,

$$p^+ > 0\,, \qquad p^- > 0\,.$$

• Integration over the mass shell:

$$(2\pi)^{-3} \int \frac{d^3\vec{p}}{2\sqrt{\vec{p}^{\,2} + m^2}} \cdots = (2\pi)^{-3} \int d^2\mathbf{p}_T \int_0^\infty \frac{dp^+}{2p^+} \cdots.$$

• Fourier transform:

$$p \cdot x = p^+x^- + p^-x^+ - \mathbf{p}_T \cdot \mathbf{x}_T.$$

So x^- is conjugate to p^+ and x^+ is conjugate to p^-. (Sorry.)

Space-time picture of the singularities

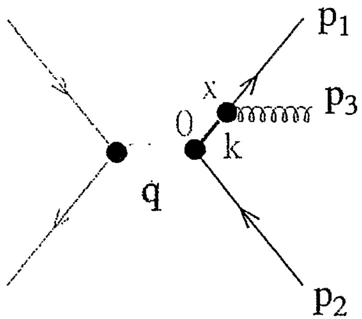

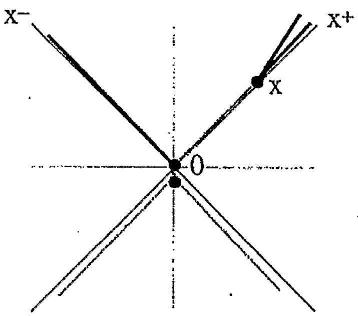

Define $p_1^\mu + p_3^\mu = k^\mu$.
Choose null-plane coordinates with k^+ large and $\mathbf{k}_1^T = \mathbf{0}$.
Then $k^2 = 2k^+k^-$ becomes small when

$$k^- = \frac{\mathbf{p}_3^2}{2p_1^+} + \frac{\mathbf{p}_3^2}{2p_3^+}$$

becomes small. (Collinear or soft singularity.)

Consider the fourier transform.

$$S_F(k) = \int dx^+ dx^- d\mathbf{x}\, \exp(i[k^+x^- + k^-x^+ - \mathbf{k}\cdot\mathbf{x}])\; S_F(x).$$

Contributing values of x have small x^- large x^+.

Long time picture

Perturbation theory suggests the generic structure of long time physics:

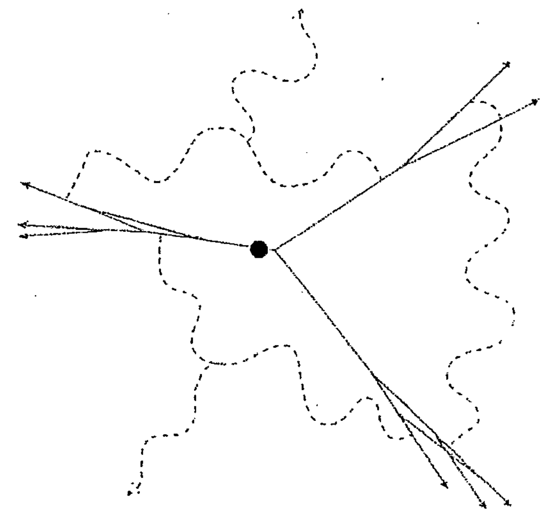

Thus QCD suggests a jet structure of final state hadrons.

• This structure is (approximately) modelled in Monte Carlo event generators (Pythia, Herwig,...).

"Summed" perturbation theory suggests this is OK.
But beware of "nonperturbative" effects!

That's a qualitative success. But can you predict reliable numbers?

The long time problem

Perturbation theory not effective for long time physics. But the detector is a long distance away!

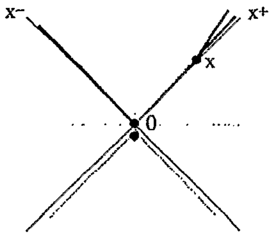

Answer

Use measurements that are not sensitive to long time physics.
Example: the e^+e^- annihilation total cross section.
Effects from $\Delta x \gg 1/\sqrt{s}$ cancel because of unitarity:

$$\begin{aligned}&\langle 0|J(y')U(y',\infty)U(\infty,y)J(y)|0\rangle\\ &\qquad = \langle 0|J(y')U(y',y)J(y)|0\rangle\end{aligned}$$

At order α_s, this works by a cancellation between real gluon emission graphs and virtual gluon graphs.

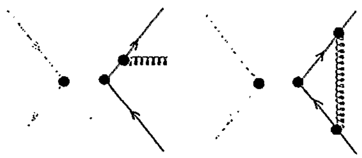

If the total cross section is all you can look at, QCD physics will be a little boring!

Infrared safe quantities

Some quantities are not sensitive to infrared effects.

$$\begin{aligned}\mathcal{I} = &\frac{1}{2!}\int d\Omega_2\ \frac{d\sigma[2]}{d\Omega_2}\ \mathcal{S}_2(p_1^\mu,p_2^\mu)\\ &+\frac{1}{3!}\int d\Omega_2 dE_3 d\Omega_3\ \frac{d\sigma[3]}{d\Omega_2 dE_3 d\Omega_3}\ \mathcal{S}_3(p_1^\mu,p_2^\mu,p_3^\mu)\\ &+\frac{1}{4!}\int d\Omega_2 dE_3 d\Omega_3 dE_4 d\Omega_4\\ &\qquad\times\frac{d\sigma[4]}{d\Omega_2 dE_3 d\Omega_3 dE_4 d\Omega_4}\ \mathcal{S}_4(p_1^\mu,p_2^\mu,p_3^\mu,p_4^\mu)\\ &+\cdots.\end{aligned}$$

Need (for $\lambda = 0$ or $0 < \lambda < 1$)

$$\mathcal{S}_{n+1}(p_1^\mu,\dots,(1-\lambda)p_n^\mu,\lambda p_n^\mu) = \mathcal{S}_n(p_1^\mu,\dots,p_n^\mu).$$

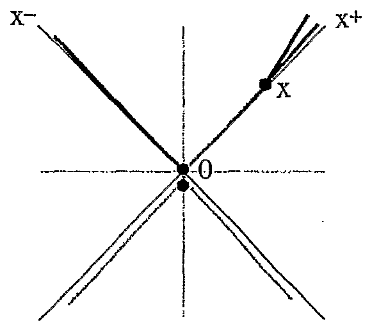

What does infrared safety mean?

$$\mathcal{S}_{n+1}(p_1^\mu, \ldots, (1-\lambda)p_n^\mu, \lambda p_n^\mu) = \mathcal{S}_n(p_1^\mu, \ldots, p_n^\mu).$$

The physical meaning is that for an IR-safe quantity a physical event with hadron jets should give approximately the same measurement as a parton event:

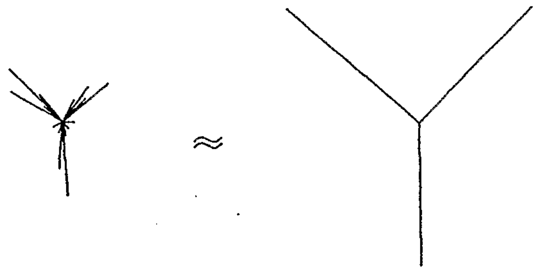

The calculational meaning is that infinities cancel.

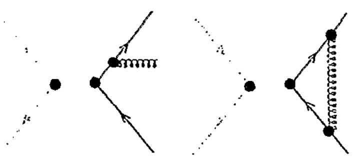

Examples: total cross section, thrust distribution, energy-energy correlation function, jet cross sections.

Deeply inelastic scattering

The effect of partons

A) Kinematics of deeply inelastic scattering.
B) Structure functions for DIS.
C) Space-time structure of DIS.
D) Factored cross section.
E) The hard scattering cross section.
F) Factorization for the structure functions.

Kinematics of deeply inelastic lepton scattering

$$\ell(k) + h(p) \to \ell'(k') + X.$$
$$q^\mu = k^\mu - k'^\mu$$

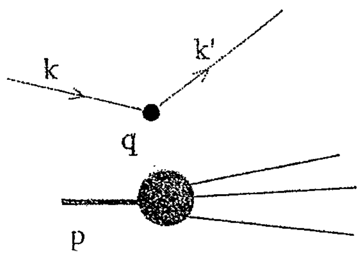

$$Q^2 = -q^2$$
$$x_{\rm bj} = \frac{Q^2}{2p\cdot q} \quad \text{or} \quad A\,\frac{Q^2}{2p\cdot q}$$

"Deeply inelastic" $\Rightarrow Q^2 \to \infty$, x fixed.
Then also

$$W^2 = (p+q)^2 = m_h^2 + \frac{1-x}{x} Q^2 \to \infty.$$

Lepton variables related to hadron variables by

$$y = \frac{p\cdot q}{p\cdot k}.$$

Structure functions for DIS

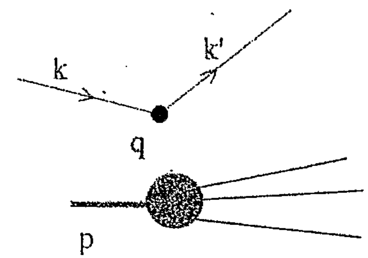

Included here: γ or W exchange. For HERA need also Z exchange.

Analysis does not require QCD, just electroweak theory:

$$d\sigma = \frac{4\alpha^2}{s}\frac{d^3\mathbf{k}'}{2|\mathbf{k}'|}\frac{1}{(q^2-M^2)^2}\, L^{\mu\nu}(k,q)\, W_{\mu\nu}(p,q).$$

$$L^{\mu\nu} = \frac{1}{2}{\rm Tr}\left(k\cdot\gamma\, \Gamma^\mu k'\cdot\gamma\, \Gamma^\nu\right).$$

$$\begin{aligned} W_{\mu\nu} = &-\left(g_{\mu\nu} - \frac{q_\mu q_\nu}{q^2}\right) F_1(x,Q^2) \\ &+ \left(p_\mu - q_\mu\frac{p\cdot q}{q^2}\right)\left(p_\nu - q_\nu\frac{p\cdot q}{q^2}\right)\frac{1}{p\cdot q}\, F_2(x,Q^2) \\ &- i\epsilon_{\mu\nu\lambda\sigma}p^\lambda q^\sigma \frac{1}{p\cdot q}\, F_3(x,Q^2). \end{aligned}$$

Cross section in terms of structure functions

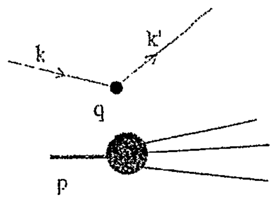

Result (neglecting m_h^2/Q^2):

$$\frac{d\sigma}{dx\,dy} = \tilde{N}(Q^2)\left[yF_1 + \frac{1-y}{xy}F_2 + \delta_V\,(1-\frac{y}{2})F_3\right].$$

Here

$$\tilde{N} = \frac{4\pi\alpha^2}{2Q^2}, \qquad \delta_V = 0, \quad e^- + h \to e^- X,$$

$$\tilde{N} = \frac{\pi\alpha^2 Q^2}{4\sin^2(\theta_W)\,(Q^2+M)^2}, \qquad \delta_V = 1, \quad \nu + h \to e^- X,$$

$$\tilde{N} = \frac{\pi\alpha^2 Q^2}{4\sin^2(\theta_W)\,(Q^2+M)^2}, \qquad \delta_V = -1, \quad \bar{\nu} + h \to e^+ X.$$

Use y dependence to determine F_1, F_2, F_3.

Space-time structure of DIS

A convenient reference frame

A convenient frame is [components $(v^+, v^-, \mathbf{v}_T)$]:

$$(q^+, q^-, \mathbf{q}) = \frac{1}{\sqrt{2}}\,(-Q, Q, \mathbf{0})$$

$$(p^+, p^-, \mathbf{p}) \approx \frac{1}{\sqrt{2}}\,(\frac{Q}{x}, \frac{x m_h^2}{Q}, \mathbf{0})$$

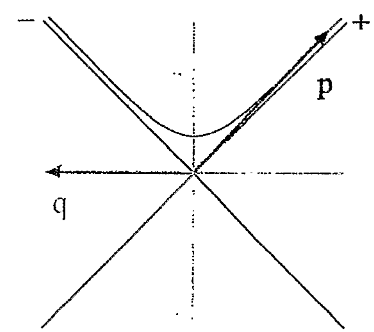

- Hadron momentum is big.
- Momentum transfer is big.

Interactions within a fast moving hadron

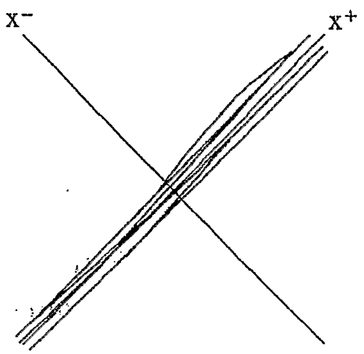

Lorentz transformation spreads out interactions. Hadron at rest has separation between interactions

$$\Delta x^+ \sim \Delta x^- \sim \frac{1}{m}.$$

Moving hadron has

$$\Delta x^+ \sim \frac{1}{m} \times \frac{Q}{m} = \frac{Q}{m^2}, \qquad \Delta x^- \sim \frac{1}{m} \times \frac{m}{Q} = \frac{1}{Q}.$$

The virtual photon meets the fast moving hadron

Moving hadron has

$$\Delta x^+ \sim Q/m^2.$$

Interaction with photon with $q^- \sim Q$ is localized to within

$$\Delta x^+ \sim 1/Q.$$

Thus quarks and gluons = "**partons**" are effectively free.

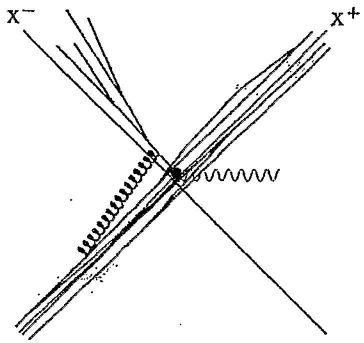

At a given x^+, find partons with an amplitude

$$\psi(p_1^+, \mathbf{p}_1; p_2^+, \mathbf{p}_2; \cdots), \qquad 0 < p_i^+.$$

The $\mathbf{p}_i$ are negligible. For p_i^+, use momentum fractions

$$\xi_i = p_i^+/p^+, \qquad 0 < \xi_i < 1.$$

$\Rightarrow$ Hadron is like a collection of free massless partons with $v = 1$, parallel momenta.

Summary so far

Final states

- Collinear parton splitting and joining $\rightarrow$ singularities.
- Soft gluon emission and absorption$\rightarrow$ singularities.
- This suggests a jet structure of final states.

- The singularities reflect long time physics.
- For short time physics, use infrared safe observables.

DIS

- One photon exchange $\rightarrow$ structure functions.

- Collinear splitting and joining in initial hadron
- Partons are effectively nearly free.

Factored cross section

Treat hadron as a collection of free massless partons with parallel momenta.

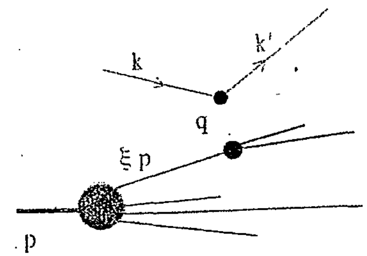

$$\frac{d\sigma}{dE'\,d\omega'} \sim \int_0^1 d\xi \sum_a f_{a/h}(\xi,\mu)\,\frac{d\hat{\sigma}_a(\mu)}{dE'\,d\omega'} + \mathcal{O}(m/Q).$$

$f_{a/h}(\xi,\mu)\;d\xi =$ probability to find a parton
with flavor $a = g, u, \bar{u}, d, \ldots$,
in hadron h,
carrying momentum fraction $\xi = p_i^+/p^+$.

$d\hat{\sigma}_a/dE'\,d\omega' =$ cross section for scattering that parton.

We delay discussion of the μ dependence.

The hard scattering cross section

To calculate $d\hat{\sigma}_a(\mu)/dE'\,d\omega'$ use diagrams like

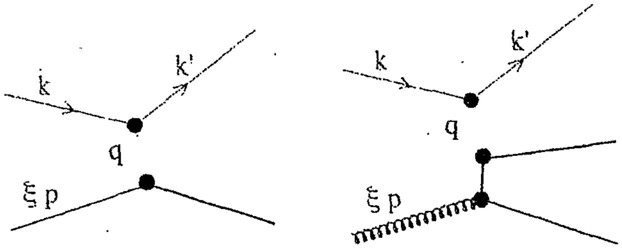

Lowest order. Higher order.

Kinematics of lowest order diagram:

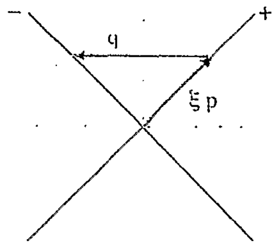

$\xi p^+ + q^+ = 0.$
$p^+ = Q/(x\sqrt{2}),\; q^+ = -Q/\sqrt{2}.$
So

$$\xi = x.$$

Factorization for the structure functions

We will look at DIS in a little detail since it is so important. Our object is to derive a formula relating the measured structure functions to structure functions calculated at the parton level. Then we will look at the parton level at lowest order. Start with

$$\frac{d\sigma}{dE'\,d\omega'} \sim \int_0^1 d\xi \sum_a f_{a/h}(\xi)\, \frac{d\hat{\sigma}_a}{dE'\,d\omega'} + \mathcal{O}(m/Q).$$

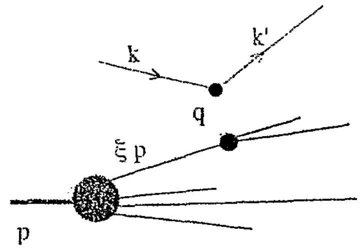

Write this in terms of x and y variables:

$$y = \frac{p\cdot q}{p\cdot k} = \frac{\xi p\cdot q}{\xi p\cdot k}.$$

$$x = \frac{Q^2}{2p\cdot q} = \xi\,\frac{Q^2}{2\xi p\cdot q} = \xi\hat{x}.$$

$$\frac{d\sigma}{dx\,dy} \sim \int_0^1 d\xi \sum_a f_{a/h}(\xi)\,\frac{1}{\xi}\left[\frac{d\hat{\sigma}_a}{d\hat{x}\,dy}\right]_{\hat{x}=x/\xi} + \mathcal{O}(m/Q).$$

Relate cross sections to structure functions

$$\frac{d\sigma}{dx\,dy} \sim \int_0^1 d\xi \sum_a \; f_{a/h}(\xi)\; \frac{1}{\xi} \left[\frac{d\hat\sigma_a}{d\hat x\, dy}\right]_{\hat x = x/\xi} + \mathcal{O}(m/Q).$$

For γ exchange,

$$\frac{d\sigma}{dx\,dy} = \tilde N(Q^2)\left[yF_1(x,Q^2) + \frac{1-y}{xy} F_2(x,Q^2)\right] + \mathcal{O}(m/Q).$$

$$\frac{d\hat\sigma_a}{d\hat x\,dy} = \tilde N(Q^2)\left[y\hat F_1^a(x/\xi,Q^2) + \frac{1-y}{(x/\xi)y} \hat F_2^a(x/\xi,Q^2)\right].$$

So the structure functions can be factored as

$$F_1(x,Q^2) \sim \int_0^1 d\xi \sum_a \; f_{a/h}(\xi)\; \frac{1}{\xi} \hat F_1^a(x/\xi,Q^2) + \mathcal{O}(m/Q).$$

$$F_2(x,Q^2) \sim \int_0^1 d\xi \sum_a \; f_{a/h}(\xi)\; \hat F_2^a(x/\xi,Q^2) + \mathcal{O}(m/Q).$$

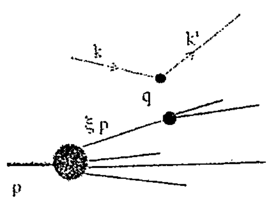

Structure functions at lowest order

A simple calculation gives

$$\hat F_1^a(x/\xi,Q^2) = \frac{1}{2} Q_f^2\; \delta(x/\xi - 1) + \mathcal{O}(\alpha_s),$$

while we recall

$$F_1(x,Q^2) \sim \int_0^1 d\xi \sum_a \; f_{a/h}(\xi)\; \frac{1}{\xi} \hat F_1^a(x/\xi,Q^2) + \mathcal{O}(m/Q).$$

So

$$F_1(x,Q^2) \sim \frac{1}{2} \sum_a \; Q_a^2\; f_{a/h}(x) + \mathcal{O}(\alpha_s) + \mathcal{O}(m/Q).$$

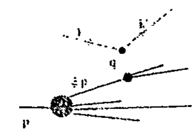

Similarly, a simple calculation gives

$$\hat F_2^a(x/\xi,Q^2) = Q_a^2\; \delta(x/\xi - 1) + \mathcal{O}(\alpha_s),$$

while we recall

$$F_2(x,Q^2) \sim \int_0^1 d\xi \sum_a \; f_{f/h}(\xi)\; \hat F_2^a(x/\xi,Q^2) + \mathcal{O}(m/Q).$$

So

$$F_2(x,Q^2) \sim \sum_a \; Q_a^2\; x\, f_{a/h}(x) + \mathcal{O}(\alpha_s) + \mathcal{O}(m/Q).$$

Factor 1/2 between F_1 and F_2: quarks have spin 1/2.

Preview of parton distributions

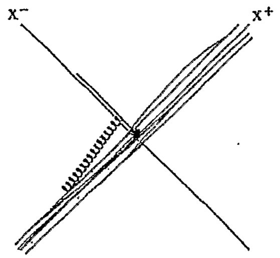

- There is a definition in terms of operators so they are process independent.
- Sum rules are automatic. Eg.

$$\sum_a \int_0^1 d\xi\ \xi\ f_{a/h}(\xi, \mu) = 1.$$

- We don't calculate f, but the definition adopted determines how $d\hat{\sigma}$ is calculated.
- The parton distributions appear in the QCD formula for any process with one or two hadrons in the initial state.
- Comparison of theory with experiment allows one to fit the parton distributions.
- The evolution with scale is predicted, so one has only to fit the parton distributions at a starting scale μ_0.
- There are lots of experiments, so this program won't work unless QCD is right.

Renormalization and factorization scales

What QCD looks like depends on the time scale at which you look.

A) What renormalization does.
B) The running coupling.
C) The choice of renormalization scale.
D) The scale dependent parton distributions.
E) The choice of factorization scale.
F) Some comments on parton distribution functions.

What renormalization does

Use $\overline{\mathrm{MS}}$ renormalization with renormalization scale μ:

- Physics of time scales $|t| \ll 1/\mu$ removed from perturbative calculation.
- Effect of small time physics accounted for by adjusting value of the coupling*: $\alpha_s = \alpha_s(\mu)$.

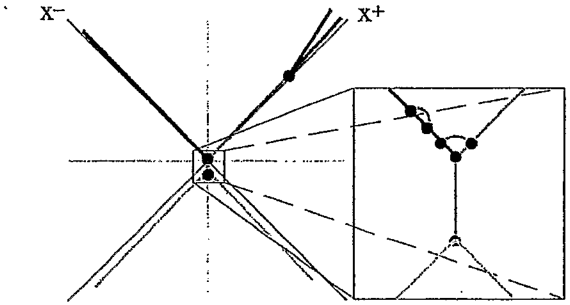

*This is not exactly the truth. There are also running masses $m(\mu)$ and there are μ dependent adjustments to the normalizations of the field operators. In addition, renormalization by dimensional regularization and minimal subtraction is not exactly the same as imposing a cutoff $|\Delta x| > 1/\mu$.

The running coupling

We account for time scales much smaller than $1/\mu$ (but bigger than a cutoff M at the "GUT scale") by using the running coupling.

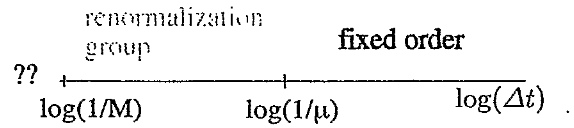

This sums the effects of short time fluctuations of the fields.

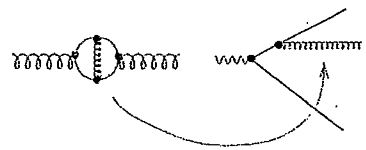

Renormalization group equation for α_s:

$$\frac{d}{d\ln\mu^2}\,\alpha_s(\mu) = \beta(\alpha_s(\mu))$$

with

$$\beta(\alpha_s(\mu)) = -\beta_0\,\frac{\alpha_s(\mu)}{\pi} - \beta_1\left(\frac{\alpha_s(\mu)}{\pi}\right)^2 + \cdots.$$

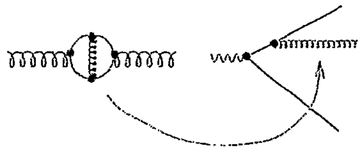

Result of one-loop renormalization group equation,

$$\frac{d}{d\ln\mu^2}\,\alpha_s(\mu) = -\beta_0\,\frac{\alpha_s(\mu)}{\pi}$$

can be written three ways:

$$\begin{aligned}\alpha_s(\mu) &\sim \alpha_s(M) - (\beta_0/\pi)\log(\mu^2/M^2)\ \alpha_s^2(M)\\ &\quad + (\beta_0/\pi)^2\log^2(\mu^2/M^2)\ \alpha_s^3(M) + \cdots\\ &= \frac{\alpha_s(M)}{1+(\beta_0/\pi)\alpha_s(M)\log(\mu^2/M^2)}\\ &= \frac{\pi}{\beta_0\log(\mu^2/\Lambda^2)}.\end{aligned}$$

- $\alpha_s(\mu)$ decreases as μ increases.

But what should the scale μ be?

The choice of scale

Example: Cross section for $e^+e^- \to$ hadrons via virtual photon:

$$\sigma_{\rm tot} = \frac{12\pi\alpha^2}{s}\left(\sum_f Q_f^2\right)[1+\Delta]$$

$$\begin{aligned}\Delta(\mu) = \frac{\alpha_s(\mu)}{\pi} &+ \left[1.4092 + 1.9167\ \log\left(\mu^2/s\right)\right]\left(\frac{\alpha_s(\mu)}{\pi}\right)^2\\ &+ \left[-12.805 + 7.8179\ \log\left(\mu^2/s\right) + 3.674\ \log^2\left(\mu^2/s\right)\right]\\ &\quad\times\left(\frac{\alpha_s(\mu)}{\pi}\right)^3\\ &+ \cdots\end{aligned}$$

Clearly, $\log\left(\mu^2/s\right)$ should not be big.

- α_s depends on μ.
- Coefficients depend on μ.
- Physical cross section does not depend on μ.
- The harder we work, the less the calculated cross section depends on μ:

$$\frac{d}{d\log\mu}\sum_{n=1}^{N} c_n(\mu)\ \alpha_s(\mu)^n \sim \mathcal{O}(\alpha_s(\mu)^{N+1})$$

Choosing μ

Recall $\Delta(\mu)$ defined by

$$\sigma_{\rm tot} = (12\pi\alpha^2/s)\left(\sum Q_f^2\right)[1+\Delta].$$

Take $\alpha_s(M_Z) \approx 0.117$, $\sqrt{s} = 34$ GeV, 5 flavors. I plot $\Delta(\mu)$ versus p defined by

$$\mu = 2^p\sqrt{s}.$$

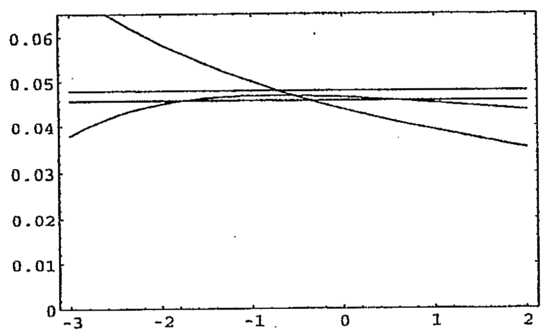

First curve: $\Delta_1(\mu) = \alpha_s(\mu)/\pi$.
Second curve (note improvement):

$\Delta_2(\mu)$ including α_s^2 term.

- Possible choice:

$$\Delta_{PMS} = \Delta(\hat{\mu}), \qquad \left[\frac{d\Delta(\mu)}{d\log\mu}\right]_{\mu=\hat{\mu}} = 0.$$

Error band: estimated using $\mu = 2\hat{\mu}$ or $\mu = (1/2)\hat{\mu}$.

One more order

I plot again $\Delta(\mu)$ versus p ($\mu = 2^p\sqrt{s}$).

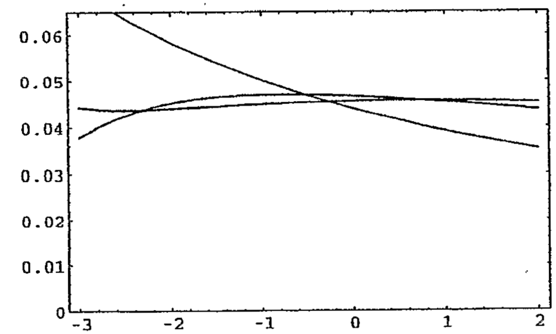

Three curves: $\Delta_1(\mu)$, $\Delta_2(\mu)$, $\Delta_3(\mu)$.

Magnified view (including our $\Delta_2(\mu)$ error band):

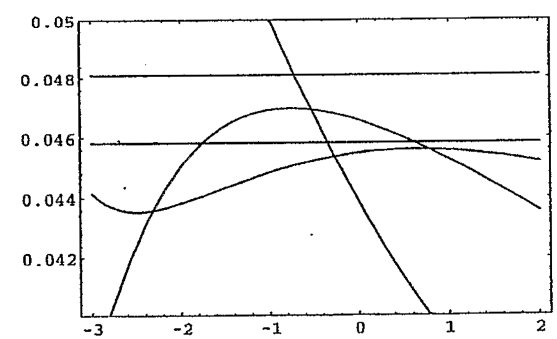

Was the error estimate valid?

Summary so far

DIS

- Collinear splitting and joining in initial hadron
- This long distance physics → parton distributions.
- Hard scattering factor is calculated.
- At lowest order, the hard scattering part of DIS is trivial, so measured structure functions ≈ parton distributions.

Renormalization

- Renormalization removes from the theory effects from $\Delta t \ll 1/\mu$.
- The coupling α_s *etc.* depend on how much you removed.
- Choose $\mu \sim p$ to avoid $\ln(\mu^2/p^2)$.

126

pole mass
running mass

each mass depends on μ
{ k }

$\frac{k+m}{k^2+m^2+i\varepsilon}$

$\beta_0 \propto 33 - 2N_f$

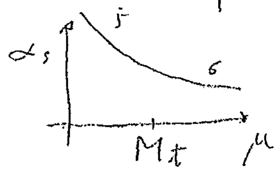

$\alpha_s(M_Z) = 0.118$

$\Lambda^{(5)}_{QCD} + \Lambda^{(4)}_{QCD}$

Scales in the factored cross section

Recall the expression for the factored cross section in DIS:

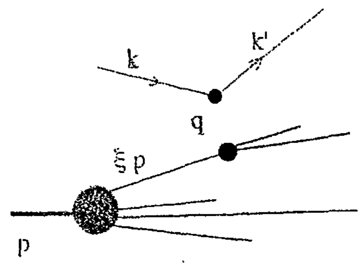

$$\frac{d\sigma}{dE'\,d\omega'} \sim \int_0^1 d\xi \sum_a f_{a/h}(\xi,\mu)\,\frac{d\hat\sigma_a(\mu)}{dE'\,d\omega'} + \mathcal{O}(m/Q).$$

$f_{a/h}(\xi,\mu)\,d\xi$ = probability to find a parton
with flavor $a = g, u, \bar u, d, \ldots$,
in hadron h,
carrying momentum fraction $\xi = p_i^+/p^+$.

$d\hat\sigma_a/dE'\,d\omega'$ = cross section for scattering that parton.

What about the μ dependence?

Look at the definition of the parton distribution functions.

· $\overline{MS}$ $\int d^{4-2\varepsilon}k$ $A(\varepsilon) - \frac{\text{const}}{\varepsilon}$

· space like subtraction pt. q — $-q^2,\mu^2$ + value

· subtraction at $q^2 = 0$

$\overline{\text{MS}}$ definition of parton distribution functions

Quarks:

$$f_{i/h}(\xi,\mu) = \frac{1}{2}\int \frac{dy^-}{2\pi}\, e^{i\xi p^+ y^-} \langle p|\bar{\psi}_i(0,y^-,\mathbf{0})\gamma^+ F \psi_i(0)|p\rangle.$$

$$F = \mathcal{P}\exp\left(-ig\int_0^{y^-} dz^- A_a^+(0,z^-,\mathbf{0})\, t_a\right).$$

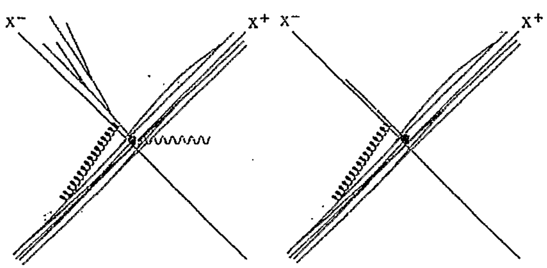

DIS Parton distribution

This is renormalized ($\overline{\text{MS}}$) with scale μ:

$$\mathbf{k}^2 < \mu^2 \text{ included in } f_{i/h}(\xi,\mu).$$

Gluons: similar definition using gluon field.

Evolution of the parton distributions

There is a renormalization group equation that gives the μ_F dependence:

Kernel

$$\frac{d}{d\log\mu_F} f_{a/h}(x,\mu_F) = \sum_b \int_x^1 \frac{d\xi}{\xi}\, P_{ab}(x/\xi,\alpha_s(\mu_F))\; f_{b/h}(\xi,\mu_F).$$

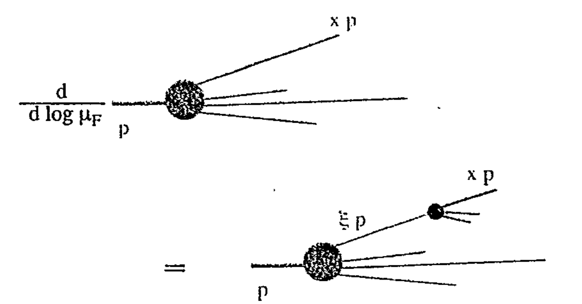

$$P_{ab}(x/\xi,\alpha_s(\mu_F)) = P_{ab}^{(1)}(x/\xi)\,\frac{\alpha_s(\mu_F)}{\pi} + P_{ab}^{(2)}(x/\xi)\left(\frac{\alpha_s(\mu_F)}{\pi}\right)^2 + \cdots.$$

Summation of perturbative effects

One often needs to sum the most important part of each of an infinite number of graphs. The differential equation

$$\frac{d}{d\log\mu_F} f_{a/h}(x,\mu_F) = \sum_b \int_x^1 \frac{d\xi}{\xi}\, P_{ab}(x/\xi, \alpha_s(\mu_F))\, f_{b/h}(\xi,\mu_F)$$

accomplishes such a summation. (*cf.* the renormalization group equation for the running coupling.)

The physical effect that we account for here is fluctuations within fluctuations within ....

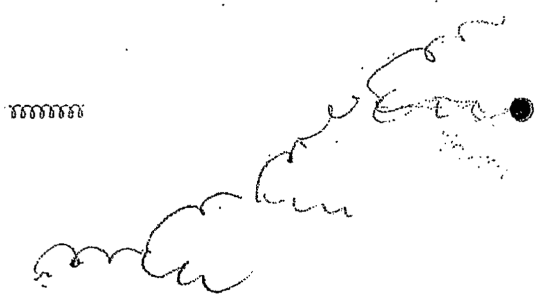

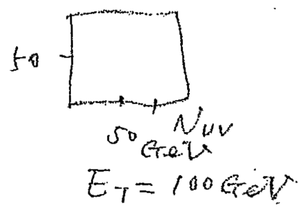

parton dist. ⊗ hard satt. cross section

ultra-violet divergence

μ_F dependence

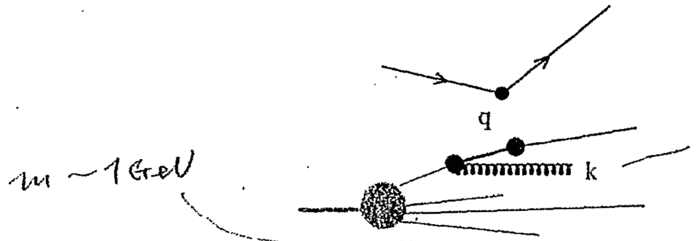

Δx^+'s cover a range from Q/m^2 to $1/Q$ to $\ll 1/Q$.

A gluon emission with $\mathbf{k}^2 \sim m^2$ is part of $f(\xi)$.

A gluon emission with $\mathbf{k}^2 \sim Q^2$ is part of $d\hat{\sigma}$.

When calculating $\hat{\sigma}$, we (roughly speaking) count it as part of $\phi(\xi)$ for $\mathbf{k}^2 < \mu_F^2$ and as part of $d\hat{\sigma}$ for $\mu_F^2 < \mathbf{k}^2$.

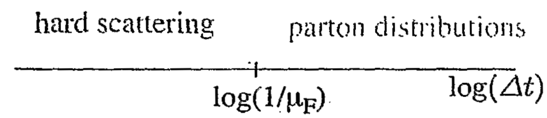

$\Rightarrow d\hat{\sigma}_a(\mu_F)/dE'\,d\omega'$ and $f_{a/h}(\xi,\mu_F)$ depend on μ_F.

- μ_F in $f_{f/h}(\xi,\mu_F)$ = "factorization scale."
- μ in $\alpha_s(\mu)$ = "renormalization scale."

As with μ, the higher order calculation you use, the less dependence on μ_F there is.

- Often one sets $\mu_F = \mu$.

lattice: $f_n = \int_0^1 dx\, x^n f(x) = \langle p|\bar{\psi}(0)\gamma^+ (D^+)^n \psi(0)|p\rangle$

$\partial^+ - eA^+$

Contour graphs of scale dependence

As an example, look at the one jet inclusive cross section in proton-antiproton collisions at $\sqrt{s} = 1800$ GeV.
How does it depend on μ in $\alpha_s(\mu)$ and μ_F in $f_{a/p}(x, \mu_F)$?

$\mu = (E_T/2) \times 2^{N_{UV}}$, $\mu_F = (E_T/2) \times 2^{N_{CO}}$

$d\sigma/dE_T\, d\eta$ at rapidity $\eta = 0$ with arbitrary normalization, 5% contour lines.

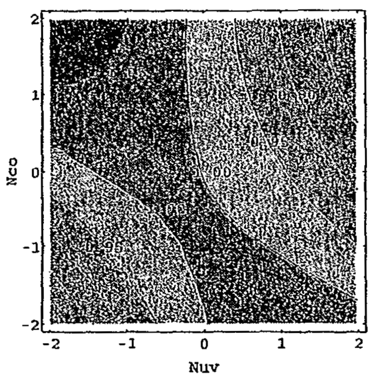

$E_T = 100$ GeV

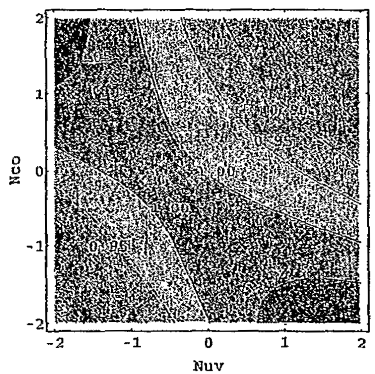

$E_T = 500$ GeV

- Variation with scale is roughly $\pm 10\%$ both for medium and large E_T.

QCD in hadron-hadron collisions

Initial state, hard scattering, final state

A) Kinematics: rapidity.
B) Production of γ^*, W, Z.
C) Heavy quark production.
D) Jet production and jet definitions.

Kinematics: rapidity

Rapidity y (or η) is useful for hadron-hadron collisions.
Choose c.m. frame with z-axis along the beam direction.

Massive particle (e.g. Z-boson production):

- Momentum $q^\mu = (q^+, q^-, \mathbf{q})$.

$$y = \frac{1}{2}\log\left(\frac{q^+}{q^-}\right).$$

transverse

$$q^\mu = (e^y\sqrt{(\mathbf{q}^2 + M^2)/2},\ e^{-y}\sqrt{(\mathbf{q}^2 + M^2)/2},\ \mathbf{q}).$$

- Transformation property under a boost along z-axis:

$$q^+ \to e^\omega q^+, \quad q^- \to e^{-\omega} q^-, \quad \mathbf{q} \to \mathbf{q}.$$

$$y \to y + \omega.$$

- Good because the c.m. frame isn't so special.

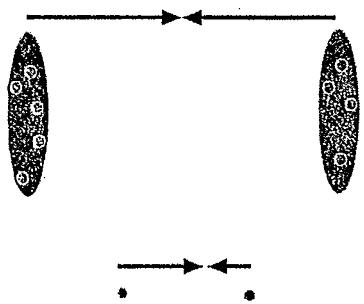

Pseudorapidity

Recall the definition of rapidity:

$$y = \frac{1}{2}\log\left(\frac{q^+}{q^-}\right).$$

For a massless particle this is

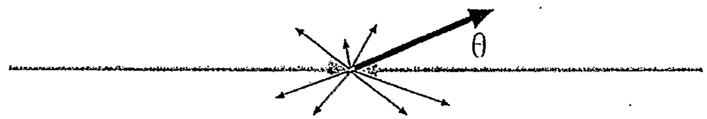

$$y = -\log\left(\tan(\Theta/2)\right)$$

If the particle isn't quite massless, $-\log\left(\tan(\Theta/2)\right)$ is the "pseudorapidity."

γ^*, W, Z production in hadron-hadron collisions

Consider the process ("Drell-Yan")

$$A + B \to Z + X. \qquad \overrightarrow{A} \quad \overleftarrow{B}$$

Let

$$x_A = e^{y}\sqrt{M^2/s}, \qquad x_B = e^{-y}\sqrt{M^2/s}.$$

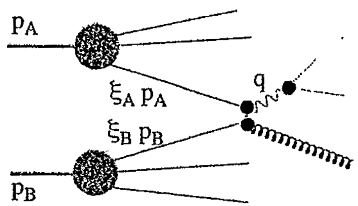

Factored form of cross section:

factorization formula with correction 2 loop m_Z

$$\frac{d\sigma}{dy} \approx \sum_{a,b}\int_{x_A}^{1} d\xi_A \int_{x_B}^{1} d\xi_B\; f_{a/A}(\xi_A,\mu)\; f_{b/B}(\xi_B,\mu)\; \frac{d\hat{\sigma}_{ab}(\mu)}{dy}.$$

This has corrections of order m/M.

When $d\hat{\sigma}_{ab}/dy$ is calculated to order α_s^N then there are corrections of order α_s^{N+1}.

We integrate over $\mathbf{q}$; Z's are mostly at $\mathbf{q} \ll M$.

transverse momentum

Historical importance of vector boson production

For $A + B \to \mu^+ + \mu^- + X$ one has the formula.

virtuality

$$\frac{d\sigma}{dQ^2 dy} \approx \sum_{a,b}\int_{x_A}^{1} d\xi_A \int_{x_B}^{1} d\xi_B\; f_{a/A}(\xi_A,\mu)\; f_{b/B}(\xi_B,\mu)\; \frac{d\hat{\sigma}_{ab}(\mu)}{dQ^2 dy}$$

where Q^2 is the squared mass of the muon pair.

- Before QCD, one had partons and QED. Partons and QED did a good job explaining deeply inelastic scattering.
- But there were other ways to explain DIS.
- Drell and Yan proposed to explain the Lederman *et al.* experiment using the lowest order version of this formula.

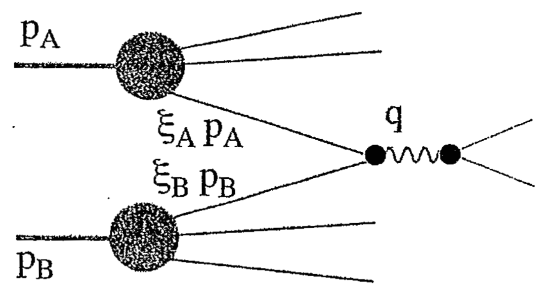

- It worked!

lowest,
なし グルーオン emission

1970's アルジェから 出した

132

Factorization is not so obvious

For $A + B \to \mu^+ + \mu^- + X$ one has the formula

$$\frac{d\sigma}{dQ^2 dy} \approx \sum_{a,b} \int_{x_A}^{1} d\xi_A \int_{x_B}^{1} d\xi_B \; f_{a/A}(\xi_A, \mu)\; f_{b/B}(\xi_B, \mu)\; \frac{d\hat{\sigma}_{ab}(\mu)}{dQ^2 dy}$$

up to m^2/Q^2 corrections.

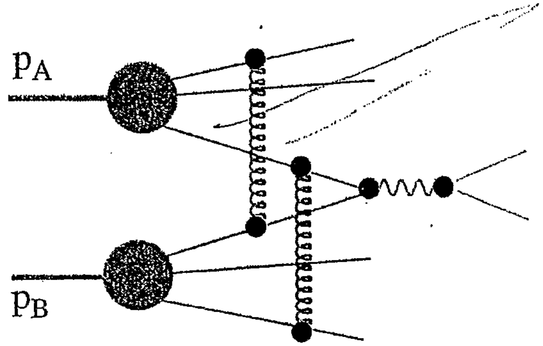

This result is not so obvious, and in fact does not hold graph by graph.

- Need unitarity.
- Need causality.
- Need gauge invariance.

Heavy quark production

$B\bar{B}$

$$A + B \to Q + \bar{Q} + X.$$

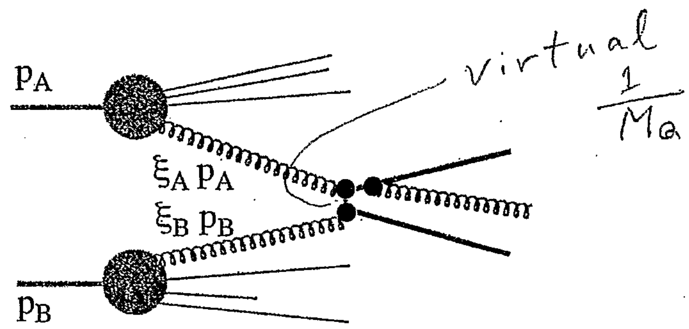

Here the big momentum scale (like Q in DIS) is M_Q.

$$\sigma_T \approx \sum_{a,b} \int_{x_A}^{1} d\xi_A \int_{x_B}^{1} d\xi_B \; f_{a/A}(\xi_A, \mu)\; f_{b/B}(\xi_B, \mu)\; \hat{\sigma}_T^{ab}(\mu).$$

Is this really perturbative?

The crucial point is that even if the final state heavy quarks are on-shell, the "exchanged" heavy quark has virtuality at least as big as M_Q^2.

Jet production

One can also measure cross sections to make jets,

$$A + B \to jet + X.$$

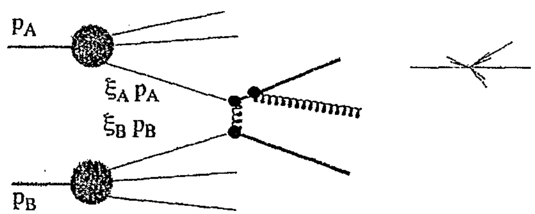

The idea is that the partons in the final state turn into collimated sprays of physical particles ("jets"). The cross section has the factored form

$$\frac{d\sigma}{dE_T d\eta} \approx$$

$$\sum_{a,b} \int_{x_A}^{1} d\xi_A \int_{x_B}^{1} d\xi_B\; f_{a/A}(\xi_A;\mu)\; f_{b/B}(\xi_B;\mu)\; \frac{d\hat{\sigma}^{ab}(\mu)}{dE_T d\eta}.$$

α

$+O\left(\frac{m}{E_T}\right)$

$\frac{m}{Q}$

higher twist

But what do you mean by a jet?

What does one mean by a jet?

Consider

$$\frac{d\sigma}{dE_T\, d\eta}\,,$$

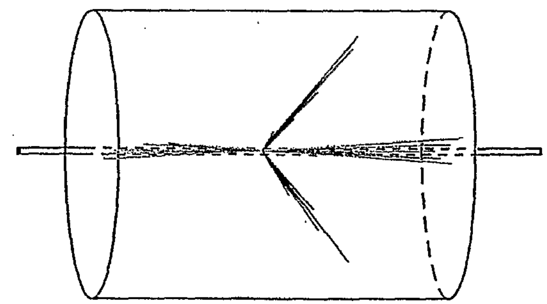

E_T = transverse energy [$\sim$ transverse momentum] of jet.
η = rapidity [$\sim -\log(\tan(\theta/2)$] of jet .

- Substantial E_T at large angles $\Rightarrow$ care with the definition.
- In particular, the definition should be infrared safe.
- There are several possibilities. The one most used in hadron-hadron collisions is based on cones.

infrared safe ?

jet from e^+e^- annihilation

"Snowmass Accord" definition

Define jet cone of radius R in η-ϕ space.

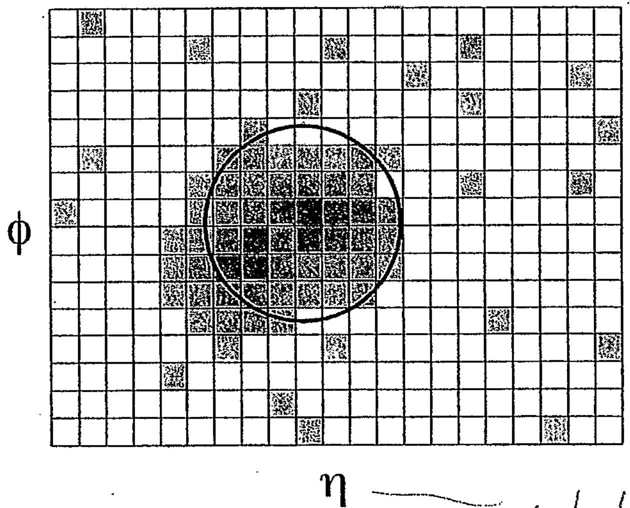

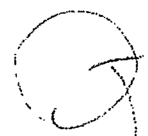

0.7 rad.

pseudo rapidity

$$E_{T,J} = \sum_{i \in \text{cone}} E_{T,i}$$

Jet axis:

$$\phi_J = \frac{1}{E_{T,J}} \sum_{i \in \text{cone}} E_{T,i}\, \phi_i$$

$$\eta_J = \frac{1}{E_{T,J}} \sum_{i \in \text{cone}} E_{T,i}\, \eta_i$$

- The cone axis must agree with the jet axis.

then move the cone axis

k_T algorithm

In application, the Snowmass definition has a lot of "fine print" that I have not discussed.

It is possible to use an iterative successive combination algorithm, as used in e^+e^- annihilation.

The main idea is to use E_T, η and ϕ as variables, and to take the many low E_T particles into account.

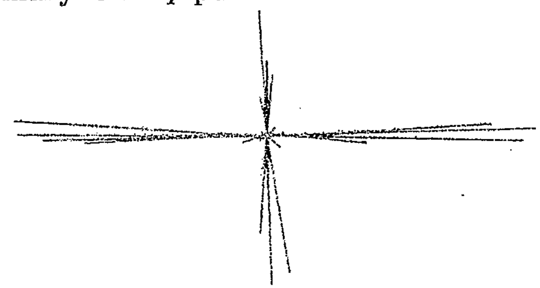

- Choose a merging parameter R.
- Start with a list of "protojets" with momenta $p_1^\mu, \ldots, p_N^\mu$.
- We also start with an empty list of finished jets.

- Result is a list of momenta p_k of jets, ordered in E_T.
- Many will have small E_T and are really minijets, or just part of low E_T debris.
- For an exclusive n jet cross section, use an $E_{T,\min}$

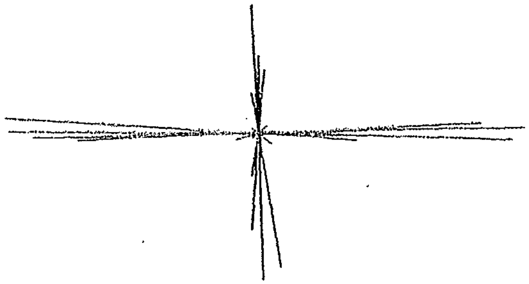

1. For each pair of protojets define

$$d_{ij} = \min(E_{T,i}^2, E_{T,j}^2)\,[(\eta_i - \eta_j)^2 + (\phi_i - \phi_j)^2]/R^2$$

$R \sim 1$ rad

For each protojet define

$$d_i = E_{T,i}^2$$

2. Find the smallest of all the d_{ij} and the d_i. Call it $d_{\min}$
3. If $d_{\min}$ is a d_{ij}, merge protojets i and j into a new protojet k with

$$\begin{aligned} E_{T,k} &= E_{T,i} + E_{T,j} \\ \eta_k &= [E_{T,i}\,\eta_i + E_{T,j}\,\eta_j]/E_{T,k} \\ \phi_k &= [E_{T,i}\,\phi_i + E_{T,j}\,\phi_j]/E_{T,k} \end{aligned}$$

4. If If $d_{\min}$ is a d_i, then protojet i is "not mergable." Remove it from the list of protojets and add it to the list of jets.
5. If protojets remain, go to 1.

infrared safe definition
because merging

Summary of today's topics

- Parton distributions defined as matrix elements of certain operators.
- A scale, μ_F, divides Δt included in parton distributions and Δt included in hard scattering.
- Parton distributions depend on μ_F.
- Choose $\mu \sim p$ to avoid $\ln(\mu_F^2/p^2)$.
- Hard processes in hadron-hadron collisions factor into

parton dist. $\times$ *parton dist.* $\times$ *hard scattering*

- Examples: γ^*, W, Z; heavy quarks; jets.
- Jet cross sections need a definition.

Heavy Ion Physics at RHIC

Y. Akiba (KEK, High Energy Accelerator Research Organization)
RIKEN Winter School, Wako, Japan, March 29-31

Abstract

Lattice QCD predicts that a phase transition from ordinary hadronic matter to a deconfined phase of quark and gluons, the quark-gluon plasma (QGP), should occur at sufficiently high energy density. Such high energy density state can be created in central collision of heavy nuclei at high energy. The main goal of heavy ion physics at RHIC is to find evidences of the QGP and to study its properties. RHIC started its first physics run in year 2000 (RUN-1), and data of Au+Au collision at 130GeV were obtained. After an introduction to heavy ion physics, the lecture summarized the results of RUN-1 obtained by PHENIX experiment at RHIC in the following six topics.

(1) Global measurements
Charged particle multiplicity density $dN_{ch}/d\eta$ and total transverse energy density dE_T/dy are measured as function of number of participant nucleons (N_{part}). The data shows that both quantity increases faster than N_{part}. The result suggests that initial state parton-parton collision has significant contribution to those global variables.

(2) Flow effects in semi-central collisions
The initial space anisotropy of reaction zone in semi-central collision leads to final state momentum anisotropy (flow). The strength of this elliptic flow at RHIC energy was found to be much stronger than that at lower energies. This result is consistent with a scenario of early thermalization and hydro-dynamical evolution.

(3) Space-time structure of reaction zone measured by two pion correlation
Two-pion correlation is used to measure the size and the duration time of reaction zone at the freeze-out stage. The data shows that duration time of the freeze-out is consistent with zero, and it contradicts with naive hydro-dynamical model predictions.

(4) Measurement of identified hadrons
Hadron production yield dN/dy and momentum distribution dN/dp_T are measured. The ratios of hadron yields are consistent with thermal model with T~170 MeV and μ_B~30MeV. The momentum spectra of K/p/p are also described by a thermal distribution with a radial flow, with parameters Tth~120 MeV and $\beta_T = 0.7$. Those results suggest the realization of thermal and chemical equilibrium at RHIC.

(5) Measurement of high pt particle production
High pt particle production was measured, and found to be suppressed relative to the scaling with number of binary collisions. This results is consistent with prediction of jet quenching effect, and suggests that scattered quark and gluon suffer significant energy loss in dense matter created at RHIC.

(6) Measurement of single electrons and implications for charm production
Single electron spectra in Au+Au collision show an excess over background from light hadron decays and photon conversions. The excess is consistent with semi-leptonic decay of charm.

RHIC and PHENIX has just completed its second RUN (RUN-2). More results are expected from RUN-2 data of RHIC.

Heavy Ion Physics at RHIC

Y. Akiba (KEK)

Outline

- RHIC and PHENIX experiment
- Results from RHIC Run-1 (2000)
  - Global observables
  - Flow
  - Two particle correlation
  - Hadron spectra and ratios
  - High pt particle production
  - Single electron and charm
- Outlook
- For more…
  - RHIC http://www.rhic.bnl.gov
  - PHENIX http://www.phenix.bnl.gov

PHENIX Q: Why RHIC? A: Quark Gluon Plasma

In cold matter: quark and gluons are confined in nucleon

In hot matter: quarks are de-confined.

Lattice QCD predicts that the de-confinement phase transition at T~200 MeV

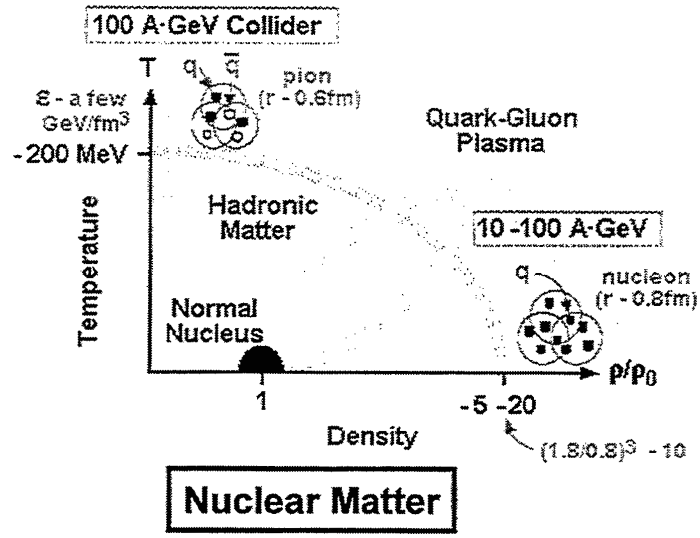

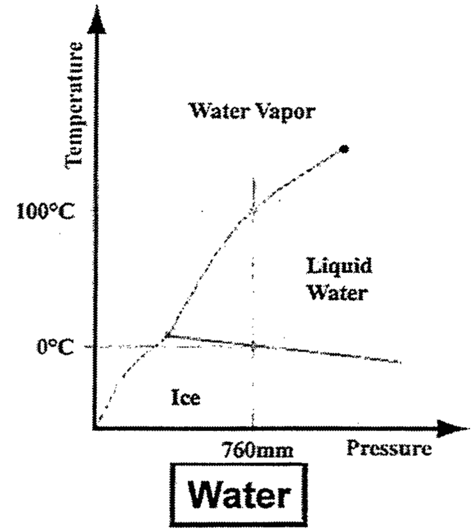

3

PHENIX Phase transition in early Universe

- The Universe is in Quark Gluon Plasma Phase just after the Big Bang.
- There was a phase transition from QGP to Hadron phase at a few micro-second after the Big Bang.

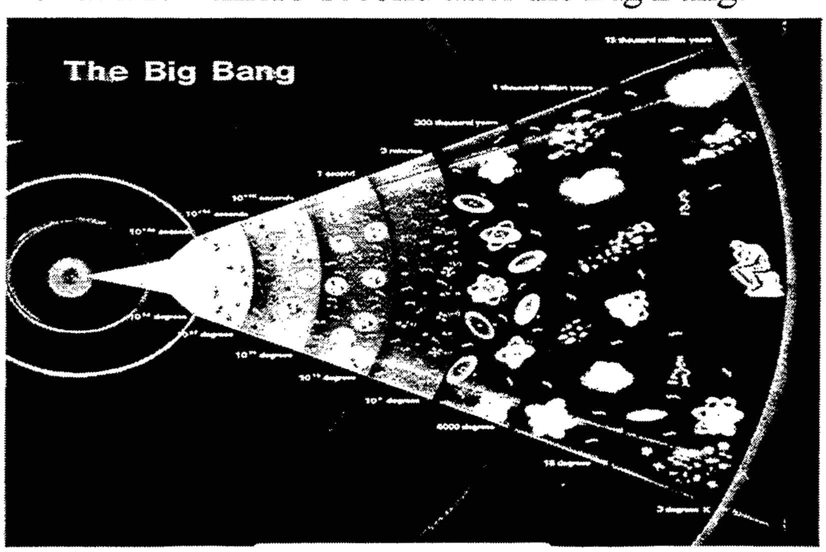

PHENIX — Recreate QGP by High Energy Nucleus-Nucleus Collision

- Collide heavy nucleus as high energy as possible
- Purpose:
  - ❑ Produce very high energy density matter
  - ❑ Re-create QGP phase in the laboratory

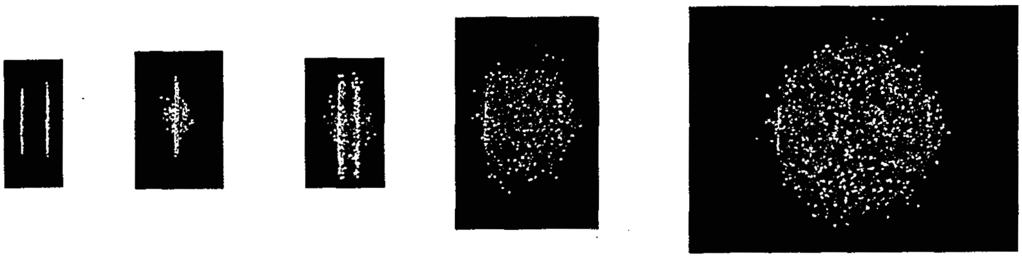

5

PHENIX — Space Time evolution of Au+Au collisions

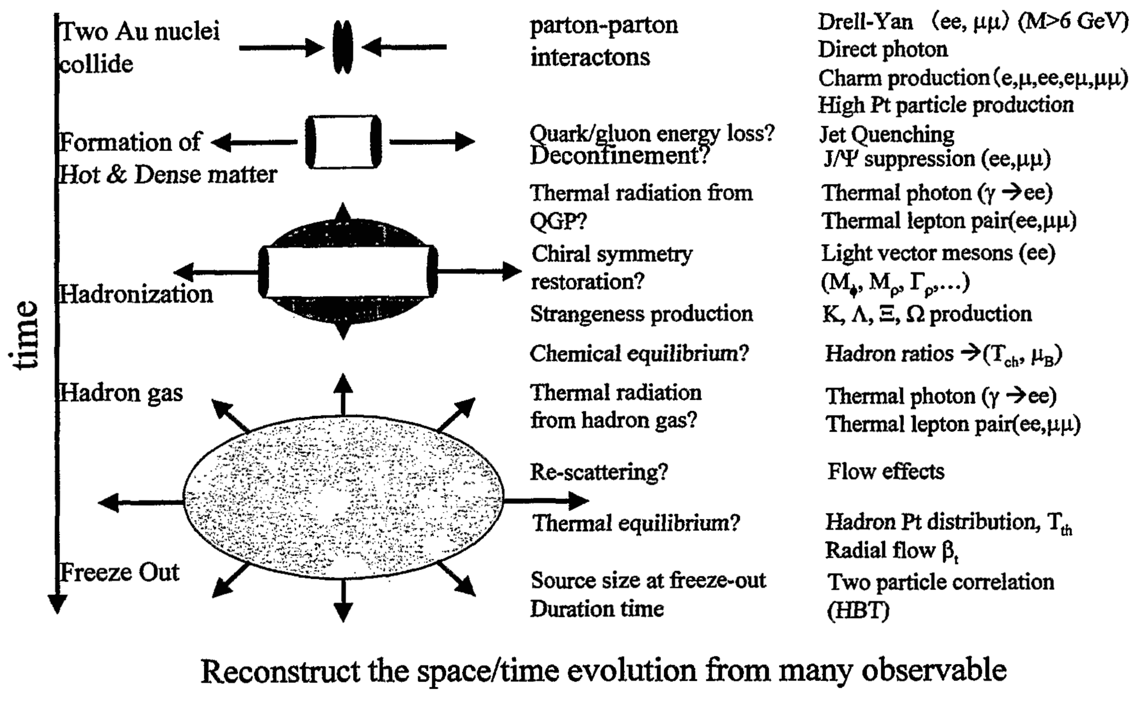

Reconstruct the space/time evolution from many observable

PHENIX Relativistic Heavy Ion Collider

- Located at BNL
- The first collider of heavy ion
- Two super-conducting rings
  - 3.83 km circumference
  - 120 bunches/ring
  - 106 ns bunch crossing time
- Top Energy:
  - ➧ $s^{1/2}$ = 500 GeV for p-p
  - ➧ $s_{NN}^{1/2}$ = 200 GeV for Au-Au (total $s^{1/2}$ = 40 TeV for Au+Au)
- Luminosity
  - Au-Au: 2 x 10^{26} cm^{-2} s^{-1}
  - p-p : 2 x 10^{31} cm^{-2} s^{-1} (*polarized*)
- Started physics run in spring 2000 at $s_{NN}^{1/2}$=56 and 130 GeV

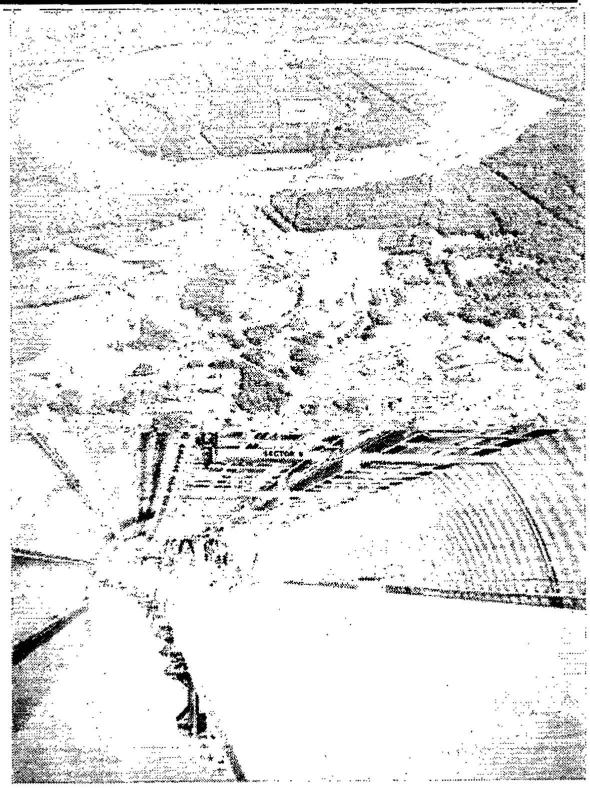

7

PHENIX Experiments at RHIC

- Two "small" experiment
  - Phobos
    - ◆ Detector to measure low pt charged particles and $dN_{ch}/d\eta$
  - Brahms
    - ◆ Detector to measure hadron spectra in wide range of rapidity
- Two "large" experiments
  - STAR
    - ◆ "4π" tracking detector based on a large TPC
    - ◆ Limited capability in paricle identification
  - PHENIX
    - ◆ Detector to measure electrons, muons, photons, and hadrons
    - ◆ High resolution, high granularity
    - ◆ Smaller solid angle coverage than STAR

PHENIX PHOBOS

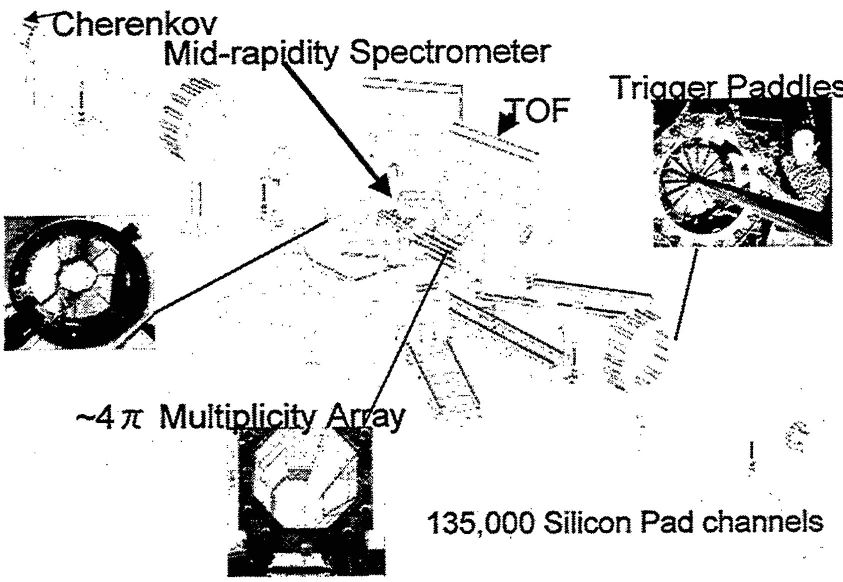

- Detector for low global phenomena
- Specialized for
  - dN/dη
  - Low pt

9

PHENIX BRAHMS

- Two magnetic spectrometers in "classic" fixed-target configuration
- Identified single hadron measurements over a broad range of rapidity and p_T

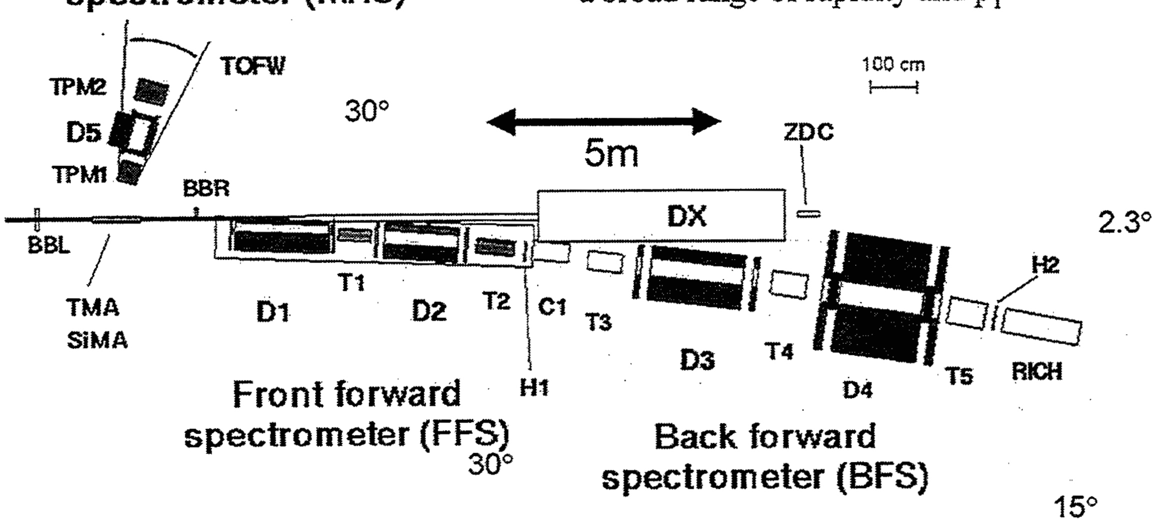

PHENIX STAR

- "4π" detector (measure ~2000 tracks/events)
- Limited rate and PID capability

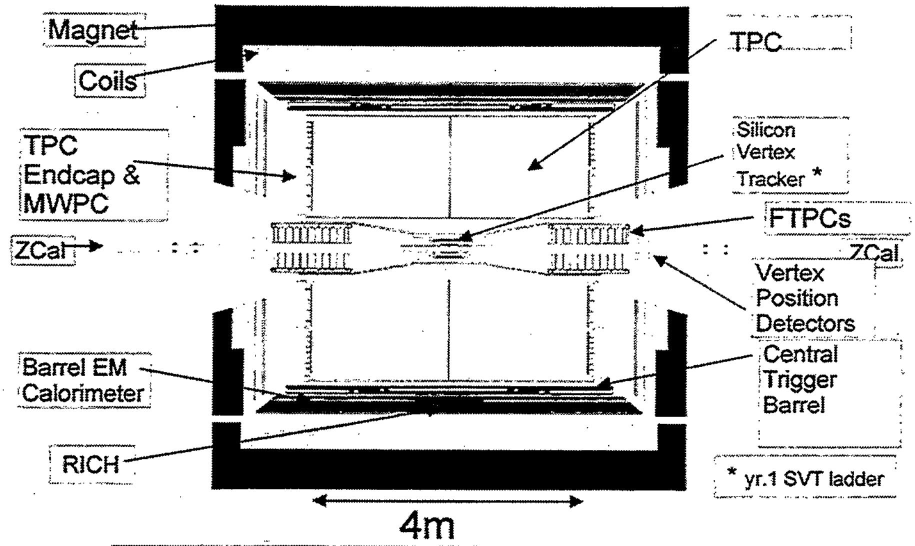

Operation in 2000, 2001, 2003

11

PHENIX PHENIX

Two central arms to measure electron, photon, and hadrons

Three Global detectors for trigger and event characterization

Two forward muon spectrometers

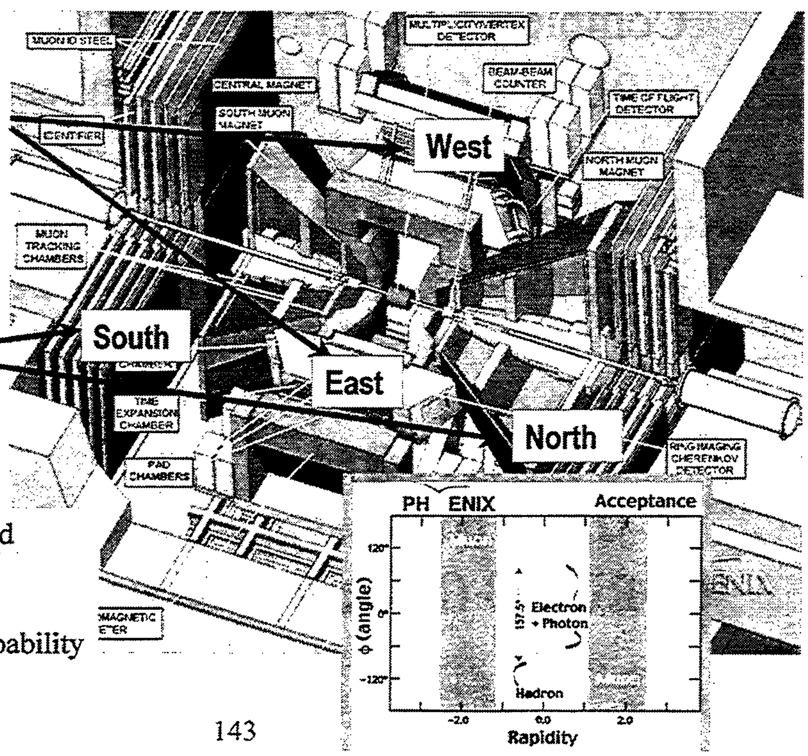

Measure lepton, photon, and hadron
Limited solid angle
High rate and good PID capability

PHENIX Experimental Challenge at RHIC

- Very high multiplicity of produced particles
  - $dN_{ch}/d\eta \sim 1000$
  - High segmentation of detector is required
- STAR approach
  - "4π" coverage with a large TPC
  - Event rate and Particle ID capabilities are limited
- PHENIX approach
  - Multiple detector subsystem with very high segmentation to identify hadrons, photons, and leptons
  - High event rate
  - Limited solid angle coverage

Event recorded by STAR detector on June 25, 2000.

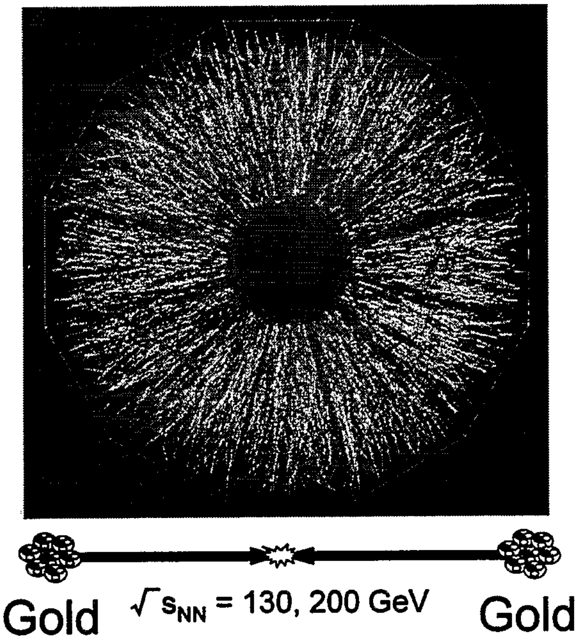

13

PHENIX RHIC operation

Completed and started physics in 2000

- RUN-1 (August – September, 2000)
  - Au + Au at $s_{NN}^{1/2} = 130$ GeV
  - Achieve ~10% of design luminosity
- RUN-2 (August 2001 – January 2002)
  - Au + Au at $s_{NN}^{1/2} = 200$ GeV
    - Achieve design luminosity
  - short (1 day) run Au+Au at $s_{NN}^{1/2} = 22$ GeV
  - First polarized p+p run at $s^{1/2} = 200$ GeV
- RUN-3 (November 2002 (?) -)

PHENIX Run-1 Results of PHENIX

- Global Measurements —
  - Charged Multiplicity — PRL 86 (2001) 3500
  - Transverse Energy — PRL 87 (2001) 052301
- Elliptic flow measurement — paper in preparation
- Event fluctuation
  - Charge fluctuation — nucl-ex/0203014, submitted to PRL
  - <Pt>, <et> fluctuation — nucl-ex/0203015, submitted to PRC
- Two particle correlation — nucl-ex/0201008, accepted in PRL
- Hadron production
  - K,π,p spectra — nucl-ex/0112006, submitted to PRL
  - Particle ratios — paper in preparation
  - Λ production — paper in preparation
- High pt particle production
  - Suppression of high pt hadrons — PRL 88 (2002) 022301
  - Centrality dependence — paper in preparation
- Electron and charm — nucl-ex/0202002, accepted in PRL

15

PHENIX Global measurements

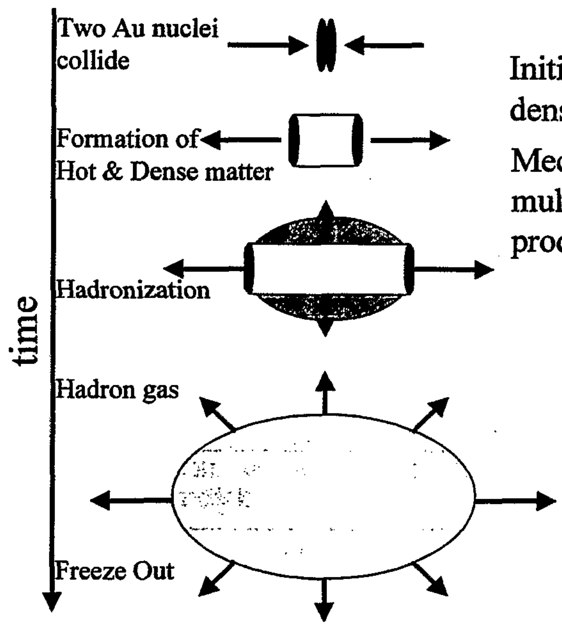

Initial energy density ε ⟷ $d\Sigma E_T/dy$

Mechanism of multi-particle production ⟷ N_{part} dependence of N_{ch}, ΣE_T

Parton scattering contribute to Nch and ΣE_T?

Parton saturation effect?

PHENIX — Transverse Energy and Energy Density

Bjorken estimate for energy density

$$\varepsilon_{Bj} = \frac{1}{\pi R^2}\frac{1}{c\tau_0}\left(\frac{dE_T}{dy}\right)$$

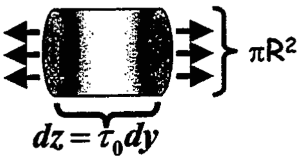

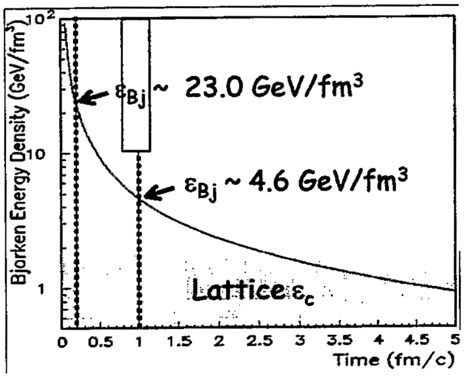

formation time: 0.2 - 1 fm

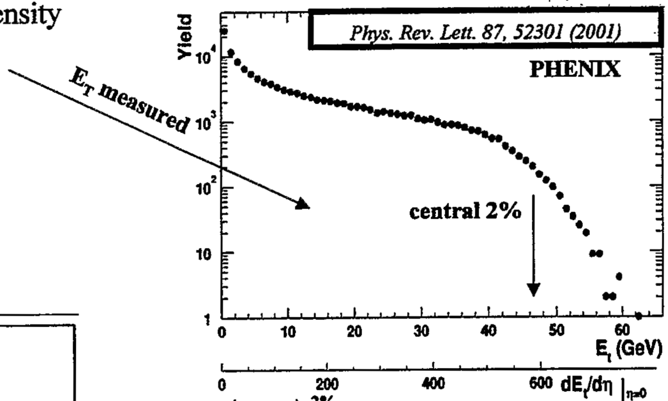

$$\left\langle \frac{dE_T}{dy} \right\rangle^{2\%}_{y=0} = \left(578^{+26}_{-39}\,\mathrm{GeV}\right)\times\left(1.19\pm0.01\right)$$

Initial condition: energy density

- significantly above expected critical density

  lattice: ε_c ~ 0.6 - 1.2 GeV/fm³
- > 1.6 increase compared to CERN

17

PHENIX — Multiplicity

- Measured by PC1-PC3
  - $|\eta| < 0.35$
  - $\Delta\phi = 90^o$
  - Minimum bias ~ 92% of s_{GEOM} = 6.8b
- Multiplicity density in central collision

$dN/d\eta = 622 \pm 41$

(60 % increase from Pb+Pb collisions at CERN SPS)

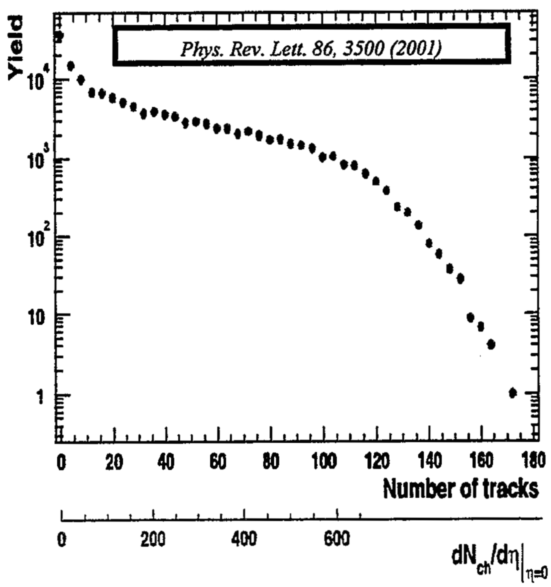

PHENIX RHIC : $dN_{ch}/d\eta$ at $\sqrt{s_{NN}}$ = 130 GeV

PHOBOS: $|\eta|<1$, $\Delta\Phi \approx 1\%$?

$dN_{ch}/d\eta$ = 555 ± 12 ± 35 (6% most central) PRL

$dN_{ch}/d\eta$ = 579 ± 1 ± 22 (6% most central)

PHENIX: $|\eta|<0.35$, $\Delta\Phi = 90°$

$dN_{ch}/d\eta$ = 622 ± 1 ± 41 (5% most central)

STAR: $|\eta|<1.8$, $\Delta\Phi = 2\pi$

$dN_{ch}/d\eta$ = 567 ± 1 ± 38 (5% most central)

BRAHMS $|\eta|<4.7$

$dN_{ch}/d\eta$ = 553 ± 1 ± 36 (5% most central)

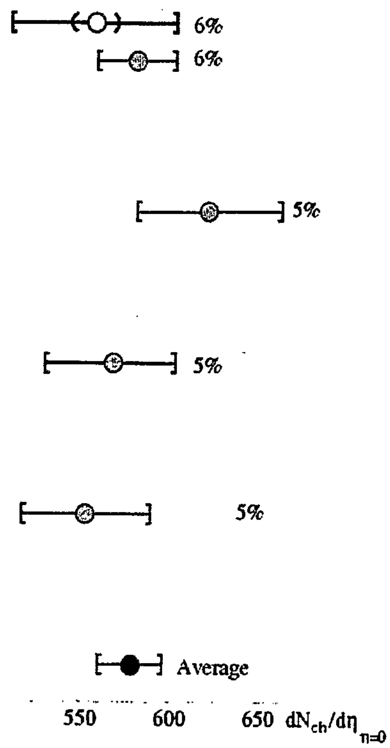

19

PHENIX $dN_{ch}/d\eta$: pp and AA (central)

Collection of data points from pp and AA experiments.
AA values are divided by Number of participants

AA Fixed-target:
$dN_{ch}/d\eta$ approx.
equal to dN_{ch}/dy

AA Collider:
$dN_{ch}/d\eta$ *not*
equal to dN_{ch}/dy

- A+A dN/dh is higher than p+p
- Note large spread at SPS

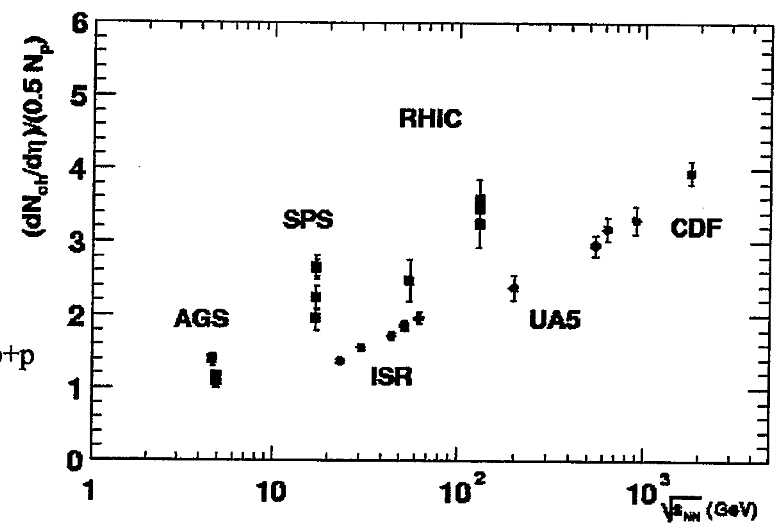

Basics: N_{part}, N_{coll}

- p+p: $N_{part} = 2$, $N_{coll} = 1$
- p+A: $N_{part} = N_{coll} + 1$
  ($N_{part} \sim 6$ for Au)
- Geometrical Model (Glauber Model)
  - Number of collsion (N_{coll})
  - Participants (N_{part})
    - Nucleons that collide with nucleus
  - Spectators ($2A - N_{part}$)
    - Nucleons that do not collide
- A+A: $N_{coll} \propto N_{part}^{4/3}$

QUESTION:

How dN/dy behaves as function of Npart ?

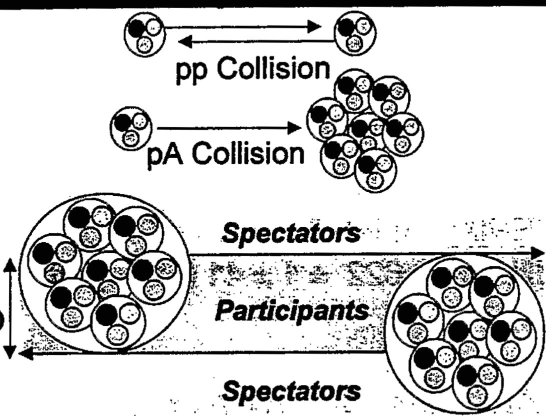

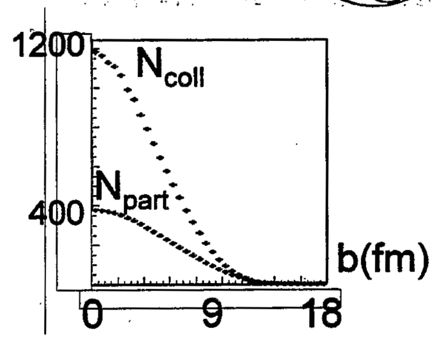

21

Determining N_{part}

- Use combination of ZDC and BBC
  - ZDC measures number of spectator neutrons
  - BBC measures charged multiplicity (~ # of participants)
- Use Glauber model (geometrical model) to determine centrality classes

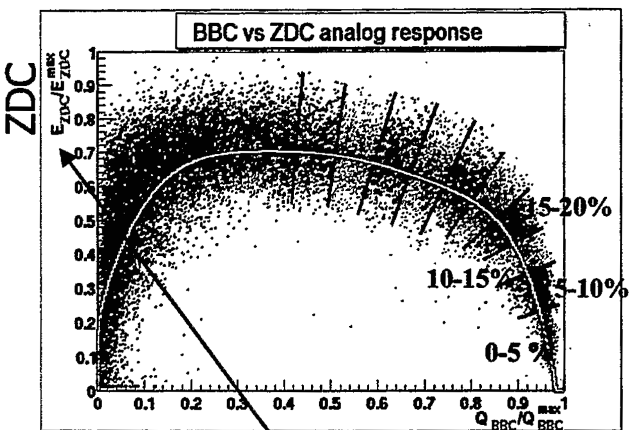

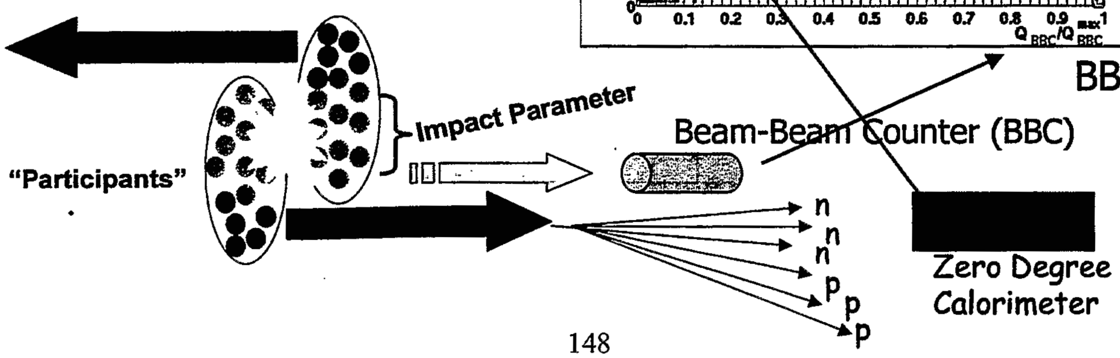

148

PHENIX N_{ch}, ΣE_T per N_{part}

- Measure N_{ch} and ΣE_T per N_{part}
- Both quantities increases faster than Npart

$$dX/d\eta\big|_{\eta=0} = A \times N_{part} + B \times N_{coll}$$

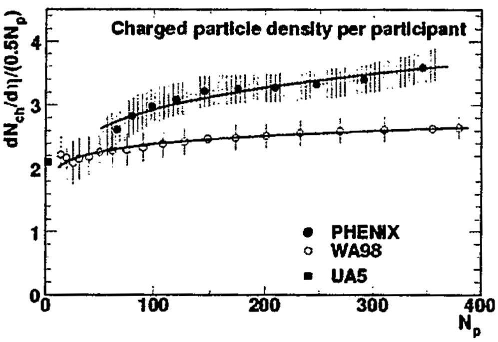

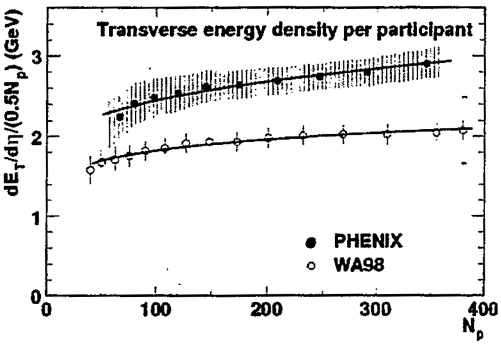

$A = 0.88 \pm 0.28$
$B = 0.34 \mp 0.12$
$B/A = 0.38 \pm 0.19$

$A = 0.80 \pm 0.24 (GeV)$
$B = 0.23 \mp 0.09 (GeV)$
$B/A = 0.29 \pm 0.18$

23

PHENIX Globals: Summary

- ΣE_T
  - Bjorken energy density $\varepsilon = 4.6$ GeV/fm^3
    - Initial density can be as high as 20 GeV/fm^3
    - Well beyond Lattice estimate of ε_{crit}
- $dN_{ch}/d\eta$
  - 60 % higher than Pb+Pb at SPS
  - Non-linear increase with N_{part}
    - Hard scattering contribution (~ Ncoll)
    - Parton saturation?

PHENIX Flow effects

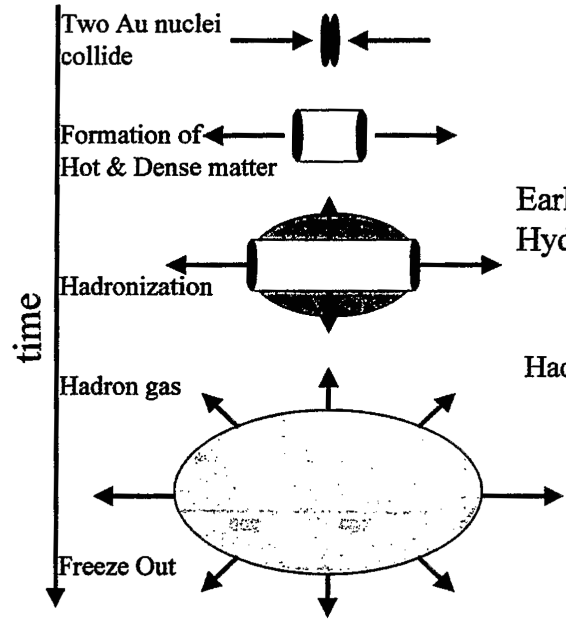

Early thermailzation? ⟷ Stronger flow
Hydrodynamics? effect

Hadron re-scattering? ⟷ Weaker flow
effect

PHENIX Flow effects in H.I.C.

- In non-central A+A collisions, “flow” effect has been observed.
- The flow effect is caused by conversion of spatial anisotropy to momentum anisotropy by particle re-scattering
- The flow becomes strong in the hydrodynamic limit (strong re-scattering limit).

Non-central Collisions

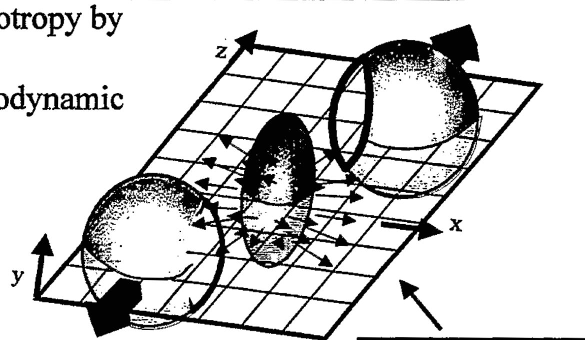

Reaction plane

Elliptic Flow

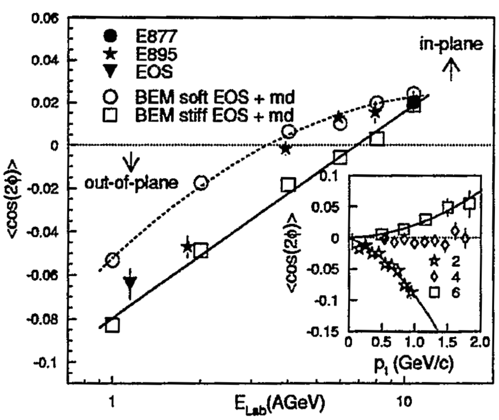

Low Energy: ---- Squeeze-out
High Energy : In-plane Emission

PHENIX — Flow measurements by two particle correlation

Study $\Delta\phi$ Correlation between particles:

$$\boxed{\frac{dN_{pairs}}{d\Delta\phi} \propto \left(1+\sum_{n=1}^{\infty} 2v_n^2 \cos(n\Delta\phi)\right)}$$

- **Event by event reaction plane determination & Dispersion Corrections Circumvented**
- **Uncertainties associated with Acceptance, efficiency Reduced**

PHENIX Detector - First Year Physics Run

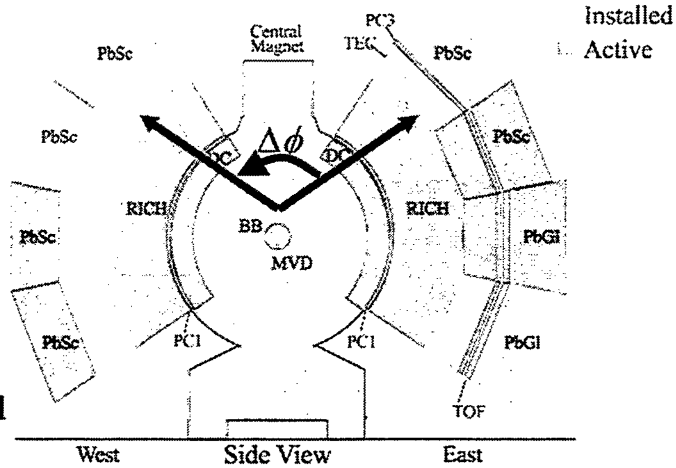

Measured quantity: Fourier coefficient v_n
V_1: (Directed flow): small at RHIC
V_2: (Eliptic flow): large at RHIC

PHENIX — Correlation Functions

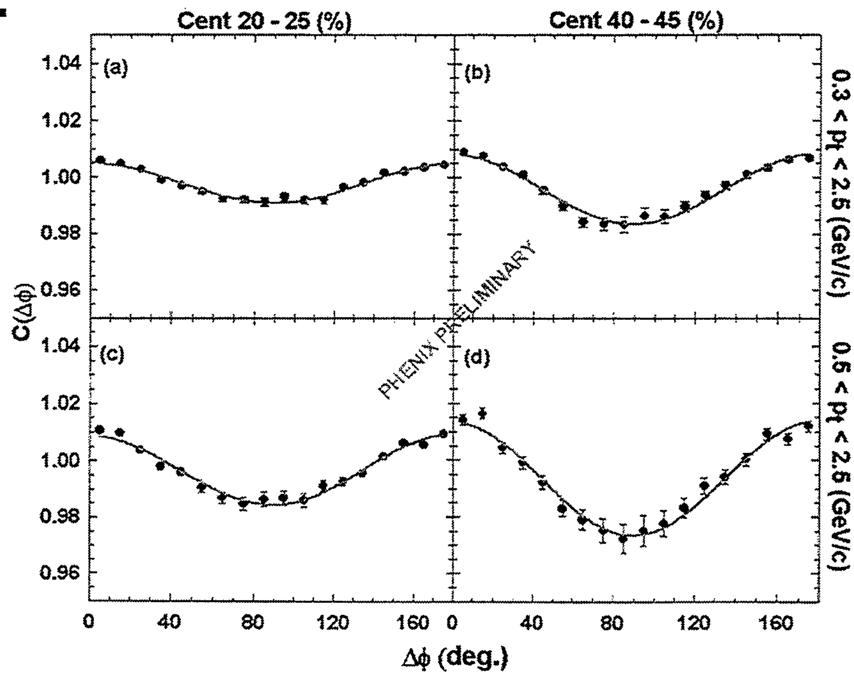

V_2 shows clear centrality and p_T dependence

PHENIX

V_2 vs. Pt

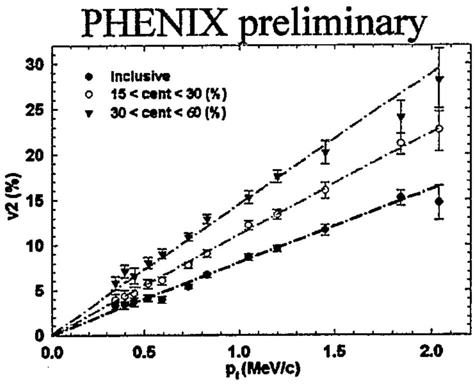

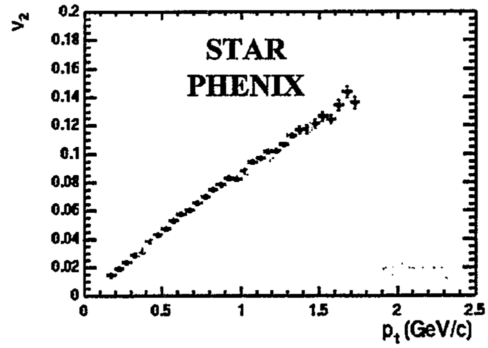

Very strong Elliptic flow (V_2) signal at RHIC
(V_2 increase from 3-4% at SPS to 6-7% at RHIC)
Strong pt Dependence
Consistent results from PHENIX and STAR

Strong flow effects suggests early thermalization at RHIC

29

PHENIX

Scaled Eliptic Flow

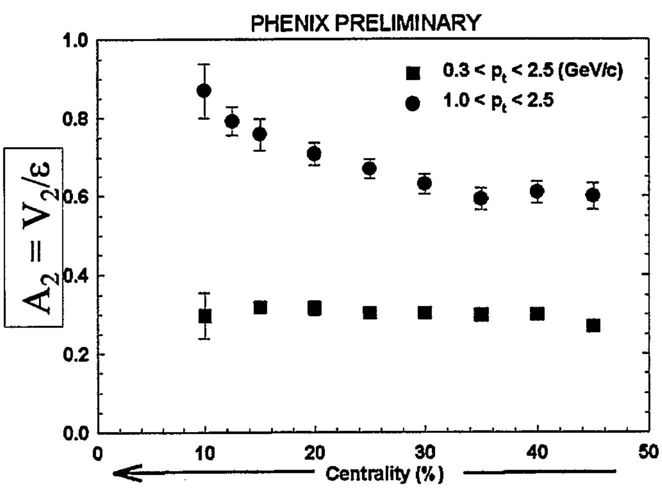

Scaled Eliptic flow
$A_2 = v_2/\varepsilon$

Here
ε: eccentlicity or initial spatial anisotropy of "participants"
$\varepsilon = (\langle y^2\rangle - \langle x^2\rangle)/(\langle y^2\rangle + \langle x^2\rangle)$
(calculated from a Glauber model)

In low pt, v_2 scaled with e
At high pt, the scaling breaks down

PHENIX Two particle correlation

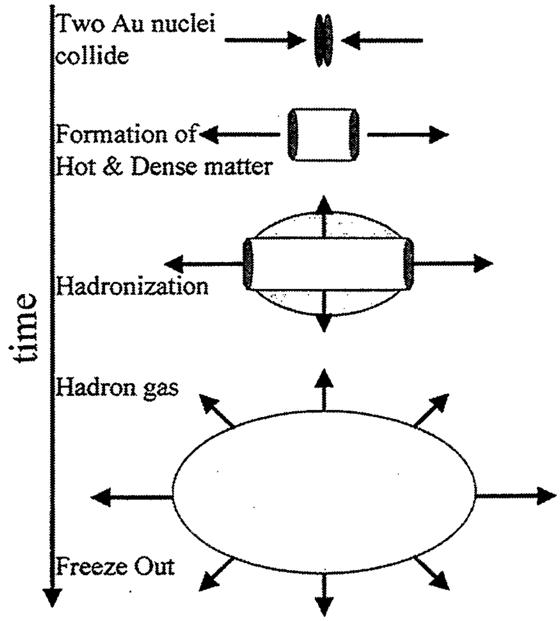

1st order phase transition?

Duration time and Source size at Freeze-out ⟷ Two particle correlation measurement (HBT)

Source size and duration time of freeze-out can be Extracted from two particle interference measurement.

In some model, a very long duration time is predicted if there is a first order phase transition.

Does it observed at RHIC?

PHENIX HBT measurements

$$
\begin{aligned}
C_2 &= P_2(p_1,p_2)/P(p_1)P(p_2) \\
&= 1+\lambda \exp\left(-q_{inv}^2 R_{inv}^2\right) \\
&= 1+\lambda \exp\left(-q_X^2 R_X^2 - q_Y^2 R_Y^2 - q_Z^2 R_Z^2 - q_t^2 \sigma_t\right) \\
&= 1+\lambda \exp\left(-q_{side}^2 R_{side}^2 - q_{out}^2 R_{out}^2 - q_{long}^2 R_{long}^2\right)
\end{aligned}
$$

Assuming a source density is a Gaussian distribution

Bertsch-Pratt parameterization scheme

1D correlation function

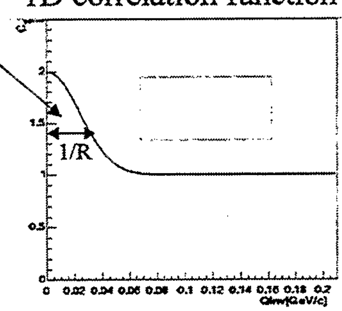

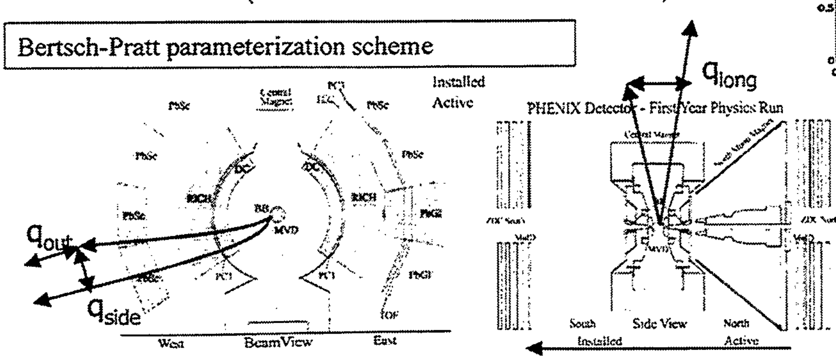

⊗ Beam direction

Beam direction

If we use LCMS frame…

The duration time

$$\Delta\tau = \sqrt{R_{To}^2 - R_{TS}^2}/\beta$$

PHENIX 3-D correlation result

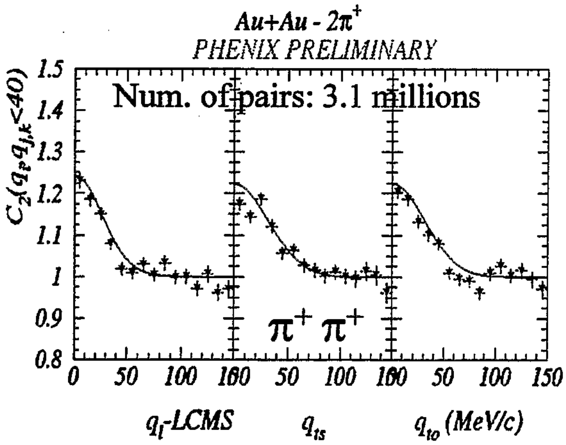

$\lambda = 0.395 \pm 0.026$
$R_{side} = 4.42 \pm 0.22$
$R_{out} = 4.45 \pm 0.22$ [fm]
$R_{long} = 5.28 \pm 0.32$

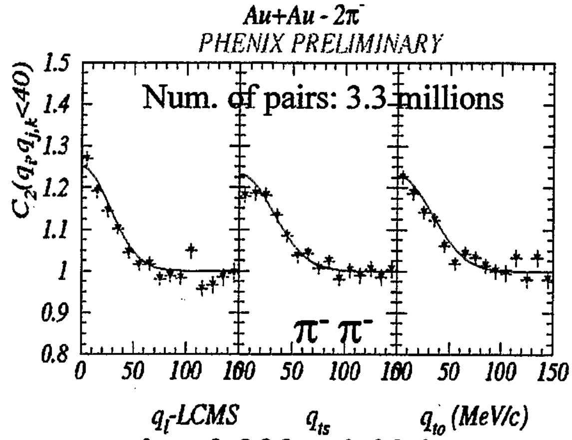

$\lambda = 0.399 \pm 0.026$
$R_{side} = 4.41 \pm 0.22$
$R_{out} = 4.30 \pm 0.24$ [fm]
$R_{long} = 5.13 \pm 0.26$
(Errors are statistical only)

nucl-ex/0201008, accepted in PRL

PHENIX Comparison with other experiments

	$\sqrt{s_{NN}}$
PHENIX,STAR	130GeV
NA44,NA49,CERES	17.2GeV
AGS-E866	4.6GeV

Radii parameters depend on K_T
- Transverse radii (R_{side} and R_{out}) have very little dependence on beam energy

- Almost all energy dependence is in longitudinal radius (R_{long})

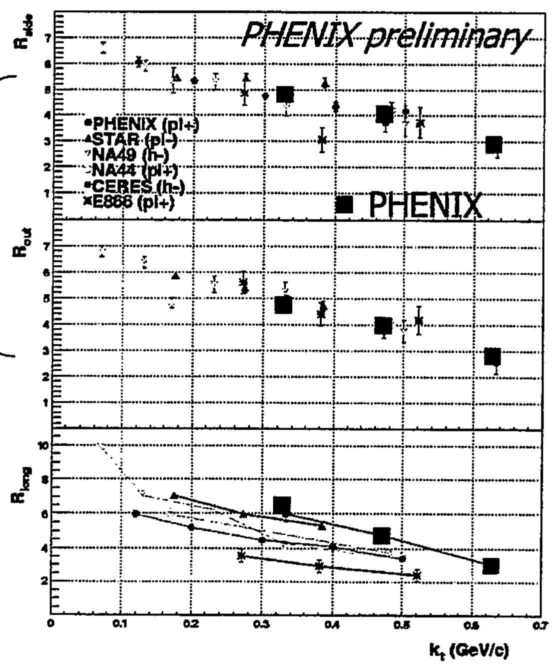

nucl-ex/0201008, accepted in PRL

PHENIX HBT puzzle

In Hydrodynamical models

1^{st} order phase transition → long duration time τ

For *static* and *transparent* source

$t = \text{sqrt}(R_{out}^2 - R_{side}^2)$

→ Prediction:

$R_{out} >> R_{side}$

PHENIX and STAR result:

Rout = Rside

→Naïve hydrodynamic models are excluded

Possibile solutions to the puzzle

- Dynamic effects
- Opacity? (reduce Rout)
- Frame dependence?

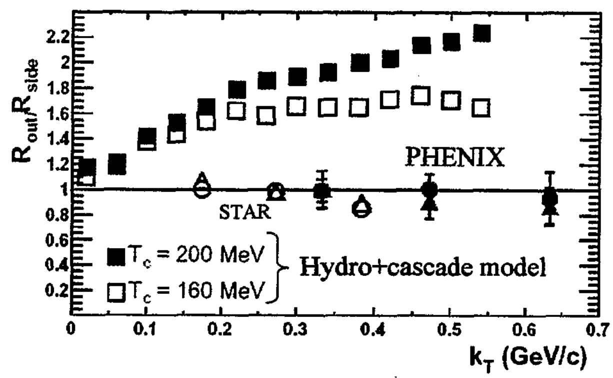

nucl-ex/0201008, accepted in PRL

35

PHENIX Hadron measurements

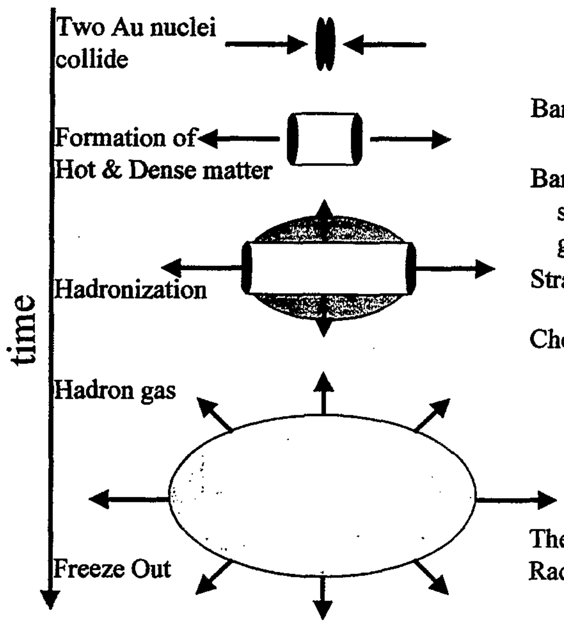

Baryon transport ↔ Net proton density dN/dy(p) – dN/dy(pbar)

Baryon pair produciton ↔ dN/dy(pbar)
string fragmentation?
gluon junction model?

Strangeness production ↔ K, Λ, Ξ, Ω

Chemical freeze-out ↔ Hadron dN/dy ratios Thermal fit (T_{ch}, μ_B)

Thermal freeze-out ↔ dN/dpt of K, π, p, Λ, etc
Radial flow? Thermal fit (T_{th}, β_t)

PHENIX Hadron measurement

Combined
- Tracking
- Beam-Beam Counter
- Time-of-Flight array

provides excellent hadron identification over broad momentum band:

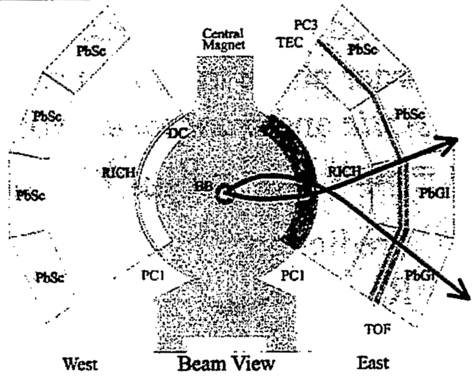

DC resolution
$\sigma p/p \sim 0.6\% \oplus 3.6\%\, p$

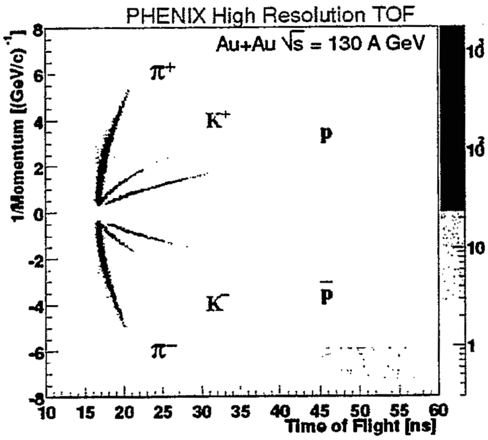

TOF resolution 115 ps

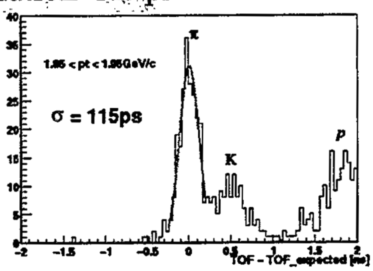

37

PHENIX 10% Central PHENIX Spectra

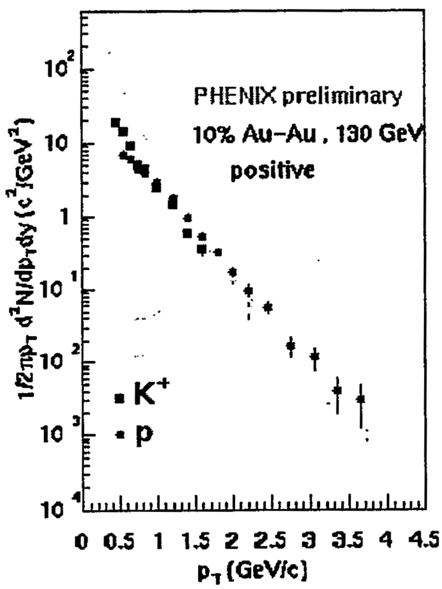

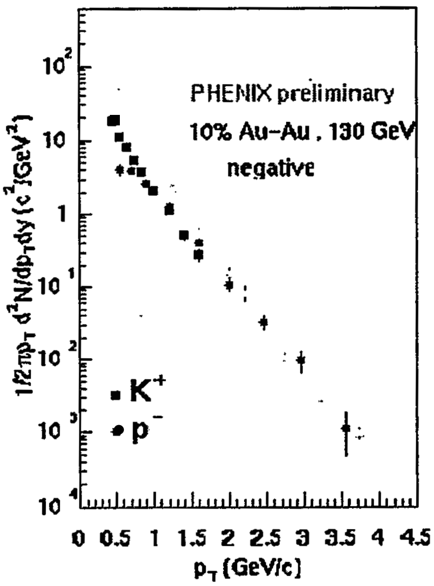

nucl-ex/0112006, submitted to PRL

PHENIX Hadron Yield

- dN/dy scaled by N_p pair rises faster for (anti)p than pions with N_{part}
- Note: scaled for clarity

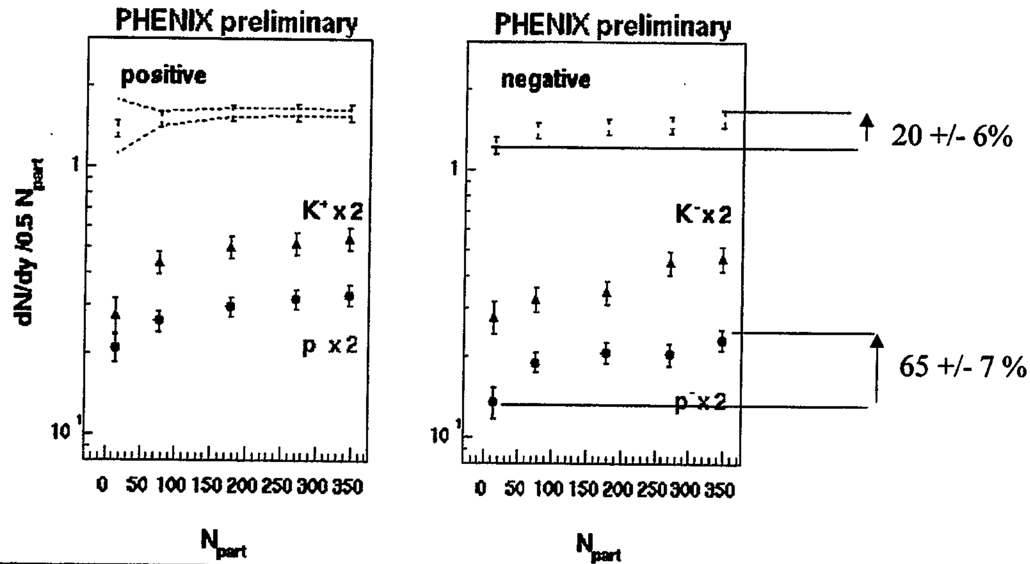

nucl-ex/0112006, submitted to PRL

39

PHENIX K/π ratio in central collisions vs $\sqrt{s_{NN}}$

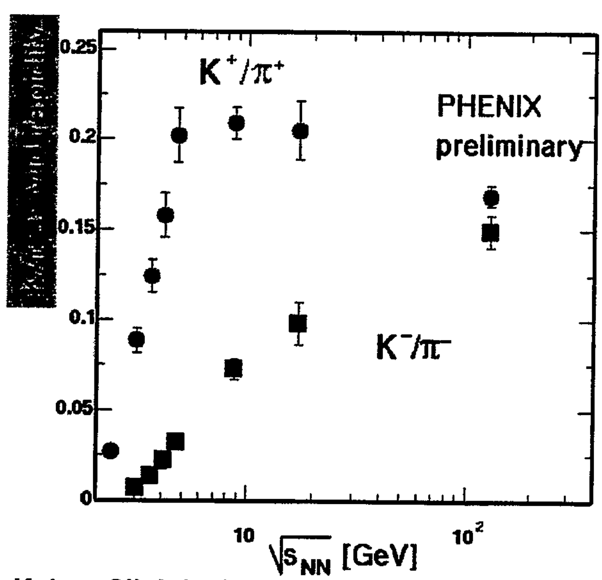

- Strangeness enhancement with respect to p+p collisions

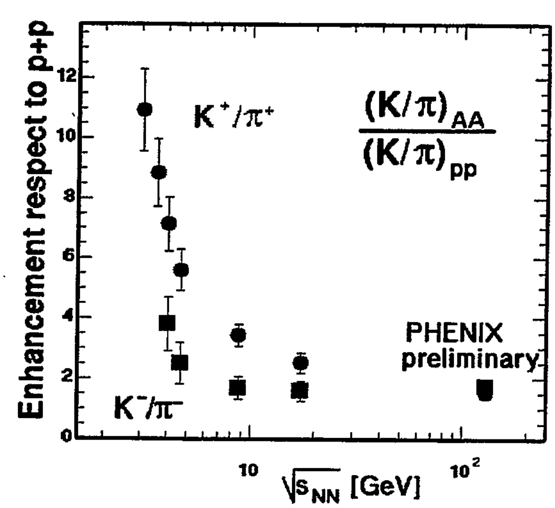

- K+/π+ : Slightly decreases from top SPS energy.
- K-/π- : monotonically increases from AGS/SPS

Paper in preparation

PHENIX Collision energy dependence

- p-/p+, K-/K+ and pbar/p vs. collision energy.
  - anti-particle/particle ratios are dramatically increasing from SPS and AGS energies and approaching unity.

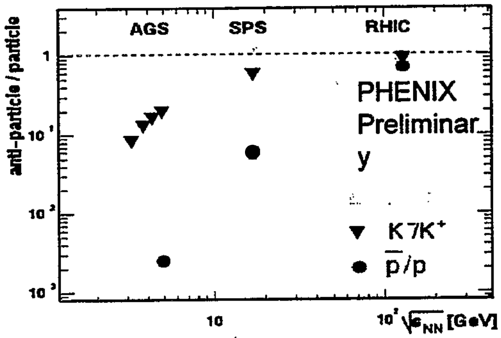

- (p-p)/(Npart pair) is dramatically decreasing from AGS and SPS energy

  RHIC : factor 7 smaller than AGS energy.

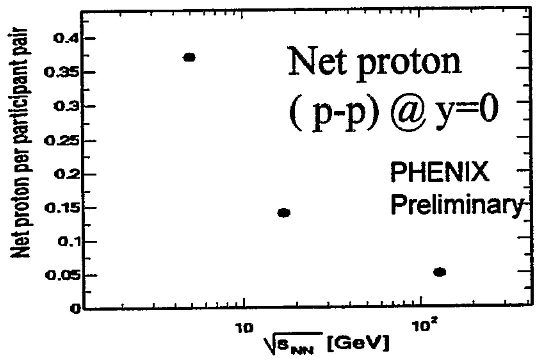

Paper in preparation

PHENIX Thermal fit to particle ratios

Hadron resonance ideal gas

Refs. J.Rafelski PLB(1991)333
J.Sollfrank et al. PRC59(1999)1637

$$\rho_i = \gamma_s^{|s_i|} \frac{g_i}{2\pi^2} T_{ch}{}^3 \left(\frac{m_i}{T_{ch}}\right)^2 K_2(m_i/T_{ch})\ \lambda_q{}^{Q_i}\ \lambda_s{}^{s_i}$$

$$\lambda_q = \exp(\mu_q/T_{ch}), \quad \lambda_s = \exp(\mu_s/T_{ch})$$

T_{ch} : Chemical freeze-out temperature
μ_q : light-quark chemical potential
μ_s : strangeness chemical potential
γ_s : strangeness saturation factor

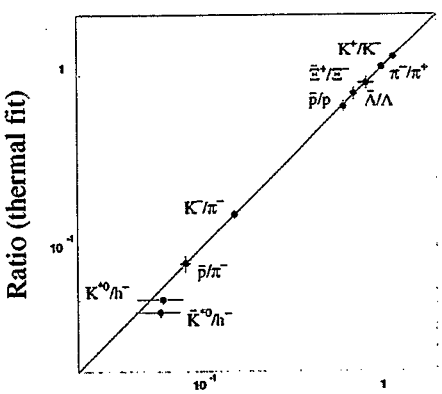

Fit by M. Kaneta to RHIC data
Similar fits by other groups

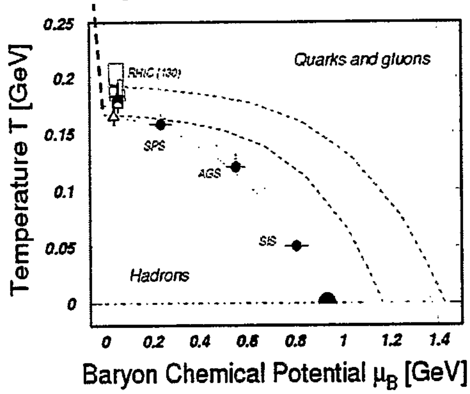

- Fit results: T_{ch}~170MeV~T_{crit}
  μ_B~30 MeV

PHENIX — Mean transverse momentum

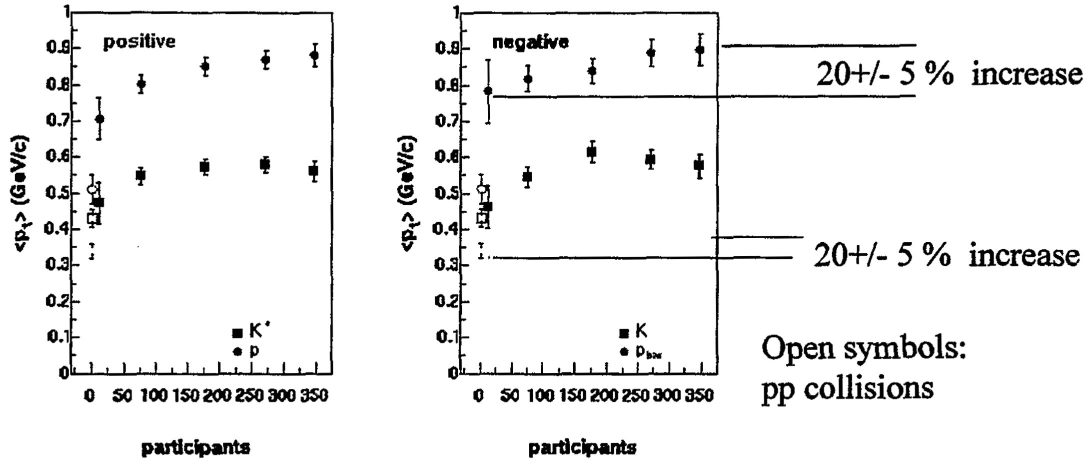

- Mean p_t ↑ with N_{part}, m_0 → radial flow
- Relative increase from peripheral to central same for π, K, (anti)p
- (Anti)proton significant ↑ from pp collisions

nucl-ex/0112006, submitted to PRL

43

PHENIX — Hydrodynamics model fit: M_T distribution

Local thermalized fluid, with radial expanding flow

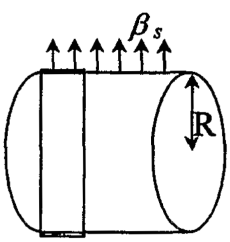

$$E\frac{d^3n}{dp^3} \propto \int_\sigma e^{-(u^\nu p_\nu)/T_{th}} p^\lambda d\sigma_\lambda \qquad u^\nu(t,r,z=0) = (\cosh\rho, e_r \sinh\rho, 0) \qquad \rho = \tanh^{-1}\beta_r \quad \beta_r = \beta_s f(r)$$

↓ Integral over fluid volume

$$\frac{dn}{m_T dm_T} \propto \int_0^R r\,dr\,m_T K_1\left(\frac{m_T \cosh\rho}{T_{th}}\right) I_0\left(\frac{p_T \sinh\rho}{T_{th}}\right)$$

Ref. : E.Schnedermann et al, PRC48 (1993) 2462

Flow profile used

$(\beta_r = \beta_s (r/R_{max}))$

This simple model predicts the shapes of Mt distribution of π, K, p, Λ, etc for only two parameters (T_{th}, β_s) (if you chose a profile)

Can model describe the data?

PHENIX Fit to Single Particle Spectra

Simultaneous fit ($m_t - m_0$) < 1 GeV (see arrows)

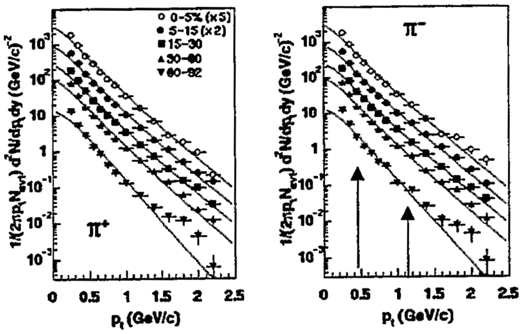

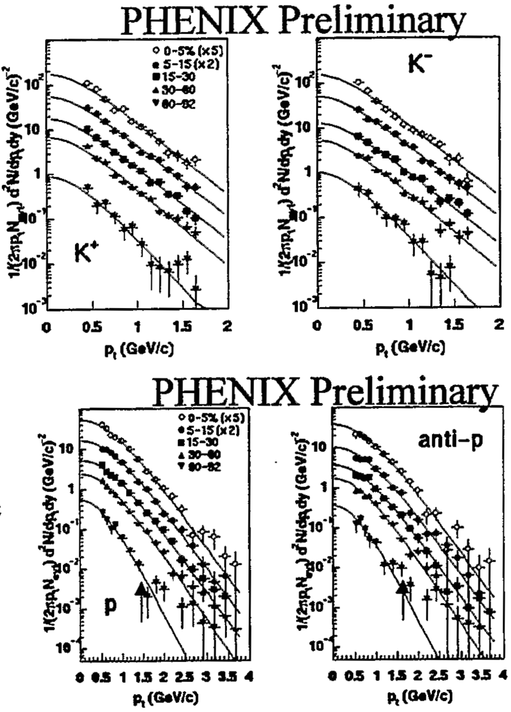

Exclude π resonances by fitting $p_t > 0.5$ GeV/c

The resonance region decreases T by ~20 MeV.

Paper in preparation

PHENIX Hydrodynamics fit resut

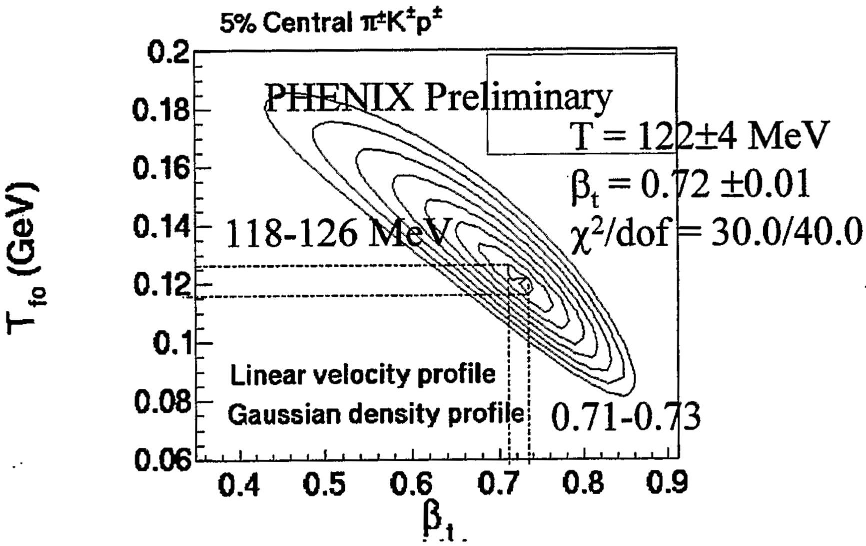

Paper in preparation

PHENIX High Pt particle production

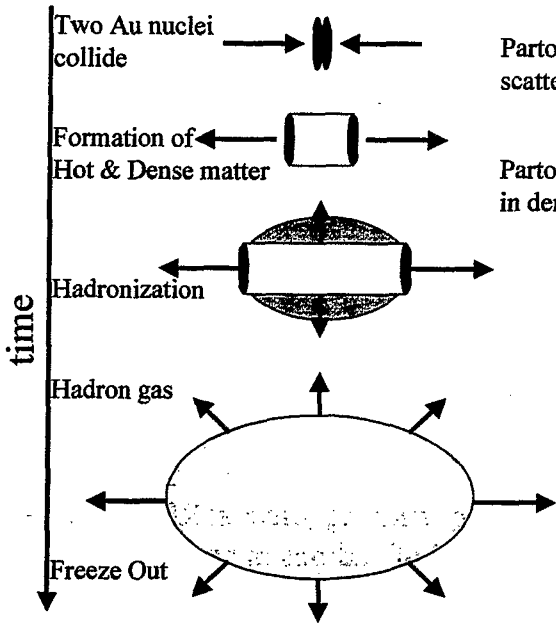

Parton-parton scattering	High pt particle production
Parton energy loss in dense matter	Suppression of high pt particles (jet quenching)

47

PHENIX High pt particle production

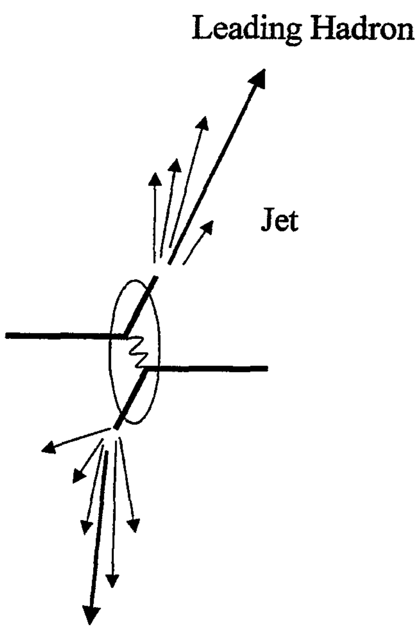

- In high energy collisions, scattered quarks and gluons are observed as high energy jets.
- Due to very high multiplicity, jets can not be directly observed at RHIC. However, jets can be observed by their leading hadrons
- In the absence of nuclear effects Yield of high pt hadrons should scale with number of binary collisions
- PHENIX measures high pt charged particles and π^0

PHENIX — Jet Quenching

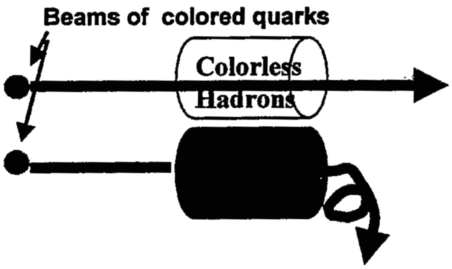

Little energy loss of quarks and gluons in hadronic matter

A large energy loss due to gluon radiation in high density matter is predicted
→Jet Quenching

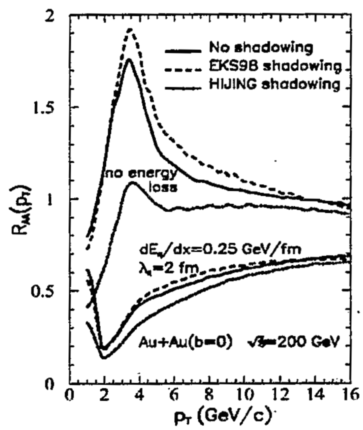

At RHIC, jet quenching can be observed as suppression of high pt particle production.

A prediction of jet quenching effect at RHIC by X.N.Wang. The yield of hadrons in pt=2-6 GeV/c is suppressed relative to scaling with number of binary collisions (Ncoll).

PHENIX — Nuclear effects in high pt particle production

In the absence of nuclear effects, high pt particle production should scale with number of binary collisions (Ncoll).

$$R_{AA} = \frac{1}{Ncoll}\frac{Yield(AA)}{Yield(NN)} = 1 \qquad R_{pA} = \frac{1}{A}\frac{\sigma(pA)}{\sigma(pp)} = 1$$

A+A p+A

Known nuclear effects

Cronin Effect

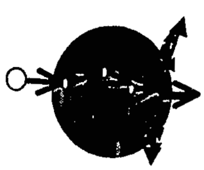

Multiple scattering of partons
→Increase of high pt particle
→R_{AA}>1

Nuclear Shadowing

Reduction of parton density q(x),G(x) in nucleus.
→ R_{AA}<1

- All p+A data shows that high pt particle production in nuclear target is larger than the binary (Ncoll) scaling. This implies that the Cronin effect is greater than the nuclear shadowing.

"Ordinary" Nuclear Effects Modifying p_t Spectra

- Nuclear shadowing at small x→ at RHIC $x \sim 2p_t/\sqrt{s} < 0.02$
- initial state multiple scattering of partons: "Cronin effect

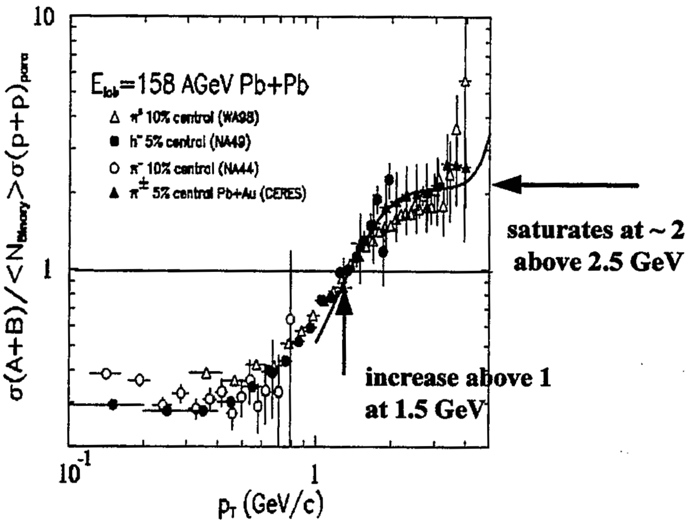

traditional analysis:

$$\sigma_{pA} = A^{\alpha(p_t)}\,\sigma_{pp}$$

"anomalous" nuclear enhancement
$\alpha > 1$ above ~ 2 GeV/c

Nuclear Modification Factor:

$$R_{AB} = \frac{1}{\langle N_{binary}\rangle}\left(\frac{d^2\sigma_{AB}}{dydp_t^2}\right)\Big/\left(\frac{d^2\sigma_{pp}}{dydp_t^2}\right)$$

increase above one at same p_t

51

High pt measurements with PHENIX

- Neutral Pion
  - EMCal
  - (east & west)

- Charged Particles
  - DC, PC1, PC3

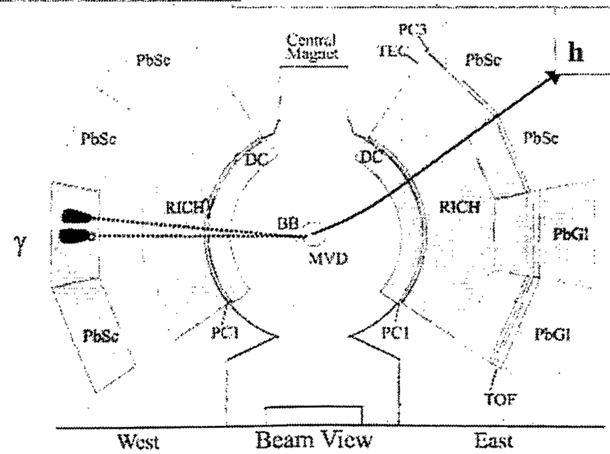

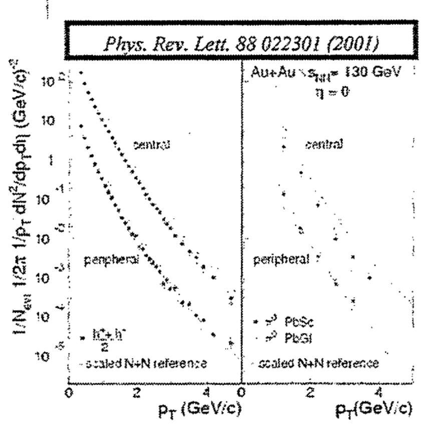

Nuclear Modification Factor Au-Au to p-p

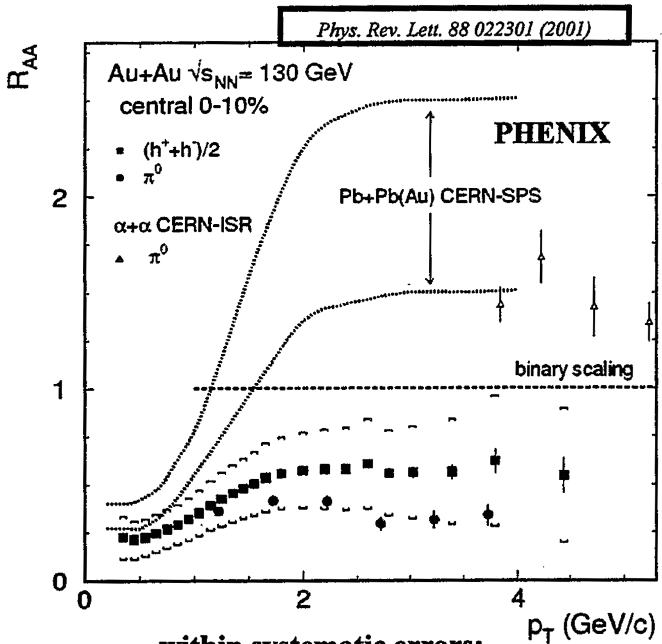

within systematic errors:

$R_{AA} < 1$

- Ratio exhibits characteristic features:
  - charged:
    - increases up to ~ 2 GeV
    - saturates at R_{AA} ~ 0.6
  - neutral pions:
    - ~ constant at R_{AA} ~ 0.4
- Estimate of systematic error
  - data:

charged	16 - 30 %
π^0	21 - 35 %
$\langle N_{binary} \rangle$	11 %
NN ref.	20 - 35 %
total	30 - 50 %

(depending on p_t)

Nucleon to Pion Ratios and Soft to Hard Transition

empirical determination of soft/hard transition at ISR

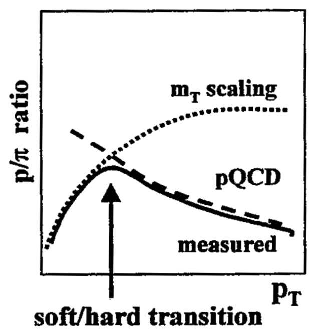

particle ratios have different p_T dependence for soft and hard component

p/π rising with p_T up to 3 GeV

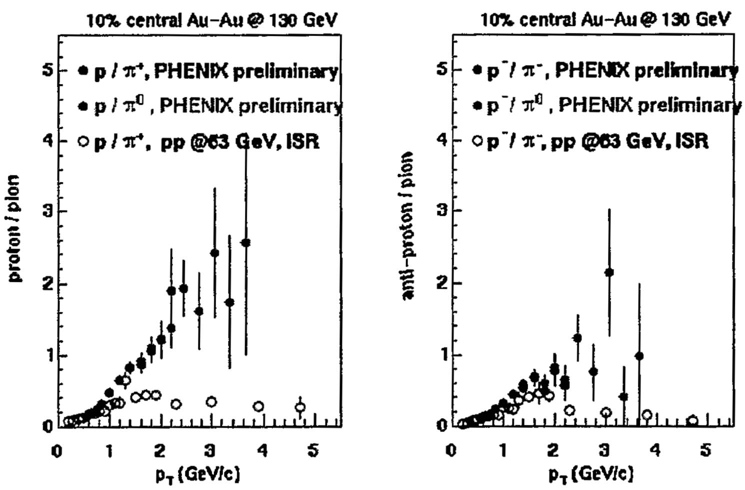

- ISR p-p soft/hard transition below 2 GeV
- RHIC Au-A soft/hard transition above 3 GeV?

PHENIX Single electron and Charm

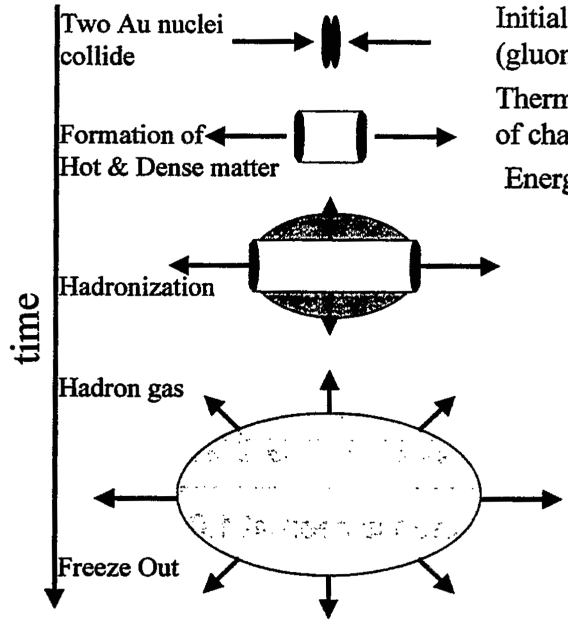

Initial gluon density (gluon shadowing?) ⟷ Charm production

Thermal production of charm ⟷ Charm enhancement?

Energy loss of charm ⟷ Charm pt distribution

Charm is a very good probe of initial stage of heavy ion collisions.

Charm production at RHIC can be studied from its decay to single electrons

55

PHENIX single electrons at high pt

- At ISR($s_{NN}^{1/2}$~60GeV), "prompt" electron signal is observed at $e/\pi \sim 2 \times 10^{-4}$.
  - The most likely source of the electrons is charm semi-leptonic decay
- At RHIC ($s_{NN}^{1/2}$~200GeV), the electron signal from charm is expected at $e/\pi \sim$ 3-4 $\times 10^{-4}$ in p+p
- The e/π ratio can be as high as 10^{-3} in Au+Au collision
  - Production of charm quark is expected to scale with binary collisions.
  - Production of the high pt pions is suppressed relative to binary scaling by about factor 3

(Simulation)

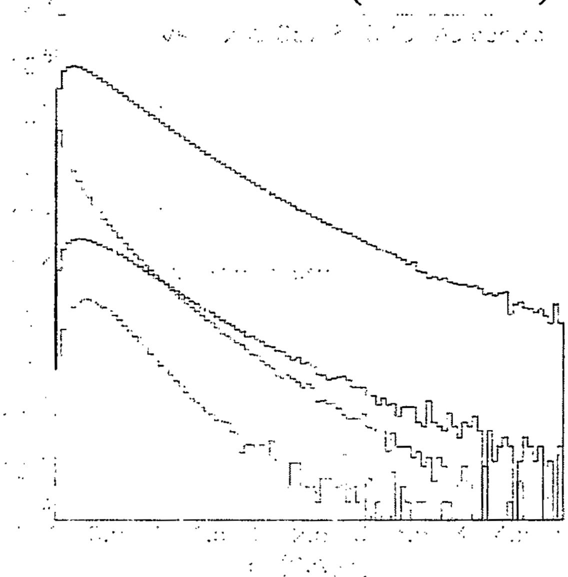

PHENIX Electron measurment in PHENIX

- Electrons are identified by RICH and EMCAL

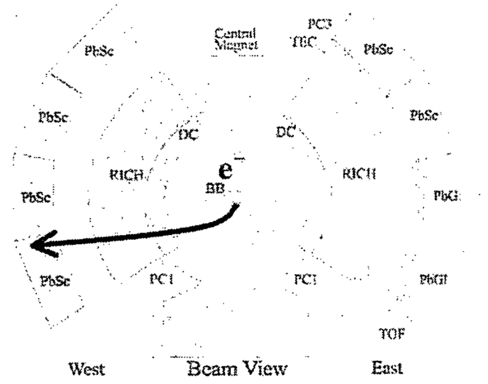

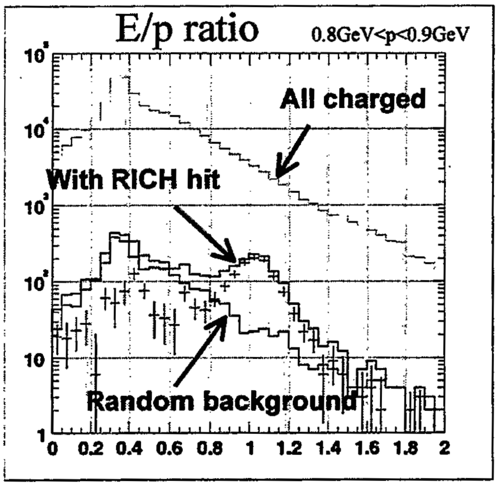

- A clear peak in the energy/momentum (E/p) ratio is seen at 1.0 after RICH hit is required
- EMCAL E/p cut cleans up the rest of the background.
- Random background is also subtracted by an event mixing method

57

PHENIX Single electron spectrum

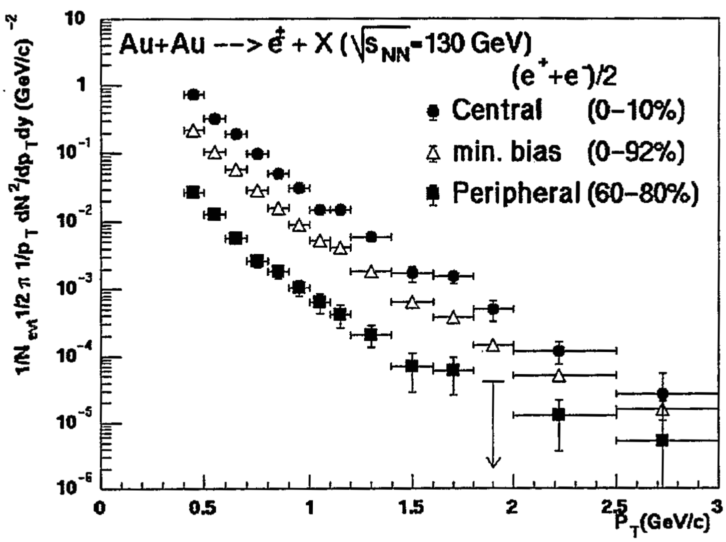

- Fully corrected single electron spectra in PHENIX.
- The spectra includes background such as Dalitz decays and photon conversions.

PHENIX — Background from light hadron decays

$\pi^0 \rightarrow e^+e^- \gamma$
$\pi^0 \rightarrow \gamma\gamma$
$\quad\quad \hookrightarrow e^+e^-$

- ~80% of background
- Proportional to pion
- conversion ~ 1.9 x Dalitz in PHENIX

$\eta \rightarrow e^+e^- \gamma$
$\eta \rightarrow \gamma\gamma$
$\quad\quad \hookrightarrow e^+e^-$

~20% of π^0 contribution at high pt

Other contributions: small

- The measured electron spectra includes trivial background from light hadron decays such as π^0 Dalitz decay and photon conversions.
- The background is estimated using a hadron decay generator that is constrained by pion measurement by PHENIX

59

PHENIX — Data/background ratio

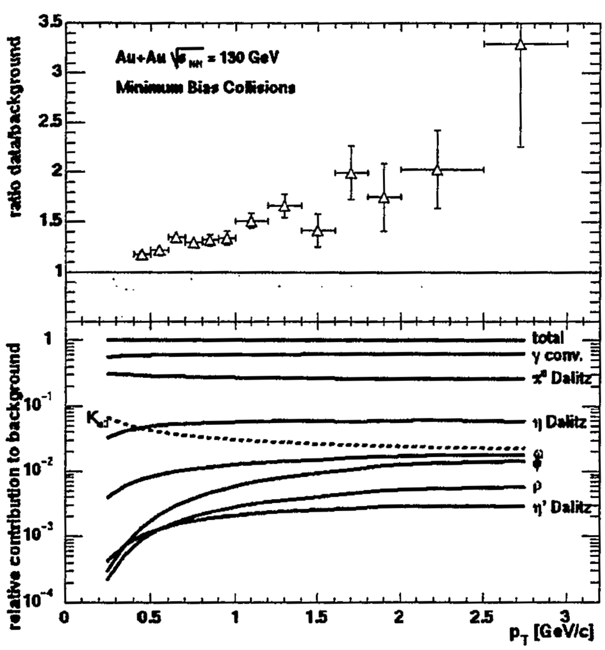

- The Upper panel shows data/background ratio as function of p_t for min. bias collisions.
- The data show excess above background in pt>0.6 GeV/c.
- Central collision data also show similar excess.
- Peripheral data do not have enough statistics
- The low panel shows the relative contribution to the background from various sources.

PHENIX Charm contribution to the signal

- Semi-leptonic decay of charm is an expected source of the electron signal above the background.
- The electron spectrum from charm decay is evaluated by PYTHIA
- PYTHIA parameters are tuned such that fixed target charm data and ISR single electron data are well reproduced.
  - ❑ PYTHIA6.152+CTEQ5L, Mc=1.25 GeV, K=3.5, $<k_t>$=1.5 GeV/c
  - ❑ $\sigma(pp \rightarrow cc)$=330 μb at 130 GeV by this PYTHIA calculation

61

PHENIX Background-subtracted single electron spectra

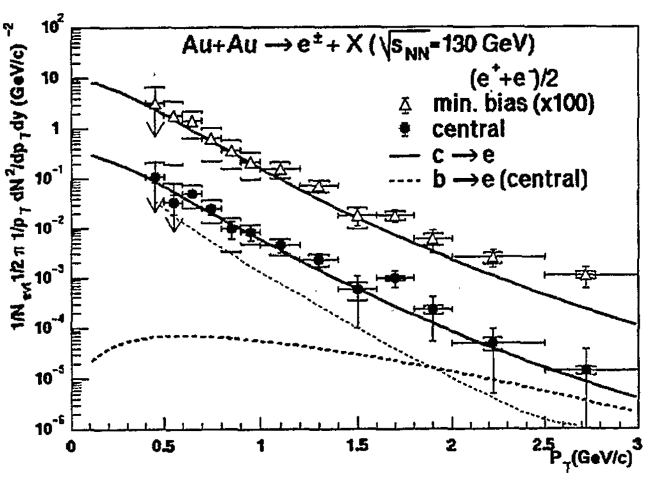

- Spectra of single electron signal is compared with the calculated charm contribution.
- Charm contribution calculated as
  $EdN_e/dp^3 = T_{AA} Ed\sigma/dp^3$
  - ❑ T_{AA}: nuclear overlap integral
  - ❑ $Ed\sigma/dp^3$: electron spectrum from charm decay calculated using PYTHIA
- The agreement is reasonably good.

Charm cross section from the electron data

- We can estimate the charm yield by assuming that all single electrons above the background are from charm
  - Neglect other possible sources such as thermal γ and di-leptons
  - Charm yield can be over-estimated.
- By fitting the PYTHIA electron spectrum to the data for pt>0.8 GeV/c, we obtained charm yield Ncc per event.
- The charm cross section per binary NN collision is obtained as

$$\sigma_{c\bar{c}} = \frac{1}{T_{AA}} N_{c\bar{c}}$$

- T_{AA} is nuclear overlap integral ~ NN integrated luminosity per event
  - T_{AA}=22.6±1.6/mb (central 0-10%)
  - T_{AA}=6.2±0.4/mb (min. bias 0-92%)
- Charm cross section per NN collision in central and minimum bias collision are obtained as

$$\sigma_{c\bar{c}}(0-10\%) = 380 \pm 60 \pm 200 \mu b$$
$$\sigma_{c\bar{c}}(0-92\%) = 420 \pm 33 \pm 250 \mu b$$

Comparison with other experiments

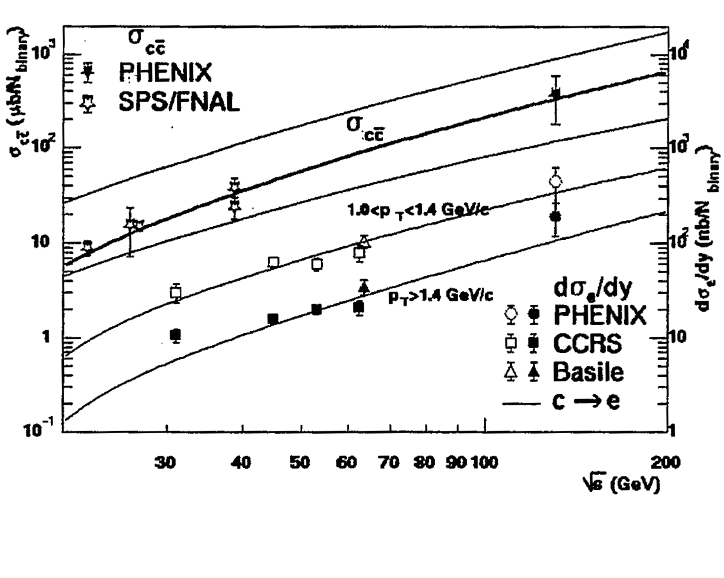

- PHENIX single electron cross section is compared with the ISR data
- Charm cross section derived from the electron data is compared with fixed target charm data
- Solid curves: PYTHIA
- Shaded band: NLO pQCD

PHENIX Summary

- RHIC started the physics run in 2000, and opened a new era in high energy nucleus-nucleus collision
- From RUN-1 data, many interesting results are obtained
  - Transverse energy → $\varepsilon_{BJ} = 4.6$ GeV/fm (>> ε_{crit})
  - Charged multiplicity→ Increase of Nch/Npart
  - Elliptic flow → Stronger than SPS. Early thermalization?
  - Two pion HBT measurement → No duration time?
  - Hadron measurements
    - Tch ~170 MeV ~ Tcrit (@chemical freeze-out)
    - T_{th} ~ 120 MeV; β_T ~ 0.7 (@thermal freeze-out)
  - High p_T spectra → Evidence for Jet quenching?
  - Inclusive electron spectrum → Charm production
    - σ_{cc} ~ 380 +-60+-200 μb at 130 GeV

PHENIX Outlook

- RHIC RUN-2 has just been completed.
  - Au+Au collision at full energy ($s_{NN}^{1/2}$=200 GeV).
  - p+p comparison run at 200 GeV
- PHENIX took data with an improved detector
  - Two full cenral arms
  - South muon arm
  - Much improved DAQ and trigger system
  - >100 times more statistics in Au+Au data (170 M events)
- Expected results from RUN-2 data sets
  - Study of hadron production in much higher statistics
  - High pt paritcle produciton in pt > 10 GeV/c
  - More precise open charm measurement by single electrons
  - J/Psi→e^+e^-, J/Psi→$\mu^+\mu^-$ (deconfinement signal?)
  - ϕ→e^+e^-, ρ→e^+e^- (chiral restoration?)
  - Thermal photons?
  - And much more!

PHENIX The PHENIX Collaboration

- About 400 collaborators from 50+ institutions in 11 nations
- 10 Institutions from Japan

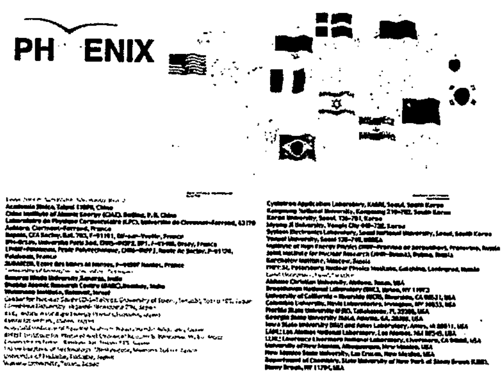

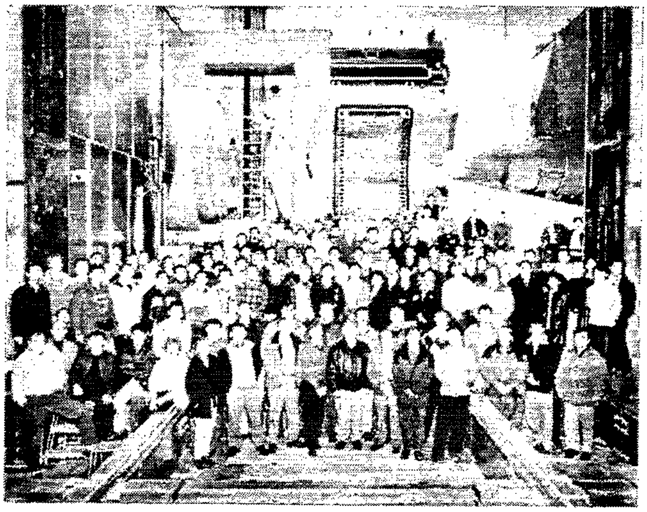

67

First Polarized Proton Collisions at RHIC

Yuji Goto

RIKEN BNL Research Center

RHIC started to be operated as the first polarized proton collider in the 2001–2002 run as well as the relativistic heavy-ion collider. With the polarized proton collisions, we perform investigations of polarized structures of the proton and interactions at high-Q^2 by utilizing symmetry.

In this run, we measured the single transverse-spin asymmetries,

$$A_N = \frac{d\sigma_L - d\sigma_R}{d\sigma_L + d\sigma_R}$$

of many channels in wide kinematical regions at $\sqrt{s} = 200$ GeV. Luminosity $L = 1.5 \times 10^{30}\mathrm{cm}^{-2}\mathrm{sec}^{-1}$ and polarization of 25% were achieved at maximum. As inclusive channels, we measured forward-region A_N (large x_F, p_T ¿ 1 GeV/c) of photons and π^0s in the STAR experiment and that of muons in the PHENIX experiment, mid-rapidity region A_N ($x_F = 0$, p_T ¡ 8 GeV/c) of jets, photons, π^0s, charged hadrons and electrons at STAR and PHENIX, and very forward-region A_N (large x_F, p_T ¡ 0.2 GeV/c) of photons, π^0s and neutrons at IP12. As elastic scatterings, we measured the Coulomb-nuclear interference (CNI) region A_N and the slope of proton-proton collisions in the PP2PP experiment, and those of proton-carbon scatterings at the RHIC polarimeter.

This lecture covers,

- Introduction to the RHIC spin programs
- Physics of A_N measurement
- Commissioning of the RHIC polarized proton acceleration in this run
- Performance of detectors

Slides for A_{LL} physics to be performed in the next run, which was not covered in the talk, are also included. We cannot show any physics results yet. Many A_N measurements will be shown soon after finalizing analyses. Further and updated information can be obtained from following web pages.

RHIC Spin Collaboration	http://spin.riken.bnl.gov/rsc
RHIC	http://www.bnl.gov/rhic
PHENIX experiment	http://www.phenix.bnl.gov
STAR experiment	http://www.star.bnl.gov
PP2PP experiment	http://www.rhic.bnl.gov/pp2pp

RHIC

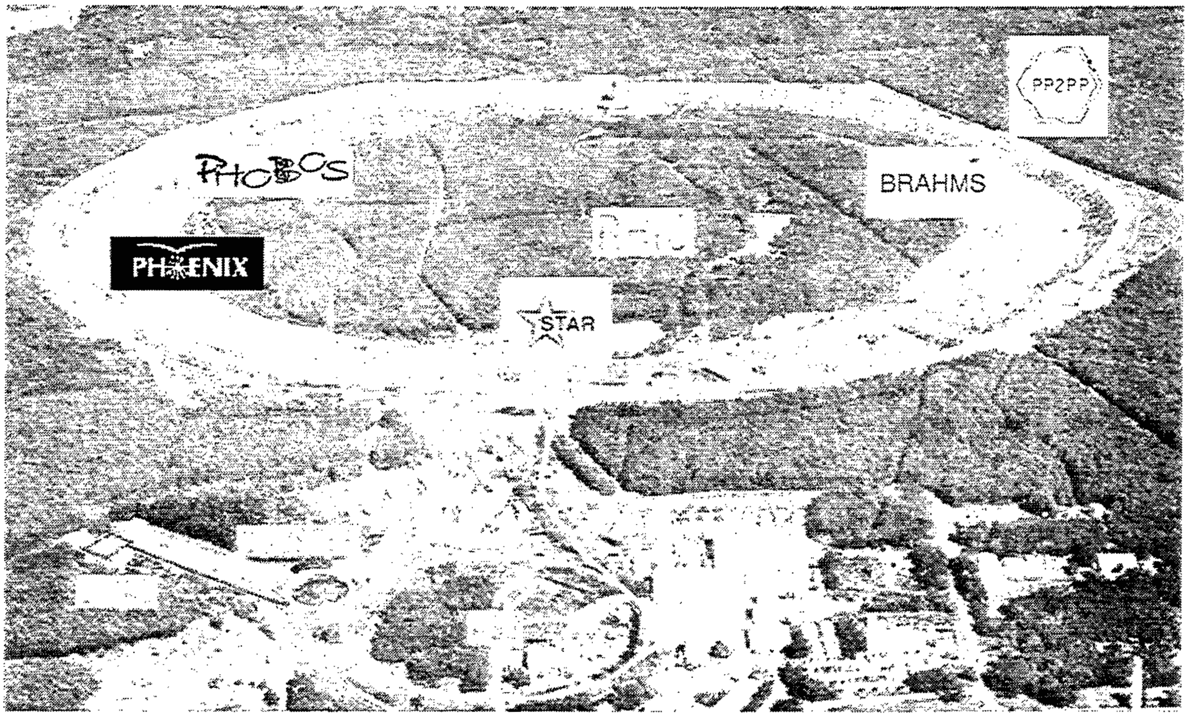

RHIC Spin project

- 1990 Polarized Collider Workshop at Penn State Univ.
- 1991 RHIC Spin Collaboration formed
- 1993 both STAR and PHENIX consider spin physics as a major part of program
- 1995 BNL–RIKEN Collaboration on RHIC spin physics started
  - Muon Arm for PHENIX
  - Siberian Snake and Spin Rotators for PHENIX and STAR
- 1997 RIKEN BNL Research Center established
- as well as
  - DOE funds for STAR Barrel Calorimeter
  - NSF funds for STAR Endcap Calorimeter
  - KEK contribution for OPPIS
  - DOE general supports for spin physics

RHIC polarized proton collider

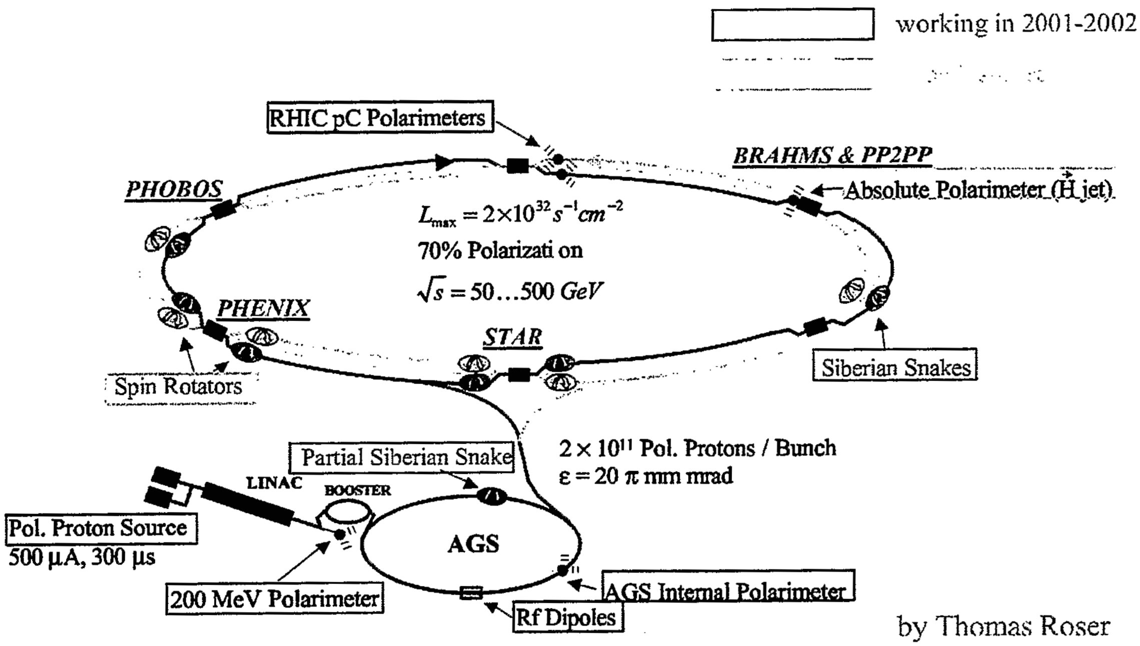

by Thomas Roser

Spin physics

- A_{LL} $$A_{LL} = \frac{d\sigma_{++} - d\sigma_{+-}}{d\sigma_{++} + d\sigma_{+-}}$$
  - double longitudinal-spin asymmetry
  - helicity distribution
- A_L $$A_L = \frac{d\sigma_{+} - d\sigma_{-}}{d\sigma_{+} + d\sigma_{-}}$$
  - parity-violating asymmetry
  - helicity distribution, BSM, …
- A_{TT} $$A_{TT} = \frac{d\sigma_{\uparrow\uparrow} - d\sigma_{\uparrow\downarrow}}{d\sigma_{\uparrow\uparrow} + d\sigma_{\uparrow\downarrow}}$$
  - double transverse-spin asymmetry
  - transversity
- A_N $$A_N = \frac{d\sigma_{L} - d\sigma_{R}}{d\sigma_{L} + d\sigma_{R}}$$
  - single transverse-spin asymmetry / left-right asymmetry
  - higher-twist effect, k_T effect, …

A_{LL}

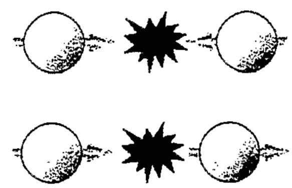

A_N

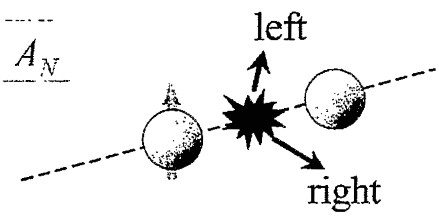

Proton spin 1/2

- Proton spin 1/2 by polarized DIS experiments
  - the quark helicity distribution contributes only 10-20% of the proton spin 1/2

$$\frac{1}{2}=\frac{1}{2}\Delta\Sigma+\Delta g+L$$
$$\Delta\Sigma=0.1\sim0.2$$

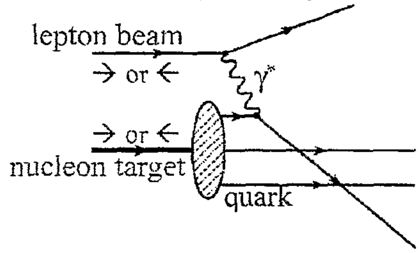

  - contribution of the gluon helicity distribution – next-to-leading order
    - Q^2-evolution (global analysis by SMC group)

$$\Delta g=1.0^{+1.0}_{-0.3}(\mathrm{stat})^{+0.4}_{-0.2}(\mathrm{sys})^{+1.4}_{-0.5}(\mathrm{th})\quad(Q^2=1\mathrm{GeV}^2)$$

    - photon-gluon fusion process
      - HERMES, COMPASS

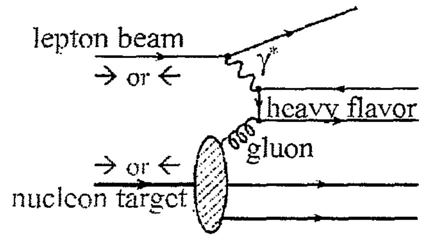

Proton spin 1/2

- Proton spin 1/2 by polarized proton collisions
  - contribution of the gluon helicity distribution – leading order
    - prompt photon production – gluon Compton

$$gq\to q\gamma$$

    - heavy flavor production – gluon fusion

$$gg\to c\bar{c},b\bar{b}$$

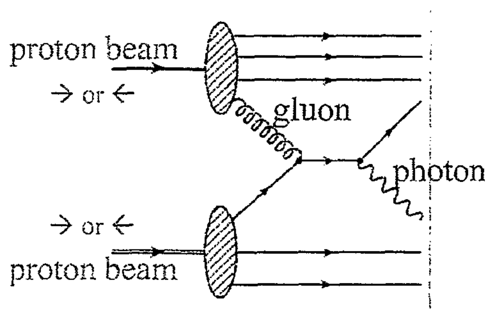

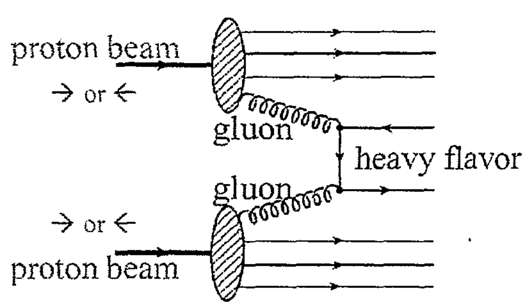

Proton spin 1/2

$$\frac{1}{2} = \frac{1}{2}\Delta\Sigma + \Delta g + L$$

- Polarized distribution functions
  - quark polarization $\Delta q(x)$
  - gluon polarization $\Delta g(x)$
    - pol. DIS in the next-to-leading order
    - pol. hadron collision in the leading order
  - flavor decomposition of the quark polarization
    - semi-inclusive pol. DIS
    - $W^{\pm}$ etc. in the pol. hadron collisions
- Other contributions
  - orbital angular momentum
  - transversity $\delta q(x)$
  - higher-twist effect
  - k_T effect & time-reversal odd fragmentation function
  - ...

Gluon polarization

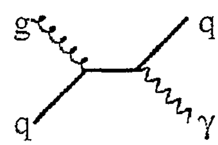

- Prompt photon production
  - gluon Compton process dominant $gq \rightarrow q\gamma$
    - clear interpretation
    - $\Delta g(x_g)$ – gluon polarization measurement in the polarized proton collision
  - asymmetry measurement

$$\boxed{A_{LL} = \frac{d\sigma_{++} - d\sigma_{+-}}{d\sigma_{++} + d\sigma_{+-}}} \qquad A_1^p(x_q, Q^2) = \frac{g_1^p(x_q, Q^2)}{F_1^p(x_q, Q^2)} = \frac{\sum_i e_i^2 \cdot \Delta q_i(x_q, Q^2)}{\sum_i e_i^2 \cdot q_i(x_q, Q^2)}$$

$$\Updownarrow \qquad i = u, \bar{u}, d, \bar{d}, s, \bar{s}, \ldots$$

$$\boxed{A_{LL}(p_T) = \frac{\Delta g(x_g, Q^2)}{g(x_g, Q^2)} \cdot A_1^p(x_q, Q^2) \cdot a_{LL}(\cos\theta^*)}$$

  - experimentally challenging
    - major background - 2γ decay of π^0

Gluon polarization

- Prompt photon production
  - PHENIX inclusive γ
  - STAR γ+jet

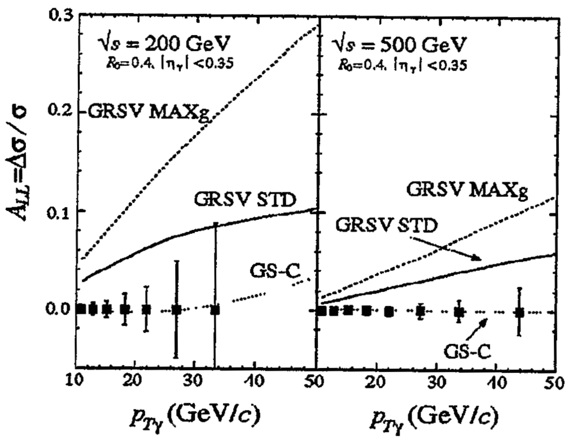

W. Vogelsang *et al.*

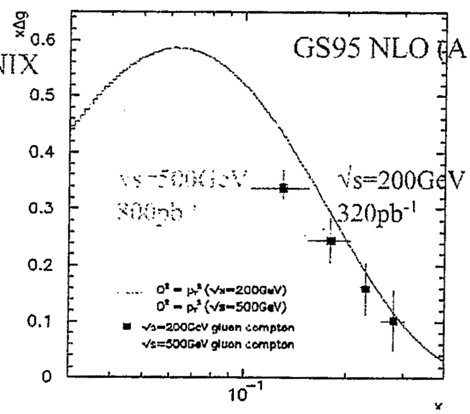

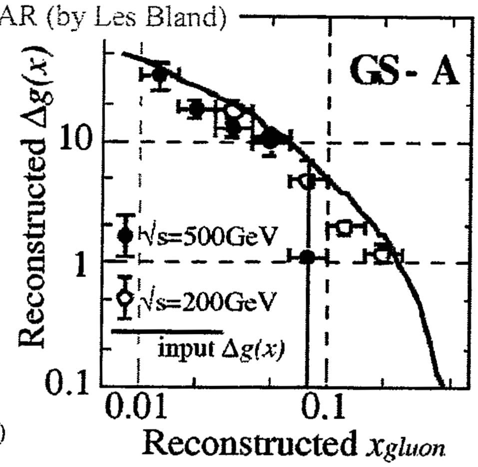

Yuji Goto (RBRC)

Gluon polarization

- Jet production
  - complementary to the prompt photon production
    - mixture of *gg/gq/qq* scatterings
    - very high statistics
  - very sensitive to the gluon polarization

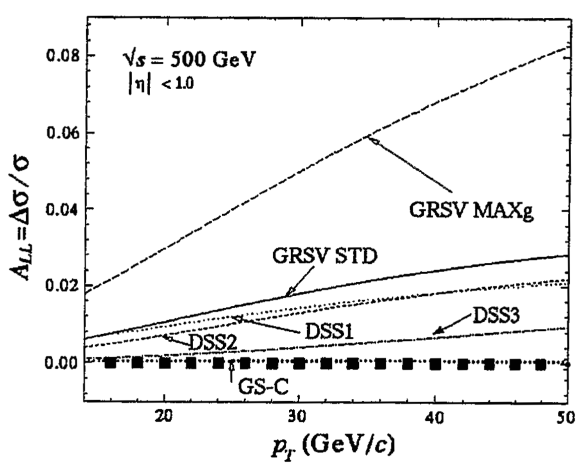

W. Vogelsang *et al.*

Gluon polarization

- Neutral/charged pions
  - ➔ gluon polarization measurement
  - – alternative to jet measurement in the small acceptance
    - $gg + gq + qq$ mixture
  - – different asymmetry between neutral and charged pions
  - ➔ input for the flavor decomposition of the quark polarization

PHENIX

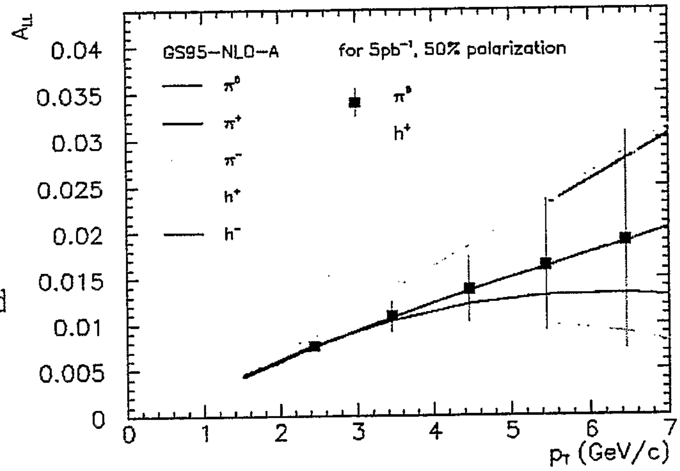

Asymmetry

Gluon polarization

- Single electron
  - – open heavy-flavor production
    - gluon fusion

$$gg \to c\bar{c}, b\bar{b}$$

    - background from conversion and π^0 Dalitz decay reduced with MVD
  - – QCD-jet study & background study
    - selected with MVD
  - ➔ input for the gluon polarization measurement

PHENIX

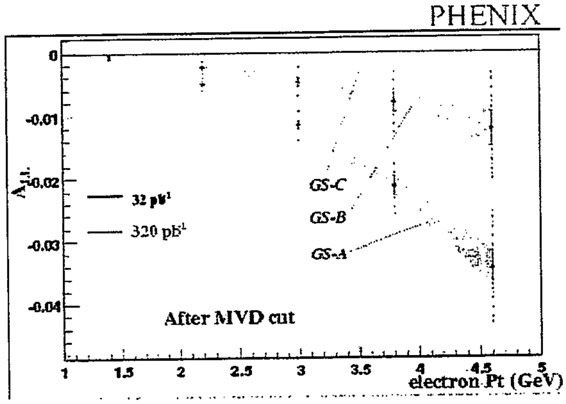

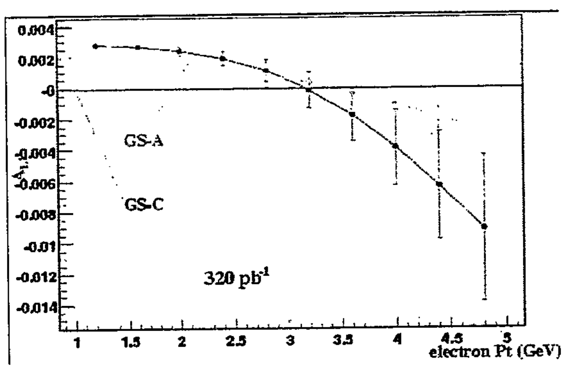

by Wei Xie

Gluon polarization

- Muons
  - J/Ψ
    - gluon fusion
    - 50K $J/\Psi \rightarrow \delta A_{LL}$~0.02
  - single muon
    - $p_T < 3\text{GeV}/c$
    - decay of π/K dominant
  - ➔ input for the gluon polarization measurement

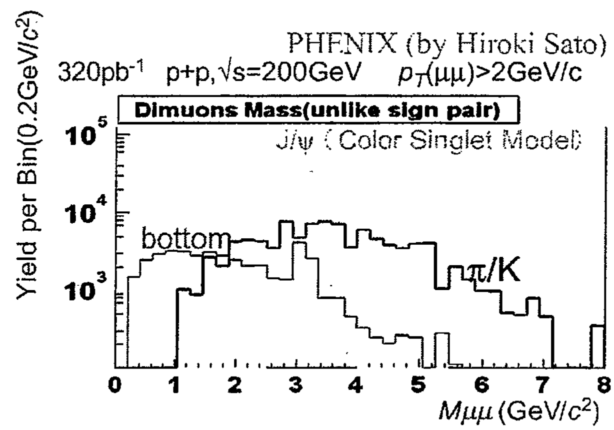

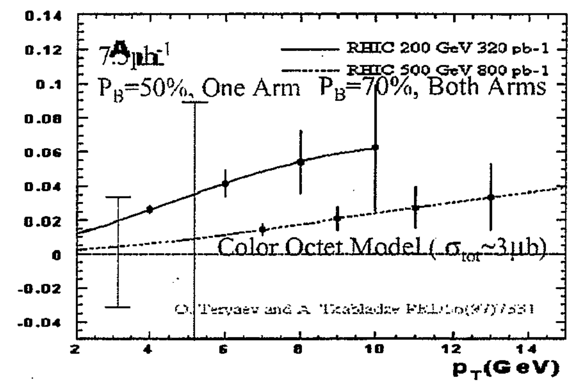

Gluon polarization

- eμ coincidence
  - open heavy flavor production $c\bar{c}, b\bar{b} \rightarrow e\mu X$

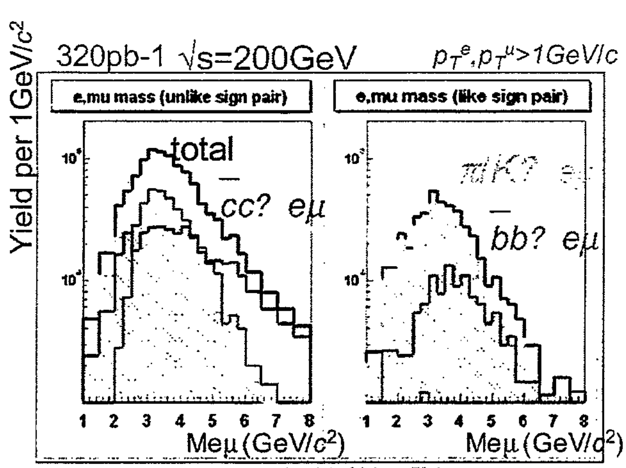

eμ invariant mass

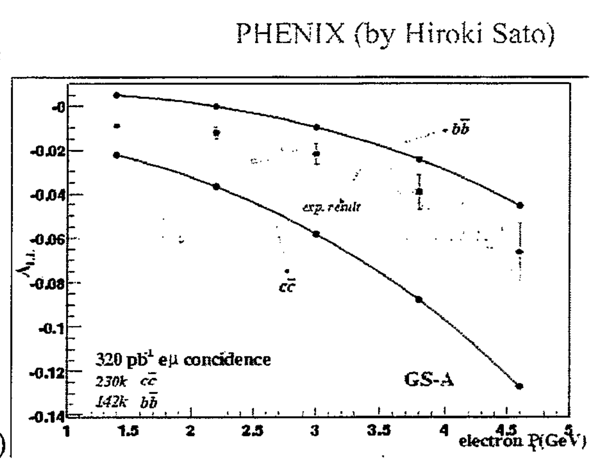

asymmetry

Gluon polarization

- Gluon polarization at RHIC
  - RHIC spin is the best measurement among currently running experiments, even only with 1 exp. & 1 chan.

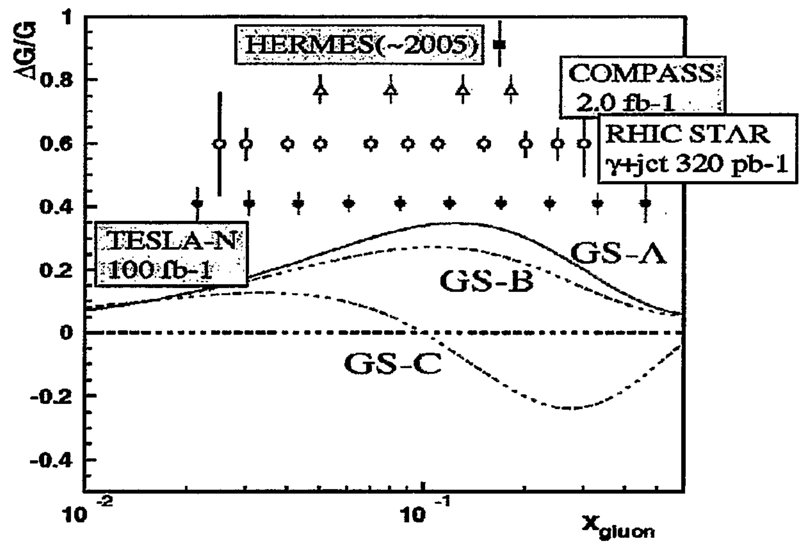

Yuji Goto (RBRC) 17

Gluon polarization

- Gluon polarization at RHIC
  - prompt photon, photon+jet
  - jet, jet+jet
  - heavy flavor – electron, muon, e-μ coincidence

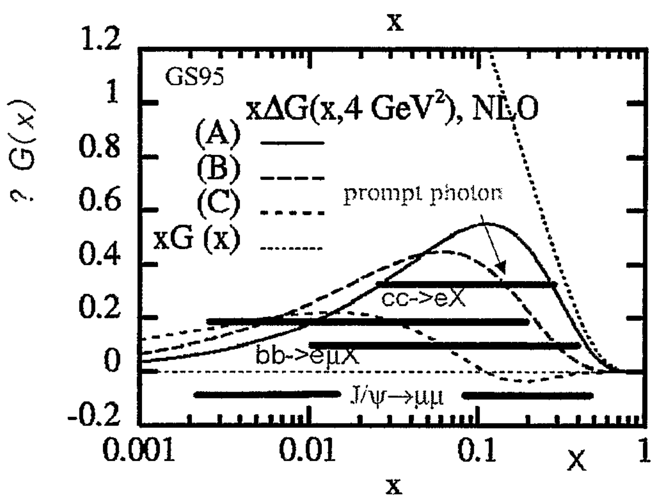

Yuji Goto (RBRC) 18

Gluon polarization

- Gluon polarization at RHIC
  - If we include PHENIX Prompt Photon Data in Global QCD Analysis…

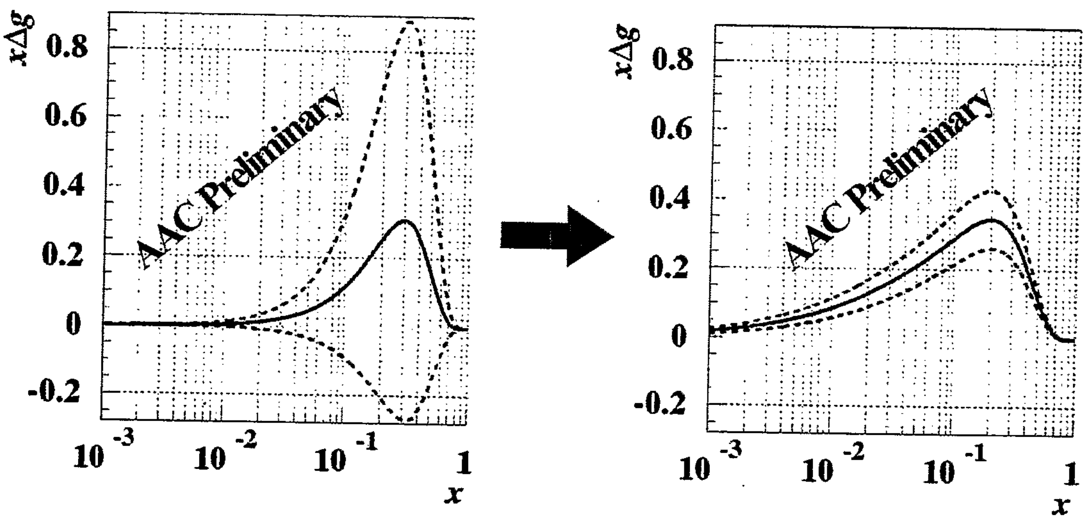

M. Hirai, H.Kobayashi, M. Miyama *et al.*

Flavor decomposition

- $W^{\pm}$ production
  - parity-violating asymmetry A_L

$$A_L^{W^+} = \frac{\Delta u(x_a)\bar{d}(x_b) - \Delta\bar{d}(x_a)u(x_b)}{u(x_a)\bar{d}(x_b) + \bar{d}(x_a)u(x_b)}$$

  - PHENIX Muon Arms
  - STAR Endcap Calorimeter provides similar sensitivity
  - A_L~$\Delta u/u(x)$~0.7-0.9 at large-x

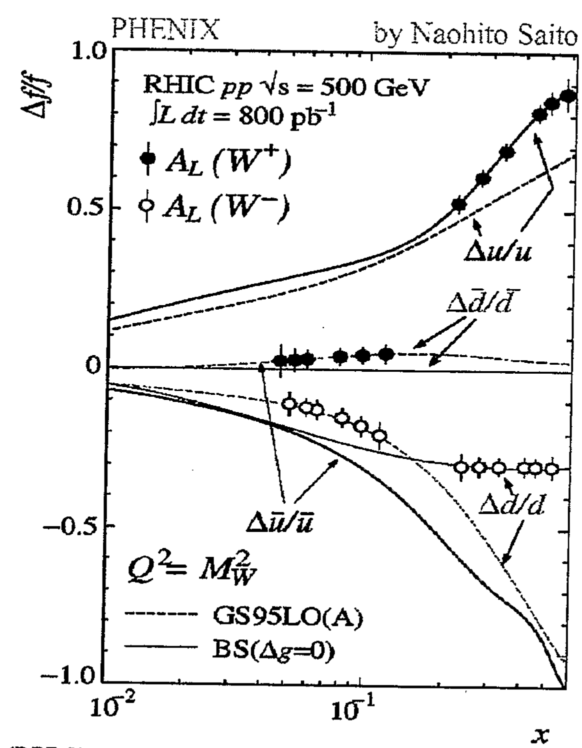

Flavor decomposition

- $W^{\pm}$ production
  - no fragmentation ambiguity
  - x-range limited
- – complementary to HERMES semi-inclusive DIS
  - wide x-range
  - limited sensitivity to sea flavors

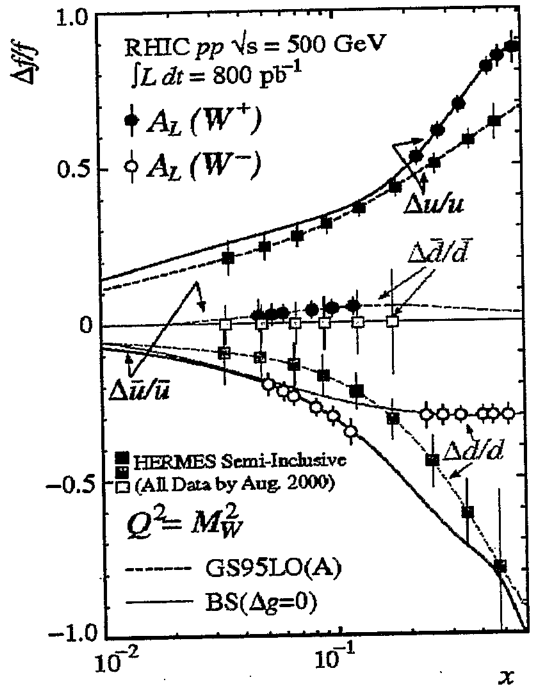

Yuji Goto (RBRC) 21

Flavor decomposition

- Neutral/charged pions
  - – fragmentation function

$$\boxed{D^{\pi^0}_{u,d} \neq D^{\pi^+}_{u,d} \neq D^{\pi^-}_{u,d}}$$

  - – asymmetry

$$\boxed{A^{\pi^0}_{LL} \neq A^{\pi^+}_{LL} \neq A^{\pi^-}_{LL}}$$

  - – *cf.* DIS semi-inclusive h^+/h^- measurement
    - HERMES & SMC experiments
    - flavor decomposition of the quark polarization

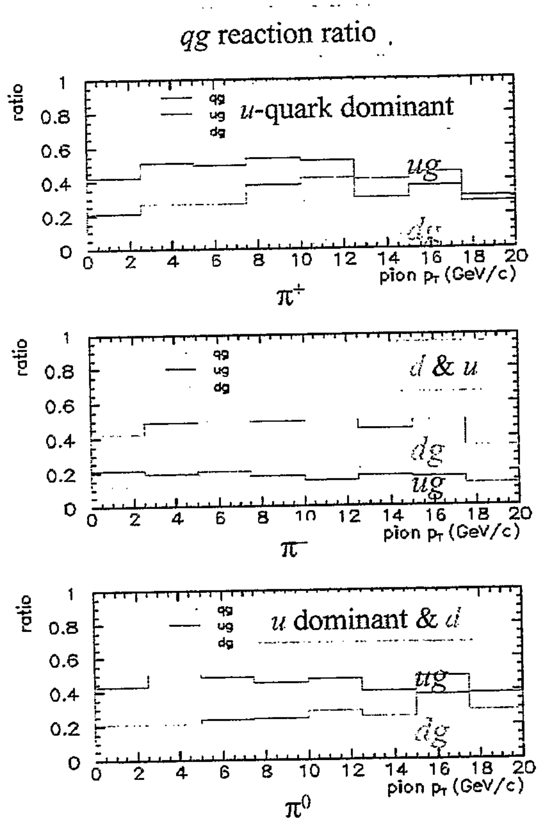

Yuji Goto (RBRC) 22

Flavor decomposition

- Neutral/charged pions
  - flavor & quark/gluon decomposition ➔ Δu_v, Δd_v, Δq_s, Δg

$$A^h(p_T) = \frac{\sum\limits_{f_1 f_2 f_3} \int dx_1 \int dx_2 \Delta f_1(x_1) \Delta f_2(x_2) d\Delta\hat{\sigma}(f_1 f_2 \to f_3 X) D^h_{f_3}(z)}{\sum\limits_{f_1' f_2' f_3'} \int dx_1 \int dx_2 f_1'(x_1) f_2'(x_2) d\hat{\sigma}(f_1 f_2 \to f_3 X) D^h_{f_3'}(z)} \qquad f = u, \bar{u}, d, \bar{d}, s, \bar{s}, g$$

purity functions

$$\boxed{P^h_{f_1 f_2}(x_1, x_2, p_T) = \frac{\sum\limits_{f_3} f_1(x_1) f_2(x_2) d\Delta\hat{\sigma}(f_1 f_2 \to f_3 X) D^h_{f_3}(z)}{\sum\limits_{f_1' f_2' f_3'} \int dx_1 \int dx_2 f_1'(x_1) f_2'(x_2) d\hat{\sigma}(f_1' f_2' \to f_3' X) D^h_{f_3'}(z)}}$$

uncertainties: fragmentation functions, PDFs, scale, …

$$A^h(p_T) = \sum_{f_1 f_2} \int dx_1 \int dx_2 P^h_{f_1 f_2}(x_1, x_2, p_T) \cdot \frac{\Delta f_1(x_1)}{f_1(x_1)} \cdot \frac{\Delta f_2(x_2)}{f_2(x_2)}$$

kinematic acceptance need to be considered

  - HERMES

$$\boxed{\begin{array}{l} A_1(p), A_1^{h^+}(p), A_1^{h^-}(p) \\ A_1(^3He), A_1^{h^+}(^3He), A_1^{h^-}(^3He) \end{array}} \Rightarrow \boxed{\Delta u_v, \Delta d_v, \Delta q_s}$$

Single transverse-spin asymmetry

- Kinematic regions
  - forward
    - A_N of photons and π^0s (p_T 1-2GeV/c, $x_F > 0.2$)
    - A_N of muons
  - mid-rapidity
    - A_N of jets, photons, π^0s, charged hadrons, and electrons ($p_T < 8$GeV/c)
  - very forward
    - A_N of photons, π^0s and neutrons ($p_T < 0.5$GeV/c, $x_F > 0.2$)
  - elastic scatting
    - proton-proton CNI A_N and slope
    - proton-carbon CNI A_N and slope vs. t ($-t = 0.005 - 0.04$)

Single transverse-spin asymmetry

- Forward region
  - Fermilab-E704
  - $\sqrt{s} = 20$ GeV
  - unexpected large asymmetry at large-x_F
    - $0.2 < p_T < 2.0$ GeV/c
  - many theoretical model calculations
    - high-twist effect
    - time-reversal odd fragmentation function
    - ...
  - experimental evolution
    - energy dependence
    - other kinematical region

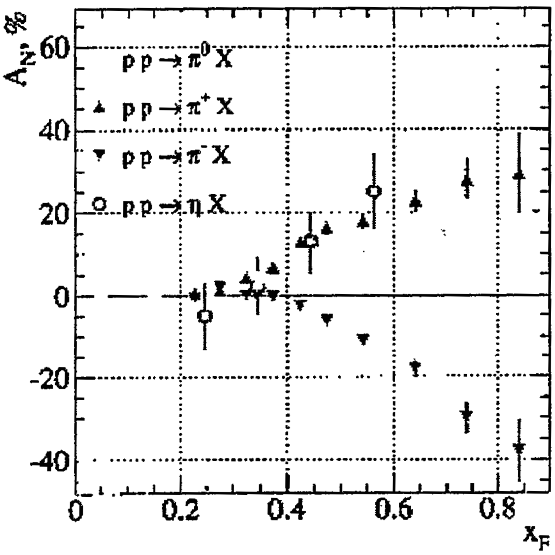

Single transverse-spin asymmetry

- Forward region
  - Qiu & Sterman's model
  - PRD59 (99) 014004
  - twist-3 effect

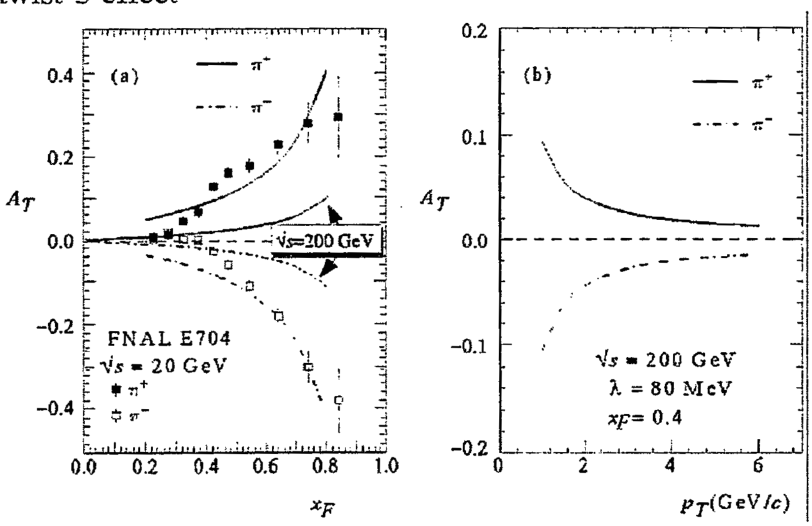

Single transverse-spin asymmetry

- Mid-rapidity region
  - Fermilab-E704
  - PRD53 (96) 4747
  - $\sqrt{s} = 20$ GeV
  - small (consistent with zero) asymmetry at $x_F \sim 0$
  - no large asymmetry like lower energy data
  - perturbative QCD expectation at high energy
  - small higher-twist contribution
  - ➔ but, small statistics, especially at high-p_T …(> 10% error)

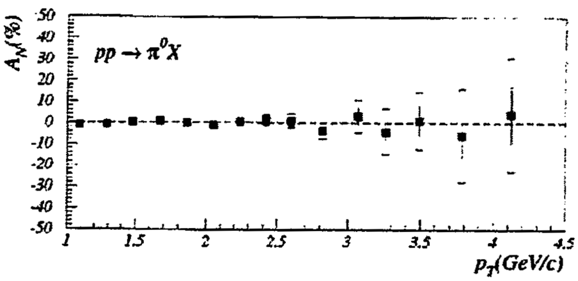

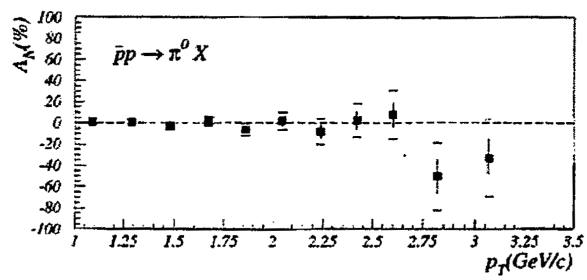

Single transverse-spin asymmetry

- Mid-rapidity region
  - PHENIX central arm
    - $x_F \sim 0$
    - neutral pion calculation with Qiu & Sterman's model
    - charged hadrons
  - PHENIX muon arm
    - $x_F > 0$
    - decay of π/K

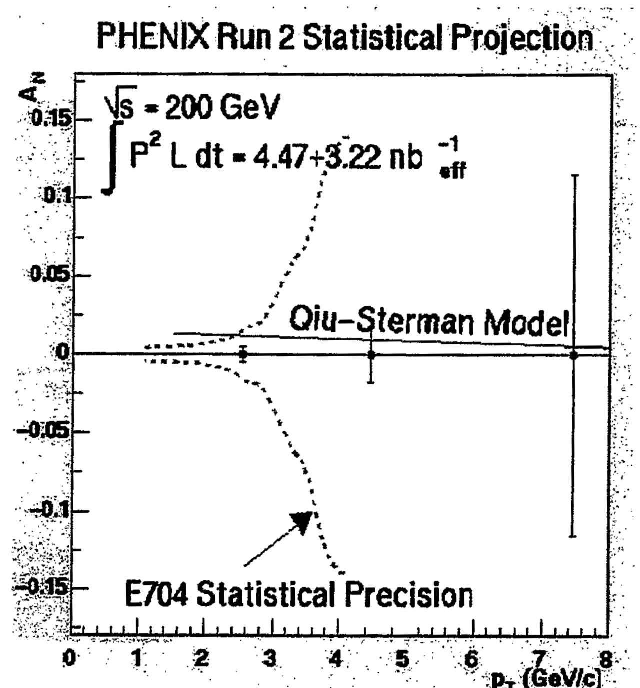

Double transverse-spin asymmetry

- Transversity measurement
  - Drell-Yan production of lepton pairs
    - clean, but low statistics (QED process)
    - precision will be improved by luminosity upgrade

PHENIX muon 200GeV

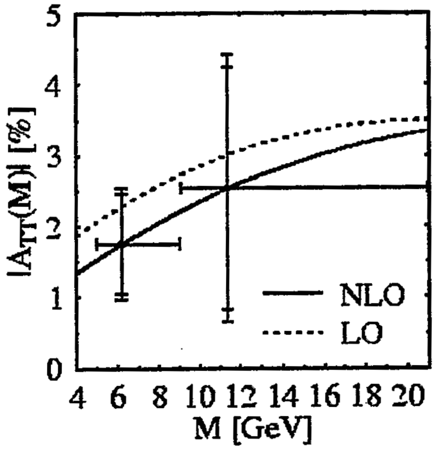

PRD60 (99) 117502

Polarized H^- source

- KEK OPPIS
  - upgraded at TRIUMF
  - 75 - 80 % Polarization

  ➔ more than 70% this year
  - 15×10^{11} protons/pulse at source

  ➔ several$\times10^{11}$ this year
  - 6×10^{11} protons/pulse at end of LINAC

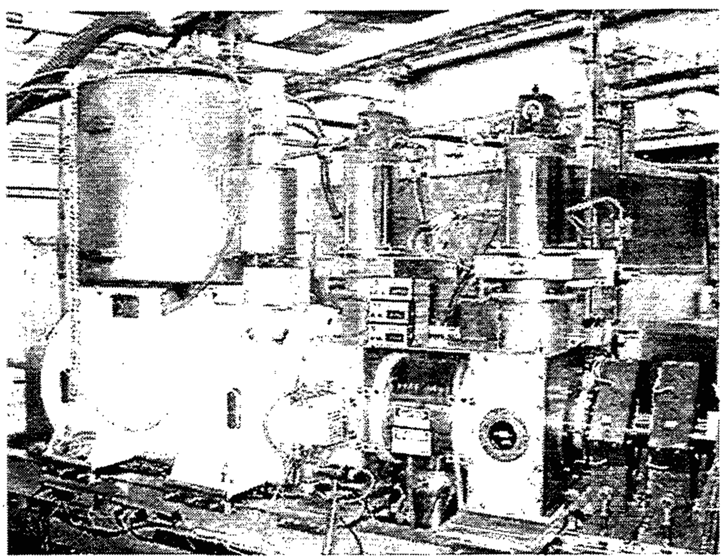

AGS

- Partial Siberian snake
  - full spin flip at all imperfection resonances
- Rf dipole
  - full spin flip at strong intrinsic resonances

➔ 25–30% polarization this year
  - slow ramp rate with backup motor generator

➔ 70% polarization in the future
  - 30% snake necessary

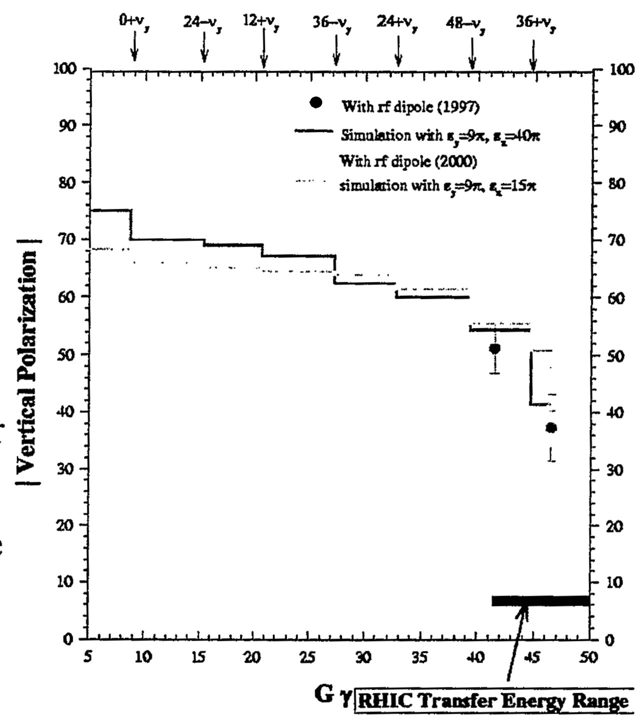

RHIC

- $\sqrt{s}$=200GeV
- 4×10^{12} polarized protons in 55 bunches in each ring
- with alternating polarization in each bunch
  - blue ring: 0+−+−+−+−...
  - yellow ring: 0++−−++−−...

➔ 25% polarization

➔ transverse-spin run only in this year

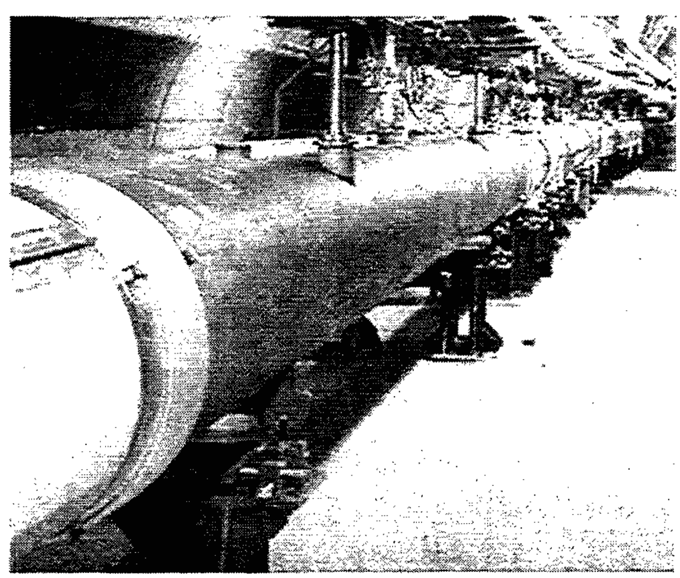

Snake magnet

- Helical dipole magnet

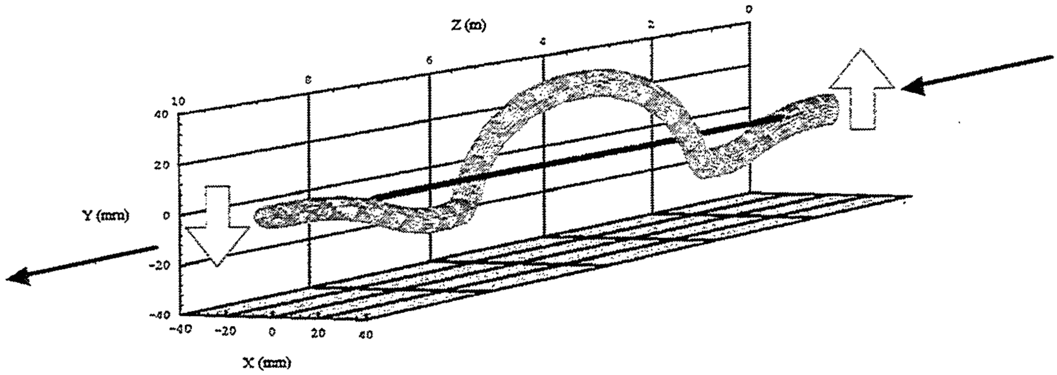

Picture of a helical dipole magnet coil

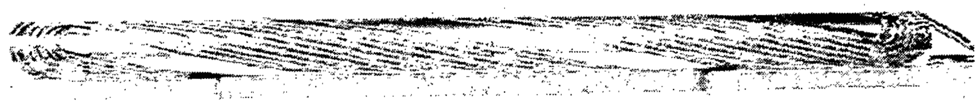

Yuji Goto (RBRC) 33

RHIC polarimeter

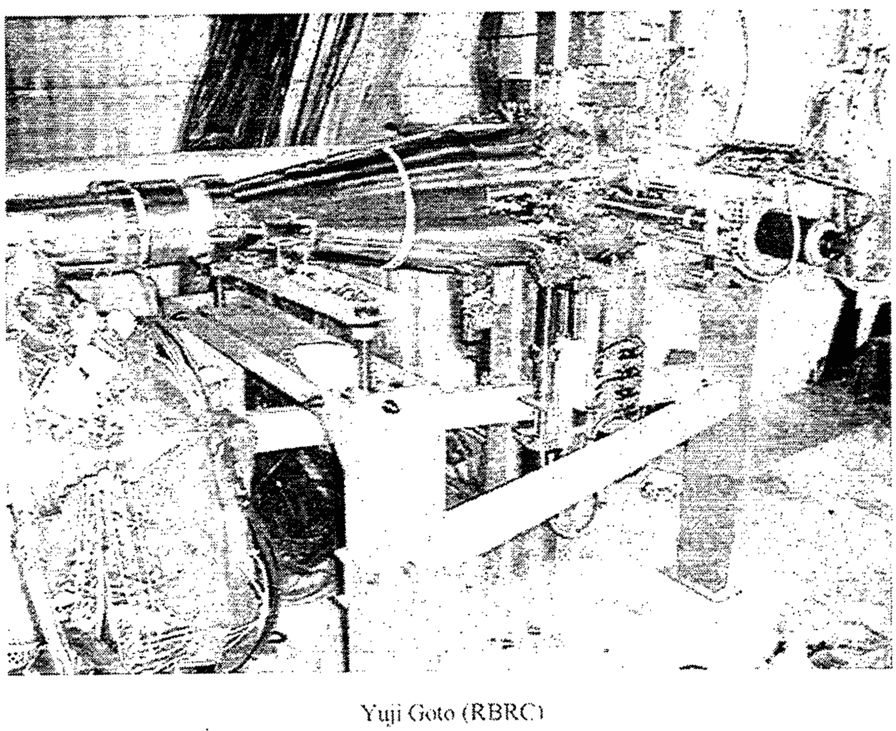

Yuji Goto (RBRC) 34

RHIC polarimeter

- Proton-carbon CNI polarimeter
  - raw asymmetry ~2×10^{-3} with 10% statistical error in 1 min.
  - $-t = 0.005 - 0.04$

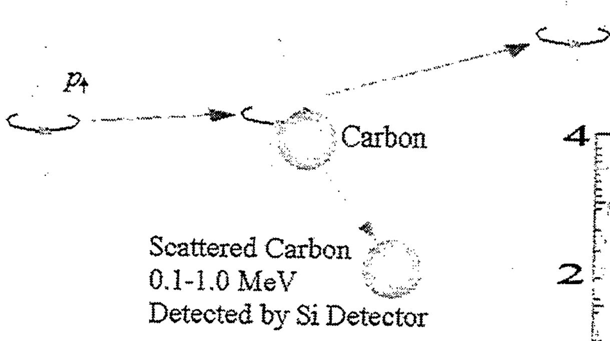

proof of feasibility
at AGS-E950
with a 22GeV/c pol. p beam

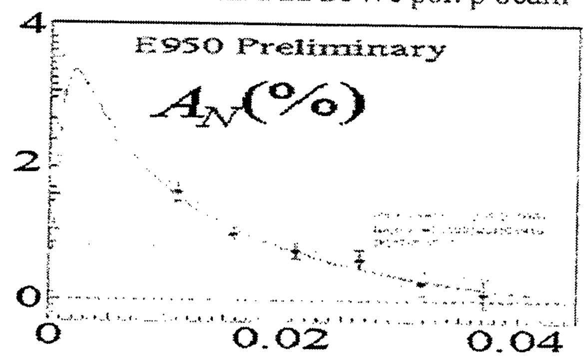

RHIC polarimeter

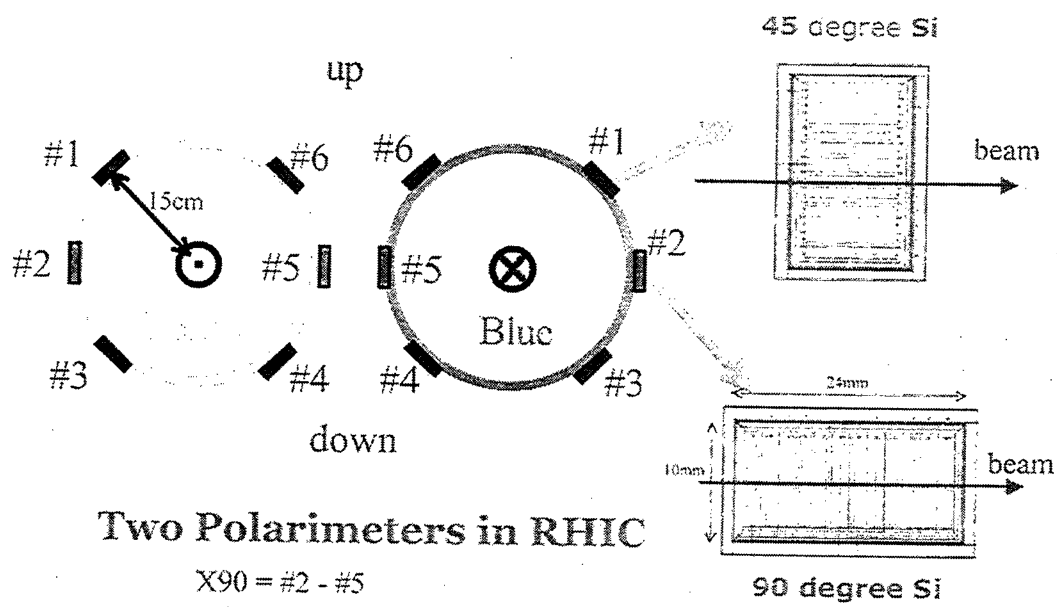

Two Polarimeters in RHIC

X90 = #2 - #5
X45 = (#1+#3) – (#4+#6)
Y45 = (#1+#4) – (#3+#6)

by Osamu Jinnouchi

RHIC polarimeter

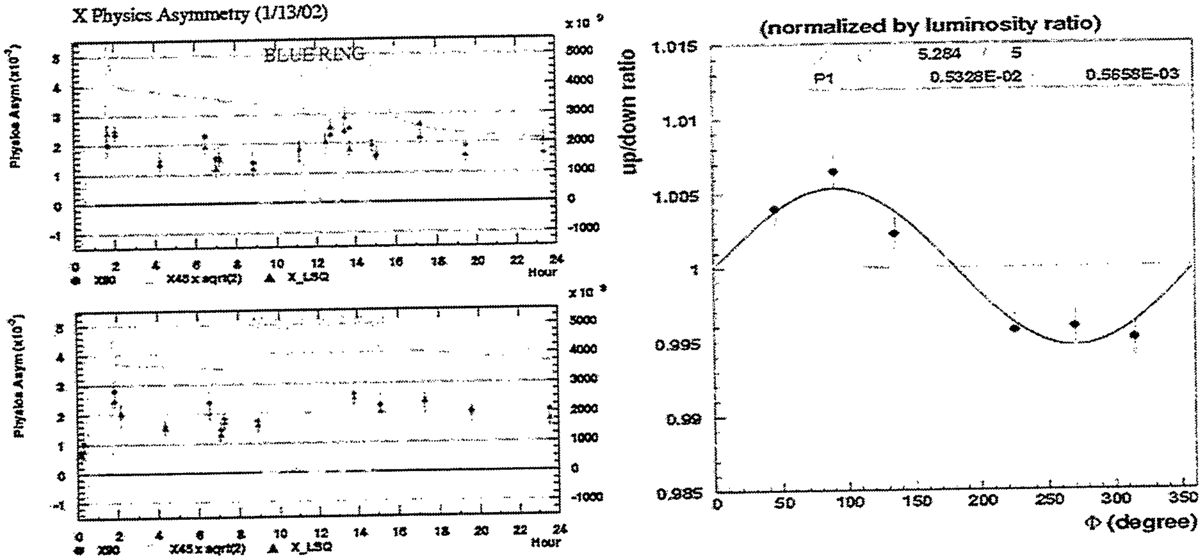

Yuji Goto (RBRC) 37

First polarized proton collisions

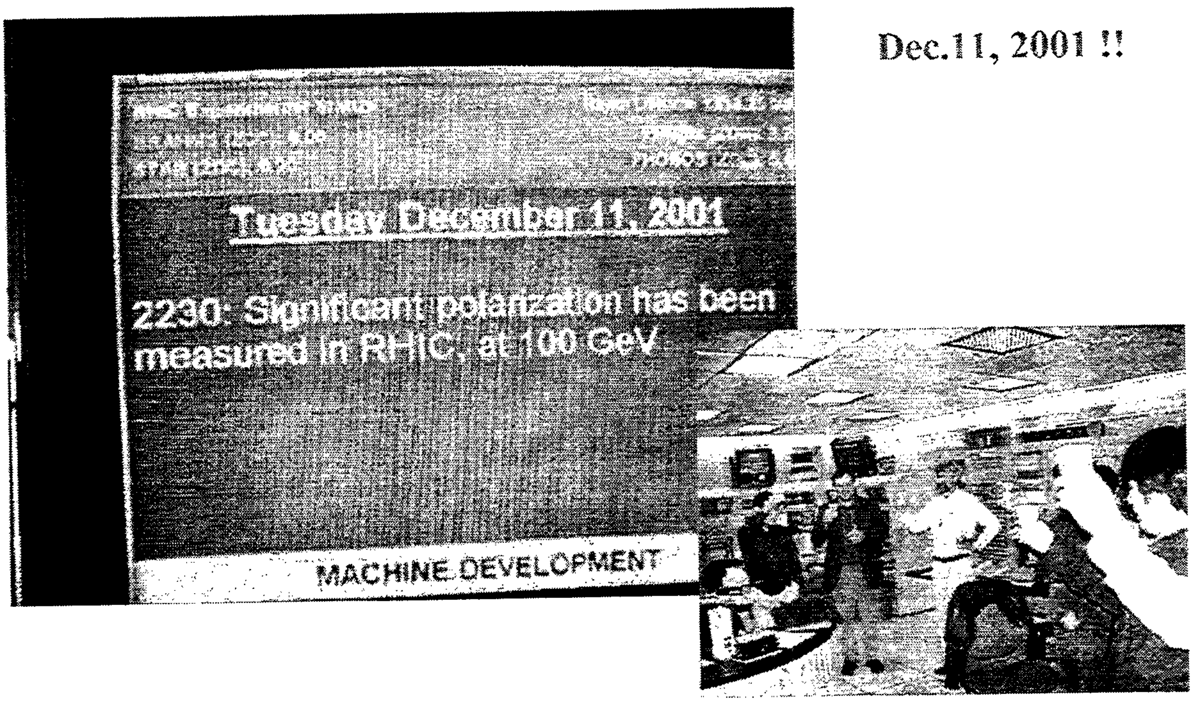

Dec.11, 2001 !!

Yuji Goto (RBRC) 38

Luminosity and polarization

PHENIX Run2 pp Recorded Luminosity

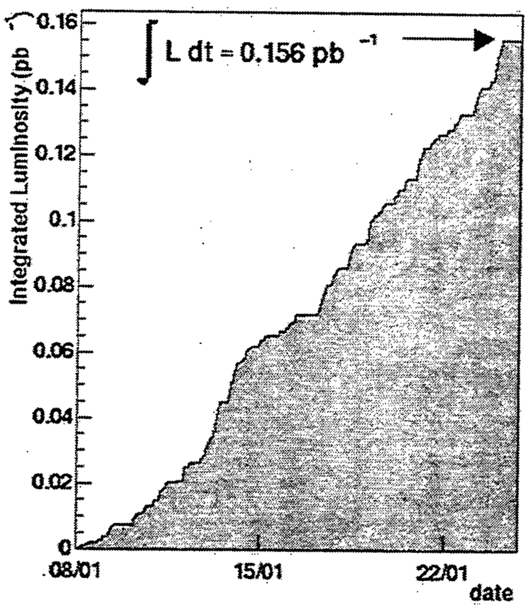

PHENIX Run2 Figure of Merit for A_N

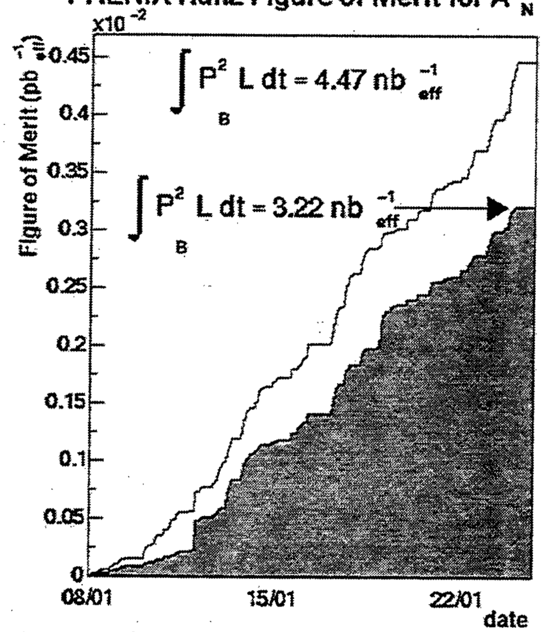

$L \sim 1.5 \times 10^{30}\,\text{cm}^{-2}\text{sec}^{-1}$ $\quad$ $\langle P_{yellow} \rangle = 17\%$ $\langle P_{blue} \rangle = 14\%$

Yuji Goto (RBRC) 39

PHENIX

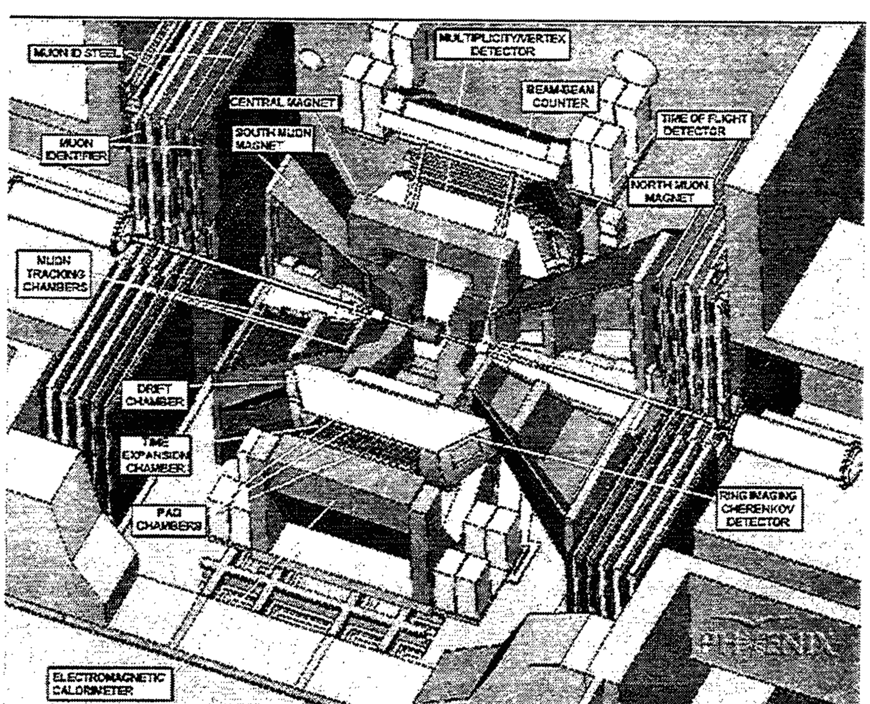

Yuji Goto (RBRC) 40

PHENIX

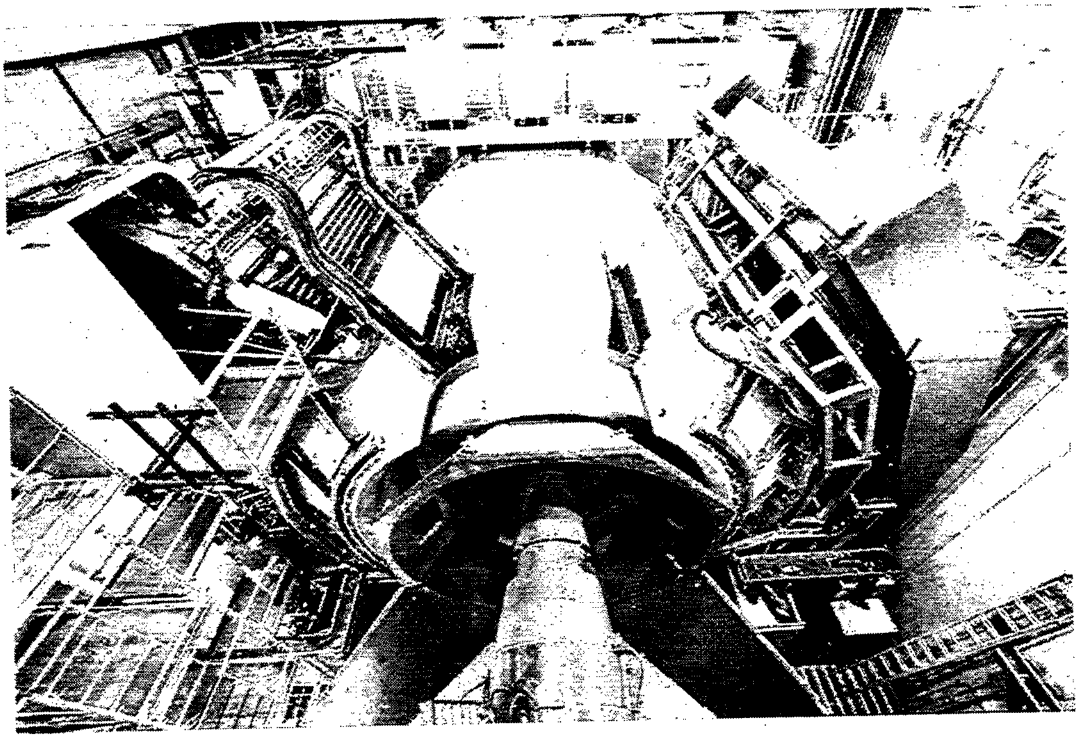

PHENIX

- $\sqrt{s_{NN}}$=200GeV heavy-ion collision

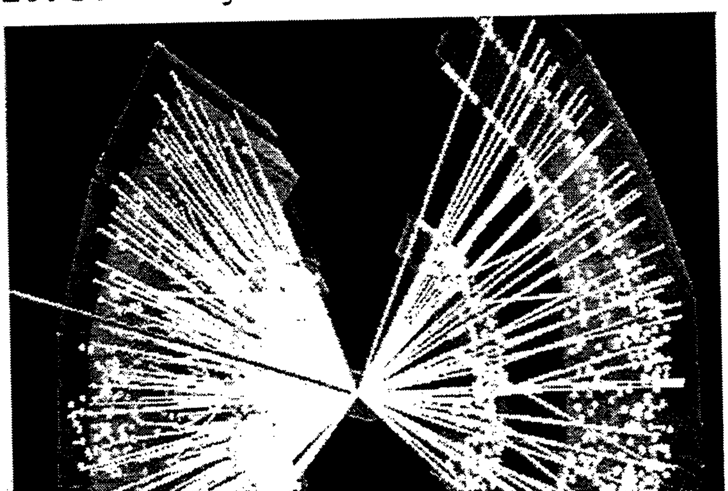

PHENIX

- Full Central Arms
- South Muon Arm
- New items for pp run
  - NTC
    - additional beam counters
  - T0/PCR
    - TOF start counter
  - EMCal/RICH trigger
  - MuID trigger
  - GL1P scaler
    - crossing-by-crossing 4×120 scalers
  - DAQ 1kHz & 70MB/sec

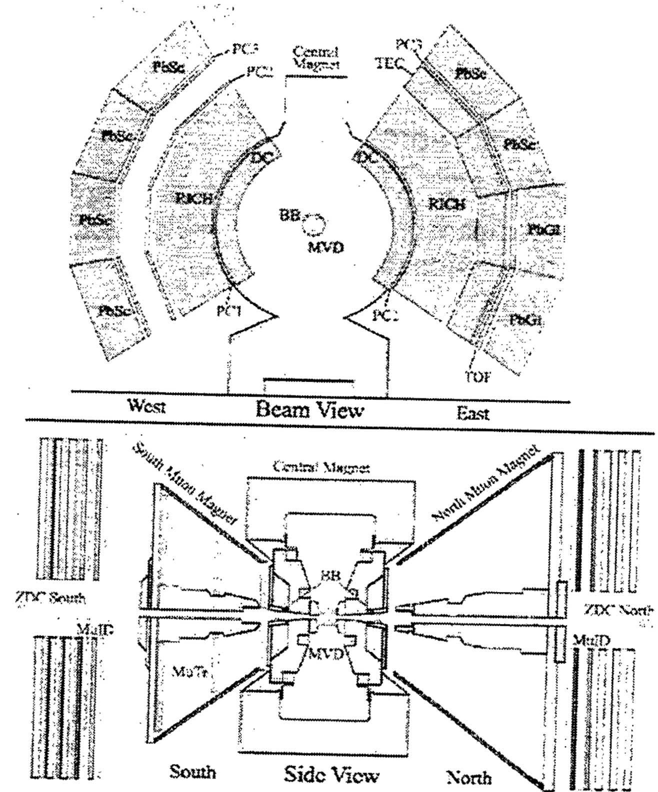

Yuji Goto (RBRC) 43

PHENIX

- EMCal/RICH trigger

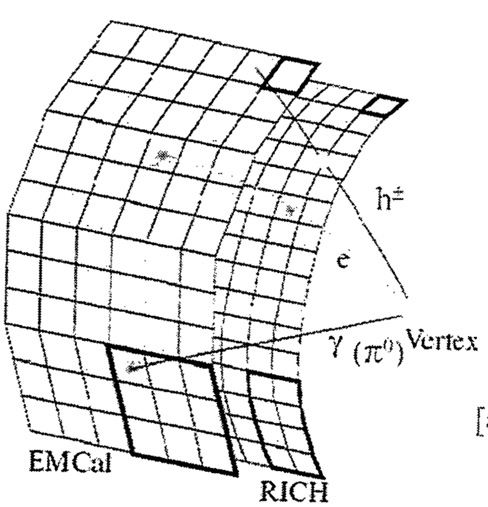

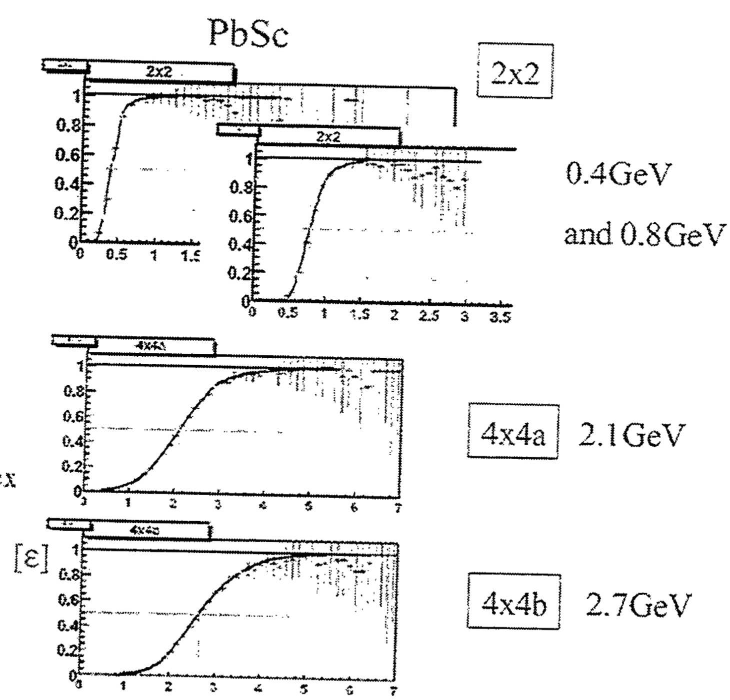

Yuji Goto (RBRC) 44

PHENIX

- Minimum-bias =BBC.or.NTC
  - comparison with heavy-ion data
  - 190M events
- EMCal trigger 900MeV threshold
  - π^0 and charged hadron
  - 50M events
- MuID 1-deep trigger
  - single muon
  - 30M events

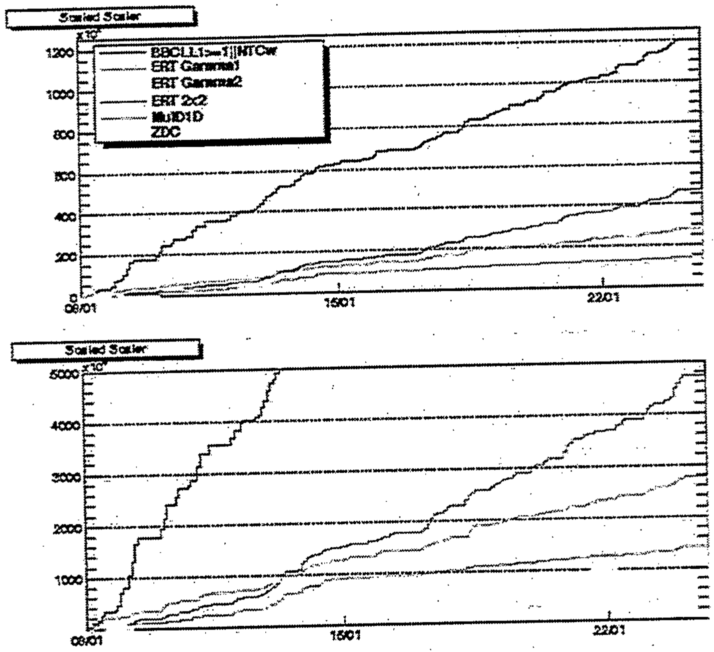

Yuji Goto (RBRC)

PHENIX

- EMCal π^0
  - EMCal trigger
  - minimum-bias
  - enhancement of high-p_T π^0 by the EMCal trigger

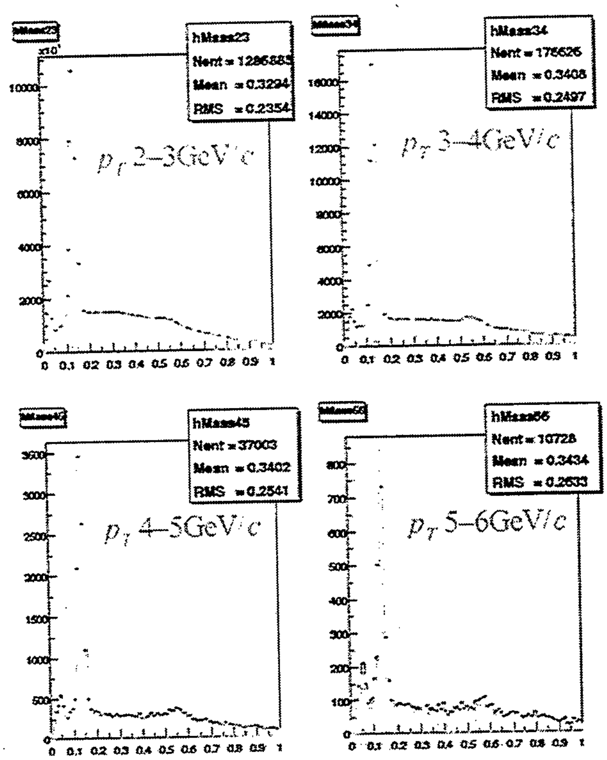

by Sasha Bazilevsky

Yuji Goto (RBRC)

PHENIX

- Charged hadrons

Comparison of minimum-bias and Charged Hadron trigger

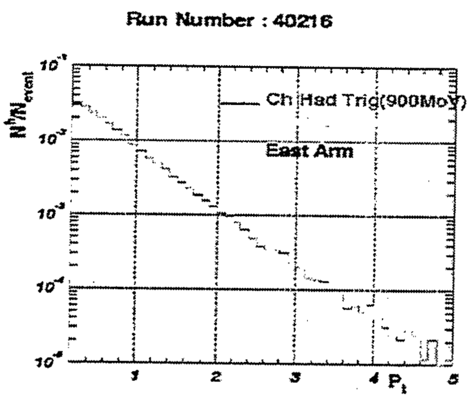

by Basanta Nandi

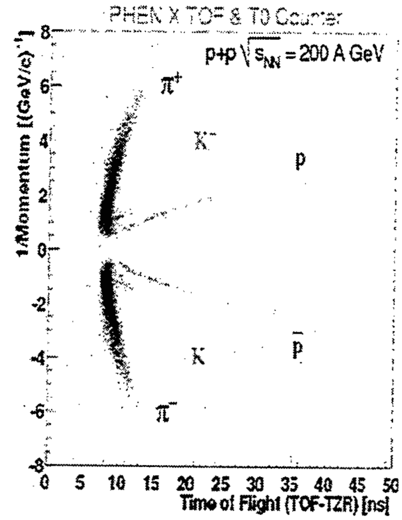

Time-of-Flight with <100 ps resolution
Separate p/K up to ~2.4 GeV/c

STAR

STAR Detector

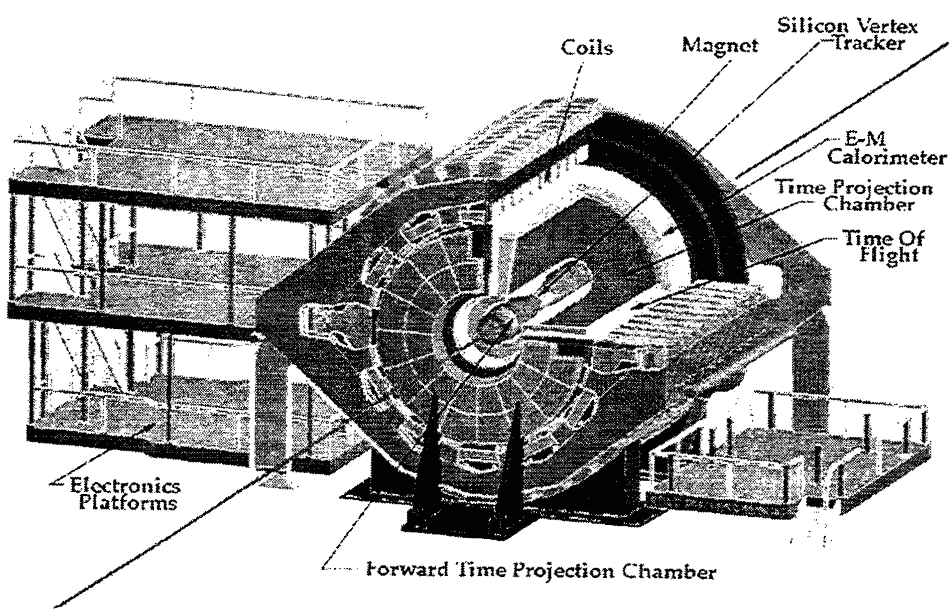

STAR

- $\sqrt{s_{NN}}$=200GeV heavy-ion collision

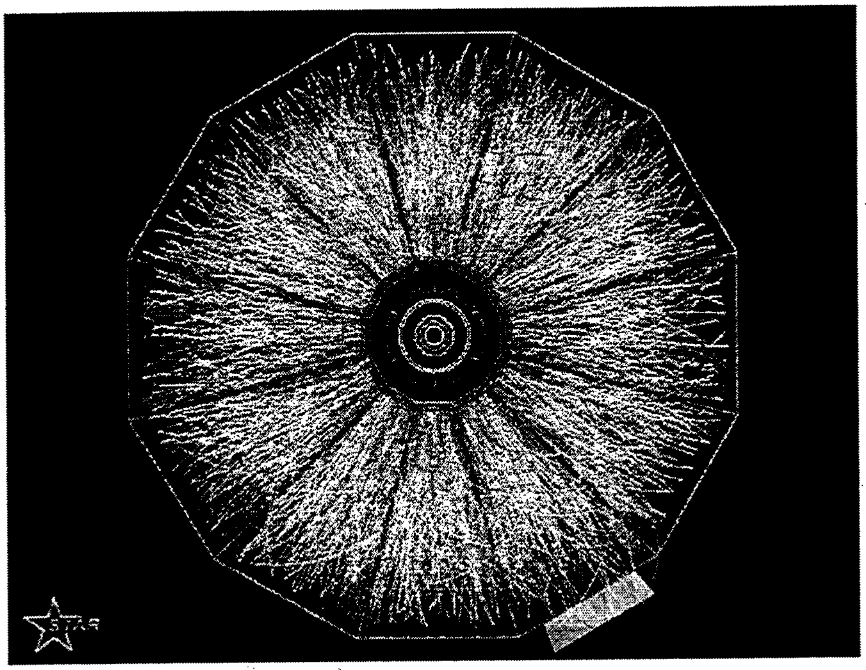

STAR

- New items for pp run
  - BBC
    - beam-collision counter
    - 36 small hex = 16 PMT for trigger $3.3<\eta<5$
    - 12 large hex = 8PMT $2.1<\eta<3.3$
  - FPD
    - forward π^0 calorimeter
  - EMC high tower energy trigger

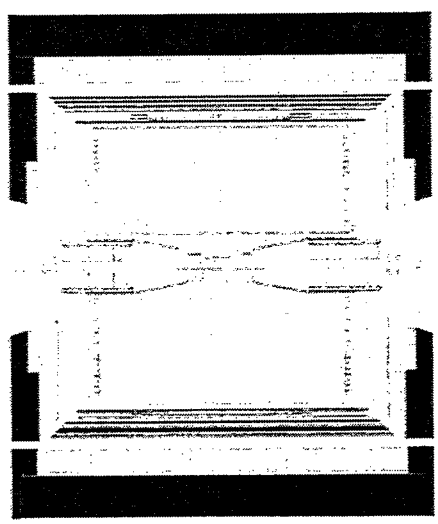

STAR

- FPD (Forward Pizero Detector)
  - $x_F \sim 0.1$ to 0.6 or -0.1 to -0.6
  - $p_T \sim 1$ to 4 GeV
  - $E \sim 10$ to 60 GeV

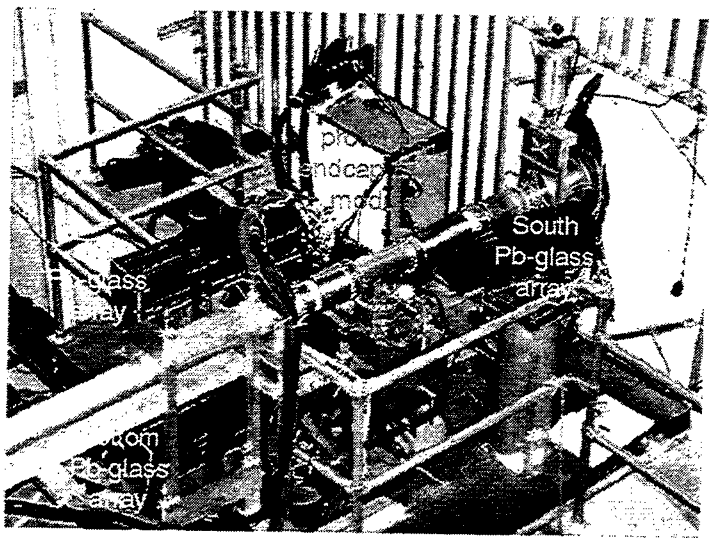

Online Results :

π^0 reconstruction

up to 60 GeV

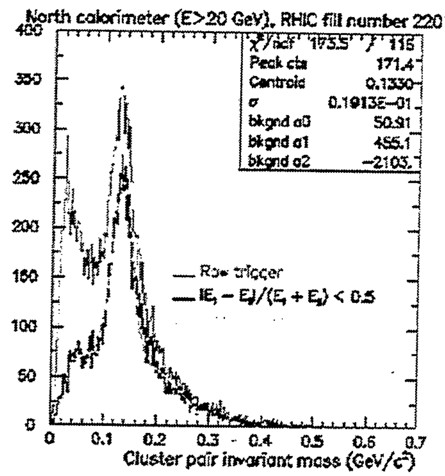

Yuji Goto (RBRC)

51

PP2PP

- 2 Roman pot stations (4 pots) with silicon tracking
- Beam-beam inelestic counters
- proton-proton CNI A_N and slope

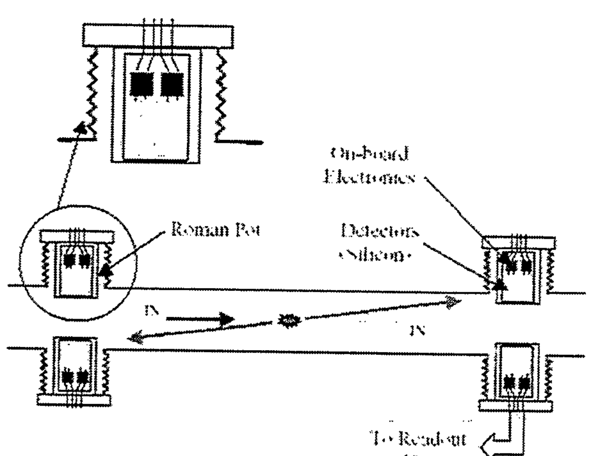

Yuji Goto (RBRC)

52

Local polarimeter at IP's

- Confirm spin dynamics in RHIC ring
  - especially for the operation with spin rotators
    - spin dynamics between spin rotators is completely transparent to the rest of accelerator by design

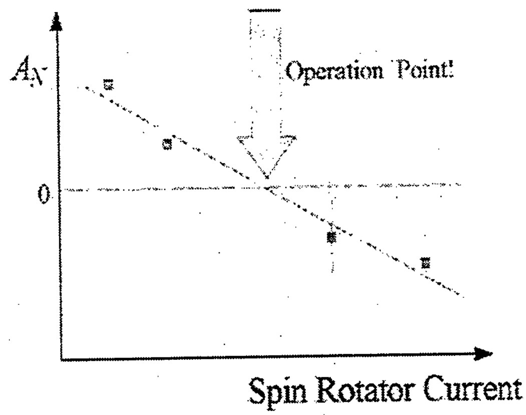

Local polarimeter at IP's

- Test at IP12
  - 5x12 array of $PbWO_4$ calorimeter
- No prediction
  - Qiu & Sterman's model not applicable

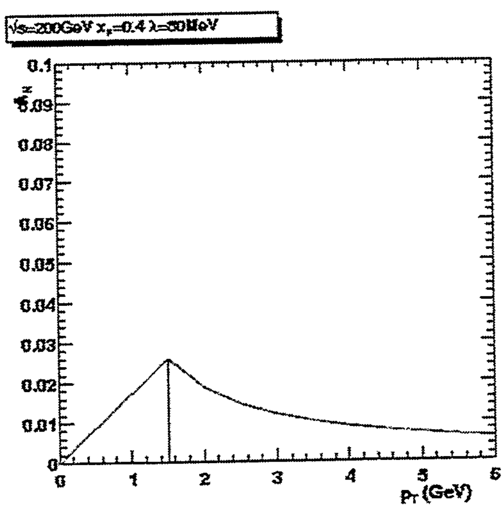

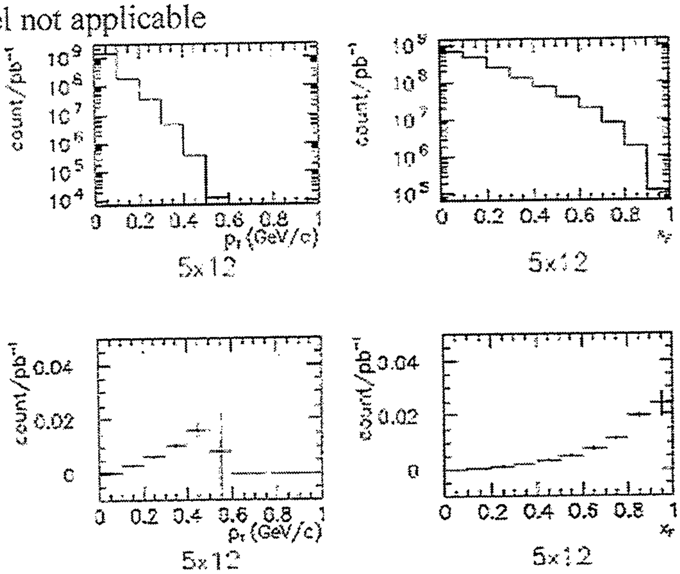

Local polarimeter test at IP12

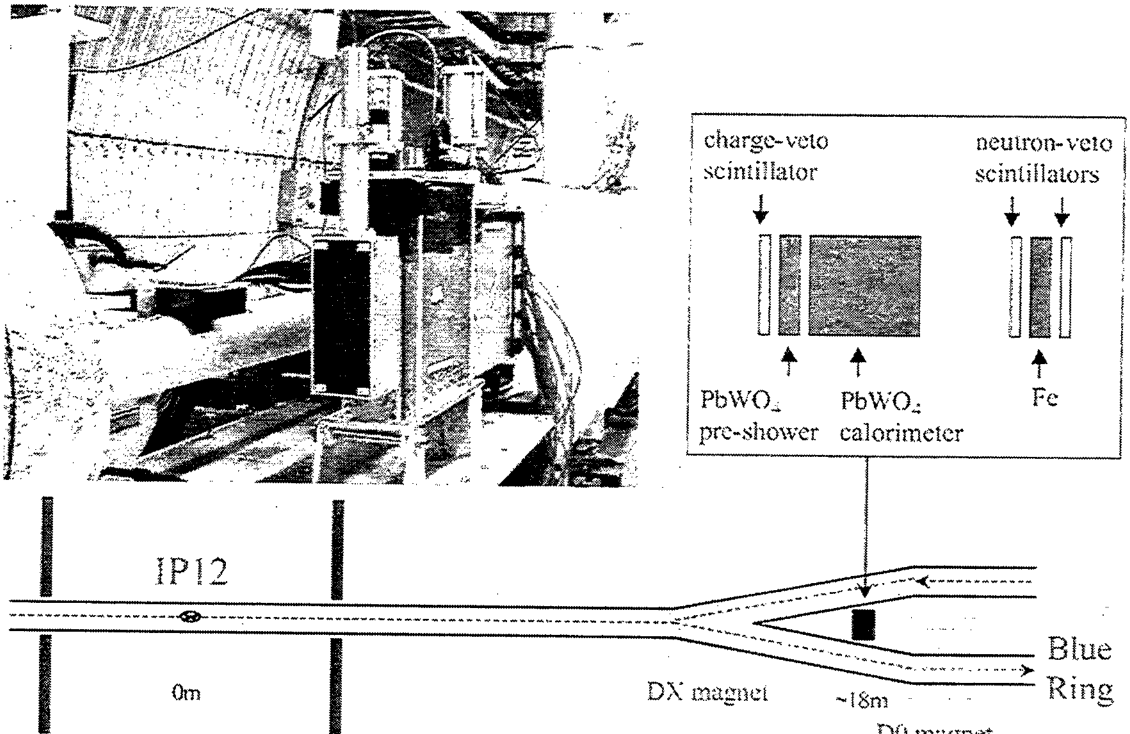

Yuji Goto (RBRC) 55

Local polarimeter test at IP12

- 2-photon mass reconstruction

exp. data PYTHIA simulation

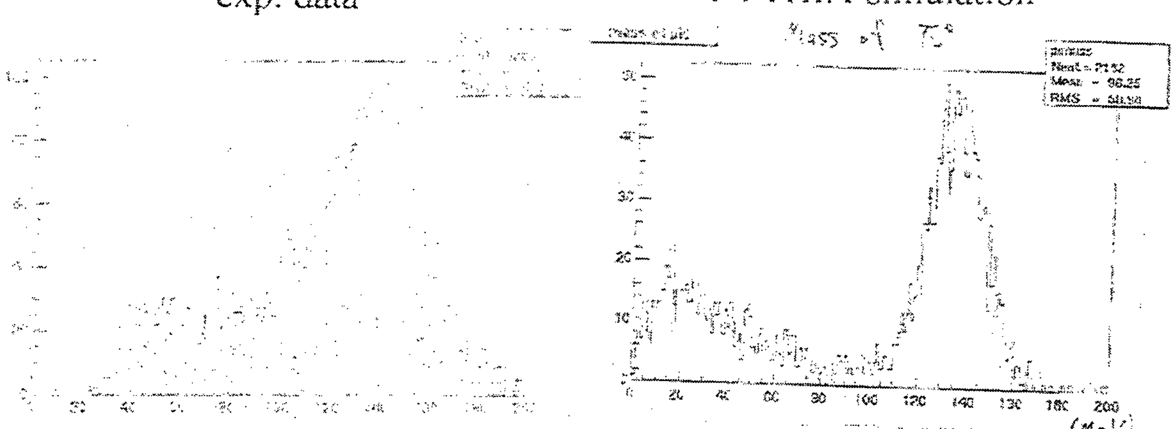

- A_N of photons, π^0s and neutrons (p_T< 0.5GeV/c, x_F > 0.2) will be obtained …

Yuji Goto (RBRC) 56

Summary

- RHIC started to be operated as the first polarized proton collider as well as the heavy-ion collider !!
  - commissioning very successful
    - pol-H^- source, AGS, RHIC, polarimeter, ...
- Transverse-spin proton collision data were accumulated in this year
  - luminosity: $L \sim 1.5 \times 10^{30} cm^{-2} sec^{-1}$
  - polarization: $\langle P \rangle \sim 15\%$
- Many A_N measurements at $\sqrt{s}$=200GeV will be obtained soon
  - forward / mid-rapidity / very forward / CNI
    - photon, π^0, jet, charged hadrons, electron, muon, neutron, ...

The Gluon Polarization Measurement by COMPASS and the Experimental Test of GDH Sum Rule

— The Story of Spin Structure of the Nucleon from High Energy to Low Energy —

Naoaki Horikawa

Center for Integrated Research in Science and Engineering, Nagoya University

RIKEN Winter School, RIKEN / JAPAN, March 29-31,2002

Abstract

The lecture includes two different subjects which concern the study of the spin structure of the nucleon, that is, the experimental studies of the gluon spin contribution to the nucleon spin by COMPASS in the high energy region and that of the GDH sum rule in low energy region.

At the beginning of the lecture ,the definition and the meaning of the spin dependent structure function $G_1(x)$ is introduced, which makes an important role in the investigation of the quark spin contribution and the understanding of the GDH sum rule. The former half of the lecture is devoted to the introduction of the COMPASS, that is , two physics objectives (muon program and hadron one), the experimental method to use the open charm process for the gluon polarization measurement, the estimation of the event rates and the requirements to the equipments.

The COMPASS has provided quite new experimental equipments including beam channel for the increase of the luminosity and the detection efficiency. Special explanations are given to the RICH detector and the polarized target system which characterize the measurement of the gluon spin polarization. RICH is necessary for the particle identification to the produced charged particles by which the open charm process has to be determined. The polarized target system consists of superconducting solenoid and dipole magnets with a specially wide aperture is now under construction.

The COMPAS has finished the installation of the 1st phase detection system in 2001 and performed the real measurement using the polarized muon beam (160GeV, 2.2×10^8ppp) and the polarized target (SMC-magnet, ^{6}LiD material). It was reported that 1.6×10^9 events were recorded and the data analysis is now going on.

In the latter half of the lecture , the physical meaning of the GDH sum rule, its derivation, the experimental results which have been already performed and the new experimental plans are introduced. Special attention has been given to the GDH integral measured by Mainx and Bonn for the energy regions 200-800 MeV and 800-1350 MeV, respectively. Although the obtained value by Bonn is still preliminary, the running GDH sum up to 1350MeV from 200MeV gives a larger value than the prediction.

It tells us the importance to know the contribution to the GDH sum from the higher energy region than Bonn energy. Finally, the experimental plan at SPring-8 up to 2900Mev in connection with above requirement has been explained.

COMPASS Experiment and Experimental Test of GDH Sum Rule

(RIKEN School on "Quark-Gluon Structure of the Nucleon and QCD")

March 30, 2002

Naoaki Horikawa

CIRSE, Nagoya University

CONTENTS

1. Definition of DIS(Deep Inelastic Scattering)
2. Spin Dependent Structure Functions
3. Measurement of the Quark Spin Contribution to Nucleon Spin
4. Measurement of Gluon Spin Contribution by COMPASS
5. What is the GDH(Gerasimov-Drell-Hearn) Sum Rule?
6. Experiments to test the GDH Sum Rule

Microscopic View of Matter

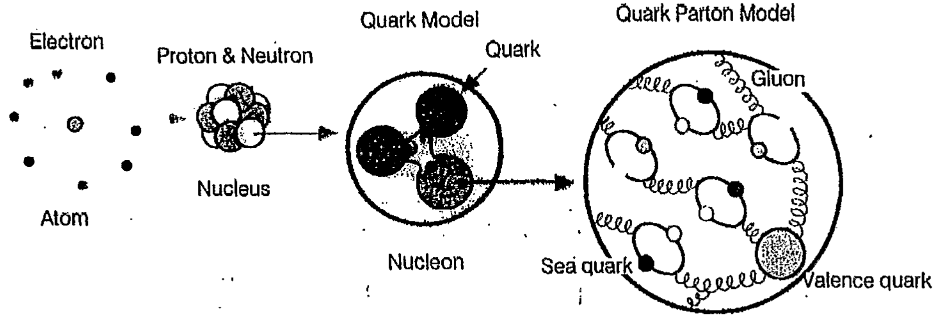

Detailed structure of Nucleon

Self rotation(Spin) of Particle and Magnetic Moment

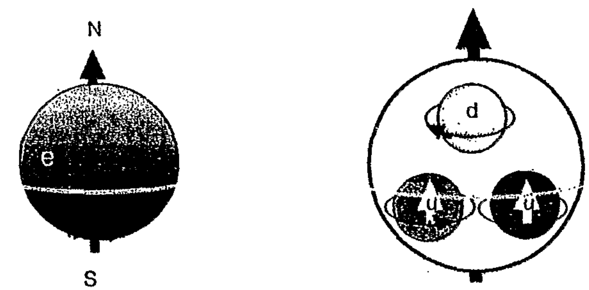

Rotation of current produces magnetic moment

3 quarks form nucleon spin in quark model

Possible Carrier of Nucleon Spin

Nucleon spin		Quark spin		Gluon spin		Angular momentum
$\frac{1}{2}$	=	$\frac{1}{2}(\Delta\Sigma)$	+	ΔG	+	$L_q + L_g$
		$(\Delta\Sigma = 0.2\text{-}0.3)$		?		?

Kinematics and Spin Dependent Structure Function g_1

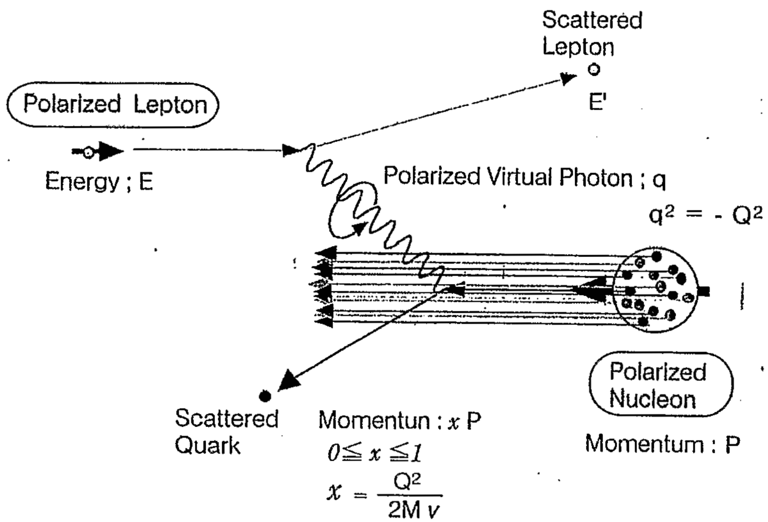

$$A_{meas} = \frac{N^{\rightarrow\leftarrow} - N^{\rightarrow\rightarrow}}{N^{\rightarrow\leftarrow} + N^{\rightarrow\rightarrow}}$$

$$A_{\parallel} = \frac{\sigma^{\rightarrow\leftarrow} - \sigma^{\rightarrow\rightarrow}}{\sigma^{\rightarrow\leftarrow} + \sigma^{\rightarrow\rightarrow}} = \frac{A_{meas}}{P_{\mu} \cdot P_T \cdot f}$$

$$= D(A_1 + \eta A_2) \rightarrow DA_1 \quad : \quad \eta A2 \rightarrow \text{neglect}$$

$$A_1 = (g_1 - \gamma^2 g_2) \frac{(1+R)}{F_1(x)} \quad : \quad \gamma^2 g_2 \rightarrow \text{neglect}$$

$$g_1(x) = \frac{A_1 \cdot F_1(x)}{(1+R)} = \frac{F_2(x) A_{\parallel}}{2xD(1+R)} \quad : \quad R = \frac{\sigma^L}{\sigma^T}$$

$$\Gamma_1 = \int_0^1 g_1{}^p(x)\, dx \quad : \quad 1_{st} \text{ moment}$$

Ref.s : Spin in Particle Physics(by E. Leader), Cambridge
The Structure of the Proton(by R.G.Roberts),Cambridge
Ph.D. Thesis(Y. Miyachi), Nagoya Univ.

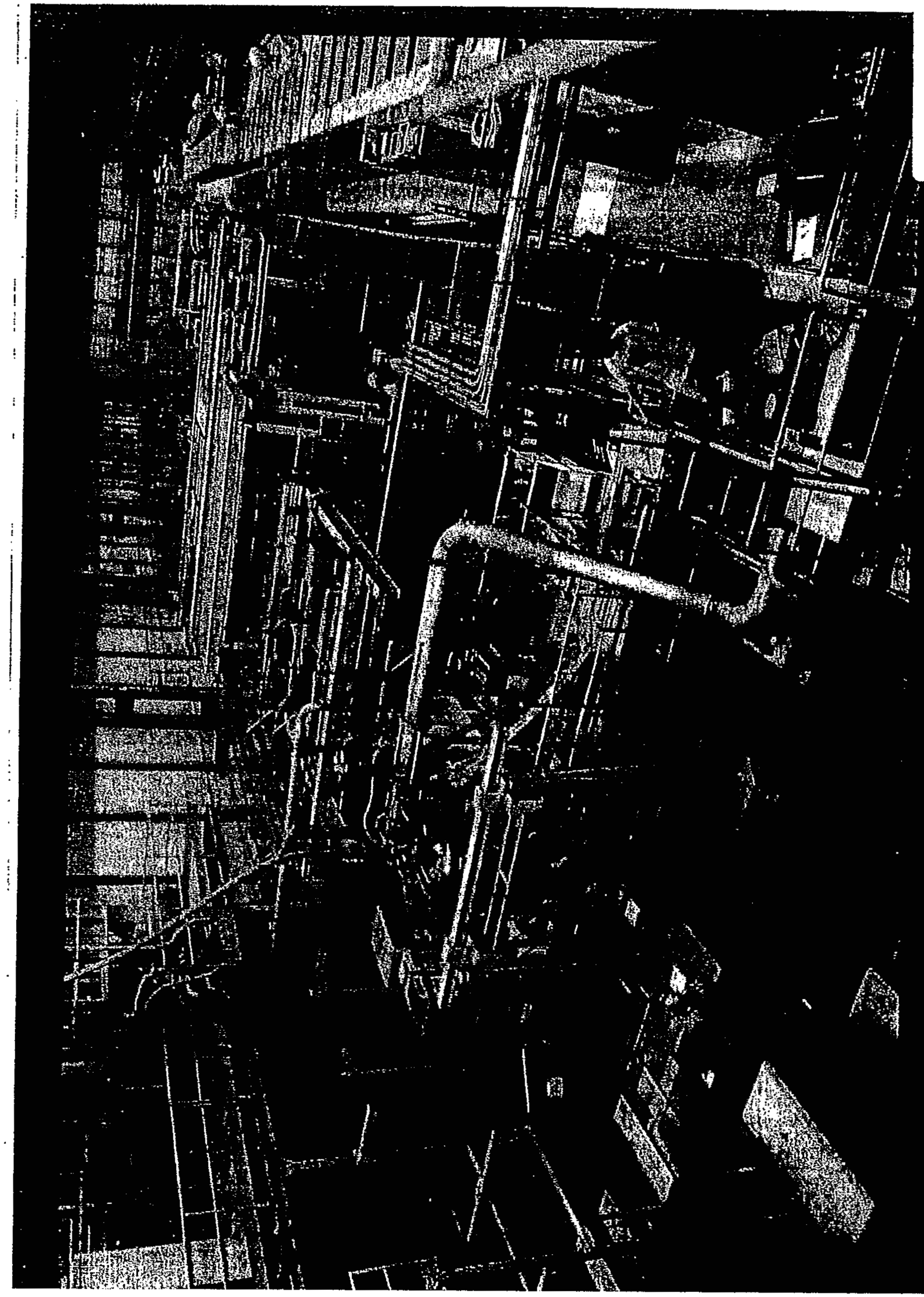

$$g_1(x,Q^2) = \frac{\langle e^2\rangle}{2}\left[C_S^q(x,\alpha_s(t))\otimes\Delta\Sigma(x,Q^2) + 2n_f C^g(x,\alpha_s(t))\otimes\Delta g(x,Q^2)\right] + \frac{1}{2}C_{NS}^q(x,\alpha_s(t))\otimes\Delta q_{NS}(x,Q^2), \tag{2.39}$$

where $\langle e^2\rangle = n_f^{-1}\sum_q e_q^2$ is the averaged quark charge, n_f is the number of quark flavors, $t = \ln(Q^2/\Lambda_{QCD}^2)$ with Λ_{QCD} being the QCD scale parameter, $\Delta\Sigma$ and Δq_{NS} are the singlet and non-singlet polarized quark distributions,

$$\Delta\Sigma(x,Q^2) = \sum_q \Delta q(x,Q^2); \qquad \Delta q_{NS}(x,Q^2) = \sum_q (e_q^2 - \langle e^2\rangle)\Delta q(x,Q^2), \tag{2.40}$$

and $C_{S,NS}^q(x,\alpha_s(t))$ and $C^g(x,\alpha_s(t))$ are the quark and gluon coefficient functions.

The x and Q^2 dependences of the polarized quark and gluon distributions are given by the DGLAP equations [8, 29, 30]:

$$\frac{d}{dt}\Delta q_{NS}(x,Q^2) = \frac{\alpha_s(t)}{2\pi}P_{NS}^{qq}(x,\alpha_s(t))\otimes\Delta q_{NS}(x,Q^2),$$

$$\frac{d}{dt}\begin{pmatrix}\Delta\Sigma(x,Q^2)\\ \Delta g(x,Q^2)\end{pmatrix} = \frac{\alpha_s(t)}{2\pi}\begin{pmatrix}P_S^{qq}(x,\alpha_s(t)) & 2n_f P_S^{qg}(x,\alpha_s(t))\\ P_S^{gq}(x,\alpha_s(t)) & P_S^{gg}(x,\alpha_s(t))\end{pmatrix} \otimes\begin{pmatrix}\Delta\Sigma(x,Q^2)\\ \Delta g(x,Q^2)\end{pmatrix} \tag{2.41}$$

where P^{ij} are the polarized splitting functions. The full set of coefficient functions [11, 26] and splitting functions [31, 32] has been computed up to next-to-leading order in α_s in the framework of Operator Product Expansions (OPE) and the renormalization group equations [33].

The n-th moment of $g_1(x,Q^2)$ which is defined by the Mellin transformation can be represented as

$$\boxed{\begin{aligned}\Gamma_1(N,Q^2) &\equiv \int_0^1 x^{N-1}g_1(x,Q^2)dx\\ &= \frac{\langle e^2\rangle}{2}\left[C_S^q(N,\alpha_s(t))\underline{\Delta\Sigma}(N,Q^2) + 2n_f C^g(N,\alpha_s(t))\underline{\Delta g}(N,Q^2)\right]\\ &\quad + \frac{1}{2}C_{NS}^q(N,\alpha_s(t))\underline{\Delta q_{NS}}(N,Q^2),\end{aligned}} \tag{2.42}$$

with the coefficient functions, $C(N,\alpha_s)$, and the parton distributions, $\Delta\Sigma(N,Q^2)$, $\Delta g(N,Q^2)$ and $\Delta q_{NS}(N,Q^2)$, transformed in the momentum space, analogously. The Mellin transformation of the DGLAP equations are also rewritten in the simple multiplication using the anomalous dimensions,

$$\gamma(N,\alpha_s) \equiv \int_0^1 x^{N-1}P(x,\alpha_s)dx. \tag{2.43}$$

In particular the first moment of the structure function, $\Gamma_1(Q^2) = \Gamma_1(1,Q^2)$, is expressed in a simple form as

$$\boxed{\begin{aligned}\Gamma_1(Q^2) &= \frac{\langle e^2\rangle}{2}\left[C_S^q(\alpha_s(t))\underline{\Delta\Sigma}(Q^2) + 2n_f C^g(\alpha_s(t))\underline{\Delta g}(Q^2)\right]\\ &\quad + \frac{1}{2}C_{NS}^q(\alpha_s(t))\underline{\Delta q_{NS}}(Q^2)\end{aligned}} \tag{2.44}$$

QCD fit to polarized parton distribution functions

$Q^2 = 1\ GeV^2$

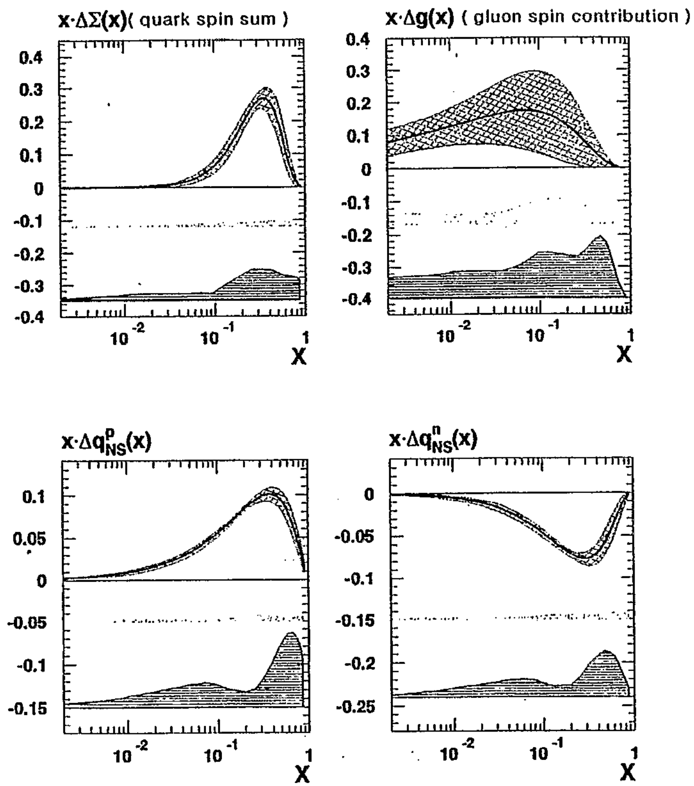

cross hatched band : error from QCD fit

vertically hatched band: experimental systematic error

horizontally hatched band: theoretical uncertainty

SMC Summary

- $\Delta\Sigma$, Δs

Quantity		Regge approach	QCD analysis
$\Delta\Sigma(=a_0)$	Proton	0.34 ± 0.17	0.22 ± 0.17
$\Delta\Sigma(=a_0)$	Deuteron	0.30 ± 0.08	
a_0	for all p,d data		$0.19 \pm 0.05 \pm 0.04$
Δs	Proton	-0.08 ± 0.06	
Δs	Deuteron	-0.09 ± 0.03	

- Bjorken sum rule is valid
- Ellis-Jaffe sum rule is violated
- A_2^p, A_2^d are consistent with 0
- Δu_v, Δd_v, Δq were measured
- The role of ΔG
  NLO QCD analysis indicates

  $\Delta G = 1.7(Q^2=5\text{GeV}^2)$, $2.0(Q^2=10\text{GeV}^2)$

  Direct measurement of ΔG !!

The COMPASS Experiment

Univ. Bielefeld, Univ. Bochum, ISKP Bonn, Phys. Inst. Bonn, Burdwan Univ., JINR Dubna, Univ. Erlangen, Univ. Freiburg, CERN, MPI Heidelberg, Univ. Heidelberg, Helsinki Univ., Univ. Mainz, Univ. Mons, INR Moscow, Lebedev Inst. Moscow, Univ. Moscow, TU-München, Univ. München, **Nagoya Univ.**, **Univ. Osaka**, IHEP Protvino, Saclay, Tel Aviv Univ., INFN-Univ. Torino, INFN-Univ. Trieste, Warsaw Univ + Technical Univ.

Physics: Study of Hadron Structure and strong interaction

- **muon** beam (100 & 200 GeV/c)
  - Spin structure of the nucleon
    - measurement of gluon-polarisation ($\Delta G/G$) using
      - open charm
      - high p_T hadrons
    - vector meson production (QCD factorization tests/ OFPD)

- **hadron** beam (140-280 GeV/c) (π,K, p)
  - 'glue-balls' and hybrid-mesons
    - diffractive/central production of gluonic excitations of hadrons
  - χPT - tests using Primakoff reaction (scattering off virtual photons)
  - D-meson physics with leptonic final states

DIS in SMC and COMPASS

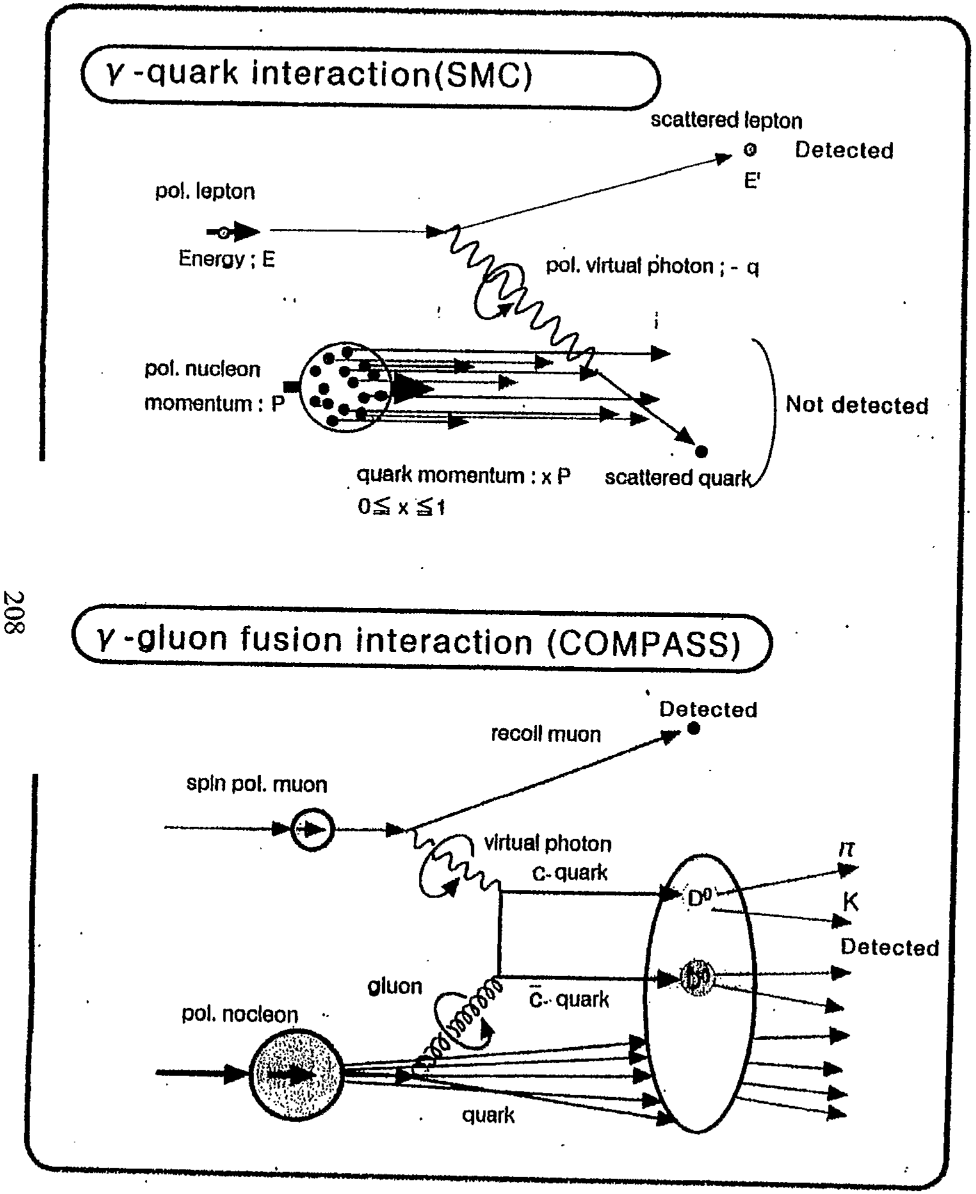

Physics Goal of COMPASS

A : Spin Structure of Nucleon
B : Spectroscopy of Hadron

A - Program(muon program)

1. Gluon Spin Polarization in Nucleon through
   open charm production by polarized muon and nucleon
   separate detection of π and K

2. Valence quark and Sea quark Contribution
   Semi-inclusive processes

3. Transverse Spin Distribution Function
   Structure function $h_1(x)$ and Jaffe-Ji sum rule

4. s-quark and Gluon Polarization
   produced Λ Polarization

Photon Gluon Fusion

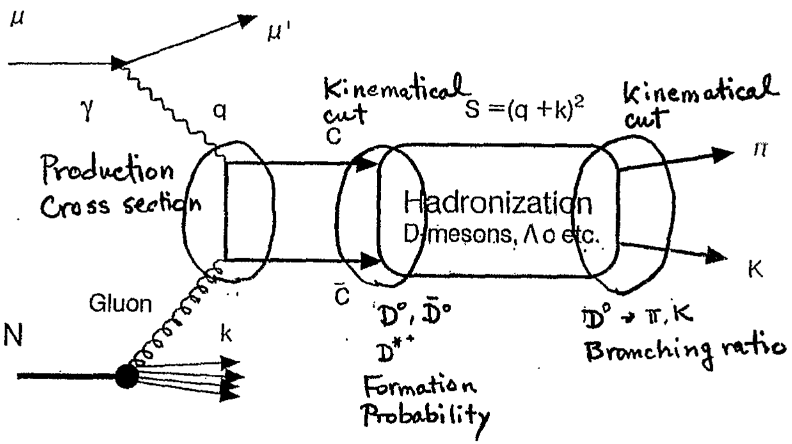

★ Hard process : scale $s \geqq 4m_c^2 \sim 10\text{GeV}^2$

★ Proportinal to Gluon Distribution

★ γ-g Subprocess is known : Unpolarized NLO

Polarized LO (NLO at Large Q^2)

Open Charm Production

★ Large Cross Section : 4% of σ_γ at 60 GeV

★ No(Large) Diffractive Contribution

★ No Constituent Charm

★ Small Contribution from resolved Photons(≦a few %)

Measurement of Asymmetry

$$\frac{N_{c\bar{c}}\uparrow\downarrow - N_{c\bar{c}}\uparrow\uparrow}{N_{c\bar{c}}\uparrow\downarrow + N_{c\bar{c}}\uparrow\uparrow} = A^{\text{meas.}} = P_b\, P_T\, f\, A_{\mu N}^{c\bar{c}}(E,y)$$

$$A_{\mu N}^{c\bar{c}}(E,y) = D\, A_{\gamma* N}^{c\bar{c}}(E,y)\,, \quad D\text{ ; Depolarization factor}$$

$$A_{\gamma* N}^{c\bar{c}}(E,y) = (\Delta\sigma^{\gamma* N \to c\bar{c}X}) / (\sigma^{\gamma* N \to c\bar{c}X})$$

$$= \frac{\int ds\, \Delta\sigma(s) \Delta G(\eta,s)}{\int ds\, \sigma(s)\, G(\eta,s)} = \langle a_{||} \rangle \langle \Delta G/G \rangle$$

$\eta = s/2ME\gamma$; Gluon momentum fraction

$s = (q + k)^2$; invariant mass of photon-gluon system

Charm Production Cross Section v.s. Photon Energy(ν)

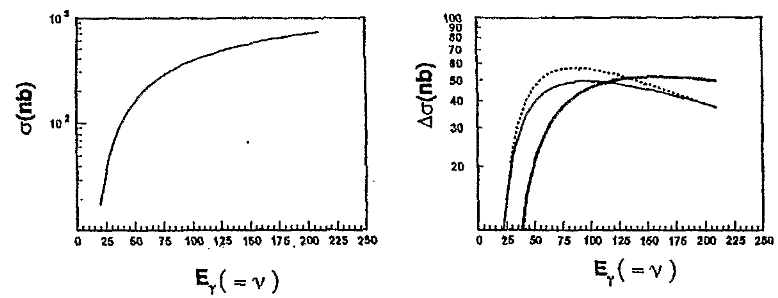

Charm production cross sections as a function of the photon energy $E_\gamma = \nu$. a) unpolarised cross section $\sigma^{\gamma N \to c\bar{c}X}$, b) polarised cross section $\Delta\sigma^{\gamma N \to c\bar{c}X}$.

Photon Gluon Cross Section(LO)

At CM

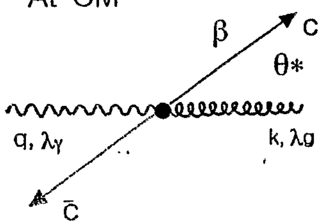

$s=(q+k)^2$

$\beta=[1-4(m_c^2/s)]^{1/2}$

Cross Section : $\gamma\, g \rightarrow c\, \bar{c}$

$$\sigma^{c\bar{c}}(s) = \sigma(s) + \lambda_\gamma \lambda_g \Delta\sigma(s)$$

$(1/2)(\sigma^+ + \sigma^-)$ ± 1 $(1/2)(\sigma^+ - \sigma^-)$

by A. D. Watson (Z. Phys. C12 (1982) 123)

$$\Delta\sigma(s) = (4/9)(2\pi\alpha\alpha_s/s)[3\beta - \ln(1+\beta)/(1-\beta)]$$

$$\sigma(s) \mp (4/9)(2\pi\alpha\alpha_s/s)[-\beta(2-\beta)^2 + (1/2)(3-\beta^4)\ln\{(1+\beta)/(1-\beta)\}]$$

- Calculation is done under the conditions
  - ★ (Quasi) real photon
  - ★ Leading Order
  - ★ Integrated over θ^*
  - ★ β ; charm quark velocity

Hadronization of $c\bar{c}$

Luminosity : 4.3×10^{37} cm^{-2} day^{-1}

Charm Events : 82,000/day (1.9nb) for $35 < \nu < 85$ GeV

DIS Events : 20,000,000/day (463nb).

D^0 : 60 % Dominates(1/3 from $D^{*+} \rightarrow D^0\pi^+$)
D^+ : 20 %
D_s : 10 %
Λ_c : 10 %

Concentrate on D^0, $\bar{D}^0$

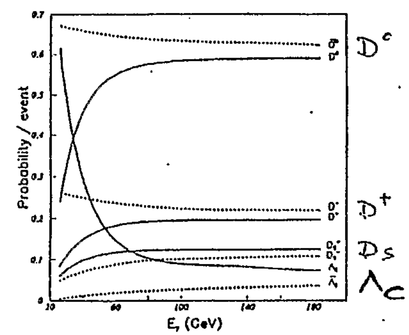

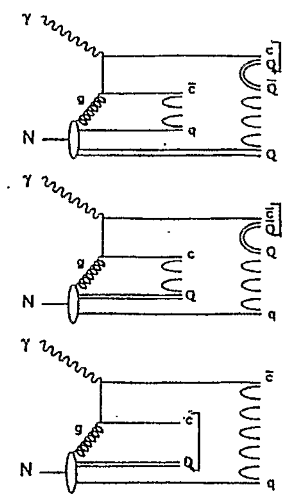

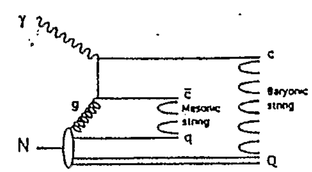

Acceptance cuts

CM: isotropic

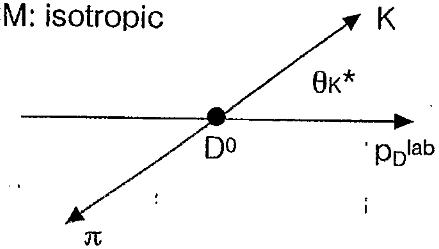

Monte Carlo Simulation

★ $|\cos\theta_K^*| \leqq 0.5$
★ $z > 0.25$
★ Mass window : $\pm$ 20MeV, $\sigma_M = 10$ MeV
★ $35 < \nu < 85$ GeV

D^0 Decays   Combinatorial BG

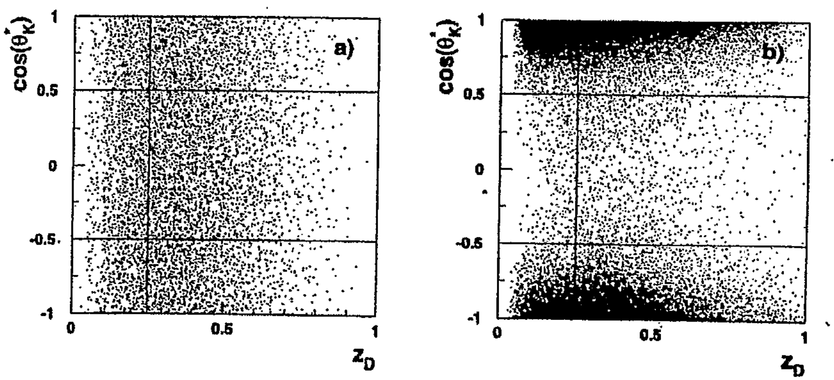

Reconstruction of D^0

★ Cleanest Decay Channel

$$\left.\begin{array}{l} D^0(c\bar{u}) \rightarrow K^-\pi^+ \\ \bar{D}^0(\bar{c}u) \rightarrow K^+\pi^- \end{array}\right\} \quad \text{BR : } 0.04$$

★ Acceptance cuts

$35 < \nu < 85$, $|\cos\theta_K^*| < 0.5$

$z > 0.25$ ($z = E_D/\nu$; energy fraction carried by D^0 from photon)

$\varepsilon^{c\bar{c}}$: Detection probability of D^0 from charmed events

ε^{BG}: Background

N^D : D-meson events

$N^{c\bar{c}}$: $c\bar{c}$ events

a : Detector acceptance

$$\varepsilon^{c\bar{c}} = (N^D/N^{c\bar{c}}) \cdot BR \cdot a$$

ε^{BG} : Depends on μ scattering events, width of D-meson cut

$$\left.\begin{array}{l} a = 0.3 \\ N^D/N^{c\bar{c}} = 1.2 \\ BR = (4.01 \pm 0.14)\% \end{array}\right\} \quad \varepsilon^{c\bar{c}} = 0.014$$

Events Estimation

★ Parameters of the Experiment

Muon Beam : 100 GeV, $P_\mu = 80\%$, 2×10^8/spill ($5\times$"SMC")

Target : 2×60cm (twin cell), 3cmϕ
Material : NH_3 : $P_T = 85\%$, f=0.176
: ^6LiD : $P_T = 50\%$, f=0.5

Acceptance : ±180mrad, $\Delta p / p = 1\sim2\%$
Particle ID : 3σ K, π Separation, p>3GeV/c

Nominal Luminosity : 5×10^{32} cm^{-2}s^{-1}
Assuming overall Efficiency : 0.25

★ Event Rates/day : $N^{c\bar{c}} = 94{,}700$

$N^{signal} = N^{cc} \cdot \varepsilon^{cc} \cdot \varepsilon^{signal}_{target}$ = 877 events/day ($\varepsilon^{signal}_{target} = 0.76$)

$N^{BG} = N\mu \cdot \varepsilon^{BG} \cdot \varepsilon^{BG}_{target} \cdot r_s$ = 3269 events/day for NH3
= 3450 events/day for LiD

2.5 years	:	1 year (150 days)	NH_3
		1.5 years	^6LiD
66K		Reconstructed	$D^0 \to K\pi$
250K		Background	

$$\boxed{\delta A_{\gamma N^{cc}} = 0.076 \Leftrightarrow \delta(\Delta G/G) = 0.21}$$

Scatter Plot of produced K and π
Energy v.s. Angle

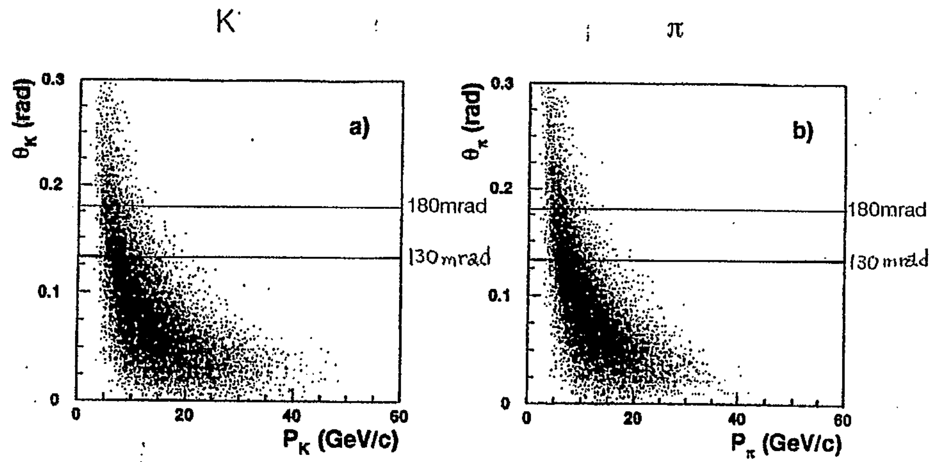

Projected Error to Asymmetry for Open Charm Production

Error corresponds to $\delta A_{\gamma N}^{cc} = 0.051$

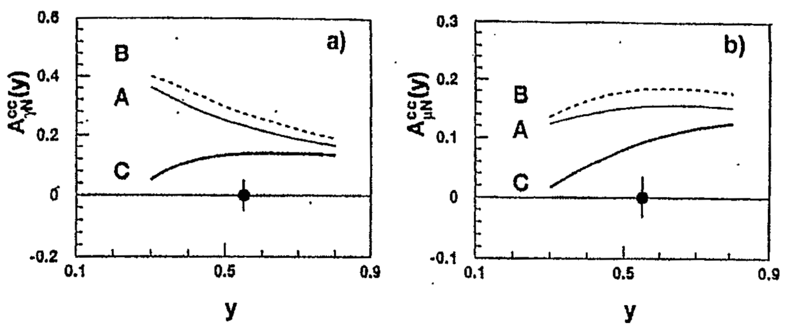

Figure 3.6: a) Asymmetry $A^{c\bar{c}}_{\gamma N}$ and b) asymmetry $A^{c\bar{c}}_{\mu N}$ for open charm as a function of y. The curves refer like in Fig. 3.1 to the three sets of ΔG from Ref. [4]. The projected precision of the measurement in the range $0.35 < y < 0.85$ is indicated by the error bars of the data points shown at $A = 0$.

Curves correspond to prediction by T.Gehrmann and W.J.Stirling
Z. Phys. C65(1994)461

Further D^0 Purification

D* Tagging : $D^{*+} \rightarrow D^0 + \pi^+_{(s)}$
30% of D^0's

$\Delta M = M(\pi^+_{(s)},\pi^+,K^-) - m(\pi^+,K^-) = 145$MeV
Detect soft pion($\pi^+_{(s)}$) > 1 GeV/c
Cut : ΔM : ± 5 MeV

Essentially Background free
Release z and $\cos\theta_K^*$ cuts

$$\boxed{\delta A_{\gamma N}^{cc} = 0.051 \Leftrightarrow \delta(\Delta G/G) = 0.14}$$

P_T Cut

event loss 20%
$P_T(D^0) < 1.0$ GeV/c → Increases Analyzing Power 50%

$$\boxed{\delta(\Delta G/G) = 0.11}$$

Other Channels are investigated

$D^0 \rightarrow K^-\pi^+\pi^0$	13.8%
$D^0 \rightarrow K^-\pi^+\pi^+\pi^-$	8.1%
$D^+ \rightarrow K^-\pi^+\pi^+$	9.1%

New Channel for Gluon Polarization High P_T Kaons and Hadrons

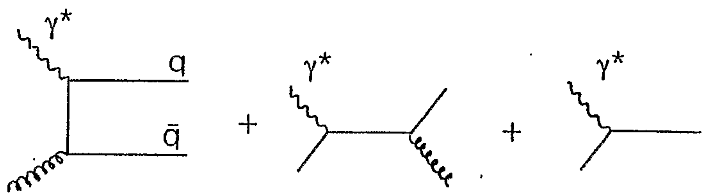

PGF Compton LO

Subprocess Compton Contribution
Simulation by "JETSET + LEPTO"

- ★ 2 High P_T Hadrons
- ★ Opposite Charge
- ★ Flavour Tagging ; $ss \rightarrow K^+K^-$

	S:B	LO	Compton	PGF	TOT
all	1: 5	0.60	0.22	0.18	1
K^+K^- ($P_T>0.5$ GeV)	1: 2.5	0.42	0.29	0.29	0.025
K^+K^- ($P_T>0.8$ GeV, $m_{K^+K^-} > 3$ GeV, $z > 0.1$)	2: 1	0.05	0.30	0.65	1.5×10^{-4}
h^+h^- ($P_T>0.8$ GeV, $m_{K^+K^-} > 3$ GeV, $z > 0.1$)	1: 1	0.05	0.49	0.46	2×10^{-3}

Results of Preliminary Study

Estimates using GS96, GRV94LO
for E_μ : 200GeV, $0.5 < y < 0.9$

$$\left.\begin{array}{l} \delta A_{LL}^{KK} \sim 0.02 \\ \delta A_{LL}^{hh} \sim 0.005 \end{array}\right\} \text{statistical error only !}$$

$$A_1 = A_{LL} = \underset{-1}{<a_{LL}>}\underset{0.36}{<\Delta g/g>}\underset{0.3}{<\sigma^{PGF}/\sigma^{tot}>}$$

$$+\underset{0.5}{<a_{LL}^{comp}>}\underset{0.25}{<\Delta u/u>}\underset{0.65}{<\sigma^{comp}/\sigma^{tot}>}$$

($x_g = 0.1$, $Q^2 = 10\text{GeV}^2$)

Rough Estimate

$$\left.\begin{array}{l} \delta(\Delta G/G)_{KK} \sim 0.05 \\ \delta(\Delta G/G)_{hh} \sim 0.10 \end{array}\right\} \text{statistical error only !}$$

Looks promising !

Further Monte Carlo studies needed!

Time schedule and Participants

1. Time schedule of COMPASS

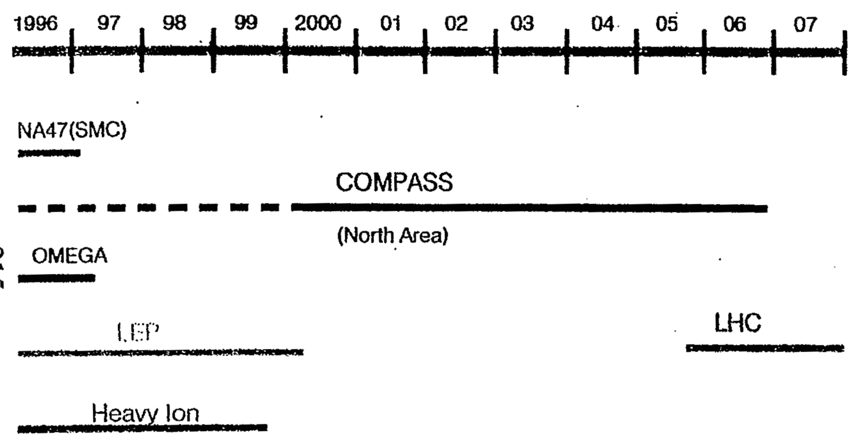

2. Collaboration

Countries : 11
Belgium, Finland, France, Germany, India, Israel, Italy, Japan, Poland, Russia, Switzerland,

Institutes : 26

Participants : 168(Jan. 1998)

Requirements for COMPASS Experiment

1. New Spectrometer :

Wide Aperture : 2 sets of spectrometer
Essentially new 2-stage spectrometer!!

Particle ID : 2 RICHs
2 Ele-Mag Calorimeters

2. Larger Target Solenoid (180mrad opening angle)

3. Polarized Target Materials

Ammonia for proton
^{6}LiD for Deuteron

4. Posible highest beam flux:

μ-flux (5 times higher than SMC: $2x10^{8}$ppp)

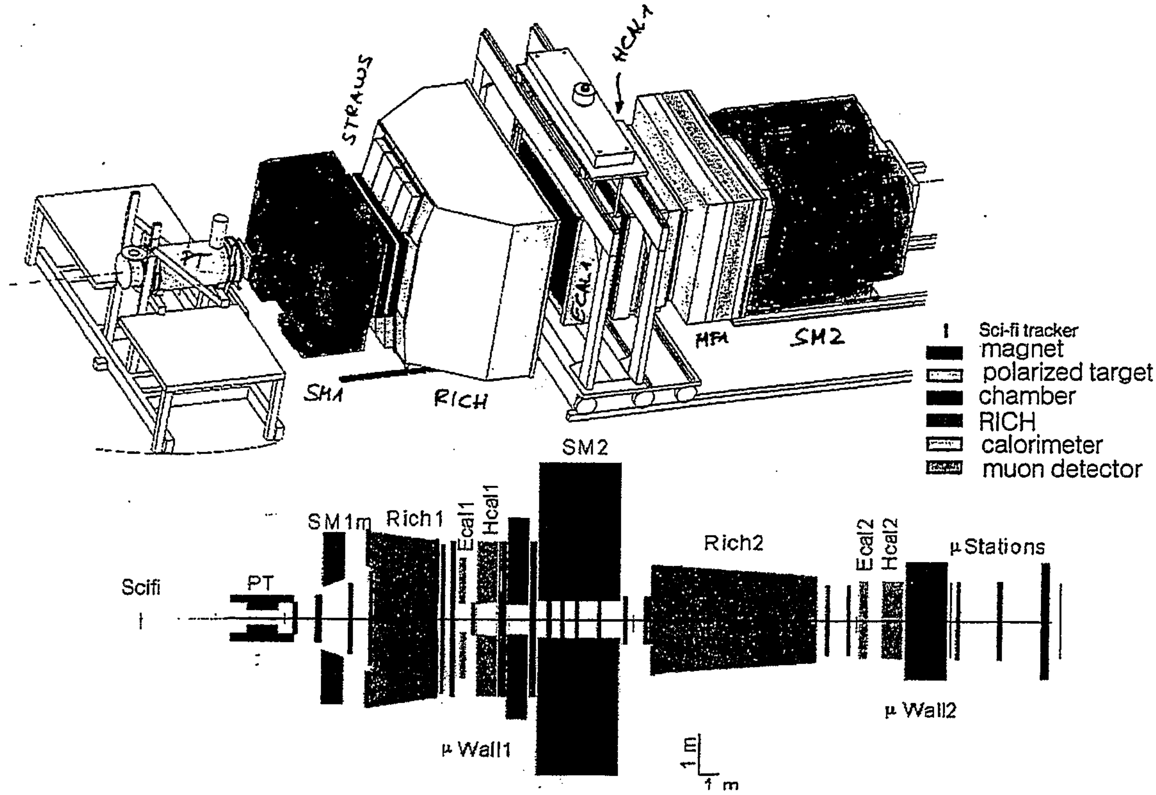

COMPASS Spectrometer

RICH 1 in the COMPASS Experiment Hall

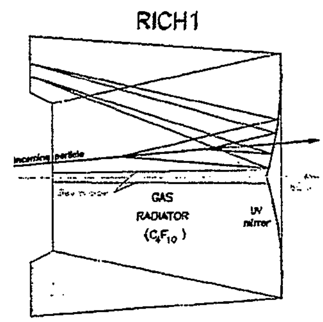

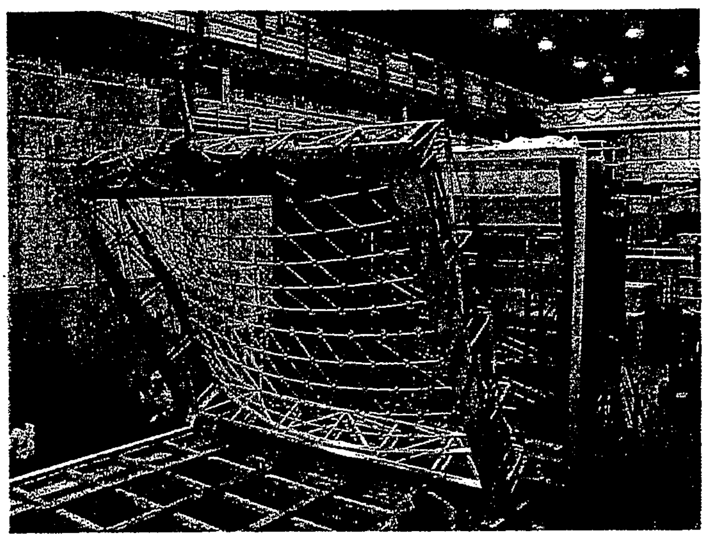

RICH 1 backwall mounting, May 10, 2000

Size; H 5.3 m x W 6.6 m x D 3.3 m

π, K Separation; up to ~ 60 GeV

Gas Radiator; C4F10

2 Mirrors; total surface > 20 m^2, focalize the Cherenkov photons onto 2 sets of photon detector.

Photon detectors; MWPCs equipped with CsI photocathodes.

RICH 1 project

University of Bielefeld, INFN Trieste, University of Trieste, ICTP Trieste, INFN Torino, University of Torino, Charles University Prague, JINR Dubna

COMPASS PT System

COMPASS Polarized Target

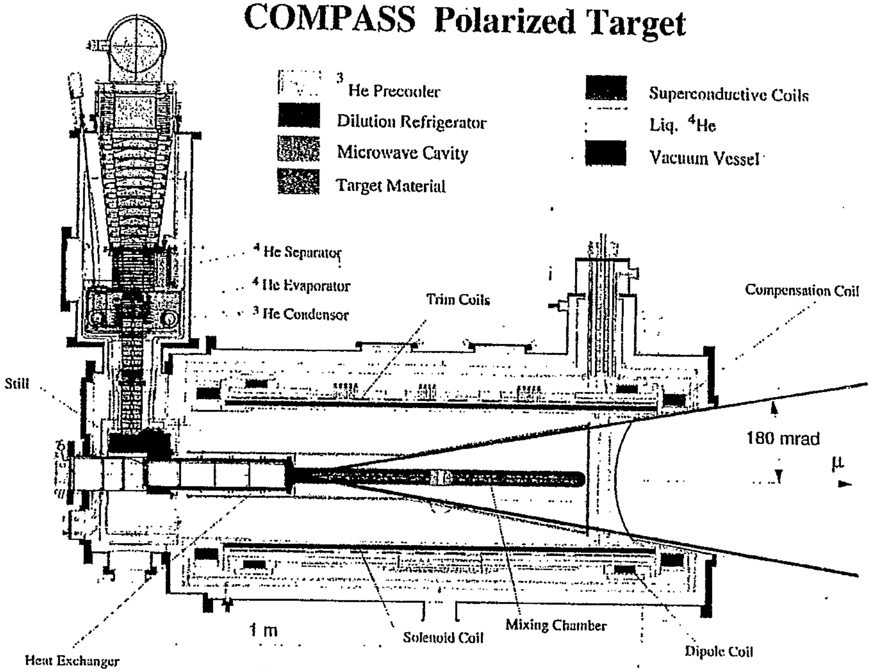

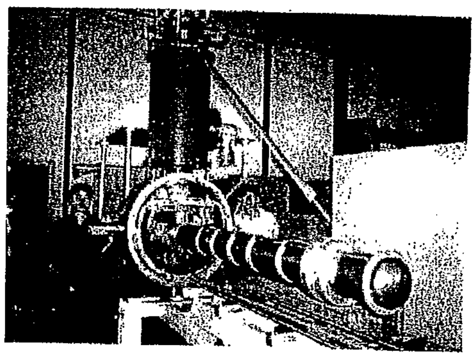

ilution Refrigerator and Microwave Cavity

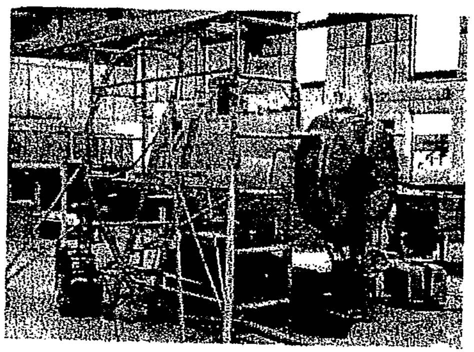

Superconducting Magnet in Test

Experimental Hall and Preparation

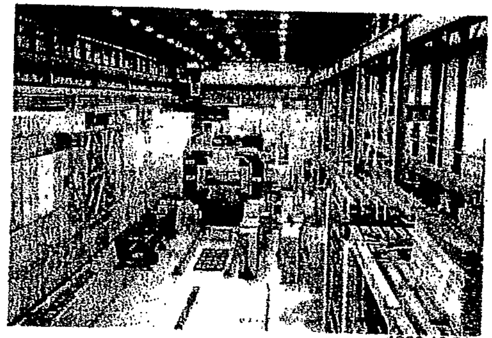

1999.10.31

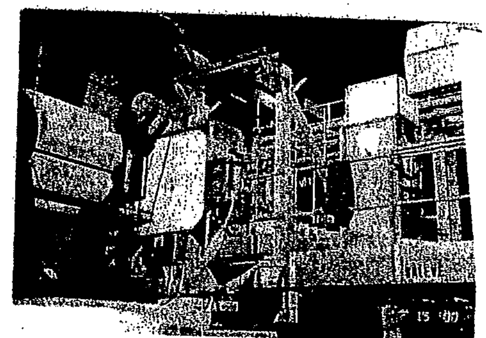

2000.7.15

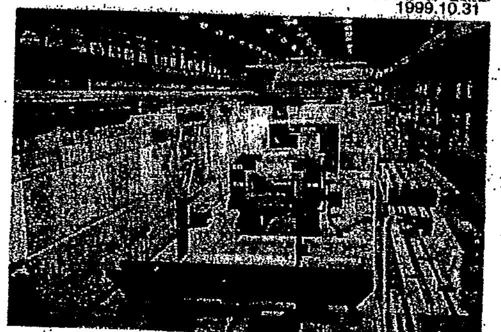

2000.3.14

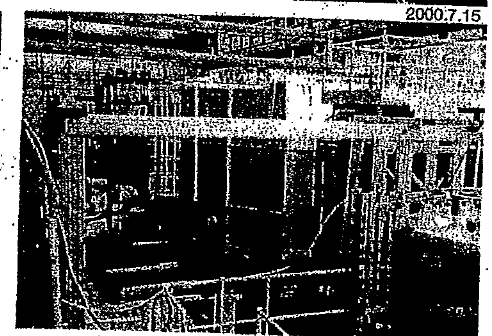

2000.7.15

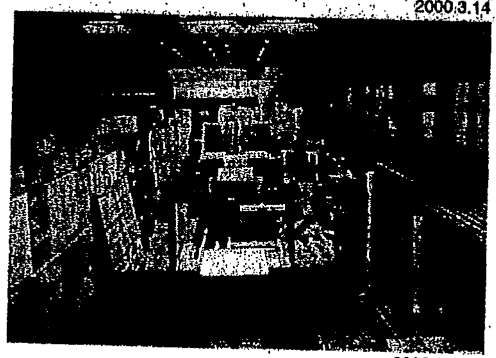

2000.4.13

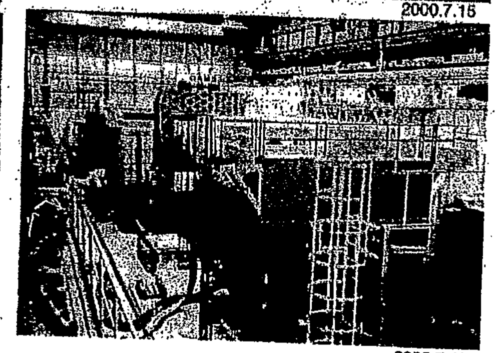

2000.7.15

Target materials

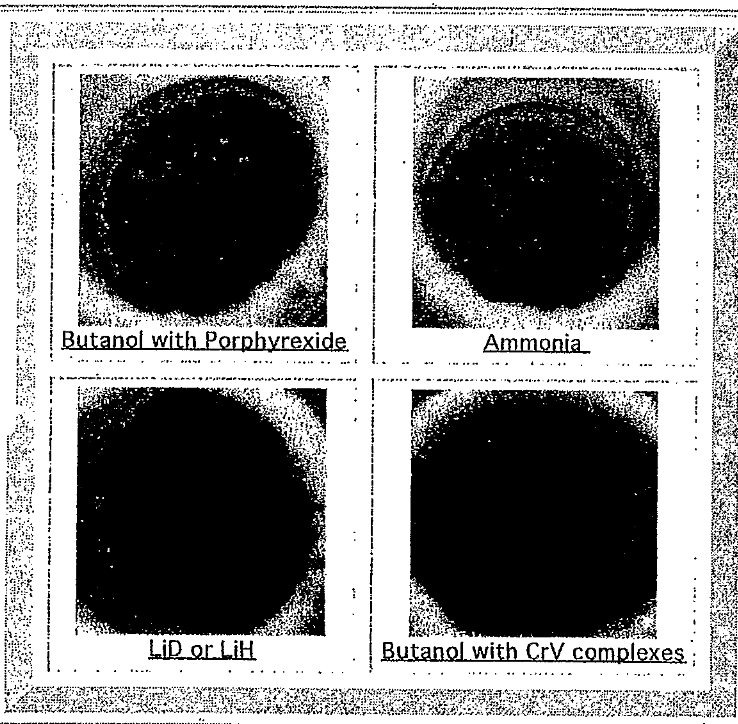

Butanol with Porphyrexide

Ammonia

LiD or LiH

Butanol with CrV complexes

24.Sep.2001

COMPASS Polarized Target

Successful Dynamic Nuclear Polarization of Deuteron (^{6}LiD) in two cells.

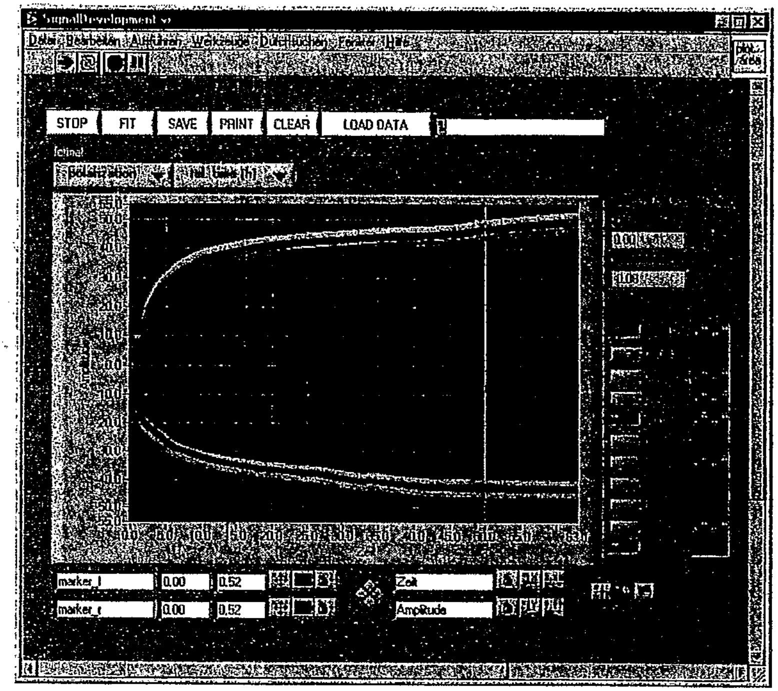

On-monitor, Polarization (%) vs time (h)

NMR_1, ..., NMR_3: Polarization measurement in upstream cell

NMR_5, ..., NMR_9: Polarization measurement in downstream cell

Preliminary values

Pupstream = ~ -43%, Pdownstream = + 48 %

(more optimization and precise calibration/analysis will come.)

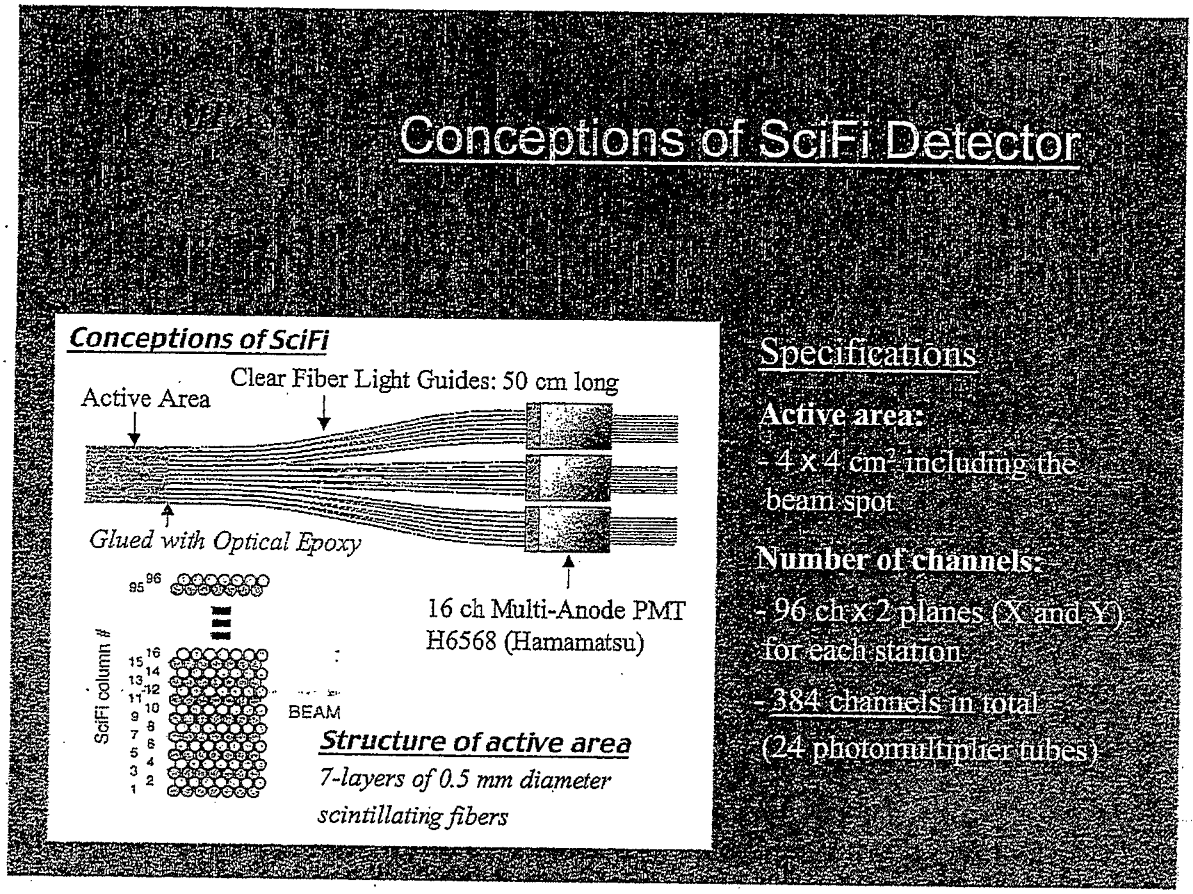
Conceptions of SciFi Detector
Conceptions of SciFi
Clear Fiber Light Guides: 50 cm long
Active Area
Glued with Optical Epoxy
16 ch Multi-Anode PMT
H6568 (Hamamatsu)
SciFi column #
BEAM
Structure of active area
7-layers of 0.5 mm diameter
scintillating fibers
Specifications
Active area:
- 4 x 4 cm² including the beam spot
Number of channels:
- 96 ch x 2 planes (X and Y) for each station
- 384 channels in total
(24 photomultiplier tubes)

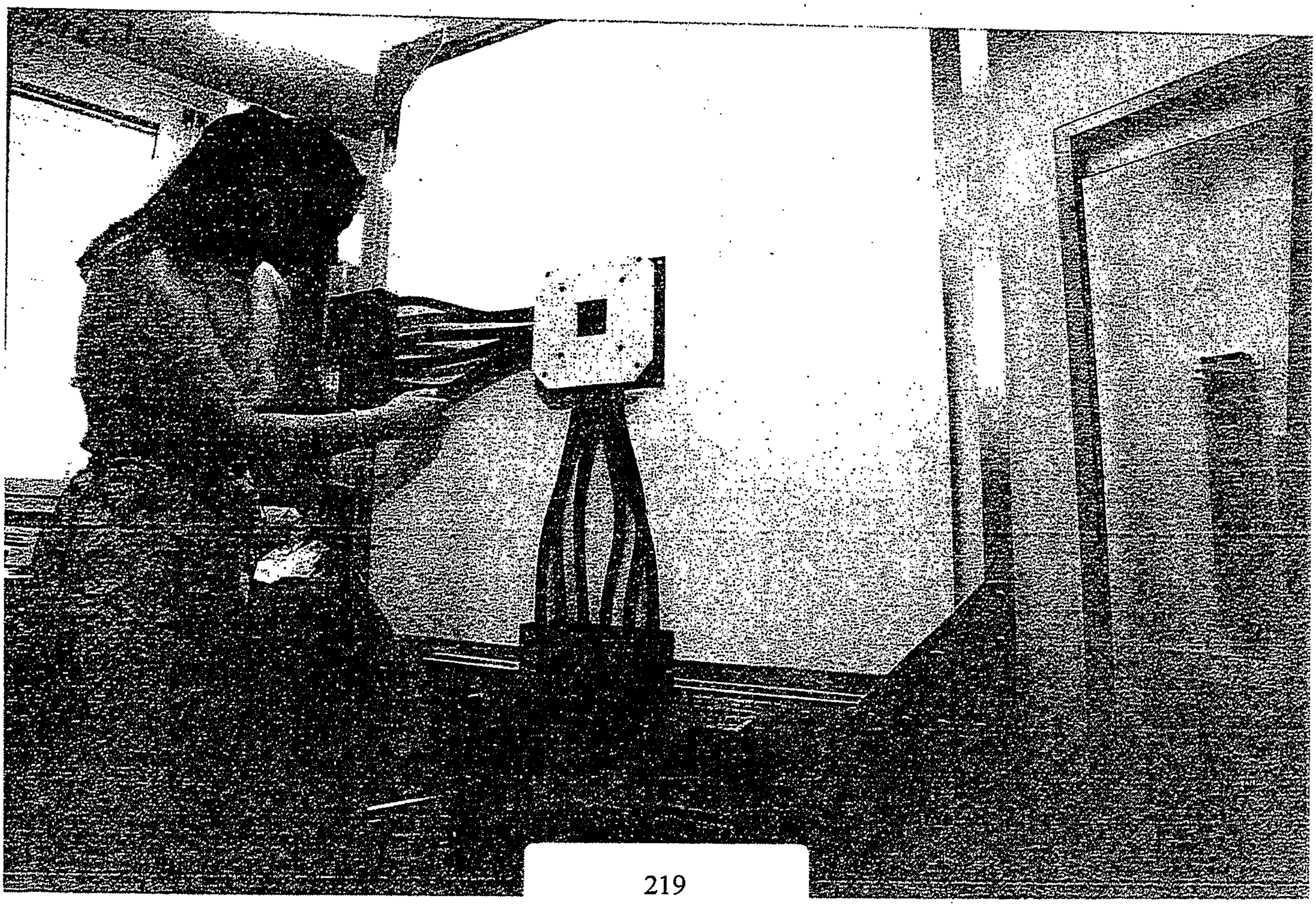

COMPASS 2001 Run

- Overview - 1 -

- Beam time: 12 July - 23 October 2001
  - **About 360 shifts (starting from 15 August)**
- Setup Period (12/Jul - 06/Oct)
  - **12/July - 04/Sep: Major installation work**
    - Beam - only during night and weekend
      - SciFi-J/G and MWPC fully commissioned
      - DAQ test, first alignment etc...
  - **05/Sep - 02/Oct: Detector commissioning**
    - Default Beam ON
      - Spectrometer growing up...
      - PT (LiD) operation started!!

COMPASS 2001 Run

- Overview - 2 -

- Physics Data Taking (07 - 23/Oct)
  - **07-13/Oct; Lower trigger rate (< 7,000 events/spill)**
  - **14-23/Oct; Nominal trigger rate (18,000 events/spill)**
- Collected Data:
  - **During the "setup period" - 14 TB**
  - **During the "physics data taking" - 14 TB**
  - **Total 1.6 x 10^9 events**

COMPASS 2001 Run

- Overview - 3 -

- Beam Parameters:
  - **Momentum: 160 GeV/c; Spot size: 9 x 7 mm^2 (sigma)**
  - **Intensity: 2.2 x 10^8 particles/spill (after 12/Sep)**
  - **Spill duration: 5.2 sec (in 16.8 sec cycle)**
- Trigger
  - **3 trigger systems:**
    - **Inner (IT) < Meddle (MT) < Ladder (LT)**

      Small Q^2 <<<<<<<<<<<<<<<< Large Q^2
  - **Veto (V)**
  - **Calorimeter (C)**
  - **ITCV + MTV + LTCV ->> 18,000 triggers**

GDH Sum Rule and Spin Structure Function g_1

Pol. Photon & Pol. Nucleon Reaction

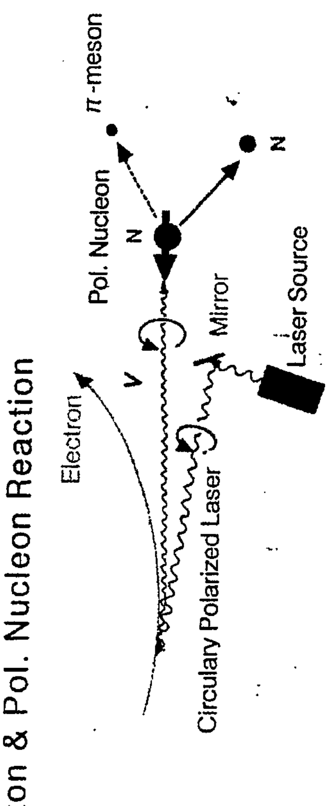

Reaction Cross Section : $\sigma^{\uparrow\uparrow}, \sigma^{\uparrow\downarrow}$

$$I \propto \int_{\pi\text{-Threshold}}^{\infty} \frac{\sigma^{\uparrow\uparrow} - \sigma^{\uparrow\downarrow}}{\nu} \cdot d\nu \propto \kappa^2$$

Photon Energy

Anomalous Magnetic Moment of Nucleon

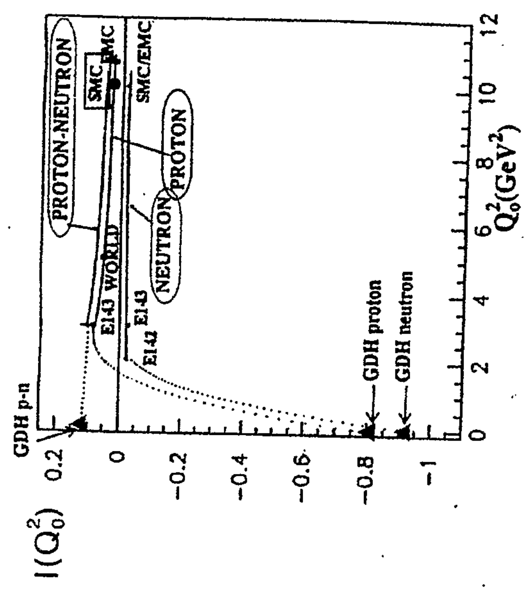

Drell-Hearn, Gerasimov(DHG) sum rule

- Hosoya & Yamamoto

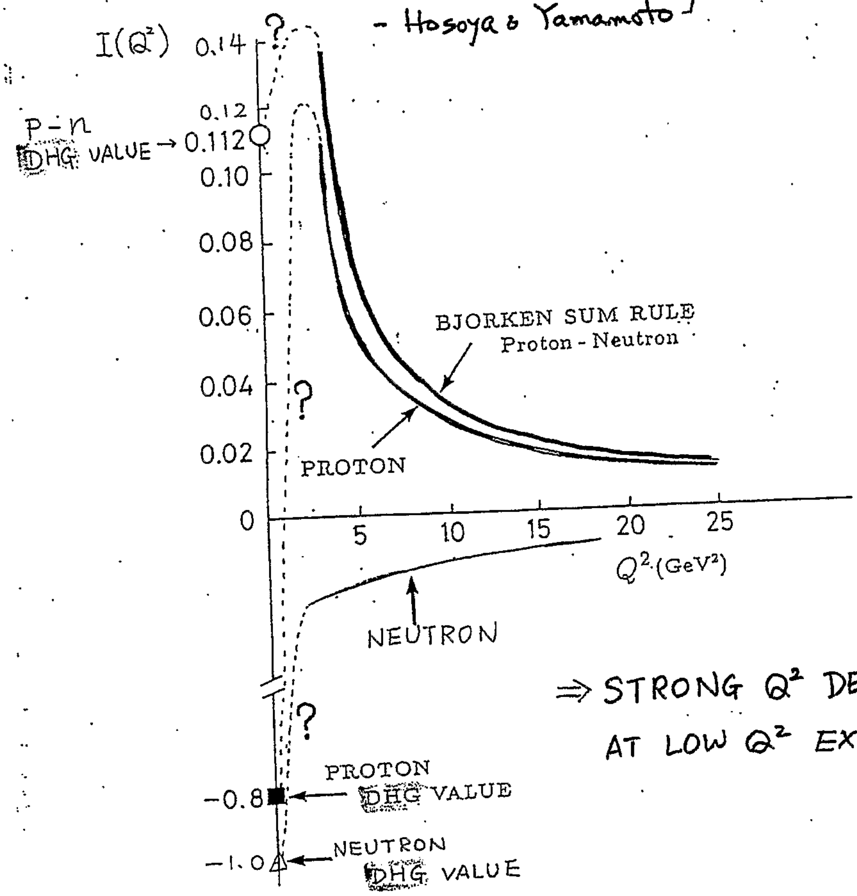

⇒ STRONG Q^2 DEPENDENCE AT LOW Q^2 EXPECTED

$$\int_0^1 d\nu \frac{\sigma_{3/2} - \sigma_{1/2}}{\nu} = \frac{2\pi^2\alpha}{m^2}\kappa^2 \qquad \kappa\text{: 陽子の異常磁気能率}$$

$$\sigma_{1/2} - \sigma_{3/2} = \frac{8\pi^2\alpha}{\nu - Q^2/2m}[m\nu G_1(\nu, Q^2) - Q^2 G_2(\nu, Q^2)]$$

$$I(Q^2) = m^3 \int_{Q^2/2m}^{\infty} d\nu \frac{G_1(\nu, Q^2)}{\nu} = \frac{2m^2}{Q^2}\int_0^1 dx\, g_1(x, Q^2)$$

$$I(0) = \frac{m^2}{8\pi^2\alpha}\int_0^{\infty} d\nu \frac{\sigma_{1/2} - \sigma_{3/2}}{\nu} = -\frac{\kappa^2}{4}$$

GDH sum rule and nucleon spin structure

Nucleon spin structure function g1 has been measured in polarized deep inelastic scattering

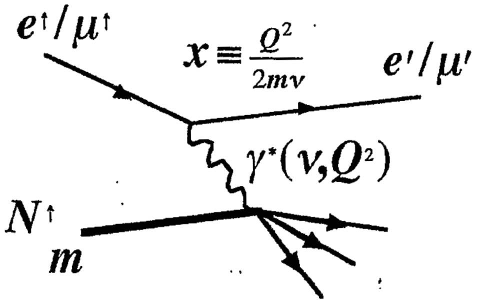

First Moment of g_1:

$$\boxed{\Gamma_1(Q^2) \equiv \int_0^1 g_1(x, Q^2)\,dx}$$

$\longrightarrow$ Bjorkrn sum rule
Ellis-Jaffe sum rule

virtual photon transverse asymmetry

$$1/2\,\Delta\sigma^T = \frac{1}{2}\left(\sigma^T_{3/2} - \sigma^T_{1/2}\right) = -\frac{4\pi^2\alpha}{\nu - \frac{Q^2}{2m}}\left(m\nu G_1(\nu, Q^2) - Q^2 G_2(\nu, Q^2)\right)$$

in Bj. limit: $m\nu G_1(\nu,Q^2) \to g_1(x)/m$, $\quad Q^2 G_2(\nu,Q^2) \to g_2(x)/m\nu^2$

$Q^2 \to 0$ real photon absoption

$\Delta\sigma(\nu) = \sigma_{3/2}(\nu) - \sigma_{1/2}(\nu)$ $\longleftarrow$ difference of helicity dependent photo-absorption crosssections

$$\Delta\sigma = -\frac{8\pi^2\alpha}{\nu}\frac{g_1(x, Q^2 \to 0)}{m} \longleftarrow$$

$$\boxed{I(Q^2) \equiv \frac{2m}{Q^2}\Gamma_1(Q^2)} = m\int_{Q^2/2m}^{\infty} g_1\left(\frac{Q^2}{2m\nu}, Q^2\right)\frac{d\nu}{\nu^2}$$

$$I(0) = m\int_0^{\infty} -\frac{\nu m}{8\pi^2\alpha}\frac{\Delta\sigma}{\nu^2}d\nu = -\frac{m^2}{8\pi^2\alpha}\boxed{\int_0^{\infty}\frac{\Delta\sigma}{\nu}d\nu}$$

$$= -\frac{1}{4}K^2$$

GDH

$$\frac{2\pi^2\alpha}{m^2}K^2$$

M.Anselmino et al., Sov. J:Nucl.Phys. 49(1989)136

Generalized GDH Sum Rule

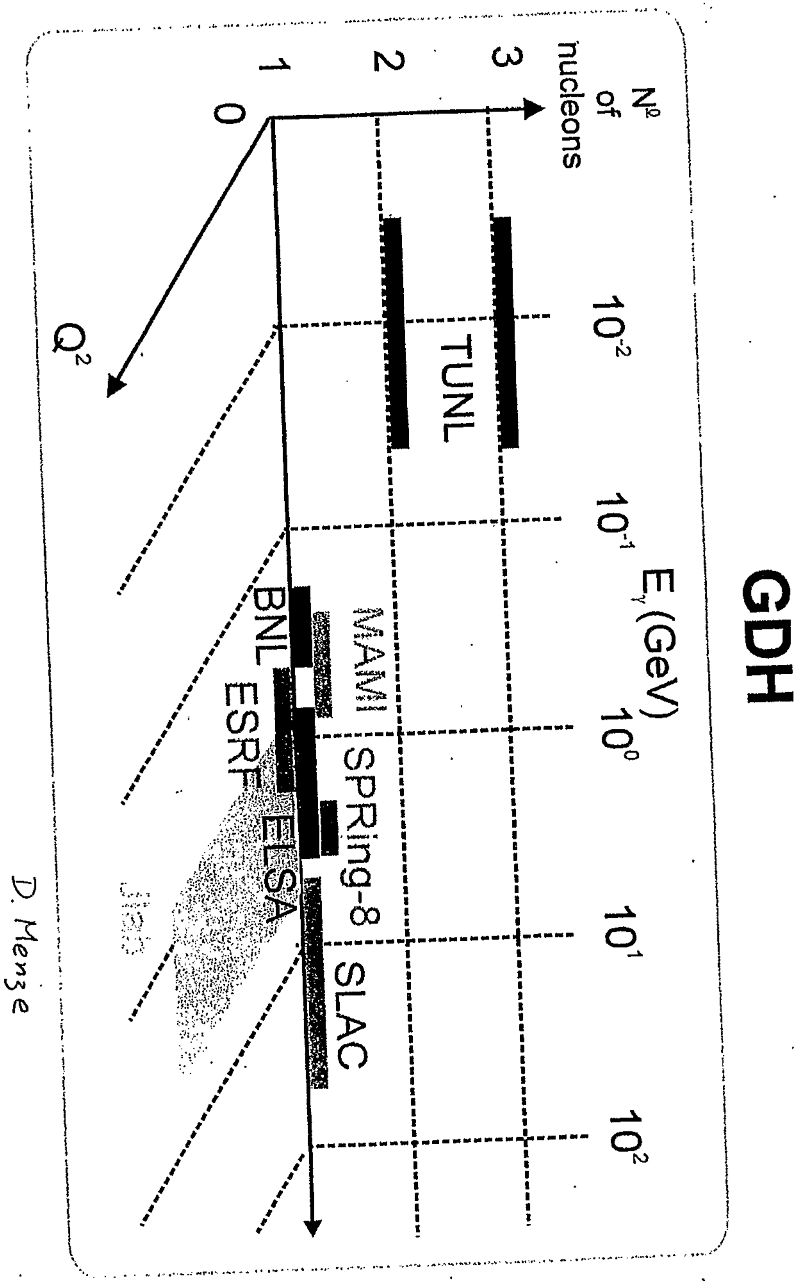

Derivation of the GDH sum rule

Forward Compton amplitude

$$f(\nu)=\chi_f^{\dagger}\left[f_1(\nu)\vec{\varepsilon}_f^{\,*}\cdot\vec{\varepsilon}_i+if_2(\nu)\sigma\cdot(\vec{\varepsilon}_f^{\,*}\times\vec{\varepsilon}_i)\right]\chi_i$$

General Principles
- Lorentz invariance
- gauge invariance
- causality relativity
- crossing symmetry
- analicity of amplitude

ASSUMPTION

$$\lim_{\nu\to\infty} f_2(\nu)=0$$

unsubtracted dispersion relation

$$\mathrm{Re}\, f_2(\nu)=\frac{\nu}{\pi}P\int_0^{\infty}\frac{\mathrm{Im}\, f_2(\nu')}{\nu'^2-\nu^2}d\nu'$$

Optical theorem

$$\mathrm{Im}\, f_2(\nu)=\frac{\nu}{8\pi}(\sigma_{3/2}(\nu)-\sigma_{1/2}(\nu))$$

Low energy theorem

$$f_2'(0)=\left.\frac{\partial f_2}{\partial\nu}\right|_{\nu=0}=\frac{\alpha}{2m^2}K^2$$

GDH sum rule

$$\int_{\nu_{th.}}^{\infty} d\nu\frac{\sigma_{3/2}(\nu)-\sigma_{1/2}(\nu)}{\nu}=\frac{2\pi^2\alpha}{m_{p,n}^2}(K_{p,n})^2$$

D. Menze
2001. 春. JPS meeting.

19.Oct.2001 JPS-APS joint meeting at Maui

Mainz GDH Experiment

- Tagged photon facility of the Mainz MAMI accelerator
  [illegible]: suitable for pol. electron acceleration

- Circularly polarized photons
  produced by bremsstrahlung of longitudinally polarized electrons

  polarized electrons
  $Pe \sim 70 - 80$ % (strained GaAs source), pol. reversal 2Hz

  electron beam energies; 525 and 855 MeV

  polarization measurement ⇒ Möller polarimeter(in tagging spectrometer)

- Tagging spectrometer(Glasgow, Mainz)
  352 ch hodoscope, $\delta E_\gamma \sim 2$ MeV
  tagging range: $50MeV \leq E_\gamma \leq 800MeV$

- Longitudinally polarized protons: frozen spin target(Bonn-Bochum-Nagoya)

  polarized butanol ($C_4H_9^\uparrow OH^\uparrow$), $\phi 20mm \times 19mm$

  $P_{max.} = 90$ % at 2.5 T(movable polarizing coil)

  data taking in frozen spin mode
  $\tau \sim 200$ hours at T ~50mK, B=0.4T(internal thin coil)

- detector system
  geometrical acceptance:

  DAPHNE ($159° \leq \Theta \leq 21°$) (Saclay, Pavia)

  MIDAS ($17° \leq \Theta \leq 7°$) (Pavia) , = micro-strip detector

  STAR-FFW ($\Theta \leq 5°$) (Tübingen, Mainz)

  Cherenkov ($e^\pm$ veto) (Gent)

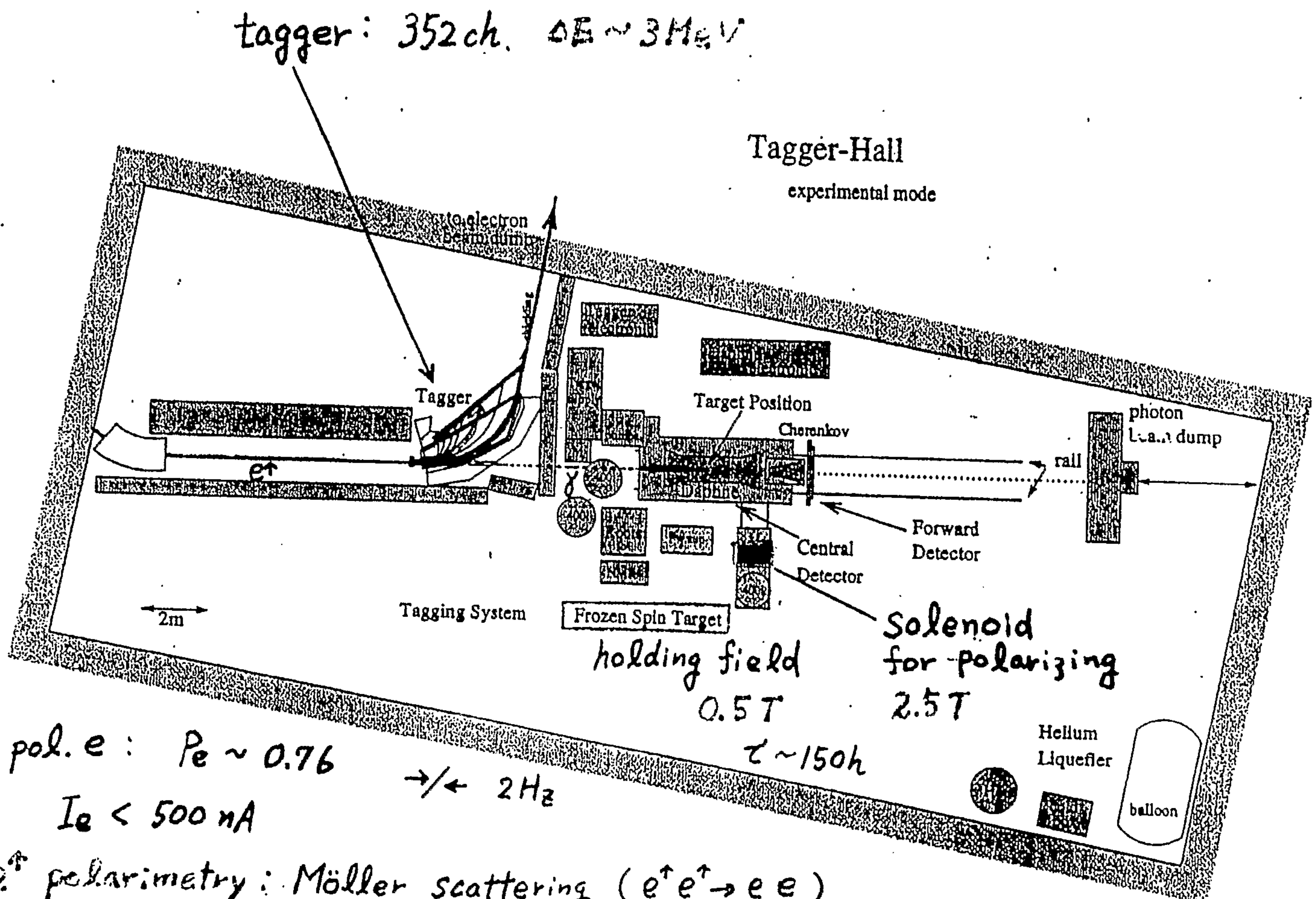

pol. e: $P_e \sim 0.76$

$I_e < 500$ nA

$e^\uparrow$ polarimetry: Möller scattering ($e^\uparrow e^\uparrow \to e e$)

$\gamma^\uparrow$ polarimetry: Compton Scattering ($\gamma^\uparrow e^\uparrow \to \gamma e$)

Figure 1:

Experimental Setup

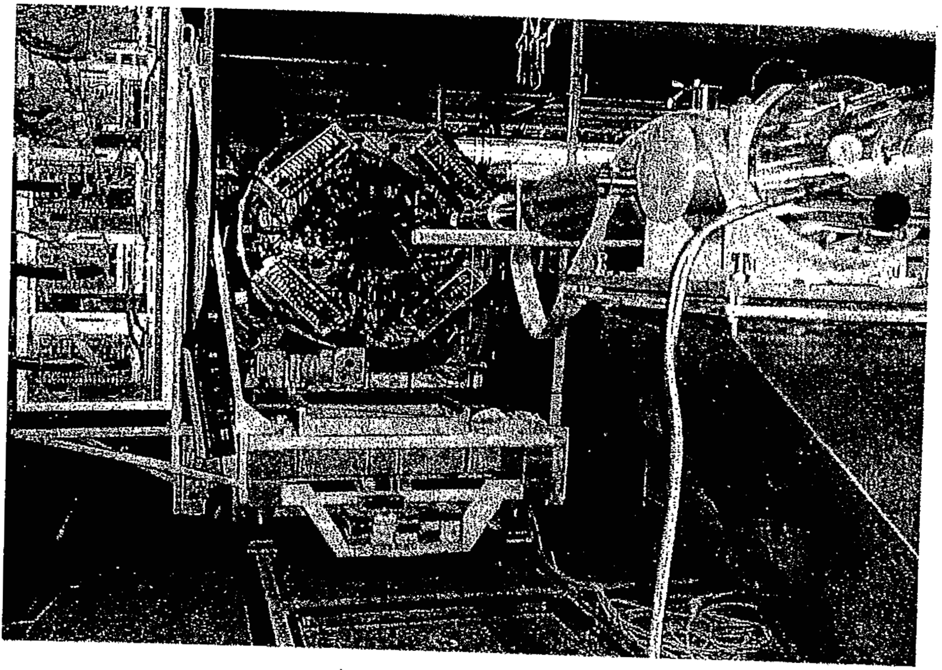

DAPHNE and Dilutioncryostat

Results

Inclusive $\vec{\gamma}\vec{p} \rightarrow hadrons$

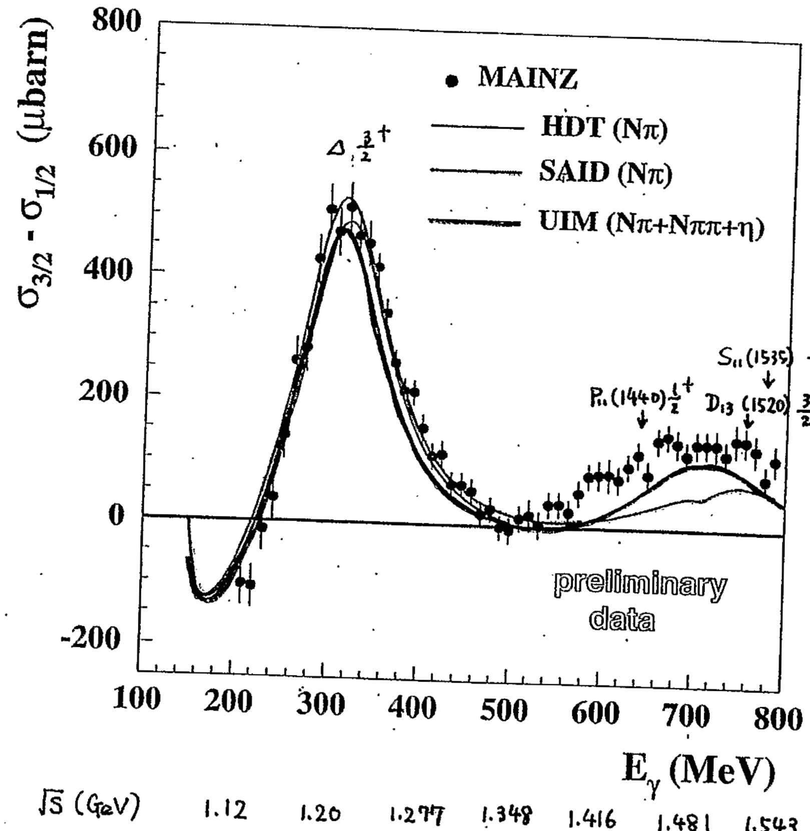

HDT: dispersion theory, Hanstein, Drechsel, Tiator, NPA 632 (99), 521

SAID: phenomenological multipole analysis, solution SM99k

UIM: unitary isobar model, Drechsel, Kamalov, Krein, Tiator, PRD 59 (99) 094021

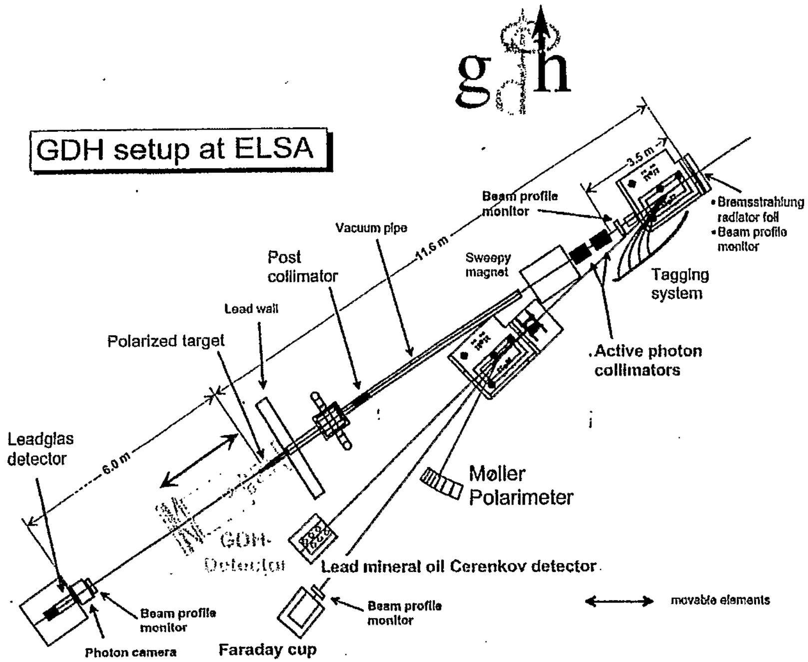

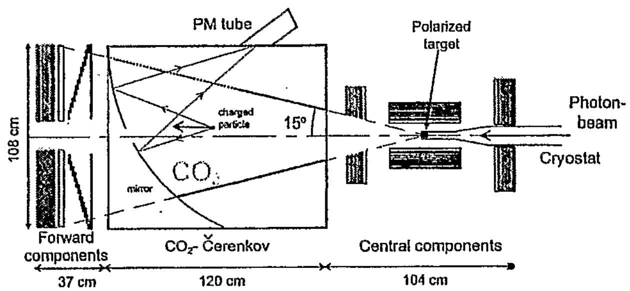

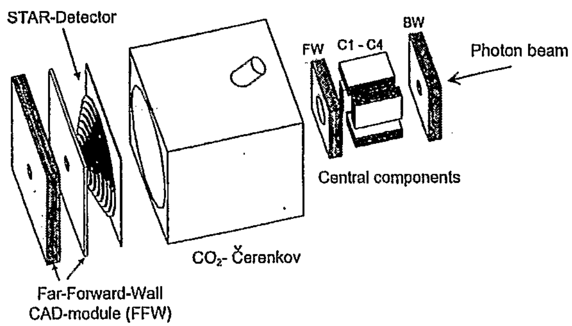

Johannes Gutenberg-Univ. Mainz
Rheinische Friedrich-Wilhelm-Univ. Bonn

Helicity-Dependent Total Cross-Section on the Proton

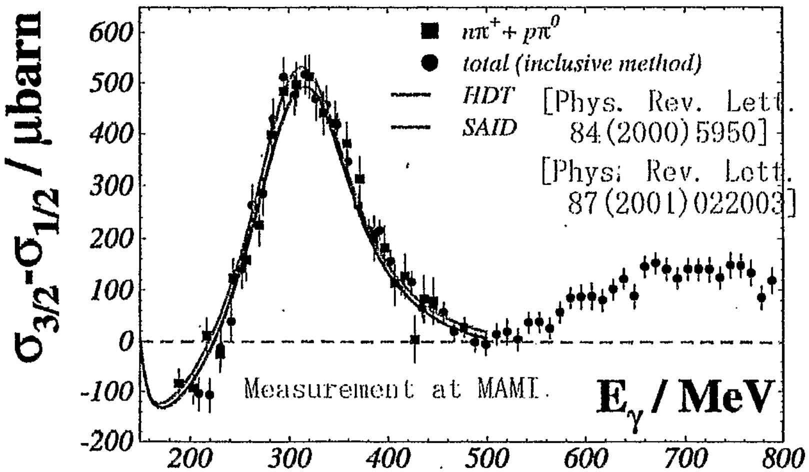

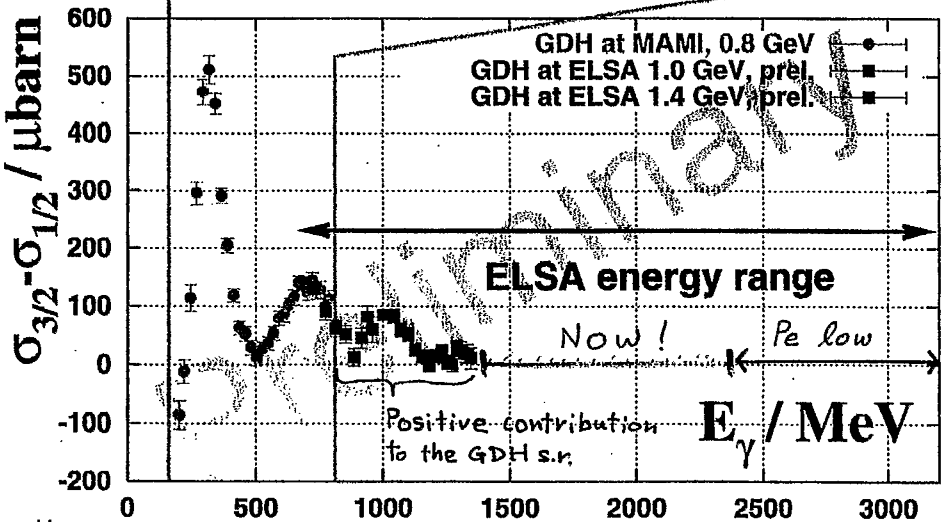

7.Nov.2001 EMI2001 Osaka

g h

The running GDH integral from 200 MeV to Bonn energy

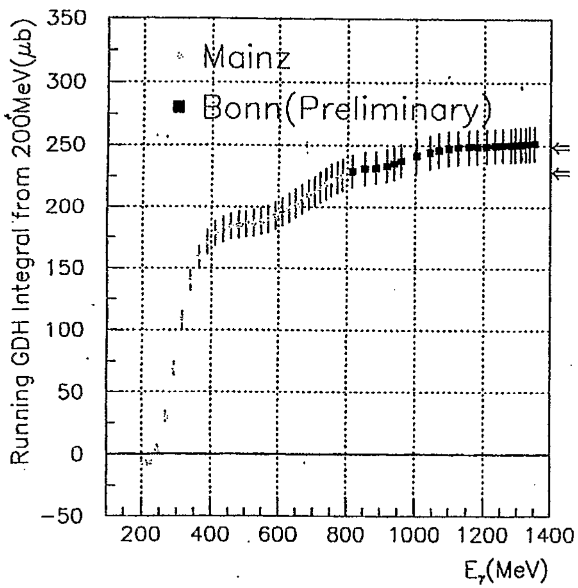

$$\int_{200MeV}^{1350MeV} (\sigma_{3/2} - \sigma_{1/2}) \frac{d\nu}{\nu}$$

at 1.35 GeV

c.f.
$I_{GDH} - I(\nu \leq 200MeV)$
$= 205\mu b - (-30\mu b) = 235\mu b$
Assuming no additional contribution in higher energy range

SPring8 ACCELERATOR COMPLEX

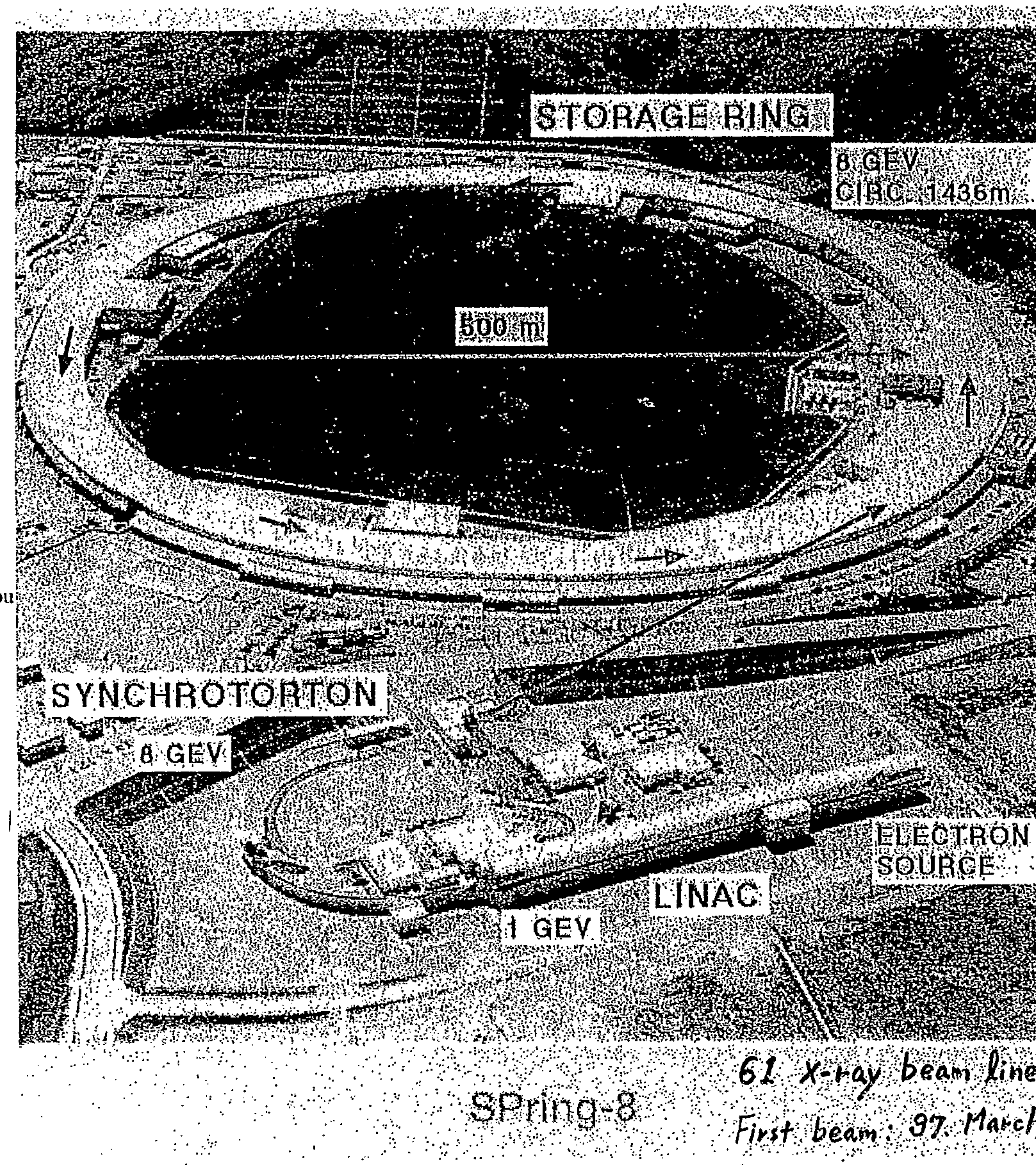

61 X-ray beam lines
First beam: 97. March
Commission: 97. Sept.

GDH Experiment at SPring-8

- Proposed experiment to study the GDH sum rule at SPring-8
  energy range: $1.8GeV \leq E_\gamma \leq 2.8GeV$
- Laser Electron Photon(LEP) beam line at SPring-8

  circularly polarized photons by laser backward Compton scattering
  polarization; $P = 100\%$ at $E_{\gamma,max}$
  $E_{\gamma,max}$=2.4 GeV ($\lambda = 350nm$) with $I_\gamma \sim 10^6\gamma/s$
  $E_{\gamma,max}$=2.8 GeV ($\lambda = 275nm$) with $I_\gamma \sim 10^5\gamma/s$
  tagging range: $E_\gamma \geq 1.5GeV$

  small divergence : $\sigma_\theta \sim 100\mu rad$
  beam profile: $\sigma_x = 3mm$, $\sigma_y = 1.5mm$ without collimators
  low background
- Proposed experiment

  measurements of $(\sigma_{3/2} - \sigma_{1/2})$ on proton
  phase 1 : $1.8GeV \leq E_\gamma \leq 2.4GeV$, $< P_\gamma >= 85\%$
  phase 2 : $2.3GeV \leq E_\gamma \leq 2.8GeV$, $< P_\gamma >= 80\%$

  polarized target with polyethylene($-CH_2^\dagger-$)
  polarizing continuously by microwave(no frozen spin mode)
  superconducting solenoid magnet with a large bore(ϕ60cm)
  reuse of KEK dilution refrigerator

  detector system
  geometrical acceptance: $0.97 \times 4\pi$
  sensitive to charged particles and photons
  e veto by a gas Cherenkov counter
  central detectors in the bore of the PT magnet(2.5T)

  status
  collaboration
  Nagoya, Miyazaki, UCLA, KEK, RMIT, Bonn, Florida Int., (Melbourne)
  proposal submitted to PAC (July 2001) —— Accepted !
  R & D for detectors in progress (central detectors)
  some parts of PT system completed (NMR for pol. measurement)

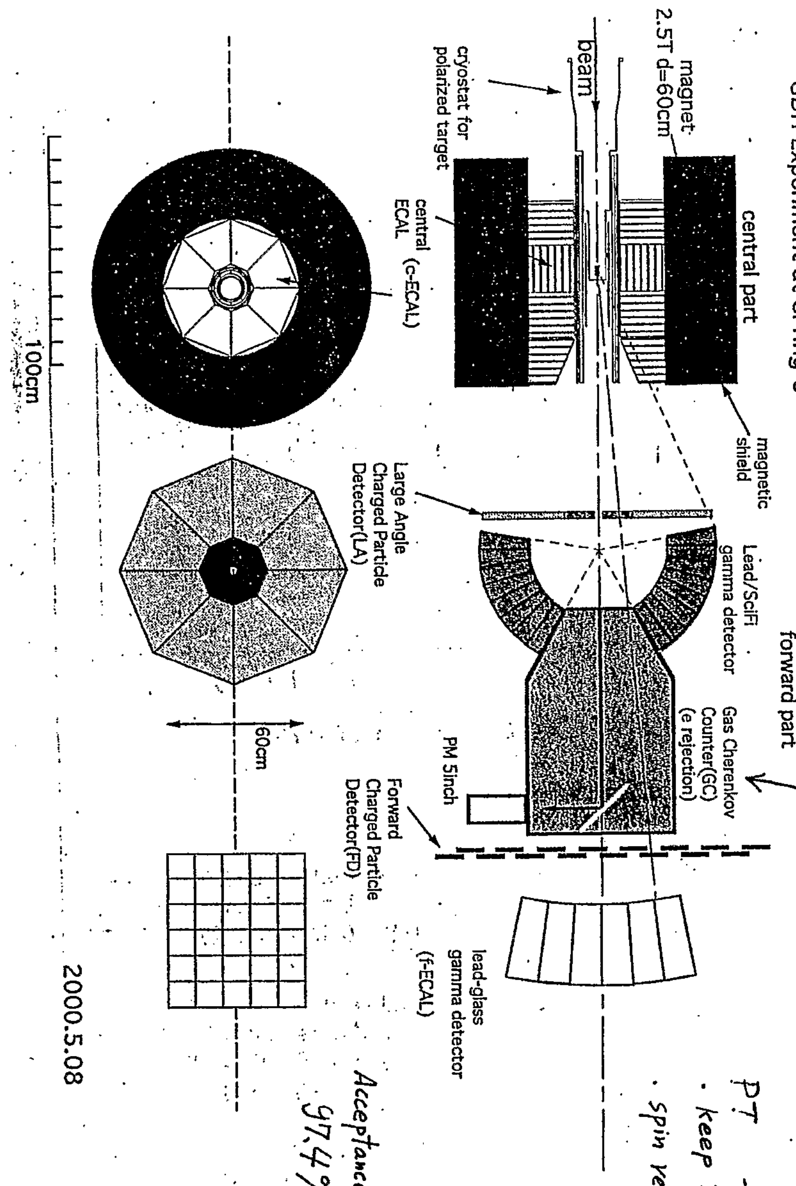

shower suppressed × 10^{-4}
eff. > 99% for 1 track

PT - no removal of magne
· keep DNP
· spin reversal by μ-wave

Yield Estimation

	1st phase		2nd phase	
energy range (GeV)	1.8-2.4		2.3-2.9	
laser wave length	351nm		266 nm	
laser power	1W		0.3W	
tagged photon intensity(full spectrum, /s)	2.5x10^6		5.7x10^5	
tagged photon energy(GeV)	1.8-2.1	2.1-2.4	2.3-2.6	2.6-2.9
tagged photon intensity(/s/100MeV)	1x10^5	1.3x10^5	2.1x10^4	2.3x10^4
tagged photon polarization	70%	90%	80%	95%
hadronic rate (full spectrum/s)	850		180	
hadronic rate (/s/100MeV)	34	42	6.8	7.8
e+ e- pair rate(full spectrum, /s)	1.5x10^5		3.6x10^4	
triggered e+ e- rate(/s/100MeV)	6	7.5	1.2	1.5

$\times 10^{-3}$
by Č
↓
$\varepsilon = 99.9\%$

beam condition:

electron beam current: 100mA

length of the interaction region: 4m

laser spot size: phi=1mm

target condition:

CH2,L=4cm

Nt=2.4x10^24 nucleons/cm^2

laser:

1st phase : Ar laser (UV)

2nd phase : diode pumped Nd:YVO4 + SHG

GDH@Jlab

Real photons

Virtual photons

E91-023

Measurement of Polarized Structure Functions in Inelastic Electron Proton Scattering using CLAS

E93-009

The polarized Structure Function G_1 and the Q^2-dependence of the Gerasimov-Drell-Hearn Sum Rule for the Neutron

The GDH Sum Rule and the Spin Structure of He and the Neutron Using Nearly Real Photons

HALL A

HALL B

Polarized e⁻: Strained GaAs source, P = 75%

Jlab microtron E < 6.0 GeV

HALL A:

E = 1.6 - 4 GeV
I_e = 1 - 15 μA
Q^2 = 0.01 - 1 $(GeV/c)^2$

Moeller polarimeter

SLAC type
high pressure polarized ^3He gas target
10 atm., P_{max}=40% at B = 20 G

Electron detection in 2 single arms
High Resolution Electron Spectrometer
High Resolution Hadron Spectrometer
scattering angles: 6, 15, 25, 35°

HALL B:

E = 0.8 - 4.0 GeV
I_e = 1 - 5 nA
Q^2 = 0.15 - 2 $(GeV/c)^2$

Jlab-Univ. of Virginia polarized target
NH_3/ND_3, P = 60/40%
@ B = 5T, T = 1K

CLAS detector
γ, n and charged particle detection
$8^0 < \vartheta < 140^0$, 0.1 < p < 4 GeV/c
$\Delta p/p < 1\%$, $\Delta\vartheta = 1^0$

Moeller polarimeter

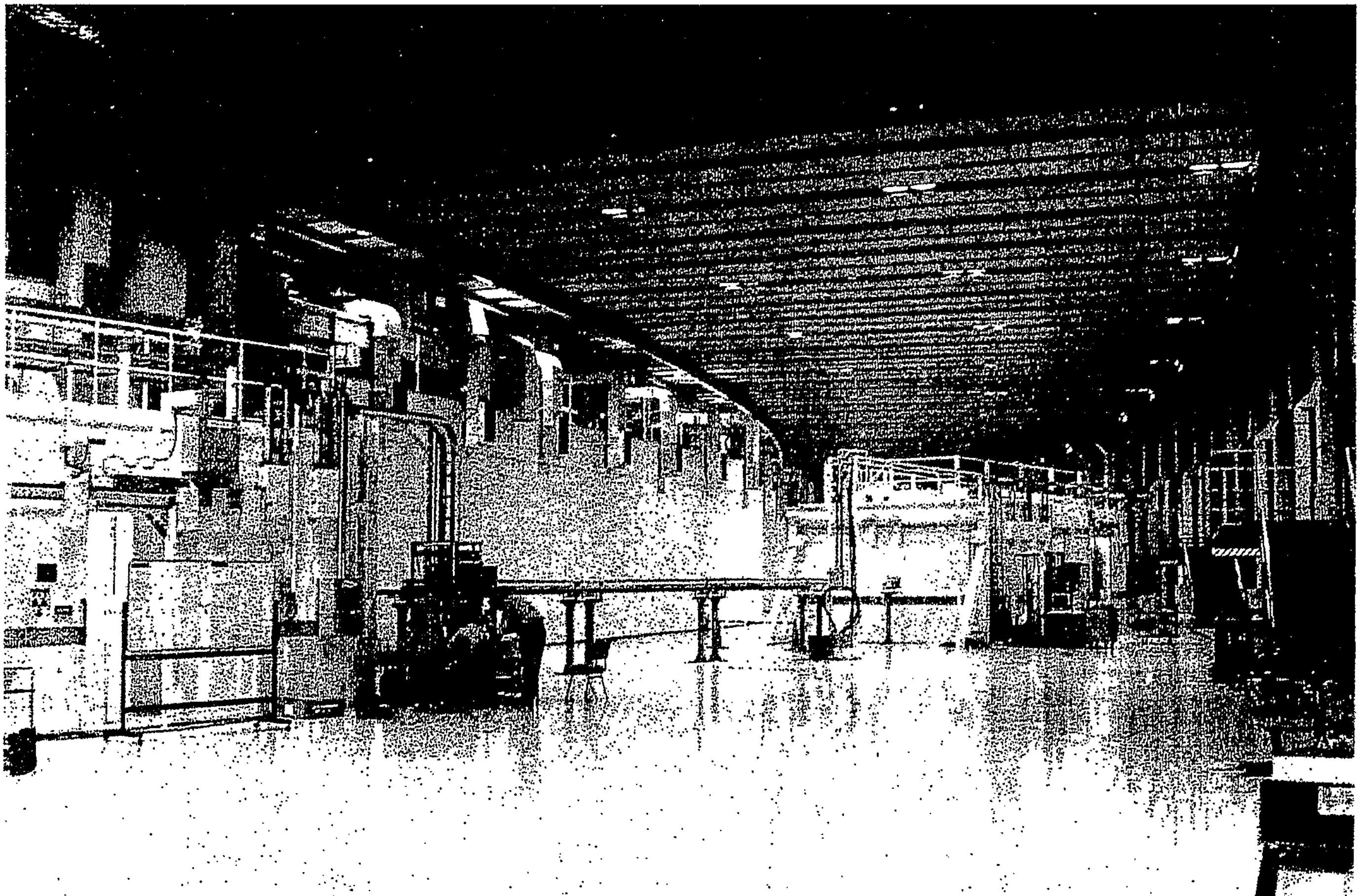

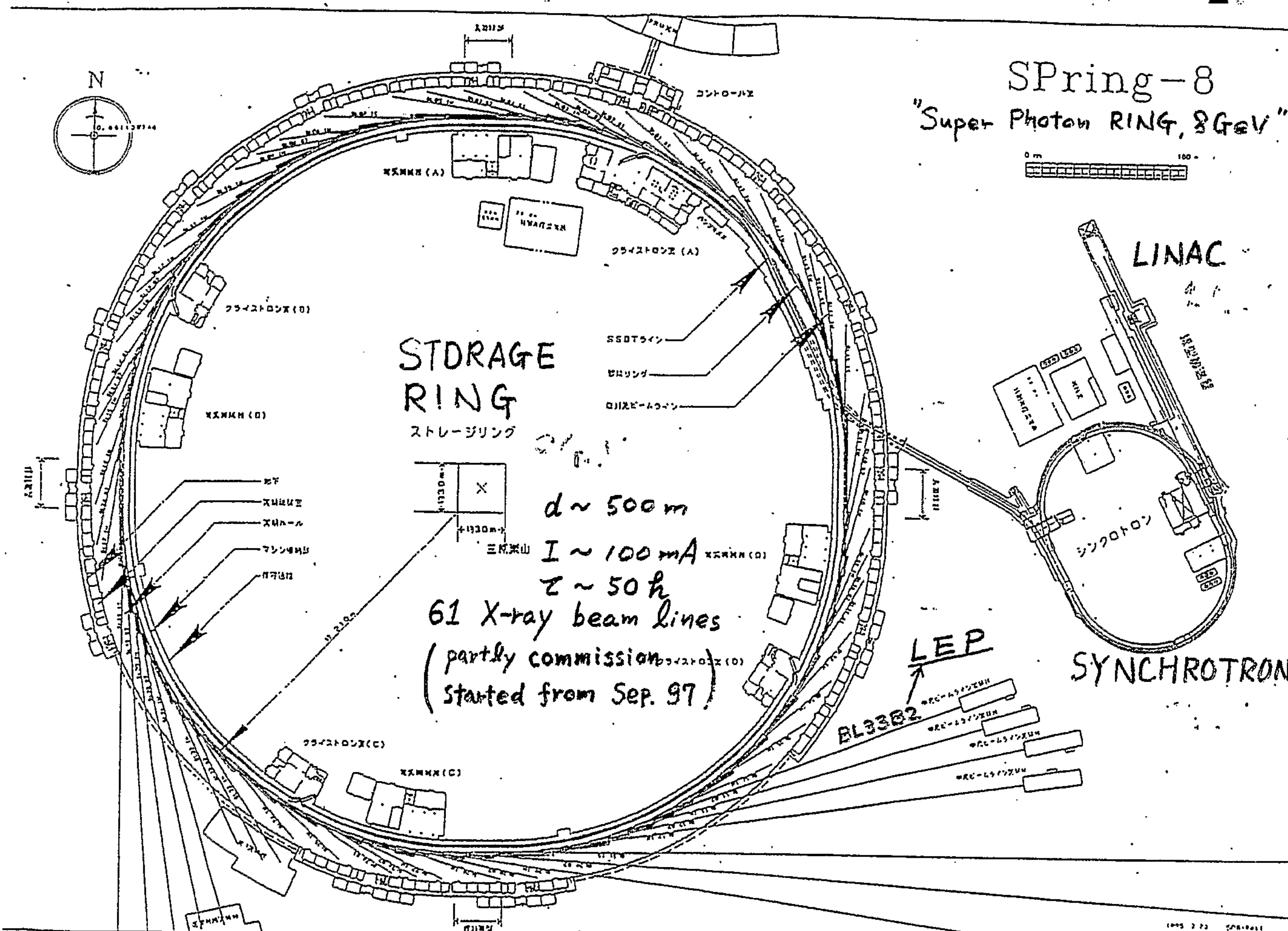

N
SPring-8
"Super Photon RING, 8GeV"
LINAC
STORAGE
RING
ストレージリング
d ~ 500 m
I ~ 100 mA
τ ~ 50 h
61 X-ray beam lines
(partly commission started from Sep. 97)
LEP
BL33B2
SYNCHROTRON
シンクロトロン

Summary

1. COMPASS Experiment

* Muon Program has started.

*All necessry equipments have been installed in the hall (in Sep. 2001). Some of those were not 100% (still missing).

*Muon beam(I=$2x10^8$ppp) has been realized and polarized target with ^{6}LiD achieved the highest polarization +58% and -48%.

*Physics data-taking for 7, Oct. - 23, Oct. has obtained $1.6x10^9$ events. Data analysis is going on.

2. GDH-Sum Rule

*The importance of the GDH sum rule test has been recognized in connection with structure function $g_1(x)$.

*The helicity dependent cross sections have been measured at Mainz and Bonn. The running GDH-sum(preliminary) gives a little bit larger than that estimated.

*The experiment at SPring-8 has been accepted. I t will cover the energy region 1.5 -2.9GeV.
Hopefully, the measurement will be performed in 2004.

Laser Electron Photon Experiments at SPring-8

Tomoaki Hotta[1] — *RCNP, Osaka University*

RIKEN School, Wako/Japan, Mar. 29-31, 2002

Abstract

This lecture describes the status and prospects of the Laser Electron Photon experiments at SPring-8 (LEPS). SPring-8 is the highest-energy third-generation synchrotron radiation facility, located in Hyogo, Japan. The LEPS beamline was constructed for studying non-perturbative nature of QCD in a few GeV energy region. The beamline produces the maximum energy 2.4 GeV polarized photon beam by means of Compton backscattering of laser light off the electron beam circulating in the ring. The first data was taken with a linearly polarized beam from December 2001 and the analysis is underway. An overview of the LEPS experiments is given and related physics topics are discussed. Photoproduction of ϕ can be a good tool to study gluon-exchange interaction at low energies because the process is well described as a Pomeron-exchange at high energies and meson-exchange is suppressed by the OZI rule. In order to study contributions from meson-exchange, glueball-exchange, and $s\bar{s}$ knock-out, precise measurements of the cross section and the decay asymmetry have been carried out. N* physics is another major subject in the LEPS experiments. Recent measurements for K^+ photoproduction at SAPHIR and GRAAL and theoretical works suggested the contribution of a "missing" nucleon resonance at 1.9 GeV to the process. The LEPS measurement covers the energy region just above the GRAAL. Photoproduction of ω at large angles also has been measured to study contributions from "missing resonance" coupling weakly to πN but strongly to ωN channel. For studying the nature of $\Lambda(1405)$, $\pi^+\Sigma^-$ and $\pi^-\Sigma^+$ decay modes are analyzed. Significant difference of the resonance shape for these decay channels is predicted by a theoretical model describing the $\Lambda(1405)$ as a meson-baryon resonance state. A time projection chamber has been constructed for the further study. For the reactions with multi-γ final states, such as $\sigma \to \pi^0\pi^0$, a γ detector array which covers the sideward and backward directions was constructed and tested.

[1] hotta@rcnp.osaka-u.ac.jp

RIKEN-QCD-School, March 2002

Laser Electron Photon Experiments at SPring-8

T. Hotta (RCNP, Osaka University)

- **Laser Electron Photon Beam at SPring-8**
- **Overview of the LEPS Experiments**
- **Physics Topics and the Recent Status**

SPring-8 (Super Photon ring-8 GeV)

- Third-generation synchrotron radiation facility
- Circumference: 1436 m
- Electron Energy: 8 GeV
- Max. beam current: 100 mA
- 62 Beamlines

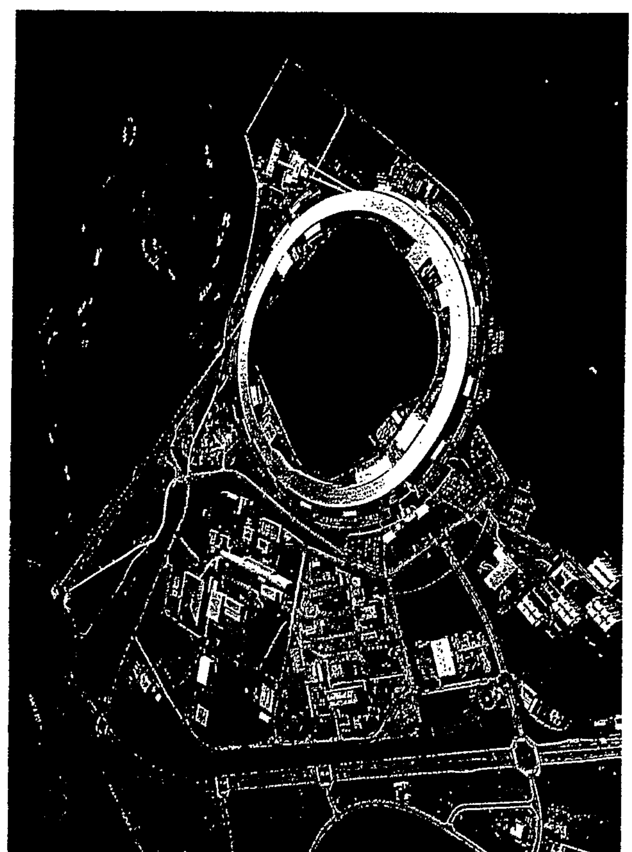

SPring-8 (Super Photon ring-8 GeV)

- Third-generation synchrotron radiation facility
- Circumference: 1436 m
- Electron Energy: 8 GeV
- Max. beam current: 100 mA
- 62 Beamlines

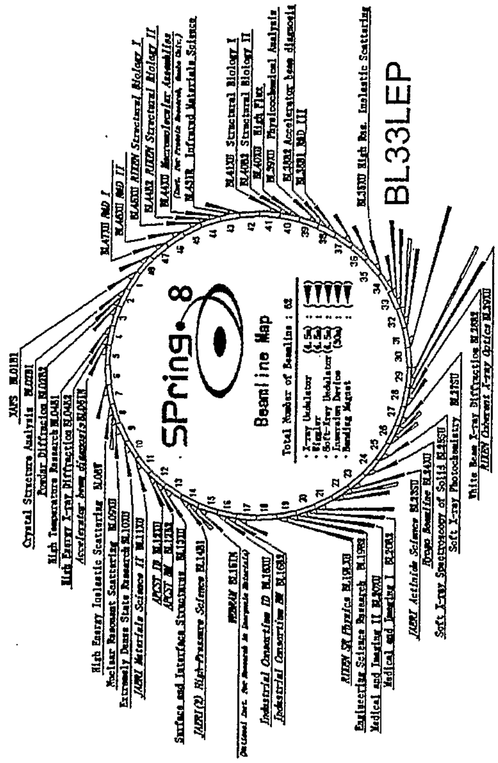

Laser Electron Photon at SPring-8

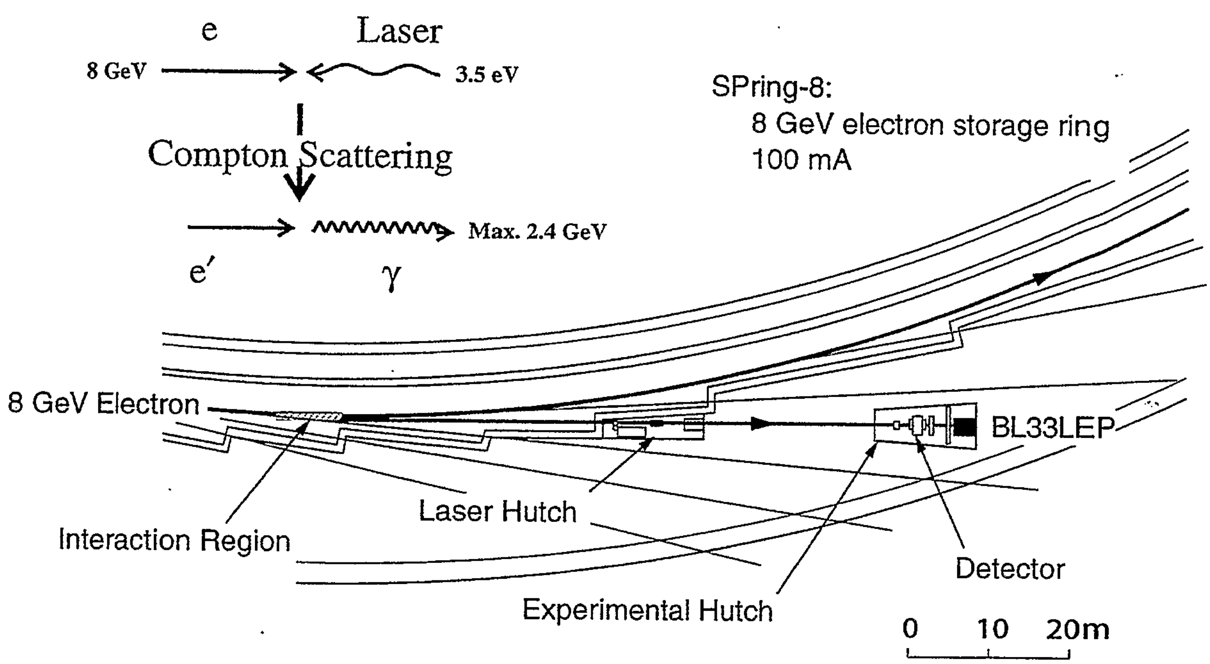

Energy Spectrum of the LEPS beam

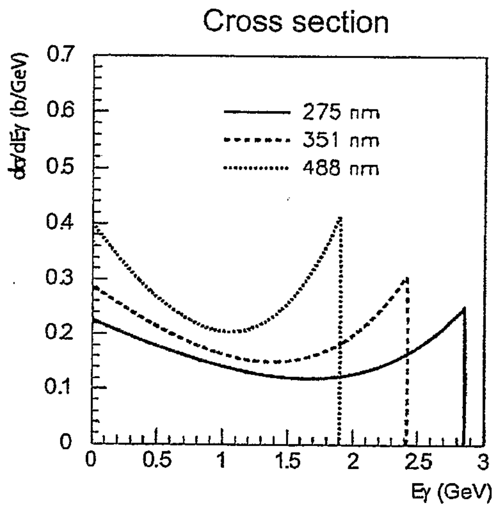

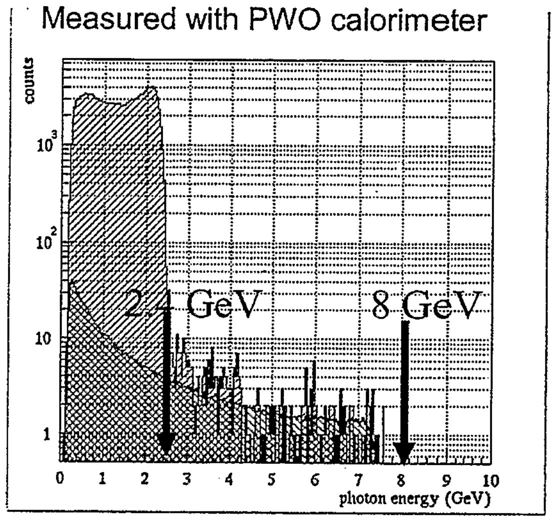

Intensity (Typ.): 2.5×10^{6} cps

Polarization of LEP Beam

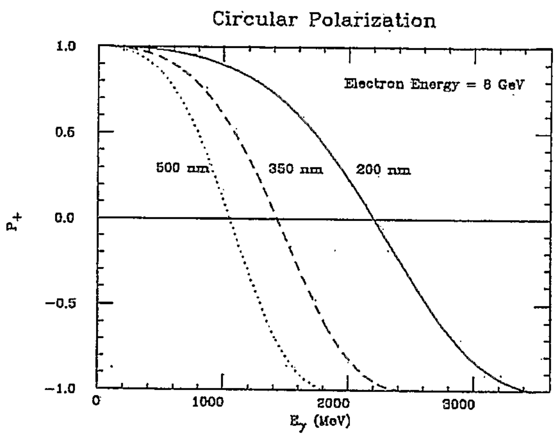

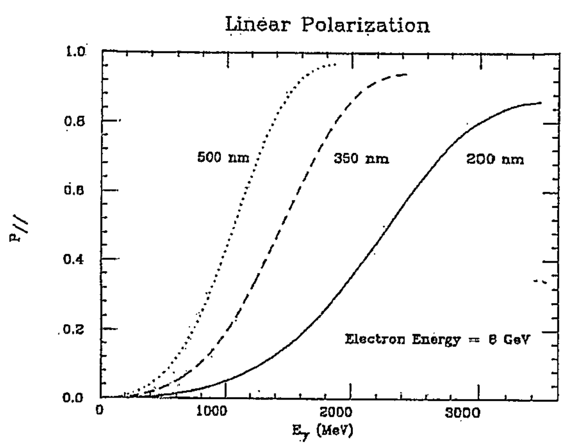

Linear Polarization : 95 % at 2.4 GeV

Photon Energy Tagging

$$E_\gamma = E_e + E_{laser} - E_{e'}$$

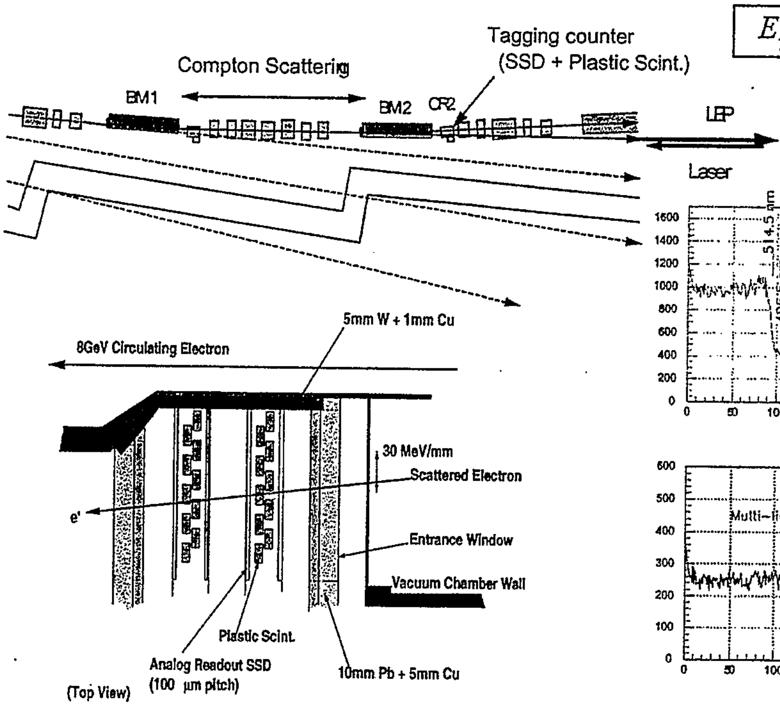

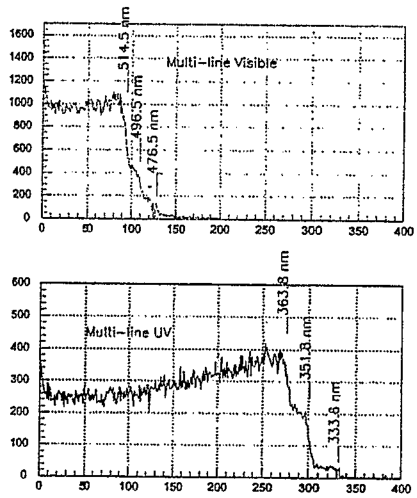

·Tagging Region : 1.5 GeV< E_γ < 2.4 GeV

Vector Meson Photoproduction

Vector Meson Dominance

γ fluctuates into quark-antiquark, interacting as hadron

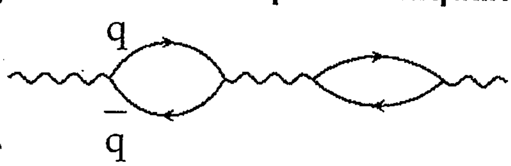

$q\bar{q} = \rho,\ \omega, \phi$ ...

Meson Exchange

Dominant at low energies

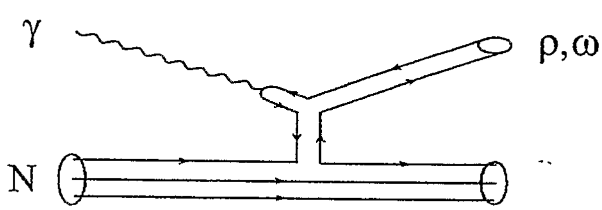

Pomeron Exchange

Small energy dependence

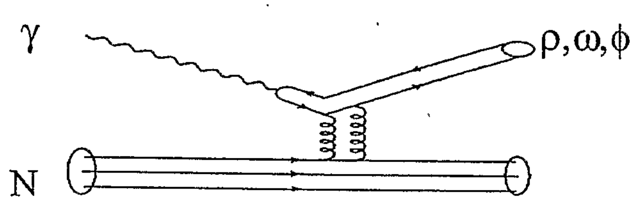

Cross section of Vector Meson Photoproduction

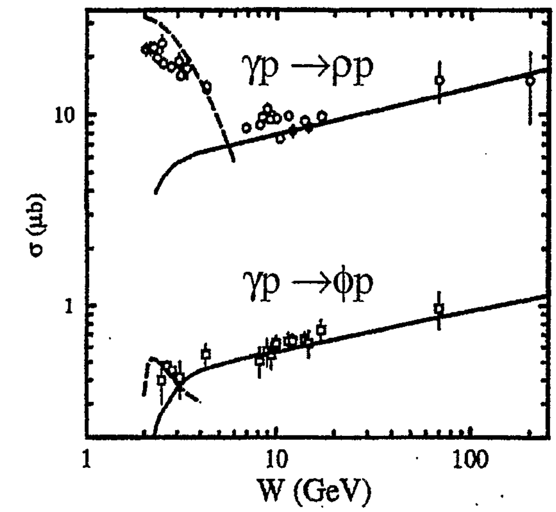

FIG. 15. Energy dependence of ρ- (top) and ϕ-meson (bottom) photoproduction cross sections. The solid curves are the predictions from our quark-nucleon Pomeron-exchange interaction. The dashed curves are the predictions of the meson-exchange model discussed in the text. The ρ-meson data (triangles) are from Refs. [35,36,44–47]. The ϕ-meson data (squares) are from Refs. [41,44,46,48].

M.A. Pichowsky and T.–S. H. Lee
PRD 56, 1644 (1997)

—— Prediction from Pomeron exchange

- - - Prediction from meson exchange

Data from: LAMP2('83), DESY('76), SLAC('73), CERN('82), FNAL('79,'82), ZEUS('95,'96)

ϕ photoproduction mechanism

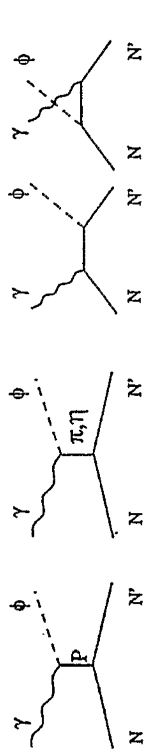

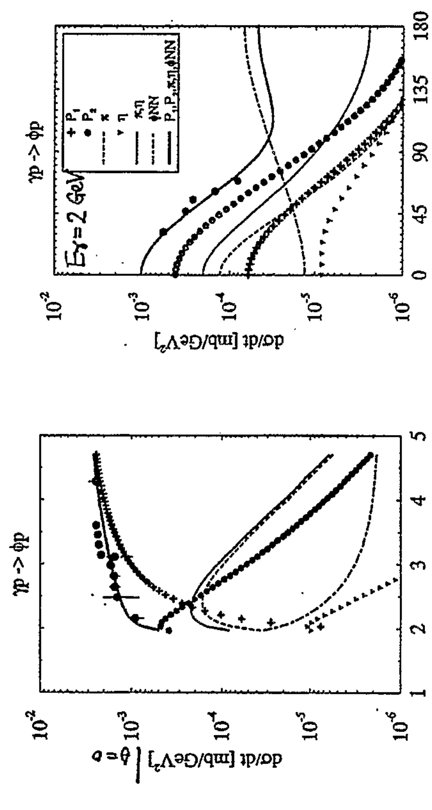

Titov, Lee and Toki, PRC 59,2993(1999)

(Data from: DESY('78), SLAC('73), Bonn('73))

○ P_2 : 2nd Pomeron ~ 0^+ glueball
(Nakano, Toki, EXPAF97 Proc.)

LEPS detector

Large acceptance in the forward directions

$\gamma p \to \phi p$
$\hookrightarrow K^+K^-$

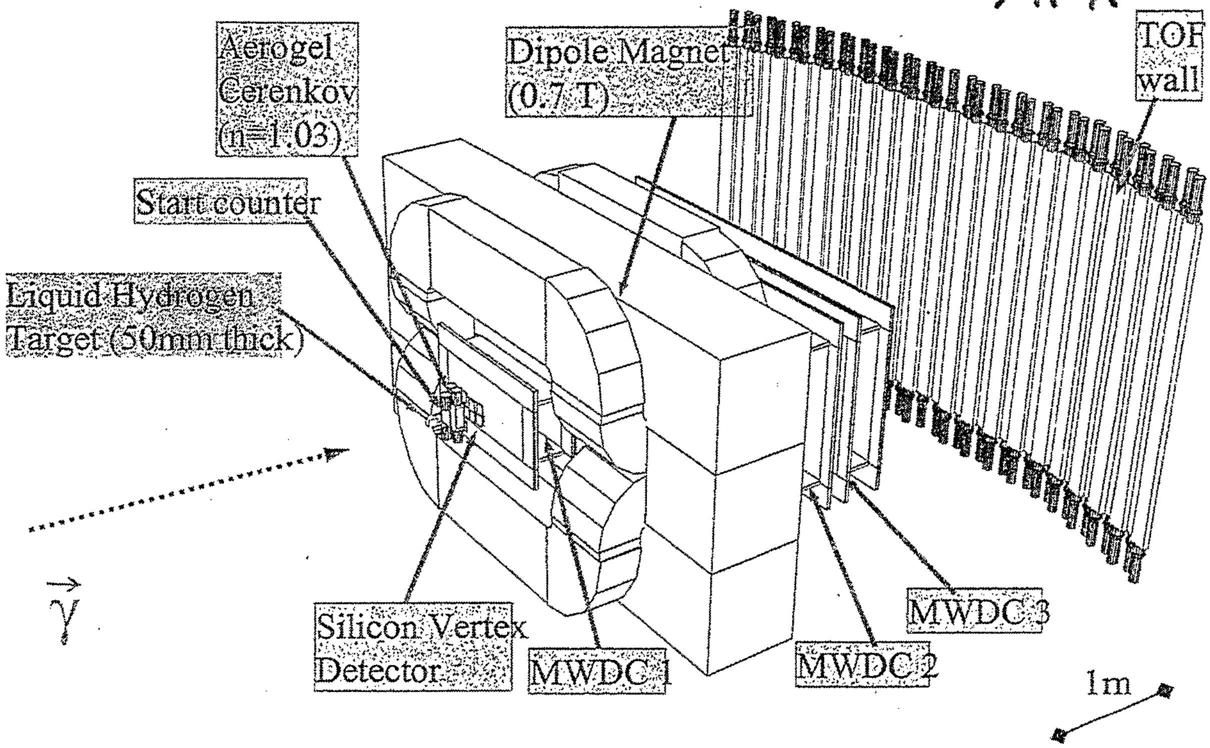

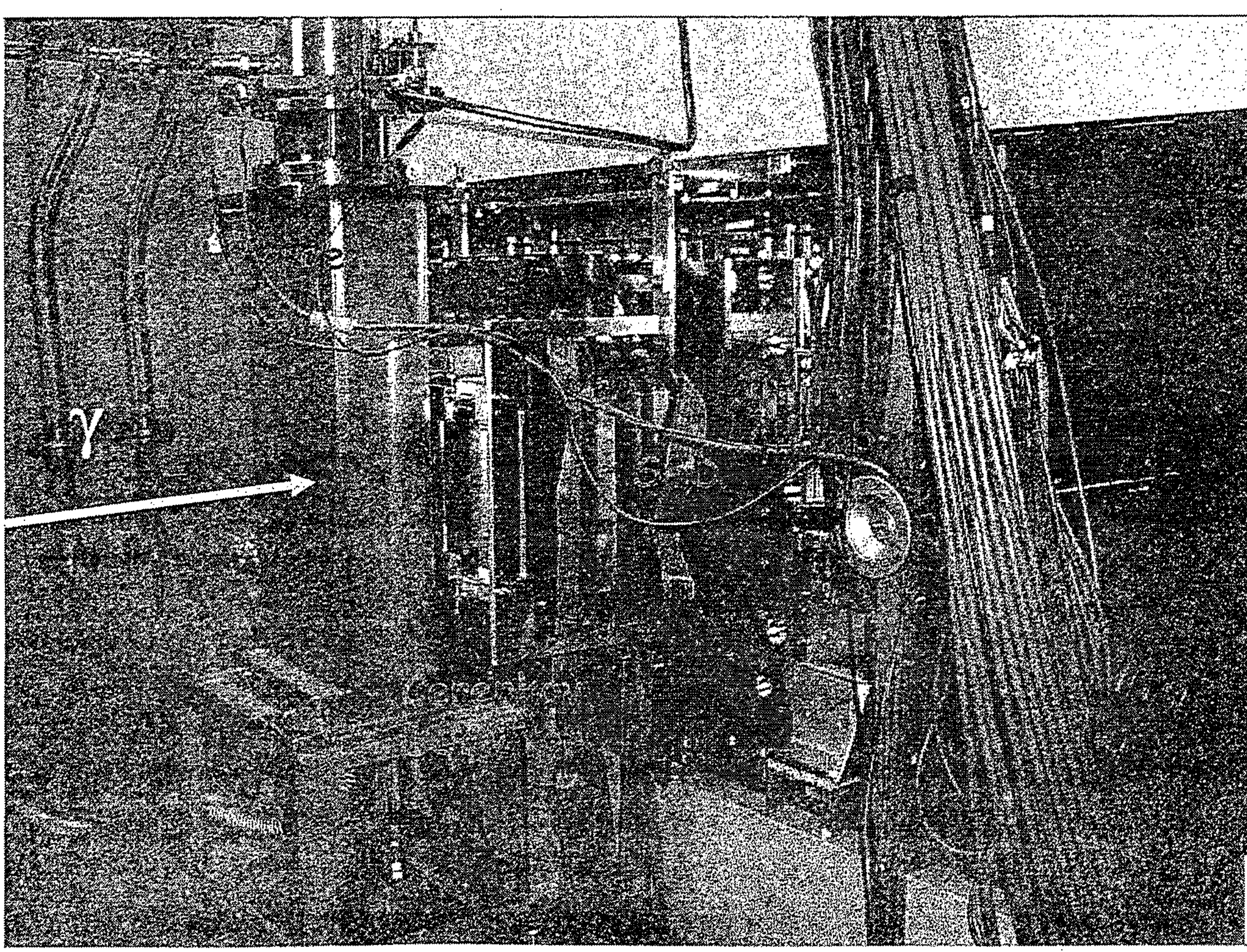

Trigger

- Photon requirement
  - Tagger hit
  - No signal in charge veto

about 30 Hz for 800 kHz at tagger

- Charged particle production
  - Start counter
  - TOF hit

- $e^+ e^-$ veto
  - AC (n = 1.03)
    - $p_\pi < 0.6$ GeV/c

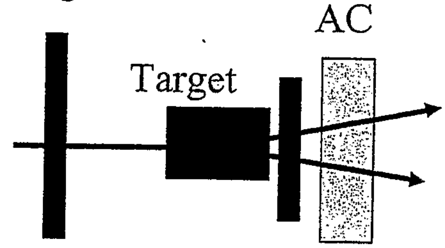

Particle Identification

Velocity vs momentum

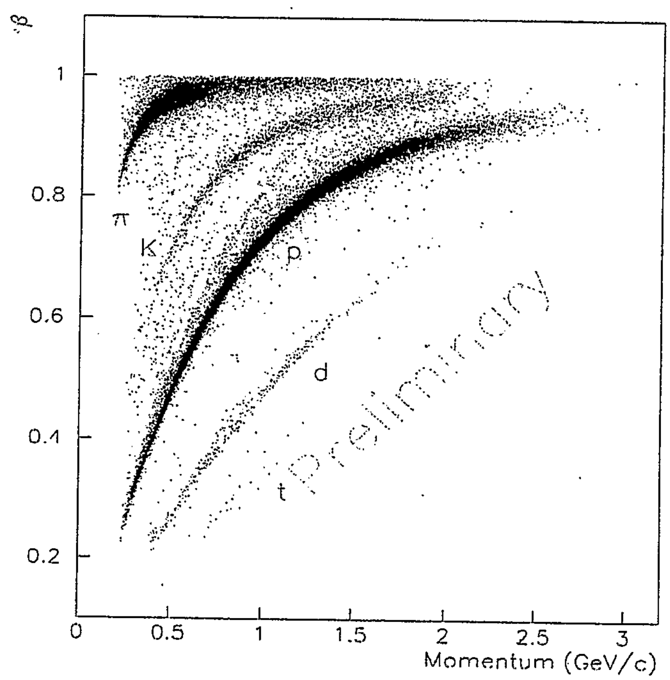

Reconstructed mass spectrum

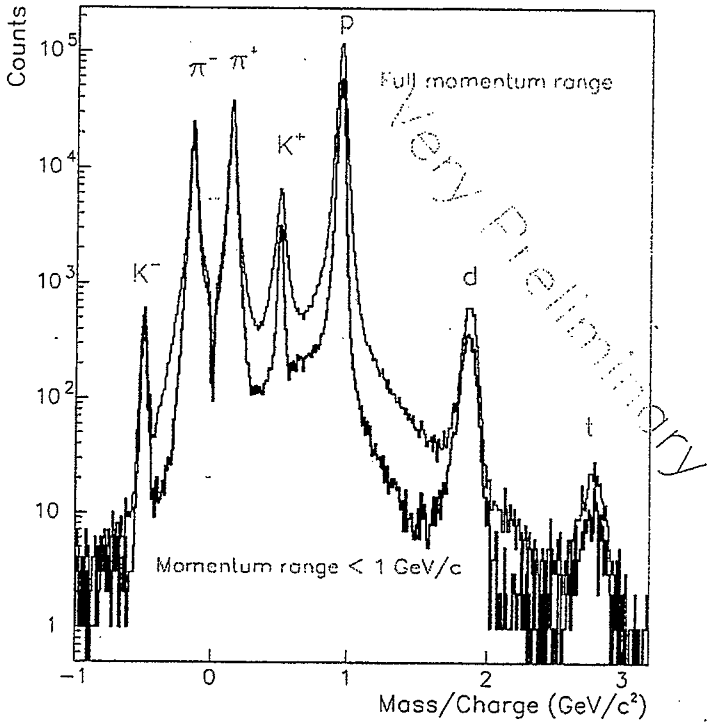

Physics Programs

- July 1999, First Laser Electron Photon Beam at SPring-8
- March 2000, Detector construction completed
- December 2000, Physics runs with Liq. H_2 target

- **Photoproduction of ϕ meson near threshold.**
  - Forward angles
  - Proton target, Nuclear target
- **Photoproduction of K**
- **Photoproduction of ω**
- **Photoproduction of $\Lambda(1405)$**

ϕ photoproduction near production threshold

Titov, Lee, Toki Phys.Rev C59(1999) 2993

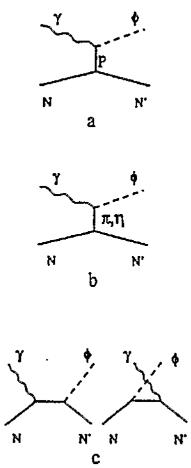

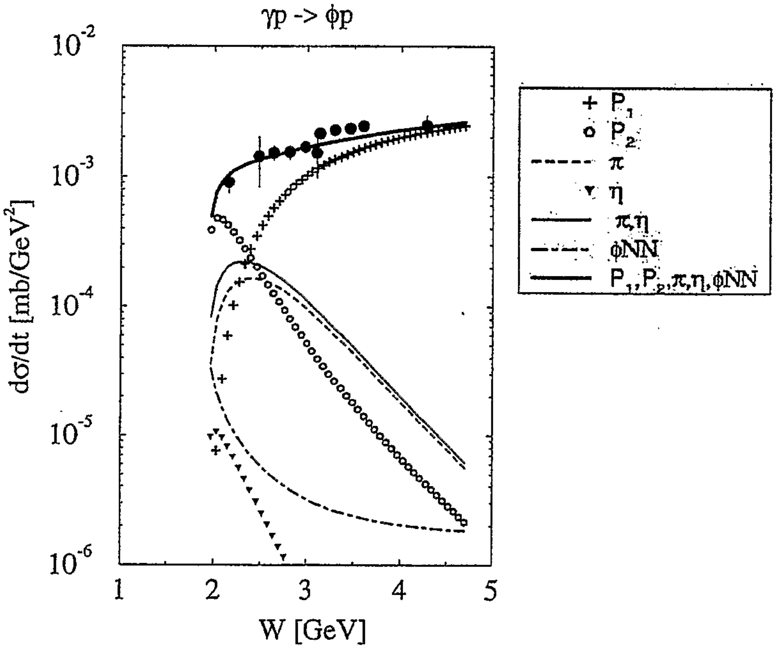

P2 : 2nd pomeron ~ 0^+ glueball (Nakano, Toki (1998))

Photoproducion by linearly polarized photon

In ϕ rest frame (Helicity frame)

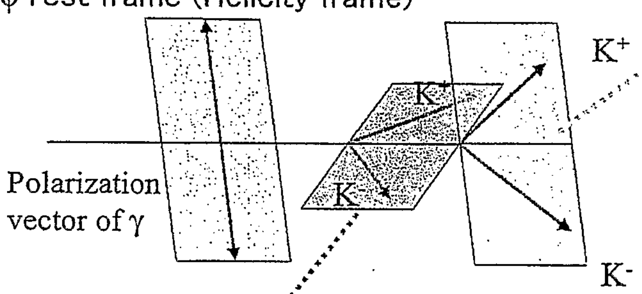

Decay Plane // $\vec{\gamma}$

if natural parity exchange

$(-1)^J$

(Pomeron, Scaler mesons)

Decay Plane $\perp$ $\vec{\gamma}$

if unnatural parity exchange

$-(-1)^J$ (Pseudoscaler mesons)

Decay Angular distribution of ϕ

↓

Decomposition of

- natural parity exchange
- unnatural parity exchange

At high energies...

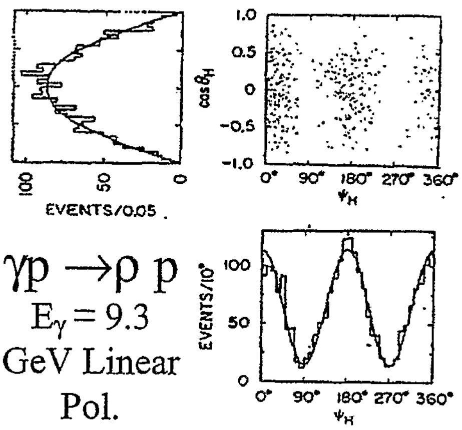

$\gamma p \rightarrow \rho\ p$
$E_\gamma = 9.3$ GeV Linear Pol.
Ballam et.al. PLD 7(1973) 3150

ρ tends to decay into direction of the photon polarizaion.

- Natural parity exchange dominate
- s−channel helicity is conserved.

What is the situation in $\gamma p \rightarrow \phi p$ near threshold ???

LEPS,Spring−8
CLAS,J.lab.

$\phi \rightarrow K^+K^-$ events

Reconstructed mass distributions from K^+K^- tracks

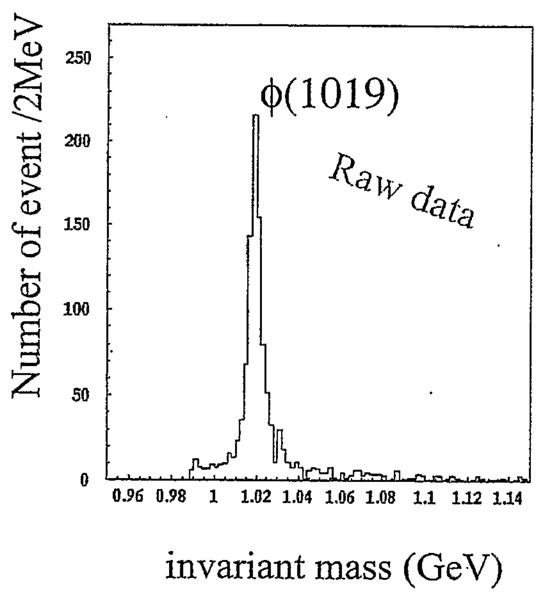

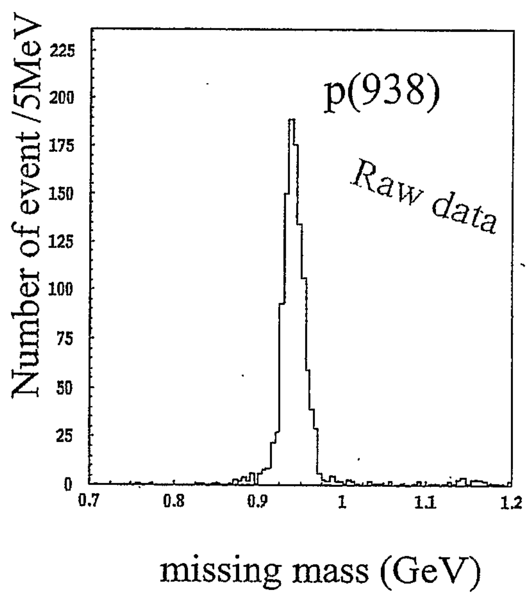

Decay angular distribution of K^+ in Helicity frame

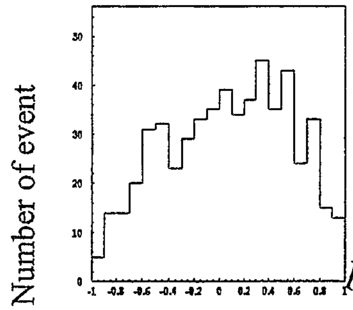

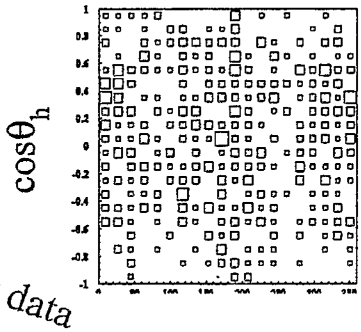

$\gamma p \to \phi p$

554 events (Vert +Hori)

$1.004 < M_\phi < 1.034$ GeV

0.88<Missing mass<1.00 GeV

$-0.2 < t < t_{min}$ GeV^2

w/o Acceptance Correction

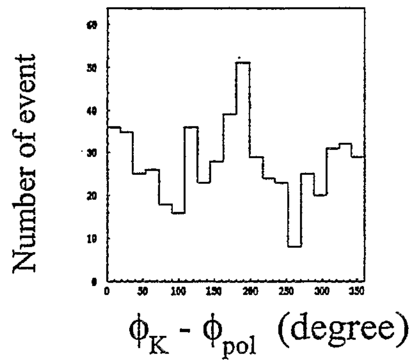

Physics programs

- **Photo-production of ϕ meson near threshold in the forward angles.**
  - **Pomeron (multi-gluon) exchange > meson exchange.**
  - **Search for additional multi-gluon (0^+ glueball) exchange.**
  - **Linearly polarized photons help to decompose natural and un-natural parity exchange contributions.**
  - **Complementary to the CLAS (Jlab) experiments.**

Strangeness Inside Nucleon

$$|p\rangle = A|uud\rangle + B|uud\,s\bar{s}\rangle$$

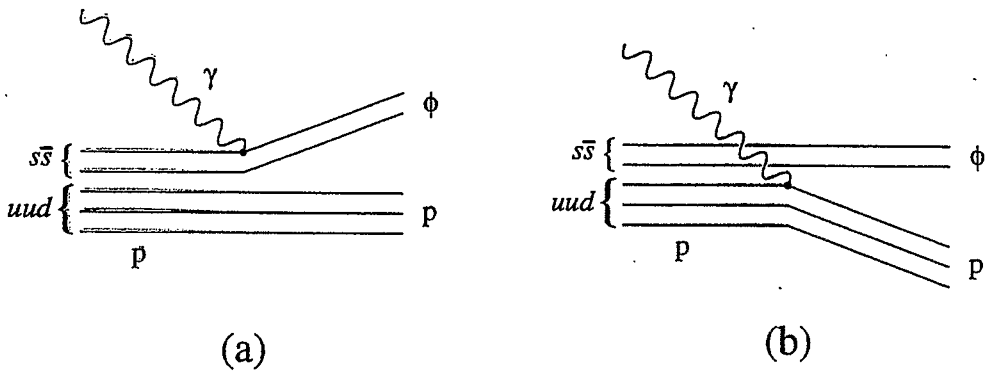

φ-knock out Process

Unpolarized cross section

A.I. Titov et al., PRL 79, 1634

$B^2 = 1\%$

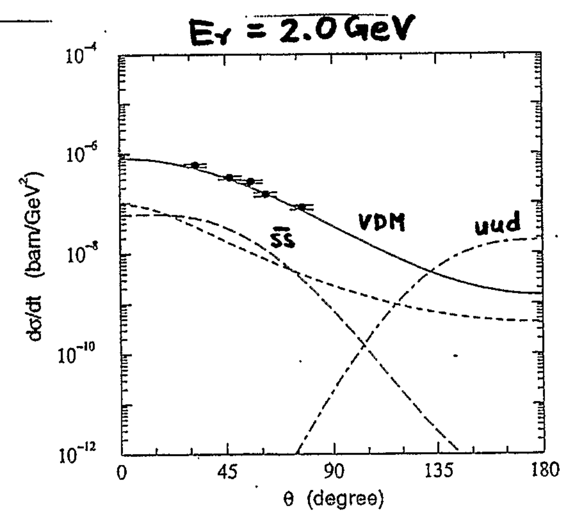

FIG. 8. The unpolarized photoproduction cross section $d\sigma/dt(\theta)$ at $W = 2.155$ GeV ($E_\gamma^L = 2.0$ GeV). The solid, dotted, dashed, and dot-dashed lines give the cross section of VDM, OPE, $s\bar{s}$-knockout, and uud-knockout, respectively, with strangeness admixture $B^2 = 1\%$ and $|b_0| = |b_1| = B^2/\sqrt{2}$. The experimental data are from Ref. [59].

Polarized Photon + Polarized Target

$$L_{BT} = \frac{\sigma_{T=+z}^{B=+z} - \sigma_{T=+z}^{B=-z}}{\sigma_{T=+z}^{B=+z} + \sigma_{T=+z}^{B=-z}}$$

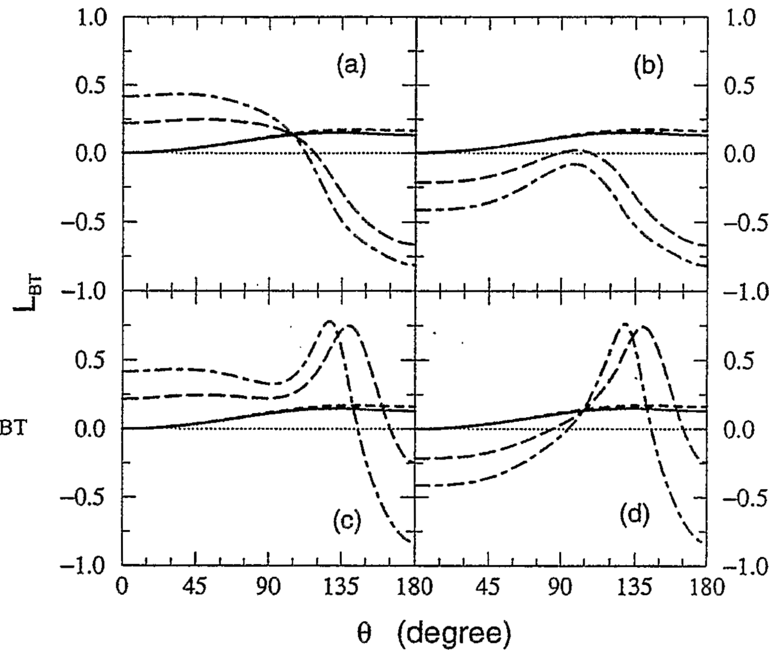

Double polarization variable L_{BT} is sensitive to the strangeness content in nucleons.

A.I.Titov et. al., PRL 79, 1634.

N* physics

- Properties of N*
  - Understanding of the quark structure of the matter
- Missing resonance problem
  - Nucleon resonances

    Constituent quark models >> Observed (in πN scattering)
    - Photoproduction
    - weakly couple to πN, but strongly to ωN or KΛ?

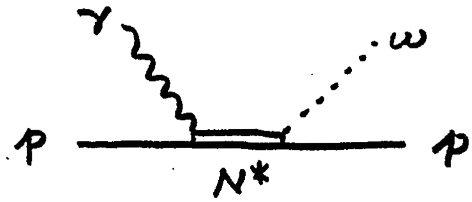

Kaon photoproduction

"missing resonance problem"

Bennhold *etal.*, nucl-th/0008024 , PRC 61 , 012201

(Data from: SAPHIR('98))

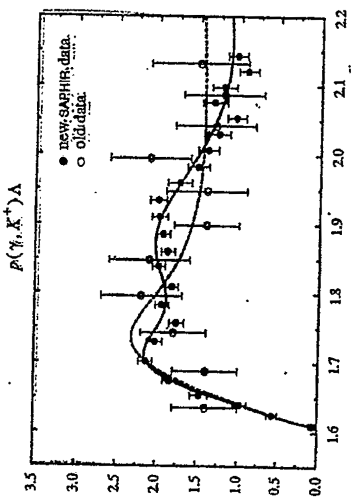

Structure around $W = 1.9$ GeV

— new $D_{13}(1960)$ resonance

Polarized photon asymmetry

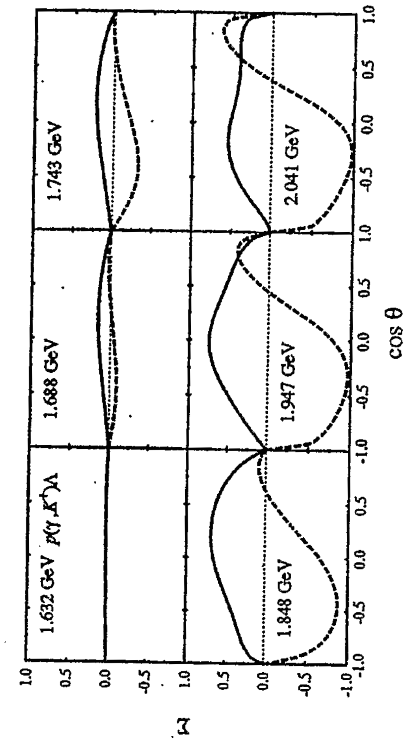

Measurement by GRAAL collaboration $E_\gamma < 1.5$ GeV

K⁺ Photo-production

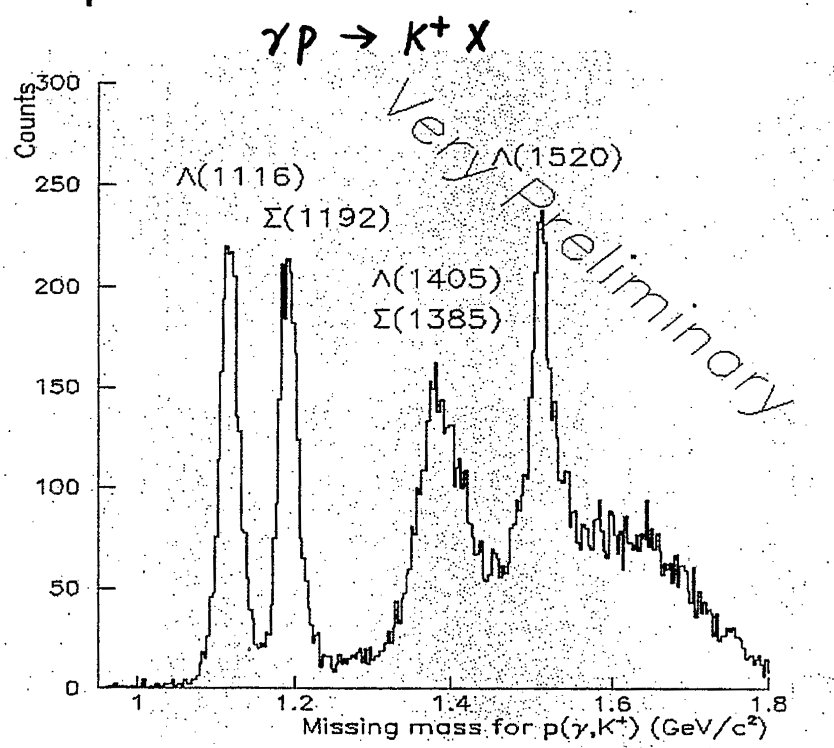

Photon-beam asymmetry

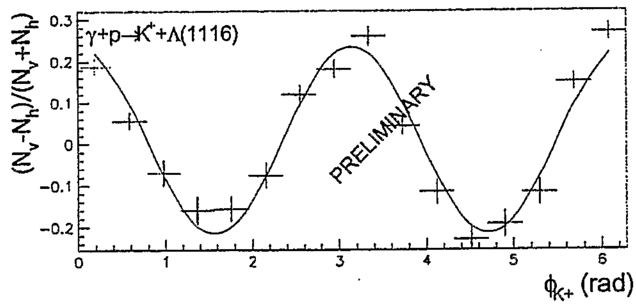

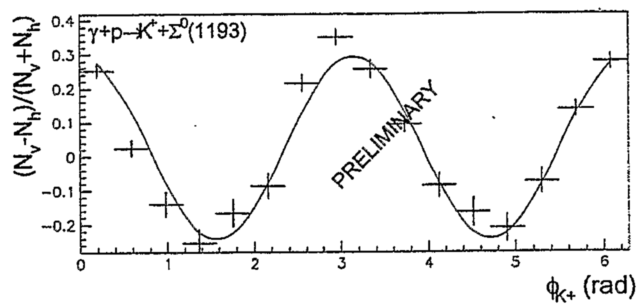

K^+ Photo-production with linearly polarized photons.

- Search for missing baryon resonances.
- SAPHIR and JLAB data indicate a structure in the $p(\gamma, K^+)\,\Lambda$ cross-section around W=1.9 GeV.
- Photon-beam asymmetry is sensitive to the existence of the baryon resonance.
- Complementary to the experiment at GRAAL.

Photo-production of ω meson in u-channel.

- Detect p in the forward angle and identify ω in the missing mass spectrum.
- Very sensitive to the $g_{\omega NN}$ coupling.
- Sensitive to the missing baryon resonances.
- Old data shows a structure around u=-0.2 GeV.

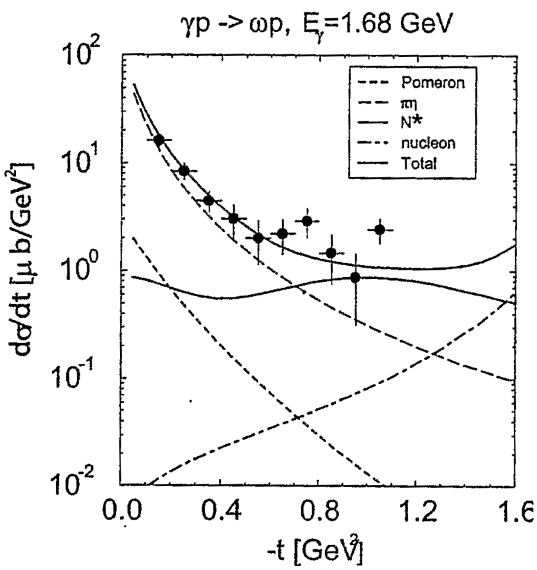

Oh, Titov, and Lee, nucl-th/0012012, Data from: SAPHIR('96)

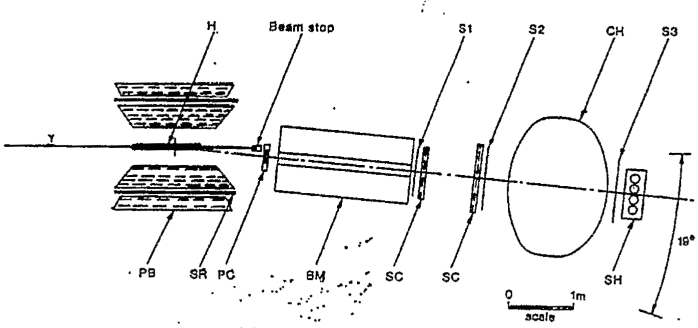

Experiment at Daresbury

Clifft et al. PL 72B, 144('97)

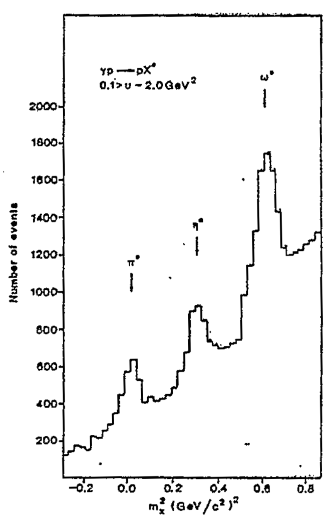

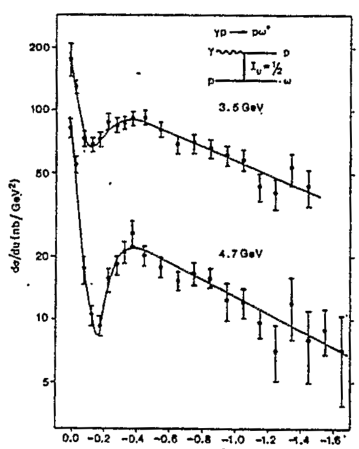

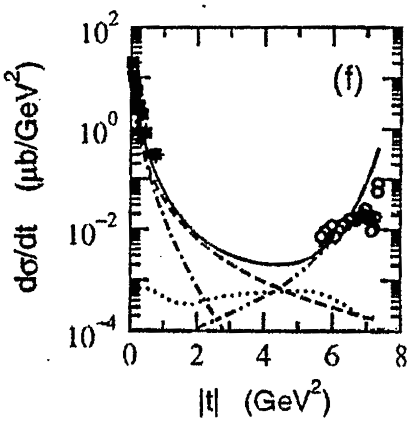

Oh, Titov, Lee

nucl-th/0104046

mx

u (GeV/c)²

Missing mass for p(γ,p)

Liq. H_2 target

$1.5 < E_\gamma < 2.4$ GeV

$|t| > 0.6\ (\mathrm{GeV})^2$

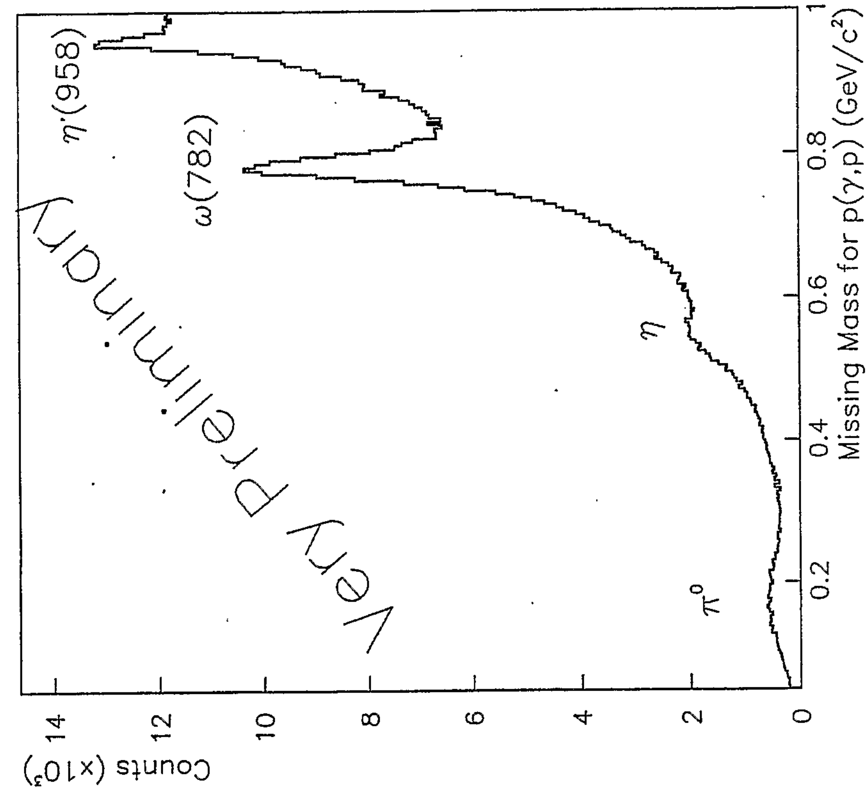

Photo-production of ω

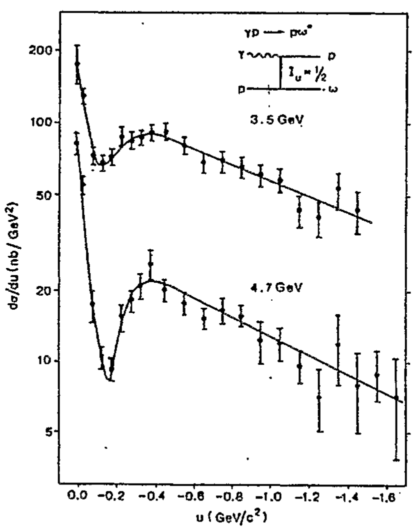

Phys. Lett. 72B (1977) 144

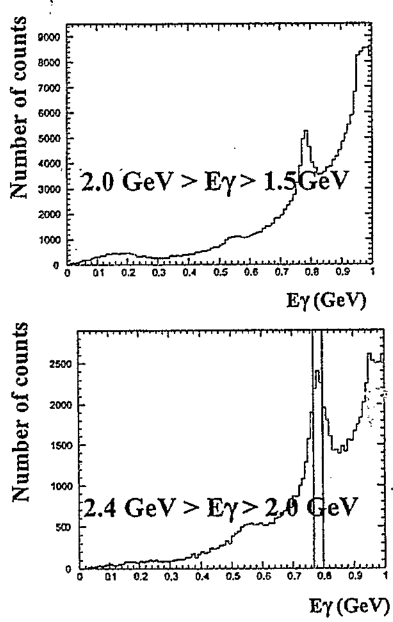

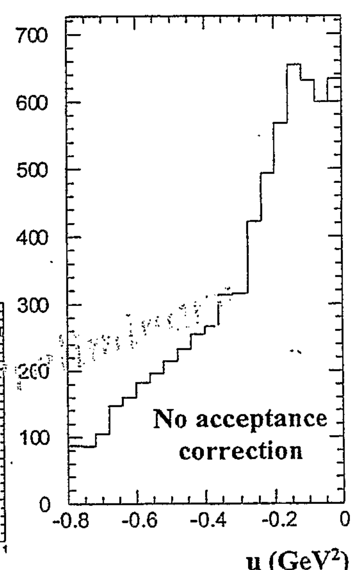

Photo-production of $\Lambda(1405)$

- qqq state vs. meson-baryon resonance.
- Big change of the decay width in nuclear medium for the meson-baryon case .

  Chiral unitary model .
- Need to identify the decay products ($\Sigma\pi$)
- Time Projection Chamber is constructed.

Nacher, Oset, Toki, Ramos, PLB455(1999)55

Chiral Unitary Model

$K^-\pi, K^0n, \pi^0\Lambda, \pi^0\Sigma^0, \eta\Lambda, \eta\Sigma^0, \pi^+\Sigma^-, \pi^-\Sigma^+, K^+\Xi^-, K^0\Xi^0$

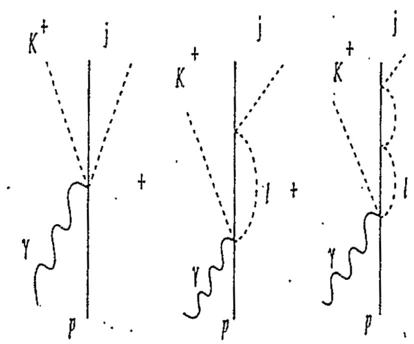

Fig. 2. Diagrammatic representation of the meson-baryon state interaction in the $\gamma p \to K^+\Lambda(1405)$ process.

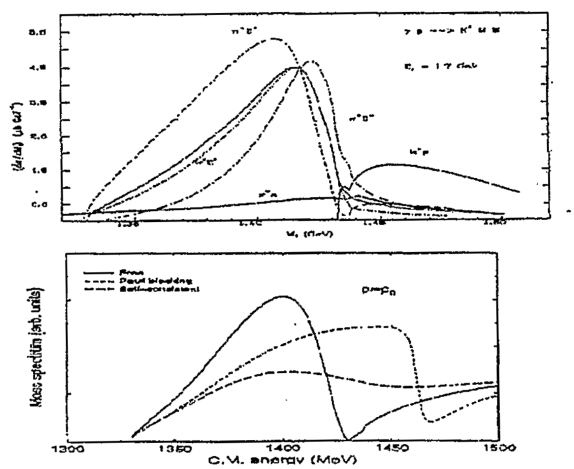

Preliminary Analysis for

$$\gamma p \longrightarrow \Lambda(1405)\, K^{+} \longrightarrow \Sigma\, \pi\, K^{+}$$

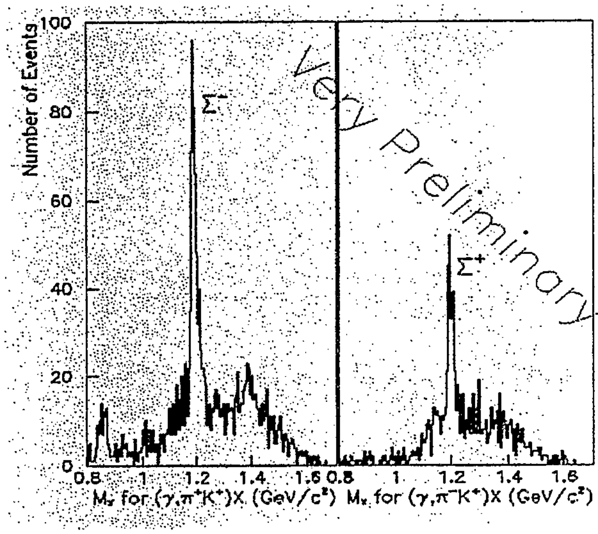

Missing-mass technique to reconstruct Σ from $p(\gamma, K^{+}\pi)X$

Possible to reconstruct $\Lambda(1405)$ from invariant mass of π and Σ

$\Sigma(1385) \rightarrow \Lambda\pi$ (88%)
$\Sigma\pi$ (12%)

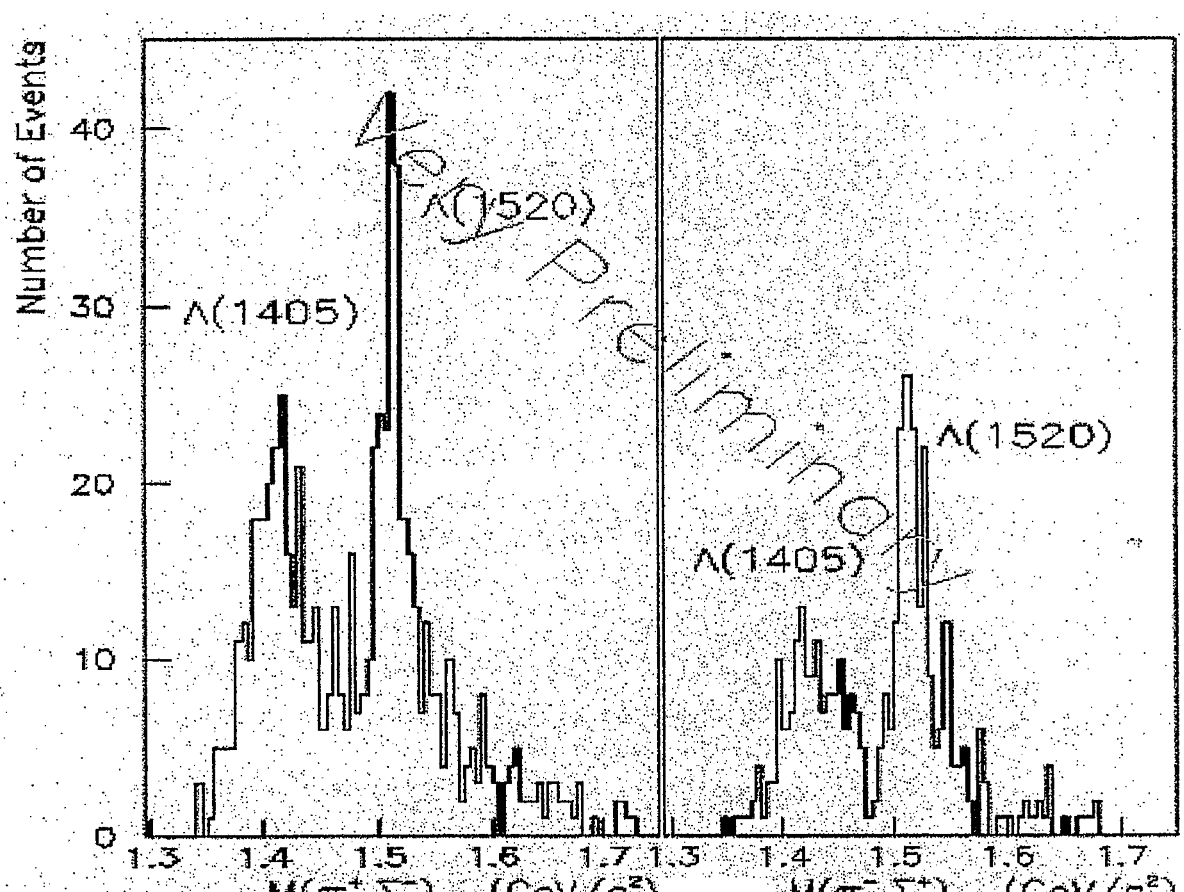

TPC Readout Chamber

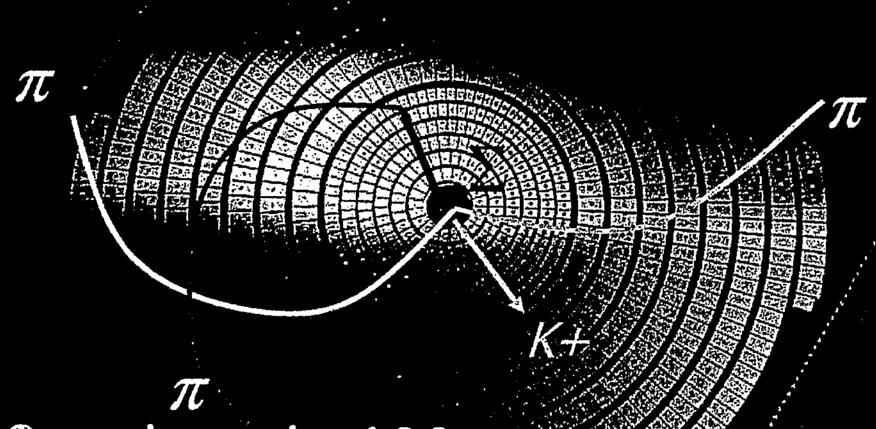

- ~1000 pads and ~100 wires for readout
  σ_{xy} ~350μm and σ_z ~ 500μm
- B = 1.5 ~ 2.5T
  ΔM/M ~ 0.5% for Λ(1405) mass

Experimental Setup with TPC

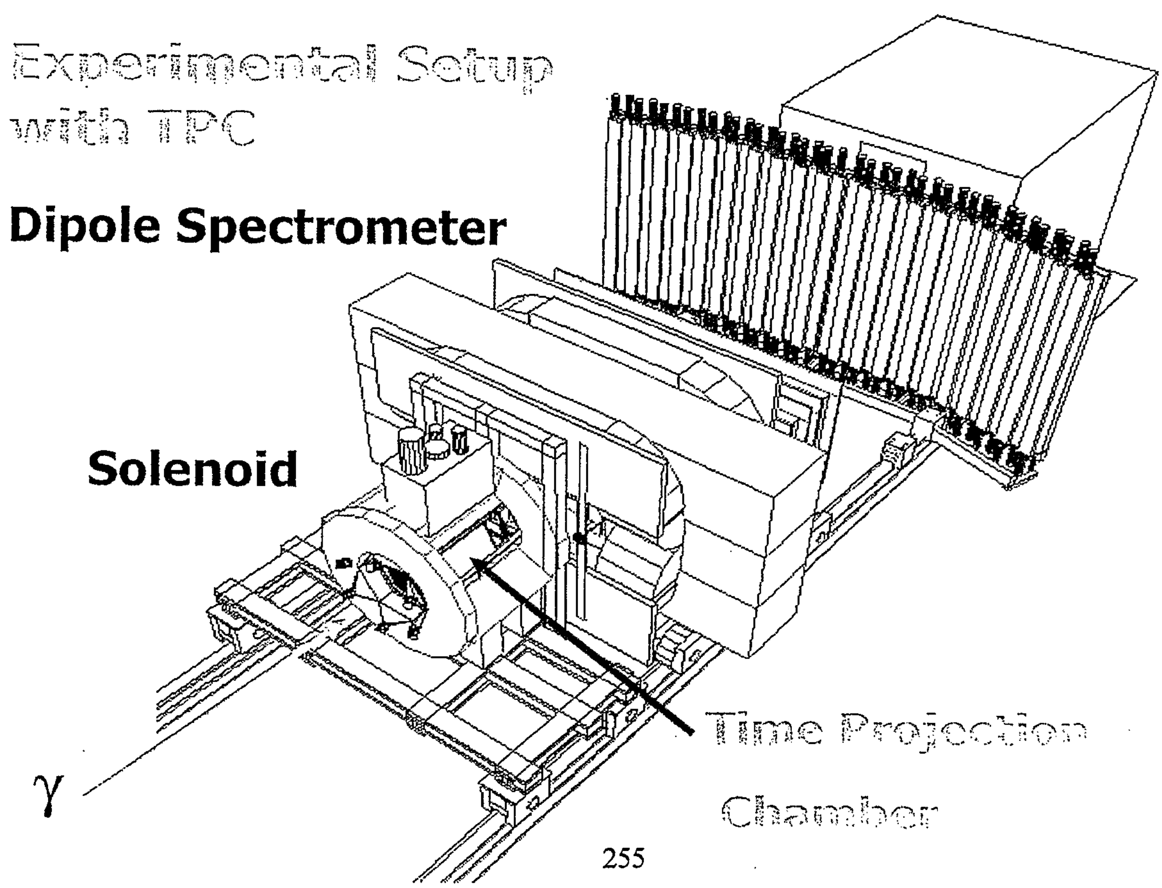

LEPS backward γ calorimeter

To detect the multi photons produced by $\pi^0\pi^0$ decay, segmented calorimeter is used.

$\sigma \rightarrow \pi^0\pi^0$

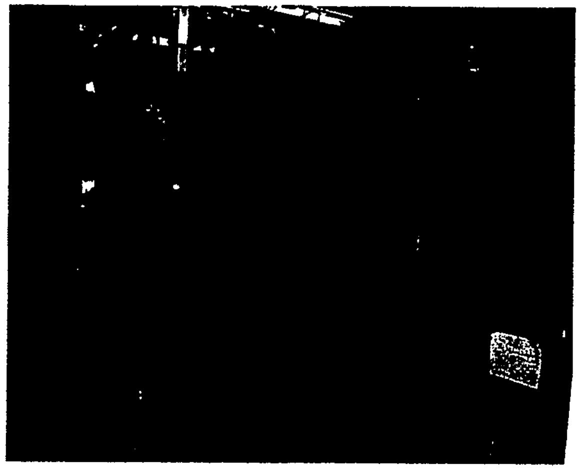

- **Main detector**
  Lead scintillating fiber
  252 modules
- Covered solid angle
  2.08π (str)
  θ : 30° ~ 100°
  ϕ : 0° ~ 360°
- Length of each module
  22cm (13.7 X_0)

Reconstructed 2γ event

- 2γ cluster selection
- π^0 mass resolution : 19.8 ± 0.1 MeV
  $\sigma_{\pi 0}/m_{\pi 0}$: ~ 15%
- η mass resolution : 54.5 ± 1.5 MeV
  σ_η / m_η : ~ 10%

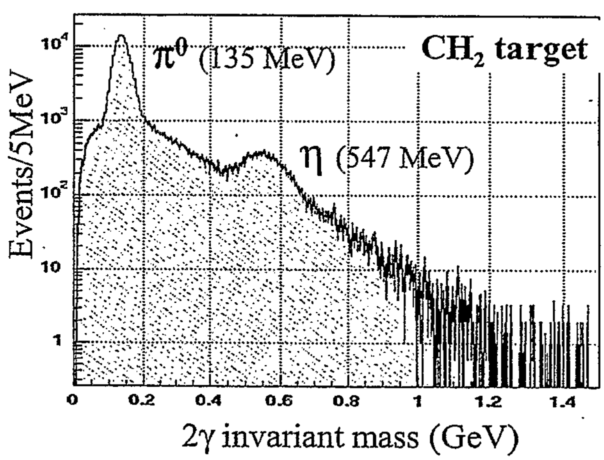

4γ cluster events

- Six entries per event ($_4C_2 = 6$)
- $\pi^0\pi^0$ and $\pi^0\eta$ events are observed.

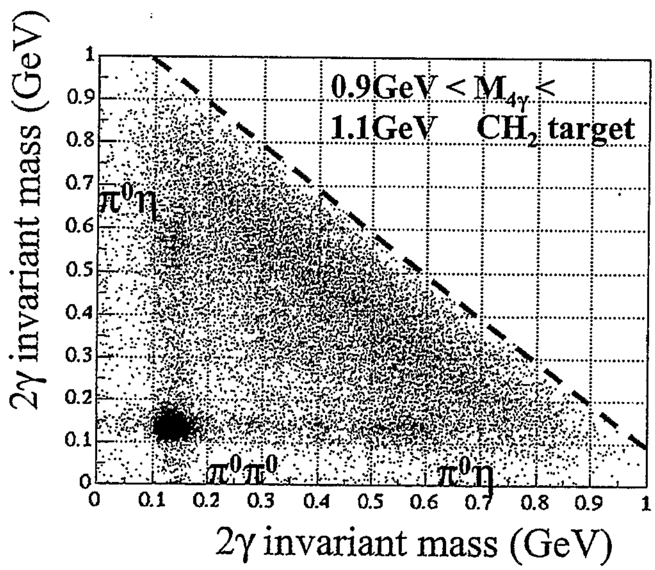

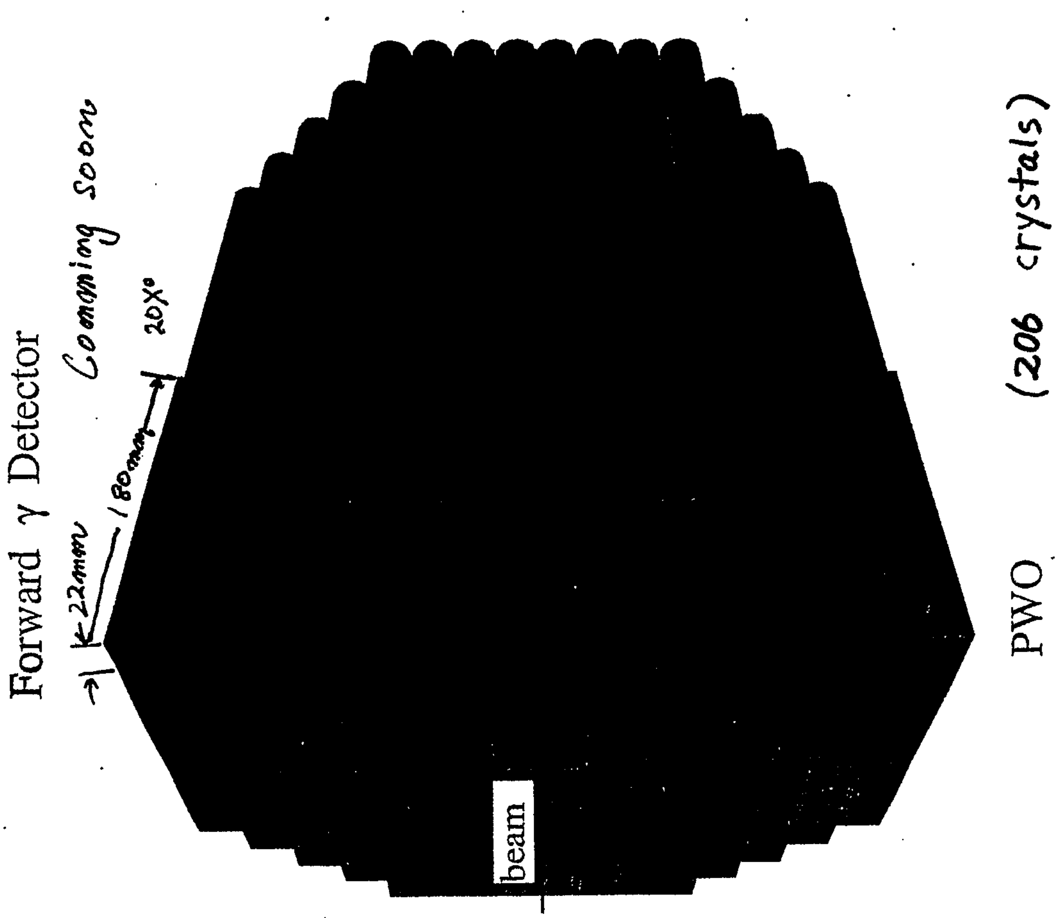

Summary

- New photon beam facility in Japan.
  - 2.4 GeV linearly polarized photons.
  - Forward-angle spectrometer .
  - Complementary to Jlab and GRAAL.
- Physics programs.
  - Photoproduction of ϕ meson near threshold.
    - Decay asymmetry measurement to separate various contributions.
    - Search for strangeness content of nucleon.
  - K^+ Photoproduction.
    - Photon beam asymmetry sensitive to N* contribution.
  - Photoproduction of ω meson in u-channel.
    - sensitive to N* and $g_{\omega NN}$..
  - Photoproduction of $\Lambda(1405)$.
    - Pin down the nature of $\Lambda(1405)$.
    - TPC to study the medium effect.

Summary

  - $2\pi^0$ photo-production
    - Search for σ meson
    - Gamma detector.

Recent Results on Spin Structure of the Nucleon from HERMES

Toshi-Aki Shibata
Tokyo Institute of Technology / RIKEN

Abstract

The spin structure of the nucleon has extensively been explored by HERMES experiment in the last seven years. HERMES is an polarized electron scattering experiment off the polarized internal gas targets (H, D, 3He). It uses 27.6 GeV electron (positron) beam of DESY-HERA.

The study of the spin structure of the nucleon was triggered by the result of EMC experiment published in 1988. Since then numerous experiments were and are being carried out at CERN, SLAC, DESY, TJNAL, and BNL.
The success of HERMES experiment was, first of all, due to the polarized electron beam and the polarized gas targets. The both were important innovations. The electron beam becomes polarized by means of Sokolov-Ternov effect after it is injected to HERA and accelerated to the highest energy. The polarization of the H and D targets were as high as 85-90%. The Ring Imaging Cherenkov Counter enabled us to identify hadrons in the momentum range of 2 − 20 GeV/c. Produced hadrons were detected in coincidence with the scattered electron.

By HERMES experiment the flavor decomposition of the polarized quark distributions was carried out with the world-best precision. Hard exclusive processes such as deeply virtual Compton scattering and exclusive meson productions were studied in detail. Single spin azimuthal asymmetry was observed in pion production for the first time. This has opened a new possibility to study the transverse quark distributions in the nucleon. Gluon spin in the nucleon spin was also studied.
HERMES will continue pioneering in the field of spin structure of the nucleon.

shibata@nucl.phys.titech.ac.jp

1. Introduction

Deep Inelastic Scattering, e, μ, ν + N

E > 20 GeV

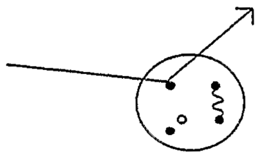

e, μ : electromagnetic + weak

ν : weak

$q(x)$: quark distribution

$G(x)$: gluon distribution

...

Bjorken x is determined from lepton kinematics event by event: a beauty of DIS

Deep Inelastic Scattering

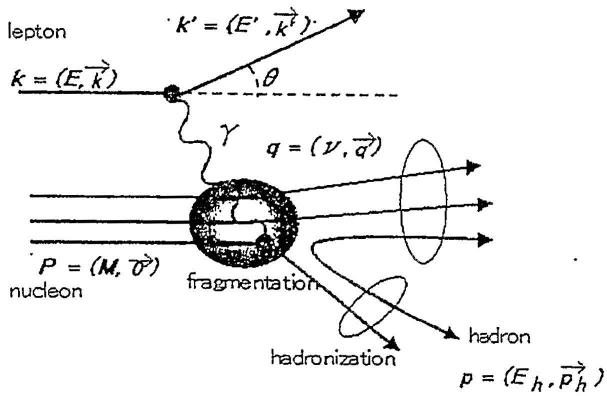

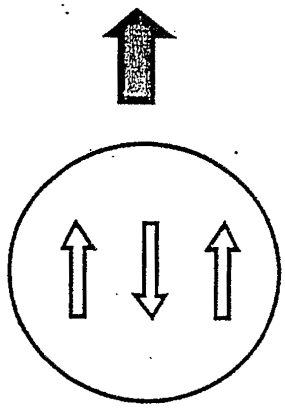

proton u, u, d

$$\frac{1}{2} = \frac{1}{2} \Delta \ \Sigma + \ldots$$
$$\Delta\Sigma = \Delta u + \Delta d + \Delta s$$

Flavor SU(3)

Magnetic Moments:

μ (p) = 4/3 μ (u) $-$ 1/3 μ (d),

μ (n) = 4/3 μ (d) $-$ 1/3 μ (u),

μ (n) / μ (p) = $-2/3$, Experiment -0.685

Spin:

$\langle p \mid S(u) \mid p \rangle = \langle p \mid 1/2 \ \sigma(u) \mid p \rangle = 2/3$

$\langle p \mid S(d) \mid p \rangle = \langle p \mid 1/2 \ \sigma(d) \mid p \rangle = -1/6$

$\langle p \mid S(u) + S(d) \mid p \rangle = \langle p \mid 1/2 \, (\sigma(u) + \sigma(d)) \mid p \rangle = 1/2$

EMC (European Muon Collaboration)

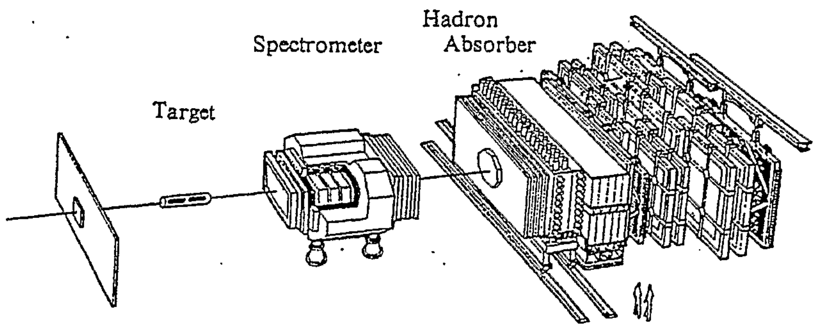

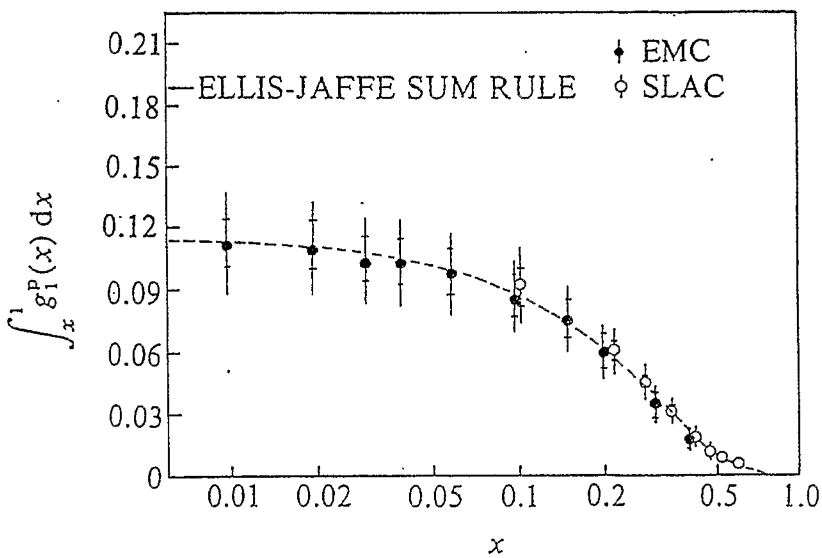

J. Ashman et al., Phys. Lett. B206 (1988) 364,
J. Ashman et al., Nucl. Phys. B328 (1989) 1.

$$\varDelta\Sigma = \varDelta u + \varDelta d + \varDelta s = 0.120 \pm 0.094 \pm 0.138$$

together with SMC, SLAC Experiments

$$\varDelta\Sigma = 0.2-0.3$$

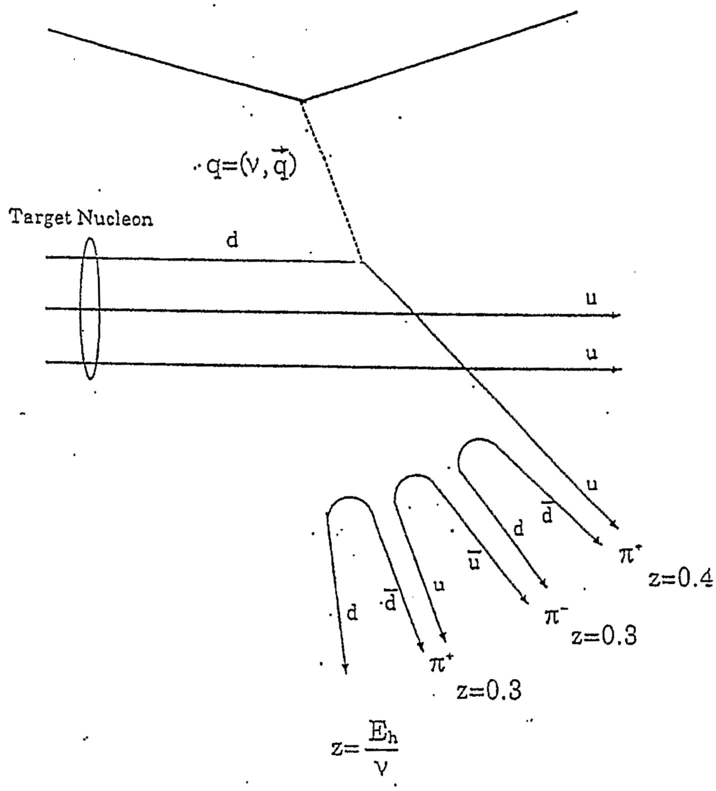

DIS data are used also for Analysis of pp Collider Data

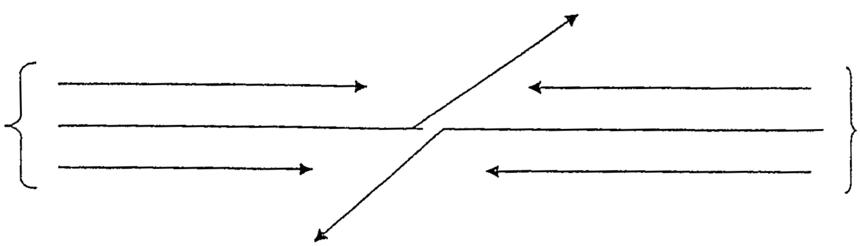

Parton-parton collision

$$A_{LL} \propto \frac{\Delta q(x)}{q(x)} \cdot \frac{\Delta G(x)}{G(x)}, \quad etc$$

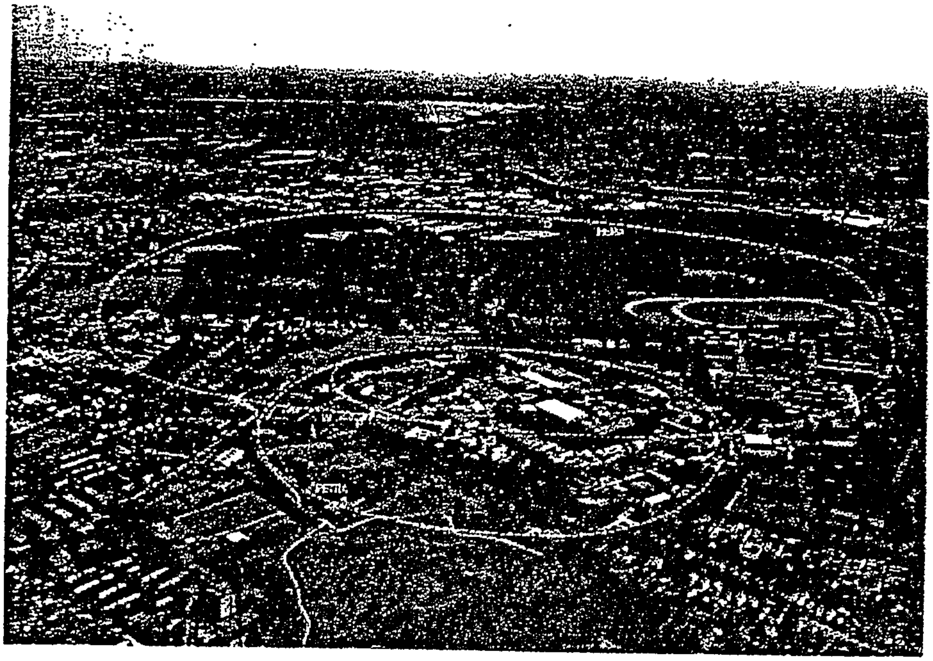

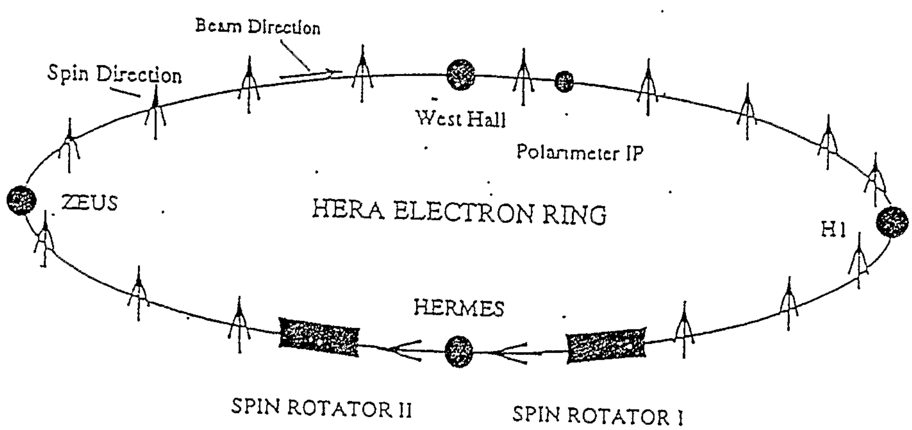
Beam Direction
Spin Direction
West Hall
Polarimeter IP
ZEUS
HERA ELECTRON RING
H1
HERMES
SPIN ROTATOR II
SPIN ROTATOR I

The polarized electron beam at HERA

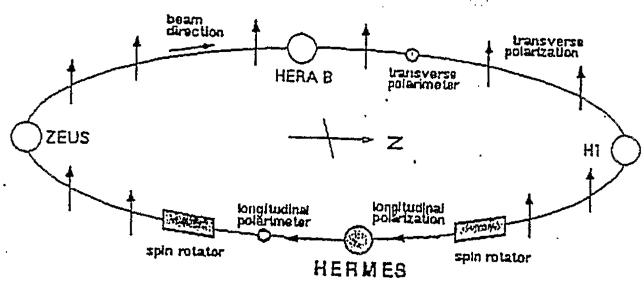

- Self-polarization by emission of synchrotron radiation
  - $p_b(t) = P_b^{max}[1-exp(-t/\tau)]$
- Spin rotators → longitudinal polarization at HERMES IP
- 2 Compton polarimeters
- Average beam polarization $<p_b> \sim 55$ %

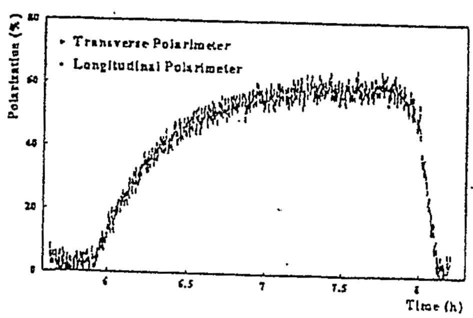

hermes

Tokyo Tech

hermes

HERMES Spectrometer

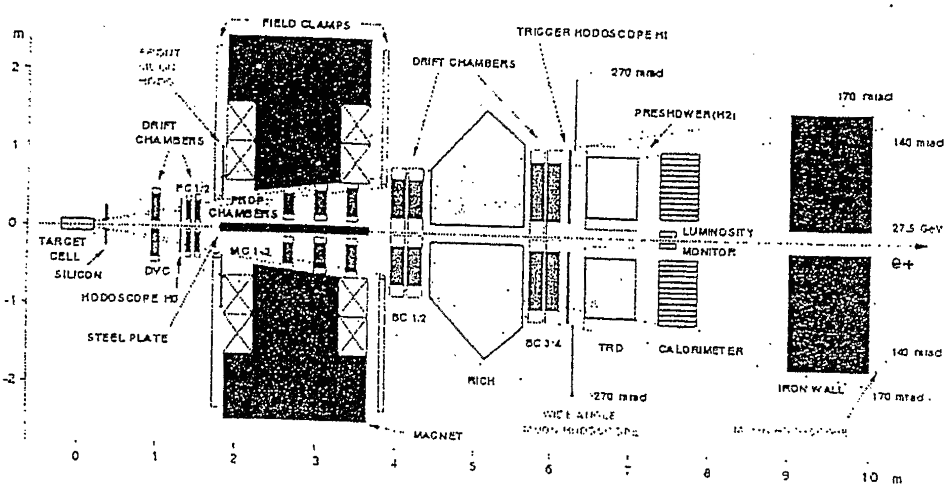

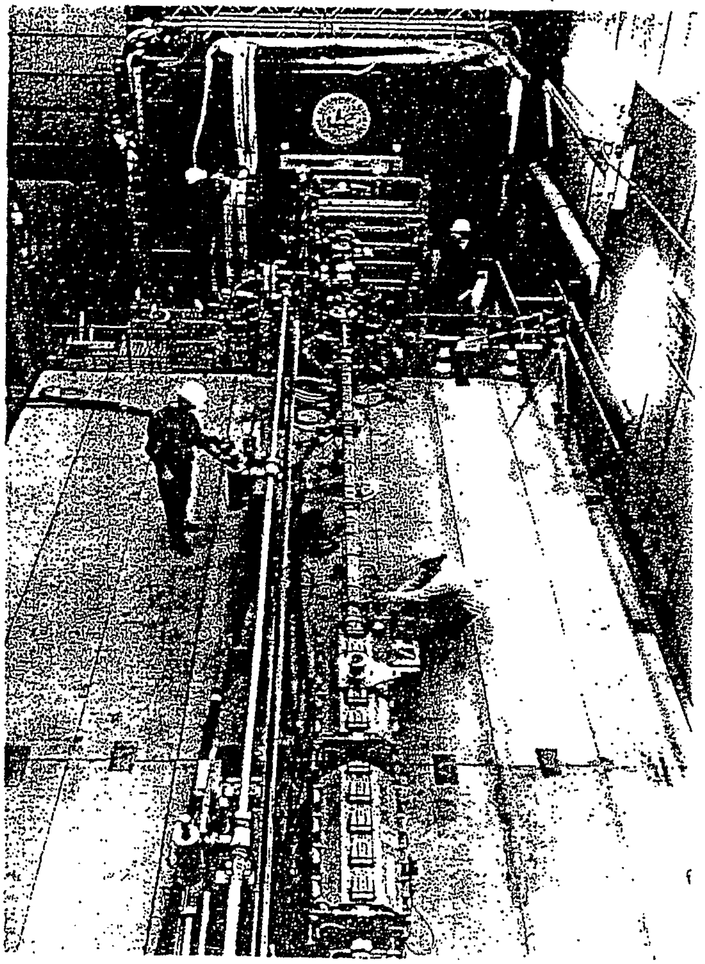

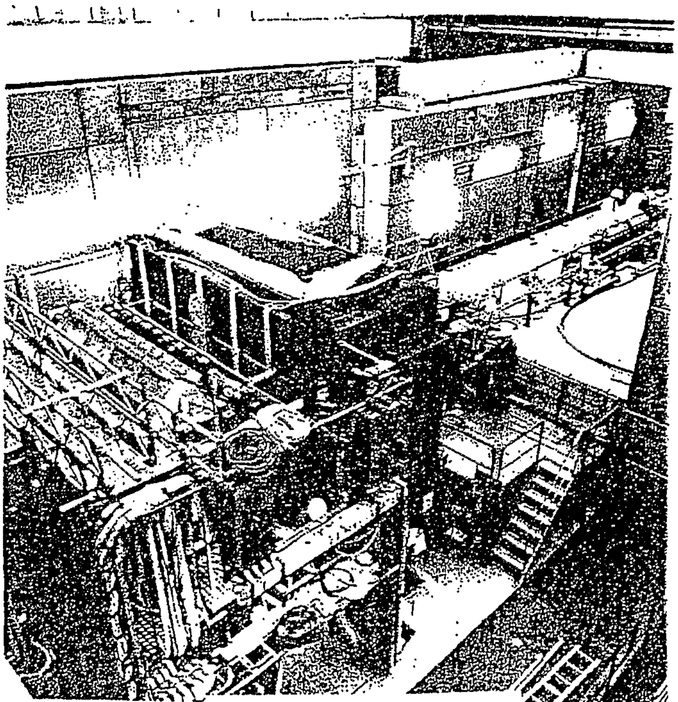

Polarized target

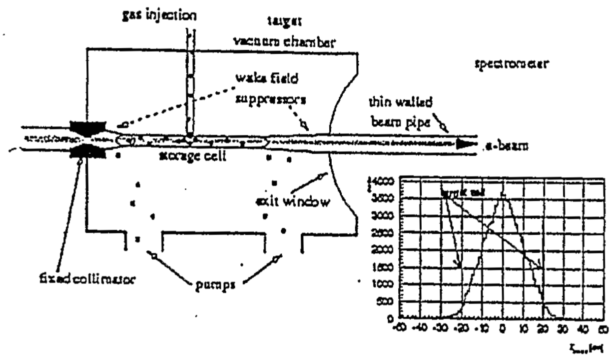

- 40 cm long open-ended storage cell
- Undiluted internal targets :
  - *H,D,^{3}He longitudinally polarized atoms*
- Laser driven polarized ^{3}He (1995) :
  - P_T=46 %, =10^{15} N/cm^2, $\Delta t_{flip} \sim 10$ min
- Atmic beam source for polarized H/D (1996 ~ 1999) :
  - P_T=92 %, =$7 \cdot \times 10^{13}$ N/cm^2; $\Delta t_{flip} \sim 1$ min
- Unpolarized gases :
  - *H,D,^{3}He,^{14}N,^{83}Kr..., $10^{15} \sim 10^{17}$ N/cm^2*

hermes

Tokyo Tech.

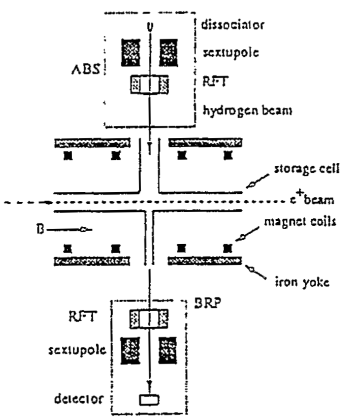

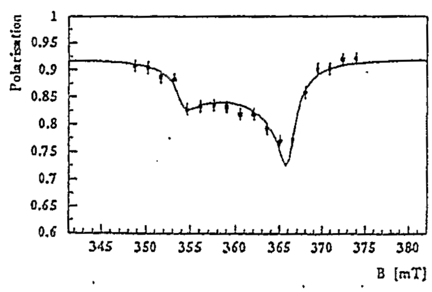

Beam-Induced Nuclear Depolarisation in a Gaseous Polarised Hydrogen Target
Phys. Rev. Lett. 82 (1999) 1164-1168

Dual-Radiator Ring Imaging Cherenkov (RICH) Detector

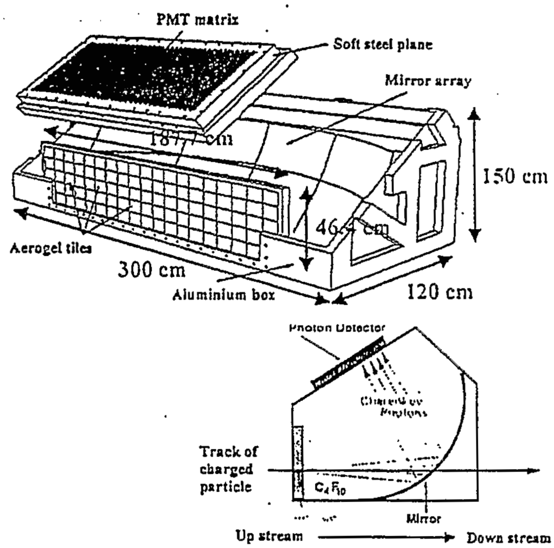

- Dual-radiators
  - Silica aerogel : index of refraction n = 1.0304
  - C_4F_{10} gas : index of refraction n = 1.00137
- Photon detector :
  - 1934 PMTs with diameter 3/4 inch for each half

Particle Identification with RICH

Reconstructed angle:

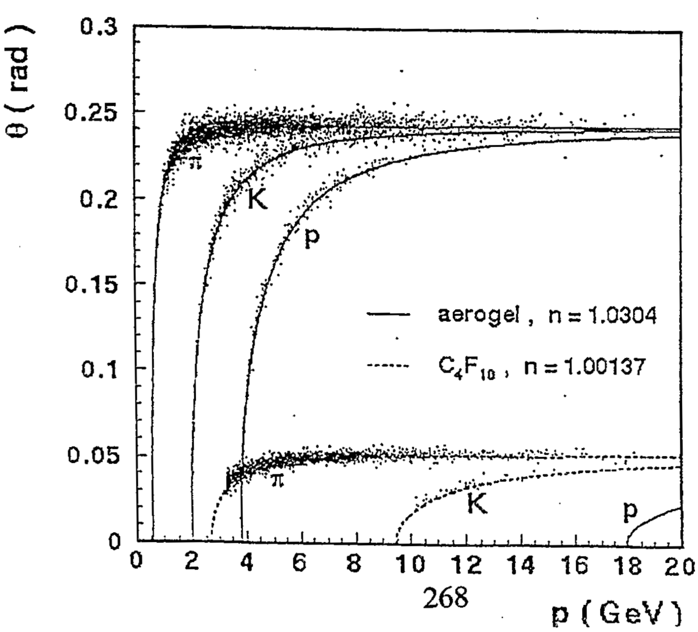

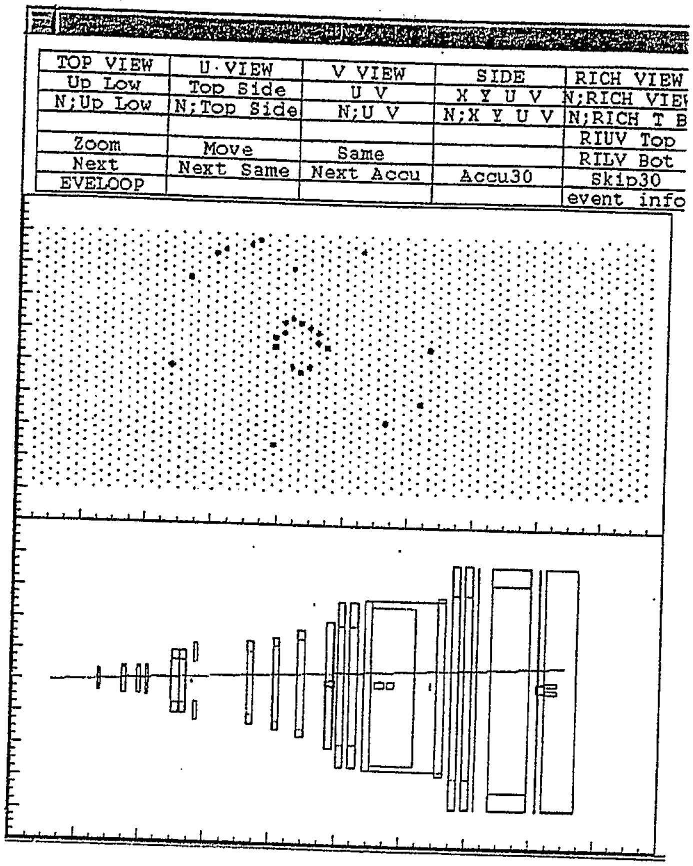
TOP VIEW
U·VIEW
V VIEW
SIDE
RICH VIEW
Up Low
Top Side
U V
X Y U V
N;RICH VIE
N;Up Low
N;Top Side
N;U V
N;X Y U V
N;RICH T B
RIUV Top
Zoom
Move
Same
RILV Bot
Next
Next Same
Next Accu
Accu30
Skip30
EVELOOP
event info

Spin Physics from HERMES

Inclusive Measurement: $g_1(x)$

Semi Inclusive Measurement:
Hadron identification -> Δu, Δd, Δs ..
Pairs of Mesons -> ΔG
Single Spin Azimuthal asymmetry -
Collins fragmentation function
-> $h_1(x)$

Quark Transversity Distribution

Deeply Virtual Compton Scattering,
Exclusive Meson Production ->

Off Forward (skewed) Parton Distribution and *J*

Physics Output from HERMES

Unpolarized Scattering

Violation of Gottfried Sum Rule
-> Flavour Asymmetric Sea

Nuclear Physics:

Coherence Length of ρ Production,
Heavy Targets (D, He, Ne, Ar, Kr, Xe)

Instrumental:

K. Ackerstaff et al., Beam-induced Nuclear Depolarization in a Gaseous Polarized Hydrogen Target, Phys. Rev. Lett. 82, 1164-1168 (1999).

K. Ackerstaff et al., HERMES Spectrometer, Nucl. Instrum. Methods A 417, 230-265 (1998).

N. Akopov et al., The HERMES Dual-Radiator Ring Imaging Cerenkov Detector, Nucl. Instrum. Meth. A479, 511-530 (2002)

< Flavour Asymmetry of the Sea Quarks >

$u(x) < d(x)$ in the sea of prot

Discovery of Violation of Gottfried Sum Rule by NMC:

Phys. Rev. Lett. 66 , 271 (1991)
Phys. Rev. D50, R1-R3 (1994)

x-dependence of the Sea Quarks by HERMES:

K. Ackerstaff et al., Phys. Rev. Lett. 81, 5519-5523 (1998).

< Inclusive Measurements >

K. Ackerstaff et al.: Measurements of the neutron spin structure function g_1^n with a polarized ^{3}He target, Phys. Lett. B404, 383-389 (1997).

A. Airapetian et al.:Measurement of the proton spin structure function g_1^p with a pure hydrogen target, Phys. Lett. B442, 484-492 (1998).

< Flavour Decomposition >

K. Ackerstaff et al.:Flavor decomposition of the polarized quark distribtuions in the nucleon from inclusive and semi-inclusive deep-inelastic scattering, Phys. Lett. B464, 123-134 (1999).

< Gluon Polarization >

A. Airapetian et al.:Measurement of the spin asymmetry in the photoproduction of pairs of high p_T hadrons at HERMES, Phys. Rev. Lett. 84, 2584-2588 (2000).

< Single Spin Azimuthal Asymmetry in Semi-Inclusive Measurements >

A. Airapetian et al.: Evidence for a single-spin azimuthal asymmetry in semi-inclusive pion electroproduction, Phys. Rev. Lett. 84, 4047-4051 (2000).

< GDH Sum Rule >

K. Ackerstaff et al.:Determination of deep inelastic contribution to the generalized Gerasimov-Drell-Hearn integral for the proton, Phys. Lett. B444, 531-538 (1998).

K. Airapetian et al.:The Q^2-dependence of the generalized Gerasimov-Drell-Hearn integral of the proton, Phys. Lett. B 494, 1 (2000).

Proton Spin Structure Function $g_1^p(x)$

$$A_1 \simeq \frac{g_1^h(x,Q^2)}{F_1^h(x,Q^2)} = \frac{\Sigma_f e_f^2 \Delta q_f(x,Q^2)}{\Sigma_f e_f^2 q_f(x,Q^2)}$$

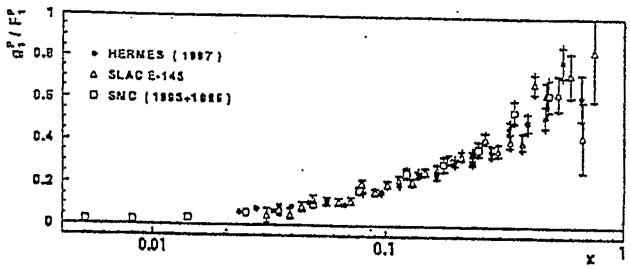

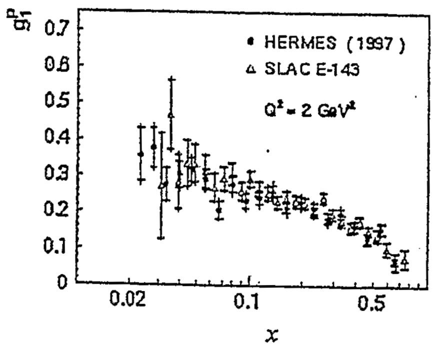

hermes

Tokyo Tech.

Quark Polarisations

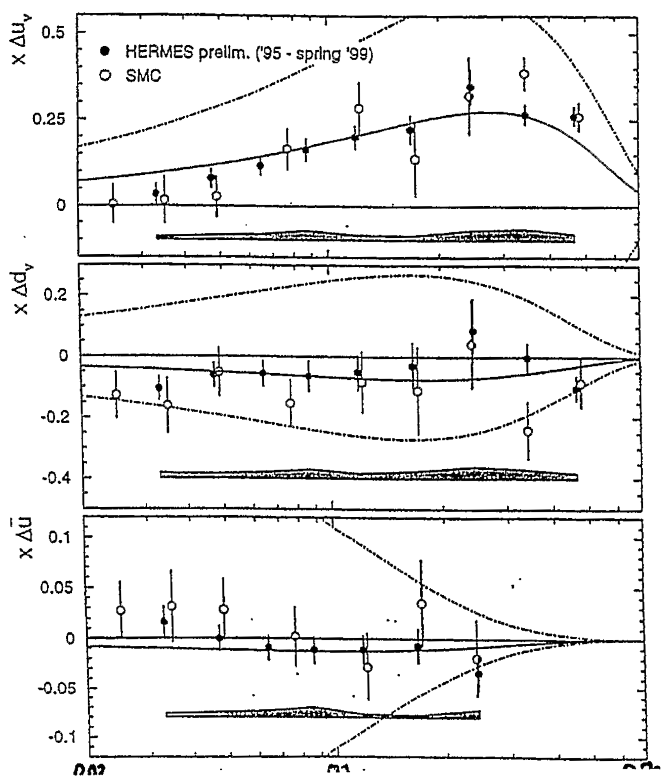

Hard Exclusive Process
Experiment:

HERMES, A. Airapetian et al., Phys. Rev. Lett. 87 182001 (2001), 'Measurement of the Beam-Spin Azimuthal Asymmetry Associated with Deeply-Virtual Compton Scattering'

HERMES, A. Airapetian et al., hep-ex/01122022, submitted to Phys. Lett., 'Single-Spin Azimuthal Asymmetry in Exclusive Electroproduction of $\pi+$ Mesons'

Theoretical Motivations:

Off-forward (skewed, generalized) Parton Distribution
$J = 1/2\ \Delta\ \Sigma + L$

F.-M. Dittes et al., Phys. Lett. B 209, 325 (1988).
D. Mueller et al., Fortsch. Phys. 42, 101 (1994).
A.V. Radyushkin, Phys. Lett. B 385, 333 1996).
X. Ji, Phys. Rev. D 55 , 7114 (1997).
.....

Exclusive Processes

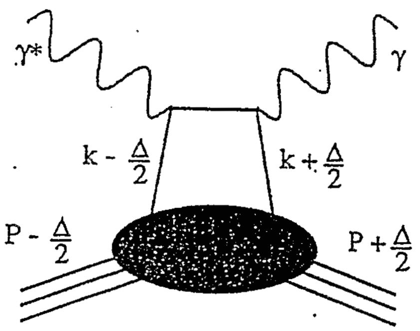

Deeply Virtual Compton Scattering

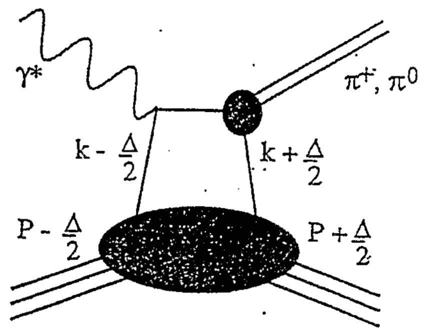

Pion Production

Exclusive Photon Production

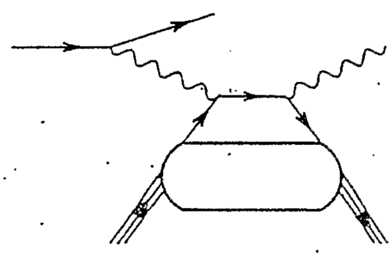

Deeply Virtual Compton Scattering

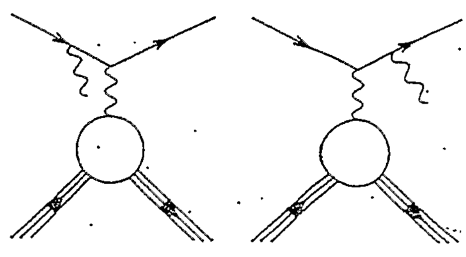

Bethe-Heitler Process

Azimuthal Angle ϕ

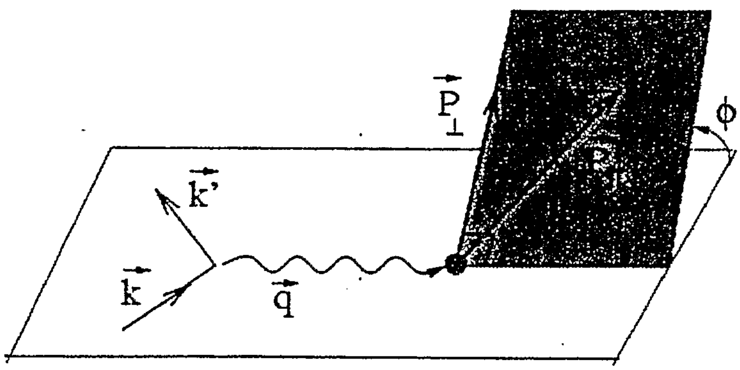

Dependence on Azimuthal Angle ϕ

Dependence on Beam Helicity

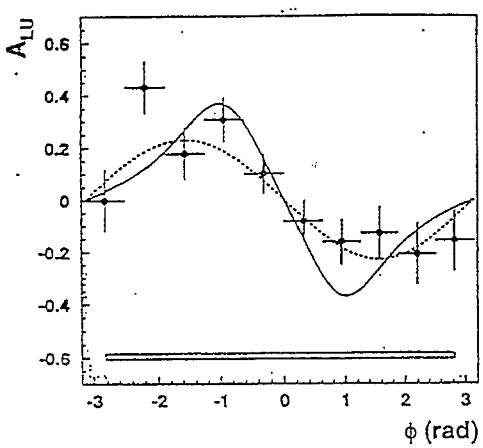

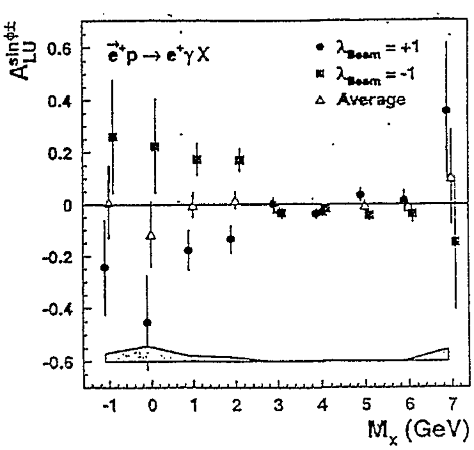

Missing Mass Distribution

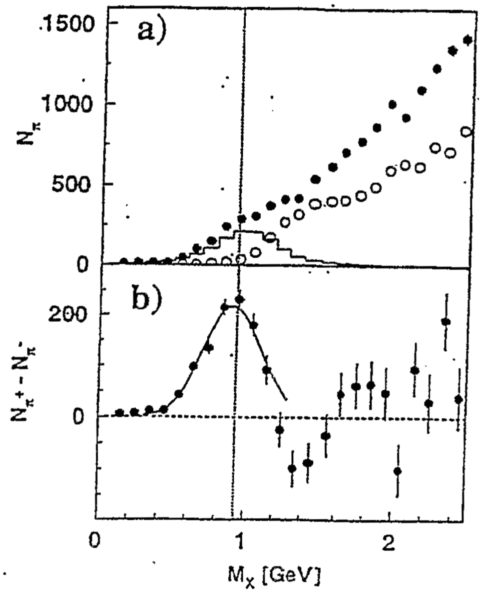

Exclusive Pion Productions

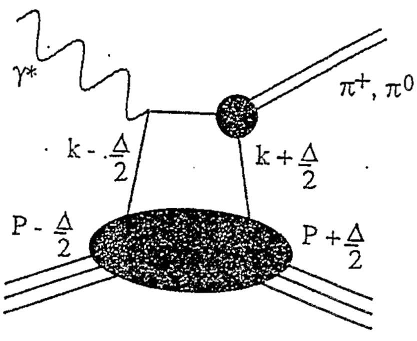

Dependence on Azimuthal Angle ϕ

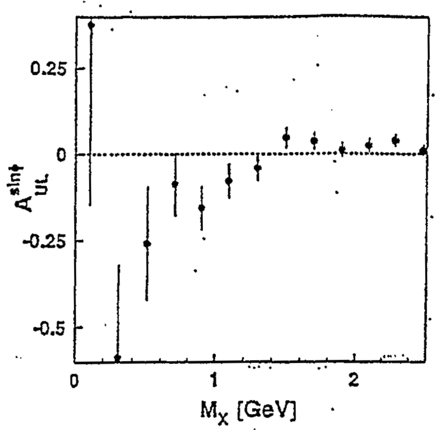

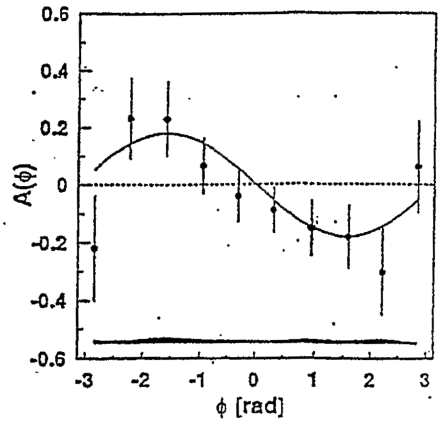

Summary

- HERMES is a Polarized Deep Inelastic Scattering Experiment at DESY-HERA with 27.6 GeV positrons(1995 -). The longitudinally polarized targets were used. The transversely polarized target will also be used.
- With RICH Identification of π, K, p is possible. Inclusive and Semi-Inclusive Measurements were done.
- Quark flavor decomposition of Spin Structure Function was done.
- Azimuthal asymmetry in semi-inclusive measurement was observed.
- Exclusive Processes (Deeply Virtual Compton Scattering and Pion Productions) were identified with the HERMES Detector
- HERMES will continue pioneering the Nucleon Spin Structure.

Hadron Physics in Kakuriken

- $S_{11}(1535)$ in nuclei observed with the (γ, η) reaction -

H. Yamazaki - *Laboratory of Nuclear Science, Tohoku University*

RIKEN School on 'Quark-Gluon Structure of the Nucleon and QCD'
RIKEN, Mar. 29-31, 2002

Abstract

This lecture describes the recent results obtained at Laboratory of Nuclear Science (Kakuriken), Tohoku University on the property of the $S_{11}(1535)$ nucleon resonance in nuclear medium.

$S_{11}(1535)$ nucleon resonance is one of the candidates of the chiral partner of the nucleon. It is very important to investigate the property of the S_{11} in nuclear medium to explore the chiral property of the nucleon. The η photoproduction reaction can be used as a probe for the $S_{11}(1535)$ in nuclei because the low energy behaviour of the η photoproduction is governed by the $S_{11}(1535)$. In order to investigate the property of $S_{11}(1535)$ resonance in nuclei, we have carried out the (γ, η) experiment on C, Al and Cu at Kakuriken, Tohoku University.

Since 1998, 1.2 GeV electron synchrotron called STretcher-Booster-ring (STB) has been in operation at Kakuriken. We constructed the photon tagging system which provides the tagged photon beam with its energy range from 0.8 GeV to 1.1 GeV. The tagged photon beam bombards the nuclear targets and produces η mesons. Two γ-decay of η meson is detected by the pure CsI calorimeter. The η photoproduction events were identified from the other background by using invariant mass analysis of 2-γ. The cross section of the (γ, η) reaction on C, Al and Cu have been deduced. Our results suggest that the width of $S_{11}(1535)$ becomes about 70 MeV broader than the natural width in all target nuclei, i.e. C, Al and Cu.

Hadron Physics at Kakuriken

- $S_{11}(1535)$ in nuclei observed with the (γ, η) reaction -

Hirohito Yamazaki

(Kakuriken - Laboratory of Nuclear Science -, Tohoku Univ.)

+ Introduction
    - Photoabsorption
    - Pion photoproduciton
    - Eta photoproduction
+ Experiment
    - Accelerators in Kakuriken
    - Photon tagging system, LNS Tagger
    - Photon detector, SCISSORS and more
+ Results
    - Yeild and cross section
    - QMD calculation and resonance in nuclei

Introduction

How dose the N* behave in Nuclei?

Total photoabsorption on nuclei

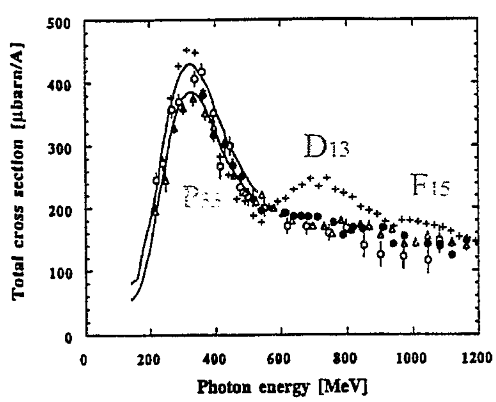

Total photoabsorption cross section par nucleon (D, Be, C, U)
[N. Bianchi et al. Phys.Lett.B309(1993)5 etc.]

Three u and/or d quarks
- N (isospin 1/2)
- Δ (isospin 3/2)

Two u and/or d quarks
- Λ (isospin 0)
- Σ (isosipn 1)

One u or d quark
- Ξ (isospin 1/2)

No u or d quark
- Ω (isospin 0)

Orbital angular momentum of N-π

D_{13}

isospin spin

Disappearance of N* and collision broadening

Large collision broadening ~ 300 MeV

L.A. Kondratyuk et al., Nucl. Phys. A579 (1994) 453

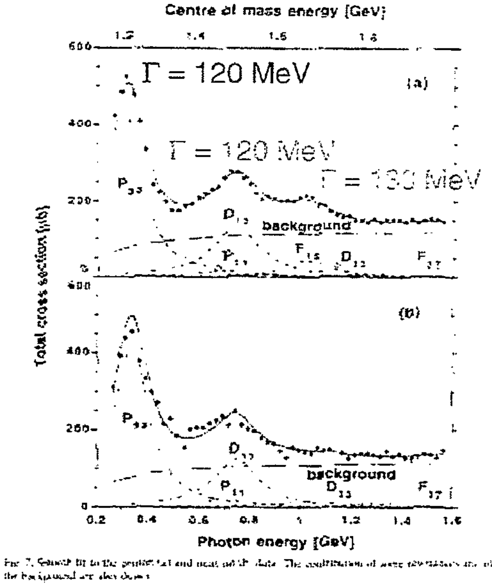

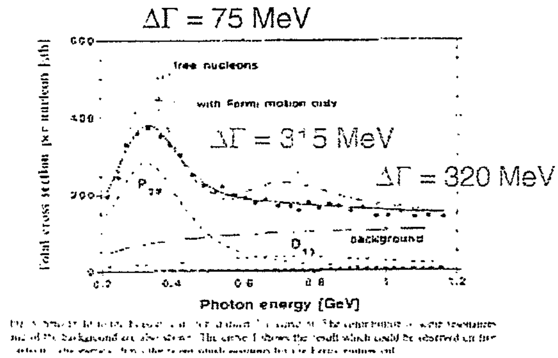

$\Delta\Gamma$ = 315 MeV $\Rightarrow$ σ_{NN^*} = 180 mb

cf. σ_{NN^*} = 90 mb (from the inverse reaction)

Pion photoproduction and N*

Cooperative effect of collision broadening,
π distortion and interference of 2π production

M. Hirata et al. Phys. Rev. Lett. 80(1998)5068

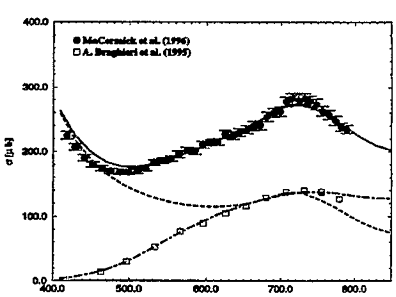

Single pion production
(Δ, N* dominant)

Double pion produciton
(Δ-KR etc.)

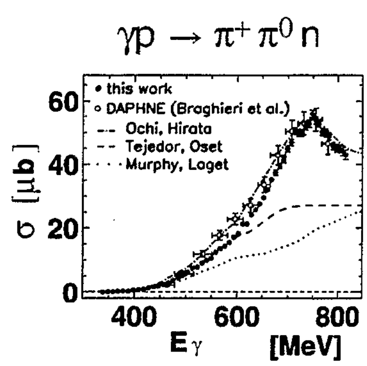

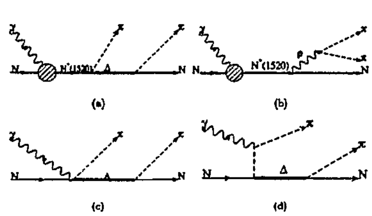

It is important to investigate
the properties of each N*
exclusively in this energy region

S_{11}(1535) resonance in nuclei

Chiral symmetry with spontaneous breakdown: Important concept in the hadron dynamics

S_{11}(1535) :
A candidate of a chiral partner of nucleon?

Partially restoration of chiral symmetry in nuclear medium
Mass, coupling and so on

C. DeTar and T. Kunihiro Phys. Rev. D39 2805(1989),
D. Jido et al. Nucl. Phys. A671(2000)471

Mass and width of S_{11} in Nuclei?
Chiral structure of nucleon and nuclear resonance

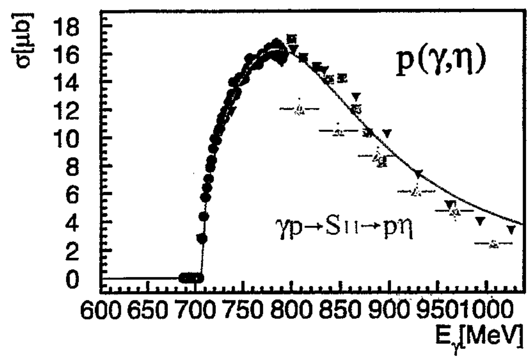

[B. Krusche et al., Phys. Rev. Lett. 74 (1995) 3736]
[M. Wilhelm. Ph.D. Thesis, Bonn, BN-IR-93-43]
[S. Homma et al., J. Phys. Soc. JPN. 57 (1988) 828]
[D. Rebreyend et al., Nucl. Phys. A663&664 (2000) 436c]

Large branching ratio to N-η (35 ~ 55 %)
Most of the η photoproduction occur via S11 resonance up to 1 GeV

S_{11}(1535) resonance in Nuclei

(γ, η) reaction cross section on C at KEK(Tanashi)

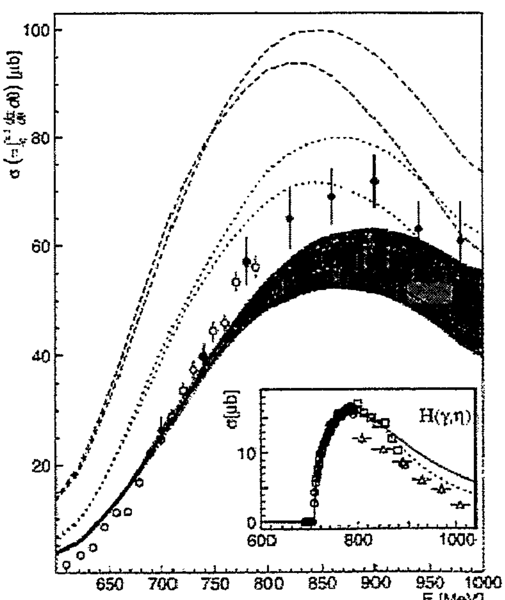

T. Yorita, H. Yamazaki et al.
Phys. Lett B476(2000)226

Basically the cross section can be explained by the well known effect; Fermi motion, Pauli blocking, η absorption and Collision broadening with M_R = 1544 MeV, Γ_R = 212 MeV

Discrepancies around 900 MeV?

Precise and systematical study in LNS, Tohoku University

Accelerators at Kakuriken

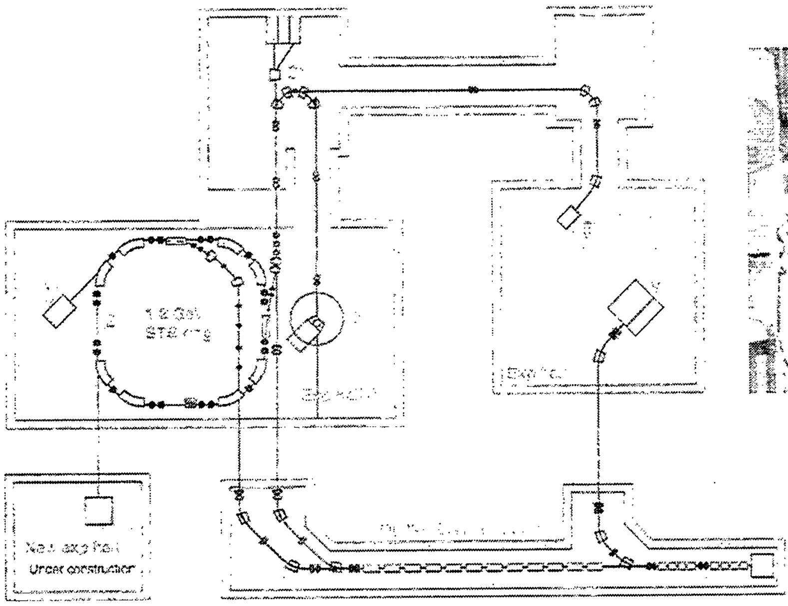

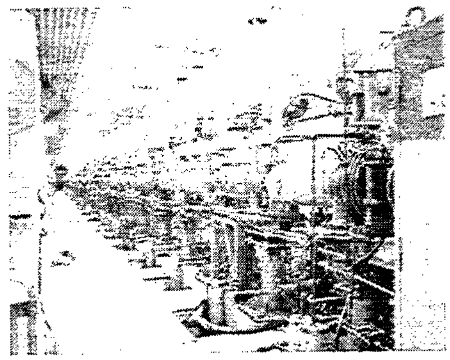

300 MeV electron linac
(35 years old)

(1) 1.2 GeV tagged photon beamline. SCISSORS. NKS spectrometer
(2) 1.2 GeV electron beamline : Internal target
(3) 300 MeV pulse electron beam line : Coherent SOR
(4) 300 MeV continuous electron beam line: LDM
(5) 300 MeV Tagged photon beam line : NE213 neutron counters
(6) 60 MeV high intensity pulse beam line : Material science

LNS Tohoku 1.2 GeV STB ring

(STretcher Booster ring)

Liniac electron beam
(200 MeV Maxmum)

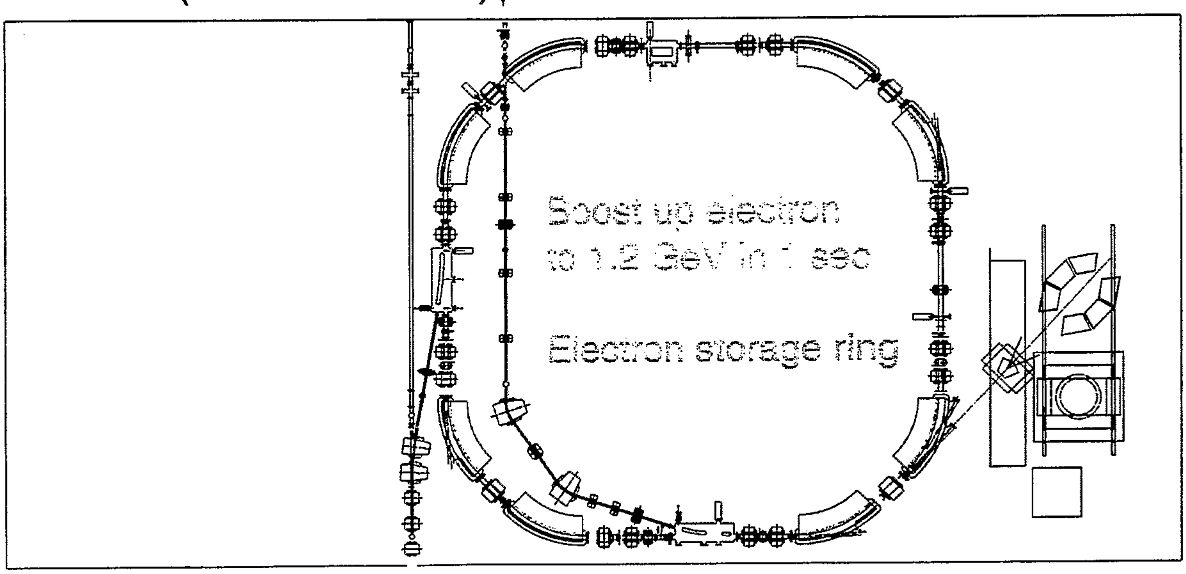

Photon tagging system → STB Tagger
High energy photon detector → SCISSORS

Setup

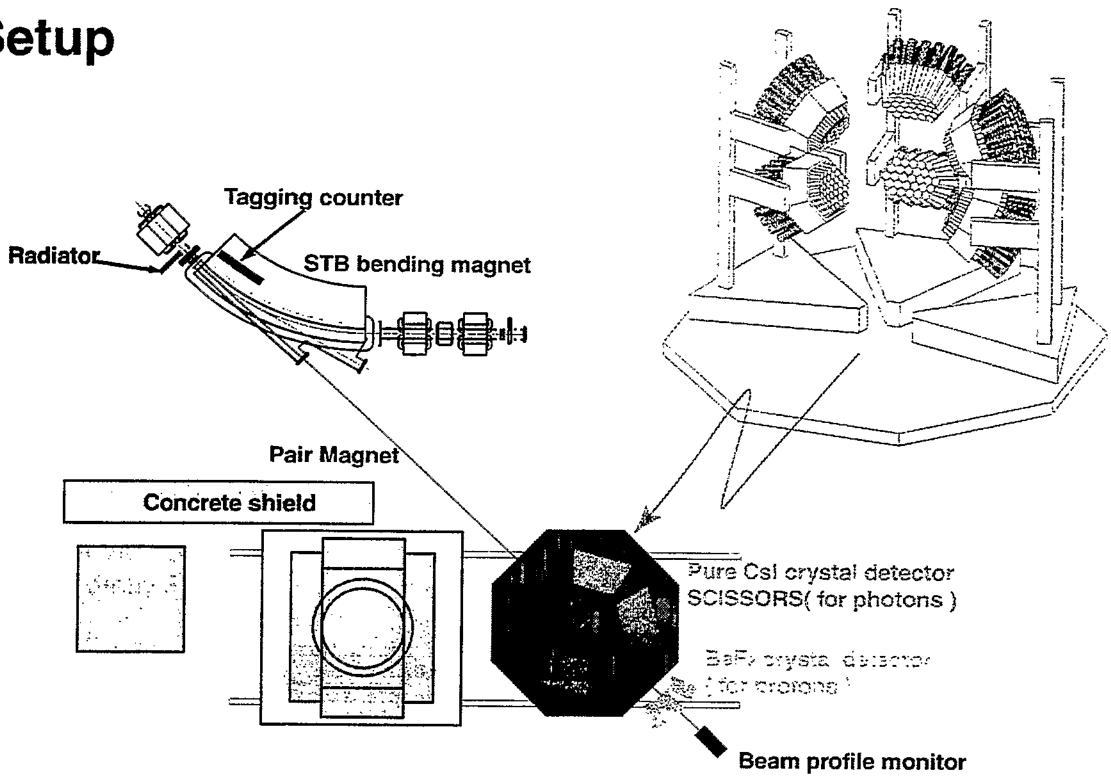

Tagging counters and tagging magnet

Momentum of recoil electrons ⟶ STB bending magnet

$$E\gamma = Ee - Ee'$$

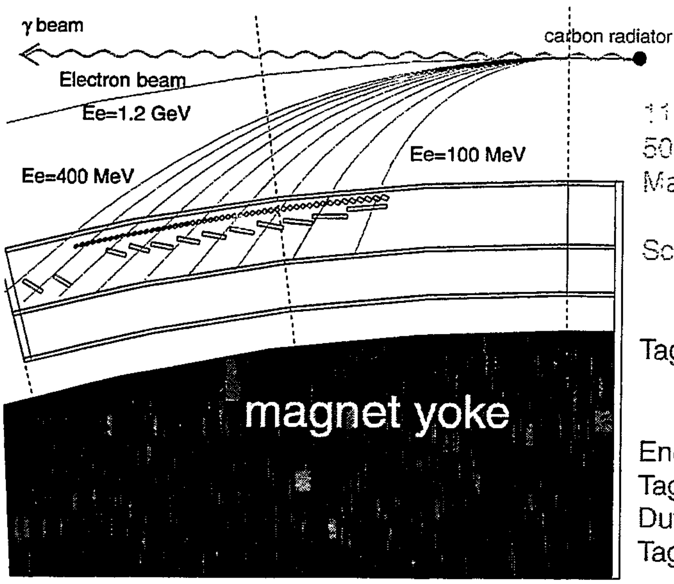

11 μm carbon fiber as the radiator
50 ch main counters + 12 ch backup counters
Main counter : 5mm in thickness
5~8 mm in width
Scintillation : Extracted through
3.5m optical plastic fibers

Tagging range :
0.8 ~ 1.1 GeV (Ee = 1.2 GeV)
0.62 ~ 0.85 GeV (Ee = 0.93 GeV)
Energy bin : 6 MeV (Ee = 1.2 GeV)
Tagged photon flux : 10^7 tagged γ / sec
Duty factor : ~ 0.8
Tagging efficiency : about 90 %

Radiator Control

1.2 GeV flat top
(5 ~ 30 sec)

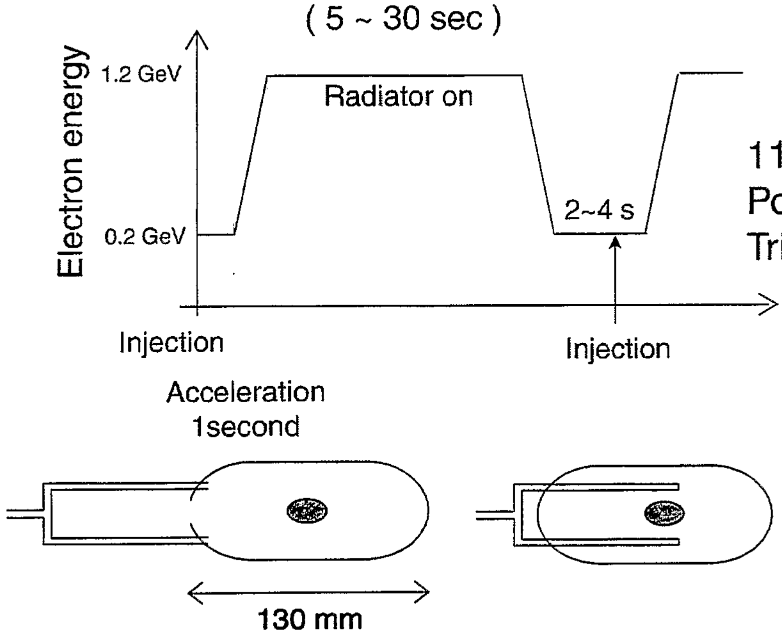

11 μm carbon fiber
Position resolution 2 μm
Triggered by the accelerator

Radiator position and counting rate of tagging counters

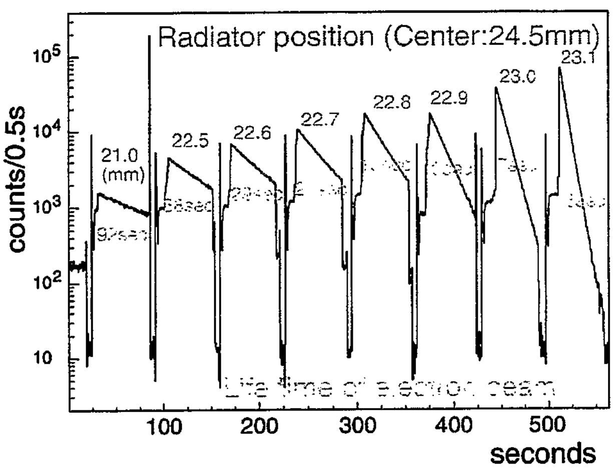

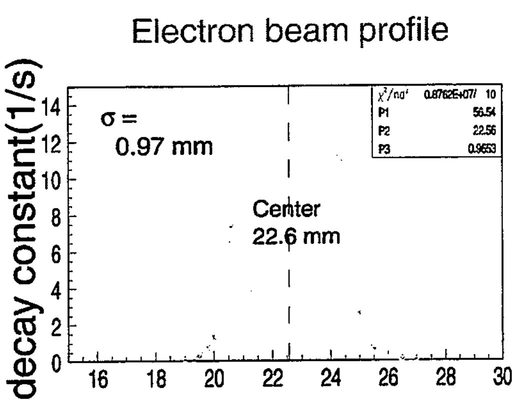

Beam intensity:
reduced exponentially with fixed radiator position

Radiator position control
Constant photon flux

Photon flux control

Radiator position : 3.6 mm to 3.0 mm from the beam center
(σ = 1.0 mm)

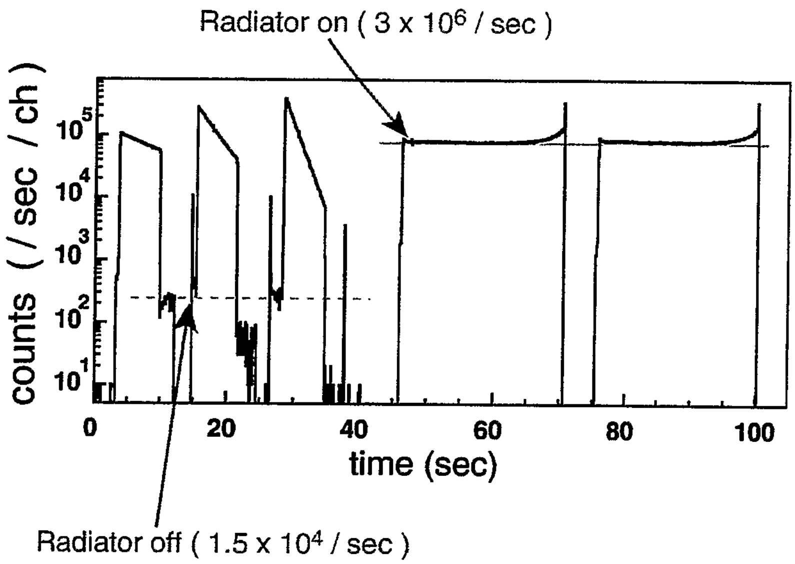

Photon flux : 6×10^6 / s
(0.8 ~ 1.1 GeV tagged γ)
Radiator off background :
less than 0.5 %
Duty factor : ~ 0.8
(for flat top of 25 s)
Tagging efficiency
~ 90 %

very stable

Tagged photon beam profile

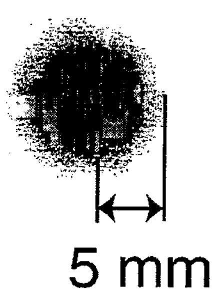

Polaroid picture taken at the target positon

FWHM ~ 10 mm

SCISSORS

(Sendai CsI Scintillator System On Radiation Search)

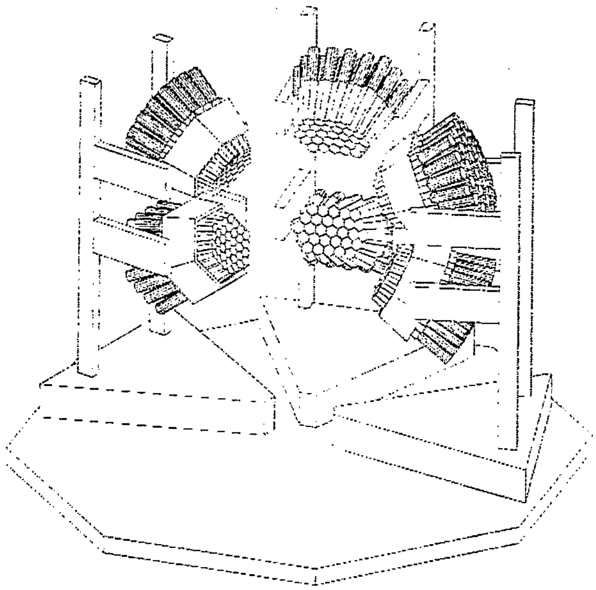

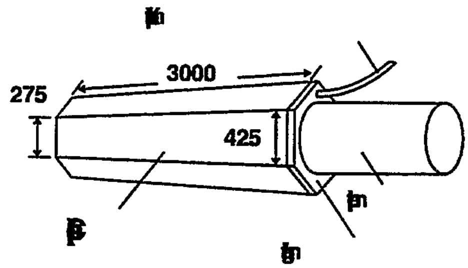

206 ch pure CsI crystal array
(about 1 sr.)
Energy resolution ~ 2% at 1 GeV
Position resolution ~ 3 cm
(Energy weighted average)

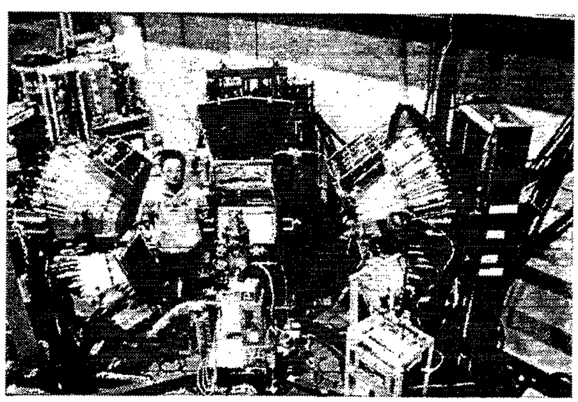

Detection of eta mesons

$\eta \rightarrow 2\gamma$ decay

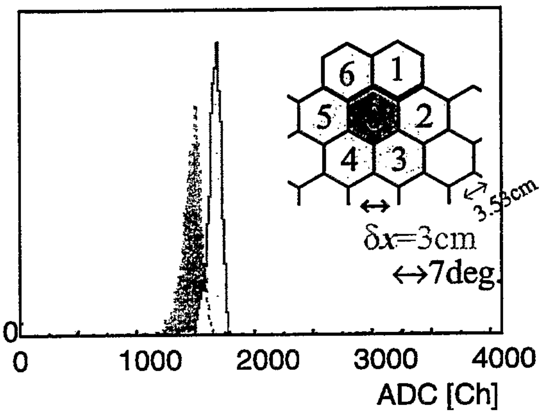

Particle IDentification :
  Plastic scintillators for charged particle veto

Energy :
  Sum of light outputs of 7 crystals

Position and momentum vector :
  Energy weighted average of crystal centers

$$x = \frac{\sum_{i=0}^{6} E_i x_i}{\sum_{i=0}^{6} E_i} \quad , \quad p_\gamma = E_\gamma \frac{x}{\|x\|}$$

Invariant mass of 2γ events

$$M_{\gamma\gamma} = \sqrt{(E_{\gamma_1} - E_{\gamma_2})^2 - (p_{\gamma_1} - p_{\gamma_2})^2}$$

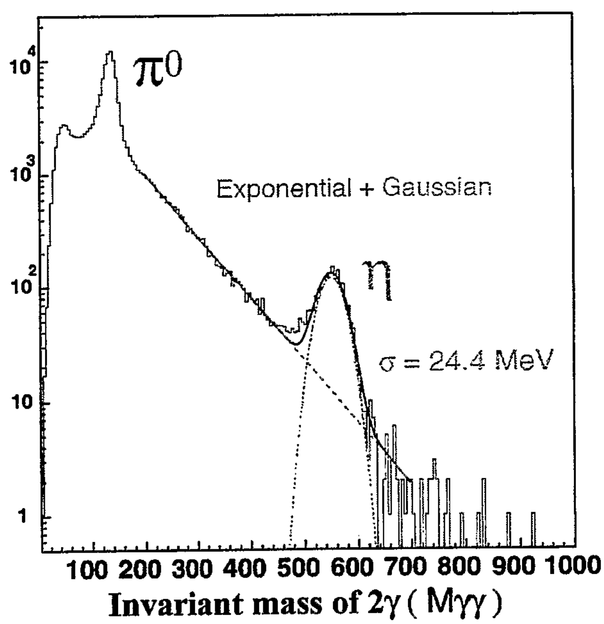

$M\gamma\gamma \sim$ 140 MeV/c^2 π^0
550 MeV/c^2 η

$\Delta M(\eta) \sim 22.4$ MeV/c^2
(~ 4 %)

Subtracting the background as the exponential function

↓

Double differential cross section

↓

Total cross section of (γ,η)

Double differential cross section

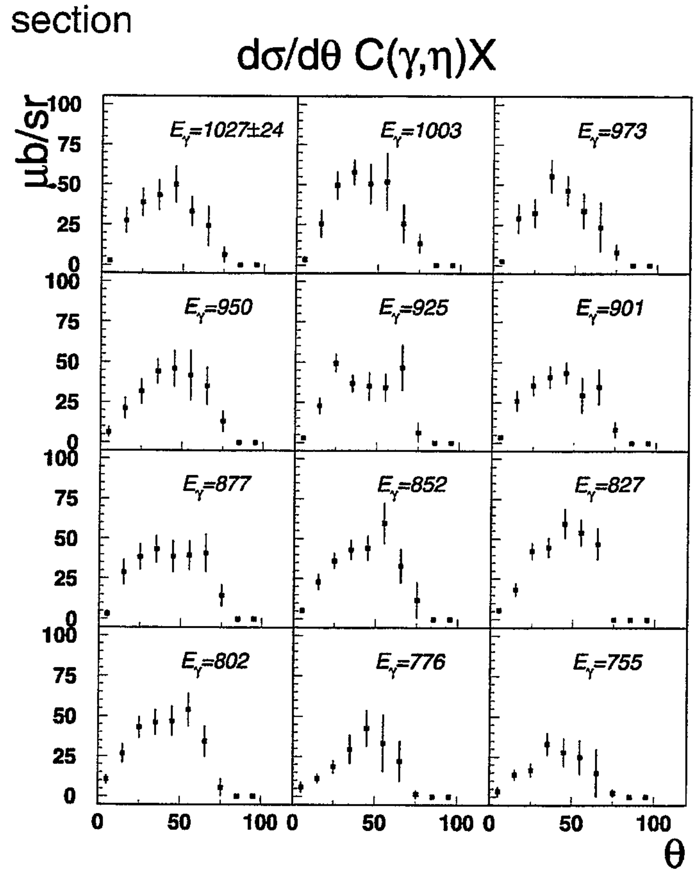

C(γ,η) reaction cross section

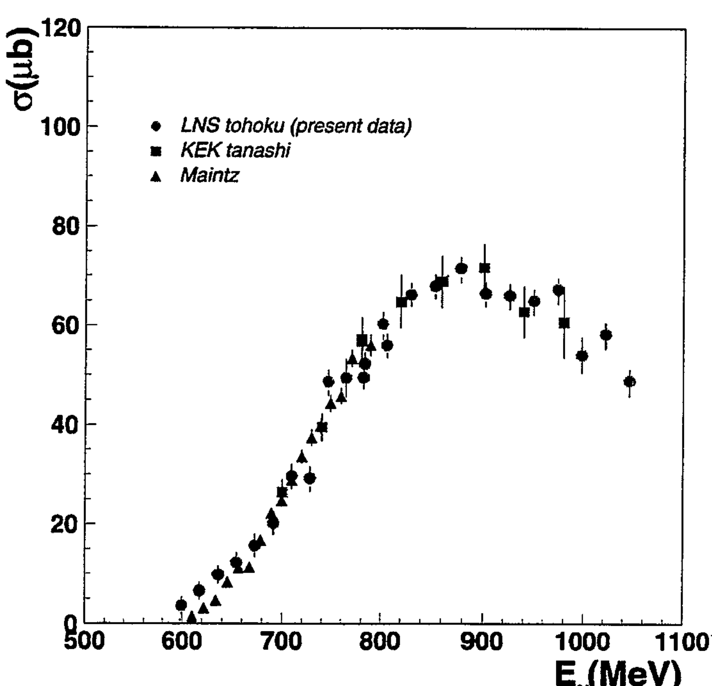

Consistent with previous data measured in Mainz and KEK

Better statistics than KEK data at around 900 MeV

New data points over 1.0 GeV of photon energy

N* property in nuclear medium?

QMD(Quantum Molecular Dynamics)

Initial state

Ground state $\rightarrow$ Fermi motion, charge dist.

$$\phi_i(\mathbf{R}_i,\mathbf{P}_i) = \frac{1}{(2\pi L)^{2/3}} \exp\left[\frac{(\mathbf{r}-\mathbf{R}_i)^2}{2L} + \frac{i}{\hbar}\,\mathbf{r}\cdot\mathbf{P}_i\right]$$

$$\frac{d\mathbf{R}_i}{dt} = \frac{\partial H}{\partial \mathbf{P}_i}, \quad \frac{d\mathbf{P}_i}{dt} = -\frac{\partial H}{\partial \mathbf{R}_i}$$

$$\begin{aligned} H = & \sum_i \sqrt{m_i^2 + \mathbf{P}_i^2} \\ & + \frac{1}{2}\frac{A}{\rho_0}\sum_i \langle\rho_i\rangle + \frac{1}{1+\tau}\frac{B}{\rho_0^\tau}\sum_i \langle\rho_i\rangle^\tau \\ & + \frac{1}{2}\sum_{i,j(\neq i)} \frac{e_i e_j}{|\mathbf{R}_i-\mathbf{R}_j|}\,\mathrm{erf}\left(|\mathbf{R}_i-\mathbf{R}_j|/\sqrt{2L}\right) \\ & + \frac{C_s}{2\rho_0}\sum_{i,j(\neq i)} c_i c_j \rho_{ij} \end{aligned}$$

$L = 0.6$ fm, $A = -248$ MeV, $B = 141$ MeV,
$\rho_0 = 0.168\ \mathrm{fm}^{-3}$, $C_s = 25$ MeV, $\tau = 4/3$

Ground state (^{12}C)

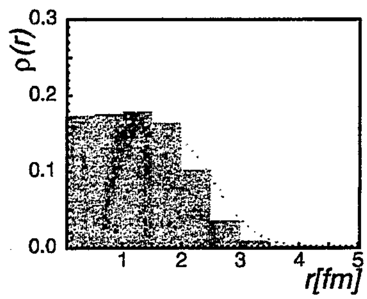

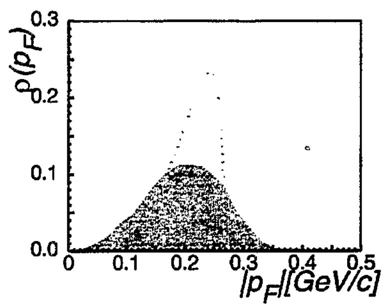

QMD(Quantum Molecular Dynamics)

Excite one nucleon

$\gamma N \rightarrow S_{11}$ (initial channel)

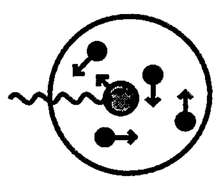

$$\sigma_{\gamma p\rightarrow\eta p} = A\left(\frac{k_0}{k}\right)^2 \frac{s\Gamma_\gamma\Gamma_\eta}{(s - M_{S_{11}}^2)^2 + s\Gamma_{tot}^2}$$

$$\Gamma_\gamma = b_\gamma\left(\frac{k}{k_0}\right)\Gamma_0$$

$$\Gamma_\pi = b_\pi\, x_\pi\, \Gamma_0,\ \Gamma_\eta = b_\eta\, x_\eta\, \Gamma_0$$

$$\Gamma_{tot} = \Gamma_\pi + \Gamma_\eta = (b_\pi\, x_\pi + b_\eta\, x_\eta)\,\Gamma_0$$

$$x_{\pi(\eta)} = \frac{q_{\pi(\eta)}}{q_{R,\pi(\eta)}}\,\frac{c^2 + q_{R,\pi(\eta)}^2}{c^2 + q_{\pi(\eta)}^2}$$

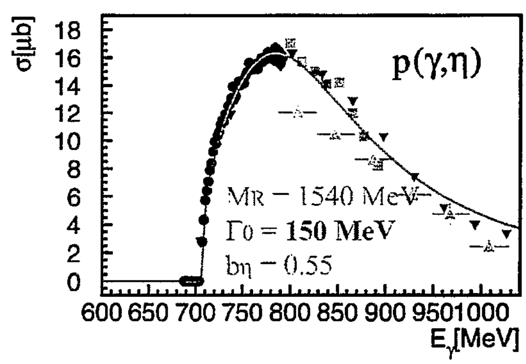

[B. Krusche et al., Phys. Rev. Lett. 74 (1995) 3736]
[M. Wilhelm, Ph.D. Thesis. Bonn. BN-IR-93-43]
[S. [illegible] et al., J. Phys. Soc. JPN. 57 (1988) 828]
[D. Rebreyend et al., Nucl. Phys. A663&664 (2000) 436c]

Recent result of (e,e'p)η at Jlab ~ 154 MeV

QMD(Quantum Molecular Dynamics)

Time evolution

$S_{11} \rightarrow \eta + N, \pi + N$ (decay)
$S_{11} + N \rightarrow N + N$ (collision)
$\eta + N \rightarrow S_{11} \rightarrow \eta + N, \pi + N$ (FSI)

η absorption

$$\eta N \rightarrow \pi N: \quad \sigma_{\eta N \rightarrow S_{11} \rightarrow \pi N} = \frac{q_\pi^2}{q_\eta^2} \cdot \sigma_{\pi N \rightarrow \eta N}$$

$$\eta N \rightarrow \eta N: \quad \sigma_{\eta N \rightarrow S_{11} \rightarrow \eta N} = \sigma_{\eta N \rightarrow S_{11} \rightarrow \pi N} \cdot \frac{\Gamma_\eta}{\Gamma_\pi}$$

RN collision

$$\Gamma_{RN \rightarrow NN} = 4\gamma \int_0^{p_F} \frac{dp_N}{(2\pi)^2} v_r \int d\Omega \, \frac{d\sigma_{RN \rightarrow NN}}{d\Omega} \, P_N P_N S$$

S : upper limit of the NR $\rightarrow$ NN cross section (80 mb)

Nuclear medium effects in QMD

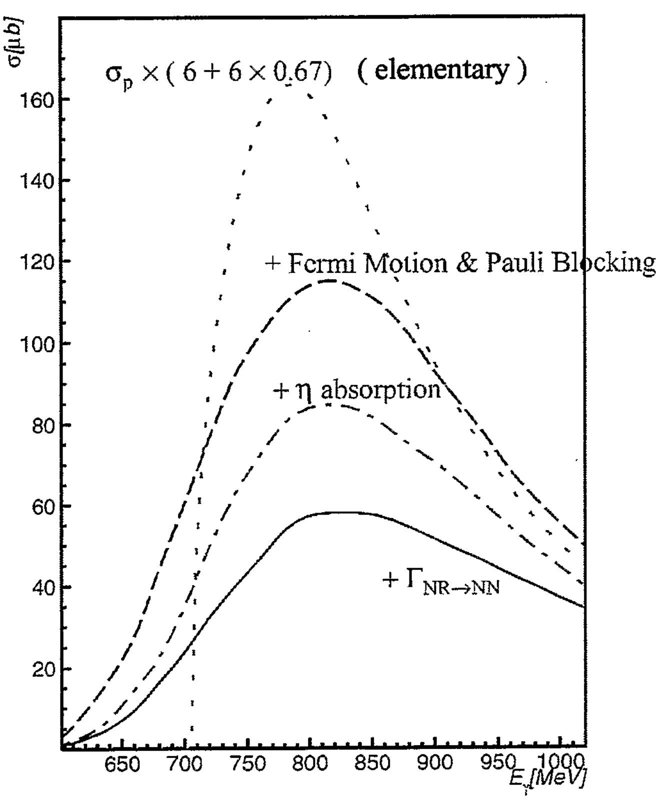

$$\sigma_{\gamma p \rightarrow \eta p} = A \left(\frac{k_0}{k}\right)^2 \frac{s\Gamma_\gamma \Gamma_\eta}{(s - M_{S_{11}}^2)^2 + s\Gamma_{tot}^2}$$

$$\Gamma_\gamma = b_\gamma \left(\frac{k}{k_0}\right) \Gamma_0$$

$$\Gamma_\pi = b_\pi x_\pi \Gamma_0, \; \Gamma_\eta = b_\eta x_\eta \Gamma_0$$

$$\Gamma_{tot} = \Gamma_\pi + \Gamma_\eta = (b_\pi x_\pi + b_\eta x_\eta) \Gamma_0$$

$$\Gamma_{tot} = \Gamma_\pi + \Gamma_\eta = (b_\pi x_\pi + b_\eta x_\eta) \Gamma_0 + \Gamma_{col}$$

Γ_R = 150 MeV
230 MeV

Comparison ith QMD

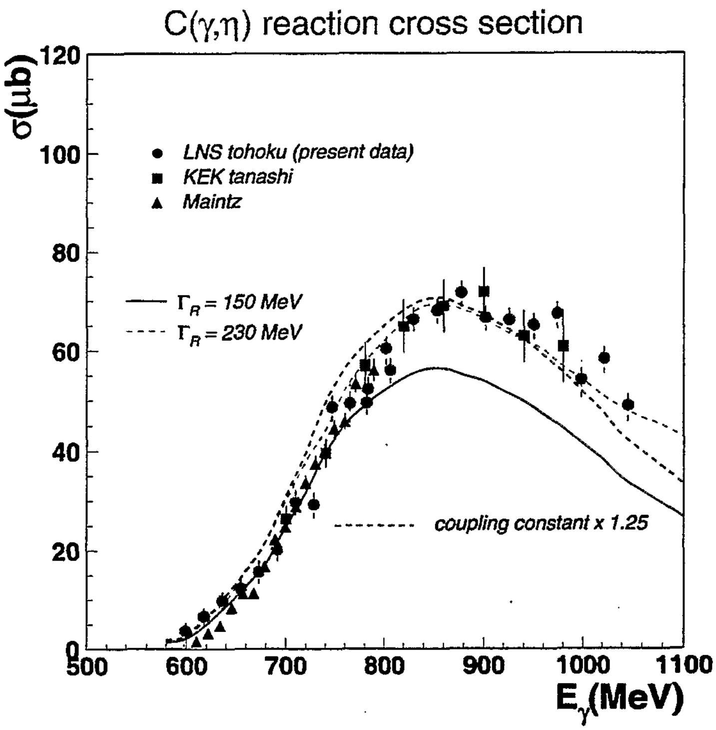

—— $\Gamma_R = 150$ MeV
Cannot reproduce the data

To explain the data

------ $\Gamma_R = 230$ MeV
Other parameters are same

------ $\Gamma_R = 150$ MeV
Increase Helicity amplitude
125→140 x 10^{-3} $GeV^{-1/2}$ (12%)
or
S_{11}→ Nη branch
0.55→0.69 (25%)

Other effect
Coherent production (iso-scaler) : samll
Two step (via $D_{13}(1520)$) : less than 5%

Summary

(γ, η) cross section on C
Fermi motion, Pauli blocking, η-absorption and collision broadening could not explain the data

Increase Γ_0 (150 MeV to 230 MeV)
or
Increase helicity amplitude or Nη decay branch

Width or Coupling or something else : changed in nuclei

(γ,η) reaction on other Nuclei (Al, Cu)
ηN interaction

Upgrade programs

Large solid angle
crystal array complex

CsI (existent)
+ PWO (forward)
+ BSO (barrel)

$\sigma \rightarrow 2\pi^0 \rightarrow 4\gamma$ detection
D13(1520) $\rightarrow 2\pi^0 + N$

Proton and deuteron target

Solid Hydrogen Target

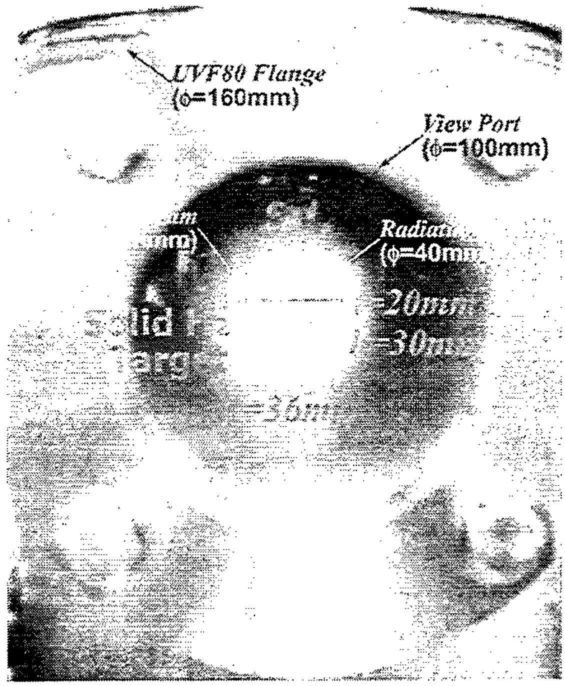

Large solid angle crystal array complex

CsI + PWO (forward)
+ BSO (barrel)

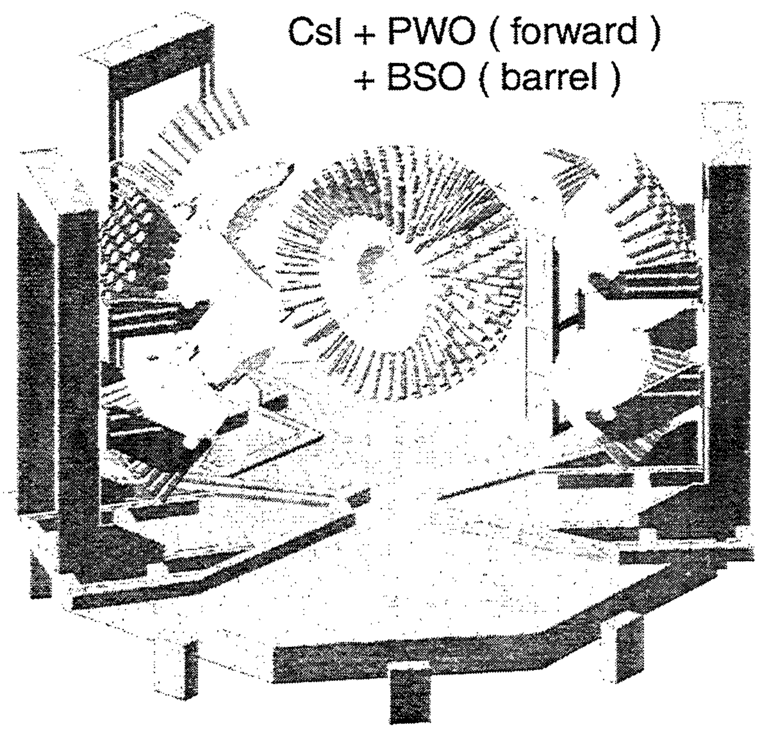

$\sigma \rightarrow 2\pi^0 \rightarrow 4\gamma$ detection
D13(1520) $\rightarrow 2\pi^0 + N$

List of Participants

Abuki, Hiroaki (University of Tokyo)
Akiba, Yasuyuki (KEK)
Akimura, Yuka (Saitama University)
Baba, Hidetoshi (Kyoto University)
Qiao, Cong Feng (Hiroshima University)
En'yo, Hideto (RIKEN/RBRC)
Fueki, Yuko (Nara Women's University)
Fujii, Hirotsugu (University of Tokyo)
Goi, Kazuhiro (Waseda University)
Goto, Yuji (RIKEN/RBRC)
Hatsuda, Tetsuo (University of Tokyo)
Hatta, Yoshitaka (Kyoto University)
Hidaka, Yoshimasa (KEK)
Hirai, Masanori (RIKEN)
Hirano, Tetsufumi (University of Tokyo)
Horaguchi, Takuma (Tokyo Institute of Technology)
Horikawa, Naoaki (Nagoya University)
Hotta, Tomoaki (Osaka University)
Ichikawa, Kazuhide (University of Tokyo)
Iida, Hideaki (Tokyo Institute of Technology)
Iio, Masami (Miyazaki University)
Ishida, Takashi (Kyushu University)
Ishii, Noriyoshi (RIKEN)
Kagawa, Shinji (University of Tokyo)
Kajihara, Fukutaro (CNS, University of Tokyo)
Kamano, Hiroyuki (Osaka City University)
Kamihara, Nobuyuki (Tokyo Institute of Technology/BNL)
Kitazawa, Masakiyo (Kyoto University)
Kiyomichi, Akio (Tsukuba University)
Kohama, Akihisa (RIKEN)
Kohara, Munetsugu (Hiroshima University)
Kohno, Takanori (KEK)
Matsuo, Mamoru (University of Tokyo)
Matsuura, Taeko (University of Tokyo)
Mawatari, Kentaro (Kobe University)
Miyahara, Fusashi (Tohoku University)
Muto, Ryotaro (Kyoto University)
Nagai, Yukoh (University of Tokyo)
Nagashima, Junji (Niigata University)
Nakabayashi, Tadashi (Tohoku University)
Naruki, Megumi (Kyoto University)
Nasu, Takashi (Tokyo Institute of Technology)
Nishikawa, Miyuki (University of Tokyo)
Oka, Makoto (Tokyo Institute of Technology)
Osuga, Hiroshi (Tokyo Institute of Technology)
Oyama, Ken (CNS, University of Tokyo)

Oyama, Satoshi (Kobe University)
Saito, Naohito (RIKEN/RBRC)
Saito, Takuya (Hiroshima University)
Sakuma, Fuminori (Kyoto University)
Sasaki, Chihiro (Nagoya University)
Sawada, Shinya (KEK)
Shibata, Toshi-Aki (Tokyo Institute of Technology)
Shimizu, Hirotaka (Hiroshima University)
Shindo, Miki (University of Tokyo)
Soper, David (University of Oregon)
Sudou, Kazutaka (Kobe University)
Suzuki, Ken (University of Tokyo)
Suzuki, Tomokazu (Yamagata University)
Takahashi, Takeshi (Saitama University)
Tanaka, Hidekazu (Tokyo Institute of Technology)
Tanushi, Yuichiro (Nagoya University)
Toi, Yuya (Miyazaki University)
Tsutsumi, Yohei (University of Tokyo)
Watanabe, Yasushi (RIKEN/RBRC)
Watanabe, Yoshiki (University of Tokyo)
Yamazaki, Hirohito (Tohoku University)
Yasui, Yoshiaki (KEK)
Yazaki, Koichi (Tokyo Woman's Christian University/RIKEN)
Yokokawa, Kazuo (University of Tokyo)
Yokoya, Hiroshi (Hiroshima University)

Program of the School

March 29 (Fri)	
9:30 - 10:00	Registration
Beginning of School	
10:00 - 10:15	Orientation
10:15 - 11:15	Soper (1)
11:35 - 12:35	Oka (1)
Lunch	
14:00 - 15:00	Yamazaki
15:30 - 16:30	Goto
16:50 - 17:50	Hatsuda (1)
18:00 -	Reception
March 30 (Sat)	
9:30 - 10:30	Oka (2)
10:50 - 11:50	Soper (2)
Lunch	
13:00 - 14:00	Shibata
14:20 - 15:20	Horikawa
15:50 - 16:50	Hatsuda (2)
17:10 - 18:10	Oka (3)
March 31 (Sun)	
9:30 - 10:30	Soper (3)
10:50 - 11:50	Hatsuda (3)
Lunch	
13:00 - 14:00	Hotta
14:20 - 15:20	Akiba
15:30 - 16:00	Summary
End of School	

Winter School

Pictures

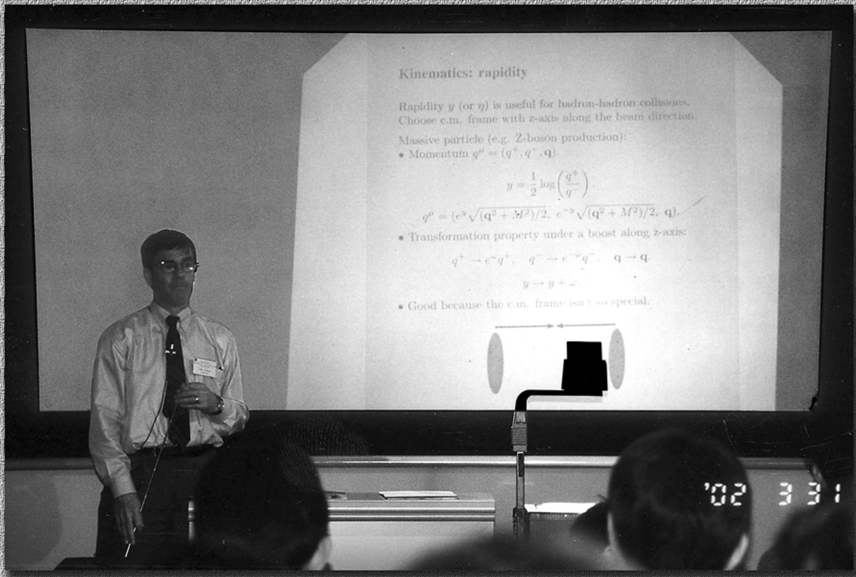
Kinematics: rapidity
Rapidity y (or η) is useful for hadron-hadron collisions.
Choose c.m. frame with z-axis along the beam direction.
Massive particle (e.g. Z-boson production):
• Momentum $q^\mu = (q^+, q^-, \mathbf{q})$.
$$y = \frac{1}{2}\log\left(\frac{q^+}{q^-}\right).$$
$$q^\mu = (e^y\sqrt{(\mathbf{q}^2+M^2)/2},\ e^{-y}\sqrt{(\mathbf{q}^2+M^2)/2},\ \mathbf{q}).$$
• Transformation property under a boost along z-axis:
$$q^+ \to e^\omega q^+,\quad q^- \to e^{-\omega} q^-,\quad \mathbf{q} \to \mathbf{q}.$$
$$y \to y + \omega.$$
• Good because the c.m. frame isn't so special.
'02 3 31


'02

Additional RIKEN BNL Research Center Proceedings:

Volume 43 – RIKEN Winter School – Quark-Gluon Structure of the Nucleon and QCD – BNL-
Volume 42 – Baryon Dynamics at RHIC – BNL-52669
Volume 41 – Hadron Structure from Lattice QCD – BNL-
Volume 40 – Theory Studies for RHIC-Spin – BNL-52662
Volume 39 – RHIC Spin Collaboration Meeting VII – BNL-52659
Volume 38 – RBRC Scientific Review Committee Meeting – BNL-52649
Volume 37 – RHIC Spin Collaboration Meeting VI (Part 2) – BNL-52660
Volume 36 – RHIC Spin Collaboration Meeting VI – BNL-52642
Volume 35 – RIKEN Winter School – Quarks, Hadrons and Nuclei – QCD Hard Processes and the Nucleon Spin – BNL-52643
Volume 34 – High Energy QCD: Beyond the Pomeron – BNL-52641
Volume 33 – Spin Physics at RHIC in Year-1 and Beyond – BNL-52635
Volume 32 – RHIC Spin Physics V – BNL-52628
Volume 31 – RHIC Spin Physics III & IV Polarized Partons at High Q^2 Region – BNL-52617
Volume 30 – RBRC Scientific Review Committee Meeting – BNL-52603
Volume 29 – Future Transversity Measurements – BNL-52612
Volume 28 – Equilibrium & Non-Equilibrium Aspects of Hot, Dense QCD – BNL-52613
Volume 27 – Predictions and Uncertainties for RHIC Spin Physics & Event Generator for RHIC Spin Physics III – Towards Precision Spin Physics at RHIC – BNL-52596
Volume 26 – Circum-Pan-Pacific RIKEN Symposium on High Energy Spin Physics – BNL-52588
Volume 25 – RHIC Spin – BNL-52581
Volume 24 – Physics Society of Japan Biannual Meeting Symposium on QCD Physics at RIKEN BNL Research Center – BNL-52578
Volume 23 – Coulomb and Pion-Asymmetry Polarimetry and Hadronic Spin Dependence at RHIC Energies – BNL-52589
Volume 22 – OSCAR II: Predictions for RHIC – BNL-52591
Volume 21 – RBRC Scientific Review Committee Meeting – BNL-52568
Volume 20 – Gauge-Invariant Variables in Gauge Theories – BNL-52590
Volume 19 – Numerical Algorithms at Non-Zero Chemical Potential – BNL-52573
Volume 18 – Event Generator for RHIC Spin Physics – BNL-52571
Volume 17 – Hard Parton Physics in High-Energy Nuclear Collisions – BNL-52574
Volume 16 – RIKEN Winter School - Structure of Hadrons - Introduction to QCD Hard Processes – BNL-52569
Volume 15 – QCD Phase Transitions – BNL-52561
Volume 14 – Quantum Fields In and Out of Equilibrium – BNL-52560

Additional RIKEN BNL Research Center Proceedings:

Volume 13 – Physics of the 1 Teraflop RIKEN-BNL-Columbia QCD Project First Anniversary Celebration – BNL-66299

Volume 12 – Quarkonium Production in Relativistic Nuclear Collisions – BNL-52559

Volume 11 – Event Generator for RHIC Spin Physics – BNL-66116

Volume 10 – Physics of Polarimetry at RHIC – BNL-65926

Volume 9 – High Density Matter in AGS, SPS and RHIC Collisions – BNL-65762

Volume 8 – Fermion Frontiers in Vector Lattice Gauge Theories – BNL-65634

Volume 7 – RHIC Spin Physics – BNL-65615

Volume 6 – Quarks and Gluons in the Nucleon – BNL-65234

Volume 5 – Color Superconductivity, Instantons and Parity (Non?)-Conservation at High Baryon Density – BNL-65105

Volume 4 – Inauguration Ceremony, September 22 and Non -Equilibrium Many Body Dynamics – BNL-64912

Volume 3 – Hadron Spin-Flip at RHIC Energies – BNL-64724

Volume 2 – Perturbative QCD as a Probe of Hadron Structure – BNL-64723

Volume 1 – Open Standards for Cascade Models for RHIC – BNL-64722

For information please contact:

Ms. Pamela Esposito
RIKEN BNL Research Center
Building 510A
Brookhaven National Laboratory
Upton, NY 11973-5000 USA

Phone: (631) 344-3097
Fax: (631) 344-4067
E-Mail: pesposit@bnl.gov

Ms. Tammy Heinz
RIKEN BNL Research Center
Building 510A
Brookhaven National Laboratory
Upton, NY 11973-5000 USA

(631) 344-5864
(631) 344-2562
theinz@bnl.gov

Homepage: http://quark.phy.bnl.gov/www/riken.html
http://penguin.phy.bnl.gov/www/riken.html

RIKEN BNL RESEARCH CENTER

RIKEN Winter School

Quark-Gluon Structure of the Nucleon and QCD

March 29-31, 2002

核子重如牛對撞生新態

Li Keran

Nuclei as heavy as bulls
Through collision
Generate new states of matter.
T.D. Lee

Speakers:

Y. Akiba	Y. Goto	T. Hatsuda	N. Horikawa	T. Hotta
M. Oka	T.-A. Shibata	D. E. Soper	Y. Watanabe	H. Yamazaki

Organizers: H. En'yo, N. Saito, T.-A. Shibata, & K. Yazaki